Université de Toulouse

THÈSE

En vue de l'obtention du

DOCTORAT DE L'UNIVERSITÉ DE TOULOUSE

Délivré par :

Université Toulouse 3 Paul Sabatier (UT3 Paul Sabatier)

Présentée et soutenue par :
Nicolas CHASSAING

le jeudi 12 décembre 2013

Titre :

Génétique des micro-anophtalmies : revue des phénotypes et des génotypes ; stratégies d'identification de nouveaux gènes impliqués dans le développement oculaire

---

École doctorale et discipline ou spécialité :

ED BSB : Gènes, cellules et développement

Unité de recherche :

EA-4555, Université Paul-Sabatier Toulouse III

Directeur(s) de Thèse :

Professeur Patrick CALVAS (PU-PH)
Docteur Heather ETCHEVERS (CR1)

Jury :

Professeur Stéphane BEZIEAU (PU-PH) - Rapporteur
Professeur Patrick CALVAS (PU-PH) - Directeur
Professeur Mireille CLAUSTRES (PU-PH) - Examinateur
Docteur Erica E. DAVIS (PhD) - Examinateur
Docteur Heather ETCHEVERS (CR1) - Co-Directeur
Professeur Cyril GOIZET (PU-PH) - Rapporteur
Professeur Sylvie ODENT (PU-PH) - Examinateur

Université de Toulouse

THÈSE

En vue de l'obtention du

DOCTORAT DE L'UNIVERSITÉ DE TOULOUSE

Délivré par :

Université Toulouse 3 Paul Sabatier (UT3 Paul Sabatier)

Présentée et soutenue par :
Nicolas CHASSAING

le jeudi 12 décembre 2013

Titre :

Génétique des micro-anophtalmies : revue des phénotypes et des génotypes ; stratégies d'identification de nouveaux gènes impliqués dans le développement oculaire

---

École doctorale et discipline ou spécialité :

ED BSB : Gènes, cellules et développement

Unité de recherche :

EA-4555, Université Paul-Sabatier Toulouse III

Directeur(s) de Thèse :

Professeur Patrick CALVAS (PU-PH)
Docteur Heather ETCHEVERS (CR1)

Jury :

Professeur Stéphane BEZIEAU (PU-PH) - Rapporteur
Professeur Patrick CALVAS (PU-PH) - Directeur
Professeur Mireille CLAUSTRES (PU-PH) - Examinateur
Docteur Erica E. DAVIS (PhD) - Examinateur
Docteur Heather ETCHEVERS (CR1) - Co-Directeur
Professeur Cyril GOIZET (PU-PH) - Rapporteur
Professeur Sylvie ODENT (PU-PH) - Examinateur

A Marie, Paul et Carmen

A mes parents

Patrick,

Ce travail est l'occasion pour moi de te remercier pour la formation de généticien que tu m'as donnée. Tu m'as enseigné l'importance d'une vision englobant les différents aspects de notre spécialité (clinique, moléculaire et chromosomique) ainsi que les aspects éthiques et sociétaux indissociables de notre métier. Tu m'as appris à réfléchir aux implications potentielles de chaque analyse prescrite et à réfléchir aux bénéfices, mais aussi aux limites et aux conséquences éventuelles de celles-ci. Merci également de m'avoir fait confiance et de m'avoir ainsi permis rapidement de m'autonomiser que ce soit dans le cadre de la génétique clinique, du laboratoire hospitalier ou du laboratoire de recherche. J'ai ainsi pu apprendre à développer des projets tout en sachant pouvoir compter sur tes conseils en cas de doute ou difficulté.

Je te suis reconnaissant pour tout cela.

Sommaire

LISTE DES FIGURES ET TABLEAUX

Figures

Tableaux

LISTE DES PUBLICATIONS

PRESENTATION GENERALE

Les anophtalmies et microphtalmies (AM) sont les plus sévères des malformations de l'œil. Leur incidence est estimée entre 1 sur 5000 et 1 sur 10000 naissances[1]. La microphtalmie est définie par une diminution de la longueur axiale de l'œil inférieure à -2 déviations standard (19 mm à un an et 21 mm à l'âge adulte)[2, 3], l'anophtalmie par une absence de structure oculaire. Les AM peuvent être isolées, associées à d'autres malformations oculaires (AM complexes), et parfois à une déficience intellectuelle, ou à des malformations d'organes (AM syndromiques). Ces malformations oculaires sont une cause importante de malvoyance et la prévalence des AM chez les aveugles est estimée entre 3,2 % et 11,2 %[1].

Bien que certaines causes environnementales soient connues pour être impliquées dans les AM (rubéole, acide rétinoïque, thalidomide, alcool…) elles ne rendent compte que d'une minorité des AM. Les causes génétiques sont prépondérantes, et le risque de récurrence d'AM dans la fratrie d'un cas index est estimé entre 10 % et 15 %. Des mutations dans plusieurs gènes ont été décrites dans ces anomalies du développement oculaire. Différentes voies métaboliques ont ainsi été impliquées, mais les principaux gènes codent pour des facteurs de transcription (PAX6, SOX2, OTX2, RAX, VSX2/CHX10 et FOXE3). Tous ces gènes sont fortement conservés au cours de l'évolution et jouent un rôle dans le développement des yeux et de la tête, même chez les invertébrés. Des mutations du gène *SOX2* expliquent 10 à 20 % des AM[4, 5], alors que les autres gènes ne sont impliqués que beaucoup plus rarement. Notre laboratoire hospitalier s'est spécialisé dans le diagnostic moléculaire des anomalies du développement embryonnaire oculaire, et j'ai participé pendant ma formation médicale à mettre au point les analyses moléculaires de plusieurs des gènes d'AM et à analyser des patients. Mon travail de thèse a consisté pour partie à analyser les résultats moléculaires obtenus dans une cohorte de 150 patients atteints d'AM. Ceci nous a permis de préciser la fréquence de l'implication de chaque gène et d'analyser les phénotypes associés.

A partir de deux familles particulières, nous avons pu explorer plus précisément les phénotypes liés aux mutations des gènes *OTX2* et *STRA6* :

- nous avons, en effet, observé la présence de patients présentant un défaut sévère du développement de la mâchoire inférieure (agnathie ou otocéphalie) dans une famille où une mutation du gène *OTX2* avait été identifiée chez plusieurs membres atteints d'AM. Nous avons pu recruter, en collaboration avec le Pr Ethylin Jabs (New York, USA), d'autres patients otocéphales et confirmer l'implication du gène *OTX2* chez certains. Nous avons de plus essayé de comprendre, en collaboration avec l'équipe du Pr. Nicholas Katsanis et du Dr. Erica Davis (Université de Duke, Durham, USA), les facteurs pouvant expliquer ces variations

phénotypiques intra familiales et avons apporté des arguments pour un modèle de gènes modificateurs.

- Les mutations du gène *STRA6* ont été impliquées dans une AM syndromique, le syndrome de Matthew-Wood (ou PDAC pour Pulmonary, Diaphragmatic, Anophthalmia, Cardiac). Nous avons pu montrer que ce gène pouvait être à l'origine d'un spectre phénotypique plus large allant du syndrome de Matthew-Wood à une atteinte oculaire isolée. Nous avons spécifiquement étudié l'implication de ce gène dans les différentes présentations cliniques dans un projet collaboratif avec le Dr. Nicola Ragge (Oxford, UK).

Malgré des analyses moléculaires poussées, aucune cause génétique ne peut être identifiée chez plus de 3/4 des patients avec AM. L'hétérogénéité génétique déjà mise en évidence indique que seule une partie (probablement petite) des gènes d'AM avait été identifiée et que d'autres gènes d'AM restaient donc à découvrir. Pour identifier ces gènes, nous avons décidé de mener en parallèle plusieurs approches :

- Le séquençage de gènes et régions candidates
- L'identification de gènes candidats par recherche de réarrangement chromosomique en CGH-array
- L'identification de gènes candidats par une approche plus fondamentale visant à identifier les cibles des facteurs de transcription majeurs déjà impliqués dans les AM (SOX2, OTX2, RAX et PAX6)

Grâce au développement des techniques de séquençage haut débit, nous avons pu séquencer un total de 407 gènes candidats (fonctionnels, positionnels, ou cible d'un des 4 facteurs de transcription étudiés). Cette analyse nous a permis d'identifier un 2eme gène majeur impliqué dans les défauts du développement oculaire, le gène *PTCH1*. Le caractère délétère des mutations identifiées dans notre cohorte a pu être confirmé sur un modèle de poisson zèbre (*Danio rerio*) grâce à une collaboration entreprise avec le Dr. Erica Davis (Université de Duke, Durham, USA). L'implication de ce gène est particulièrement intéressante car elle permet de confirmer un faisceau d'éléments qui laissait suspecter l'implication importante de la voie *SHH* dans le développement oculaire. Cette analyse a également pointé d'autres gènes dont l'implication dans les défauts du développement embryonnaire oculaires reste à démontrer.

Enfin, nous avons participé, dans le cadre de projets collaboratifs à l'identification de nouveaux gènes impliqués dans des AM isolées (*TMX3*) ou syndromiques (*ALDH1A3*, *RARB*).

Nous avons initié plus récemment un nouveau projet collaboratif avec le Dr. Nicola Ragge (Oxford, UK) et avons étudié par séquençage d'exome 24 patients atteints d'AM (12 trio chez des cas sporadiques et 12 patients issus de parents apparentés). D'autres projets collaboratifs similaires (utilisant le séquençage haut débit) ont également été entrepris pour identifier des gènes impliqués dans des anomalies du développement oculaire isolées (anomalies de la chambre antérieure) ou syndromiques (microphtalmie de Lenz, syndrome de Gillespie, syndrome PDAC).

Afin de bien montrer la diversité des différentes approches employées, j'ai décidé de subdiviser cet exposé en 6 grandes parties :

1- Une introduction à l'anatomie de l'œil, à son embryologie, à la génétique des AM et une description des 4 facteurs de transcription sélectionnés pour notre approche expérimentale.
2- La présentation des résultats obtenus par analyse des gènes d'AM précédemment identifiés dans notre cohorte de 150 patients souffrant d'AM
3- Une description plus spécifique des phénotypes associés aux mutations des gènes *OTX2* et *STRA6*
4- La recherche de nouveaux gènes d'AM avec la description des différentes stratégies utilisées en parallèle. Un sous chapitre sera dédié à chaque approche méthodologique.
5- Un exposé des travaux collaboratifs finalisés
6- Une discussion générale récapitulant les principaux résultats et soulignant le lien entre ces différents chapitres. Il y sera associé une partie sur les perspectives de poursuivre ce travail.

CHAPITRE I

INTRODUCTION

I-1 : Anatomie de l'œil

Introduction

L'œil est l'organe de la vision. Il permet de capter la lumière pour l'analyser et interagir avec l'environnement. C'est est un organe complexe comprenant des structures aux fonctions très différentes. Ces structures assurent une fonction de protection (sclérotique), de réfraction (cornée, cristallin), d'accommodation (le cristallin et ses annexes), de diaphragme (iris et pupille) et de réception et transmission de l'image (rétine) vers les structures cérébrales au travers du nerf optique.

Anatomie de l'œil

L'œil humain est constitué d'un globe oculaire, formé de 3 enveloppes (de l'extérieur vers l'intérieur): la scléro-cornée, l'uvée (iris, corps ciliaire et choroïde), et la rétine. Il est divisé en deux parties situées de part et d'autre du cristallin : le segment antérieur et le segment postérieur (Fig. 1).

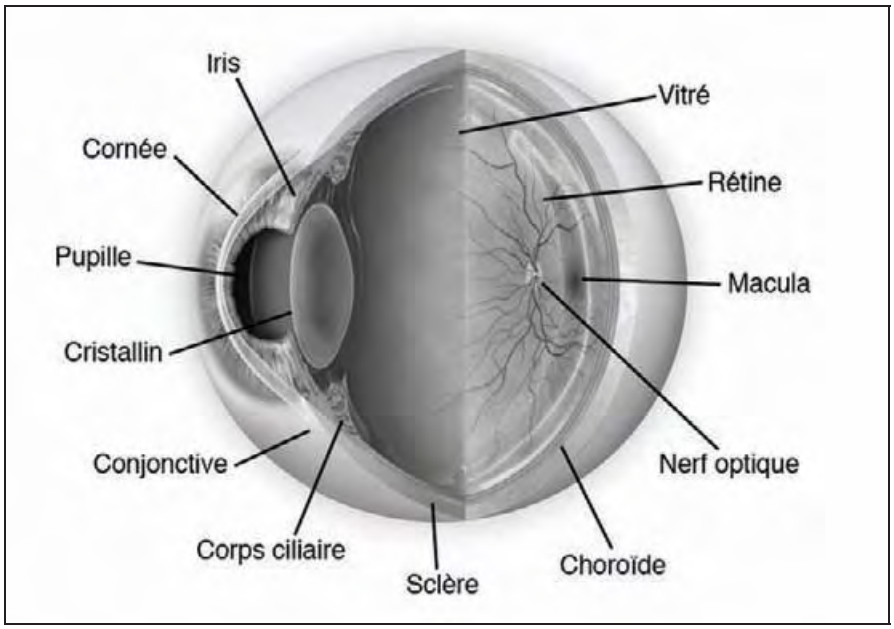

Figure 1: Anatomie de l'œil.[1]

Les différentes structures oculaires sont indiquées. Le segment antérieur comprend l'humeur aqueuse, l'iris et la pupille, la cornée et le cristallin. Le segment postérieur comprend l'humeur vitrée et la rétine.

[1] http://tpeveil.e-monsite.com/medias/images/anatomie-oeil-1.jpg

1. Le segment antérieur
    a. La cornée

La cornée prolonge la sclérotique dans sa partie antérieure. Il s'agit d'un tissu conjonctif transparent recouvrant en avant la pupille et l'iris. Elle a un rôle de dioptre convergent.

La cornée se compose de 5 couches qui sont de l'extérieur vers l'intérieur :

- *Un épithélium cornéen* qui joue un rôle de barrière avec le milieu extérieur. Il s'agit d'un épithélium pavimenteux stratifié non kératinisé, qui repose sur une membrane basale. Sa surface apicale, tapissée de microplis retient un film aqueux de larmes humidifiant en permanence la cornée.
- *La membrane de Bowman* située entre la membrane basale épithéliale et le stroma.
- *Le stroma cornéen*, collagène et dense. Il occupe plus de 90 % de la cornée. Il est limité en avant par la membrane de Bowman et en arrière par la membrane de Descemet. Les microfibrilles de collagène sont groupées en lamelles empilées parallèlement, entre lesquelles se disposent les fibroblastes du stroma, ou kératocytes. D'une lamelle à l'autre, l'orientation des microfibrilles est différente. Les microfibrilles ont toutes le même diamètre, et leur indice de réfraction est identique à celui de la substance fondamentale, conditions essentielles au maintien de la transparence de la cornée.
- *La membrane de Descemet*, membrane basale épaissie de l'endothélium cornéen.
- *L'endothélium cornéen*, pavimenteux simple.

    b. L'iris

L'iris a une forme de disque perforé en son centre par la pupille. Le stroma irien est formé de tissu conjonctif qui prolonge le stroma du corps ciliaire. On trouve dans ce stroma

- deux muscles lisses responsables des variations du diamètre de la pupille : le dilatateur et le constricteur de la pupille.
- des cellules pigmentaires responsables des différences de couleur des yeux.

La face postérieure du stroma irien est revêtue par un épithélium bistratifié poursuivant l'épithélium des procès ciliaires qui prolonge la rétine (Fig. 2).

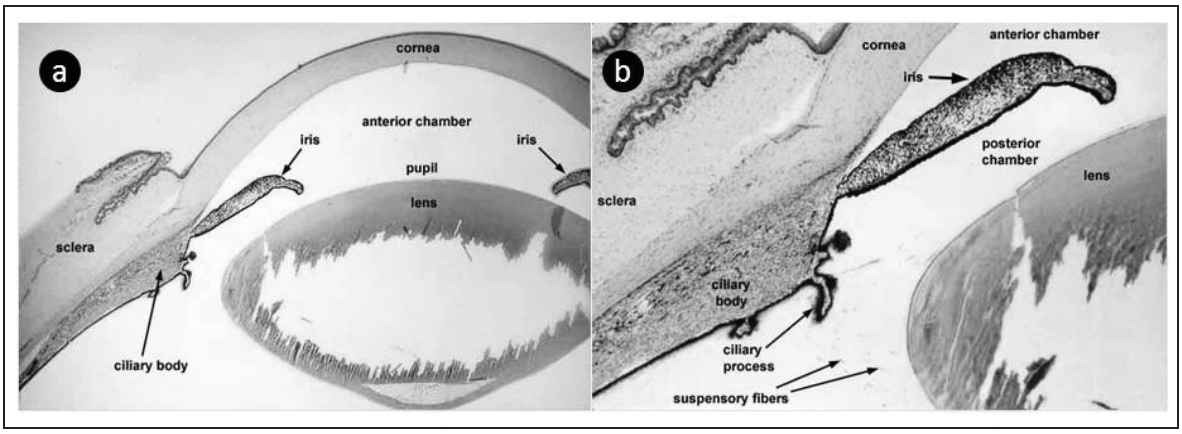

Figure 2: Coupe histologique d'un œil.[2]

(**a**) Les différentes structures de la chambre antérieure sont visibles et indiquées sur la coupe histologique. (**b**) Agrandissement au niveau du corps ciliaire. On remarque la continuité entre le stroma irien et le stroma du corps ciliaire et entre l'épithélium postérieur des procès ciliaire et celui de l'iris. Les ligaments suspenseurs liant le cristallin au corps ciliaire sont également visibles.

c. La pupille

La pupille est l'ouverture dans l'iris qui a un rôle de diaphragme : elle module la quantité de lumière pénétrant dans l'œil qui atteindra la rétine.

d. Le cristallin

C'est la structure postérieure du segment antérieur de l'œil. De forme d'une lentille biconvexe, il assure une fonction d'accommodation. Le cristallin est un massif épithélial transparent, non vascularisé. Ce massif épithélial est constitué de cellules dont le noyau a disparu et contenant des protéines spécifiques (cristallines) dont la fonction est d'assurer la transparence du cristallin et d'absorber les UV pour protéger la rétine. Les cellules cristalliniennes sont tassées les unes contre les autres avec un grand axe grossièrement antéro-postérieur. Le cristallin est relié par les ligaments suspenseurs du cristallin au corps ciliaire. Celui-ci, par le jeu de la contraction des muscles ciliaires contenus dans son stroma conjonctif, peut ainsi modifier la forme du cristallin et permettre l'accommodation à la distance (Fig. 2).

e. Les procès ciliaires

Ce sont des franges formées d'un axe conjonctif riche en vaisseaux et revêtu d'un épithélium cubique bistratifié. Cet épithélium est le prolongement vers l'avant de la rétine. Les procès ciliaires sécrètent

[2] Adaptée de http://www.siumed.edu/~dking2/ssb/

l'humeur aqueuse qui assure la nutrition de la cornée, de l'iris et du cristallin. L'humeur aqueuse est drainée au niveau de l'angle irido-cornéen.

2. Le segment postérieur

Le segment postérieur de l'œil est limité en avant par le cristallin et en arrière par la rétine. Il contient un gel transparent, l'humeur vitrée.

a. L'humeur vitrée

C'est un milieu gélatineux transparent, fait d'eau à 90 %, de glycosaminoglycanes et de collagène. Il assure un rôle de maintien de la rétine contre la paroi de l'œil, ainsi qu'un rôle de réservoir de facteurs trophiques pour le cristallin et la rétine.

b. La rétine

La rétine est composée de deux feuillets : l'épithélium pigmentaire rétinien (RPE) et la neurorétine :

- Le RPE est formé par un épithélium simple, fait de cellules pavimenteuses, hexagonales, synthétisant de la mélanine. La face apicale de ces cellules présente des expansions qui enveloppent le segment externe des photorécepteurs. Le bon fonctionnement du RPE est essentiel pour l'intégrité de la neurorétine (rôle dans le renouvellement des photorécepteurs, dans le renouvellement de la rhodopsine et des pigments, dans le transport transépithélial, absorption des photons n'ayant pas interagi avec les photopigments, sécrétion de facteurs de croissance ou d'immunomodulateurs…). La face basale du RPE repose sur la membrane de Brüch qui réunit la choroïde à la rétine.
- La neurorétine constitue un récepteur des signaux lumineux (photons). Elle les capte et les transforme en signaux électro-chimiques grâce à des photorécepteurs : cônes (vision diurne et colorée) et bâtonnets (vision crépusculaire et nocturne en noir et blanc). Ces signaux électro-chimiques sont alors envoyés vers les aires visuelles cérébrales par le nerf optique après transduction du signal au travers des différentes couches de la neurorétine.

Histologiquement la rétine est composée de 10 couches (Figure 3) listées ci-dessous de l'extérieur vers l'intérieur :

- *Epithélium pigmentaire rétinien*
- Segments externes des photorécepteurs
- *Membrane limitante externe*

- *Couche granulaire externe* (contient les corps cellulaires des photorécepteurs)
- *Couche plexiforme externe* (contient les connexions entre les cellules des couches granulaires externe et interne)
- *Couche granulaire interne* (contient les corps cellulaires des cellules bipolaires)
- *Couche plexiforme interne* (contient les connexions entre les cellules de la couche granulaire interne et les cellules de la couche ganglionnaire)
- *Couche ganglionnaire* (contient les corps cellulaires des cellules ganglionnaires)
- *Couche des fibres optiques* (contient les axones des cellules ganglionnaires qui convergent vers la papille pour rejoindre le nerf optique. Les vaisseaux artériels et veineux sont également situés au sein de cette couche)
- *Membrane limitante interne*

En plus de cette organisation générale, il faut signaler la présence de deux zones particulières dans la rétine, la papille optique et la macula. La papille, ou tête du nerf optique, correspond à la zone où convergent les fibres optiques issues des cellules ganglionnaires. Cette zone est dépourvue de cellules photoréceptrices et est donc une zone "aveugle". La macula, ou rétine centrale, correspond au point d'intersection avec l'axe visuel. Au centre de la macula, dans la *fovea*, la rétine est amincie et composée uniquement de cônes, permettant une meilleure résolution optique.

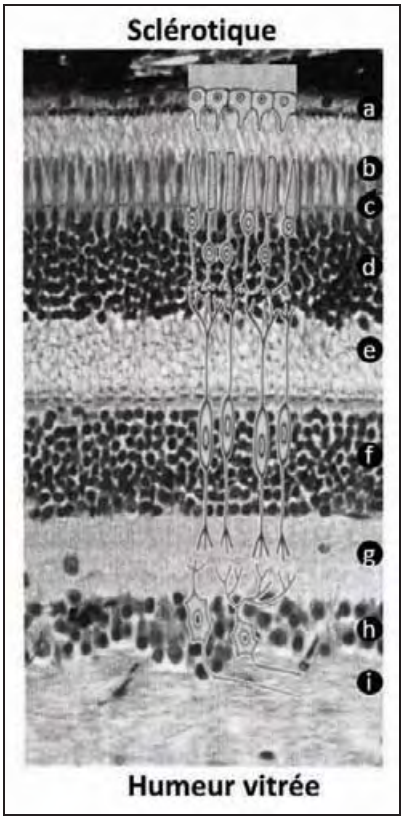

Figure 3: Les différentes couches de la rétine.[3]

Coupe histologique d'une rétine. Les différentes couches indiquées sur la figure: épithélium pigmentaire rétinien (**a**), prolongements sensoriels des cellules photoréceptrices (**b**), la membrane limitante externe (**c**), la couche granulaire externe (**d**), la couche plexiforme externe (**e**), la couche granulaire interne (**f**), la couche plexiforme interne (**g**), la couche ganglionnaire (**h**) et la couche des fibres optiques (**i**).

3. Les tuniques de l'œil

a. La sclérotique

La sclérotique est la membrane la plus extérieure de l'œil. Elle est très résistante et permet de contenir la pression interne de l'œil et de protéger celui-ci contre les agressions mécaniques. Elle se prolonge en avant par la cornée (Figure 1).

b. La choroïde

La choroïde est une mince couche de tissu conjonctif lâche contenant de nombreux vaisseaux sanguins et des nerfs. C'est la couche de la paroi du globe oculaire située entre la sclérotique à l'extérieur, et la rétine à l'intérieur. De la partie externe à la partie interne, on distingue 3 couches :

- *Couche des vaisseaux* (contenant artères et veines)
- *Couche choriocapillaire* (contenant un important réseau capillaire dépendant des vaisseaux de la couche précédente)
- *Membrane de Brüch* (mince couche de microfibrilles collagènes et élastiques recouverte d'un côté par la membrane basale des capillaires de la couche choriocapillaire et de l'autre par la membrane basale de l'épithélium pigmentaire de la rétine)

[3] Adaptée de http://sciences.exp.free.fr/cours/cours_svt/premiere_es_l/representation-visuelle/images/couperetine.jpg

I-2 : Embryologie de l'œil

Introduction

Les yeux se forment dès la 4eme semaine du développement. Il s'agit d'un organe complexe d'origine embryologique variée. L'ébauche neurale (*vésicules optiques*) dérivée du cerveau antérieur forme la rétine et l'ébauche ectodermique (*placodes optiques*) est à l'origine du cristallin. Les autres structures de l'œil dérivent du mésenchyme environnant, colonisés par la crête neurale. L'origine embryologique des différentes structures oculaires est résumée dans le tableau 1. Les principales étapes du développement oculaire sont décrites dans le tableau 2.

Tableau 1: Origine embryologique des différentes structures oculaires

Origine Embryologique	Structures Oculaires
Neurectoderme	Neurorétine Epithélium pigmenté rétinien Epithélium irien Epithélium des corps ciliaires Nerf optique
Crête neurales	Endothélium cornéen Trabéculum Stroma de la cornée, de l'iris et des corps ciliaires Muscle ciliaire Choroïde et sclérotique Cellules musculaires lisses Gaine du nerf optique Os et cartilage de l'orbite Tissu conjonctif des muscles extrinsèques Vitré secondaire
Ectoderme de surface	Epithélium de la cornée et de la conjonctive Cristallin Glandes lacrymales Epiderme des paupières Cils Epithélium des glandes annexes Epithélium du canal nasolacrimal
Mésoderme	Cellules musculaires extraoculaires Endothélium vasculaire Endothélium du canal de Schlemm

Les étapes précoces du développement oculaire

- Premières ébauches

L'ébauche des yeux apparait vers le 22eme jour de développement. Deux sillons, les *gouttières optiques*, se dessinent de part et d'autre de la ligne médiane sur l'extrémité encore ouverte du cerveau antérieur (Figures 4 et 5). Lors de la fermeture du tube neural, le développement du cerveau antérieur va placer les gouttières optiques au niveau du diencéphale.

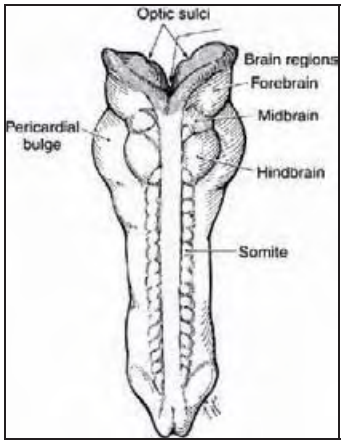

Figure 4: Vue générale d'un embryon de 23 jours.[4]

Les premières ébauches oculaires (*gouttières optiques*) apparaissent sur la face interne du cerveau antérieur.

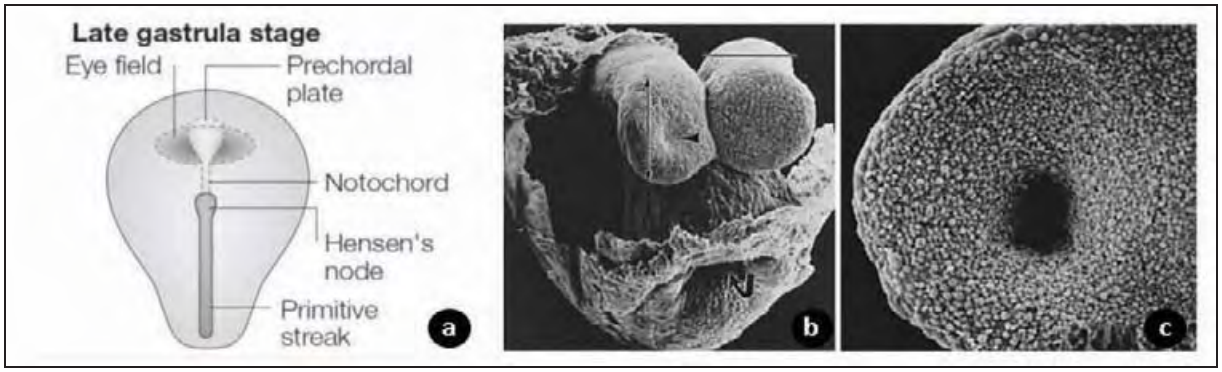

Figure 5: Formation des gouttières optiques.[5] [6]

Apparition des premières ébauches oculaires (*gouttières optiques*) au niveau du cerveau antérieur. Représentations schématique (**a**) et en microscopie électronique (**b**,**c**) chez un embryon de souris au 8eme jour (E8, équivalent de 4 semaines chez l'homme).

[4] http://www.oculist.net/downaton502/prof/ebook/duanes/pages/v7/v7c002.html#t1
[5] Les figures 5, 6,7, 9 et 10 sont adaptées de Graw J. Nat Reviews Genetics 2003 et http://www.oculist.net/downaton502/prof/ebook/duanes/pages/v7/v7c002.html#t1

- Les vésicules optiques et cristalliniennes

A partir du 24eme jour, avec la fermeture du tube neural, les gouttières optiques vont progressivement s'élargir et s'éloigner du système nerveux central pour former les *vésicules optiques* (Figure 6). Entre les vésicules optiques et le diencéphale se développe le *pédicule optique*. Les vésicules optiques se développent vers l'ectoderme de surface, et le contact entre ces deux structures va entrainer l'apparition d'un épaississement de l'ectoderme de surface qui correspond à la formation des *placodes cristalliniennes* (27eme jour). Les placodes cristalliniennes vont secondairement s'invaginer pour former les *vésicules cristalliniennes* (29eme jour) (Figure 7).

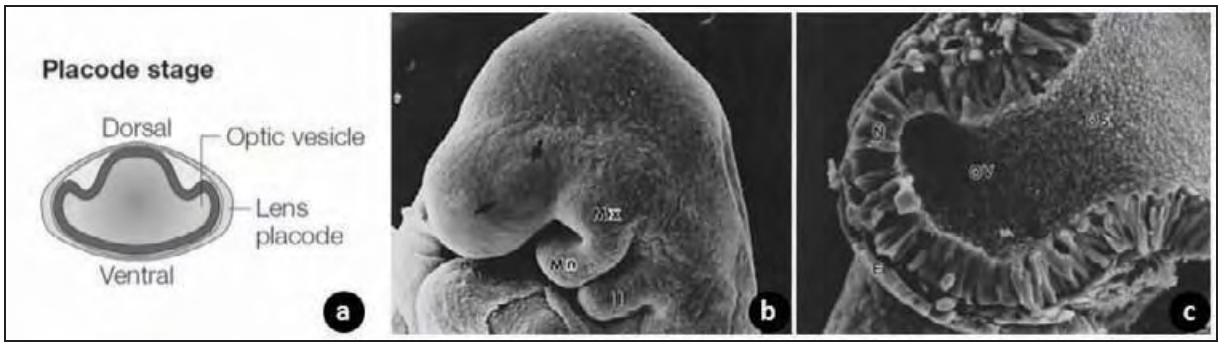

Figure 6: Les vésicules optiques.

L'élargissement des gouttières optiques et leur éloignement du diencéphale entraîne l'apparition des vésicules optiques. Représentations schématique (**a**) et en microscopie électronique (**b**,**c**) chez un embryon de souris à un développement équivalent de la fin de la 4eme semaine chez l'homme.

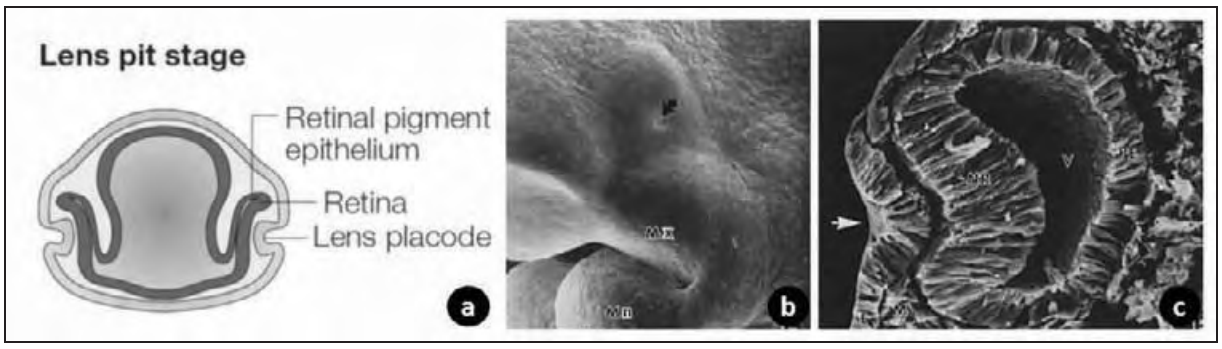

Figure 7: Les placodes cristalliniennes.

Au contact des vésicules optiques et de l'ectoderme de surface, ce dernier va s'épaissir pour former les *placodes cristalliniennes* qui vont secondairement s'invaginer pour former les *vésicules cristalliniennes*. Représentations schématique (**a**) et en microscopie électronique (**b**,**c**) chez un embryon de souris à un développement équivalent du début de la 5eme semaine chez l'homme.

Devenir des vésicules optiques et cristalliniennes

Les vésicules optiques et cristalliniennes vont subir des transformations qui vont permettre la différentiation de la rétine et du cristallin. Les principales étapes de ces transformations sont résumées dans la figure 8.

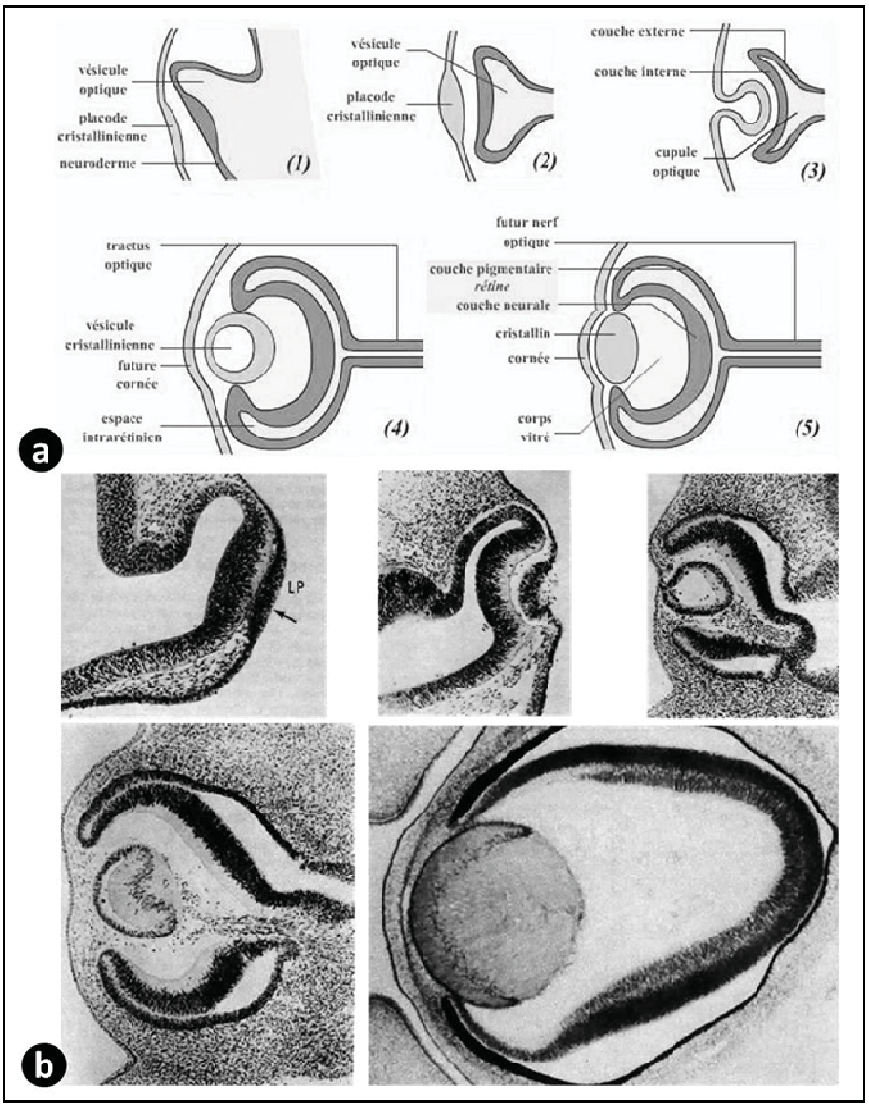

Figure 8: Les grandes étapes du développement oculaire.[6]

Sous l'action de signaux provenant des vésicules optiques, l'ectoderme de surface s'épaissi puis s'invagine pour former les *vésicules cristalliniennes* qui vont se détacher progressivement de l'ectoderme de surface et donneront naissance au cristallin. Les vésicules optiques s'invagineront également et formeront secondairement la rétine. Représentations schématique (**a**) et coupes histologiques correspondantes (**b**) chez un embryon humain.

[6] (**a**) http://legacy.futura-sciences.com/uploads/tx_oxcsfutura/comprendre/d/images/667/vision_038big.jpg
(**b**) adapté de http://www.oculist.net/downaton502/prof/ebook/duanes/pages/v7/v7c015.html

- Devenir des vésicules cristalliniennes

La vésicule cristallinienne va progressivement (entre le 33eme et le 36eme jour de développement) se détacher de l'ectoderme de surface pour former une structure arrondie qui se différentiera en cristallin (Figures 8 et 9). L'ectoderme de surface reformé donnera secondairement la cornée.

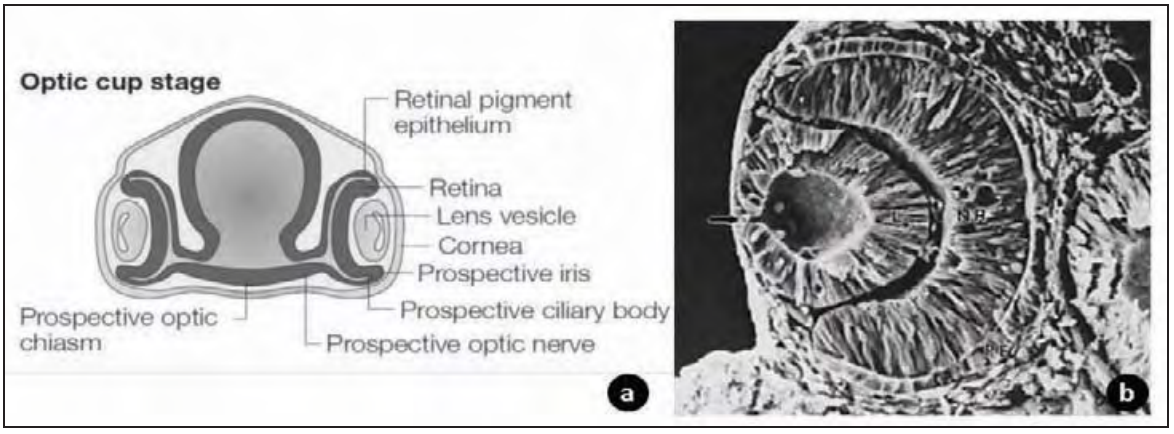

Figure 9: Formation des vésicules cristalliniennes.

Les *vésicules cristalliniennes* qui donneront naissance au cristallin se détachent progressivement de l'ectoderme de surface. Représentations schématique (**a**) et en microscopie électronique (**b**) chez un embryon de souris.

La différentiation de la vésicule cristallinienne en cristallin nécessite des changements de forme et de composition afin de permettre la formation d'une structure transparente (Figure 10). Ces changements débutent au 37eme jour du développement. Les cellules de la face postérieure de la vésicule cristallinienne vont s'allonger pour former les fibres cristalliniennes primaires. Ces cellules vont sécréter des protéines spécifiques, les cristallines, et perdre leur noyaux. Les cellules de la paroi antérieure de la vésicule cristallinienne constituent un épithélium germinatif qui continue à se diviser. Ces cellules vont donner naissance aux fibres cristalliniennes secondaires qui vont former des couches concentriques autour des fibres primaires.

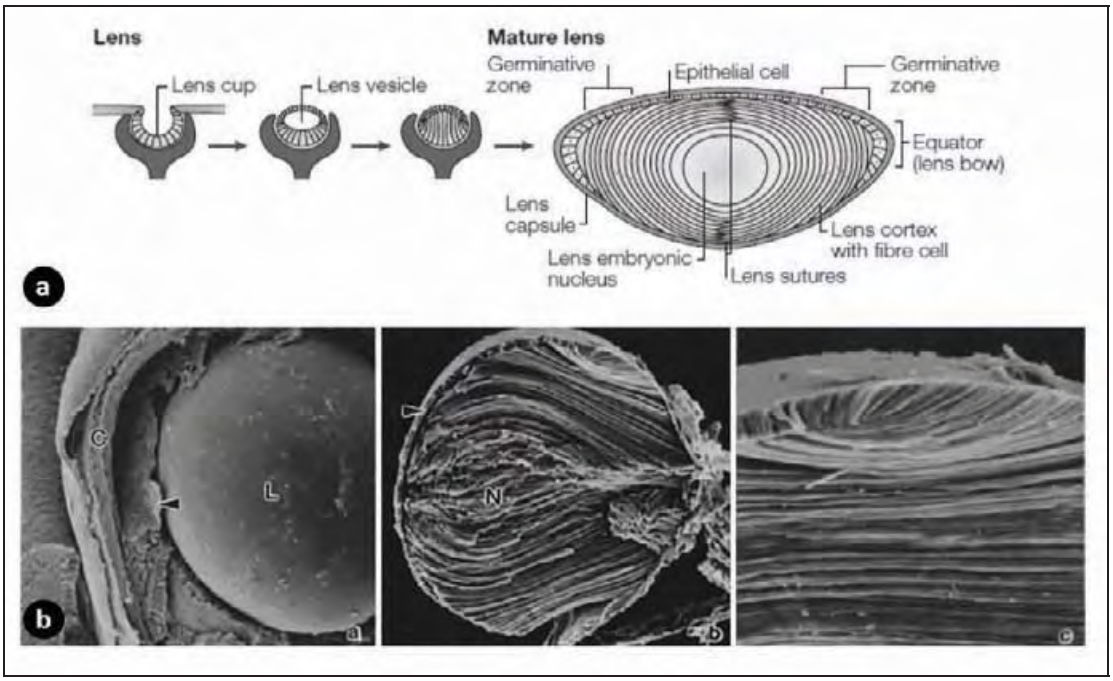

Figure 10: Différentiation du cristallin.

Vue schématique (**a**) et en microscopie électronique (**b**) chez un embryon de souris de la formation des fibres cristalliniennes. Ces cellules, allongées, orientées dans un sens antéro postérieur deviennent transparentes grâce à la perte de leur noyaux et à la production de protéines spécifiques.

- Devenir des vésicules optiques

Au fur et à mesure de la formation de la placode puis vésicule cristallinienne, la vésicule optique s'aplatit et finalement devient concave pour former la *cupule optique* (à partir du 29eme jour du développement). Les deux feuillets de la cupule optique séparés par une cavité primitive rétinienne vont progressivement s'accoler au cours de l'invagination et la cavité va devenir virtuelle (Figures 8 et 11). Le feuillet le plus externe va se différentier en *épithélium rétinien pigmentaire*, tandis que le feuillet interne va se différentier en *neurorétine*. A la jonction entre ces deux feuillets se formera l'iris et le corps ciliaire.

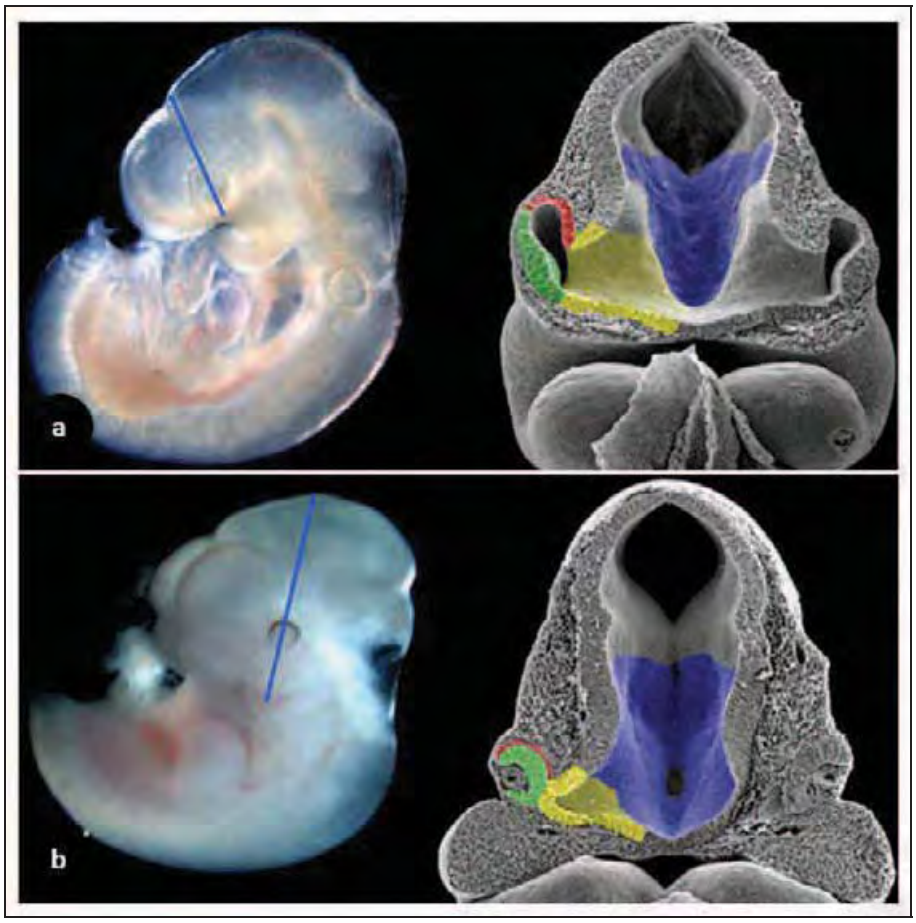

Figure 11: Mise en place de la rétine.[7]

Coupes en microscopie électronique d'embryon de souris à E9.5 (**a**) et E10.5 (**b**). Les vues de l'embryon entier montrent les plans de coupe. Certaines structures ont été colorées : futur hypothalamus (en bleu), pédicule optique (en jaune), neurorétine (en vert) et épithélium rétinien pigmentaire (en rouge).

La cupule optique s'invagine en s'enroulant autour de l'artère hyaloïdienne, laissant ainsi une ouverture inférieure sur la face ventrale de la cupule optique et du pédicule optique, la *fente colobomique*. Progressivement, les deux lèvres de la fente colobomique vont se rapprocher et fusionner au cours de la 7eme semaine de développement. L'artère hyaloïdienne initialement présente dans le vitré va disparaître au cours de ce processus (Figure 12).

[7]http://www.google.fr/imgres?imgurl=http://www.unc.edu/~pevny/Langer3.jpg&imgrefurl=http://www.unc.edu/~pevny/langer.html&usg=__ETYNG2MBDJqo2xnxAD68330To5s=&h=575&w=527&sz=256&hl=fr&start=6&zoom=1&tbnid=IHSycmYeNH7BZM:&tbnh=134&tbnw=123&ei=K9cmUqisIsLW0QXrgoCQDg&prev=/images%3Fq%3Ddevelopment%2Beye%2Belectronic%2Bmicroscopy%26hl%3Dfr%26gbv%3D2%26tbm%3Disch&itbs=1&sa=X&ved=0CDgQrQMwBQ

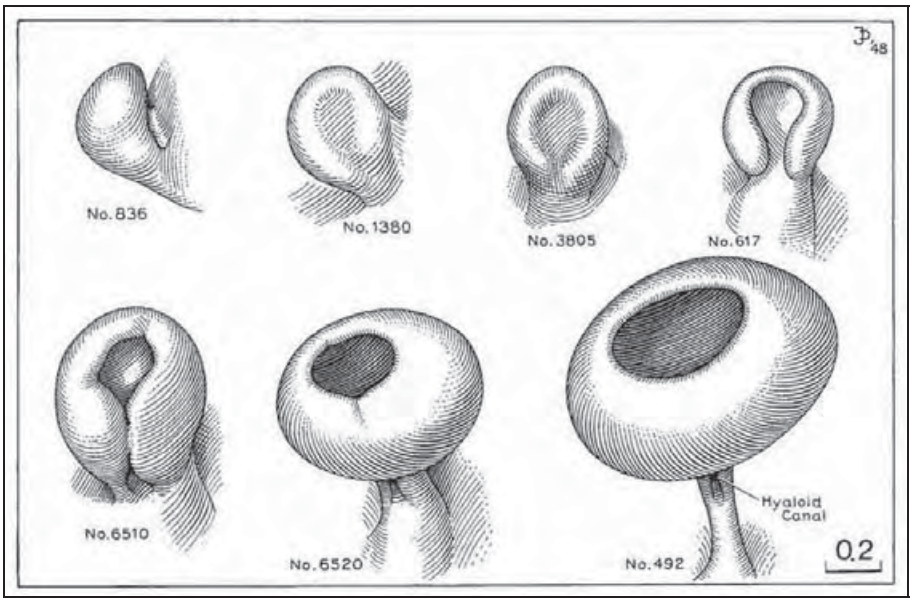

Figure 12: Fermeture de la fente colobomique.[8]

Représentation schématique de la progression de l'invagination de la cupule optique à partir de la vésicule optique et de la fermeture progressive de la fente colobomique entre la 5eme et 7eme semaine de développement.

Les autres structures oculaires

La différentiation des autres structures oculaires (chambre antérieure, sclérotique et choroïde) vont être sous l'influence notamment de la migration des crêtes neurales au cours de trois vagues successives.

- Chambre antérieure

Les structures de la chambre antérieure (cornée, iris, corps ciliaires, et à sa partie postérieure le cristallin) sont issues de cellules issus de l'ectoderme de surface, du neurectoderme et de la crête neurale (Figure 13).

[8] Adaptée de http://www.ehd.org/developmental-stages/stage18.php

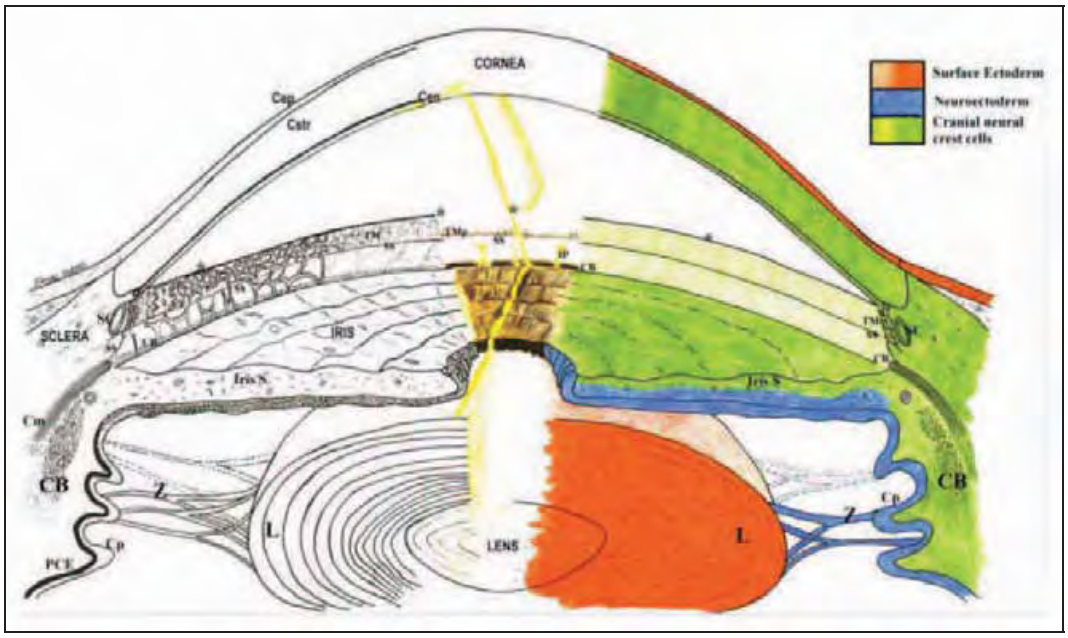

Figure 13: Origine embryologique des structures de la chambre antérieure.[9] [7]

Représentation schématique de la chambre antérieure. Sur la droite de la figure, les couleurs indiquent les différentes origines embryologiques. La cornée a un épithélium de surface (Cep) d'origine ectodermique, un stroma (Cstr, Cen) et un endothélium issus de la crête neurale. Les structures de l'angle irido-cornéen ainsi que le stroma de l'iris (Iris S) et des corps ciliés (CB) sont issus de la crête neurale. L'épithélium irien, ainsi que celui des corps ciliés et les procès ciliaires (Cp) sont d'origine neurectodermique. Le cristallin (L) à une origine ectodermique.

Cornée et angle irido-cornéen

L'épithélium pigmentaire de la cornée (couche externe) se différentie à partir de l'ectoderme de surface sous l'induction de signaux provenant du cristallin. Le cristallin sécrète également les constituants du stroma primaire acellulaire de la cornée qui va permettre la migration de la crête neurale et la constitution du stroma cornéen (deux premières vagues de migration). Enfin, la cornée est délimitée en interne par un endothélium lui aussi issue de la différentiation de la crête neurale (Figure 13).

Les crêtes neurales de la première vague de migration situées dans la partie postérieure et périphérique de la cornée se différentient en angle irido-cornéen, trabéculum et en canal de Schlemm.

[9] Idrees F *et al.* Survey Of Ophthalmology 2006

Iris et corps ciliés

La troisième vague de cellules originaires des crêtes neurales migre entre l'endothélium cornéen en avant et le cristallin en arrière pour former les stromas irien et des corps ciliés. A la partie postérieure des stromas irien et des corps ciliés se différentie un épithélium originaire du neurectoderme (Figure 13).

- Sclérotique et choroïde

La sclérotique et la choroïde dérivent du mésenchyme entourant la cupule optique formé par les crêtes neurales. A partir de ce mésenchyme péri-oculaire s'individualisent deux couches. L'une est située contre l'épithélium pigmentaire rétinien et va former la choroïde et le stroma irien. La choroïde est richement vascularisée et contient des mélanocytes. La seconde couche, plus externe, et riche en fibre de collagène et va former la sclérotique prolongée en avant pat le stroma cornéen et en arrière par la gaine du nerf optique.

Tableau 2: Récapitulatif des principales étapes du développement embryonnaire de l'œil humain.

Month	Week(s)	Day(s)	CR Length (mm)	Neuroectodermal Derivatives Posterior iris epithelium, ciliary body epithelium, pupillary muscles, neural retina, retinal pigment epithelium (RPE), secondary vitreous, and optic nerve	Neural Crest Derivatives Corneal endothelium, stroma of cornea, iris, and ciliary body, ciliary muscle, trabecular meshwork, choroid, sclera, secondary vitreous, and orbit	Surface Ectoderm Derivatives Corneal and conjunctival epithelium, lens, eyelid epidermis, eyelid cilia and glands, lacrimal gland, nasolacrimal duct	Mesodermal Derivatives Endothelium of Schlemm's canal, vascular (hyaloid, tunica vascula lentis (TVL) endothelium, extraocular muscles
1	3	20	1–2	Neural plate thickens		Gastrulation (formation of mesoderm)	
	4	22	2–3.5	Optic sulci present in forebrain			
		24	2–3	Neural tube closed Optic stalk formed			
		25	3–4	Optic sulci converted into optic vesicles	Mesenchyme surrounds optic vesicle		
		27	4–5	Optic vesicle contacts surface ectoderm		Lens placode begins to thicken Eyelid territory determined	
2	5	29	5–7	Optic vesicle begins to invaginate forming optic cup with optic fissure		Lens pit forms as lens placode invaginates Cord of ectoderm buried by maxillary processes to later form nasolacrimal duct	Hyaloid artery enters through the optic fissure
		33	7–9	Optic fissure closed Pigment in outer layer of optic cup (future RPE) Oculomotor nerve present Trochlear and abducens nerves appear		Lens pit closed forming lens vesicle surrounded by intact basement membrane (lens capsule) Corneal epithelium formed	
	6	37	8–11	Ciliary ganglion present	Choriocapillaris formed around the optic cup	Primary lens fibers fill lens vesicle forming embryonal nucleus	
		40	11–14	Retina consists of: external limiting membrane (with zonula adherens), proliferative zone, primitive zone, marginal zone, and internal limiting membrane	Corneal endothelium formed	Secondary lens fibers form Lid folds present	
	7	42–45	13–17	Retina consists of: inner neuroblastic layer, transient fiber layer of Chievitz, proliferative zone, and outer neuroblastic layer			
		45–48	16–18	Ganglion cells give rise to nerve fiber layer	Anterior chamber beginning to form First orbital bone formation (ethmoid) Optic sheath formation begins		

	8	48–54	18–22	Optic cup measures 1 mm Optic fissure within the optic stalk closed Optic stalk cavity obliterated by optic nerve fibers which now reach the brain	Secondary vitreous forming Acellular corneal stroma present		Levator muscle forming
3	9	54–57	23–31	Transient fiber layer of Chievitz disappears, except in macula	Cellular corneal stroma forming (5–7 layers) Descemet's membrane present (not continuous) Pupillary membrane formed Scleral condensation present	Epithelial buds of lacrimal gland present	
	10	63	43–48		Tenon's capsule present	Eyelids fuse	Hyaloid vasculature reaches maximal development
	11	71–77	50–5	Inner plexiform layer formed Cilia within developing inner segments		Conjunctival goblet cells present	
	12–14	78–90	60–80	Outer plexiform layer separates horizontal and bipolar nuclei from rudimentary rods and cones Synapses develop between photoreceptors, ganglion cells, and bipolar cells in central retina First indication of ciliary processes	Lamina cribrosa formation begins Marginal bundle of Drualt/vitreous base present	Glands of Moll, meibomian glands present	Rectus muscle tendons fuse with sclera Branches of ophthalmic artery accompany hyaloid artery Iridal major arterial circle formed
4	15		90–100	Orbital axis 105°	Ciliary muscle appears	Glands of Zeiss present	
	16		100–120	Mitosis ceases in the neural retina	Corneal endothelium exhibits zonulae occludentes Aqueous humor formation begins Regression of corneal endothelium covering iridocorneal angle recess	Schlemm's canal present Tunica vasculosa lentis begins to atrophy	
			120–130	Pupillary sphincter develops	Scleral spur developing Bowman's membrane present	Short eyelashes appear	Hyaloid artery begins to atrophy to the disc, branches of the central retinal artery form
5			120–180	Outer segments formation begins Differentiation of macula begins	Layers of the choroid complete Cloquet's canal formed		
6			175–230	Pupillary dilator muscle develops Ora serrata distinct nasally	Pupillary membrane begins to atrophy axially Capsulohyaloidal ligament present	Eyelids begin to open, light perception	
7			220–260		Iris pigmentation present Lamina cribrosa mature Myelination begins at the chiasm and progresses to the lamina cribrosa		
8			240–280	Retinal layers developed except at macula	Regression of pupillary membrane nearly complete		Retinal vessels reach the ora serrata
9–term			310–350	Orbital axis 71°		Lacrimal duct canalized	

I-3 : Génétique des AM

Introduction

Les microphtalmies et anophtalmies correspondent respectivement à une réduction de taille ou une absence de globe oculaire. Ce sont les malformations les plus sévères du développement embryonnaire oculaire. C'est sur ces malformations oculaires sévères qu'a porté l'essentiel de mon travail de thèse. Ce chapitre a pour but de bien définir ces malformations, certains éléments épidémiologiques (fréquence, malformations associées), et de discuter les différentes étiologies. Une grande partie de ce chapitre sera consacré à une revue des bases moléculaires connues dans ces malformations oculaires. Ce chapitre sera clôturé par une brève discussion sur la prise en charge de ces patients et le conseil génétique.

Définition

L'anophtalmie correspond à une absence de structure oculaire dans l'orbite (*anophtalmie vrai*). Ce diagnostic ne pourrait être porté que par une analyse histologique. En pratique, ce terme d'anophtalmie est utilisé en pratique devant l'absence de structure oculaire lors de l'examen clinique. On parle alors d'*anophtalmie clinique*. La microphtalmie correspond à un œil de petite taille (inférieur à deux déviations standards par rapport à une population du même âge). Cela correspond à une longueur axiale de l'œil <16 mm à la naissance, <19 mm à un an et <21 mm chez l'adulte[2, 3]. La microphtalmie peut être associée à d'autres malformations oculaires (dysgénésie du segment antérieur et/ou postérieur). On parle alors de *microphtalmie complexe* par opposition à la *microphtalmie simple* ou la microphtalmie n'est pas associée à d'autre malformation oculaire[1]. La *microphtalmie colobomateuse* associe une anomalie de fermeture de la fente colobomique à la microphtalmie. Les AM peuvent être des *AM isolées* ou associées à d'autres malformations d'organes (*AM syndromiques*). Quelques exemples de présentations cliniques d'AM sont montrés figure 14. La *nanophtalmie* est une forme particulière de microphtalmie : elle est sévère et associée à une microcornée, une hypermétropie forte et fréquemment un glaucome. La *microphtalmie postérieure* est une microphtalmie ne touchant que le segment postérieur de l'œil.

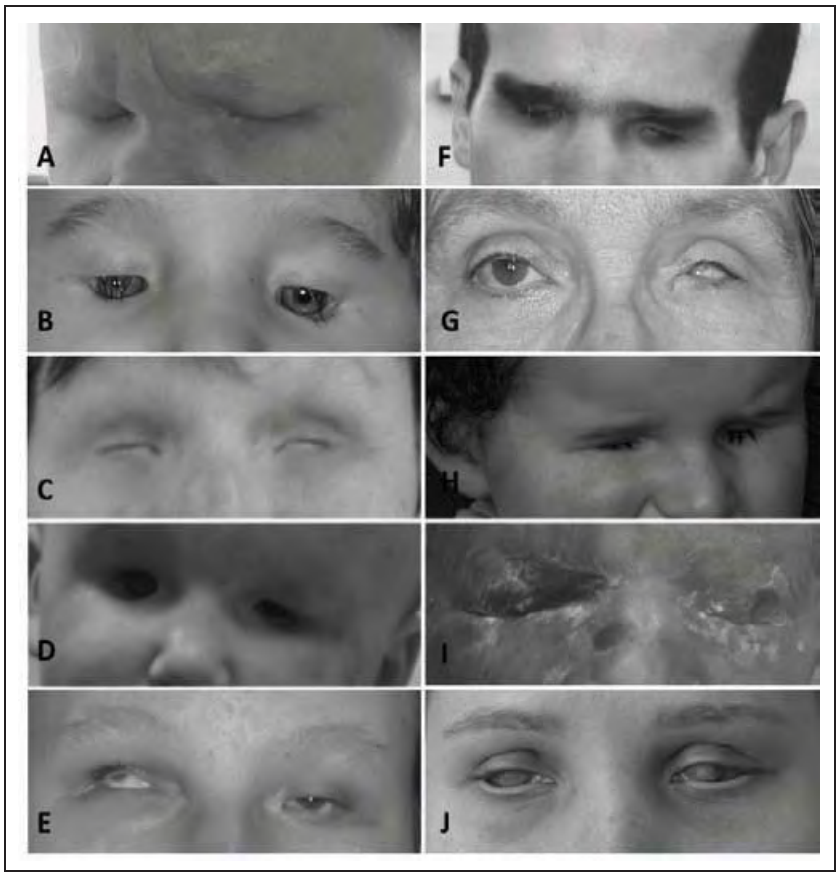

Figure 14: Exemples d'atteintes oculaires de patients AM.

Présence d'une AM (**A-F**, **H-J**) ou unilatérale (**G**). Les patients **B** et **D** portent des prothèses. Une sclérocornée est présente chez **J**.

Les mécanismes physiopathologiques à l'origine des AM restent mal connus. Il a été proposé que les AM pourraient résulter d'un défaut d'induction au niveau de tube neural primitif ou des gouttières optiques[8]. Secondairement a été suggéré la possibilité d'une régression secondaire d'une structure oculaire en formation, hypothèse expliquant ainsi la présence parfois retrouvée de nerfs optiques ou reliquats rétiniens retrouvés lors de l'analyse histologique sur des anophtalmies[9].

Epidémiologie

Plusieurs études épidémiologiques ont essayé de définir la prévalence des AM. La plupart se basant sur les registres nationaux de malformations donnent une incidence des AM autour de 1 pour 10.000[10-16], les chiffres variant entre 0.3 et 2 pour 10.000[15, 16]. Des malformations d'autres organes sont présentes dans 33 à 93 % des AM[17, 18]. Les associations malformatives les plus fréquemment

décrites dans une étude récente[18] sont représentées figure 15. Un retard des acquisitions est présent chez 20 % des enfants présentant une AM et/ou un colobome[16].

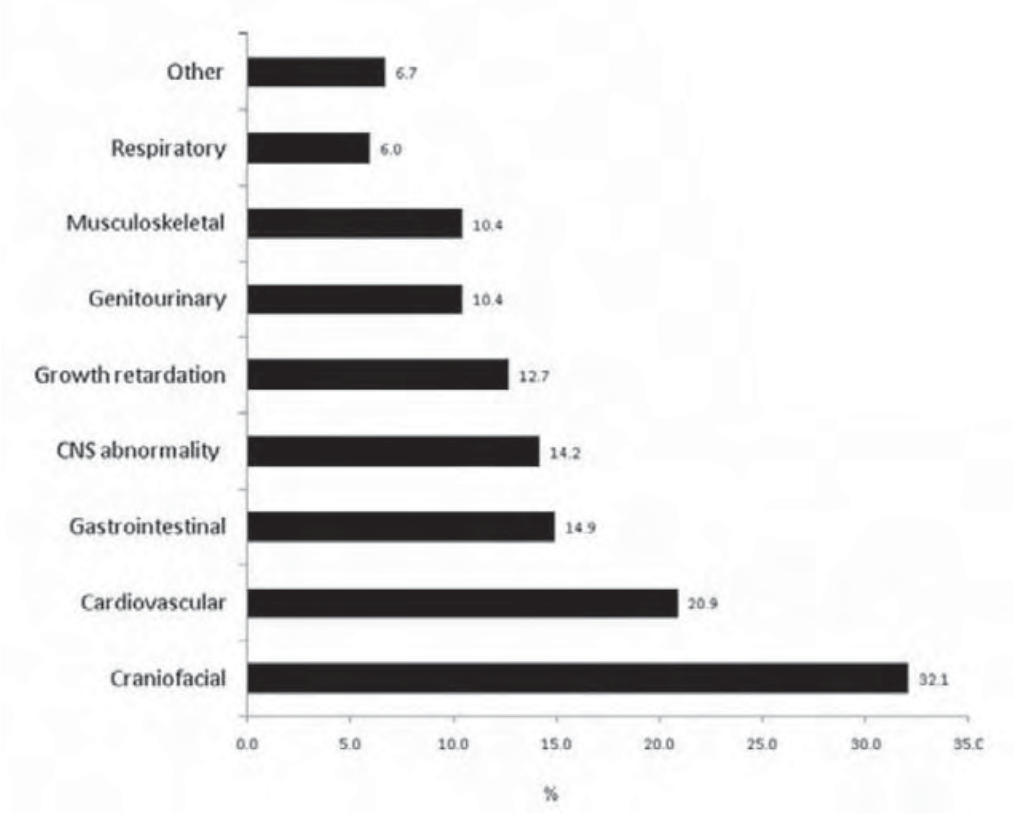

Figure 15: Fréquence des malformations identifiées chez les patients avec AM et/ou colobomes.

Les malformations identifiées chez de patients avec AM et/ou colobome (n=137) dépistés au Royaume Uni sur une période de 18 mois.[10]

Etiologies

Les étiologies des AM sont diverses et comprennent des causes environnementales, chromosomiques et géniques. A partir d'une population de plus de 1 million de personne, avaient identifiés 240 patients AM, et avaient estimés que 16 % des AM étaient liés à une cause monogénique, 22 % à une cause chromosomique (en incluant les aneuploïdies fréquentes comme les trisomies 13 ou 18) et 2 % à l'environnement[15]. Dans 60 % des cas aucune cause n'avait été identifiée.

Les causes environnementales sont supposées ne représenter qu'une petite partie des causes d'AM[1, 15]. Les causes environnementales les mieux connues sont certains agents infectieux comme la rubéole, le CMV, ou la toxoplasmose[19-21]. Des substances toxiques et des médicaments ont

[10] Shah SP et al. *Ophthalmology* 2011

également été impliqués dans les AM, et notamment l'alcool, le tabac, l'acide folique, les rétinoïdes, et l'hydantoïne[13, 22-25].

De nombreuses anomalies chromosomiques ont été associées aux AM. Ces anomalies peuvent être visible sur un caryotype standard ou être identifiées par analyse en cytogénétique moléculaire. Le taux de détection d'anomalie chromosomique chez des patients avec atteinte oculaire syndromique est entre 7 et 10 % par cytogénétique conventionnelle[24, 26]. Les principales anomalies retrouvées étant les trisomies 13 et 18 et certains syndromes délétionnels comme les 4p-, 5p-, 18q-[1]. L'apport de la CGH-array permet d'identifier 10 % à 15 % d'anomalies chromosomiques cryptiques chez les patients avec atteinte oculaire syndromique[27, 28]. Dans les formes non syndromiques, la part d'anomalie chromosomique identifiée par CGH-array est faible, de l'ordre de 3 %[29].

Enfin, de nombreux gènes ont été associées aux AM dans des formes syndromiques ou non syndromiques. Les principaux gènes impliqués codent majoritairement pour des facteurs de transcription (*SOX2, OTX2, PAX6, RAX, VSX2, FOXE3, VAX1, ATOH7*), des régulateurs d'expression (*BCOR*), ou des gènes impliqués dans des voies de signalisation (*BMP4, BMP7, SHH, GDF6*)[6]. Plus récemment, des mutations dans des gènes codant pour des protéines impliqués dans le métabolisme de l'acide rétinoïque (*STRA6, ALDH1A3 et RARB*) ont été identifiées chez des patients AM. De nombreux gènes ne rentrant pas dans ces catégories ont également été impliqués dans les AM (*SMOC1, HCCS, c12orf57, ODZ3, TMX3, FNBP4*…).

Pour décrire les bases moléculaires des AM, je séparerais le prochain chapitre en deux parties ; les gènes des AM non syndromiques et des AM syndromiques. Cette dichotomie est artificielle, et n'est pas le reflet exact de la réalité car des formes syndromiques et non syndromiques peuvent être décrites pour un même gène.

Bases moléculaires des AM isolées

SOX2

SOX2 (SRY [sex determining region Y]-box 2) code pour un facteur de transcription très exprimé au cours du développement oculaire[30, 31]. La fonction de cette protéine sera détaillée dans le chapitre suivant ("Introduction aux facteurs de transcription étudiés").

L'implication de SOX2 dans les AM a été mise en évidence à partir d'une patiente porteuse d'une translocation d'allure équilibrée apparue *de novo*. Des analyses complémentaires ont permis de mettre en évidence une délétion de 600 kb comprenant le gène *SOX2*[4]. Des mutations ponctuelles

dans ce gène ont été recherchées et retrouvées par la même équipe, confirmant l'implication de ce gène dans les AM[4]. Des mutations sont identifiés chez 10-15 % des patients AM[5, 32, 33] ce qui en fait à l'heure actuelle le gène majeur dans cette pathologie. A l'heure actuelle, 58 mutations différentes ont été décrites[32, 34-40], et correspondent à des petites insertions et/ou délétion nucléotidiques (32/58), des mutations non-sens (13/58) et des mutations faux sens (13/58). Des délétions du gène *SOX2* sont fréquentes et correspondent à 25 ou 50 % des mutations identifiées[33, 40]. La plupart des mutations intra géniques sont des mutations privées.

Le phénotype lié aux mutations de *SOX2* initialement décrit comprenait des malformations oculaires (typiquement sévères et bilatérales), un retard des acquisitions, de l'épilepsie, des malformations mineures cérébrales, un retard de croissance, des anomalies génitales chez le garçon et quelques critères faciaux mineurs[5]. Il a secondairement été montré que les mutations de *SOX2* pouvaient être à l'origine d'une forme syndromique d'AM, le syndrome AEG (pour Anophthalmia-Esophageal-Genital)[31]. Différentes malformations ont été associées rarement à ces mutations[41, 42]. Le phénotype oculaire s'est progressivement élargi, et des atteintes moins sévères ont été décrits chez des patients porteurs de mutation de *SOX2* : colobomes iriens et rétiniens, hypoplasie irienne[41, 43]. Nous avons même pu montrer l'absence d'atteinte macroscopique et microscopique chez un patient porteur d'une mutation de délétère[41]. Dans notre expérience, les mutations sont bilatérales (17 patients sur 18) et sévères (anophtalmie chez 15 patients sur 18). Les éléments extra-oculaires retrouvées les plus fréquemment sont le retard des acquisitions présent chez la grande majorité des patients vivants décrits (déficience légère à sévère), des atteintes cérébrales (ventriculomégalie, hypoplasie du corps calleux), hypogonadisme et retard de croissance. Dans notre cohorte de 18 patients mutés, 3 présentaient une atrésie de l'œsophage[44].

Une corrélation génotype/phénotype a été suggérée[35] mais les patients porteurs de mutations similaires ont des atteintes oculaires et extra-oculaires variables. Une variabilité de sévérité intra familiale a également été décrite a plusieurs reprises[34, 41, 42, 45]. De plus, les atteintes peuvent être très asymétriques entre les deux yeux chez un même patient, rendant difficile ces tentatives de corrélation.

Le syndrome anophtalmie lié à *SOX2* est transmis selon un mode autosomique dominant, avec la grande majorité des patients porteurs de mutations apparues *de novo*. Cependant, la description de trois cas de mosaïques germinales dans la littérature[35, 41, 46] doit faire modérer le conseil génétique plutôt rassurant habituellement en cas de mutation *de novo*.

OTX2

OTX2 (orthodenticle protein homolog 2) code pour un facteur de transcription impliqué dans la mise en place des différentes structures oculaires, et particulièrement au cours de la différentiation de la rétine[30]. La fonction de cette protéine sera détaillée dans le chapitre suivant ("Introduction aux facteurs de transcription étudiés").

L'implication de ce gène dans les AM a été démontrée par Ragge et al. Par une approche gène candidat ont identifié les premières mutations de ce gène chez 8 patients AM[47]. Ce gène a été impliqué dans 0.7 à 10 % des AM[32, 47-50]. Dans notre laboratoire, des mutations ont été identifiées chez 5/150 patients AM (3 %). Un total de 31 mutations différentes ont été décrites, comprenant des mutations décalant le cadre de lecture (14/31), des mutations non-sens (9/31), des faux-sens (7/31) et des délétions du gène[32, 40, 53]. Les délétions du gène *OTX2* semblent représenter une 30 à 40 % des mutations de ce gène[40, 51].

Le phénotype oculaire de ces patients est variable et souvent asymétrique. Il va de l'anophtalmie bilatérale à une absence de malformation oculaire[40, 47] et peut inclure des colobomes (iriens et/ou rétiniens), une cataracte ou une sclérocornée. Les malformations extra-oculaires sont également inconstantes et sont représentées essentiellement par une déficience intellectuelle, un retard statural et une atteinte pituitaire[47, 48, 50]. Des mutations du gène *OTX2* ont été décrites chez quelques patients présentant un pan hypopituitarisme isolé[52]. Nous avons également démontré le rôle des mutations de ce gène dans une malformation majeure du développement embryonnaire de la mandibule, l'agnathie (voir chapitre correspondant)[53, 54]. Il n'y a pas d'arguments pour une corrélation génotype/phénotype.

La transmission de l'atteinte clinique liée aux mutations du gène *OTX2* est autosomique dominante. La pénétrance est incomplète et la variabilité d'expression est importante. Les mutations peuvent être héritées d'un des deux parents ou survenir *de novo* (environ une fois sur deux). Des cas de mosaïques germinales ont été décrits à trois reprises[47, 50].

RAX

RAX (retina and anterior neural fold homeobox) code pour un facteur de transcription dont le rôle au cours du développement oculaire a été étudié dans différents modèles de vertébrés[55]. La fonction de cette protéine sera détaillée dans le chapitre suivant ("Introduction aux facteurs de transcription étudiés").

Des mutations récessives ont été identifiées dans 7 familles[40, 56-58]. Ces mutations (10 mutations différentes, 4 faux-sens, 3 non-sens, 1 frameshift, 1 mutation d'épissage et une délétion du gène) ont un effet supposé perte de fonction. Dans notre expérience, les mutations du gène *RAX* sont identifiées chez 2.5 % des patients AM (4/150). Une déficience intellectuelle a été décrite dans 3 des 7 patients impliqués. Il n'y a pas de phénotype extra-oculaire rapporté, en dehors d'anomalies des sinus frontaux et sphénoïdaux décrite chez deux patients[58]. Des mutations hétérozygotes ont été décrites chez des patients avec colobome chorio-rétinien[59] ou AM[60]. Pour ces patients, l'analyse parentale de ces mutations n'a pas été faite et le caractère hérité ou non n'est donc pas connu. Nous avons identifié deux mutations hétérozygotes dans notre cohorte d'AM, dont une, p.Thr50Pro, déjà décrite associée à une AM à l'état hétérozygote[60]. Cette variation n'est pas prédite comme délétère par les outils *in silico* (SIFT, Polyphen-2) et était chez notre patiente héritée d'une mère asymptomatique. Les porteurs hétérozygotes pour une mutation du gène *RAX* dans les familles de patients AM ne sont pas symptomatiques. Il est difficile d'exclure totalement la possibilité de mutation dominante à pénétrance incomplète chez les patients hétérozygotes, mais les arguments dont nous disposons doivent orienter le conseil génétique à l'heure actuelle dans le sens d'une transmission purement autosomique récessive.

PAX6

PAX6 (paired box 6) code pour un facteur de transcription très important au cours du développement oculaire[30]. La fonction de cette protéine sera détaillée dans le chapitre suivant ("Introduction aux facteurs de transcription étudiés").

PAX6 a été le premier gène dont les mutations ont été associées à l'AM en 1994[61]. Cependant, les mutations de *PAX6* ne sont que rarement associées à l'AM[30, 40, 62]. Le phénotype associé classiquement aux mutations de ce gène est l'absence d'iris (aniridie). Plus généralement, les mutations hétérozygotes du gène *PAX6* entraîne un défaut de développement pouvant toucher les différentes structures oculaires (cornée, iris, cristallin, rétine)[63]. Des présentations atypiques, (anomalie de Peters, correctopie, nystagmus, hypoplasie fovéale, malformations du nerf optique), ont été associées aux mutations de *PAX6*[30, 63]. Plus de 300 mutations différentes ont été décrites (The Human *PAX6* mutation Database, http://lsdb.hgu.mrc.ac.uk). Des patients porteurs de mutations hétérozygotes composites du gène *PAX6* ont été rapportés[61, 64] : ils présentent un phénotype associant AM et un phénotype cérébral évoquant l'holoprosencéphalie). Les délétions emportant le gène *PAX6* peuvent s'étendre au gène *WT1* et se traduire cliniquement par l'association d'une aniridie, d'anomalies génitales et d'une tumeur de Wilms (syndrome WAGR). La transmission des

mutations *PAX6* est autosomique dominante avec une pénétrance forte mais une expressivité variable. Dans 1/3 des cas environ, la mutation identifiée est *de novo*[65].

VSX2

VSX2 (visual system homeobox 2 gene), anciennement appelé *CHX10*, code pour un facteur de transcription jouant un rôle majeur dans le développement oculaire des mammifères[66]. *VSX2* est exprimé dès le stade de la vésicule optique. Son expression au sein des progéniteurs rétiniens permet leur prolifération et la différentiation en cellules neurorétiniennes[66].

Les premières mutations du gène *VSX2* ont été décrites chez des patients AM en 2000[67]. Des mutations ont été décrites dans 13 familles[40, 68-71]. L'AM est généralement bilatérale et y est parfois associée une cataracte ou un glaucome. Un patient avec atteinte oculaire atypique a été récemment décrit ; son phénotype comprenait une subluxation du cristallin, une dystrophie rétinienne et une myopie forte[71]. Dans notre expérience, les mutations de *VSX2* ne sont identifiées que chez 1/150 patients. L'association à un retard des acquisitions et des troubles autistiques a été rapportée une fois chacun. Il n'y a pas d'atteinte extra-oculaire associée à ces mutations. L'AM liée aux mutations du gène *VSX2* est de transmission autosomique récessive.

FOXE3

FOXE3 (forkhead box E3) code pour un facteur de transcription exprimé au cours du développement cristallinien dès le stade de la placode cristallinienne[72]. Son expression est limitée au cristallin. A la fin de la mise en place du cristallin, son expression va ne concerner que l'épithélium cristallinien ou il permet la prolifération cellulaire, et empêche la différentiation de ces cellules en fibres cristalliniennes[73].

Les mutations de ce gène ont initialement été décrites dans des dysgénésies du segment antérieure transmises selon un mode autosomique dominant[74, 75], puis secondairement des mutations récessives ont été associées à l'aphakie[76], et à l'AM[77]. Il a été suggéré après une étude de 26 patients, que des mutations de ce gène pouvaient être impliquées dans 15 % (4/26) des AM[78]. Ces mutations semblent cependant être plus rares et dans une grande série de 236 patients porteurs d'anomalies du développement oculaire, des mutations n'ont été identifiées que chez deux patients[77]. Nous avons identifié des mutations de *FOXE3* chez deux patients parmi nos 150 cas index[40]. Ces deux patients présentent une AM bilatérale avec sclérocornée. Une sœur d'un des cas index de notre

série, également porteuse des mutations et de l'atteinte oculaire présentait de plus une déficience intellectuelle et des troubles autistiques. 13 mutations différentes ont été décrites dans *FOXE3*[37, 77-81]. De manière intéressante, 8 sont responsables d'anomalies oculaires sur un mode autosomique récessif (4 frameshift, 3 faux-sens et une mutation non-sens) alors que 5 sont associés avec un phénotype se transmettant selon un mode autosomique dominant (dont 4 mutations non-stop). Il semblerait donc exister une corrélation entre la nature de la mutation et le mode de transmission et le phénotype clinique. Les mutations à transmission dominante donnent des phénotypes moins sévères (dysgénésie du segment antérieur) que celles à transmission récessive (AM et dysgénésie du segment antérieur).

ALDH1A3

ALDH1A3 (A3 isoform of the aldehyde dehydrogenase 1) code pour une enzyme impliquée dans le métabolisme la vitamine A en acide rétinoïque[82].

Nous avons pu participer à la description des premières mutations de ce gène dans 3 familles d'AM[83]. Depuis, ce gène a été impliqué dans 6 familles[84-87]. Différents type de mutation ont été décrites et ce sont des mutations perte de fonction. Le phénotype oculaire associé aux mutations de ce gène est souvent bilatéral et variable en sévérité (du colobome isolé à l'anophtalmie). Certains des patients présentent des troubles autistiques et/ou un retard des acquisitions. Une atteinte cardiaque n'a été décrite que chez un patient, et il n'y a pas d'autre phénotype extra-oculaire connu à l'heure actuelle.

ODZ3

Par une stratégie de séquençage d'exome et d'analyse de liaison, des mutations récessives du gène *ODZ3* (ODZ homolog of drosophilia, 3) ont été décrites dans une famille consanguine[88] ou deux enfants étaient atteints de microphtalmie colobomateuse isolée. La mutation c.2083dup (p.Thr695Asnfs*5) a été identifiée à l'état homozygote. En dehors d'une expression oculaire embryonnaire de ce gène connue chez la souris, peu d'arguments fonctionnels ne démontrent le lien entre cette mutation et le phénotype oculaire. Ce gène reste donc à être confirmé par l'identification de mutations chez d'autres patients AM.

ATOH7

ATOH7 (Atonal homolog of drosophilia 7) a été impliqué, par séquençage d'exome puis séquençage Sanger de 105 patients, dans des anomalies oculaires variables de deux familles consanguines[89] associant sclérocornée, nystagmus, microphtalmie, cataracte, décollements rétiniens, persistance du vitré primitif, hypoplasie des nerfs optiques, et calcifications du vitré et de la rétine. La microphtalmie n'étant pas l'élément majeur du tableau oculaire. Cette atteinte oculaire est strictement isolée. Une mutation homozygote a été secondairement identifiée une famille consanguine dont trois membres étaient atteints de persistance du vitré primitif[90].

SIX6

Par une stratégie de séquençage d'exome et d'analyse de liaison, des mutations récessives du gène *SIX6* (sine oculis homeobox 6) ont été décrites dans une famille consanguine[91] ou deux enfants étaient atteints de microphtalmie complexe (glaucome chez un patient) sans signes extra-oculaires. La mutation c.532_536del a été identifiée à l'état homozygote. Les arguments présentés dans cet article, et notamment le phénotype murin d'anophtalmie chez les souris KO pour *Six6*, sont en faveur de l'implication de ce gène dans l'AM.

Bases moléculaires des AM syndromiques

Des AM sont décrites associées à de nombreux syndromes (la London Dysmorphology Database comprend 269 syndromes comprenant microphtalmie ou anophtalmie). Seuls les principaux syndromes, où l'atteinte oculaire est au premier plan du syndrome, seront traités ici.

BCOR

Des mutations du gène BCOR ont été identifiées chez des patients atteints de syndrome Oculo-Facio-Cardio-Dentaire (OFCD) et une partie des patients atteints de microphtalmie de Lenz[92, 93], ce pourquoi ces deux syndromes sont traités ensemble.

L'acronyme OFCD reprend les principales atteintes de ce syndrome : Œil, Face, Cœur et Dents. Au niveau oculaire, l'atteinte est caractérisée par une cataracte constante et souvent une microphtalmie ou une microcornée (82 % des cas). Différentes autres atteintes oculaires sont possibles. Au niveau

facial, on retrouve une face allongée, une hypoplasie malaire et une pointe du nez élargie. L'atteinte cardiaque est présente chez 75 % des patients et correspond essentiellement à des CIA et CIV. Enfin, l'atteinte dentaire est quasi-constante, et elle est caractérisée par une radiculomégalie (racines extrêmement longues) touchant préférentiellement les canines. D'autres signes (anomalies des extrémités, fente palatine, déficience intellectuelle légère, surdité, défaut de latéralité) ont été associés à ce syndrome[17, 92]. Le syndrome OCFD est lié à des mutations nulles (non-sens, frameshift, mutation d'épissage) du gène *BCOR*. *Il* ne touche que les femmes, ces mutations étant supposées être létales chez les garçons, *BCOR* étant localisé sur le chromosome X[92].

Une mutation faux-sens (p.Pro85Leu) du gène *BCOR* a été identifiée dans deux familles chez des garçons atteints de microphtalmie de Lenz. Ce syndrome se caractérise par une AM avec souvent un colobome et/ ou une cataracte, une microcéphalie, une déficience intellectuelle, une atteinte cardiaque, squelettique (extrémités et clavicules), rénale et génitale[17]. Cependant, seule une faible proportion de patients atteints de microphtalmie de Lenz semble être liée à des mutations du gène *BCOR*[92].

STRA6

Les mutations du gène *STRA6* (stimulated by retinoic acid 6) sont impliquées dans le syndrome de Matthew-Wood ou spectre PDAC (pour Pulmonary-Diaphragmatic-Anophthalmia-Cardiac). Un chapitre de cette thèse est dédié au spectre phénotypique lié aux mutations de ce gène.

RARB

Nous avons participé en collaboration avec l'équipe du Pr Michaud (Montréal) à la description de mutations dominantes et récessives dans le gène *RARB* (retinoic acid receptor beta) chez des patients présentant une AM avec d'autres malformations du spectre PDAC. L'article issu de ce travail[94] est présenté dans la section "Travaux collaboratifs".

GDF6

GDF6 (growth differentiation factor 6) code pour une protéine faisant partie des voies de signalisation des bone morphogenetic proteines (BMP). Des mutations de ce gène ont été retrouvées chez des patients présentant des anomalies squelettiques, et principalement des anomalies des

premières vertèbres[95, 96]. Une mutation de *GDF6* a été identifiée chez un patient présentant un colobome chorio-rétinien bilatéral[97], ce qui a motivé la recherche de mutations de ce gène dans une cohorte de 489 patients avec atteintes oculaires diverses et 81 avec atteinte squelettique. Des variations hétérozygotes ont été identifiées chez 9 patients présentant des atteintes oculaires (AM, colobome), squelettiques ou oculo-squelettiques[95]. Les mutations de ce gène sont dominantes avec une pénétrance incomplète. Ce gène a été décrit comme pouvant expliquer jusqu'à 8 % des AM (4/50 patients[60]). Dans notre cohorte, nous n'avons retrouvé une mutation que chez un patient (1/150), mutation héritée d'un père asymptomatique, confirmant le caractère très incomplet de la pénétrance[40].

BMP4

L'implication du gène *BMP4* (bone morphogenetic protein 4) dans les défauts du développement de l'œil chez l'homme a été suspectée devant l'identification d'une délétion emportant ce gène chez un patient présentant une AM avec glaucome congénital et sclérocornée, une poly-syndactylie et un retard des acquisitions[98]. Des mutations ponctuelles hétérozygotes de *BMP4* ont été depuis décrites dans 5 familles associées à une variabilité phénotypique importante intrafamiliale (d'une atteinte oculaire majeure avec malformations cérébrales et des extrémités, à des myopies fortes isolées ou des polydactylies isolées)[99, 100] et une pénétrance incomplète[78, 101]. Le phénotype lié aux mutations de ce gène a secondairement été étendu au syndrome SHORT (Short stature; Hyperextensibility of joints and/or Hernia (inguinal); Ocular depression (deep-set eyes); Rieger anomaly; and Teething delay)[78].

BMP7

Par une approche gène-candidat, Wyatt *et al.* ont pu en 2010 identifier l'implication du gène *BMP7* (bone morphogenetic protein 7) chez trois patients AM associé à une combinaison variable de signes extra-oculaires (fente palatine, retard des acquisitions, surdité, fistule trachéo-oesophagienne, hémi-vertèbre, RCIU)[102]. Dans les trois cas, les mutations hétérozygotes étaient héritées de parents asymptomatiques.

SMOC1 et FNBP4

Des mutations du gène *SMOC1* (SPARC related modular calcium binding 1), et plus récemment *FNBP4* (formin binding protein 4) ont été décrites chez des patients atteints de syndrome d'anophtalmie de Waardenburg associant AM (90 % des patients) et des anomalies des extrémités (oligodactylie, syndactylies, synostose des IV^{ème} et V^{ème} métacarpiens, 90 % des patients). Des atteintes plus rare sont également décrits dans ce syndrome (déficience intellectuelle chez 1/3 des patients, fente palatine, dents néonatales, anomalies génitales et/ou urinaires)[17]. La transmission de ce syndrome est autosomique récessive et des mutations perte de fonction ont été identifiées dans douze familles[103-105].

Plus récemment, dans une famille consanguine avec un phénotype similaire (avec ectrodactylie), une mutation faux-sens homozygote du gène *FNBP4* a été identifiée[106]. En dehors d'une expression oculaire, peu d'arguments fonctionnels ne démontrent le lien entre cette mutation et le phénotype. Ce gène reste donc à être confirmé par l'identification de mutations chez d'autres patients avec ce phénotype.

HCCS et *COX7B*

Les mutations du gène HCCS (holocytochrome c synthase) sont à l'origine du syndrome MLS (microphthalmia with linear skin defects) aussi connu sous l'acronyme MIDAS (microphthalmia, dermal aplasia, and sclerocornea) qui se transmet selon un mode dominant lié à l'X. Les filles sont donc atteintes en majorité, l'anomalie génétique étant supposée létale chez le garçon. L'atteinte clinique est caractérisée par une microphtalmie et une atteinte cutanée à type de zones d'aplasie cutanée linéaires touchant principalement la face et le cou. De nombreuses autres malformations ont été rapportées chez certains patients (cardiopathies, anomalies cérébrales pour les plus fréquentes)[17]. L'anomalie génétique en cause est souvent une délétion de la région Xp22 emportant *HCCS*, et la taille de ces délétions (et donc les gènes également impliqués) peut expliquer une partie de la variabilité phénotypique. Cette variabilité de la taille des délétions n'explique pas toutes les différences de sévérité de présentation clinique puisque des variabilités phénotypiques intrafamiliales sont également notées[107]. Des mutations ponctuelles d'*HCCS* ont secondairement été décrites[107].

Plus récemment, par une approche gène candidat, des mutations du gène *COX7B* (cytochrome c oxidase 7B) ont également été impliquées dans le syndrome MLS. La transmission y est également dominante liée à l'X[108].

VAX1

Par une approche gène candidat, Slavotinek *et al.* ont identifiés une variation faux-sens (p.Arg152Ser) homozygote dans le gène *VAX1* (ventral anterior homeobox 1) chez un patient AM (sur 80 testés) issu de parents apparentés[109]. Ce patient présentait une microphtalmie bilatérale, une fente labio-palatine bilatérale, des malformations cérébrales (malformations des hippocampes, agénésie du corps calleux et de l'épiphyse), un retard de croissance et un décalage des acquisitions.

c12orf57

Des mutations récessives de ce gène ont récemment été décrites dans un nouveau syndrome associant une AM colobomateuse, agénésie du corps calleux avec retard des acquisitions chez deux enfants[110]. Secondairement, des mutations de ce gène ont été rapportées dans 4 familles multiplexes consanguines d'agénésie ou hypoplasie du corps calleux[111]. Une atteinte oculaire était rapportée chez la moitié des patients. Enfin, dans une autre famille consanguine 3 des 4 enfants porteurs homozygotes d'une mutation délétère du gène *c12orf57* avaient une atteinte du corps calleux, et deux des enfants un colobome oculaire[112].

Prise en charge des patients

Comme nous l'avons vu dans la description des AM, la dichotomie entre forme "isolées" et "syndromiques" et artificielle. Des malformations d'autres organes sont présentes dans 33 à 93 % des AM[17, 18], et vont toucher de façon prédominante le cerveau, le cœur et les extrémités. La recherche de signes associés à l'AM peut orienter la recherche étiologique, même s'il existe des chevauchements entre les différents syndromes. Compte tenu des variabilités extrêmes des phénotypes entre les différents syndromes, et même pour des mutations dans un même gène, il est difficile de définir a priori une prise en charge commune à tous les patients. En dehors de la prise en charge ophtalmologique (qui vise à perfectionner la vision existante et à améliorer l'esthétique par la stimulation simultanée de la croissance des tissus mous et des cavités orbitales osseuses), une prise en charge multidisciplinaire est souvent nécessaire. Une surveillance du développement psychomoteur semble également importante pour pouvoir proposer une prise en charge précoce et adaptée pour les enfants qui le nécessiteront.

Le bilan initial et les grandes lignes de la prise en charge oculaire et extra-oculaire ne sont pas définis pour les AM, et il sera nécessaire pour élaborer un protocole de soin de réunir les différents

intervenants. L'élaboration d'un protocole de soin standardisé risque cependant de se heurter en pratique à la diversité des présentations cliniques rencontrée dans le cadre des AM (microphtalmie *vs* anophtalmie ; microphtalmie simple *vs* microphtalmie complexe, AM unilatérale *vs* AM bilatérale, AM isolée *vs* AM syndromique etc……).

Conseil génétique

Là aussi, l'hétérogénéité génétique rend difficile le conseil génétique. On estime à 10-15 % le risque de récurrence des AM dans la fratrie[1]. Dans la majorité des cas, le dépistage va reposer sur un suivi échographique anténatal orienté. L'identification d'une anomalie génétique causale (environ un quart des patients) permet de préciser ce conseil génétique, et éventuellement de pouvoir proposer un diagnostic prénatal voire préimplantatoire. Cependant, même dans les familles ou une cause génétique a pu être identifiée, le conseil génétique est rendu difficile par la grande variabilité phénotypique observée pour la plupart des gènes (y compris au sein d'une même famille), la pénétrance incomplète de mutations de certains gènes, et la possibilité de mosaïque germinale pour les gènes à transmission autosomique dominant. Tous ces aspects, et les difficultés qu'elles entraînent en termes de conseil génétique, doivent être discutés avec les familles.

I-4 : Introduction aux facteurs de transcription étudiés

Introduction

L'une des différentes approches utilisées pour identifier de nouveaux gènes d'AM a consisté à identifier les gènes régulés par des facteurs de transcription impliqués dans le développement oculaire (voir chapitre correspondant). Nous avons sélectionné quatre FTs à étudier : OTX2, PAX6, RAX et SOX2. *SOX2*, *OTX2*, et *RAX* sont les principaux gènes dans lesquels des mutations sont retrouvées chez les patients AM. *PAX6*, n'est que plus rarement impliqué dans les AM, mais il a été défini comme le "master regulator" du développement oculaire. Ces gènes sont impliqués dans les différents temps du développement oculaire (Fig. 16). Nous allons dans ce chapitre résumer les principales données connus sur nos 4 FTs d'intérêt, et leur rôle au cours du développement oculaire.

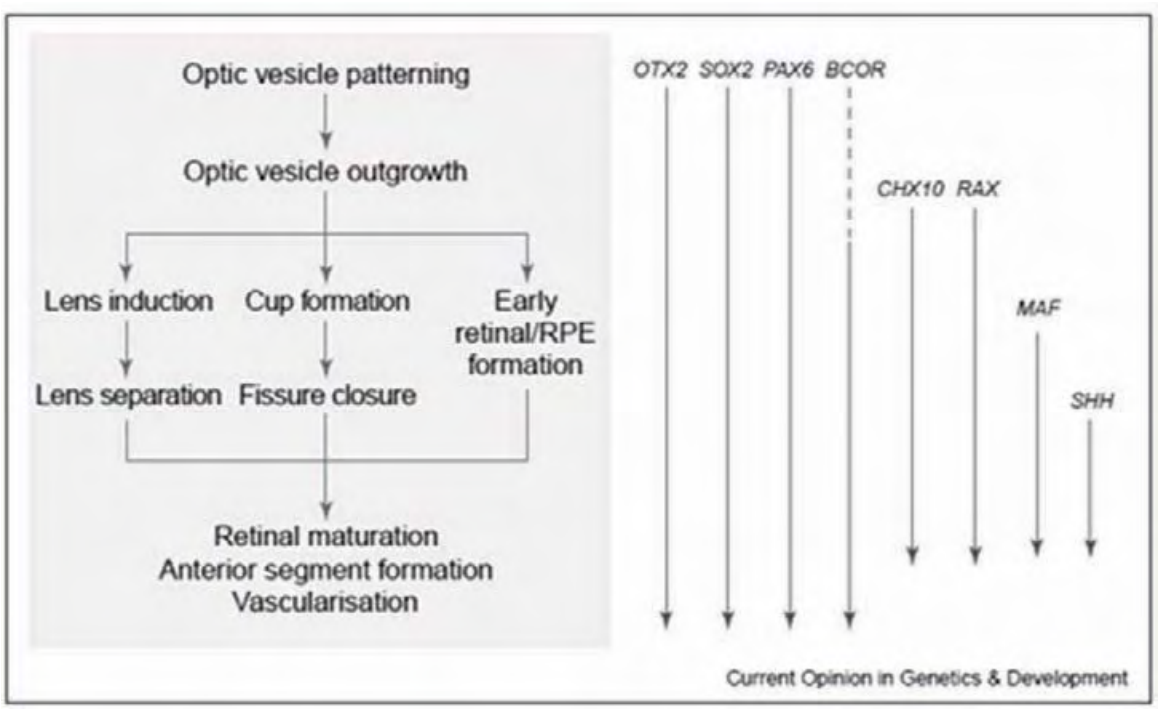

Figure 16: Implication des facteurs de transcription étudiés au cours du développement oculaire.

Cette figure est tirée de [9]. Elle montre les différentes grandes étapes de la formation oculaire et l'implication de différents facteurs de transcription et de SHH au cours de ces étapes. Trois des 4 FTs que nous avons sélectionnés (*OTX2*, *SOX2*, *PAX6*) sont exprimés pendant l'induction de la vésicule optique puis la différenciation des différentes structures oculaires. *RAX* lui est exprimé pendant la formation des différentes structures.

SOX2

- Généralités

SOX2 [SRY (sex determining region Y)-box 2] est localisé sur le chromosome 3 (3q27) et code pour une protéine de 317 acides aminés[30]. SOX2 appartient à la famille des facteurs de transcription SOX caractérisée par la présence d'un domaine de liaison à l'ADN de type HMG (high-mobility group) initialement décrite pour la protéine SRY. Il existe 20 protéines appartenant à cette famille de protéine et qui sont réparties en 8 sous famille en fonction de leur homologie de structure. SOX2 appartient au sous-groupe SOXB1 avec SOX1, SOX3, SOX14 et SOX21 constituant le sous-groupe SOXB2[113].

- Fonction

SOX2 est un facteur de transcription et régule donc l'expression de gènes cibles. La liaison à l'ADN des domaines HMG est faible, et la co-régulation avec d'autres protéines permet d'apporter la stabilité au FT. De plus, cette utilisation de protéines partenaires permet de modifier la régulation d'expression médiée par SOX2 sur les plans spatial et temporel (l'expression des différentes protéines partenaires étant variable dans le temps et en fonction des types cellulaires)[30]. SOX2 est impliqué dans de nombreux mécanismes parfois opposés, et son action va être dépendante du niveau d'expression et du contexte cellulaire: maintenance du caractère indifférencié des cellules souches embryonnaires et adultes (Fig. 17)[113, 114]; rôle dans la spécification, morphogénèse et prolifération dans de nombreux tissus fœtaux[113]. La spécification tissulaire va être déterminée par le niveau d'expression de *SOX2* et d'autres facteurs de transcription spécifiques de lignées (Fig. 18).

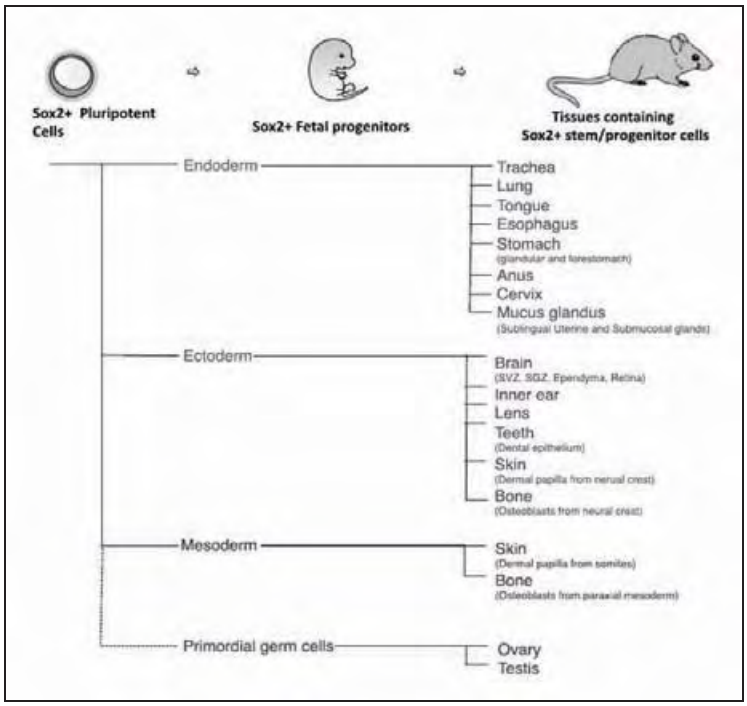

Figure 17: Expression de *Sox2* dans les cellules pluripotentes embryonnaires et adultes.

Sox2 est exprimé dans les cellules souches pluripotentes puis tout au long du développement fœtal et chez l'adulte dans les cellules progénitrices de dérivés endodermiques, ectodermiques, mésodermiques et des cellules germinales. Son expression est également retrouvée dans certaines cellules différentiées. Tirée de [113].

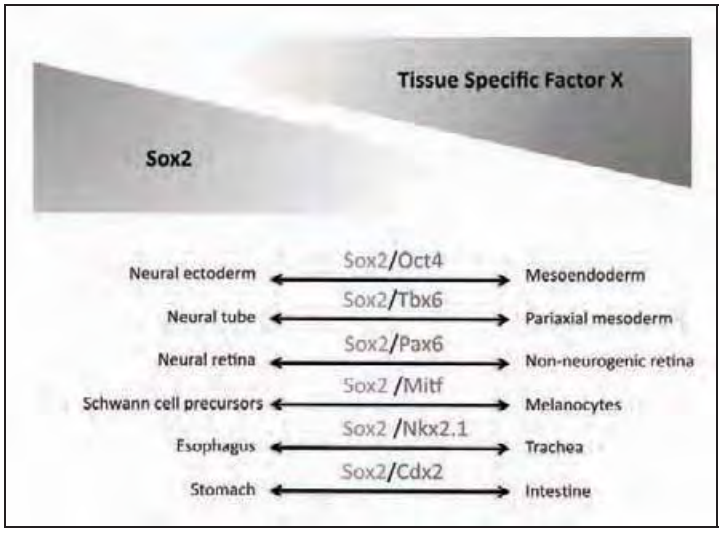

Figure 18: L'antagonisme entre *Sox2* et d'autres facteurs de transcription spécifiques de tissus détermine le devenir des cellules.

Durant l'organogénèse, le niveau d'expression de *Sox2* détermine la spécification cellulaire par antagonisme à d'autres facteurs de transcription spécifiques de lignées. Tirée de [113].

- Expression au cours du développement oculaire

Sox2 est exprimé dans les cellules souches embryonnaires et après la gastrulation, son expression concerne essentiellement les cellules à l'origine du neurectoderme, des placodes sensorielles, des arcs branchiaux, de l'endoderme intestinal, et des cellules germinales [115-117]. L'expression de Sox2 va augmenter de façon importante au stade la cupule optique ainsi que dans l'ectoderme de surface après le contact avec cette dernière. Cette surexpression dans l'ectoderme de surface semble être médiée par des signaux moléculaires issus de la cupule optique et permettre ainsi la formation de la placode cristallinienne puis son invagination[118, 119]. Secondairement, *Sox2* reste très exprimé dans la vésicule cristallinienne et la rétine (Fig. 19).

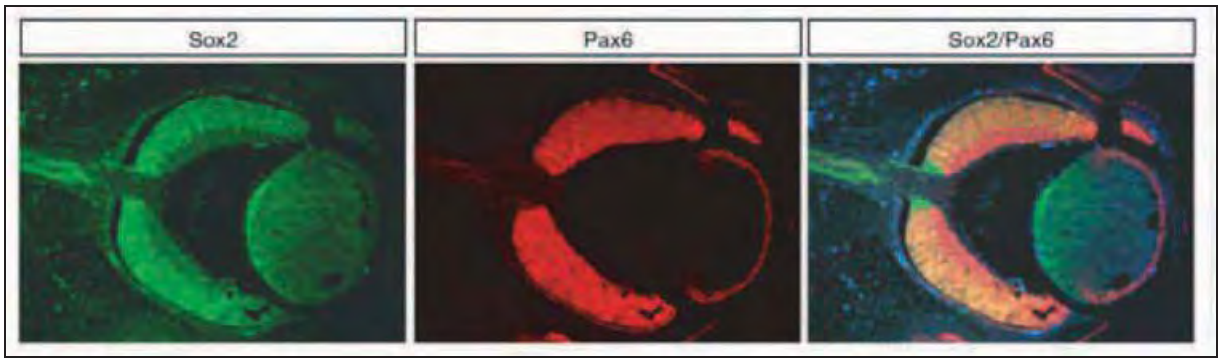

Figure 19: Patron d'expression des gènes *Sox2* et *Pax6* à E13.5 chez la souris.

Figure tirée de [30]. L'expression de *Sox2* concerne les fibres cristalliniennes et la neurorétine (avec un gradient de l'intérieur vers l'extérieur). *Pax6* lui est exprimé à ce stade dans l'épithélium cristallinien, sur l'ectoderme de surface à proximité de la structure oculaire et dans la neurorétine (avec un gradient opposé à *Sox2*).

- Modèles animaux

Les mutations nulles homozygotes ne permettent pas le développement embryonnaire[115]. Au contraire, les souris hétérozygotes n'ont qu'un phénotype modéré (infertilité des mâles, insuffisance hypophysaire)[42, 115] dépendant du fond génétique. L'association d'une délétion hétérozygote de *Sox2* à une délétion des régions régulatrices spécifiques du système nerveux central sur le second allèle entraine des malformations cérébrales sévères[120]. Taranova *et al.* ont montrés que l'hétérozygotie composite chez les souris pour des mutations nulles sur un allèle et hypomorphes sur l'autre était à l'origine de défaut du développement oculaire à type d'AM à partir d'une diminution d'expression de 60 % et dont la sévérité était dépendante de l'activité résiduelle de SOX2[121].

PAX6

- Généralités

PAX6 (paired box 6) est localisé en 11p13. Il code principalement pour une protéine de 422 acides aminés contenant deux domaines de liaison à l'ADN, un domaine *paired* box et un domaine *homeobox*. PAX6 appartient à la famille des facteurs de transcription PAX caractérisée par la présence d'un domaine de liaison à l'ADN de type *paired*. Il existe 9 protéines appartenant à cette famille de protéine et qui sont réparties en 4 sous-groupes en fonction de leur homologie de structure.

Il existe différentes isoformes de *PAX6*. L'une contenant 14 acide aminés supplémentaires dans le domaine *paired* et modifiant ainsi sa capacité de liaison à l'ADN. Trois isoformes sont produites par l'utilisation de codons d'initiation alternatifs après le domaine *paired* et entrainent donc la production de protéines délétées pour ce domaine. La présence de ces différentes isoformes aux capacités de fixation sur l'ADN différents pourrait avoir un rôle dans les différentes fonctions de *PAX6*[122]. Comme SOX2, PAX6 peut co-réguler l'expression de gènes cibles avec d'autres facteurs de transcription, expliquant également la variabilité fonctionnelle de PAX6[123].

- Fonction

PAX6 a un rôle majeur dans le développement du système nerveux central, de l'hypophyse, de l'épiphyse, des yeux, du nez, et du pancréas[124-127]. Au cours de la neurogénèse, il va être important pour le maintien des cellules souches neuronales sous forme indifférenciée, favoriser la prolifération de ces progéniteurs, mais également pour favoriser leur différentiation en fonction du contexte cellulaire et leur migration[123, 128] (Fig. 20). Au niveau oculaire, PAX6 a un rôle spécifique dans la formation du cristallin et de la rétine[129-131]. Au niveau du système nerveux central, il joue donc un rôle majeur dans la mise en place du cortex (différentiation, migration) et dans la mise en place des connexions entre cortex et thalamus[132, 133], dans le développement de l'épiphyse et l'hypophyse, dans le développement cérébelleux[134] et celui des motoneurones[135]. PAX6 est également exprimé au niveau pancréatique où il joue un rôle dans le développement[136].

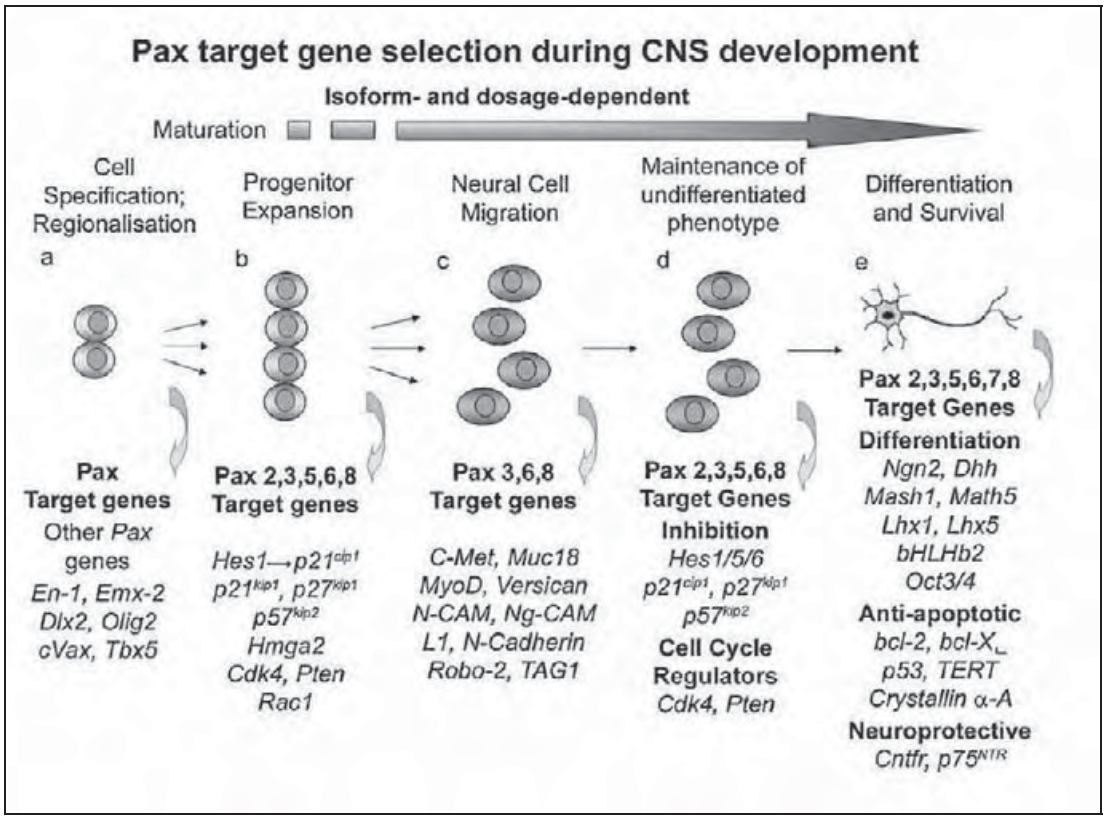

Figure 20: Différentes fonctions de PAX6 au cours du développement neuronal.

Figure tirée de [128]. Les gènes *PAX*, et notamment *PAX6* ont un rôle au cours du développement du système nerveux au cours de la régionalisation et spécification, l'expansion, la migration, la maintenance d'un état indifférencié ou la différentiation. Ces processus sont doses dépendants et dépendants du contexte cellulaire.

- Expression au cours du développement oculaire

L'expression de *Pax6* commence à E8 au niveau de la plaque neurale. A E10, l'expression se confine au prosencephale, rhombencephale et à la moelle[137]. Au niveau oculaire, l'expression de *Pax6* est détectée à E8.5 au niveau de l'ectoderme de surface, ainsi que dans les gouttières optiques[138]. A E10.5, cette expression au niveau de l'ectoderme de surface se restreint dans la région oculaire et au niveau de la neurorétine apparait un gradient, *Pax6* étant plus exprimé dans les couches internes de la neurorétine (Fig. 19).

- Modèles animaux

Il a été montré que l'absence d'un des allèles de *pax6* chez la drosophile entraîne un phénotype *eyeless*[139], et chez la souris un phénotype *small eyes*[140]. De même, les souris surexprimant *Pax6* présentent également un phénotype d'AM[141] montrant bien le caractère dose dépendant de la

régulation médiée par ces facteurs de transcription. Les souris homozygotes pour un allèle nul décèdent en période périnatale. Elles ont un phénotype associant une absence d'œil, de structures nasales et des malformations cérébrales[140]. Les souris porteuses d'un allèle hypomorphe ne présentent que peu d'atteinte clinique à l'état hétérozygote, alors qu'à l'état homozygote, le développement oculaire stoppe précocement pour aboutir à un phénotype AM[142].

L'expression ectopique de *pax6* chez la drosophile[143] ou le xénope[144] est capable de faire se développer des structures oculaires bien différentiées. Ces éléments ont fait que *PAX6* a été défini comme le "maître régulateur" du développement oculaire.

OTX2

- Généralités

OTX2 (orthodenticle homeobox 2) est localisé en 14q22.3. Il code pour un facteur de transcription contenant un homéodomaine qui est un orthologue du gène *orthodenticle* de la drosophile. Il existe deux transcrits de ce gène aboutissant à la formation de protéines de 289 et 297 acides aminés.

- Fonction

Otx2 va jouer plusieurs fonctions au cours du développement embryonnaire, et plus particulièrement au niveau du système nerveux central, de l'épiphyse et de l'œil. Otx2 est nécessaire à l'induction du cerveau antérieure et du pole céphalique chez les vertébrés. Au niveau cérébral, les fonctions essentielles sont la spécification du prosencéphale et du mésencéphale, ainsi que d'une aire à la limite du mésencéphale et du rhombencéphale qui donnera le cervelet[145]. Au niveau oculaire, l'expression d'*Otx2* pourrait permettre l'expression de facteurs de transcription nécessaires à la spécification oculaire d'une partie du cerveau antérieur[146]. L'expression d'*Otx2* est également importante au cours du développement oculaire. Elle permet la spécification et la maintenance des photorécepteurs[145, 147]. Ces différents rôles au niveau oculaire sont résumés figure 21.

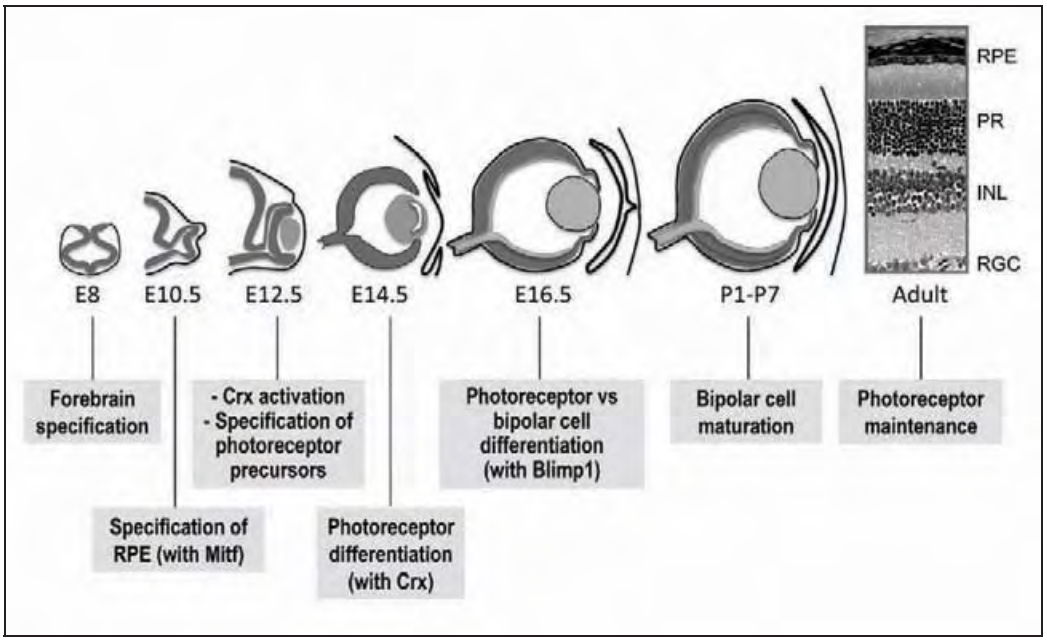

Figure 21: Différentes fonctions d'Otx2 au cours du développement oculaire.

Figure tirée de [145]. Illustration schématique des différentes étapes du développement oculaire, et implication d'Otx2 au cours de celles-ci.

- Expression au cours du développement oculaire

Otx2 est initialement exprimée dans le neurectoderme à la partie antérieure de l'embryon pendant la gastrulation[148], puis est exprimé dans le prosencéphale et le mésencéphale. Son patron d'expression dans le mésencéphale s'arrête net permettant de définir le rhombencéphale[149, 150]. *Otx2* est exprimé dans la vésicule optique ou il a un rôle clef dans l'évagination après contact avec l'ectoderme de surface[151]. L'expression est ensuite restreinte à la rétine pigmentaire ou elle se poursuit à l'âge adulte.

- Modèles animaux

Les délétions homozygotes d'*Otx2* sont létales en raison de l'absence de développement du prosencéphale et mésencéphale[148]. Les souris hétérozygotes ont des phénotypes très variables et dépendants du fond génétique. On peut observer chez ces souris des anomalies cérébrales (acéphalie, holoprosencéphalie), des anomalies oculaires (microphtalmie, anophtalmie) et/ou des anomalies mandibulaires (micrognathie, agnathie)[152]. L'utilisation d'un KO conditionnel (recombinase *Cre* soumis au promoteur de *Crx*) a permis de démontrer le rôle d'Otx2 dans le déterminisme cellulaire des cellules photoréceptrices, ainsi que dans le développement de l'épiphyse[153].

RAX

- Généralités

RAX (retina and anterior neural fold homeobox) est un gène localisé en 18q21.32 qui code pour un facteur de transcription possédant un homéodomaine et un domaine *paired-like* ou OAR (opt, aristaless and rax domain). Il code pour une protéine de 346 acides aminés

- Fonction

RAX a pour fonction initiale de déterminer la spécification des futures cellules rétiniennes[154, 155]. Il a secondairement été démontré que RAX jouait également un rôle spécifiquement dans la maintenance des cellules progénitrices des photorécepteurs, ainsi que leur différentiation[156, 157]. RAX aurait également un rôle dans la régénération rétinienne[156].

- Expression au cours du développement oculaire

Rax est initialement exprimé dans la partie antérieure de la plaque neurale au niveau du futur prosencéphale[158]. L'expression de *Rax* est ensuite scindée en deux au niveau des cupules optiques qui donneront la rétine. Plus tard, l'expression est majoritairement détectée au niveau de la neurorétine, même si une expression faible est retrouvée dans l'épiphyse et des régions du prosencéphale[158] (Fig. 22).

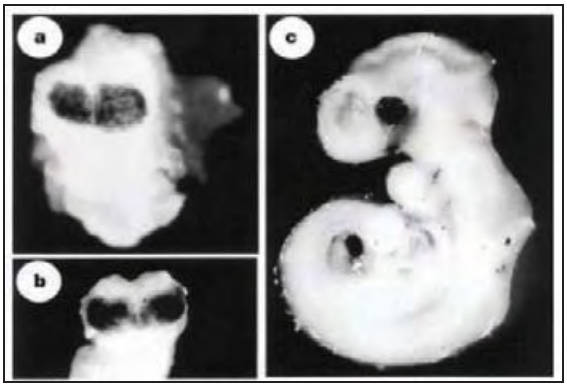

Figure 22: Expression du gène Rax au cours du développement embryonnaire murin.

Figure tirée de [158]. Expression du gène *Rax* étudié par hybridation *in situ*. (**a**) Expression dans la plaque neurale antérieure dans un embryon à E8.5. (**b**) Expression dans les futures régions oculaires à E9.5. (**c**) Expression dans les cupules optiques.

- Modèles animaux

Il existe un modèle naturel de mutation hypomorphe de *Rax* chez la souris entraînant un phénotype AM et des anomalies de l'hypothalamus[159, 160]. La présence homozygote de mutations nulles du gène *Rax* chez la souris entraîne des AM sévères associées à des atteintes cérébrales variables avec une réduction des structures prosencéphaliques et à un moindre degré mésencéphalique[158]. Les souris hétérozygotes n'ont pas de phénotype apparent. Un phénotype AM est également rencontré dans d'autres modèles animaux comme le poisson *medaka*[161], le poisson zèbre[162], et le xénope[163]. De façon intéressante, la surexpression de *Rax* entraîne également une prolifération excessive de la rétine et parfois une duplication du prosencéphale chez le xénope[158, 163] et le poisson zèbre[154].

OBJECTIFS

Mon travail de thèse s'inscrit en complément du travail réalisé dans le service de Génétique Médicale du Professeur Calvas. Notre service s'est spécialisé sur le diagnostic moléculaire des anomalies du développement embryonnaire de l'œil depuis de nombreuses années. Le travail réalisé a donc été transversal entre le laboratoire hospitalier et le laboratoire de recherche.

Les objectifs fixés au début de ma thèse d'Université portaient sur trois points essayant de répondre à différentes problématiques posées dans le cadre de ces anomalies du développement oculaire:

- Le premier objectif concernait la description de la fréquence d'implication des principaux gènes d'AM dans une cohorte constituée de 150 patients AM.
- Le deuxième objectif visait à étudier la variabilité phénotypique associée aux mutations des gènes connus d'AM. Je me suis plus particulièrement intéressé aux spectres phénotypiques secondaires aux mutations des gènes *STRA6* (initialement impliqué dans une forme syndromique d'AM) et *OTX2* (initialement impliqué dans une forme isolée d'AM).
- Enfin, le troisième objectif de mon travail avait pour but d'identifier de nouveaux gènes d'AM. Quand j'ai débuté ce travail, plusieurs approches avaient été définies en parallèle :
    - approche par gène candidat,
    - recherche de remaniement chromosomique par CGH-array,
    - et une approche fondamentale visant à identifier les gènes régulés par les facteurs de transcription déjà impliqués dans les AM.

Concernant cette dernière approche, nous avions initialement prévus de sélectionner les meilleurs gènes candidats pour les séquencer chez nos patients. La révolution du séquençage haut débit apparue pendant mon travail de thèse a fait évoluer les modalités d'analyse et nous a permis de séquencer un grand nombre de ces gènes candidats simultanément. Des analyses pan-génomique de type séquençage d'exome ont également été utilisées.

CHAPITRE II

ANALYSE MOLECULAIRE

DES GENES CONNUS

Introduction

La première partie de mon travail a consisté à étudier la fréquence de l'implication des gènes d'AM dans notre cohorte de patient. J'ai pu au cours de ma formation médicale dans le service de Génétique Médicale de Toulouse participer à la mise au point des analyses moléculaires de certains gènes d'AM (*SOX2*, *OTX2*, *RAX*, *FOXE3*, *STRA6*) et séquencer les premières séries de patients. Ces diagnostics sont maintenant proposés dans un cadre diagnostic en routine dans notre laboratoire. Pour les patients sans mutation identifiée, il leur a été proposé de participer à notre projet de recherche d'identification de nouveaux gènes d'AM dans le cadre d'un PHRC national obtenu en 2009 (PHRC 09 109 01).

Méthodes et Résultats

De nombreux gènes ont été identifiés dans des formes syndromiques et non syndromiques d'AM. Nous avons progressivement mis au point l'analyse moléculaire des gènes d'AM au fur et à mesure de leur description dans la littérature. Sept gènes (*GDF6*, *FOXE3*, *OTX2*, *PAX6*, *RAX*, *SOX2*, et *VSX2*) ont été étudiés de manière systématique dans notre cohorte de patients. Les gènes plus récemment décrits n'ont pas été systématiquement étudiés dans cette cohorte.

Nous avons analysé ces sept gènes (*GDF6*, *FOXE3*, *OTX2*, *PAX6*, *RAX*, *SOX2*, et *VSX2*) dans une cohorte de 150 cas index. Parmi les patients, 41 avaient une anophtalmie clinique d'au moins un œil, 53 une microphtalmie, et 56 une microphtalmie colobomateuse. L'atteinte était unilatérale chez 41 patients et bilatérale (parfois asymétrique) chez 109. L'atteinte était considérée comme " isolée" (strictement isolée, associée à une autre atteinte oculaire [microphtalmie complexe], ou associé à une déficience intellectuelle sans malformation cérébrale) chez 86 patients, et "syndromique" (associée avec d'autres malformations) chez 64 patients. La majorité des cas (122/150) étaient sporadiques. Une histoire familiale était présente pour 28 patients, évoquant 13 fois une transmission dominante (un parent atteint), douze fois une transmission récessive (atteinte dans la fratrie). Dans 3 familles le mode de transmission était inconnu (atteinte chez des cousins au premier degré). Dans notre cohorte, 14 cas index avaient des parents apparentés.

L'analyse de ces sept gènes a permis d'identifier des mutations causales chez 32 des 150 patients (21%).

Les résultats de ces analyses moléculaires sont décrits dans les 2 articles suivants:

- Article n°1

N. Chassaing *et al*. "Molecular findings and clinical data in a cohort of 150 patients with anophthalmia/microphthalmia." Clin Genet *Sous Presse*

- Article n°2

L. Lequeux *et al*. (2008). "Confirmation of *RAX* gene involvement in human anophthalmia." Clin Genet 74(4): 392-5.

D'autres anomalies génétiques causales ont été recherchées, et des anomalies ont pu être mises en évidence par CGH-array, ou lors de l'analyse moléculaire de certains gènes impliqués initialement dans des formes syndromiques (comme *STRA6*), ou dans des gènes plus récemment décrits et exclus de l'analyse systématique (comme *ALDH1A3* et *RARB*). Ces analyses supplémentaires n'ont cependant pas été réalisées chez tous les patients de la cohorte, et il est donc difficile de tirer des conclusions générales. Les phénotypes de ces patients sont discutés dans les chapitres correspondants (phénotype liée aux mutations du gène *STRA6*, recherche de nouveaux gènes par CGH-array, travaux collaboratifs).

Un troisième article décrivant les résultats moléculaires obtenus dans une anomalie du développement syndromique de la chambre antérieure (syndrome de Peters-plus) est également associé à ce travail :

- Article n°3

Dassie-Ajdid J *et al*. (2009). "Novel *B3GALTL* mutation in Peters-plus Syndrome." Clin Genet 76(5): 490-2.

Figures supplémentaires

Deux figures supplémentaires, non présentes dans les articles publiés ont été rajoutées avant les articles. Ces figures montrent les résultats complémentaires obtenus en QMPSF et en CGH-array.

- Figure 23 : Exemple de résultats obtenus lors de la recherche de remaniement génique par QMPSF dans notre cohorte de patients.
- Figure 24 : Analyse par CGH-array Agilent 180K des délétions identifiées par QMPSF dans la cohorte de patients AM.

Conclusion

La spécificité de notre laboratoire hospitalier de Génétique Médicale a permis un recrutement national et international d'un grand nombre de patients. Nous avons au fil des années développés des analyses moléculaires secondairement à la découverte de nouveaux gènes et ainsi pu colliger les résultats d'une analyse moléculaire poussée dans le plus grande série de patient rapportée. En plus de définir la fréquence de l'implication de chaque gène dans les AM, nous avons pu reprendre les phénotypes et décrire certaines particularités (cf. chapitre suivant). Malgré l'analyse systématique de 7 gènes, nous n'avons identifié une anomalie génétique que chez environ 25 % des patients. Cette proportion devrait pouvoir être améliorée avec le développement des techniques de séquençage haut ou moyen débit qui permettront de tester des lots de gènes plus important pour chaque patient. Malgré cela, il reste à l'heure actuelle de nombreux gènes d'AM non identifiés et ce travail d'identification de nouveaux gènes correspond à la plus grande partie de mon travail de thèse.

Outre l'intérêt fondamental en biologie du développement, la connaissance de la cause de la malformation oculaire est un élément important dans la prise en charge des patients (en connaissant le spectre phénotypique associé au gène en cause) et de leurs familles (en permettant un conseil génétique précis et éventuellement la possibilité d'un diagnostic prénatal précoce ou préimplantatoire).

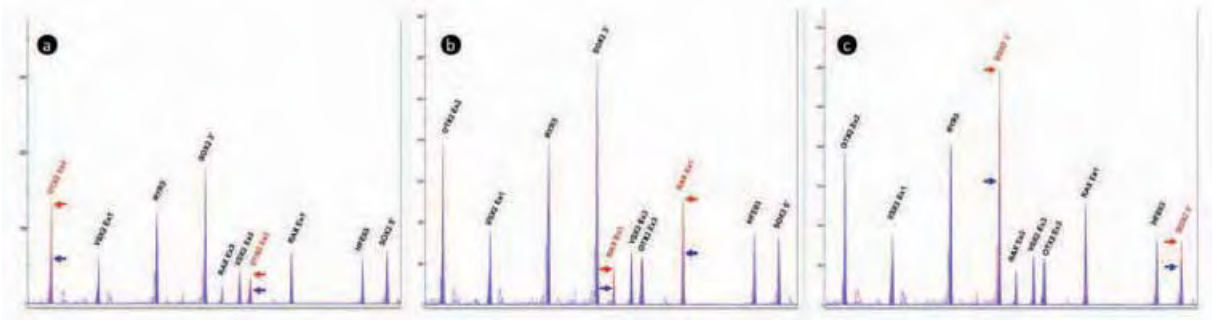

Figure 23: Exemple de résultats obtenus lors de la recherche de remaniement génique par QMPSF dans notre cohorte de patients.

Profils d'amplification de trois patients différents (**a**, **b**, **c**). Deux fragments des gènes *OTX2*, *RAX*, *SOX2* et *VSX2* et deux fragments témoins (*RYR3* et *HFE63*) sont amplifiés simultanément au cours d'une PCR multiplexe. Les intensités des différents pics sont comparés entre les patients (en bleu) et le témoin (en rouge) et normalisés par rapport aux amplifiés témoins. Les délétions sont visualisées par une diminution de moitié de la hauteur des pics et indiqués par des flèches. Cette analyse a permis la mise en évidence de délétion des gènes *OTX2* (**a**), *RAX* (**b**) et *SOX2* (**c**).

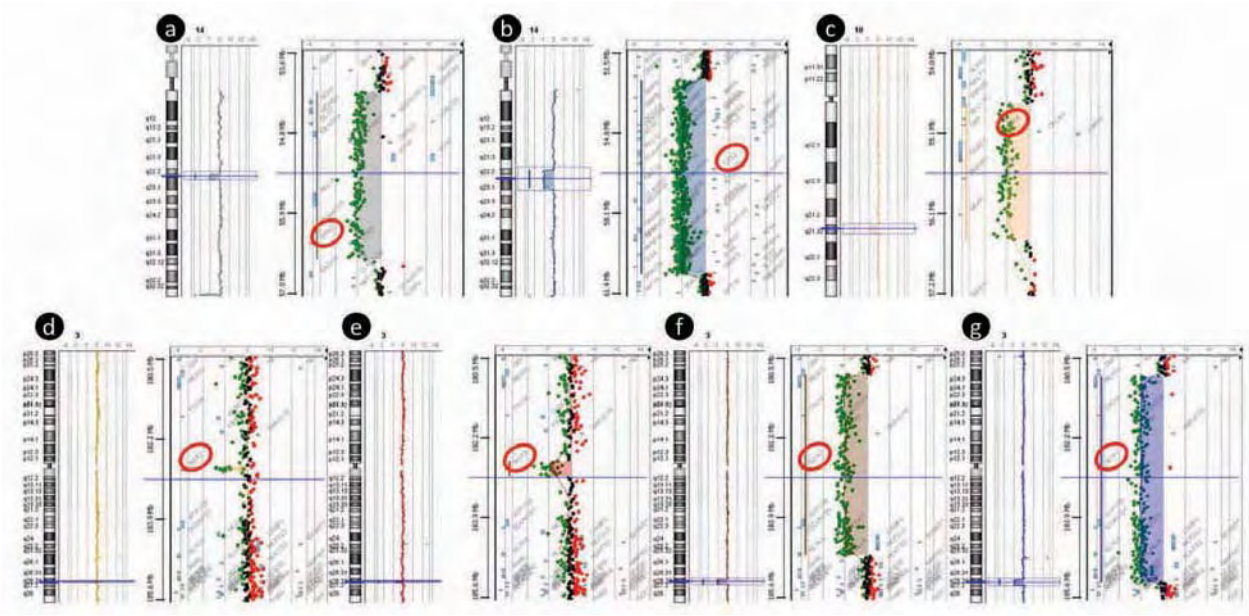

Figure 24: Analyse par CGH-array Agilent 180K des délétions identifiées par QMPSF dans la cohorte de patients AM.

Présence de délétions emportant le gène *OTX2* (**a**, **b**), le gène *RAX* (**c**) et le gène *SOX2* (**d**, **e**, **f**, **g**). Les positions des gènes d'AM situés dans les régions délétées ont été entourées d'un cercle rouge. Cette analyse a permis de confirmer la présence des délétions précédemment identifiées par QMPSF et de caractériser précisément la taille (variable) de ces délétions.

ARTICLE 1

Molecular findings and clinical data in a cohort of 150 patients with anophthalmia/microphthalmia

Clinical Genetics

Sous Presse

N. Chassaing, A. Causse, A. Vigouroux, A. Delahaye, J.-L. Alessandri, O. Boute-Benejean, H. Dollfus, B. Duban-Bedu, B. Gilbert-Dussardier, F. Giuliano, M. Gonzales, M. Holder-Espinasse, B. Isidor, M.-L. Jacquemont, D. Lacombe, D. Martin-Coignard, M. Mathieu-Dramard, S. Odent, O. Picone, L. Pinson, C. Quelin, S. Sigaudy, A. Toutain, C. Thauvin-Robinet, J. Kaplan and P. Calvas

---

Comme nous l'avons vu en introduction sur les aspects moléculaires impliqués dans les anomalies du développement oculaire de type AM, des mutations dans de nombreux gènes ont été décrites associées aux AM. Dans cet article, nous décrivons les résultats de l'analyse moléculaire de sept gènes réalisés dans une cohorte de 150 patients index atteints d'AM.

Le premier résultat de cette étude concerne le taux de détection de mutations dans ces gènes. Des mutations ont été identifiées chez 32 patients (21 %). Ce taux de détection augmente avec la sévérité de l'atteinte oculaire et atteint 54% dans l'anophtalmie. Il s'accroit légèrement en présence d'une histoire familiale (32%). A contrario, lorsque l'atteinte ophtalmologique est unilatérale, des mutations sont identifiées seulement chez 10 % des patients contre 26 % des patients dont l'atteinte est bilatérale.

Cette étude montre également la fréquence de l'implication de chacun des sept gènes étudiés. Nous confirmons ainsi l'implication prépondérante du gène *SOX2*, à l'origine du phénotype oculaire chez 18/150 patients (12 %). *OTX2* et *RAX* arrivent ensuite en terme de fréquence avec respectivement 5 (3,5 %) et 4 (2,5 %) patients porteurs de mutations délétères. Les autres gènes sont plus rarement en cause chez nos patients.

Sur le plan du diagnostic moléculaire, nous montrons dans cette étude l'apport du dosage génique par la QMPSF pour rechercher des remaniements. Ils représentent une part non négligeable des mutations causales. Par exemple, plus d'un quart des mutations identifiées dans le gène *SOX2* (5/18) correspond à des délétions de ce gène.

Concernant le gène *SOX2*, l'analyse complémentaire en CGH-array 180K, réalisée par le Dr. Andrée Delahaye à l'hôpital Jean Verdier à Bondy, a permis de caractériser finement ces remaniements, et a montré que la taille des délétions identifiées étaient variables d'un patient à l'autre (absence de délétion récurrente).

Nous avons pu confronter les données phénotypiques des patients mutés de notre cohorte avec les données de la littérature, et avons confirmé la variabilité phénotypique inter- et intrafamiliale observée pour les différents gènes étudiés. Une description détaillée du phénotype des 32 patients mutés a été incluse dans une note additionnelle à cet article.

Enfin cette étude souligne la difficulté du conseil génétique en raison de mode de transmission variable en fonction des gènes impliqués, de la variabilité phénotypique oculaire et extra-oculaire importante, d'une pénétrance parfois incomplète, et de la description de mosaïques germinales pour les gènes à transmission autosomique dominante. Ces connaissances sont essentielles à la bonne prise en charge des patients et de leurs familles.

CLINICAL GENETICS An International Journal of Genetics, Molecular and Personalized Medicine

Clin Genet 2013
Printed in Singapore. All rights reserved

CLINICAL GENETICS
doi: 10.1111/cge.12275

Short Report

Molecular findings and clinical data in a cohort of 150 patients with anophthalmia/microphthalmia

Chassaing N, Causse A, Vigouroux A, Delahaye A, Alessandri J-L, Boespflug-Tanguy O, Boute-Benejean O, Dollfus H, Duban-Bedu B, Gilbert-Dussardier B, Giuliano F, Gonzales M, Holder-Espinasse M, Isidor B, Jacquemont M-L, Lacombe D, Martin-Coignard D, Mathieu-Dramard M, Odent S, Picone O, Pinson L, Quelin C, Sigaudy S, Toutain A, Thauvin-Robinet C, Kaplan J, Calvas P. Molecular findings and clinical data in a cohort of 150 patients with anophthalmia/microphthalmia. Clin Genet 2013. © John Wiley & Sons A/S. Published by John Wiley & Sons Ltd, 2013

Anophthalmia and microphthalmia (AM) are the most severe malformations of the eye, corresponding respectively to reduced size or absent ocular globe. Wide genetic heterogeneity has been reported and different genes have been demonstrated to be causative of syndromic and non-syndromic forms of AM. We screened seven AM genes [*GDF6* (growth differentiation factor 6), *FOXE3* (forkhead box E3), *OTX2* (orthodenticle protein homolog 2), *PAX6* (paired box 6), *RAX* (retina and anterior neural fold homeobox), *SOX2* (SRY sex determining region Y-box 2), and *VSX2* (visual system homeobox 2 gene)] in a cohort of 150 patients with isolated or syndromic AM. The causative genetic defect was identified in 21% of the patients (32/150). Point mutations were identified by direct sequencing of these genes in 25 patients (13 in *SOX2*, 4 in *RAX*, 3 in *OTX2*, 2 in *FOXE3*, 1 in *VSX2*, 1 in *PAX6*, and 1 in *GDF6*). In addition eight gene deletions (five *SOX2*, two *OTX2* and one *RAX*) were identified using a semi-quantitative multiplex polymerase chain reaction (PCR) [quantitative multiplex PCR amplification of short fluorescent fragments (QMPSF)]. The causative genetic defect was identified in 21% of the patients. This result contributes to our knowledge of the molecular basis of AM, and will facilitate accurate genetic counselling.

Conflict of interest

None.

N Chassaing[a,b], A Causse[a,c], A Vigouroux[a], A Delahaye[d,e], J-L Alessandri[f], O Boespflug-Tanguy[g], O Boute-Benejean[h], H Dollfus[i], B Duban-Bedu[j], B Gilbert-Dussardier[k], F Giuliano[l], M Gonzales[m,n], M Holder-Espinasse[h], B Isidor[o], M-L Jacquemont[p], D Lacombe[q,r], D Martin-Coignard[s], M Mathieu-Dramard[t], S Odent[u], O Picone[v], L Pinson[w], C Quelin[u], S Sigaudy[x], A Toutain[y], C Thauvin-Robinet[z,aa], Josseline Kaplan[ab,ac,ad] and Patrick Calvas[a,b]

[a]Service de Génétique Médicale, Hôpital Purpan, CHU Toulouse, Toulouse, France, [b]Université Paul-Sabatier Toulouse III, Toulouse, France, [c]CHU Toulouse, Service d'Ophtalmologie, Hôpital Purpan, Toulouse, France, [d]UFR SMBH, Université Paris-Nord, Paris 13, Bobigny, France, [e]U676, Inserm, Paris, France, [f]Service de Génétique, GHSR-CHU la Réunion, Hôpital Félix Guyon, Paris, France, [g]Service de Neurologie Pédiatrique, AP-HP, Hôpital Robert Debré, Paris, France, [h]CHRU, Lille, Service de Génétique Clinique, Hôpital Jeanne de Flandre, CHRU, Lille, France, [i]Service de Génétique Médicale, Hôpitaux Universitaires de Strasbourg, CHU de Hautepierre, Strasbourg cedex, France, [j]GHICL, Centre de Génétique Chromosomique, Lille, France, [k]Service de Génétique Médicale, CHU La Milétrie, Poitiers-Cedex, France, [l]Service de Génétique Médicale, CHU Hôpital l'Archet 2, Nice, France, [m]AP-HP, Service de Génétique et d'Embryologie Médicales, Hôpital Armand Trousseau,

Paris, France, [n]Université Pierre et Marie Curie-Paris 6, Paris, France, [o]Service de Génétique Médicale, CHU Nantes, Nantes, France, [p]Service de Génétique, Service de Néonatologie-Pôle femme-mère-enfant, GHSR-CHU la Réunion, Saint Pierre Cedex, France, [q]Service de Génétique Médicale, CHU Bordeaux, Bordeaux, France, [r]Laboratoire MRGM, Université de Bordeaux, Bordeaux, France, [s]Unité de Génétique Clinique, Centre Hospitalier du Mans, Le Mans, France, [t]Unité de génétique clinique, CHU d'Amiens, Amiens, France, [u]Service de Génétique Clinique, CHU de Rennes, Rennes, France, [v]AP-HP, Service de Gynécologie-Obstétrique, Hôpital Antoine Béclère, Clamart, France, [w]Service de Génétique Médicale et Chromosomique, Hôpital Arnaud de Villeneuve, CHRU Montpellier, Montpellier, France, [x]Département de Génétique Médicale, Hôpital Timone-Enfants, Marseille, France, [y]Département de Génétique, CHU de Tours, Hôpital Bretonneau, Tours, France, [z]EA 4271 GAD Génétique des Anomalies du Développement, Université de Bourgogne, Dijon, France, [aa]Centre de Génétique, Hôpital d'Enfants, CHU Dijon, Dijon, France, [ab]Génétique Ophtalmologique INSERM U781 Paris, Paris, France, [ac]Département de Génétique, APHP Hôpital Necker, Paris, France, and [ad]Université Paris Descartes-Sorbonne Paris Cité, Institut IMAGINE, Paris, France

Key words: anophthalmia – *FOXE3* – *GDF6* – microphthalmia – *OTX2* – *PAX6* – *RAX* – *SOX2* – *VSX2*

Corresponding author: Dr Nicolas Chassaing, Service de Génétique Médicale, Pavillon Lefebvre, CHU Purpan, Place du Dr Baylac, 31059 Toulouse Cedex 9, France.
Tel.: +33 5 61 77 90 55;
fax: +33 5 62 74 45 58;
e-mail: chassaing.n@chu-toulouse.fr

Received 12 July 2013, revised and accepted for publication 5 September 2013

Anophthalmia and microphthalmia (AM) are severe ocular developmental defects. Anophthalmia refers to the complete absence of ocular tissue in the orbit (true anophthalmia), or the absence of ocular tissue on clinical examination (clinical anophthalmia). Microphthalmia corresponds to a globe with a total axial length that is at least two standard deviations below the mean for age (<19 mm in a 1-year-old child, <21 mm in an adult) (1, 2). Colobomatous microphthalmia corresponds to microphthalmia associated with failure of closure of the ectodermal optic vesicle fissure. The prevalence of AM is estimated as being between 3 and 30 per 100,000 births (1). AM can be associated with additional malformations in 33–95% of cases (3).

The aetiology of AM is diverse and includes both environmental and heritable factors. Genetic causes are thought to account for the majority of AM and the empirical recurrence risk in siblings without a

clear aetiology or family history is estimated to be 10–15% (1). The genetic basis, either monogenic or chromosomal, is identified in about 25–30% of patients (3). In order to delineate the frequency and the phenotypes associated with mutations in AM genes better, we performed molecular screening of seven of these genes [*GDF6* (growth differentiation factor 6), *FOXE3* (forkhead box E3), *OTX2* (orthodenticle protein homolog 2), *PAX6* (paired box 6), *RAX* (retina and anterior neural fold homeobox), *SOX2* (SRY sex determining region Y-box 2), and *VSX2* (visual system homeobox 2 gene)] in a cohort of 150 AM patients.

Patients and methods

Patients

One hundred and fifty samples from patients diagnosed with unilateral or bilateral AM were sent to our laboratory for molecular screening. The study respected the principles expressed in the Declaration of Helsinki. We retrospectively reviewed the clinical records and molecular results. The age of the index patients ranged from foetuses to 52-year-old adults. Among these, 41 displayed clinical anophthalmia, 53 microphthalmia, and 56 colobomatous microphthalmia. Ocular involvement was unilateral in 41 patients and bilateral in 109. It was isolated in 86 patients, and associated with other malformations in 64 patients. Most cases (122/150) were sporadic. The family history indicated dominant inheritance (one affected parent) in 13 families, recessive inheritance (one affected sibling) in 12, and was unclear in 3 families (affected cousin). 14 patients were born to consanguineous parents. Clinical data of the patients carrying mutations are described in the Appendix S1 and summarized in Table 1. Some examples of the eye phenotypes are shown in Fig. 1.

Mutation screening

DNA was extracted from blood, frozen tissue or paraffin-embedded tissue (foetuses). The number of AM genes molecularly screened in our laboratory increased progressively as new genes were identified and seven genes (*GDF6*, *FOXE3*, *OTX2*, *PAX6*, *RAX*, *SOX2*, and *VSX2*) were studied by direct sequencing. In four of these genes (*OTX2*, *RAX*, *SOX2*, and *VSX2*), quantitative multiplex polymerase chain reaction (PCR) amplification of short fluorescent fragments (QMPSF) was performed in order to detect deletions or duplications. The size of identified deletions was evaluated by 180K array-comparative genomic hybridization (CGH) in deletion carrying patients. Other AM genes which have been identified more recently were not covered in the gene tests performed in this cohort. Detailed methods are given in the Appendix S1.

Results and discussion

The causative molecular defect was identified in 32 of 150 (21%) patients. Mutations were identified in the seven genes tested: *SOX2* ($n = 18$), *OTX2* ($n = 5$), *RAX* ($n = 4$), *FOXE3* ($n = 2$), *VSX2* ($n = 1$), *PAX6* ($n = 1$), and *GDF6* ($n = 1$). The mutation detection rate was higher in anophthalmic patients (22/41, 54%). A family history of AM only moderately increases the mutation detection rate, to 32% (9/28), when compared with sporadic cases (23/122, 19%). In addition, mutations were more frequently found in bilateral forms (28/109, 26%) than in unilateral (4/41, 10%). The presence of extra-ocular features slightly increases the mutation detection rate (16/64, 25%) compared with isolated ocular involvement (16/86, 18%)

Results from this series are described below and summarized in Table 1.

SOX2

Heterozygous *SOX2* [SRY (sex determining region Y)-box 2] mutations were identified in 18 of 150 AM patients. Sequencing identified eight small intragenic deletions/duplications, two nonsense and three missense mutations all involving conserved amino-acids located within the DNA binding domain and predicted to be probably damaging by *in silico* analyses. In addition, QMPSF analysis allowed the identification of five whole gene deletions (Fig. 2a), thus corresponding to 5 out of 18 (28%) of the *SOX2* mutations. Array-CGH of four showed that deletion sizes were highly variable between patients, ranging from 0.08 to 4.3 Mb (Fig. 2b, Table S2). In 12 of 13 cases where parents were analysed the mutation appeared *de novo*, while in the remaining case, somatic mosaicism was identified in the mother.

To date, including the 10 novel mutations reported herein, 58 different mutations have been described. Currently *SOX2*, which is mutated in about 10–15% of AM patients, represents the most frequently involved AM gene. Within this series, *SOX2* mutations were identified in 18 out of 150 (12%) of patients. The *SOX2* anophthalmia syndrome was originally described with ocular malformations (most often bilateral and severe) associated with developmental delay, seizures, mesial temporal brain malformations, growth failure, subtle facial dysmorphism and male genital tract abnormalities (4). *SOX2* mutations were also identified in the anophthalmia–esophageal–genital (AEG) syndrome (5), and various additional features were secondarily reported. The ocular phenotype has been extended to less severe malformations, and even to the absence of macroscopic or microscopic eye malformations (6). In this study, ocular involvement was often bilateral (17/18) and frequently severe with at least one absent eye (15/18). The main extra-ocular features were developmental delay, brain anomalies (mainly affecting the corpus callosum and cerebellum), hypogonadism, and short stature. Oesophageal abnormalities were present in three patients and cleft lip/palate in two.

SOX2 anophthalmia is inherited in an autosomal dominant manner, with most cases resulting from a *de novo* mutation. However, germline mosaicism leading to recurrence in siblings has been described in

Table 1. Phenotype and genotype of mutated patients[a,b]

Patient	Age	Mutated gene	Mutation (cDNA)	Mutation (protein)	Protein domain involved	Family History	Phenotype				
							Right eye	Left eye	Brain	Intellectual disability	Other
1	32 y	*SOX2*	c.(?_-30)_(*220_?)del	SOX2del		–	Ano	Ano	CCA Vermian hypoplasia	+	Short stature
2	30 wg	*SOX2*	c.(?_-30)_(*220_?)del	SOX2del		*De novo*	Micro	Ano	N		–
3	8 y	*SOX2*	c.(?_-30)_(*220_?)del	SOX2del		–	Ano	Ano	CCH Periventricular heterotopia	+	Short stature
4	5 y	*SOX2*	c.(?_-30)_(*220_?)del	SOX2del		*De novo*	Ano	Ano	N	+	GH deficiency Micropenis
5	30 wg	*SOX2*	c.(?_-30)_(*220_?)del	SOX2del		*De novo*	N	Micro Athalamia Retinal dysplasia Sclerocornea	N		Oesophageal atresia Hemi-uterus
6	2 m	*SOX2*	c.70_86del	p.Ala29Glyfs*66		Germinal mosaicism with recurrence	Ano	Ano	N		Oesophageal atresia
7	28 wg	*SOX2*	**c.86_95dup**	**p.Asn33Glyfs*66**		*De novo*	Ano	Ano	N		–
8	4 y	*SOX2*	**c.151T>C**	**p.Trp51Arg**	HMG-box domain	–	Ano	Micro Coloboma	CCH	+	Hypogonadism Micropenis
9	23 wg	*SOX2*	**c.158_174delinsATG**	**p.Arg53Hisfs*37**		*De novo*	Ano	Ano	Ventriculomegaly		–
10	24 wg	*SOX2*	**c.200delA**	**p.His67Profs*35**		*De novo*	Micro Retinal dysplasia	Micro Retinal dysplasia	N		–
11	37 y	*SOX2*	c.221G>C	p.Arg74Pro	HMG-box domain	–	Micro	Micro		+	Hypogonadism
12	17 y	*SOX2*	**c.236G>C**	**p.Trp79Ser**	HMG-box domain	*De novo*	Ano	Ano		+	GH deficiency Cleft palate
13	2 y	*SOX2*	**c.245delT**	**p.Leu82Cysfs*20**		*De novo*	Ano	Ano	N	+	Atrial septal defect Pyelic dilatation
14	8 y	*SOX2*	**c.255_256delGGinsT**	**p.Thr85Thrfs*17**		*De novo*	Ano	Ano	Left cerebellar hemisphere hypoplasia	+	Cryptorchidism
15	11 y	*SOX2*	c.310G>T	p.Glu104*		*De novo*	Ano	Micro	CCH	+	Oesophageal stenosis Micropenis
16	23.5 wg	*SOX2*	**c.476_479dup**	**p.Tyr160***		–	Ano	Ano	N		Bilateral cleft L/P
17	20 y	*SOX2*	**c.513C>G**	**p.Tyr171***		*De novo*	Ano	Ano	CCH Vermian hypoplasia	+	GH deficiency Hypogonadism
18	28 y	*SOX2*	**c.599delA**	**p.Tyr200Serfs*2**		*De novo*	Micro	Ano	N	+	GH deficiency Hypogonadism
19	33 wg	*OTX2*	c.(?_-30)_(*220_?)del	OTX2del		–	Ano	Ano	Ventriculomegaly Vermian heterotopia Cortical dysplasia		–

Table 1. Continued

Patient	Age	Mutated gene	Mutation (cDNA)	Mutation (protein)	Protein domain involved	Family History	Phenotype				
							Right eye	Left eye	Brain	Intellectual disability	Other
20	24 y	*OTX2*	c.(?_-30)_(*220_?)del	OTX2del		Three generations	Micro Coloboma	Micro Coloboma	N	+	–
21	23.5 wg	*OTX2*	c.289C>T	p.Arg97*		–	Ano	N	N		–
22	31 y	*OTX2*	c.289C>T	p.Arg97*		Four generations One son displayed otocephaly	Ano	N	N	–	–
23	22 y	*OTX2*	c.316delC	p.Gln106Asnfs*11		Five generations Three affected related displayed otocephaly	Ano	Ano	N	+	–
24	4 y	*RAX*	**c.478T>C** **c.563G>A**	**p.Tyr160His** **p.Arg188Gln**	Homeodomain Homeodomain	One affected sibling	Micro	Micro	N	+	–
25	18 m	*RAX*	**c.560G>A** **c.560G>A**	**p.Arg187Gln** **p.Arg187Gln**	Homeodomain	–	Ano	Ano	N	–	–
26	2 y	*RAX*	c.664delT c.909C>G	p.Ser222Argfs*62 p.Tyr303*		–	Ano	Ano		–	–
27	26 wg	*RAX*	**c.665C>A** **c.(?_-30)_(*220_?)del**	**p.Ser222*** ***RAX*del**		–	Ano	Ano	N		–
28	7 y	*FOXE3*	**c.685_686insTCCGGAGC** **c.685_686insTCCGGAGC**	**p.Ala230Argfs*2** **p.Ala230Argfs*2**		One affected cousin born to consanguineous parents	Micro Sclerocornea	Micro Sclerocornea	N	+	–
29	23 y	*FOXE3*	c.720C>A c.720C>A	p.Cys240* p.Cys240*		One affected sibling	Micro Sclerocornea	Micro Sclerocornea	N	–	Polycystic ovarian syndrome
30	2 y	*PAX6*	c.418G>C	p.Arg19Pro	Paired domain	One affected sibling	Micro Sclerocornea	Micro Sclerocornea	N	–	–
31	8 y	*VSX2*	**c.71_72insG** **c.667G>A**	**p.Ala25Argfs*101** **p.Gly223Arg**	CVC domain	One affected sibling	Micro Cataract Coloboma	Micro Cataract Coloboma	N	–	–
32	4.5 y	*GDF6*	c.980C>A	p.Pro327His	TGF-β prodomain	Inherited from asymptomatic father	N	Micro Coloboma	N	–	–

Ano, anophthalmia; CCA, corpus callosum agenesis; CCH, corpus callosum hypoplasia; cDNA, complementary DNA; empty box, information unknownmicro, microphthalmia; GH, growth hormone; HMG-box, high mobility group box; m, months; N, normal; empty box: absent data; TGF, transforming growth factor; wg, weeks of gestation; y, years; –, absence; +, presence.

[a]The italicized patient numbers correspond to already reported patients (Appendix S1). Novel mutations identified in this study are indicated in bold.

[b]Sequence variations were numbered considering Adenine of the ATG initiation codon as the first nucleotide (GenBank accession NM_001001557.2 [GDF6], NM_012186.2 [FOXE3], NM_021728.2 [OTX2], NM_001604.4 [PAX6], NM_013435.2 [RAX], NM_003106.3 [SOX2], and NM_182894.2 [VSX2]).

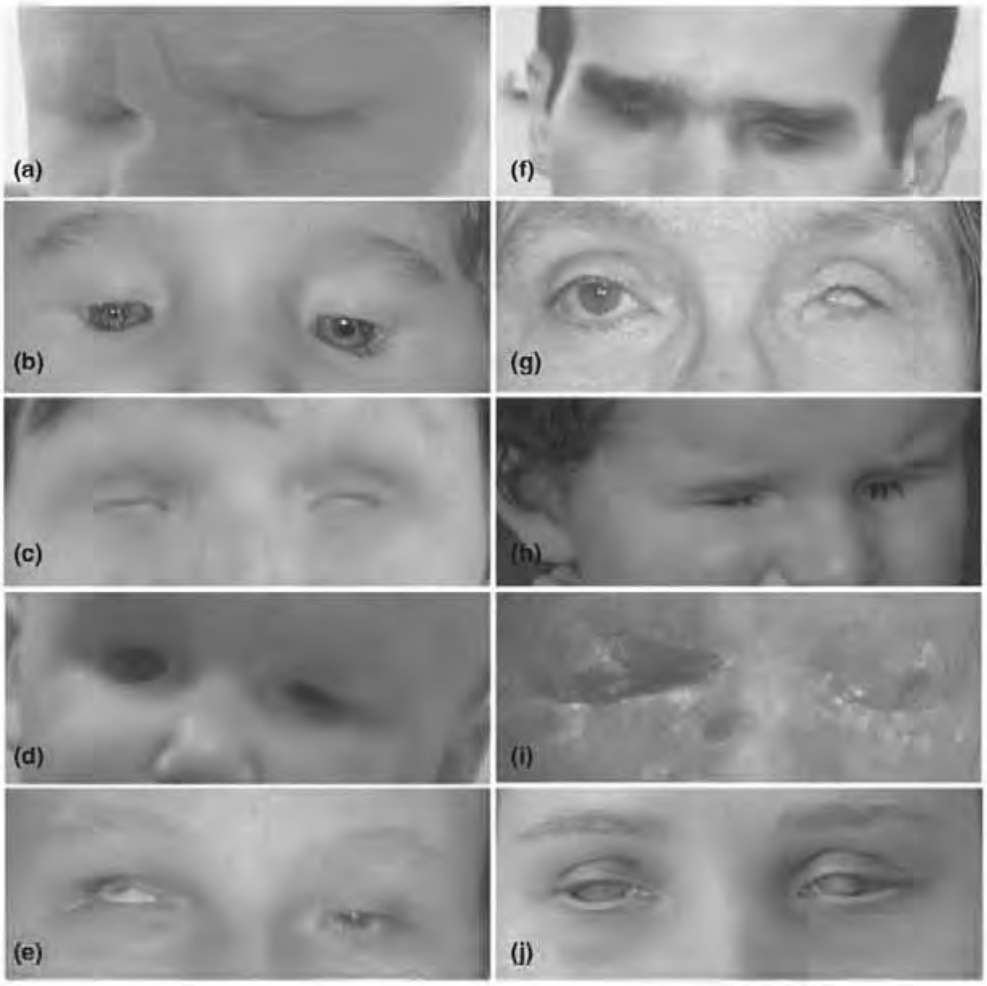

Fig. 1. Ocular involvement in patients carrying mutations. Examples of ocular involvement in patients with *SOX2* mutations (**a–e**) corresponding to P1, P3, P11, P13, and P18, respectively); *OTX2* mutations (**f, g**) corresponding to P23 and P23's aunt, respectively); *RAX* mutations (**h, i**) corresponding to P24 and P27, respectively); and *FOXE3* mutations (**j**) P29). Note unilateral (G) or bilateral anophthalmia-microphthalmia (**a–f, h–j**) associated with sclerocornea in P29 (**j**).

three families. There is no clear genotype/phenotype correlation.

OTX2

OTX2 mutations were identified in 5 of 150 (3%) AM patients including two patients with an *OTX2* gene deletion (Table S2). The *OTX2* mutation was inherited from a symptomatic parent in three families, and in two cases, no family history was mentioned but parents' samples were unavailable for analysis.

A total of 31 *OTX2* different mutations (14 frameshift, 9 nonsense, 7 missense, and whole gene deletion) have been reported. *OTX2* mutations are associated with a broad spectrum of ocular phenotypes, intellectual deficiency, seizures, brain malformations, pituitary abnormalities, and short stature (7). More recently, we described involvement of *OTX2* mutations in otocephaly-agnathia (8). In this study, clinical presentation was variable, even within families, ranging from bilateral anophthalmia to unilateral mild microphthalmia. Otocephalic cases were reported in two families.

OTX2 anophthalmia is inherited in an autosomal dominant manner with variable expressivity and incomplete penetrance. Germline mosaicism has been described in two families.

RAX

Homozygous or compound heterozygous *RAX* mutations were identified in 4 of 150 (3%) patients, bringing the number of described *RAX* mutations to 10. Including the four patients in this report, only seven patients with *RAX* mutations have been described. The ocular phenotype associated with recessive *RAX* mutations is often bilateral and severe. Neurological involvement (intellectual deficiency, autistic features) was observed in three out of seven described patients. Apart from cerebral involvement, no other extra-ocular malformation was associated with *RAX* mutations. *RAX* anophthalmia is inherited in an autosomal recessive manner.

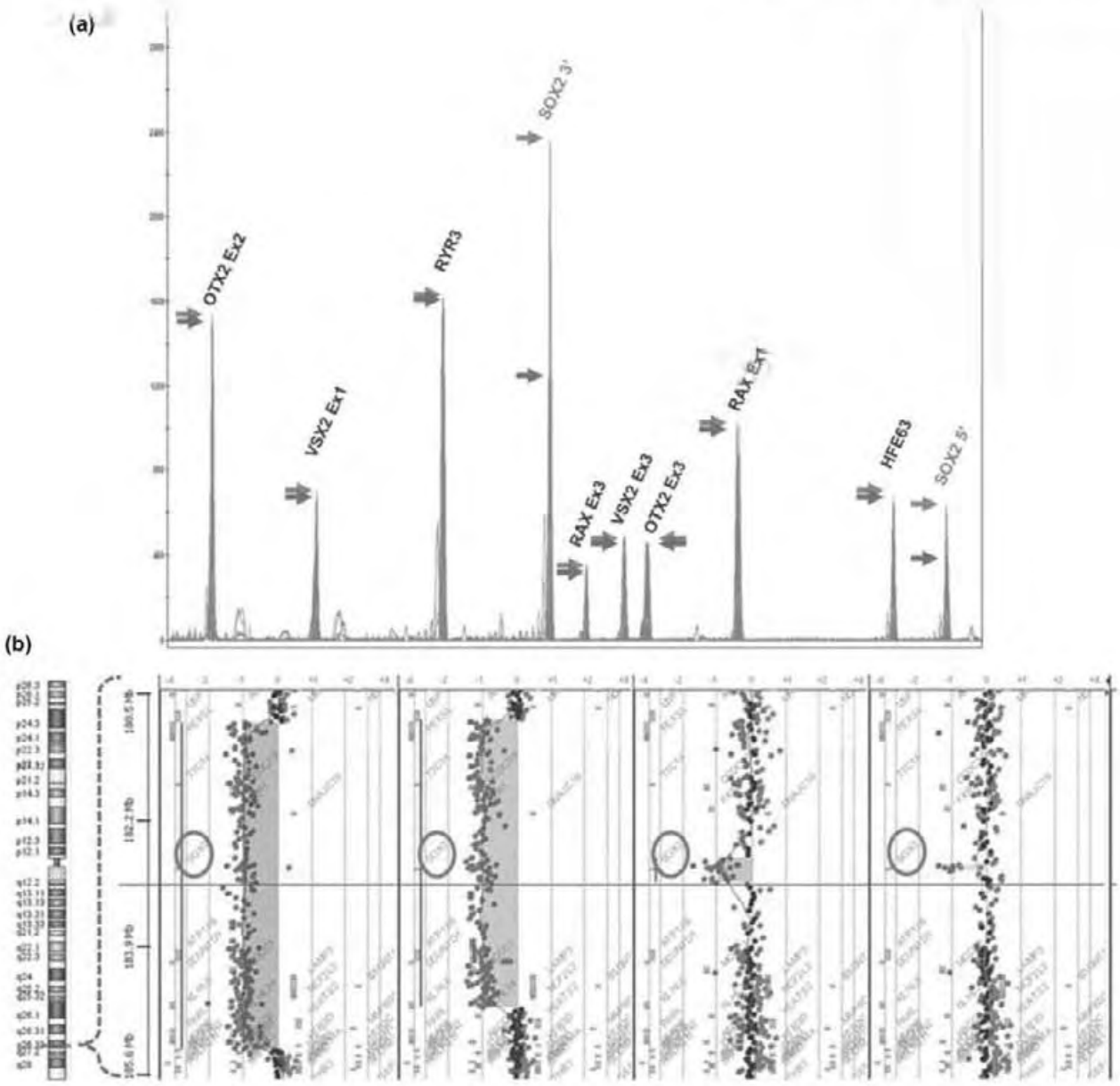

Fig. 2. Identification of *SOX2* deletion by quantitative multiplex PCR amplification of short fluorescent fragments (QMPSF) and characterization of the deletion sizes by array-comparative genomic hybridization (CGH). (**a**) Example of *SOX2* deletion revealed by QMPSF. Amplification profile of one patient sharing the deletions (in blue), and of a normal control (in red) are superimposed. Fluorescent profiles are normalized using the control amplicons *RYR3* and *HFE63*. Intensity of each peak is indicated by an arrow, blue for the patient bearing the deletion, red for the control. The twofold reduction in the intensity of *SOX2* peaks is to the result of the heterozygous deletion (**b**) Gene view of the region 3q26.33-3q27.1 (Chromosome 3: 180,556,405 – 185,680,405 – hg18 – view of 5.12 Mb) produced by the Agilent CGH ANALYTICS software and showing the aberrant deletions, which are highlighted in colour. The *SOX2* gene is surrounding in red. The dots correspond to the array targets, arranged on the y-axis according to their genomic position and on the x-axis according to their log2 intensity ratio value.

FOXE3

FOXE3 mutations were identified in 2 of 150 AM patients. Both were born to consanguineous parents One patient had a recurrent homozygous nonsense mutation (c.720C>A [p.C240*]), while the other had a novel homozygous frameshifting mutation c.685_686insTCCGGAGC. *FOXE3* mutations have previously been associated with autosomal dominant anterior segment anomalies (9), autosomal recessive primary aphakia (10), and autosomal recessive microphthalmia (11). A total of 13 different *FOXE3* mutations have been described, 8 leading to a recessively inherited phenotype and 5 associated with dominant inheritance. Interestingly, four of the five dominant mutations correspond to non-stop mutations suggesting that the extended protein may have a dominant negative effect, while the recessive mutations would be loss of function mutations. Dominant mutations mainly cause

anterior segment dysgenesis, while recessive mutations cause a more severe ocular phenotype adding microphthalmia to the anterior segment dysgenesis. No other extra-ocular malformation has previously been associated with *FOXE3* mutations. In our cohort, one patient carrying a homozygous *FOXE3* mutation displayed intellectual deficiency and autistic features.

PAX6

A heterozygous missense mutation in the *PAX6* gene was identified in 1 of 150 AM patients. This patient has bilateral microphthalmia and sclerocornea, while her sister has a left microphthalmia and sclerocornea and right partial iris hypoplasia. Both had the same missense mutation (c.418G>C [p.Arg19Pro]). This mutation involved a conserved amino-acid in the paired domain. The change was predicted to be damaging *in silico*. Neither clinical data nor samples were available for the parents. More than 300 *PAX6* mutations have been identified (The Human *PAX6* mutation Database see http://lsdb.hgu.mrc.ac.uk) and are typically associated not only with autosomal dominant aniridia but also affect the cornea, lens and retina (12). Although we have identified *PAX6* mutations in patients referred for aniridia with mild microphthalmia, this is the sole example of *PAX6* involvement in our cohort of patients referred for AM.

VSX2

VSX2 compound heterozygous mutations were identified in 1 of 150 AM patients. This patient, who had bilateral colobomatous microphthalmia and cataracts, was a compound heterozygote for two novel mutations (c.71_72insG, and p.Gly223Arg), thus bringing the total of *VSX2* mutations described to 11. The p.Gly223Arg involved a conserved amino-acid located in the conserved CVC domain of the protein, and was evaluated separately by POLYPHEN-2 (damaging) and by SIFT (tolerated). It is absent in a control population (Exome Variant Server). A missense mutation involving the same amino-acid (p.Gly223Ala) had previously been reported in association with AM, suggesting that p.Gly223Arg could be deleterious. *VSX2* mutations have previously been associated with microphthalmia and coloboma and/or anterior chamber abnormalities. *VSX2* anophthalmia is inherited in an autosomal recessive manner.

GDF6

One heterozygous *GDF6* mutation was identified in 1 of 150 AM patients. He had unilateral colobomatous microphthalmia without skeletal involvement. The missense mutation (c.980C>A [p.Pro327His]) had been previously reported in association with microphthalmia (13). The variation was inherited from the asymptomatic father in our patient as in the published case. p.Pro327His is predicted to be benign *in silico*. It is, however, absent in a control population (Exome Variant Server and (13)). Functional studies are likely to be needed to determine more conclusively whether this variant does indeed produce a deleterious effect.

GDF6 loss-of-function mutations were first associated with skeletal defects and subsequently with ocular defects (microphthalmia and coloboma) (13, 14). This oculo-skeletal syndrome is inherited in an autosomal dominant manner, with incomplete penetrance.

Conclusion

The overall mutation detection rate in this cohort is 21% (32/150) after screening the seven selected genes (*GDF6*, *FOXE3*, *OTX2*, *PAX6*, *RAX*, *SOX2*, and *VSX2*). Importantly, whole gene deletion represents a high percentage of the identified mutations, especially for *SOX2* and *OTX2*. No mutation was found in the vast majority (about 80%) of AM patients. Other genes are known to be involved. Some have been identified in syndromic and non-syndromic AM by array-CGH (e.g. *BMP4* and *TMX3*), by linkage analysis (e.g. *SMOC1* and *STRA6*) or by a candidate gene approach (e.g. *VAX1* and *BMP7*). In addition, next-generation sequencing has allowed the identification of several novel AM genes (e.g. *ALDH1A3*, *ATOH7*, *c12orf57*, *FNBP4*, *ODZ3* ...). However, mutations in each of these genes explain the symptoms in only a very small percentage of AM patients, and it seems likely that only a small proportion of AM causative genes have so far been identified. While this represents a vast genetic heterogeneity, this is not entirely surprising in the developmental process of such a complex organ.

The existence of a range of modes of inheritance, germline mosaicism, and incomplete penetrance all pose particular challenges for genetic counselling. Clinical overlaps within patients and genetic heterogeneity have led to difficulties in designing an efficient screening strategy. Advances in high throughput sequencing will allow a larger set of AM genes to be screened for diagnostic purposes (15). High throughput sequencing (whole exome and whole genome) also represent to date a better method for the identification of new AM genes.

Phenotypic variability, asymmetric ocular involvement, and incomplete penetrance reflect the complexity of the developmental process, driven by interacting networks and modulated by stochastic events and environmental influences. Identifying novel genes and deciphering factors determining the clinical presentation represent further essential steps to achieve.

Supporting Information

The following Supporting information is available for this article:

Table S1. Primers used for direct sequencing and quantitative multiplex PCR amplification of short fluorescent fragments (QMPSF) analysis

Table S2. Deletions characterized using array-comparative genomic hybridization (array-CGH) Agilent 180K

Appendix S1. Clinical spectrum and molecular findings in a cohort of 150 patients with microphthalmia/anophthalmia.

Additional Supporting information may be found in the online version of this article.

Acknowledgements

The authors would like to thank the families for their participation and the following physicians and technicians for their assistance: Ludivine Pouey, Claire Scaramouche, Beaudou Joelle, Florence Nicot, Léopoldine Lequeux, Sirine Hammoud, le CPDPN de Besançon and the SOFFOET. Authors are indebted to Samantha Leonard for her help in preparing the manuscript.

This work was supported by grants from the Clinical Research Hospital Program from the French Ministry of Health (PHRC 09 109 01), and by Retina France.

References

1. Verma AS, Fitzpatrick DR. Anophthalmia and microphthalmia. Orphanet J Rare Dis 2007: 2: 47.
2. Weiss AH, Kousseff BG, Ross E, Longbottom J. Simple microphthalmos. Arch Ophthalmol 1989: 107: 1625–1630.
3. Slavotinek AM. Eye development genes and known syndromes. Mol Genet Metab 2011: 104: 448–456.
4. Ragge NK, Lorenz B, Schneider A et al. SOX2 anophthalmia syndrome. Am J Med Genet A 2005: 135: 1–7 discussion 8.
5. Williamson KA, Hever AM, Rainger J et al. Mutations in SOX2 cause anophthalmia-esophageal-genital (AEG) syndrome. Hum Mol Genet 2006: 15: 1413–1422.
6. Chassaing N, Gilbert-Dussardier B, Nicot F et al. Germinal mosaicism and familial recurrence of a SOX2 mutation with highly variable phenotypic expression extending from AEG syndrome to absence of ocular involvement. Am J Med Genet A 2007: 143: 289–291.
7. Schilter KF, Schneider A, Bardakjian T et al. OTX2 microphthalmia syndrome: four novel mutations and delineation of a phenotype. Clin Genet 2011: 79: 158–168.
8. Chassaing N, Sorrentino S, Davis EE et al. OTX2 mutations contribute to the otocephaly-dysgnathia complex. J Med Genet 2012: 49: 373–379.
9. Semina EV, Brownell I, Mintz-Hittner HA, Murray JC, Jamrich M. Mutations in the human forkhead transcription factor FOXE3 associated with anterior segment ocular dysgenesis and cataracts. Hum Mol Genet 2001: 10: 231–236.
10. Valleix S, Niel F, Nedelec B et al. Homozygous nonsense mutation in the FOXE3 gene as a cause of congenital primary aphakia in humans. Am J Hum Genet 2006: 79: 358–364.
11. Iseri SU, Osborne RJ, Farrall M et al. Seeing clearly: the dominant and recessive nature of FOXE3 in eye developmental anomalies. Hum Mutat 2009: 30: 1378–1386.
12. Tzoulaki I, White IM, Hanson IM. PAX6 mutations: genotype-phenotype correlations. BMC Genet 2005: 6: 27.
13. Asai-Coakwell M, French CR, Ye M et al. Incomplete penetrance and phenotypic variability characterize Gdf6-attributable oculo-skeletal phenotypes. Hum Mol Genet 2009: 18: 1110–1121.
14. Tassabehji M, Fang ZM, Hilton EN et al. Mutations in GDF6 are associated with vertebral segmentation defects in Klippel-Feil syndrome. Hum Mutat 2008: 29: 1017–1027.
15. Jimenez NL, Flannick J, Yahyavi M et al. Targeted 'next-generation' sequencing in anophthalmia and microphthalmia patients confirms SOX2, OTX2 and FOXE3 mutations. BMC Med Genet 2011: 12: 172.

Clinical spectrum and molecular findings in a cohort of 150 patients with microphthalmia/anophthalmia

SUPPLEMENTARY NOTE:

- **Methods**
- **Clinical data for the mutated patients**

METHODS

- Direct sequencing

After PCR amplification of coding exons and exon-intron boundaries using pairs of primers derived from published sequences (Supp. Table 1), PCR fragments were sequenced using Big Dye 1.1 DNA sequencing kit (Applied Biosystems, UK) on a ABI3130XL sequencer (Applied Biosystems, UK). Missense mutations pathogenic effect was evaluated *in silico* by using Polyphen-2 (http://genetics.bwh.harvard.edu/pph2/) and SIFT (http://sift.jcvi.org/) softwares.

- QMPSF analysis

Oligonucleotide primer pairs for amplifying two fragments of each of *OTX2*, *RAX*, *SOX2*, and *VSX2* genes and two control fragments of reference genes (*HFE63* and *RYR3*), were used to construct the multiplex PCR set. All primers carried a 10 nucleotides sequence extension at their 5' end and all forward primers were 5'-labelled with the 6-FAM fluorochrome. Amplicon sizes range from 115 bp to 242 bp (Supp. Table 1). DNA fragments generated by QMPSF were separated on an ABI 3130XL sequencer (Applied Biosystems, UK), and the resulting fluorescence profiles were analysed with Genemapper v3.1 software (Applied Biosystems, UK). The presence of a deletion was indicated by a two-fold reduction in the height of the corresponding peak.

- Array-CGH

Seven of the eight deletions identified by QMSF analysis were subsequently analyzed by array-CGH in order to better characterize the size of these deletions. Oligonucleotide array-CGH was performed using the SurePrint G3 Human CGH Microarray Kit 180K (Agilent Technologies, Santa Clara, CA, USA). The arrays include a total of 180 880 probes, with an overall median probe spacing of 13 kb. The data were graphed and analysed using Agilent CGH Analytics software (statistical algorithm: ADM-2, sensitivity threshold: 6.1). Only gains or losses that encompassed at least three consecutive oligomers on the array were considered.

CLINICAL DATA FOR THE MUTATED PATIENTS

Patient 1 (*SOX2* deletion), Fig 1A

A 32 year old woman born to healthy unrelated parents. She had one healthy sister. She was delivered at 40 weeks gestation with normal measurements. Bilateral anophthalmia was evident at birth. She had severe developmental delay, sat at 36 months and never walked or talked. At age 28, her height was 140 cm (-4 SD), her weight 27 kg (-4.5 SD), and her head circumference was 47 cm (-5 SD). Facial dysmorphism included coarse facies, large nares, thick lips and long and thin fingers and toes. She has had seizures and MRI scans showed agenesis of the corpus callosum, optic nerve hypoplasia, and hypoplasia of the vermis. QMPSF analysis identified a deletion of *SOX2*. CGH array showed that the deletion size was 3.8 Mb (Sup Table 2). Parental DNA was unavailable.

Patient 2 (*SOX2* deletion)

A male foetus at 30 weeks gestation. The parents were unrelated and healthy. At 24.5 weeks gestation an ultrasound scan detected left anophthalmia. MRI scan confirmed the absence of the left ocular globe. No cerebral abnormality was detected. The parents decided to terminate the pregnancy. At autopsy, moderate right microphthalmia was found in addition to the left anophthalmia. Apart from a right single palmar crease, no other abnormality was detected. Measurements were normal for the gestational age (length 39.5 cm, weight 1.310 kg, and OFC 26 cm). QMPSF analysis identified a deletion of *SOX2*. Parental studies showed that this deletion occurred *de novo*.

Patient 3 (*SOX2* deletion), Fig 1B

A 8 year old boy, born to healthy unrelated parents. He had one healthy brother and one healthy sister. He was delivered at 38 weeks gestation with normal measurements (length 48.5 cm, weight 3.460 kg, and OFC 35.5 cm). At birth, bilateral anophthalmia was evident. He had developmental delay, and walked at age 4. The IQ was estimated to be 60. At age 8, his height was 107 cm (-3.5 SD), his weight 16.2 kg (-2.5 SD), and his head circumference 50 cm (-2 SD). MRI scans showed hypoplasia of the corpus callosum and periventricular heterotopia. QMPSF analysis identified a deletion of *SOX2*. CGH array demonstrated that this patient had a 3q26 microdeletion (330 kb, Sup Table 2) involving *SOX2*.

Patient 4 (*SOX2* deletion)

A 5 year old boy, born to healthy unrelated parents. At birth, bilateral anophthalmia and micropenis were noted. He had severe developmental delay, and was unable to walk alone at age 5. He had short stature secondary to GH insufficiency. No cerebral abnormality was detected by MRI. QMPSF analysis identified a deletion of *SOX2*. CGH array showed that this patient had a small deletion (80 kb, Sup Table 2) involving only one gene, *SOX2*. Parental studies showed that this deletion occurred *de novo*.

Patient 5 (*SOX2* deletion)

A female foetus at 30 weeks gestation. The parents were healthy and unrelated. She had one healthy sister and one healthy brother. At 22 weeks gestation an ultrasound scan showed suspected esophageal atresia. A karyotype performed on the amniotic fluid was normal (46, XX). At 30 weeks gestation, there was an intrauterine fetal death. Length, weight and OFC were respectively 43 cm (+1.5 SD), 1.342 kg (-1 SD) and 28 cm (median). Autopsy confirmed the presence of esophageal atresia, and identified left ocular involvement, hemi-uterus, and ante-positioned anus. Ocular involvement consisted of left microphthalmia with sclerocornea, retinal dysplasia and athalamia. The contralateral eye was normal, as were the cerebral structures. Weight, length and head circumference were all normal (0 SD). QMPSF analysis identified a deletion of *SOX2*. CGH array showed that the deletion size was 4.3 Mb (Sup Table 2). Parental studies showed that this deletion occurred *de novo*.

Patient 6 (*SOX2*, p. [Ala29Glyfs*66];[=])

This case has already been reported (1). She presented at birth with short palpebral fissures and closed eyelids, with no palpable eyeball. CT scan and post-mortem examination confirmed bilateral anophthalmia. She had type III esophageal atresia, and a diagnosis of AEG syndrome (Anophthalmia, Esophageal atresia, Genital abnormalities, MIM (206900) was made. *SOX2* molecular screening identified a heterozygous deletion (c.70_86del) leading to a frameshift and premature termination of translation (p.Ala29Glyfs*66). Direct sequencing of *SOX2* in the parents failed to identify this mutation. During her mother's subsequent pregnancy, an ultrasound scan examination detected severe and progressive triventricular hydrocephalus. The pregnancy was terminated in the 20th week. Autopsy of the female fetus demonstrated stenosis of the aqueduct of Sylvius, associated with hypoplasia of the corpus callosum, and identified the presence of 11 rib pairs. No other malformation was identified. External ocular examination was normal, and ocular length (10 mm) corresponded to that of age-matched fetuses. Furthermore, extensive microscopic examination ruled out any subtle anomaly of the ocular structures. Molecular analysis showed that the fetus was also bearing the c.70_86del mutation suggesting germinal mosaicism. Using semiquantitative capillary electrophoresis of fluorescent *SOX2* PCR fragments encompassing the deleted region, we were able to identify the presence of somatic mosaicism, corresponding to about 3 % of the cells, in the mother (2).

Patient 7 (*SOX2*, p.[Asn33Glyfs*66];[=])

A female foetus at 28 weeks gestation. The parents were healthy and unrelated. At 22 weeks gestation an ultrasound scan identified bilateral anophthalmia. An MRI scan at 27.5 weeks gestation confirmed the absence of the ocular globes. No cerebral abnormality was detected. The parents decided to terminate the pregnancy. Autopsy confirmed bilateral anophthalmia, with no other malformations. In particular, the neuropathology examination was normal. Measurements were within the normal range (+1 SD) for the gestational age. *SOX2* molecular screening identified a

heterozygous duplication (c.86_95dup) leading to a frameshift and premature termination of translation (p.Asn33Glyfs*66). Parental studies showed that this mutation occurred *de novo*.

Patient 8 (*SOX2*, p.[Trp51Arg];[=])

A 4 years old boy born to healthy unrelated parents. His mother had two miscarriages. He was delivered at 40 weeks gestation with normal measurements (length 51cm, weight 3.360 kg and OFC 34 cm). Right anophthalmia and left colobomatous microphthalmia were noted at birth. He had developmental delay, sat at 12 months, walked at 36 months and spoke his first words at 26 months. At age 3.5, his height was 104 cm (+1.5 SD), his weight 21 kg (+3 SD), and his head circumference 50 cm (-1 SD). He had micropenis, and hypogonadism which was treated with hormone therapy. MRI scans showed hypoplasia of the corpus callosum, and posterior pituitary agenesis. *SOX2* molecular screening led to the identification of a heterozygous missense mutation (p.Trp51Arg). Parental DNA was unavailable.

Patient 9 (*SOX2*, p.[Arg53Hisfs*37];[=])

A male foetus at 23 weeks gestation. The parents were consanguineous and healthy . At 22 weeks gestation an ultrasound scan identified bilateral anophthalmia and ventriculomegaly. The parents decided to terminate the pregnancy. Autopsy confirmed bilateral anophthalmia. Measurements were normal for the gestational age. Neuropathologic examination identifies atresia of the aqueduct of Sylvius. No other malformations were seen. This fetus had subtle dysmorphic features with mild hypertelorism and micrognathia. *SOX2* molecular screening identified a heterozygous deletion/insertion (c.158_174delinsATG) leading to a frameshift and premature termination of the translation (p.Arg53Hisfs*37). Parental studies showed that this mutation occurred *de novo*.

Patient 10 (*SOX2*, p.[His67Profs*35];[=])

A male foetus, at 24 weeks gestation. The parents were healthy and unrelated. At 22 weeks an ultrasound scan identified bilateral anophthalmia and hypotelorism. The parents decided to terminate the pregnancy. Autopsy showed bilateral extreme microphthalmia with absent lens and retinal dysplasia. Measurements were normal for the gestational age. In addition, a bifid xiphoid process was noted. *SOX2* molecular screening identified a heterozygous deletion (c.200delA) leading to a frameshift and premature termination of translation (p.His67Profs*35). Parental studies showed that this mutation occurred *de novo*.

Patient 11 (*SOX2*, p.[Arg74Pro];[=]), Fig 1C

A 37 year old woman born to unrelated parents. She had one healthy sister. Ultrasound scans demonstrated bilateral extreme microphthalmia. She was delivered at 40 weeks of gestation with normal measurements (length 49 cm, weight 3.600 kg). Bilateral extreme microphthalmia was

confirmed at birth. She had developmental delay, sat at 12 months, and walked at 24 months and spoke her first words at 26 months. She had moderate intellectual impairment. At age 37, her height was 154 cm (-1.25 SD), and her weight 65 kg (+2 SD). She had hypogonadism. Cerebral MRI scans did not identify additional abnormalites. *SOX2* molecular screening allows identification of a heterozygous missense mutation (p.Arg74Pro). Screening for this mutation in her mother was negative. Her father was deceased, and was thus not studied.

Patient 12 (*SOX2*, p.[Trp79Ser];[=])

A 17 year old man born to healthy unrelated parents. He had one healthy sister and one healthy brother. He was delivered at 36 weeks of gestation with a birth weight of 2.500 kg and length of 46 cm. Bilateral anophthalmia was noted at birth. He had developmental delay, and walked at 48 months. He had moderate intellectual impairment. At age 17 his height was 164 cm (-2 SD), his weight 52 kg (-1.75 SD), and his head circumference 53.5 cm (-2.5 SD). Cerebral MRI scan did not identify additional abnormalities. He had supernumerary teeth and cleft palate. *SOX2* molecular screening identified a heterozygous missense mutation (p.Trp79Ser). Parental studies showed that this mutation occurred *de novo*.

Patient 13 (*SOX2*, p.[Leu82Cysfs*20];[=]), Fig 1D

A 2 year old girl born to healthy unrelated parents. Ultrasound scans showed bilateral extreme microphthalmia, and left renal pelvic dilatation. She was delivered at 41 weeks gestation with normal birth weight (3.020 kg). Bilateral extreme microphthalmia in addition to the left renal pelvic dilatation was confirmed at birth. An atrial septal defect was also noted. She suffered respiratory distress of unknown cause and had sequelae of perinatal anoxia. She had developmental delay, and was unable to sit or speak at 26 months. At age 26 months, her height was 73 cm (-4 SD), her weight 9.220 kg (-2.25 SD), and her head circumference 44 cm (-3 SD). Dysmorphic traits included microstomia, retrognathia and chin chondrofibroma. *SOX2* molecular screening identified a heterozygous deletion (c.245delT) leading to a frameshift and premature termination of translation (p.Leu82Cysfs*20). Parental studies showed that this mutation occurred *de novo*.

Patient 14 (*SOX2*, p.[Thr85Thrfs*17];[=])

A 8 year old boy, born to healthy unrelated parents. He was delivered at 38 weeks of gestation weighing 2.830 kg (-1SD), with a length of 45 cm (-2 SD) and an OFC of 34 cm (median). At birth, bilateral anophthalmia was noted. He had developmental delay, sat at 24 months, and walked at 7 years. At 8 years his height was 115 cm (-3 SD), his weight 18 kg (-2.5 SD), and his head circumference 49.5 cm (-2.5 SD). He had bilateral cryptorchidism. Cerebral MRI scan revealed left cerebellar hemisphere hypoplasia, and moderately enlarged lateral ventricles. *SOX2* molecular screening identified a heterozygous deletion/insertion (c.255_256delGGinsT) leading to a frameshift

and premature termination of the translation (p.Thr85Thrfs*17). Parental studies showed that this mutation occurred *de novo*.

Patient 15 (*SOX2*, p.[Glu104*];[=])

A 11 year old boy, third son of healthy unrelated parents. At birth, he was noted to have left extreme microphthalmia and right anophthalmia associated with esophageal stenosis, and micropenis. A diagnosis of AEG syndrome was made. He had developmental delay, and at age 11 years, he was unable to walk alone or speak. He developed seizures. At age 11, his height was 127 cm (-2.5 SD), and his weight 27 kg (-1.25 SD). *SOX2* molecular screening identified a heterozygous nonsense mutation (p.Glu104*). Parental studies showed that this mutation occurred *de novo*.

Patient 16 (*SOX2*, p.[Tyr160*];[=])

A male foetus of 23.5 weeks gestational age. The parents were healthy and unrelated. At 22 weeks gestation an ultrasound scan identified bilateral anophthalmia and bilateral cleft lip and palate, and the parents decided to terminate the pregnancy. The length was 650g (+1 SD), height was 33cm (+2 SD) and OFC was 22 cm (+1 SD). Autopsy confirmed these abnormalities, and did not identify other malformations. Of note, the neuropathology examination was normal. *SOX2* molecular screening identified a heterozygous 4 nucleotides duplication (c.70_86del) leading to a frameshift and premature termination of translation (p.Ala29Glyfs*66).Parental DNA was unavailable.

Patient 17 (*SOX2*, p.[Tyr171*];[=])

A 20 year old woman born to healthy unrelated parents. She had one healthy brother. She was delivered at 39 weeks of gestation weighing 2.900 kg (-0.5 SD), with a length of 48 cm (-0.5 SD) and OFC at 32 cm (-1 SD). At birth, bilateral anophthalmia was noted. She had developmental delay, walked at 6 years and had language delay. At age 20, her height was 155 cm (-1.5 SD) with a weight of 40 kg (-2 SD). She had hypogonadism and GH deficiency. MRI scans showed hypoplasia of the vermis and corpus callosum. *SOX2* molecular screening identified a heterozygous nonsense mutation (p.Tyr171*). Parental studies showed that this mutation occurred *de novo*.

Patient 18 (*SOX2*, p.[Tyr200Serfs*2];[=]), Fig 1E

A 28 year old woman born to healthy unrelated parents. She had one healthy sister. She was delivered at 40 weeks of gestation with normal measurements (length 50 cm, weight 3.770 kg, and OFC 35.5 cm). Right microphthalmia and left anophthalmia were noted at birth. She had developmental delay, sat at 11 months walked at 30 months and spoke her first words at 3.5 years. She had severe intellectual deficiency. At age 28, her height was 158 cm (-0.75 SD), her weight 62 kg (+1.5 SD), and her OFC 55.5 cm (median). She had hypogonadism and GH deficiency. Dysmorphic traits included narrow auditory canals, upper labial frenulum, tapering fingers, pes planus. The MRI

was normal. *SOX2* molecular screening identified a heterozygous deletion (c.599delA) leading to a frameshift and premature termination of the translation (p.Tyr200Serfs*2). Parental studies showed that this mutation occurred *de novo*.

Patient 19 (*OTX2* deletion)

A male foetus at 33 weeks of gestation. The parents were healthy and unrelated. At 22 weeks of gestation an ultrasound scan identified bilateral anophthalmia and mild ventricular dilatation. An MRI scan confirmed the bilateral anophthalmia and the ventriculomegaly, and identified hypoplasia of the vermis and temporal pachygyria. The parents decided to terminate the pregnancy. Autopsy showed bilateral anophthalmia with absence of optic nerves and chisama. Histological analysis of the brain showed the presence of temporal cortical dysplasia, and vermian neuronal heterotopia. Measurements were normal for the gestational age (length 45 cm, weight 1.800 kg, and OFC 30 cm). No other abnormality was found. QMPSF analysis identified a deletion of *OTX2*. CGH array showed that the deletion size was 7.7 Mb (Sup Table 2). Parental DNA was unavailable.

Patient 20 (*OTX2* deletion)

This patient and his family have previously been reported (Patient 3, Family C, (3)). 8 patients shared the same 2.3 Mb deletion encompassing the *OTX2* gene (Sup. Table 2). There is wide intrafamilial phenotypic variability and patients have various combinations of colobomatous microphthalmia, palate anomalies, facial dysmorphism, renal malformation, microcephaly, and intellectual disability (some have low-normal intelligence), and speech problems sometimes associated with strabismus or nystagmus. One was asymptomatic (3).

Patient 21 (*OTX2*, p[.Arg97*];[=])

A male foetus at 23.5 weeks gestation. The parents were healthy and unrelated. At 22 weeks of gestation an ultrasound scan identified isolated unilateral anophthalmia. Measurements were normal for the gestational age. *OTX2* molecular screening identified a heterozygous nonsense mutation (p.Arg97*). Parental DNA was unavailable.

Patient 22 (*OTX2*, p.[Arg97*];[=])

This 31 year old woman had severe unilateral microphthalmia. Ocular involvement was isolated, without additional abnormality or intellectual impairment. Her father and her paternal grandmother were also affected by isolated unilateral microphthalmia. *OTX2* molecular screening identified a heterozygous nonsense mutation (p.Arg97*) inherited from the symptomatic father. She had two pregnancies interrupted, one in which the foetus had bilateral severe microphthalmia, and the other in which the foetus displayed otocephaly-dysgnathia complex (4). Both fetuses shared the *OTX2* p.Arg97* heterozygous mutation.

Patient 23 (*OTX2*, p.[Gln106Asnfs*11];[=]), Fig 1F-G

This patient and his family have been reported previously (Patient IV-7, Family A, (5)). In family A, 17 members displayed micro/anophthalmia segregating with autosomal dominant inheritance and sometimes associated with a variable degree of intellectual disability (moderate to severe), three patients were diagnosed as otocephalic, and one patient displayed clinical features overlapping both micro/anophthalmia and otocephaly, which we consider to be an intermediate phenotype. *OTX2* molecular screening identified a heterozygous deletion (c.316delC) leading to a frameshift and premature termination of translation (p.Gln106Asnfs*11). All affected members screened shared this mutation.

Patient 24 (*RAX*, p.[Tyr160His];[Arg188Gln]), Fig 1H

A 4 year old boy born to healthy unrelated parents. He was delivered at 40 weeks of gestation with normal measurements (length 50 cm, weight 3.060 kg, and OFC 34 cm). Bilateral extreme microphthalmia was noted at birth. He had developmental delay, sat at 8 months, and was unable to walk at 4 years. He had speech delay. At age 4, his height was 97.5 cm (-1 SD), his weight 15 kg (-0.5 SD), and his OFC 51.5 cm (+0.5 SD). *RAX* molecular screening identified two heterozygous missense mutations (p.Tyr160His and p.Arg188Gln). Parental studies confirmed the biparental transmission of the mutations.

Patient 25 (*RAX*, p.[Arg187Gln];[Arg187Gln])

A 18 month old boy born to healthy consanguineous parents. He had bilateral extreme microphthalmia. He had developmental delay, sat at 16 months, and was unable to walk at 18 months. He had severe constipation and a polyuria-polydipsia syndrome. At age 18 months, his height was 80 cm (0 SD), and his weight 12 kg (+1 SD). *RAX* molecular screening identified a homozygous missense mutation (p.Arg187Gln). Parental studies confirmed the biparental transmission of the mutations.

Patient 26 (*RAX*, p.[Ser222Argfs*62];[Tyr303*])

This patient has previously been reported (6). She is a 2 year old girl, the third child of non-consanguineous healthy parents. Delivery occurred at 41 weeks of amenorrhea with a birth weight of 3.200 kg. At birth, bilateral small palpebral features were noted without other malformation or dysmorphic features. Anophthalmia was subsequently confirmed. Psychomotor development was within the normal range with head held up at three months, sitting at ten months, walking at 1 year. Speech developed normally. Slight growth retardation was recorded at 14 months, with weight at -0.5 SD (9.020 kg), height at -1 SD (72 cm) and head circumference at -2 SD (44 cm). Orbital and

cranial MRI scan showed bilateral absence of the eyes with only fibrous tissue in the orbits. No cerebral malformation was observed. *RAX* molecular screening identified two heterozygous mutations (p.Ser222Argfs*62 and p.Tyr303*). Parental DNA was unavailable, but we were able to demonstrate that these two mutations were each located on a different allele.(6)

Patient 27 (*RAX*, p.[Ser222*];[*RAX* deletion]), Fig 1I

A female foetus at 26.5 weeks gestation. The parents were healthy and unrelated. At 22 weeks of gestation an ultrasound scan identified bilateral anophthalmia; this malformation was subsequently confirmed by MRI scan. No cerebral abnormality was detected. The parents decided to terminate the pregnancy. Autopsy confirmed bilateral anophthalmia, and did not find other malformations. In particular, the neuropathology examination was normal. Measurements were normal for the gestational age. *RAX* molecular screening identified an apparently homozygous nonsense mutation (p.Ser222*). Parental studies failed to identify the nonsense mutation. A microsatellite marker segregation study ruled out a sampling error. QMPSF analysis identified a heterozygous deletion of *RAX*. CGH array showed that the deletion size was 1.7 Mb (Sup Table 2). This deletion was inherited from the asymptomatic mother. These results demonstrated that patient 27 was compound heterozygous for a large deletion encompassing *RAX*, inherited from the mother, and a *de novo* nonsense mutation on the paternal allele.

Patient 28 (*FOXE3*, p.[Ala230Argfs*2];[Ala230Argfs*2])

A 7 year old girl born to healthy unrelated parents. She was delivered at 40 weeks gestation with normal measurements. Bilateral microphthalmia with sclerocornea was noted at birth. At age 7, her height was 36 cm (+3 SD), her weight 29 kg (+3 SD), and her OFC 52 cm (+0.5 SD). She sat at 7 months, walked at 17 months, and had severe speech delay associated with autistic features. She has one affected cousin born to consanguineous parents. *FOXE3* molecular screening identified a homozygous frameshift mutation (p.Ala230Argfs*2).

Patient 29 (*FOXE3*, p.[Cys240*];[Cys240*]), Fig 1J

A 23 year old woman born to healthy consanguineous parents. She had one affected sister and one healthy brother. She was delivered at 39 weeks gestation with a birth weight of 2.500 kg (-2 SD). At three weeks of age, her length was 47.5 cm (-2.5 SD) and her OFC 34 cm (-1.5 SD). She had bilateral microphthalmia with sclerocornea. She had normal motor development and no intellectual deficiency. At age 23, her height was 152 cm (-2 SD), her weight 69 kg (+2.5 SD), and her OFC 55.5 cm (median). She had polycystic ovarian syndrome. The MRI showed hypoplastic optic nerves and chiasma, without additional brain abnormalities. She had one affected sister aged 28 years, who had bilateral microphthalmia, seizures, autistic features, and severe intellectual deficiency. *FOXE3* molecular screening identified a homozygous mutation (p.Cys240*). DNA from the affected sister and the parents was not available.

Patient 30 (*PAX6*, p.[Arg19Pro];[=])

This family has previously been reported (7). The index case suffered from bilateral microphthalmia and sclerocornea, while her sister had a left microphthalmia and sclerocornea and right partial iris hypoplasia. Both sisters shared the same *PAX6* missense mutation (p.[Arg19Pro]).

Patient 31 (*VSX2*, p.[Gly24Glyfs*102];[Gly223Arg])

A 9 month old girl born to healthy consanguineous parents. She had isolated bilateral extreme microphthalmia without associated malformations. *VSX2* molecular screening identified two heterozygous mutations (p.Ala25Argfs*101 and p.Gly223Arg). Parental studies confirmed the biparental transmission of the mutations.

Patient 32 (*GDF6*, p.[Pro327His];[=])

A 4.5 year old boy born to healthy unrelated parents. He was delivered at 40 weeks gestation with normal measurements (length 51 cm, weight 3.910 kg, and OFC 34 cm). Unilateral colobomatous microphthalmia was noted at birth. He had normal psychomotor development: he walked at 13 months and spoke his first words at 13 months. At age 4.5, his height was 110 cm (+0.75 SD), his weight 18.5 kg (+0.5 SD), and his OFC 49.5 cm (-1.5 SD). There were no dysmorphic features. Heart, kidneys and vertebrae were normal. *GDF6* molecular screening identified a heterozygous missense mutation (p. Pro327His) inherited from his asymptomatic father.

REFERENCES

1. Menetrey C, Belin V, Odent S et al. Bilateral anophthalmia and oesophageal atresia in a newborn female: a new case of the anophthalmia-oesophageal-genital (AEG) syndrome. Clin Dysmorphol 2002: 11: 139-140.
2. Chassaing N, Gilbert-Dussardier B, Nicot F et al. Germinal mosaicism and familial recurrence of a SOX2 mutation with highly variable phenotypic expression extending from AEG syndrome to absence of ocular involvement. Am J Med Genet A 2007: 143: 289-291.
3. Delahaye A, Bitoun P, Drunat S et al. Genomic imbalances detected by array-CGH in patients with syndromal ocular developmental anomalies. Eur J Hum Genet 2012: 20: 527-533.
4. Patat O, van Ravenswaaij-Arts CMA, Tantau J et al. Otocephaly-Dysgnathia Complex: description of four cases and confirmation of the role of OTX2. Molecular Syndromology In Press.
5. Chassaing N, Sorrentino S, Davis EE et al. OTX2 mutations contribute to the otocephaly-dysgnathia complex. J Med Genet 2012: 49: 373-379.
6. Lequeux L, Rio M, Vigouroux A et al. Confirmation of RAX gene involvement in human anophthalmia. Clin Genet 2008: 74: 392-395.
7. Vincent MC, Pujo AL, Olivier D et al. Screening for PAX6 gene mutations is consistent with haploinsufficiency as the main mechanism leading to various ocular defects. Eur J Hum Genet 2003: 11: 163-169.

Supplementary Table 1: Primers used for direct sequencing and QMPSF analysis

SEQUENCING				
Gene	Exon	ForwardPrimer	ReversePrimer	Length (bp)
GDF6	1	GCCGGGCCCCGGCCGCTGTCCA	GTAGCCTCCAGCGGGAAC	574
	2a	GAAGAGCACCGGGCTGAT	GATAATCCAGTCGTCCCAGC	776
	2b	CGCCGCCCCCGGACCTGCGGAGTCT	GCAGGTAGAAGTTACTGGG	791
FOXE3	1a	TGTCCATATAAAGCGGGTCG	TCGTTGAGCGTGAGATTGTG	448
	1b	CCATCTACCGCTTCATCACC	GGGGACCTGCGAGTAGAGT	512
	1c	TCTGTTCAGCGTCGACAGC	ACAGGTCGCACAGGTGCCT	352
OTX2	1	TTTAAAAGCCTCTGCCTCG	GAACAGGGTGTTGCATCC	408
	2	GAGAGCATTGGTAGGCTCC	TCTCCACAGTCCCATACTCG	370
	3a	GAGCCATTCTTGTCCTTAAGG	GAAGCTGGTGATGCATAG	450
	3b	CCACTGTCAGATCCCTTGT	AATGCCTGGCTAAAACTGG	469
PAX6	4	GTTGGGAGTTCAGGCCTACC	GAAGTCCCAGAAAGACCAGA	164
	5	CTCTTCTTCCTCTTCACTCTG	AGAGGGCGTTGAGAGTGG	257
	6	TGAAAGTATCATCATATTTGTAG	GGAAGTGGACAGAAAACCA	200
	7	GTGGTTTTCTGTCCACTTCC	AGGAAGTGGACAGAAAACCAC	300
	8	CAGGAGACACTACCATTTGG	ATGCACATATGGAGAGCTGC	251
	9	GGGAATGTTTTGGTGAGGCT	CAAAGGGCCCTGGCTAAATT	380
	10	GTAGTTCTGGCACAATATGG	GTACTCTGTACAAGCACCTC	216
	11	CGTAGACACAGTGCTAACCTG	GCAAACAGGTTTAA	253
	12	TTAAACCTGTTTGCTCCGGG	TTATGCAGGCCACCACCAG	218
	13	GCTGTGGCTGTGTGATGTGTTCCTCA	TGCAGCCTGCAGAAAGCAGTG	237
	14	CATGTCTGTTTCTCAAAGGG	GAACAATTAACTTTTGCTGGCC	202
RAX	1	GCCTCTCCTCTCCGTCTCC	GGGCGCCCGAACGGCCTC	380
	2	GGAGTGCATCTGACCCTCC	GACACCCGTGAATTCCGAGAAGC	351
	3a	GAGCTGAACCGGCTCAGG	GGCGGTGGCGTGTAGCTG	355
	3b	GCTGGAGTCCTGGCTC	GGATCCCAAGACGTTCCCC	348
SOX2	1a	AGTCCCGGCCGGGCCGAG	GGTAGCCCAGCTGGTCCTG	565
	1b	GGCGTGAACCAGCGCATGG	TGAGCGTACCGGGTTTTCTCC	518
VSX2	1	GGCACCTGGGACCAACTTCGC	TCTGGTCCAGCAAGCGAGAG	548
	2	GTTTCGGCACAGCGGAGCGC	GACCTCAGATCCGTTGTCGGCG	255
	3	GTTCTGTCTTGTCTGAGACAGG	AACCCTGGAGTGGTAGATGTCAC	260
	4	GAAATCTTCACTCCAAGCCTACAAG	AGCCCGCTCTCCTCACCGCAG	318

	5	GGGAGTAAGGCTTTCTGCTCGTC	AGAGTCTTGGGGCTCCGGCATCTGA	480	
QMPSF					
Gene	Exon	ForwardPrimer	ReversePrimer	Length	Primer Final Concentration [µM]
OTX2	2	CGTTAGATAGGGAAGCACTGTTTGCCAAGACCC	GATAGGGTTATGCCCTACCTGCACCCTCGA	115	0.25
OTX2	3	CGTTAGATAGAGACATCTCCAGCTCGGGAAGTGAGT	GATAGGGTTACATGCAGGAAGAGGAGGTGGACAAGG	191	0.3
RAX	1	CGTTAGATAGCACCGCCGCACTCGGGAAGA	GATAGGGTTATGGCCTCGATGCTGTGAAGTCGC	206	0.2
RAX	3	CGTTAGATAGCGCCTCCGCCCTTCCTGAACTC	GATAGGGTTACTTGGCTTTCAGACGCAGCGCCGCG	180	0.25
SOX2	1	CGTTAGATAGTAGTTTGCTGCCTCTTTAAGACTAGGACTG	GATAGGGTTACGAGGAAAATCAGGCGAAGAATAATTTG	242	1.2
SOX2	1	CGTTAGATAGAGCCCATGCACCGCTACGACG	GATAGGGTTACGGACTTGACCACCGAACCCAT	174	0.25
VSX2	1	CGTTAGATAGGAACAGGGAGATGACGGGGAAAGCA	GATAGGGTTATCCTGGATGCCGAACCCAGTGCA	133	0.2
VSX2	3	CGTTAGATAGAGACAGGCTCTTTTAGTTTCTGGGGTCC	GATAGGGTTATCTTCCGGCAGCTCCGTTTTCATG	187	0.3
HFE	2	CGTTAGATAGGATCACATGGTTAAGGCCTGTTGC	GATAGGGTTATAGCCACATCTGGCTTGAAATT	233	0.4
RYR3	4	CGTTAGATAGATCCCAGACAGACAAACTTGCC	GATAGGGTTAGAGTAACGCATTCAGGGTCCTT	155	0.2

QMPSF PCR were performed in 25 µl with 0.2 mmol/L of each deoxynucleoside triphosphate, 1.5 mmol/L $MgCl_2$, 1.5 Units of DNA polymerase with its buffer (Abgene, Epson, UK), 5 % DMSO, 5mM TEAA, 100 ng of DNA, and 0.2 to 1.2 µM of each primers. After an initial step of denaturation at 95°C for 3 minutes, 25 cycles were performed consisting of denaturation at 95 °C for 15 seconds, annealing at 51°C for 20 seconds, and extension at 72°C for 20 seconds, followed by a final extension step at 72 °C for 7 minutes.

Patient	*Major gene involved*	*size (Mb)*	*ISCN description**	*DECIPHER patient*
P4	*SOX2*	0.08	3q26.33q26.33(182,877,971-182,958,506)x1	PAR256662
P3	*SOX2*	0.33	3q26.33q26.33(182,775,402-183,101,622)x1	PAR254663
P1	*SOX2*	3.8	3q26.33q27.1(180,960,157-184,754,546)x1	PAR254638
P5	*SOX2*	4.3	3q26.33q27.1(181,012,354-185,302,035)x1	PAR256663
P20	*OTX2*	2.3	14q22.2q23.1(54,277,920-56,570,089)x1	PAR256664
P19	*OTX2*	7.7	14q22.2q23.1(52,820,533-60,588,720)x1	PAR256665
P27	*RAX*	1.7	18q21.32q21.32(54,776,469-56,521,121)x1	PAR256666

ISCN, Internation System for Human Cytogenetic Nomenclature (2009); *NCBI (National Center for Biotechnology Information) build hg18

Supplementary Table 2 : Deletions characterized using array-CGH Agilent 180K

ARTICLE 2

Confirmation of *RAX* gene involvement in human anophthalmia

Clinical Genetics

2008-74(4): 392-5

L. Lequeux, M. Rio, A. Vigouroux, M. Titeux, H. Etchevers, F. Malecaze, **N. Chassaing** and P. Calvas

---

En 2004, Voronina et al. avaient identifié par une approche gène candidats le premier patient AM lié à des mutations du gène *RAX* (retina and anterior neural fold homeobox)[57].

Nous avons rapporté dans cet article le deuxième cas d'atteinte oculaire secondaire aux mutations du gène *RAX*. Il s'agissait d'une patiente atteinte d'AM (anophtalmie gauche et microphtalmie avec sclérocornée à droite) chez qui deux mutations délétères (c.664delT [p.Ser222Argfs*62] et c.909C>G [p.Tyr303*]) du gène *RAX* ont été retrouvées. Il n'a pas été possible d'étudier la ségrégation familiale de ces mutations, mais ces deux mutations étant situées dans le même exon, un clonage de cet exon nous a permis de confirmer que ces mutations étaient situées sur un allèle différent (en *trans*).

Il s'agit donc dans cet article de la confirmation de l'implication du gène *RAX* dans l'AM. Sur 7 familles avec une atteinte de ce gène décrites dans la littérature, 4 sont issues de notre cohorte (cf. Article 1).

Clin Genet 2008: 74: 392–395
Printed in Singapore. All rights reserved

CLINICAL GENETICS
doi: 10.1111/j.1399-0004.2008.01078.x

Short Report

Confirmation of *RAX* gene involvement in human anophthalmia

Lequeux L, Rio M, Vigouroux A, Titeux M, Etchevers H, Malecaze F, Chassaing N, Calvas P. Confirmation of *RAX* gene involvement in human anophthalmia.
Clin Genet 2008: 74: 392–395. © Blackwell Munksgaard, 2008

Microphthalmia and anophthalmia are at the severe end of the spectrum of abnormalities in ocular development. Mutations in several genes have been involved in syndromic and non-syndromic anophthalmia. Previously, *RAX* recessive mutations were implicated in a single patient with right anophthalmia, left microphthalmia and sclerocornea. In this study, we report the findings of novel compound heterozygous *RAX* mutations in a child with bilateral anophthalmia. Both mutations are located in exon 3. c.664delT is a frameshifting deletion predicted to introduce a premature stop codon (p.Ser222ArgfsX62), and c.909C>G is a nonsense mutation with similar consequences (p.Tyr303X). This is the second report of a patient with anophthalmia caused by *RAX* mutations. These findings confirm that *RAX* plays a major role in the early stages of eye development and is involved in human anophthalmia.

L Lequeux[a,b], M Rio[c], A Vigouroux[a,b], M Titeux[a], H Etchevers[a], F Malecaze[a,d,e], N Chassaing[a,b,d] and P Calvas[a,b,d]

[a]INSERM, U563, Centre de Physiopathologie de Toulouse Purpan, Toulouse, France, [b]CHU Toulouse, Hôpital Purpan, Service de Génétique Médicale, Toulouse, France, [c]Département de Génétique Médicale, Hôpital Necker-Enfants Malades, Paris, France, [d]Université Toulouse III Paul-Sabatier, Toulouse, France and [e]CHU Toulouse, Hôpital Purpan, Service d'Ophtalmologie, Toulouse, France

Key words: anophthalmia – microphthalmia – OAR transactivation domain – *RAX*

Corresponding author: Professor Patrick Calvas, Service de Génétique Médicale, Pavillon Lefebvre, CHU Purpan, Place du Dr Baylac, 31059 Toulouse Cedex 9, France.
Tel.: +33 5 61 77 90 79;
fax: +33 5 61 77 90 73;
e-mail: calvas.p@chu-toulouse.fr

Received 27 March 2008, revised and accepted for publication 3 July 2008

Microphthalmia and anophthalmia are at the severe end of the spectrum of abnormalities in ocular development. The combined occurrence rate for these two malformations is 1/10,000 births (1, 2). Mutations in several genes have been isolated in syndromic and non-syndromic anophthalmia. Heterozygous mutations in *SOX2* account for approximately 10% of anophthalmia (3, 4). Other genes have been identified as causing anophthalmia or extreme microphthalmia in humans (*PAX6*, *OTX2*, *CHX10*, *STRA6*, and *BMP4*) (5, 6). These latter genes are implicated in a very small proportion of affected individuals, implying wide genetic heterogeneity to match the phenotypic variability.

The *RAX* homeobox gene is essential for vertebrate eye development. *RAX* transcription begins in the anterior neural plate and then simultaneously in the eye field and in the ventral forebrain (7). Even before *PAX6*, its expression is critical to defining the eye field during early development in animal models (8). The lack of *RAX* expression hampers optic vesicle formation and leads to brain size reduction in mouse, while ectopic expression induces the appearance and proliferation of retinal pigment epithelium cells in *Xenopus* (9). The function of the *RAX* gene in eye development is yet not fully understood, but there is additional evidence from animal studies that it is involved in the proliferation of neural and retinal cells (10). In humans, the role of *RAX* in eye formation is clearly supported by the association of anophthalmia and sclerocornea in a patient bearing

a truncating mutation and a missense mutation, both located in the DNA-binding helix of the homeodomain and reducing the DNA-binding ability of the resulting protein (11). We report in this study the case of a new patient with bilateral anophthalmia associated with two distinct and novel truncating mutations of the *RAX* gene.

Patient, materials and methods

Patient

The proband, a 2-year-old girl, is the third child born to non-consanguineous, healthy Algerian parents. There was no relevant familial history of ocular malformation or remarkable disease. The pregnancy was uneventful, and the prenatal ultrasonography was not suggestive of anomaly. Delivery occurred at 41 weeks of amenorrhea without neonatal difficulties. Birth weight was 3200 g. At birth, bilateral small palpebral fissures were noted without other malformation or dysmorphic features. Anophthalmia was subsequently confirmed. Psychomotor development was within the normal range with head held up at 3 months, sitting at 10 months, and walking at 1 year. Speech developed normally. A slight growth defect was recorded at 14 months, with weight at −0.5 standard deviation (DS) (9020 g), height at −1 DS (72 cm) and head circumference at −2 DS (44 cm). Abdominal and pelvic ultrasonography detected no visceral anomalies. Orbital and cranial magnetic resonance imaging scan showed bilateral absence of eyes with only fibrous tissue in the orbits (Fig. 1). Optic nerves and chiasma were hypoplastic. Extraocular muscles appeared to be relatively preserved. The hypothalamus and pituitary gland were normal. No cerebral malformation was observed.

Molecular analysis

Parents gave their informed consent, according to French law, to participate in this study. DNA was isolated by standard procedures from peripheral white blood cells of the proband. Routine examination ruled out rearrangements or point mutations of *SOX2* and *PAX6* genes. The three *RAX* exons, with exon intron borders, were amplified by polymerase chain reaction (PCR) using previously published primers (11). PCR fragments were subsequently purified with QIAquick Gel Extraction Kit (QIAGEN SA, Courtaboeuf, France), and both strands were sequenced using Big Dye DNA sequencing kit (Applied Biosystems, Warrington, UK). Reactions were analyzed in an ABI 3100 sequencer (Applied Biosystems).

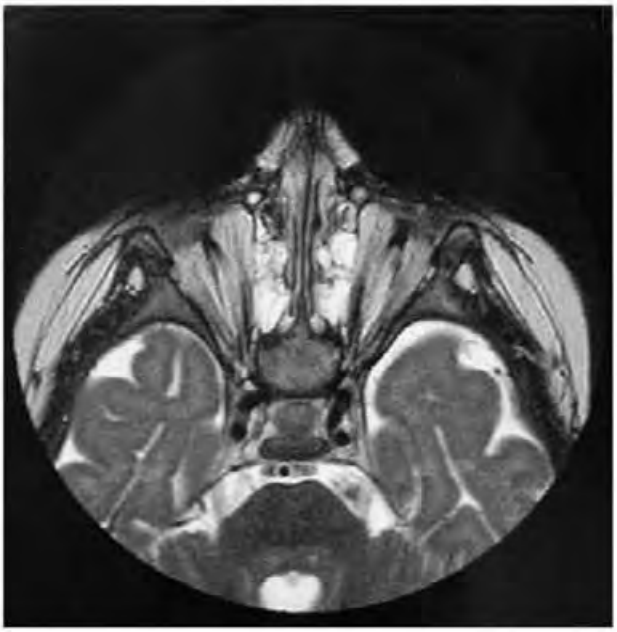

Fig. 1. Magnetic resonance imaging scan of the proband. Note absence of ocular structures replaced by fibrous tissue.

Sequence variations were numbered considering adenine of the ATG initiation codon as the first nucleotide (GenBank accession no. NM_013435.2). The changes were verified by performing independent PCR and sequencing reactions on the proband's DNA.

Exon 3 of the *RAX* gene was PCR amplified from the patient's DNA as above (11). The resulting 602-bp fragments were cloned into the pGEM-T vector (Promega, Charbonnières, France). JM109 competent cells were transformed and grown on Luria-Bertani agar plates. DNAs from 10 expanded LacZ-deficient clones were extracted using Promega Wizard miniprep purification system. Further sequencing was performed using the ABI-Big Dye terminator 3.1 on an ABI 3100 sequencer (Applied Biosystems).

Results

Sequence analysis of the proband's DNA revealed two novel mutations, both located in exon 3 of the *RAX* gene. c.664delT frameshifting deletion generates a premature stop codon (p.Ser222-ArgfsX62). c.909C>G is a nonsense mutation changing a tyrosine at position 303 to a stop codon (p.Tyr303X). These mutations were not found in a panel of 96 control chromosomes. Both are predicted to lead to a truncated protein so that, if not submitted to nonsense-mediated mRNA decay, the predicted RAX proteins lack the putative otp, aristaless, rax (OAR) transactivation domain and are non-functional (7).

As this family left the country, DNA from the proband's parents was unavailable, and thus, segregation analysis of these two mutations was impossible. Nevertheless, the c.664delT and the c.909C>G mutations were shown to lie in *trans* after sequencing of the cloned products of the patient's *RAX* exon 3 (Fig. 2).

Discussion

This is the second report of human anophthalmia-associated mutations of the *RAX* homeobox gene (11). While the parents were not carefully examined, they did not complain of any visual impairment at the time their child was evaluated. The proband was demonstrated to bear composite heterozygous mutations on both alleles of the *RAX* gene. The parents are thus likely to each be healthy carriers of a heterozygous mutation, unless one of these mutations appeared *de novo*. This would confirm the recessive inheritance of *RAX* mutations in ocular dysgenesis.

The phenotype, reported in this study, consisting in bilateral and symmetric anophthalmia is more severe than the one previously described. This first patient had right anophthalmia and left microphthalmia and sclerocornea (11). One of the causative mutations (p.Gln147X) induced, as predicted for the two mutations reported in this study, a truncation of the protein. The other was a missense p.Arg192Gln, with a milder effect on the protein, which conserved a low activity. This could suggest that the observed phenotypic variability be correlated with the mutation severity. However, definite conclusions cannot be drawn in view of the limited number of observations.

In animal models, all truncating mutations have been reported to have severe effects and lead to the absence of eye development (9, 12, 13). In contrast, antisense or morpholino inhibition in *Xenopus* acts in a dose-dependant manner, leading to graduated phenotypes ranging from eye reduction to anophthalmia (14). In this report, the location of the mutations in the last exon makes nonsense-mediated mRNA decay unlikely (15). This is in accordance with the observation that, in the cellular model used by Voronina et al (11), the more proximal p.Gln147X mutation allowed translation of a large amount of protein. These facts suggest that the two mutations we report in this study lead to truncated proteins, both lacking the C-terminal part containing the critical OAR functional domain (7). Absence of RAX C-terminus is known to abolish its proliferative effect in *Xenopus* (14). Furthermore, regulation of transcriptional activity of several other homeobox genes by the OAR domain has been suggested in other studies (7, 16, 17). Thus, p.Ser222ArgfsX62 and p.Tyr303X are thought to drastically impair RAX target genes expression. The precise delineation of the mechanistic effects of these mutations must therefore await binding studies, and an important goal for future research will be the identification of the putative genes that can modulate *RAX* activity through direct interaction.

To date, no cerebral malformation has been associated with *RAX* mutations in man. This is

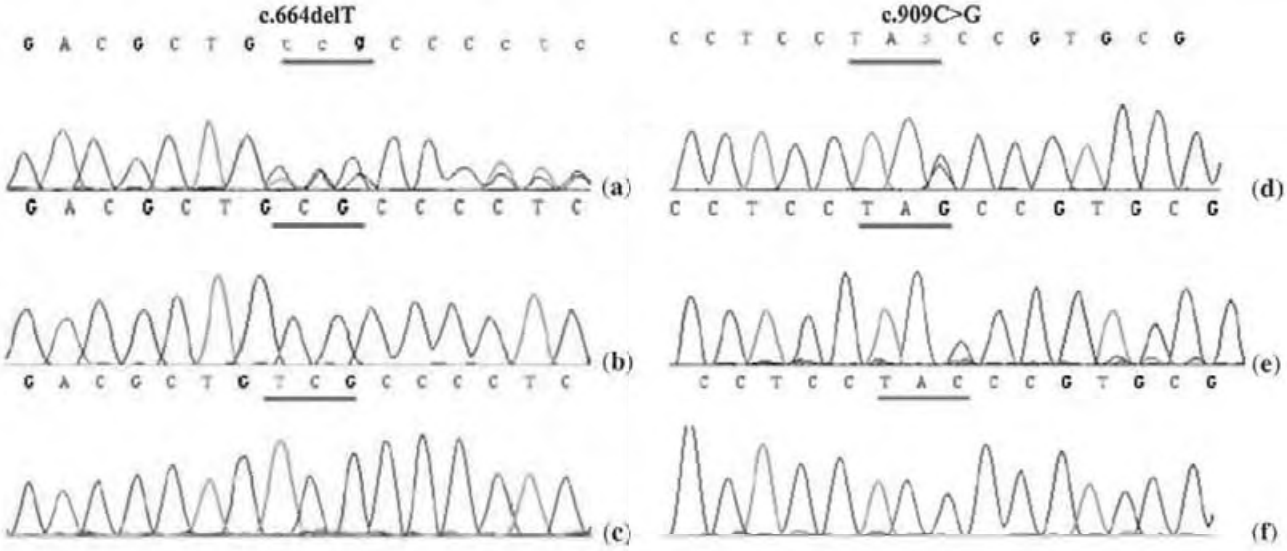

Fig. 2. Electropherograms showing the two mutations on *RAX* exon 3 (a and d) in comparison with wild-type sequence (c and f). Sequencing of cloned patient's exon 3 amplimers in a pGEM-T vector (b and e) demonstrated that mutations were not located on the same alleles. Mutated codons are underlined.

surprising in the light of the observations in insect, batracian, fish and rodent models, where *RAX* consistently participates in brain development and homozygous null alleles cause severe cerebral malformations (9, 14, 18, 19). A similar situation is seen, however, with respect to the Hesx1 homeobox-containing transcription factor, which in mice has a similar early role and an overlapping domain to that of *Rax* but is downstream of *Pax6* and *Otx2* (20) and *Rax* itself (21). While *Hesx1* mouse mutants can demonstrate anophthalmia in addition to cerebral anomalies, human patients have either isolated pituitary malformations or septo-ocular dysplasia, with no further retinal involvement (22). In a complementary fashion and unlike *SOX2* or *OTX2* mutations, no extra-ocular malformations have been observed in *RAX* ocular dysgenesis patients. The patient reported previously by Voronina et al. (11) was diagnosed as autistic. The patient reported in this study seems to have normal psychomotor development, although she is too young to exclude the possibility of developmental delay and/or autistic features. Thus, *RAX* phenotypic spectrum is still unclear, and due to the limited number of cases reported so far, the existence of *RAX* involvement in syndromic forms of anophthalmia cannot be excluded.

Acknowledgements

The authors are grateful to Dr Iba Zizen for providing magnetic resonance imaging scan pictures.

References

1. Morrison D, FitzPatrick D, Hanson I et al. National study of microphthalmia, anophthalmia, and coloboma (MAC) in Scotland: investigation of genetic aetiology. J Med Genet 2002; 39: 16–22.
2. Lowry RB, Kohut R, Sibbald B et al. Anophthalmia and microphthalmia in the Alberta Congenital Anomalies Surveillance System. Can J Ophthalmol 2005; 40: 38–44.
3. Fantes J, Ragge NK, Lynch SA et al. Mutations in SOX2 cause anophthalmia. Nat Genet 2003; 33: 461–463.
4. Ragge NK, Lorenz B, Schneider A et al. SOX2 anophthalmia syndrome. Am J Med Genet A 2005; 135: 1–7; discussion 8.
5. Bakrania P, Efthymiou M, Klein JC et al. Mutations in BMP4 cause eye, brain, and digit developmental anomalies: overlap between the BMP4 and hedgehog signaling pathways. Am J Hum Genet 2008; 82: 304–319.
6. Verma AS, Fitzpatrick DR. Anophthalmia and microphthalmia. Orphanet J Rare Dis 2007; 2: 47.
7. Furukawa T, Kozak CA, Cepko CL. rax, a novel paired-type homeobox gene, shows expression in the anterior neural fold and developing retina. Proc Natl Acad Sci U S A 1997; 94: 3088–3093.
8. Zhang L, Mathers PH, Jamrich M. Function of Rx, but not Pax6, is essential for the formation of retinal progenitor cells in mice. Genesis 2000; 28: 135–142.
9. Mathers PH, Grinberg A, Mahon KA et al. The Rx homeobox gene is essential for vertebrate eye development. Nature 1997; 387: 603–607.
10. Bailey TJ, El-Hodiri H, Zhang L et al. Regulation of vertebrate eye development by Rx genes. Int J Dev Biol 2004; 48: 761–770.
11. Voronina VA, Kozhemyakina EA, O'Kernick CM et al. Mutations in the human RAX homeobox gene in a patient with anophthalmia and sclerocornea. Hum Mol Genet 2004; 13: 315–322.
12. Tucker P, Laemle L, Munson A et al. The eyeless mouse mutation (ey1) removes an alternative start codon from the Rx/rax homeobox gene. Genesis 2001; 31: 43–53.
13. Loosli F, Staub W, Finger-Baier KC et al. Loss of eyes in zebrafish caused by mutation of chokh/rx3. EMBO Rep 2003; 4: 894–899.
14. Andreazzoli M, Gestri G, Angeloni D et al. Role of Xrx1 in Xenopus eye and anterior brain development. Development 1999; 126: 2451–2460.
15. Harries LW, Bingham C, Bellanne-Chantelot C et al. The position of premature termination codons in the hepatocyte nuclear factor-1 beta gene determines susceptibility to nonsense-mediated decay. Hum Genet 2005; 118: 214–224.
16. Amendt BA, Sutherland LB, Russo AF. Multifunctional role of the Pitx2 homeodomain protein C-terminal tail. Mol Cell Biol 1999; 19: 7001–7010.
17. Norris RA, Kern MJ. Identification of domains mediating transcription activation, repression, and inhibition in the paired-related homeobox protein, Prx2 (S8). DNA Cell Biol 2001; 20: 89–99.
18. Eggert T, Hauck B, Hildebrandt N et al. Isolation of a Drosophila homolog of the vertebrate homeobox gene Rx and its possible role in brain and eye development. Proc Natl Acad Sci U S A 1998; 95: 2343–2348.
19. Andreazzoli M, Gestri G, Cremisi F et al. Xrx1 controls proliferation and neurogenesis in Xenopus anterior neural plate. Development 2003; 130: 5143–5154.
20. Spieler D, Baumer N, Stebler J et al. Involvement of Pax6 and Otx2 in the forebrain-specific regulation of the vertebrate homeobox gene ANF/Hesx1. Dev Biol 2004; 269: 567–579.
21. Martinez-Barbera JP, Rodriguez TA, Beddington RS. The homeobox gene Hesx1 is required in the anterior neural ectoderm for normal forebrain formation. Dev Biol 2000; 223: 422–430.
22. Dattani MT, Martinez-Barbera JP, Thomas PQ et al. Mutations in the homeobox gene HESX1/Hesx1 associated with septo-optic dysplasia in human and mouse. Nat Genet 1998; 19: 125–133.

ARTICLE 3

Novel *B3GALTL* mutation in Peters-plus Syndrome

Clinical Genetics

2009-76(5): 490-2

Dassie-Ajdid, J., A. Causse, A. Poidvin, M. Granier, J. Kaplan, L. Burglen, D. Doummar, P. Teisseire, A. Vigouroux, F. Malecaze, P. Calvas and **N. Chassaing**

L'anomalie de Peters est une anomalie du développement embryonnaire du segment antérieur de l'œil liée à une absence de développement de la membrane de Descemet et de l'endothélium au centre de la cornée. Elle se caractérise par une opacité cornéenne centrale ou complète, des synéchies irido-cornéenne (adhérences de l'iris et de la cornée), et un glaucome. Cette anomalie oculaire peut être isolée ou être intégré dans des formes syndromiques. Le syndrome de Peters-plus associe à l'anomalie de Peters un retard statural, une brachydactylie, et de façon moins constante, une déficience intellectuelle, une cardiopathie, une fente labiale ou labio-palatine, des anomalies génitales et quelques critères faciaux mineurs. Des mutations du gène *B3GALTL* (β1, 3-galactosyltransferase-like) sont identifiées dans chez des patients avec syndrome de Peters-plus "classique" (associant les signes cardinaux du syndrome [anomalie de la chambre antérieure, retard statural, brachydactylie]) et ne sont pas retrouvées dans les formes incomplètes.

La première description de mutations de ce gène date de 2006 sur un modèle monogénique avec homogénéité allélique[164]. Nous avions dans notre étude inclus quatre patients : deux avec un syndrome de Peters-plus "classique" et deux avec une atteinte atypique. Nous avons retrouvés des mutations chez les deux patients "classiques" et non dans les formes atypiques, comme précédemment rapporté. Nous avons démontré une hétérogénéité allélique plus importante que décrite initialement et rapporté la première mutation faux-sens délétère du gène *B3GALTL*.

Clin Genet 2009: 76: 490–492
Printed in Singapore. All rights reserved

CLINICAL GENETICS
doi: 10.1111/j.1399-0004.2009.01253.x

Letter to the Editor

Novel *B3GALTL* mutation in Peters-plus Syndrome

To the Editor:

Peters-plus syndrome (MIM#261540) is a rare autosomal recessive genetic disorder including ocular features, systemic malformations, and variable degree of developmental delay. Ocular malformations concern the anterior chamber (98% of patients) and are mainly represented by Peters' anomaly (73%) (1), which corresponds to corneal clouding and variable degrees of iridolenticulocorneal adhesions. Other features include short stature, broad extremities, cleft lip/palate, cardiac and genito-urinary malformations (1, 2). There is also a common facial dysmorphism comprising a round face, broad neck, thin and cupid bow upper lip, long philtrum, hypertelorism, short palpebral fissures, variable external ear anomalies and prominent forehead (1).

In 2006, Lesnik Oberstein et al. identified the β1, 3-galactosyltransferase-like gene (*B3GALTL*) as the gene involved in Peters-plus syndrome (3). They found three different *B3GALTL* mutations with one, c.660+1G>A, representing 90% of the mutated alleles. These authors concluded that Peters-plus syndrome was thus a monogenic, primarily single-mutation syndrome. Reis et al. confirmed the role of *B3GALTL* in Peters-plus syndrome and identified two new mutations bringing the number of reported *B3GALTL* mutations to five (2). Further studies clearly established that *B3GALTL* mutations lead to a congenital disorder of glycosylation (4, 5).

In this study, we screened two additional patients (patients 1 and 2) with clinically defined Peters-plus syndrome for *B3GALTL* mutation. Their clinical features are summarized in Table 1, and craniofacial and extremities findings are illustrated in Fig. 1. We also included two patients with Peters' anomaly and psychomotor delay but who did not meet other Peters-plus syndrome criteria.

Two *B3GALTL* mutations were identified in the typical Peters-plus patients. Patient 1, originating from Sri Lanka, was compound heterozygous for the recurrent c.660+1G>A mutation and a novel missense mutation c.1178G>A (p.Gly393Glu) in exon 13 (Fig. 2a). This mutation was absent from a panel of 100 chromosomes from Caucasian controls, and predicted *in silico* to be probably damaging by Polyphen software (http://genetics.bwh.harvard.edu/pph/). This substituted glycine, located in the putative catalytic domain, has been shown to be one of the 12 most conserved amino acids during evolution of this protein orthologues (Fig. 2b), and to be located in one of the five most conserved functional domains of the enzyme (6). This is the first *B3GALTL* missense mutation to be involved in Peters-plus syndrome. Patient 2 was homozygous for the recently published c.459 + 1G>A splice site mutation. Parents of patients 1 and 2 were each shown to be heterozygous for one of the two mutations identified in their child. No causative mutations in *B3GALTL* were identified in patients who had Peters' anomaly and psychomotor delay but without additional features of Peters-plus syndrome, confirming previous published data (2).

Clinical presentation of patients published to date with *B3GALTL* mutations is summarized in Table 1. This table clearly shows that the major criteria of the Peters-plus syndrome, essentially always present, are anterior chamber anomalies (mainly Peters' anomaly), growth retardation, and brachydactyly. Developmental delay is frequent, whereas cleft lip and/or palate, cardiac malformation, and external ear anomalies are observed in about half of the patients. Thus, although different *B3GALTL* mutations lead to Peters-plus syndrome, the clinical presentation seems to be uniform. No *B3GALTL* mutation was found in patients with an incomplete phenotype ((2), this report). Other glycosyltransferases or proteins modified by B3GALTL may be involved in these isolated or syndromic Peters' anomalies, in which the patients do not fulfill all criteria for Peters-plus syndrome diagnosis.

In conclusion, these results confirm the implication of *B3GALTL* in Peters-plus syndrome and support clinical homogeneity in patients with *B3GALTL* mutations. Furthermore, this is the first report of a *B3GALTL* missense deleterious mutation, showing that allelic heterogeneity is wider than initially described.

Fig. 1. Clinical presentation of patients 1 (a–c) and 2 (d and e). Similar features are visible in both, including corneal clouding, prominent forehead, macrostomia with cupid bow-shaped upper lip, and broad extremities.

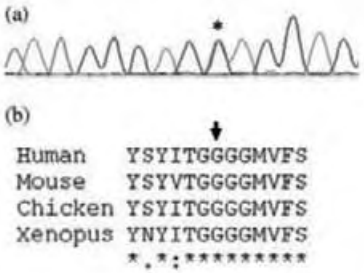

Fig. 2. Electropherogram showing the c.1178G>A (p.Gly393Glu) indicated by a star (a). Alignment of part of B3GALTL proteins from human, mouse, chicken and Xenopus, showing conservation of glycine 393 (arrow) in these species (b).

J Dassie-Ajdid[a,b,c*]
A Causse[a,b,c*]
A Poidvin[d]
M Granier[d]
J Kaplan[e]
L Burglen[f]
D Doummar[g]
P Teisseire[a,b,c]
A Vigouroux[a,b]
F Malecaze[a,c,h]
P Calvas[a,b,h]
N Chassaing[a,b,h]

[a]INSERM, U563, Centre de Physiopathologie de Toulouse Purpan, Toulouse, [b]CHU Toulouse, Hôpital Purpan, *Service* de Génétique Médicale, Toulouse, [c]CHU Toulouse, Hôpital Purpan, *Service* d'Ophtalmologie, Toulouse, [d]Service de Médecine Néonatale, CH Sud Francilien, Evry, [e]Département de Génétique, Hôpital Necker-Enfants Malades, Paris, [f]Service de Génétique Médicale, Hôpital Trousseau, APHP, Paris, [g]Service de Neuropédiatrie, Hôpital Trousseau, APHP, Paris, and [h]Université Toulouse III Paul-Sabatier, Toulouse, France.

*The authors J. D-A. and A. C. contributed equally to this article

Table 1. Clinical features of patients with Peters-plus syndrome

	Identified *B3GALTL* mutation	Peters' anomaly	Anterior chamber anomaly	Short stature	Brachydactyly	Developmental delay	Cleft lip/palate	Heart anomaly	Genito Urinary (GU) anomaly	Ear anomaly
This report Patient 1	Yes	+	+	+	+	+	−	+	−	−
This report Patient 2	Yes	+	+	+	+	+	−	+	−	−
Lesnik Oberstein et al. (3)	Yes	15/19	20/20	20/20	NR	15/19	9/20	5/19	5/20	NR
Reis et al. (2)	Yes	4/4	4/4	4/4	4/4	4/4	4/4	3/4	2/4	3/4
Maillette de Buy Wenniger-Prick et al. (1)	No	36/49	48/49	45/49	49/49	41/49	38/49	15/49	9/49	39/49
Total number of patients with *B3GALTL* mutations (%)		21/25 (84)	26/26 (100)	26/26 (100)	6/6 (100)	21/25 (84)	13/26 (50)	10/25 (40)	7/26 (27)	3/6 (50)
Total patients (%)		67/75 (91)	74/75 (99)	71/75 (95)	55/55 (100)	62/74 (84)	51/75 (68)	25/74 (34)	16/75 (21)	42/55 (76)

Review of frequency of main Peters-plus syndrome features in either patients with identified *B3GALTL* mutations, compared with a major series of clinically diagnosed patients with Peters-plus syndrome previously reported without molecular data (1).
+, presence; −, absence; NR, not reported.

References

1. Maillette de Buy Wenniger-Prick LJ, Hennekam RC. The Peters' plus syndrome: a review. Ann Genet 2002: 45: 97–103.
2. Reis LM, Tyler RC, Abdul-Rahman O et al. Mutation analysis of B3GALTL in Peters Plus syndrome. Am J Med Genet A 2008: 146A: 2603–2610.
3. Lesnik Oberstein SA, Kriek M, White SJ et al. Peters Plus syndrome is caused by mutations in B3GALTL, a putative glycosyltransferase. Am J Hum Genet 2006: 79: 562–566.
4. Heinonen TY, Maki M. Peters'-plus syndrome is a congenital disorder of glycosylation caused by a defect in the beta1,3-glucosyltransferase that modifies thrombospondin type 1 repeats. Ann Med 2009: 41: 2–10.
5. Hess D, Keusch JJ, Oberstein SA et al. Peters Plus syndrome is a new congenital disorder of glycosylation and involves defective *O-glycosylation* of thrombospondin type 1 repeats. J Biol Chem 2008: 283: 7354–7360.
6. Heinonen TY, Pasternack L, Lindfors K et al. A novel human glycosyltransferase: primary structure and characterization of the gene and transcripts. Biochem Biophys Res Commun 2003: 309: 166–174.

Correspondence:
Dr Nicolas Chassaing
Service de Génétique Médicale
Pavillon Lefebvre
CHU Purpan
Place du Dr Baylac
31059 Toulouse Cedex 9
France.
Tel.: +33 5 61 77 90 55
fax: +33 5 62 74 45 58
e-mail: chassaing.n@chu-toulouse.fr

CHAPITRE III

ANALYSE DES PHENOTYPES

Introduction

Comme nous l'avons vu dans le chapitre précédent, la variabilité phénotypique chez les patients porteurs de mutations dans les gènes d'AM est très importante. Cette variabilité s'exprime en inter- et en intra- familial, mais de façon très intéressante, également en intra-individuelle. En effet l'atteinte oculaire peut être très variable et très asymétrique d'un œil à l'autre chez un même patient. Ainsi, certains patients de notre cohorte, porteurs de mutations d'un gène du développement oculaire, présentent des atteintes (parfois sévères à type d'anophtalmie) strictement unilatérale. La variabilité clinique s'exprime au niveau oculaire et également au niveau extra-oculaire, les mêmes gènes pouvant être à l'origine d'AM isolées ou d'AM syndromiques. Les observations restent, à ce jour, trop peu nombreuses pour conclure quant aux proportions relatives des atteintes isolées ou syndromiques liées aux mutations d'un même gène.

Au cours de mon travail de thèse, j'ai pu m'intéresser plus particulièrement à la variabilité phénotypique de deux gènes :

- le premier *OTX2* était connu comme un gène d'AM "isolées" à pénétrance incomplète et expressivité variable. Nous avons pu montrer que ce gène était également impliqué dans une forme syndromique d'anomalie du développement de la mandibule, le syndrome agnathie-otocéphalie.
- les mutations du deuxième gène, *STRA6*, ont été décrites comme causales du syndrome de Matthew-Wood également décrit par l'acronyme PDAC pour résumer les principales malformations du syndrome (Pulmonary, Diaphragmatic, Anophthalmia, Cardiac). Nous avons pu montrer que le spectre phénotypique des mutations de ce gène pouvait s'étendre à des AM "isolées".

Dans ces deux exemples, les informations décrites ont été observées chez des patients (et leurs apparentés) dont les prélèvements avaient été analysés dans un cadre diagnostic de leur AM. A partir des informations observées pour ces familles, des projets spécifiques ont été élaborés pour confirmer nos hypothèses.

III-1 : Analyse des phénotypes liés aux mutations du gène *OTX2*

Introduction

L'agnathie correspond à l'absence de développement embryonnaire de la mandibule, la dysgnathie à un développement anormal de celle-ci. L'otocéphalie est définie par une agnathie associée à une fusion des oreilles sur la face antérieure du cou (synotie). Différentes malformations, et plus particulièrement des holoprosencéphalies, peuvent être associées à l'otocéphalie. Plusieurs modèles murins ont été décrits avec une agnathie, notamment ceux liés à des mutations des gènes *Pgap1*, *Twsg1* et *Otx2*[152, 165, 166]. Chez l'homme, des mutations du gène *PRRX1* ont été retrouvées chez quelques patients otocéphales[167].

Méthodes et Résultats

Nous avons émis l'hypothèse de l'implication du gène *OTX2* dans l'otocéphalie à partie d'une grande famille de patients souffrant d'AM transmise selon un mode autosomique dominant sur 4 générations (17 membres atteints). Dans cette famille, deux cousins atteints d'AM ont eu un enfant atteint d'otocéphalie. L'identification dans cette famille d'une mutation du gène *OTX2* (c.316delC), associée aux données connues sur le modèle murin *Otx2*$^{+/-}$, a suggéré le rôle des mutations de ce gène dans l'otocéphalie. Pour confirmer cette hypothèse, nous avons recruté dix cas sporadiques atteints d'otocéphalie lors d'une première étude. Des analyses fonctionnelles réalisées sur un modèle de poisson zèbre ont permis d'étayer les hypothèses émises à partir des résultats chez les patients et de démontrer le rôle probable de facteurs modulateurs d'origine génétique. En effet, l'inactivation conjointe chez le poisson zèbre d'*otx2* et d'autres gènes du développement mandibulaire potentialisait le phénotype mandibulaire.

Dans une seconde phase de ce travail, nous avons décrit quatre patients otocéphales supplémentaires dont deux étaient porteurs d'une mutation délétère du gène *OTX2*. Une de ces mutations a été retrouvée chez un fœtus otocéphale, issue d'une famille ou se transmettait une microphtalmie unilatérale sur 3 générations. Une délétion *de novo* du gène *OTX2* a également été identifiée chez un enfant décédé à la naissance, et atteint d'otocéphalie.

Les résultats de ces travaux sont décrits dans les 2 articles suivants:

- Article n°4

Chassaing, N *et al*. (2012). "*OTX2* mutations contribute to the otocephaly-dysgnathia complex." J Med Genet 49(6): 373-9.

- Article n°5

Patat et al. (2013) "Otocephaly-Dysgnathia Complex: description of four cases and confirmation of the role of OTX2." Molecular Syndromology 4: 302–305

Figure supplémentaire

Une figure supplémentaire, non présentée dans l'article n°4 a été rajoutée à sa suite. Cette figure montre le résultat de l'analyse du niveau d'expression des gènes impliqués dans les modèles humains ou animaux d'otocéphalie après transfection par une vecteur d'expression d'*OTX2* sauvage ou porteur des mutations identifiées dans les deux familles décrites dans l'article 4.

- Figure 25 : Analyse d'expression des gènes impliqués dans l'otocéphalie chez l'homme et/ou la souris après transfection par un vecteur exprimant *OTX2* normal ou muté

Conclusion

Nous avons pu montrer que des mutations du gène *OTX2* initialement décrites dans les AM "isolées" étaient impliquées dans l'otocéphalie, une anomalie majeure du développement mandibulaire. Nous n'avons pas pu dans les familles mutées identifier les facteurs expliquant la variabilité d'expression intrafamiliale, même si les expériences sur le modèle du zebrafish orientent vers la possibilité d'implication de gènes modificateurs. Une hétérogénéité génétique a été montrée dans l'otocéphalie puisque des mutations du gène *PRRX1* ont également été décrites chez l'homme. D'autres gènes sont probablement impliqués et les mutations des gènes *PRRX1* et *OTX2* ne sont retrouvées que chez une minorité de patients.

ARTICLE 4

***OTX2* mutations contribute to the otocephaly-dysgnathia complex**

Journal of Medical Genetics

2012-49(6): 373-9

N. Chassaing*, S. Sorrentino*, E. E. Davis, D. Martin-Coignard, A. Iacovelli, W. Paznekas, B. D. Webb, O. Faye-Petersen, F. Encha-Razavi, L. Lequeux, A. Vigouroux, A. Yesilyurt, S. A. Boyadjiev, H. Kayserili, P. Loget, D. Carles, C. Sergi, S. Puvabanditsin, C. P. Chen, H. C. Etchevers, N. Katsanis, C. L. Mercer, P. Calvas and E. W. Jabs

---

Nous avons identifié la mutation c.316delC du gène *OTX2* dans une famille ou une AM était transmise sur un mode autosomique dominant sur 4 générations avec une expressivité variable. Deux cousins atteints ont eu des enfants atteints d'otocéphalie suggérant un rôle potentiel d'*OTX2* dans le développement mandibulaire. Dans cette famille, on retrouvait de plus deux patients associant une atteinte oculaire et mandibulaire. Pour démontrer le rôle d'*OTX2* dans le développement de la mâchoire inférieure, nous avons recruté 10 patients otocéphales supplémentaires et recherché des mutations de ce gène. Nous avons pu identifier chez deux d'entre une mutation délétère décalant le cadre de lecture. Pour l'un des patients, la mutation frameshift était héritée d'une mère microphtalme. Cette famille n'a pas souhaité que les données les concernant soient publiées. Pour l'autre patiente, la mutation c.130delC a été identifiée à l'état hétérozygote. L'analyse des parents a montré que cette mutation était apparue *de novo*, apportant un argument fort pour confirmer notre hypothèse. Nous avons réalisé des analyses fonctionnelles des mutations identifiées dans ces deux familles (c.130delC et c.316delC) pour confirmer leur effet délétère : nous avons montré que l'expression d'*OTX2* entrainait une surexpression du gène *MSX1*, surexpression qui disparaissait lors de la transfection de des vecteurs d'expression *OTX2* mutés (Fig. 25). De plus des analyses ont été réalisées en collaboration avec l'équipe du Pr Katsanis et du Dr

Davis (Duke University, Durham NC, USA) pour confirmer le rôle d'*otx2* dans le développement mandibulaire sur un modèle de poisson zèbre. De manière intéressante, nous avons pu montrer qu'otx2 pouvait interagir avec les autres protéines précédemment impliquées chez l'homme ou la souris dans l'otocéphalie (msx1, pgap1 et prrx1) et que l'inactivation simultanée d'un de ces gènes potentialisait l'effet malformatif observé lors de l'inactivation du gène *otx2*. Nous avons recherché dans ces gènes candidats pour être potentiellement des gènes modificateurs du phénotype mandibulaire des mutations qui auraient pu expliquer la variabilité d'expression intrafamiliale observée pour les mutations d'*OTX2*.

JMG Online First, published on May 10, 2012 as 10.1136/jmedgenet-2012-100892

ORIGINAL ARTICLE

OTX2 mutations contribute to the otocephaly-dysgnathia complex

Nicolas Chassaing,[1,2,3] Susanna Sorrentino,[4] Erica E Davis,[5,6,7] Dominique Martin-Coignard,[8] Anthony Iacovelli,[4] William Paznekas,[4] Bryn D Webb,[4,9] Ona Faye-Petersen,[10] Férechté Encha-Razavi,[11] Leopoldine Lequeux,[12] Adeline Vigouroux,[1] Ahmet Yesilyurt,[13] Simeon A Boyadjiev,[14] Hülya Kayserili,[15] Philippe Loget,[16] Dominique Carles,[17] Consolato Sergi,[18,19] Surasak Puvabanditsin,[20] Chih-Ping Chen,[21,22,23] Heather C Etchevers,[2,24] Nicholas Katsanis,[5,6,7] Catherine L Mercer,[25] Patrick Calvas,[1,2,3] Ethylin Wang Jabs[4,9,26]

► Additional materials are published online only. To view these files please visit the journal online (http://jmg.bmj.com/content/early/recent).

For numbered affiliations see end of article.

Correspondence to
Dr Nicolas Chassaing, Service de Génétique Médicale, Pavillon Lefebvre, CHU Purpan, Place du Dr Baylac, Toulouse 31059, Cedex 9, France; chassaing.n@chu-toulouse.fr

NC, SS contributed equally to this work.

Received 14 March 2012
Accepted 11 April 2012

ABSTRACT

Background Otocephaly or dysgnathia complex is characterised by mandibular hypoplasia/agenesis, ear anomalies, microstomia, and microglossia; the molecular basis of this developmental defect is largely unknown in humans.

Methods and results This study reports a large family in which two cousins with micro/anophthalmia each gave birth to at least one child with otocephaly, suggesting a genetic relationship between anophthalmia and otocephaly. *OTX2*, a known microphthalmia locus, was screened in this family and a frameshifting mutation was found. The study subsequently identified in one unrelated otocephalic patient a sporadic *OTX2* mutation. Because *OTX2* mutations may not be sufficient to cause otocephaly, the study assayed the potential of *otx2* to modify craniofacial phenotypes in the context of known otocephaly gene suppression in vivo. It was found that *otx2* can interact genetically with *pgap1*, *prrx1*, and *msx1* to exacerbate mandibular and midline defects during zebrafish development. However, sequencing of these loci in the OTX2-positive families did not unearth likely pathogenic lesions, suggesting further genetic heterogeneity and complexity.

Conclusion Identification of *OTX2* involvement in otocephaly/dysgnathia in humans, even if loss of function mutations at this locus does not sufficiently explain the complex anatomical defects of these patients, suggests the requirement for a second genetic hit. Consistent with this notion, *trans* suppression of *otx2* and other developmentally related genes recapitulate aspects of the otocephaly phenotype in zebrafish. This study highlights the combined utility of genetics and functional approaches to dissect both the regulatory pathways that govern craniofacial development and the genetics of this disease group.

INTRODUCTION

Otocephaly-dysgnathia (also known as otocephaly, agnathia-holoprosencephaly, dysgnathia complex) (OMIM #202650) is characterised by mandibular hypoplasia or agenesis, ventromedial auricular malposition (melotia or synotia), microstomia, and oroglossal hypoplasia or aglossia. The mesenchyme-forming neural crest is affected, resulting in abnormal derivatives of the caudal portion of the first branchial arch.[1] Additional malformations can be associated with this condition, including, but not limited to, failure of development of the prosencephalon, resulting in midline defects as severe as alobar hemispheres or cyclopia, anophthalmia, microphthalmia, pituitary hypoplasia, situs inversus, pulmonary hypoplasia, and limb malformations.

Fewer than 150 cases have been documented, with an incidence estimated to be 1 per 70 000 births.[2] Two families have been reported with more than one affected member.[3 4] In one example of a genomic rearrangement, Pauli *et al* reported two stillborn female infants with agnathia-holoprosencephaly who harboured an unbalanced 46,XX, der18,t(6;18) (pter->p24.1 or p24.2::p11.21->qter) translocation from a parent with a balanced translocation t(6;18) (p24.1 or p24.2; p11.21).[5] Karyotypes of other cases of otocephaly described in the literature have been normal, suggesting that most causative lesions are either point mutations or copy number variants that fall below detectable thresholds for karyotype or microarray. Environmental causes such as exposure to salicylates have also been suspected contributors.[6]

Forward genetic screens in murine models have identified numerous genes involved in otocephaly. The first otocephaly locus was identified in a screen for lethal mutations on chromosome 1,[7] and the causal mutation was mapped to *Pgap1* (post-glycosylphosphatidylinositol attachment to proteins 1).[8] Ueda *et al* subsequently generated *Pgap1* deficient mice and showed that they recapitulate the otocephalic phenotype and its variable penetrance and expressivity, since the phenotype of mutant pups ranged in severity from a normal face to complete lack of mouth and jaw.[9] Loss of two other murine genes has also been shown to cause otocephaly-agnathia, in each case in a context dependent fashion. On a C57BL/6 genetic background, loss of the twisted gastrulation gene 1 (*Twsg1*$^{-/-}$) results in anomalies of the first branchial arch leading to agnathia, as well as forebrain abnormalities.[10] Finally, chimeric *Otx2*

heterozygous knockout mice also display an otocephalic phenotype, albeit with variable penetrance and expressivity attributable in part to genetic background.[11]

In humans, molecular defects leading to otocephaly are largely unknown. Recently, missense mutations in *PRRX1* (*paired-related homoeobox gene 1*) were identified in two sporadic cases of otocephaly.[12 13]

OTX2 mutations have been observed in patients with isolated severe ocular and pituitary malformations.[14 15] Here, we report the identification of a deleterious mutation in *OTX2* in a large French family in which variable expressivity extends from micro/anophthalmia to otocephaly and is inherited in a dominant manner among four generations. We subsequently performed molecular screening of *OTX2* in nine additional, non-related otocephalic cases and identified a second sibship with an *OTX2* mutation. Despite OTX2 being a known microphthalmia locus, our data suggested that this gene might also be necessary but not sufficient in some families with otocephaly. To dissect this apparently complex genetic model, we suppressed *otx2* during zebrafish development and determined that: (1) *otx2* is also necessary for correct mandible formation; and (2) *otx2* can interact genetically with other loci to modulate the severity of mandibular malformations. Taken together, our data support a causal role of *OTX2* in otocephaly in humans but indicate that other genetic factors are likely necessary for the manifestation of the otocephalic phenotype.

SUBJECTS, MATERIALS AND METHODS

Patient samples

One family and nine sporadic otocephaly patients were included in this study. Among the sporadic patients, four have been reported previously elsewhere.[16–19] Informed consents with appropriate ethics review committee approvals were obtained. DNA was extracted from blood or fresh tissue for the family, three sporadic patients, and asymptomatic parents of an otocephalic patient; DNA was extracted from paraffin embedded tissue for the remaining patients. Following DNA extraction from paraffin embedded blocks, whole genome amplification was performed using standard procedures (Sigma Aldrich, Lyon, France).

Patient phenotypes

Patient descriptions including medical history, family history, physical examinations, autopsy reports, and radiological studies were obtained. Except for one family in which some members display micro/anophthalmia, all patients were diagnosed as sporadic cases of otocephaly-dysgnathia syndrome.

Complete clinical data for the family and the patient sharing the *OTX2* mutations are described in the supplementary material. Briefly, in family A (figure 1A), 17 members display micro/anophthalmia (supplementary figure 1) segregating with an autosomal, dominant inheritance and sometimes associated with a variable degree of intellectual disability (moderate to

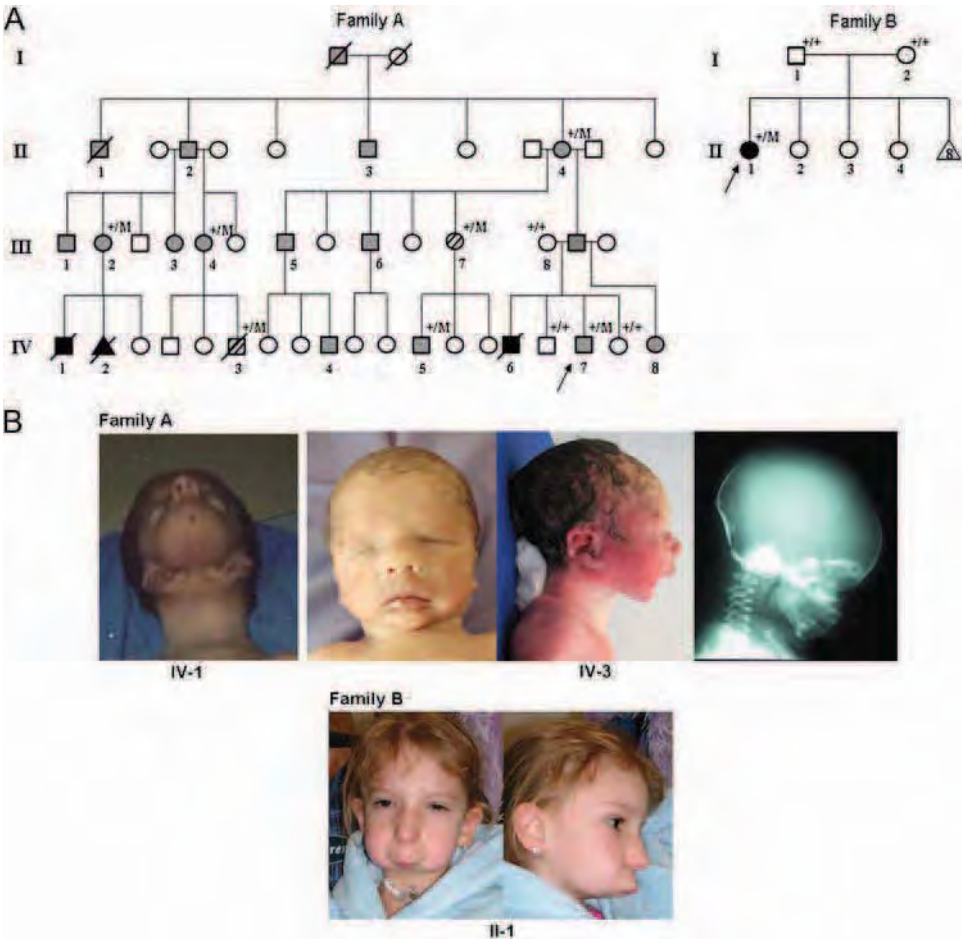

Figure 1 Families and spectrum of otocephaly-dysgnathia phenotypes. (A). Pedigrees of families with phenotypic descriptions and mutation analysis. Otocephaly is indicated by dark symbols. Patients with isolated unilateral/bilateral microphthalmia and anophthalmia are indicated by grey symbols. Patients with an intermediate phenotype (striped individuals in family A) had additional features to ocular findings including micrognathia, but did not fulfil the criteria for otocephaly. Index cases are shown by arrows. Family A, IV-7 had bilateral anophthalmia, intellectual disability, and a heterozygous *OTX2* mutation. Family B, the proband was born to unaffected parents +/M indicates heterozygous presence of the familial mutation, while +/+ represents homozygous wild type alleles. If no genotype is indicated, a DNA sample was not available for testing. (B). Phenotypic spectrum of *OTX2* mutations in otocephalic and intermediate phenotypes. In family A, patient IV-1 displayed otocephaly (agnathia, microstomia, and synotia), while patient IV-3 shared micro/anophthalmic and otocephalic (microretrognathia, rudimentary tongue, hypoplasia of the upper pharynx) features. Family B proband (II-1) has otocephaly with a tubular nose, microstomia, agnathia, and moderately low set ears.

severe), three patients were diagnosed as otocephalic (figure 1A), and one patient displayed clinical features overlapping both micro/anophthalmia and otocephaly, which we consider to be an intermediate phenotype (figure 1B and supplementary figure 2). The second otocephalic patient (figure 1B) harbouring an *OTX2* mutation was a sporadic case (figure 1A) with no familial history of ophthalmic or mandibular malformations.

Molecular analysis

Candidate gene analysis

We sequenced *OTX2* in all index cases and extended our sequencing to relatives when a change of interest was identified. Since half of the DNAs were extracted from paraffin embedded blocks, primer pairs were designed to amplify PCR products <250 bases. Patients negative for *OTX2* coding and flanking splice site mutations were also screened for *ALX4*, *MSX1*, *PGAP1*, *PRRX1*, and *TWSG1* mutations when the amount of DNA allowed such analyses (four out of eight patients). In addition, the same loci were sequenced in the two families with *OTX2* mutations in search of candidate modifier alleles. Primers and PCR conditions used are summarised in supplementary table 1. Both DNA strands were sequenced using the Big Dye Terminator Cycle Sequencing Ready Reaction Kit (Applied Biosystems, Courtaboeuf, France). GenBank accession numbers were NM_021728.2 (*OTX2*), NM_024989.3 (*PGAP1*), NM_020648.5 (*TWSG1*), NM_021926.3 (*ALX4*), and NM_002448.3 (*MSX1*).

Functional studies

Zebrafish embryo manipulation and genetic interaction studies

Splice blocking morpholinos (MOs) targeting *otx2*, *pgap1*, *prrx1a* and *prrx1b*, and a translation blocking morpholino targeting *msx1* (Gene Tools, Philomath, Oregon, USA) were diluted to appropriate concentrations with sterile, nuclease-free water (3 or 9 ng/nl for each MO for dose response; 3 ng/nl for genetic interaction studies) and injected into wild-type zebrafish embryos collected from natural matings at the 1–2 cell stage according to standard procedures. Embryos were reared at 28°C in 1-phenyl-2-thiourea beginning at 24 h post-fertilisation until harvest at 5 days post-fertilisation (dpf). All experiments (n=66–75 embryos/injection) were repeated twice. To assess cartilaginous craniofacial structures, embryos were anaesthetised with tricaine, fixed overnight in 4% paraformaldehyde, and stained overnight in Alcian blue solution (0.1% Alcian blue, 70% ethanol, 1% HCl). Embryos were cleared with acidic ethanol (70% ethanol, 5% HCl) for 4 h, dehydrated in 100% ethanol, and imaged in glycerol. All images (live and Alcian blue stained whole embryos) were acquired on a Nikon AZ100 stereoscope at 6× magnification using Nikon NIS Elements software. To assess knockdown efficiency of each splice blocking morpholino, we harvested total RNA from injected batches of 25 embryos using Trizol (Invitrogen, Grand Island, NY, USA) according to the manufacturer's instructions. Oligo-dT-primed cDNA was then synthesised using SuperScriptIII reverse transcriptase (Invitrogen) and cDNA was subsequently PCR amplified using primers flanking the MO target sites for each of *otx2*, *pgap1*, *prrx1a* and *prrx1b*.

RESULTS

OTX2 is a candidate gene for otocephaly-agnathia

In family A, we identified a c.316delC mutation in exon 3 of *OTX2* (figure 2), a deletion predicted to result in a frameshift, p. Gln106AsnfsX11. The truncated protein is predicted to terminate at the end of the homeodomain within the glutamine stretch (figure 2). Since otocephalic patients IV-1 and IV-2 died about 20 years ago, their DNAs were unavailable to investigate

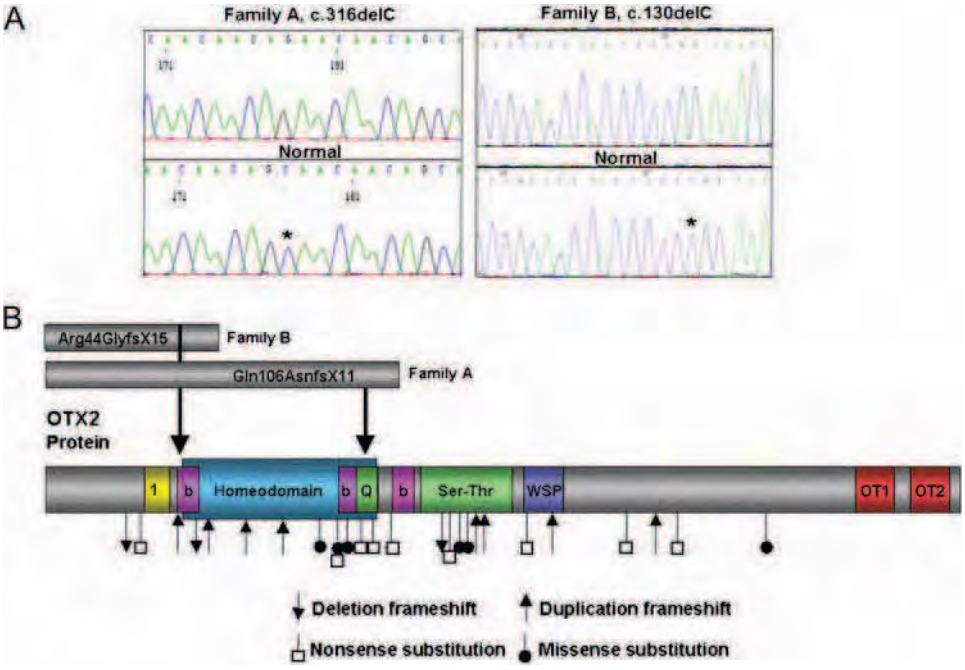

Figure 2 OTX2 mutations in otocephaly-dysgnathia complex. (A) Electropherograms showing the two *OTX2* mutations identified in otocephalic patients in comparison with wild type sequence. Mutations were identified at heterozygous state in patients and amplimers were cloned in a pGEM-T vector to better delineate sequence variations. The asterisks are positioned over the deleted nucleotides and numbered according to GenBank accession numbers NM_021728.2 (NM_172337.1). (B) The two *OTX2* mutations identified herein are predicted to result in a frameshift leading to production of a truncated protein or nonsense mediated decay. An RNA or protein source was unavailable to test the functional outcome for either mutation. The mutations and their predicted truncated proteins are indicated at the top. The type and location of the previously reported *OTX2* mutations identified in micro/anophthalmic patients are indicated relative to the protein representation of isoform a. There are two alternative transcripts that code for isoforms a (NP_068374.1, 297 amino acids) and b (NP_758840.1) that differ only in the presence or absence of eight amino acids, GPWASCPA, represented by the yellow region, 1 (33–40 aa). Labelled nucleotide regions coding for different protein domains are colour coded for the three basic amino acid regions (b: b1 44–50 aa; b2 97–102 aa; b3 115–121 aa), homeodomain (45–105 aa), glutamine stretch (Q 103–109 aa), serine and threonine rich region (Ser-Thr 125–154 aa), conserved WSP motif (WSP 158–167 aa), and repeated tails (OT1 267–275 aa and OT2 281–293 aa). The region coding for the homeodomain overlaps regions coding for b1, b2, and glutamine stretch Q.

their *OTX2* mutational burden. However, their mother (III-2) was found to have the mutation, suggesting that her two otocephalic offspring IV-1 and IV-2 likely inherited this mutation from her. Individual IV-7, with ocular abnormalities, also carried the mutation, suggesting that his otocephalic sibling IV-6 may have had the mutation, although we were unable to obtain a sample for testing from IV-6 or from their affected father III-9. Patient IV-3, with clinical features overlapping both micro/anophthalmia and otocephaly, did share the familial *OTX2* mutation.

In family B (figure 1A), we screened *OTX2* in a female patient with otocephaly (figure 1B) and detected a c.130delC mutation in exon 2 (figure 2). This deletion is predicted to result in a frameshift, p.Arg44GlyfsX15; if translated, the truncated protein would terminate before the OTX2 homeodomain (figure 2). This patient was a sporadic case with no family history of ophthalmic or mandibular malformations. Parental DNA analysis showed that the *OTX2* mutation appears de novo. No *OTX2* mutation was identified in the 8 remaining otocephalic patients. These results are summarised in supplementary table 2.

Candidate gene screening of *ALX4, MSX1, PGAP1, PRRX1, and TWSG1* in *OTX2* mutation-negative otocephaly samples

To explore further the genetic basis of otocephaly and overlapping phenotypes in the *OTX2* mutation-negative samples in our cohort, we conducted molecular analysis of five additional candidate genes known to play a role in otocephaly malformations in vertebrates (*ALX4*, *MSX1*, *PGAP1*, *PRRX1*, and *TWSG1*; possible for four out of the eight remaining patients with DNA of sufficient quality). One patient displayed two heterozygous *PGAP1* intronic variations (c.1-115C>T and c.927+31A>G), while another one displayed two heterozygous variations in *MSX1* (c.119C>G [p.Ala40Gly] and c.*+6C>T). More variants were identified in *ALX4*: c.63C>T [p.Tyr21Tyr], c.104G>C, [p.Arg35Thr], c.304C>T (p.Pro102Ser), c.621A>G [p.Ser207Ser], c.1074C>T [p.His358Gln], and c.*228C>T. All sequence variations are common single nucleotide polymorphisms (SNPs) referenced in dbSNP. These variants are thus unlikely to cause otocephaly. No *PRRX1* or *TWSG1* variation was identified. Patient genotypes are summarised in supplementary table 2.

otx2 interacts with other otocephaly loci in an in vivo developmental model

Because of the observed phenotypic variability observed among affected individuals in our families, we hypothesised that lesions in additional loci may interact with *OTX2* to cause otocephaly—an hypothesis consistent with the reported background dependent variable penetrance and expressivity of murine otocephaly mutations.[11 20] We have shown previously that the zebrafish is a useful model to dissect epistasis contributing to variable phenotypes observed in human developmental disorders.[21–23] Therefore, we investigated the potential for *otx2* to modulate specific otocephaly endophenotypes or severity by suppressing *otx2* in a sensitised, physiologically relevant context in the developing zebrafish embryo. First, we identified the single zebrafish ortholog of OTX2 (91% identity; 94% similarity vs human) and suppressed it transiently by microinjection of an antisense MO targeting the splice donor sequence of *Danio. rerio otx2* exon 2 in batches of wild-type (wt) embryos at the one-to-two cell stage. At 5 dpf, we scored embryos for craniofacial phenotypes relevant to otocephaly and we observed mild microphthalmia and shortening of the pharyngeal skeleton that increased in penetrance in a dose dependent manner (figure 3A, supplementary figure 3J). Notably, Alcian blue staining of 5dpf embryos revealed the presence of all pharyngeal components, but distinct defects in comparison to controls. These data were consistent with the specific and robust targeting of the MO as indicated by RT-PCR of cDNA generated from total RNA harvested from *otx2* morphants (supplementary figure 3A,E).

Next, we asked whether *otx2* could exacerbate the craniofacial phenotypes that result from loss of the known otocephaly loci, *PGAP1* and *PRRX1*, and an additional locus implicated in mandibular development, *MSX1*. First, we identified the zebrafish orthologs of each protein; PGAP1 (one copy; 43% identity, 64% similarity vs human), PRRX1 (two copies; a and b each, 85% identity, 91% similarity vs human), and MSX1 (one copy; 61% identity, 68% similarity vs human) could each be suppressed efficiently in developing zebrafish embryos subsequent to injection of splice blocking (*pgap1*, *prrx1a* and *prrx1b*) or translation blocking (*msx1*) MOs (supplementary figure 3B–D, F–J). Scoring of zebrafish larva at 5 dpf revealed that knockdown of *pgap1* resulted in mild microphthalmia, fusion of the eyes at the midline, and protrusion of the mandible (figure 3A, D); *prrx1a/b* double morphants and *msx1* morphants displayed reduced eye size and anterior-posterior shortening of jaw structures (figure 3A,D). Similar to *otx2*, these abnormalities in the pharyngeal skeleton were dose dependent (supplementary figure 3J). Next, to test *otx2* genetic interaction with *pgap1*, we injected subeffective doses of each MO (3 ng each of *otx2* and/or *pgap1*) either alone or in a pairwise fashion into wt zebrafish embryos at the 1–2 cell stage and scored them live for craniofacial defects at 5 dpf. Whereas we observed a modest percentage of abnormal embryos for *otx2* and *pgap1* individually (2% and 26%, respectively; n=66–74 embryos/injection, repeated at least twice with masked scoring), the combined effect resulted in a synergistic exacerbation of phenotypes when compared to either MO alone. Pairwise suppression resulted in increased mortality and a new severe class of embryos that displayed severe microphthalmia, eye fusion along the midline, and severe disorganisation of mandibular cartilage as indicated by Alcian blue staining (figure 3A,B,D). Suppression of *otx2* also exacerbated the effects of *prrx1a/b* knockdown. Through comparisons of subeffective MO injection doses targeting either *otx2* and/or *prrx1a/b* (3 ng of each MO), we saw a pronounced increase in embryos with craniofacial defects and a severe class of embryos in the *otx2/prrx1a/b* morphant injection batches (2%, 4%, and 32% affected embryos for *otx2*, *prrx1a/b* and *otx2/prrx1a/b* double morphants, respectively; n=66–74 embryos/injection; figure 3A,C,D). Similarly, pairwise interaction studies between *otx2* and *msx1* resulted in exacerbation of craniofacial defects in *otx2/msx1* injection batches compared to either single MO alone (3%, 6%, and 22% affected embryos for *otx2*, *msx1* and *otx2/msx1* double morphants respectively; n=66–75 embryos/injection; figure 3A,C,D). Together, these results indicate that suppression of *otx2*, in combination with loss of function of other loci contributing to otocephaly phenotypes, can modulate phenotypic severity in the manifestation of craniofacial malformations.

ALX4, *MSX1*, *PGAP1*, *PRRX1*, and *TWSG1* as candidate genetic interactors of *OTX2*

Informed by the in vivo functional studies, which indicated the potential for OTX2 to modulate otocephaly phenotypes, we returned to the patient cohorts for further mutational analysis. We screened the five candidate genes listed above (*ALX4*, *MSX1*, *PGAP1*, *PRRX1*, and *TWSG1*) in available family members from each of the two families bearing pathogenic *OTX2* mutations. Variants identified among *ALX4*, *MSX1*, *PGAP1*, *PRRX1*, *and*

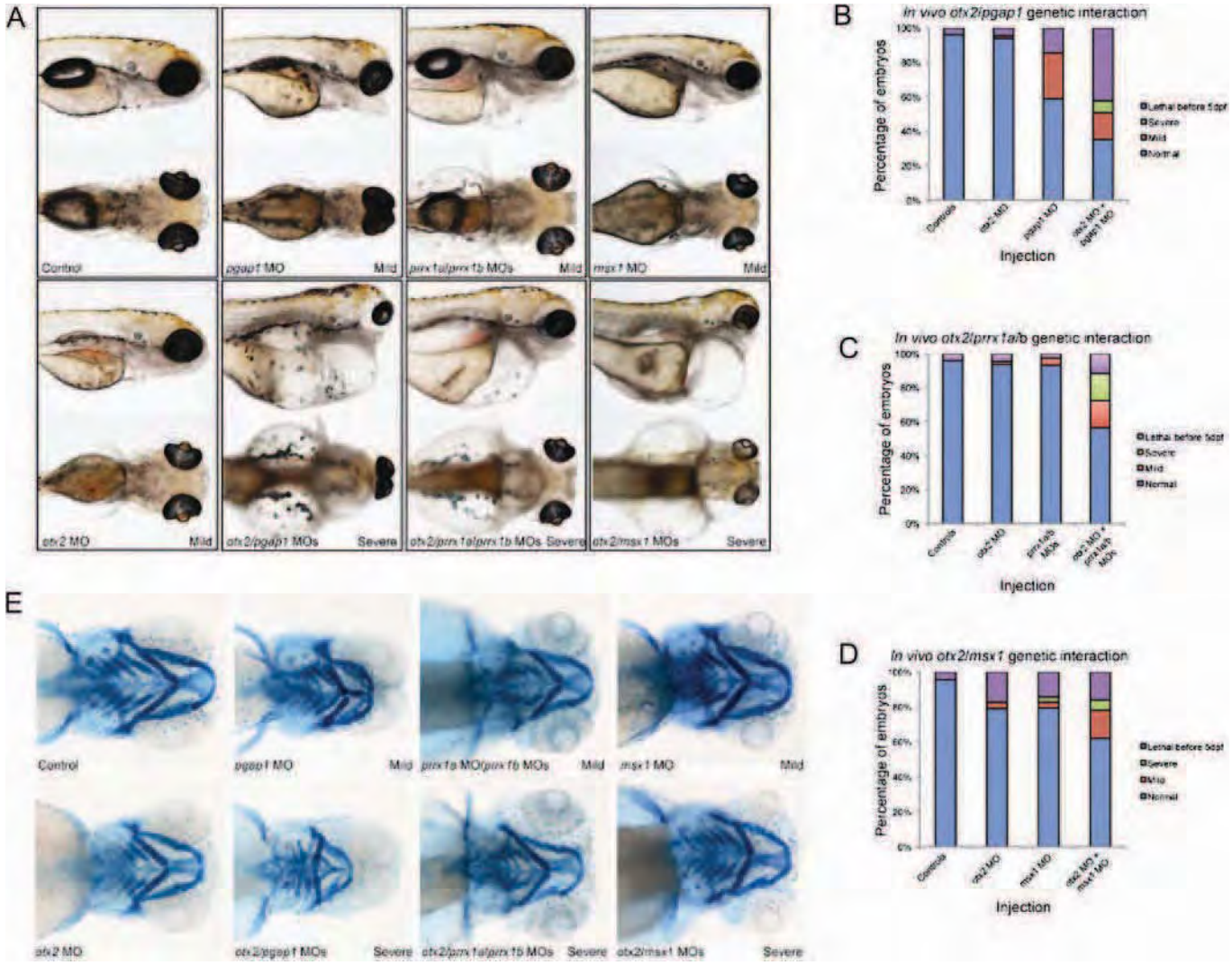

Figure 3 *otx2* interacts genetically with *pgap1*, *prrx1a/b*, and *msx1*. (A) Representative live embryo images of *otx2*, *pgap1*, *prrx1a/1b*, and *msx1* suppressed zebrafish larva. Wild-type zebrafish embryos were injected at the 1−2 cell stage with morpholinos (MO) targeting the zebrafish orthologs of OTX2, MSX1, PGAP1 (one *Danio rerio* ortholog each), or PRRX1 (two orthologs, denoted as a and b). *otx2* morphants displayed mild microphthalmia and shortening of the pharyngeal skeleton; *pgap1* morphants exhibited mild microphthalmia, fusion of the eyes at the midline, and protrusion of the mandible; *prrx1a/b* double morphants displayed reduced eye size and anterior-posterior shortening of jaw structures. Co-injection of *otx2* with candidate modifier genes *pgap1* or *prrx1a/b* resulted in classes of severely affected embryos respectively, characterised by extreme microphthalmia, fused eyes (*pgap1* only), and severe abnormalities of craniofacial structures. Lateral (top) and ventral views (bottom) are shown for each injection cocktail. (B). Quantification of *otx2* genetic interaction with *pgap1*. Subeffective doses of each MO were injected either alone or in a pairwise fashion into wt zebrafish embryos at the 1−2 cell stage and scored live for craniofacial defects at 5 days post-fertilisation (dpf). Mild and severe classes are depicted in panel A (centre column). Many double morphants die before 5 dpf (42%), but display severe craniofacial defects, including cyclopia, when evaluated at earlier stages. (C) Quantification of *otx2* genetic interaction with *prrx1a/b*. Subeffective doses of each morpholino were injected either alone or in a pairwise fashion into wt zebrafish embryos at the 1−2 cell stage and scored live for craniofacial defects at 5 dpf. Mild and severe classes are depicted in panel A (right column). (D) Quantification of *otx2* genetic interaction with *msx1*. Subeffective doses of each morpholino were injected either alone or in a pairwise fashion into wt zebrafish embryos at the 1−2 cell stage and scored live for craniofacial defects at 5 dpf. Mild and severe classes are depicted in panel A (right column). (E) Craniofacial cartilage defects in *otx2*, *pgap1*, *prrx1a/b*, *msx1* or double morphant embryos. Alcian blue staining of 5 dpf embryos revealed the presence of all pharyngeal components (ventral views are shown), but distinct defects in comparison to controls. Suppression of each gene or gene combination resulted in curving and shortening of ceratobranchial cartilage, and, in particular, *pgap1* or *otx2/pgap1* morphants exhibited severely disorganised structures including abnormally shaped Meckel's cartilage, and an increased angle of ceratohyal cartilage with respect to the midline. Note the decrease in eye size for all injected embryos shown in comparison to controls.

TWSG1 are described below and summarised in supplementary table 2. First, in *PRRX1*, we detected no novel changes. In *ALX4*, *PGAP1*, *TWSG1*, and *MSX1*, only known SNPs and all but two (c.778-11G>A in *ALX4*, and c.906T>C [p.Leu302Leu] in *PGAP1*) shared by micro/anophthalmic relatives were identified. The *ALX4* c.778-11G>A variation is not predicted to alter splicing by in silico analysis and the *PGAP1* c.906T>C variation is a neutral variation with no amino acid modification and no predicted effect on splicing by in silico analysis. Variations identified among the screened genes are thus unlikely to exert a modifier effect leading to otocephaly.

DISCUSSION

Otocephaly/agnathia is the most severe known developmental defect of the mandible. Three genes (*Otx2*, *Pgap1*, *Twsg1*) cause otocephaly when inactivated in mice, but the molecular defects

underlying this severe malformation are still largely unknown in humans. Recently, missense mutations in *PRRX1*, encoding a transcriptional co-activator, was identified in two cases of otocephaly.[12 13] Functional studies indicated that these mutations decrease the ability for the mutant protein to regulate the tenascin-C gene promoter, and thus, these mutations were considered as deleterious. *Prrx1* null mice display cleft palate and mild hypoplasia of both the mandible and the zeugopodal bones of the limbs.[24] These are the only cases reported with a plausible molecular explanation of otocephaly. However, we cannot exclude the possibility that additional mutational burden was required to manifest the severe craniofacial phenotype.

In this report, we demonstrated that *OTX2* mutations contribute to this malformation in humans. We identified an *OTX2* mutation in a large family where an autosomal dominant form of micro/anophthalmia was present. Two microphthalmic cousins of this family each gave birth to at least one child with otocephalic features. Since these otocephalic patients died prenatally or shortly after birth 20 years ago, it is not possible to establish whether they shared the familial mutation. However, we were able to show that their affected parent harboured the familial *OTX2* null mutation. Additionally, in the same family, we identified the familial *OTX2* mutation in a fetus displaying ocular (microphthalmia with retinal dysplasia and absence of the anterior chamber) and mandibular (severe micrognathia) features.

To confirm the role of *OTX2* mutations in otocephaly, we screened an additional nine unrelated otocephalic patients for *OTX2* mutations. In one patient, we found a de novo frameshifting *OTX2* mutation, thus confirming the implication of this gene in otocephaly. In our series, an *OTX2* mutation was identified in 2/10 (20%) probands, and no other *OTX2* mutations could be found in the remainder of our cohort. Despite the possibility that we missed mutations by direct sequencing (exonic rearrangements, splicing mutation located far from the coding sequence, or mutations in regulatory regions), this result supports a probable genetic heterogeneity for otocephaly.

We performed additional molecular analysis for four of the eight patients mutation-negative for *OTX2*, focusing on plausible functional candidates (*ALX4*, *MSX1*, *PGAP1*, *PRRX1*, and *TWSG1*). *Alx4*, a gene involved in skull defects, has previously been proposed to be a modifier of the otocephalic phenotype in *Otx2* heterozygous mutant mice.[20] *MSX1* is a gene involved in mandibular embryonic development,[25] and its expression is regulated directly or indirectly by TWSG1[26] and OTX2.[27] In addition, MSX1 binds a distant non-coding regulatory element of *SOX9* which, when mutated, leads to Pierre-Robin sequence, a less severe human mandibular phenotype.[28] *Pgap1* and *Twsg1* cause otocephaly when inactivated in mice.[9 10] Finally, a mutation in *PRRX1* was previously identified in two otocephalic patients.[12 13] No deleterious mutations were identified in any of these genes in the *OTX2* mutation-negative patients. However, this particular cohort is too small to rule out their possible contribution to human otocephalic phenotypes.

The major phenotype described previously in patients with *OTX2* mutations is microphthalmia/anophthalmia associated with extra-ocular defects such as brain malformations, pituitary abnormalities, short stature, and mental retardation.[15] *OTX2* mutations identified so far are listed in supplementary table 3, and represented in figure 2B. Phenotypic variability and incomplete penetrance have also been documented.[14 15] No obvious phenotype/genotype correlations for the single gene *OTX2* can be made. First, several micro/anophthalmic patients harbour frameshifting or nonsense mutations located in the same region of *OTX2* (figure 2B), indicating that haploinsufficiency at this locus is likely insufficient to cause otocephaly. Second, our epistatic analysis shows overt genetic interactions with other genes known to be required for mandibular formation in humans and/or rodents. Together, these data suggest that genetic interactions as well as the position/type of mutations at *OTX2* likely drive phenotypic expressivity.

The otocephaly-dysgnathia spectrum ranges from isolated mandibular involvement (dysgnathia or agnathia) to a broader spectrum of malformations including dysgnathia, holoprosencephaly, situs inversus, and visceral anomalies.[29] Of note, the patient with *OTX2* mutations and otocephaly whom we could examine (family B, patient II-1) was not affected by features of holoprosencephaly, situs inversus, or by visceral malformations. In one patient with an intermediate phenotype (family A, patient IV-3), thymic hyperplasia, 11 rib pairs, and micropenis were also associated with the otocephaly.

Discrete *OTX2* expression in the mammalian forebrain and retinal anlage is preceded and accompanied by transcription in the anterior mesendoderm and pharyngeal endoderm.[30] This region of pharyngeal endoderm is critical for the induction and orientation of facial skeletal elements derived from cephalic neural crest cells.[31] We speculate that the effect of *OTX2* mutations on eye formation would be direct within the neuroepithelial component, but indirect, via mis-specification of the rostral pharyngeal endoderm, on the mandibular portion of the first branchial arch.

Consistent with observations in *OTX2* null mice, the mandibular phenotype associated with *OTX2* mutation in humans is highly variable, ranging from absence of developmental defect (most of the family A members), to micrognathia (family A, patient IV-3), to agnathia (family B), to severe otocephaly (family A, patients IV-1, IV-2, and IV-6). Phenotypic variation has been attributed to modifier genes, environmental variations, and stochastic effects. To understand the phenotypic variability observed between the two families with *OTX2* mutations, we hypothesised that pathogenic alleles at epistatic loci may be involved in the otocephalic phenotype for patients bearing an *OTX2* mutation. In vivo modelling experiments in zebrafish showed that suppression of three genes in concert with *otx2*, (*pgap1*, *prrx1a/b*, and *msx1*) lead to exacerbated craniofacial defects far exceeding defects of each gene alone, suggesting that the combinatorial effect of additional molecular lesions in the genome may explain the phenotypic variability associated with *OTX2* mutations. In our families, known otocephaly-causing/contributing genes were mutation negative for the candidates screened, suggesting that the otocephaly phenotype is likely subject to additional genetic heterogeneity. Whole exome/genome sequencing of these and other families under a 'two-hit' hypothesis, coupled to epistatic analysis in zebrafish or other suitable model organisms, is likely to identify such alleles and illuminate the genetic architecture of this complex disorder.

Author affiliations
[1]Department of Medical Genetics, Purpan Hospital, CHU Toulouse, Toulouse, France
[2]GR2DE Team, Toulouse III Paul-Sabatier University, Toulouse, France
[3]INSERM, Centre de Physiopathologie de Toulouse Purpan, Toulouse, France
[4]Department of Genetics and Genomic Sciences, Mount Sinai School of Medicine, New York, USA
[5]Center for Human Disease Modeling, Duke University Medical Center, Durham, North Carolina, USA
[6]Department of Pediatrics, Duke University Medical Center, Durham, North Carolina, USA
[7]Department of Cell Biology, Duke University Medical Center, Durham, North Carolina, USA
[8]Department of Medical Genetics, CH Le Mans, Le Mans, France

[9]Department of Pediatrics, Mount Sinai School of Medicine, New York, USA
[10]Department of Pathology, University of Alabama, Birmingham, Alabama, USA
[11]Department of Histology-Embryology, Hôpital Necker, Paris, France
[12]Department of Ophthalmology, Purpan Hospital, CHU Toulouse, Toulouse, France
[13]Genetic Center, Dr Zekai Tahir Burak Women Health Training and Research Hospital, Ankara, Turkey
[14]Section of Genetics, Department of Pediatrics, University of California Davis, Sacramento, California, USA
[15]Department of Medical Genetics, Istanbul Medical Faculty, Istanbul, Turkey
[16]Department of Pathology, University Hospital of Rennes, Rennes, France
[17]Pathology Laboratory, Bordeaux University Hospital, Bordeaux, France
[18]Department of Laboratory Medicine and Pathology, University of Alberta Hospital, Edmonton, Canada
[19]Institute of Pathology, Medical University of Innsbruck, Innsbruck, Austria
[20]Department of Pediatrics, University of Medicine and Dentistry of New Jersey, Newark, New Jersey, USA
[21]Department of Medical Research, Mackay Memorial Hospital, Taipei, Taiwan
[22]Department of Biotechnology, Asia University, Taichung, Taiwan
[23]School of Chinese Medicine, College of Chinese Medicine, China Medical University, Taichung, Taiwan
[24]INSERM, Université de la Méditerranée Faculté de Médecine, Marseille, France
[25]Academic Unit of Genetic Medicine, Division of Human Genetics, University of Southampton, Southampton, UK
[26]Department of Developmental and Regenerative Biology, Mount Sinai School of Medicine, New York, USA

Acknowledgements The authors thank the families for their participation and the following physicians and scientists for their assistance: Petra Reinecke at University Hospital, Duesseldorf, Germany; Didier Lacombe at CHU Pellegrin-Enfants, Bordeaux Cedex, France; Marion Gerard at Robert Debré Hospital, Paris, France; Christine Peres, Annaïck Desmaison, Matthias Macé and Stanislas Faguer at Inserm U563, Toulouse, France, and the French Foetopathology Society (SOFFOET). NK is a Distinguished George W. Brumley Professor.

Contributors NC, SS, EED, PM, PC, HCE, NK, and EWJ contributed to the project design, analysis of data, and/or the writing of the manuscript. DM-C, BK, OF-P, PL, DC, CS, SP, CPC, AY, SAB, HK, GS, FE-R, SEB, PJT, LS, AMG, CLM, and EWJ recruited patients and family members and phenotypically characterised patients and family members. NC, SS, AI, WAP, BDW, LL, and AV performed molecular analysis. EED and NK performed zebrafish experiments.

Funding This work was supported by grants from the Clinical Research Hospital Program from the French Ministry of Health (PHRC 09 109 01), Retina France, and from National Institutes of Health (5 R01 DE13849 and -09 S1).

Competing interests None.

Patient consent Obtained.

Ethics approval Ethics approval was provided by the Comité de Protection des Personnes Sud-Ouest et Outre-Mer II.

Provenance and peer review Not commissioned; externally peer reviewed.

REFERENCES

1. **Opitz JM,** Zanni G, Reynolds JF Jr, Gilbert-Barness E. Defects of blastogenesis. *Am J Med Genet* 2002;**115**:269—86.
2. **Gekas J,** Li B, Kamnasaran D. Current perspectives on the etiology of agnathia-otocephaly. *Eur J Med Genet* 2010;**53**:358—66.
3. **Pauli RM,** Pettersen JC, Arya S, Gilbert EF. Familial agnathia-holoprosencephaly. *Am J Med Genet* 1983;**14**:677—98.
4. **Porteous ME,** Wright C, Smith D, Burn J. Agnathia-holoprosencephaly: a new recessive syndrome? *Clin Dysmorphol* 1993;**2**:161—4.
5. **Krassikoff N,** Sekhon GS. Familial agnathia-holoprosencephaly caused by an inherited unbalanced translocation and not autosomal recessive inheritance. *Am J Med Genet* 1989;**34**:255—7.
6. **Khan A,** Bourgeois J, Mohide P. Agnathia-otocephaly complex in a fetus with maternal use of topical 1% salicylate. *Clin Dysmorphol* 2008;**17**:75—6.
7. **Juriloff DM,** Sulik KK, Roderick TH, Hogan BK. Genetic and developmental studies of a new mouse mutation that produces otocephaly. *J Craniofac Genet Dev Biol* 1985;**5**:121—45.
8. **Zoltewicz JS,** Ashique AM, Choe Y, Lee G, Taylor S, Phamluong K, Solloway M, Peterson AS. Wnt signaling is regulated by endoplasmic reticulum retention. *PLoS One* 2009;**4**:e6191.
9. **Ueda Y,** Yamaguchi R, Ikawa M, Okabe M, Morii E, Maeda Y, Kinoshita T. PGAP1 knock-out mice show otocephaly and male infertility. *J Biol Chem* 2007;**282**:30373—80.
10. **Petryk A,** Anderson RM, Jarcho MP, Leaf I, Carlson CS, Klingensmith J, Shawlot W, O'Connor MB. The mammalian twisted gastrulation gene functions in foregut and craniofacial development. *Dev Biol* 2004;**267**:374—86.
11. **Matsuo I,** Kuratani S, Kimura C, Takeda N, Aizawa S. Mouse Otx2 functions in the formation and patterning of rostral head. *Genes Dev* 1995;**9**:2646—58.
12. **Sergi C,** Kamnasaran D. PRRX1 is mutated in a fetus with agnathia-otocephaly. *Clin Genet* 2011;**79**:293—5.
13. **Celik T,** Simsek PO, Sozen T, Ozyuncu O, Utine GE, Talim B, Yigit S, Boduroglu K, Kamnasaran D. PRRX1 is mutated in an otocephalic newborn infant conceived by consanguineous parents. *Clin Genet* 2012;**81**:294—7.
14. **Ragge NK,** Brown AG, Poloschek CM, Lorenz B, Henderson RA, Clarke MP, Russell-Eggitt I, Fielder A, Gerrelli D, Martinez-Barbera JP, Ruddle P, Hurst J, Collin JR, Salt A, Cooper ST, Thompson PJ, Sisodiya SM, Williamson KA, Fitzpatrick DR, van Heyningen V, Hanson IM. Heterozygous mutations of OTX2 cause severe ocular malformations. *Am J Hum Genet* 2005;**76**:1008—22.
15. **Schilter KF,** Schneider A, Bardakjian T, Soucy JF, Tyler RC, Reis LM, Semina EV. OTX2 microphthalmia syndrome: four novel mutations and delineation of a phenotype. *Clin Genet* 2011;**79**:158—68.
16. **Faye-Petersen O,** David E, Rangwala N, Seaman JP, Hua Z, Heller DS. Otocephaly: report of five new cases and a literature review. *Fetal Pediatr Pathol* 2006;**25**:277—96.
17. **Puvabanditsin S,** Garrow E, Umaru S, Padilla J, Chowdawarapu S, Biswas A. Otocephaly, and pulmonary malformation association: two case reports. *Genet Couns* 2006;**17**:167—71.
18. **Schiffer C,** Tariverdian G, Schiesser M, Thomas MC, Sergi C. Agnathia-otocephaly complex: report of three cases with involvement of two different Carnegie stages. *Am J Med Genet* 2002;**112**:203—8.
19. **Chen CP,** Chang TY, Huang JK, Wang W. Early second-trimester diagnosis of fetal otocephaly. *Ultrasound Obstet Gynecol* 2007;**29**:470—1.
20. **Hide T,** Hatakeyama J, Kimura-Yoshida C, Tian E, Takeda N, Ushio Y, Shiroishi T, Aizawa S, Matsuo I. Genetic modifiers of otocephalic phenotypes in Otx2 heterozygous mutant mice. *Development* 2002;**129**:4347—57.
21. **Badano JL,** Leitch CC, Ansley SJ, May-Simera H, Lawson S, Lewis RA, Beales PL, Dietz HC, Fisher S, Katsanis N. Dissection of epistasis in oligogenic Bardet-Biedl syndrome. *Nature* 2006;**439**:326—30.
22. **de Pontual L,** Zaghloul NA, Thomas S, Davis EE, McGaughey DM, Dollfus H, Baumann C, Bessling SL, Babarit C, Pelet A, Gascue C, Beales P, Munnich A, Lyonnet S, Etchevers H, Attie-Bitach T, Badano JL, McCallion AS, Katsanis N, Amiel J. Epistasis between RET and BBS mutations modulates enteric innervation and causes syndromic Hirschsprung disease. *Proc Natl Acad Sci U S A* 2009;**106**:13921—6.
23. **Davis EE,** Zhang Q, Liu Q, Diplas BH, Davey LM, Hartley J, Stoetzel C, Szymanska K, Ramaswami G, Logan CV, Muzny DM, Young AC, Wheeler DA, Cruz P, Morgan M, Lewis LR, Cherukuri P, Maskeri B, Hansen NF, Mullikin JC, Blakesley RW, Bouffard GG, Gyapay G, Rieger S, Tonshoff B, Kern I, Soliman NA, Neuhaus TJ, Swoboda KJ, Kayserili H, Gallagher TE, Lewis RA, Bergmann C, Otto EA, Saunier S, Scambler PJ, Beales PL, Gleeson JG, Maher ER, Attie-Bitach T, Dollfus H, Johnson CA, Green ED, Gibbs RA, Hildebrandt F, Pierce EA, Katsanis N. TTC21B contributes both causal and modifying alleles across the ciliopathy spectrum. *Nat Genet* 2011;**43**:189—96.
24. **Martin JF,** Bradley A, Olson EN. The paired-like homeo box gene MHox is required for early events of skeletogenesis in multiple lineages. *Genes Dev* 1995;**9**:1237—49.
25. **Liu W,** Selever J, Murali D, Sun X, Brugger SM, Ma L, Schwartz RJ, Maxson R, Furuta Y, Martin JF. Threshold-specific requirements for Bmp4 in mandibular development. *Dev Biol* 2005;**283**:282—93.
26. **MacKenzie B,** Wolff R, Lowe N, Billington CJ Jr, Peterson A, Schmidt B, Graf D, Mina M, Gopalakrishnan R, Petryk A. Twisted gastrulation limits apoptosis in the distal region of the mandibular arch in mice. *Dev Biol* 2009;**328**:13—23.
27. **Binato R,** Pizzatti L, Abdelhay E. Otx2 is a putative candidate to activate mice Msx1 gene from distal enhancer. *Biochem Biophys Res Commun* 2007;**358**:655—60.
28. **Benko S,** Fantes JA, Amiel J, Kleinjan DJ, Thomas S, Ramsay J, Jamshidi N, Essafi A, Heaney S, Gordon CT, McBride D, Golzio C, Fisher M, Perry P, Abadie V, Ayuso C, Holder-Espinasse M, Kilpatrick N, Lees MM, Picard A, Temple IK, Thomas P, Vazquez MP, Vekemans M, Roest Crollius H, Hastie ND, Munnich A, Etchevers HC, Pelet A, Farlie PG, Fitzpatrick DR, Lyonnet S. Highly conserved non-coding elements on either side of SOX9 associated with Pierre Robin sequence. *Nat Genet* 2009;**41**:359—64.
29. **Kauvar EF,** Solomon BD, Curry CJ, van Essen AJ, Janssen N, Dutra A, Roessler E, Muenke M. Holoprosencephaly and agnathia spectrum: presentation of two new patients and review of the literature. *Am J Med Genet C Semin Med Genet* 2010;**154C**:158—69.
30. **Bally-Cuif L,** Gulisano M, Broccoli V, Boncinelli E. c-otx2 is expressed in two different phases of gastrulation and is sensitive to retinoic acid treatment in chick embryo. *Mech Dev* 1995;**49**:49—63.
31. **Couly G,** Creuzet S, Bennaceur S, Vincent C, Le Douarin NM. Interactions between Hox-negative cephalic neural crest cells and the foregut endoderm in patterning the facial skeleton in the vertebrate head. *Development* 2002;**129**:1061—73.

OTX2 mutations contribute to the otocephaly-dysgnathia complex

Nicolas Chassaing, Susanna Sorrentino, Erica E Davis, et al.

J Med Genet published online May 10, 2012
doi: 10.1136/jmedgenet-2012-100892

OTX2 Mutations Contribute to the Otocephaly-Dysgnathia Complex

Nicolas Chassaing,[1,2,3,26,*] Susanna Sorrentino,[4,26] Erica E. Davis,[5,6] Dominique Martin-Coignard,[7] Anthony Iacovelli,[4] William A. Paznekas,[4] Bryn D Webb,[4,8] Ona Faye-Petersen,[9] Férechté Encha-Razavi,[10] Leopoldine Lequeux,[11] Adeline Vigouroux,[1] Ahmet Yesilyurt,[12] Simeon A. Boyadjiev,[13] Hülya Kayserili,[14] Philippe Loget,[15] Dominique Carles,[16] Consolato Sergi,[17,18] Surasak Puvabanditsin,[19] Chih-Ping Chen,[20,21,22] Heather C. Etchevers,[3,23] Nicholas Katsanis,[5,6] Catherine L. Mercer,[24] Patrick Calvas,[1,2,3] and Ethylin Wang Jabs,[4,8,25]

SUPPLEMENTARY NOTE

Patients:

Family A (figure 1A):

Seventeen members display micro/anophthalmia sometimes associated with a variable degree of mental retardation (moderate to severe). One affected patient (patient III-2) had two boys (IV-1 and IV-2) with otocephaly. IV-1 died soon after birth from respiratory distress and an unsuccessful intubation (figure 2) and IV-2 was electively aborted after an ultrasound scan documented recurrence of facial malformations evocative of otocephaly. Another affected member of this family (III-9) had a child (IV-6) who deceased soon after birth from respiratory distress with a probable diagnosis of otocephaly (he was reported by his mother to have “ears in the neck”). Furthermore, a first cousin once removed (III-4) had polyhydramnios during her pregnancy, and at 30.5 weeks gestation, she delivered a male IV-3 with clinical features overlapping both micro/anophthalmia and otocephaly which we define as an intermediate phenotype (figure 2). After birth, he developed respiratory distress, and intubation was difficult contributing to his demise. On physical exam he had a triangular face, hypoplasia of the maxillae, hypoplasia of the upper pharynx, non-communication between the proboscis and the hypopharynx, and a rudimentary tongue. Subsequently an autopsy was performed and multiple abnormalities were found including bilateral microphthalmia, absence of the anterior ocular chamber, cataract, and focal retinal dysplasia

(supplementary figure 2). In addition, microretrognathia, microglossia, thymic hyperplasia, 11 ribs, and micropenis were noted. Another member (III-7) had an intermediate phenotype associating unilateral anophthalmia and microgonathia. Karyotype was 46, XY normal. Other family members display a phenotype ranging from isolated micro/anophthalmia (patients I-1, II-1, II-4, II-7, III-2, III-4, III-5, III-6, IV-8), isolated bilateral anophthalmia (patient II-2, III-1), to bilateral anophthalmia associated with mental retardation (IV-4, IV-5, IV-7).

Family B (Figure 1 B):

The proband (figure 2) was a 12 year old, white Caucasian female with agnathia and aglossia. Prenatal history was significant for polyhydramnios. She was born at 32 weeks gestation via emergency Caesarian section due to fetal distress after amnioreduction. At birth, her weight was 1.86 kg (50^{th} – 75^{th} centile), and she had respiratory distress that required nasal intubation and subsequent tracheostomy at nine hours of age. She had severe reflux as an infant necessitating a fundoplication. She suffered from middle ear effusions. The patient also had repeated episodes of lethargy and malaise with no cause found. Her physical examination revealed normal growth parameters, microstomia, hypoplasia of the maxillae, agnathia, absent tongue and a long tubular nose. Her ears were normally formed with patent external auditory canals. The only eye abnormality noted was astigmatism. Speech was absent although vocal cords were present but scarred. Developmentally, she had no delay in reaching milestones and is doing well in a mainstream school. There were no known associated limb and internal organ abnormalities or hormonal dysfunction. This patient was the first child to parents who were of English descent. They were in good health, deny consanguinity and both of had normal karyotypes. The mother had eight miscarriages with most in the first trimester, but two were in the second trimester at 13 and 15 weeks. The patient had three living siblings, none of whom displayed obvious features of otocephaly, ocular, or other anomalies. However, they all had mention of overbites that were significantly milder than that found in the proband.

SUPPLEMENTARY FIGURES

Supplementary Figure 1: Ocular phenotypes observed in Family A.

Note intra-familial variability among patients with unilateral microphthalmia (patient II-4), bilateral microphthalmia (patients III-2, III-4), unilateral anophthalmia (patient III-7) and bilateral anophthalmia (patient IV-7).

Supplementary Figure 2: Ocular phenotype observed in patient IV-3 with both mandibular and ocular abnormalities.

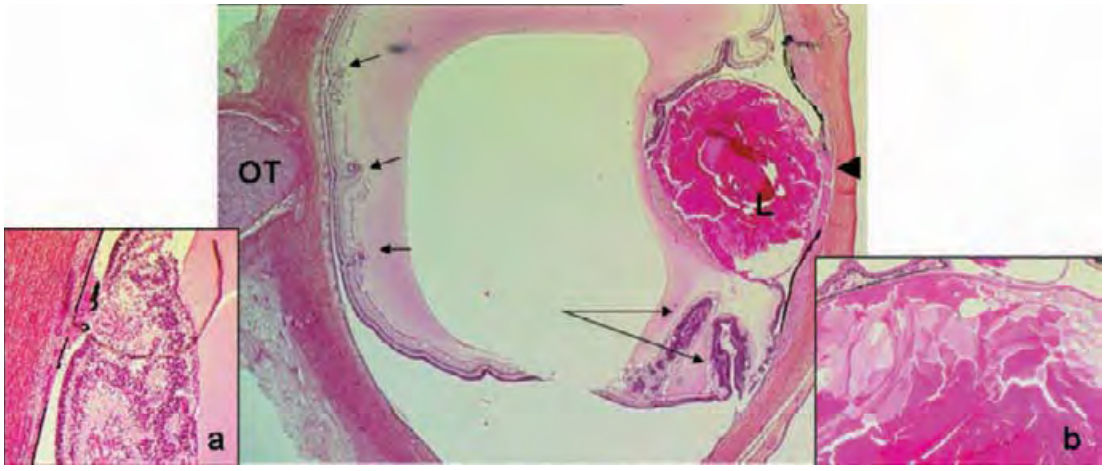

Anteroposterior sagittal section of eye through optic tract (OT), H&E staining. Note retinal dysplasia (arrows), shown with higher magnification in a; cataract (lens (L) disorganization and vacuolization, shown in higher magnification in b, absent anterior chamber (arrow head).

Supplementary Figure 3: Knockdown efficiency of *otx2*, *pgap1*, *prrx1a* and *prrx1b* morpholino antisense oligonucleotides.

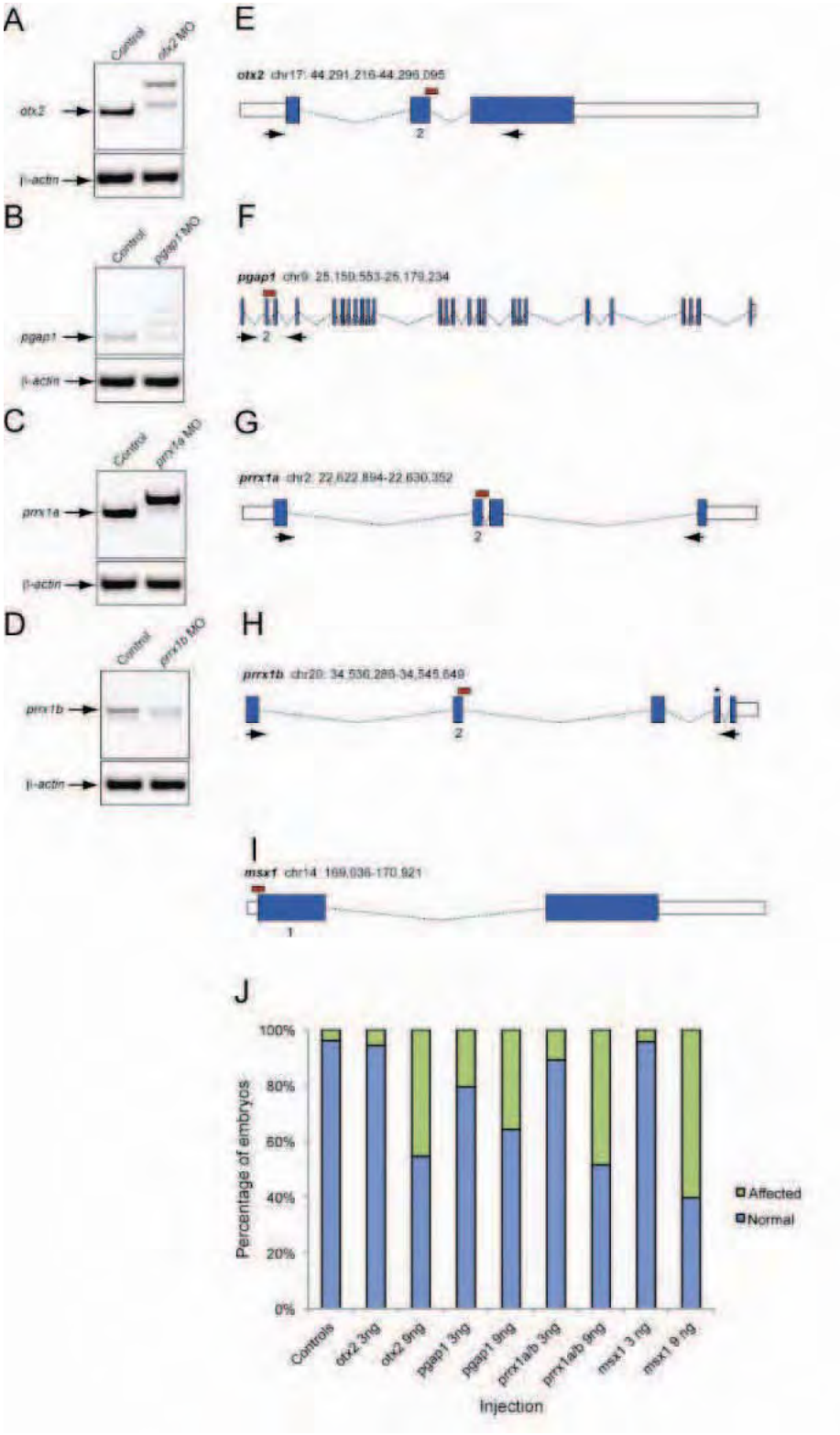

(**A-D**) We injected 9ng of each of *otx2*, *pgap1*, *prrx1a* and *prrx1b* splice-blocking morpholinos (MO)s into wild-type zebrafish embryos at the one to two cell stage and harvested embryos for total RNA extraction at 5 days post-fertilization (n=25 embryos/injection batch). cDNA was generated from oligo-dT primed reverse transcription reactions and subsequently PCR amplified for each gene of interest. 2% agarose gel electrophoresis images are shown for each reaction demonstrating aberrant splicing products in MO injected embryos in comparison to controls. Two PCR products are present for *prrx1b* in controls due to alternative splicing of exon 4 (asterisk in panel H). β-actin was amplified to control for RNA integrity.

(**E-I**) Schematic representations of each gene targeted for *otx2* genetic interaction studies. Each gene and Zv9 genomic coordinate are shown; boxes represent exons, white boxes depict untranslated regions and blue boxes depict coding regions. Red boxes indicate MO target sites and the targeted exon is indicated with the number underneath. Arrows indicate the position of primers used for RT-PCR experiments shown in panels A-D. Asterisk (*) in panel H indicates an alternatively spliced exon.

(**J**) Dose response curves for each of *otx2*, *pgap1*, *prrx1a*, *prrx1b*, and *msx1.* We injected each MO into wt zebrafish embryos at two different concentrations (3ng and 9ng each) and qualitatively scored for craniofacial defects in 5dpf Alcian blue stained embryos (n=35-53 embryos/injection, repeated twice with masked scoring).

Supplementary Table 1: Primers and PCR conditions used to amplify *OTX2*, *ALX4*, *MSX1*, *PGAP1*, *PRRX1*, and *TWSG1* genes.

Gene	Exon	Forward Primer	Reverse Primer	Length (base)	Annealing Temperature (°C)
OTX2	1-1	AAGTTAGTGCTGGAACGTGGA	TGCTAAGGTTGTTTGGAGGTG	203	56
OTX2	1-2	CCACCAAGGACTCTGAACCT	GAAGAGGGGTGCGGGAGT	232	56
OTX2	2	CGCCTATGACTGAGAAACTGC	ATCAGGAAGGATGGTTCTGC	247	56
OTX2	3-1	CCTTAAGAACTATCAAACCGAGT	ACTGCTGCTGGCAATGGT	239	56
OTX2	3-2	ACAAGTGGCCAATTCACTCC	ATGCCCCCAAAGTAGGAAGT	218	56
OTX2	3-3	GCAGAGGTCCTATCCCATGA	CTGGGTGGAAAGAGAAGCTG	211	56
OTX2	3-4	ATGGGTACCAATGCAGTCAC	TCACCCACAAAAAGAGGTTCT	236	56
ALX4	1	AAACTCCCAGCCAAGGCGCGCG	AAGCCAAGCACCCCGTGGTCCCC	596	55
ALX4	2	CTCTTGTTTGGTTCAACCATTGG	TGCTTTACCAGCCTCACTCCC	400	58
ALX4	3	TCCAGGCGGGCATCTCACCC	TTCTCAGAGCACCAGGGGCTGG	234	58
ALX4	4	AGGTGCTCTGGGGGAAGGGGCGAG	AGAGCAGAGGAGTGGGCGGG	738	60
MSX1	1-1	GAGCTGGCCTGCTGGGGAGG	CACGCTGAAGGGCAGGAGCG	346	55
MSX1	1-2	CGGTGTCAAAGTGGAGGACTCCGCC	TTGCAGCCCACGGCTCCCTA	566	55
MSX1	2-1	GAGGCACTTGGCGGCACTCA	CATGGGCTTGGCGGCCATCT	385	55
MSX1	2-2	CGCGGAGTTCTCCAGCTCGC	GCACGTCGGGGGTACAGCAC	375	55
PGAP1	1	CGC TGC AAC ACC TAC TCC TC	CGA ACC CAC AGA AGG AAA AA	473	57
PGAP1	2	TTGCATATGGTGAGGCTGAA	CACCGAGTATGGATATGATTCAA	298	60
PGAP1	3	TGAAGAAAGAATGGATGAAACC	AAAAAGGTGCCGATAGGTTG	293	60
PGAP1	4	AAAATTGGTCATATGCAGAGAGAA	CAATGGGGAGGTTAATGTTCA	294	60
PGAP1	5	TGTTTCAGGGAATGGCTACTG	TTTCATGCTCCACTGGGTCT	271	57
PGAP1	6	GAATAACAAATGTGCTTTTCGTAAG	ATTGCACCACTGTCCTCCA	248	60
PGAP1	7	AAAGGAAACTCAAATGTTCCAC	TCCATCATGGCTGTAAATGA	244	60
PGAP1	8	TGTTGGCTGTTGTCATCATT	CACAGTTTCAAAGATTTTGTCTGC	293	60
PGAP1	9	TTTCACCAGGATTCAAAGAAGAA	AAAATGGCATGCAGTTATCTTG	245	57
PGAP1	10	TCTGGATTTTTGAATGATGAAA	TTGAAAAATGAACAACAGTTAGCC	213	57
PGAP1	11/12	TTGAAAATGGGTGTTTGTTTTG	ACCAAGATAAGCTAATGAAAGAGAA	629	60
PGAP1	13	AAATTGGAAGCCTGCTTTTTA	GCATGTGTCTCCAAAACATTCT	245	60
PGAP1	14	TGATACTTTCTCCAAAGCTGAGGT	GCAATTCTTATGCTTTCCAAAA	234	60
PGAP1	15/16	AATTATTGGCATTGTCTTAATGCT	CACCTATTGAGTCTTCAAATGACA A	388	60

PGAP1	17	TTTAGGAATTCGCCATAATTTTT	TTCAAAAACACCAAAGTTTAAAGTAA	267	57
PGAP1	18	CCAGCATTTTGTATTTGAGAATTG	CATGCCACCATATATCTGAAGC	247	60
PGAP1	19	TTGCATGGTGGTTCAAAAGA	AAATAATCAACCAGCCAGGAA	237	57
PGAP1	20	GAAGAGCAACTTTTAAATTTTATGTGA	TTATGTCTCCTGATTCAATATAACAGA	296	60
PGAP1	21	GCTGTTTTAGAGAACGTGGGATA	TTGCATTATGGAACCAAATATAATG	245	60
PGAP1	22	CCTTAAATTTCAGTTGTTGGGTTT	CTTAAAGCAATAAGAAAGCTGTTAATC	291	60
PGAP1	23	GCAAGAGAGACTGGGAGGGA	TGCCTAATACAAAGCTCAATCA	282	60
PGAP1	24	CATTTCAGATTACAGTGCTTCTCA	TTTCCCCATGTTCTTTCATTTT	204	57
PGAP1	25	TGTCAGTTTGGTAATGGAAAGATG	AGGGATATTTATTGTTTGAACCAC	359	60
PGAP1	26	CAGGTCATTGTTGATTTGTGG	GGAAAAAGGCCAAGAACAGA	199	60
PGAP1	27	TGGCTCACAATGTAGTTCACA	CCCTCTTATCACTGGCCCTA	250	60
PRRX1	1	GGTGTTGATTCGAGCGGGAAGA	GCTCTAGCTGCCCTACACGGG	368	58
PRRX1	2	TGGGACTCCTACAGTGAATTTGGCT	TGGTGCCAGCCTCTCACAGC	257	58
PRRX1	3	TGCCTTCTTGCCTCCTAACAATCCT	AGCTTGAAACATGACCGACCGCT	281	58
PRRX1	4a	ATCTGGGGCACAGACTTGCAGC	CTGCTTTTCTCTGCCATGGTCCCAA	369	58
PRRX1	4b	ACATCTGCTGAACGCATTTG	CTGCAACCCCCACTTTCTTA	211	60
TWSG1	2	CCCTAGCACTTGCCTTTGAA	TGATTCAGTACCTCAGGCCC	340	59
TWSG1	3	TGCAAATATGGCAGGGTTTT	TCTTAAAGCCAAGGATTCTGTGA	251	59
TWSG1	4	GTTATAGCTCTGATTGCAAGGC	GCGGAATGGAAAAAGTCAAC	361	59
TWSG1	5	CTTTCTTGCCCTGAAATCTTAA	AGGAATTCTCTGCGCACCT	490	59

Products were amplified in 25 µl reactions containing 50 ng genomic DNA, 1X PCR buffer, 0.2 mM dNTPs, 2mM MgCl2, 100 nM forward primer, 100 nM reverse primer, and 1 U of Taq polymerase. 10 % DMSO was added in PCR for exon 1 of *PGAP1*, 1-1 and 1-2 of *MSX1*. 1 Mol Betain was added in PCR for exon 1-1 and 2-2 of *MSX1*. All PCR reactions were performed with a 5 minutes 95°C denaturing step, followed by 35 cycles of 95°C for 30 seconds, annealing temperature for 30 seconds and 72°C for 45 seconds with a final elongation step of 72°C for 7 minutes. Primer pairs and annealing temperatures are listed above. Both DNA strands were sequenced using the Big Dye™ Terminator Cycle Sequencing Ready Reaction Kit (PE Applied Biosystems). Sequence variations were numbered with the adenine of the ATG initiation codon as

the first nucleotide. GenBank accession numbers: NM_021728.2 (*OTX2*), NM_021926.3 (*ALX4)*, NM_002448.3 (*MSX1*), NM_024989.3 (*PGAP1*), NM_006902.3 and NM_022716.2 *(PRRX1),* and NM_020648.5 (*TWSG1*).

Supplementary Table 2: Summary of the sequence variations identified in *OTX2* and suspected modifier genes (*ALX4*, *MSX1*, *PGAP1*, *PRRX1*, and *TWSG1*) in otocephalic patients and their relatives.

Family	Patient	Phenotype	Genotype					
			OTX2	***ALX4***	***MSX1***	***PGAP1***	***PRRX1***	***TWSG1***
A	**II-4**	M/A	c.316delC p.Gln106AsnfsX11 heterozygous	c.621A>G (p.Ser207Ser) homozygous c.*228C>T heterozygous	-	-	nd	-
A	**III-2**	M/A	c.316delC p.Gln106AsnfsX11 heterozygous	c.621A>G (p.Ser207Ser) homozygous c.729G>A (p.Ala243Ala) heterozygous	-	-	nd	-
A	**III-4**	M/A	c.316delC p.Gln106AsnfsX11 heterozygous	c.104G>C (p.Arg35Thr) heterozygous c.304C>T (p.Pro102Ser) heterozygous c.621A>G (p.Ser207Ser) homozygous c.*228C>T homozygous	-	-	nd	c.470C>T (p.Ala157Val) heterozygous
A	**III-7**	Int	c.316delC p.Gln106AsnfsX11 heterozygous	c.621A>G (p.Ser207Ser) homozygous	-	-	nd	-
A	**III-8**	Asympt	-	c.304C>T (p.Pro102Ser) heterozygous c.621A>G (p.Ser207Ser) homozygous c.1074C>T (p.His358Gln) heterozygous	c.119C>G (p.Ala40Gly) heterozygous c.348C>T (p.Gly116Gly) heterozygous c.*+6C>T heterozygous	1-94G>A heterozygous	-	-
A	**IV-3**	Int	c.316delC	c.104G>C	c.119C>G	-	-	c.470C>T

			p.Gln106AsnfsX11 heterozygous	(p.Arg35Thr) homozygous c.304C>T (p.Pro102Ser) heterozygous c.621A>G (p.Ser207Ser) homozygous 778-11G>A heterozygous c.*228C>T heterozygous	(p.Ala40Gly) heterozygous			(p.Ala157Val) heterozygous
A	**IV-5**	M/A	c.316delC p.Gln106AsnfsX11 heterozygous	c.621A>G (p.Ser207Ser) homozygous	c.348C>T (p.Gly116Gly) heterozygous	1-94G>A heterozygous	nd	-
A	**IV-7**	M/A	c.316delC p.Gln106AsnfsX11 heterozygous	c.621A>G (p.Ser207Ser) homozygous c.729G>A (p.Ala243Ala) heterozygous	c.119C>G (p.Ala40Gly) heterozygous c.*+6C>T heterozygous	-	nd	-
B	**I-1**	Asympt	-	c.104G>C (p.Arg35Thr) homozygous c.621A>G (p.Ser207Ser) homozygous c.729G>A (p.Ala243Ala) heterozygous	c.119C>G (p.Ala40Gly) heterozygous	c.906T>C p.Leu302Leu heterozygous	nd	nd
B	**I-2**	Asympt	-	c.104G>C (p.Arg35Thr) homozygous c.621A>G (p.Ser207Ser) homozygous c.1074C>T (p.His358Gln) heterozygous	c.119C>G (p.Ala40Gly) hetrozygous	-	nd	nd

B	**II-1 (Oto1)**	Oto	c.130delC p.Arg44GlyfsX15 heterozygous	c.104G>C (p.Arg35Thr) homozygous c.304C>T (p.Pro102Ser) heterozygous c.621A>G (p.Ser207Ser) homozygous c.1074C>T (p.His358Gln) heterozygous	c.119C>G (p.Ala40Gly) heterozygous	c.906T>C p.Leu302Leu heterozygous	-	-
[1]	**Oto 2**	Oto	-	c.621A>G (p.Ser207Ser) homozygous c.1074C>T (p.His358Gln) homozygous	c.119C>G (p.Ala40Gly) heterozygous c.*+6C>T heterozygous	-	-	-

Unpublished	**Oto 3**	Oto	-	c.63C>T (p.Tyr21Tyr) heterozygous c.104G>C (p.Arg35Thr) homozygous c.304C>T (p.Pro102Ser) homozygous c.621A>G (p.Ser207Ser) homozygous c.*228C>T heterozygous	-	1-115C>T heterozygous 927+31A>G heterozygous	-	-
Unpublished	**Oto 4**	Oto	-	nd	nd	nd	nd	nd
[2]	**Oto 5**	Oto	-	nd	nd	nd	nd	nd
[3]	**Oto 6**	Oto	-	c.621A>G (p.Ser207Ser) homozygous c.*228C>T heterozygous	-	-	-	-
[4]	**Oto 7**	Oto	-	nd	nd	nd	nd	nd
[5]	**Oto 8**	Oto	-	nd	nd	nd	nd	nd
Unpublished	**Oto 9**	Oto	-	c.621A>G (p.Ser207Ser) homozygous	c.119C>G (p.Ala40Gly) heterozygous	-	-	-

M/A: microphthalmia/anophthalmia; Asympt: asymptomatic; Int; intermediate phenotype associating both ocular and mandibular features; Oto: otocephaly; -: absence of sequence variation identified; nd: not done.

REFERENCES

1. Chen CP, Chang TY, Huang JK, *et al.* Early second-trimester diagnosis of fetal otocephaly. *Ultrasound Obstet Gynecol* 2007;**29**(4):470-1.
2. Carles D, Serville F, Mainguene M, *et al.* Cyclopia-otocephaly association: a new case of the most severe variant of agnathia-holoprosencephaly complex. *J Craniofac Genet Dev Biol* 1987;**7**(2):107-13.
3. Faye-Petersen O, David E, Rangwala N, *et al.* Otocephaly: report of five new cases and a literature review. *Fetal Pediatr Pathol* 2006;**25**(5):277-96.
4. Puvabanditsin S, Garrow E, Umaru S, *et al.* Otocephaly, and pulmonary malformation association: two case reports. *Genet Couns* 2006;**17**(2):167-71.
5. Schiffer C, Tariverdian G, Schiesser M, *et al.* Agnathia-otocephaly complex: report of three cases with involvement of two different Carnegie stages. *Am J Med Genet* 2002;**112**(2):203-8.

Supplementary Table 3: Summary of *OTX2* mutations

Nucleotide Change		Mutation	Amino Acid Change		References
Variant 1 NM_021728.2	**Variant 2 NM_172337.1**	**Type**	**Isoform a NP_068374.1**	**Isoform b NP_758840.1**	
81delC	81delC	frameshift	Ser28ProfsX31	Ser28ProfsX31	[1]
93C>G	93C>G	nonsense	Tyr31X	Tyr31X	[2]
130dupC	106dupC	frameshift	Arg44ProfsX52	Arg36ProfsX52	[2]
130delC	106delC	frameshift	Arg44GlyfsX15	Arg36GlyfsX15	This study Family B
141_142delCC	117_118delCC	frameshift	Arg48GlyfsX47	Arg40GlyfsX47	[1]
160dupA	136dupA	frameshift	Thr54AsnfsX42	Thr46AsnfsX42	[3]
227G>C	203G>C	missense	Arg76Pro	Arg68Pro	[4]
238_240delGCACinsCA	214_216delGCACinsCA	frameshift	Ala80fsX86	Ala72fsX86	[5]
245_260del16	221-236del16	frameshift	Lys82fsX103	Lys74fsX103	[5]
289C>T	265C>T	nonsense	Arg97X	Arg89X	[6]
289C>G	265C>G	missense	Arg97Gly	Arg89Gly	[1]
294A>T	270A>T	missense	Arg98Ser	Arg90Ser	[7]
313C>T	289C>T	nonsense	Gln105X	Gln97X	[2]
316delC	292delC	frameshift	Gln106AsnfsX11	Gln98AsnfsX11	This study Family A
319C>T	295C>T	nonsense	Gln107X	Gln99X	[1]
337C>T	313C>T	nonsense	Gln113X	Gln105X	[3]
395_396delAG	371_372delAG	frameshift	Ser133TrpfsX11	Ser125TrpfsX11	[2]
413C>G	389C>G	nonsense	Ser138X	Ser130X	[8]
421C>A	397C>A	missense	Pro141Thr	Pro133Thr	[1]
424C>G	400C>G	missense	Pro142Ala	Pro134Ala	[1]

426dupC	402dupC	frameshift	Ser143LeufsX2	Ser135LeufsX2	[9]
428_429dupCT	404_405dupCT	frameshift	Ser144LeufsX43	Ser136LeufsX43	[10]
480_481delGAinsAT	456_457delGAinsAT	nonsense	Trp160X	Trp152X	[3]
487_488dupGC	463_464dupGC	frameshift	Ser164LeufsX23	Ser156LeufsX23	[1]
561T>A	537T>A	nonsense	Tyr187X	Tyr179X	[1]
577_580dupTATA	553_556dupTATA	frameshift	Ser194IlefsX2	Ser186IlefsX2	[3]
586G>T	564G>T	nonsense	Gly196X	Gly188X	[5]
674A>G	650A>G	missense	Asn233Ser	Asn225Ser	[11]
Whole gene deletion					[2, 5, 12]

Sequence variations were numbered with adenine of the ATG initiation codon considered as the first nucleotide. All mutations have been numbered according to GenBank accession numbers NM_021728.2 and NM_172337.1.

REFERENCES

1. Ragge NK, Brown AG, Poloschek CM, Lorenz B, Henderson RA, Clarke MP, Russell-Eggitt I, Fielder A, Gerrelli D, Martinez-Barbera JP, Ruddle P, Hurst J, Collin JR, Salt A, Cooper ST, Thompson PJ, Sisodiya SM, Williamson KA, Fitzpatrick DR, van Heyningen V, Hanson IM. Heterozygous mutations of OTX2 cause severe ocular malformations. *Am J Hum Genet* 2005;**76**(6):1008-22.
2. Wyatt A, Bakrania P, Bunyan DJ, Osborne RJ, Crolla JA, Salt A, Ayuso C, Newbury-Ecob R, Abou-Rayyah Y, Collin JR, Robinson D, Ragge N. Novel heterozygous OTX2 mutations and whole gene deletions in anophthalmia, microphthalmia and coloboma. *Hum Mutat* 2008;**29**(11):E278-83.
3. Schilter KF, Schneider A, Bardakjian T, Soucy JF, Tyler RC, Reis LM, Semina EV. OTX2 microphthalmia syndrome: four novel mutations and delineation of a phenotype. *Clin Genet* 2011;**79**(2):158-68.
4. You T, Lv Y, Liu S, Li F, Zhao Y, Lv J, Qiu G, Li-Ling J. Novel OTX2 mutation associated with congenital anophthalmia and microphthalmia in a Han Chinese family. *Acta Ophthalmol* 2012:doi: 10.1111/j.1755-3768.2011.02345.x.
5. Dateki S, Kosaka K, Hasegawa K, Tanaka H, Azuma N, Yokoya S, Muroya K, Adachi M, Tajima T, Motomura K, Kinoshita E, Moriuchi H, Sato N, Fukami M, Ogata T. Heterozygous orthodenticle homeobox 2 mutations are associated with variable pituitary phenotype. *J Clin Endocrinol Metab* 2010;**95**(2):756-64.
6. Gonzalez-Rodriguez J, Pelcastre EL, Tovilla-Canales JL, Garcia-Ortiz JE, Amato-Almanza M, Villanueva-Mendoza C, Espinosa-Mattar Z, Zenteno JC. Mutational screening of CHX10, GDF6, OTX2, RAX and SOX2 genes in 50 unrelated microphthalmia-anophthalmia-coloboma (MAC) spectrum cases. *Br J Ophthalmol* 2010;**94**(8):1100-4.
7. Ashkenazi-Hoffnung L, Lebenthal Y, Wyatt AW, Ragge NK, Dateki S, Fukami M, Ogata T, Phillip M, Gat-Yablonski G. A novel loss-of-function mutation in OTX2 in a patient with anophthalmia and isolated growth hormone deficiency. *Hum Genet* 2010;**127**(6):721-9.
8. Henderson RH, Williamson KA, Kennedy JS, Webster AR, Holder GE, Robson AG, FitzPatrick DR, van Heyningen V, Moore AT. A rare de novo nonsense mutation in OTX2 causes early onset retinal dystrophy and pituitary dysfunction. *Mol Vis* 2009;**15**:2442-7.

9. Dateki S, Fukami M, Sato N, Muroya K, Adachi M, Ogata T. OTX2 mutation in a patient with anophthalmia, short stature, and partial growth hormone deficiency: functional studies using the IRBP, HESX1, and POU1F1 promoters. *J Clin Endocrinol Metab* 2008;**93**(10):3697-702.

10. Tajima T, Ohtake A, Hoshino M, Amemiya S, Sasaki N, Ishizu K, Fujieda K. OTX2 loss of function mutation causes anophthalmia and combined pituitary hormone deficiency with a small anterior and ectopic posterior pituitary. *J Clin Endocrinol Metab* 2009;**94**(1):314-9.

11. Diaczok D, Romero C, Zunich J, Marshall I, Radovick S. A novel dominant negative mutation of OTX2 associated with combined pituitary hormone deficiency. *J Clin Endocrinol Metab* 2008;**93**(11):4351-9.

12. Delahaye A, Bitoun P, Drunat S, Gerard-Blanluet M, Chassaing N, Toutain A, Verloes A, Gatelais F, Legendre M, Faivre L, Passemard S, Aboura A, Kaltenbach S, Quentin S, Dupont C, Tabet AC, Amselem S, Elion J, Gressens P, Pipiras E, Benzacken B. Genomic imbalances detected by array-CGH in patients with syndromal ocular developmental anomalies. *Eur J Hum Genet* 2012(doi: 10.1038/ejhg.2011.233.).

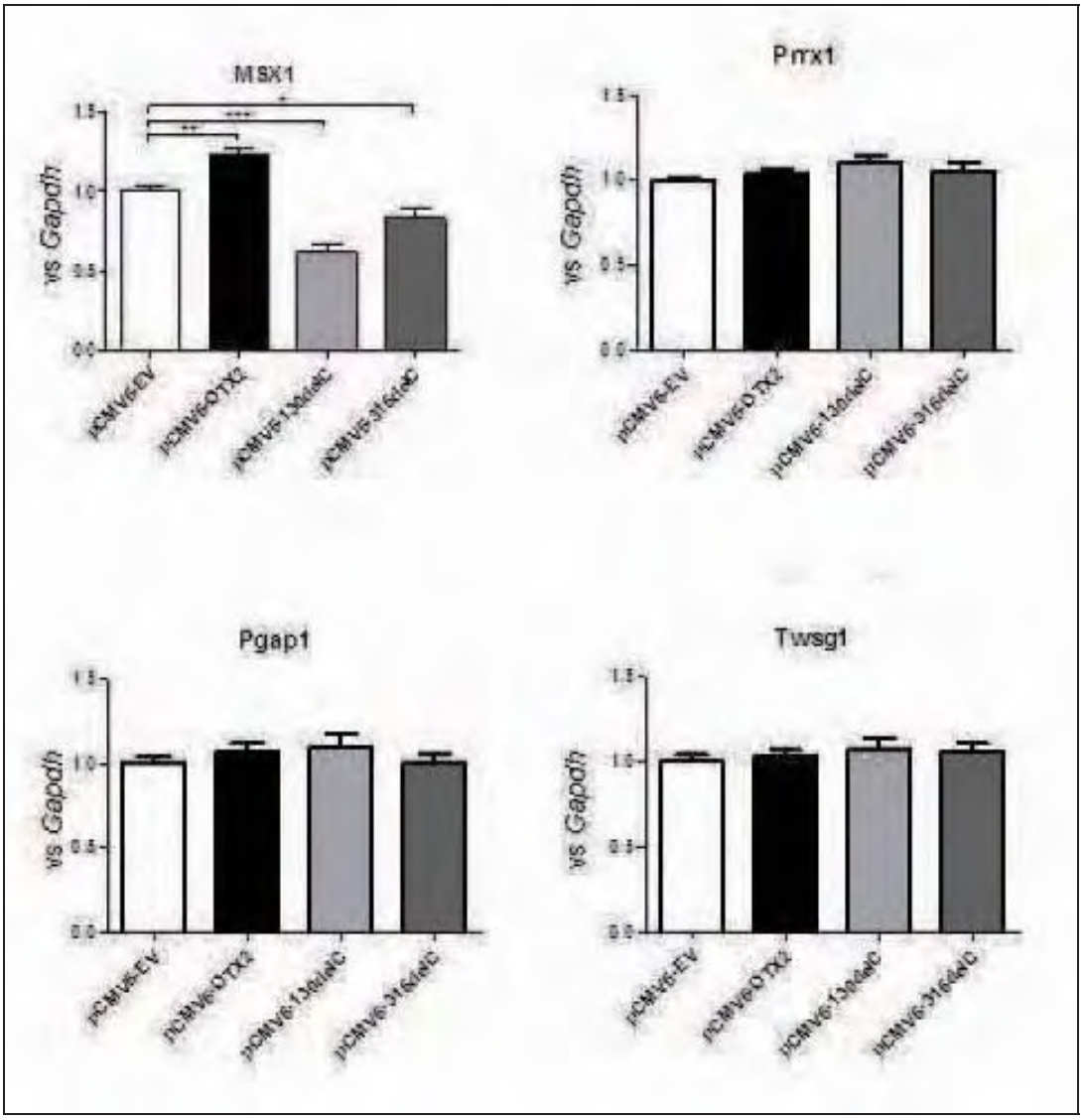

Figure 25: Analyse d'expression des gènes impliqués dans l'otocéphalie chez l'homme et/ou la souris après transfection par un vecteur exprimant *OTX2* normal ou muté

La transfection dans des cellules 3T3 du vecteur d'expression OTX2 (pCMV6-OTX2) entraine une augmentation faible, mais statistiquement significative, de l'expression du gène *Msx1* par rapport à la transfection d'un vecteur vide (pCMV-EV). La transfection par des vecteurs d'expression OTX2 porteur des mutations identifiées chez les patients otocéphales (pCMV-130delC ou pCMV-316delC) n'entraine pas de modification de l'expression du gène *Msx1* suggérant une perte de fonction de la protéine secondaire à ces mutations. L'expression des gènes *Prrx1*, *Pgap1* et *Twsg1* n'est pas modifiée quelle que soit la construction transfectée.

ARTICLE 5

Otocephaly-Dysgnathia Complex:

description of four cases and confirmation of the role of *OTX2*

Molecular Syndromology

2013-4: 302–305

O. Patat*, C. M. A. van Ravenswaaij-Arts*, J. Tantau, N. Corsten-Janssen,

J. P. van Tintelen, T. Dijkhuizen, J. Kaplan and **N. Chassaing**

Dans les suites de notre publication démontrant le lien entre *OTX2* et otocéphalie, nous avons été contactés par une équipe hollandaise pour tester trois de leurs patients otocéphales dont un était porteur d'une délétion d'environ 400 kb n'emportant que le gène *OTX2*.

Aucune mutation des gènes *OTX2* et *PRRX1* n'a pu être mise en évidence chez les deux autres patients.

Tandis que nous réalisions les analyses moléculaires sur ces trois patients, une interruption de grossesse a été réalisée chez une patiente à la suite de la découverte anténatale de signes d'otocéphalie chez l'enfant à naître. Cette patiente était atteinte de microphtalmie unilatérale, et une mutation non-sens du gène *OTX2* avait été précédemment identifiée chez elle dans notre laboratoire. L'analyse moléculaire a confirmé la présence de la mutation familiale chez le fœtus. Cette observation, confirme la variabilité d'expression clinique des mutations de ce gène. Cette donnée est importante en termes de conseil génétique.

Dans cet article, nous rapportons les données phénotypiques et moléculaires de ces quatre patients.

Short Report

Molecular Syndromology

Mol Syndromol 2013;4:302–305
DOI: 10.1159/000353727

Accepted: May 22, 2013
by M. Schmid
Published online: July 9, 2013

Otocephaly-Dysgnathia Complex: Description of Four Cases and Confirmation of the Role of *OTX2*

O. Patat[a] C.M.A. van Ravenswaaij-Arts[f] J. Tantau[c–e] N. Corsten-Janssen[f]
J.P. van Tintelen[f] T. Dijkhuizen[f] J. Kaplan[c–e] N. Chassaing[a, b]

[a]Service de Génétique Médicale, Hôpital Purpan, CHU Toulouse, and [b]EA 4555, Université Paul-Sabatier Toulouse III, Toulouse, [c]Génétique Ophtalmologique INSERM U781, [d]Département de Génétique, APHP Hôpital Necker, and [e]Institut IMAGINE, Université Paris Descartes-Sorbonne Paris Cité, Paris, France; [f]Department of Genetics, University Medical Center Groningen, University of Groningen, Groningen, The Netherlands

Key Words
Agnathia · Microphthalmia · Otocephaly · OTX2 · PRRX1

Abstract
Otocephaly-dysgnathia complex is characterized by mandibular hypo- or aplasia, ear abnormalities, microstomia, and microglossia. Mutations in the orthodenticle homeobox 2 *(OTX2)* and paired related homeobox 1 *(PRRX1)* genes have recently been identified in some cases. We screened 4 otocephalic cases for these 2 genes and identified *OTX2* mutations in 2 of them, thus confirming *OTX2* is implicated in otocephaly. No *PRRX1* mutation was identified. Interestingly, ocular involvement is not a constant feature in otocephalic cases with an *OTX2* mutation. In one case, the mutation was inherited from a microphthalmic mother. The mechanism underlying this intrafamilial phenotypic variability remains unclear, but other genetic factors are likely to be necessary for the manifestation of the otocephalic phenotype.

O.P. and C.M.A.v.R.-A. contributed equally to this work.

Otocephaly-dysgnathia complex (ODC, OMIM 202650) is a rare malformation characterized by the association of agnathia or mandibular hypoplasia, anteromedial malposition of the ears (melotia) which can be merged into one median ear (synotia), microstomia, and aglossia or lingual hypoplasia [Gekas et al., 2010]. Association with holoprosencephaly, microphthalmia or anophthalmia, pituitary hypoplasia, and malformation of the extremities have been reported [Gekas et al., 2010]. The incidence of ODC is estimated to be 1 per 70,000 births. Paired related homeobox 1 *(PRRX1)* was the first gene to be associated with ODC, and to date, *PRRX1* mutations have been identified in 4 cases [Sergi and Kamnasaran, 2011; Celik et al., 2012; Donnelly et al., 2012; Dasouki et al., 2013]. Mutations of the orthodenticle homeobox 2 *(OTX2)* gene were more recently implicated in ODC in 2 families [Chassaing et al., 2012]. Apart from a personal or family history of ocular involvement described in some ODC patients with *OTX2* mutations, the phenotypes appear similar between ODC patients mutated either in *OTX2* or *PRRX1*. The molecular basis of this severe developmental disorder remains unclear in the majority of cases [Celik et al., 2012; Chassaing et al., 2012].

KARGER

E-Mail karger@karger.com
www.karger.com/msy

1661–8769/13/0046–0302$38.00/0

Nicolas Chassaing
Service de Génétique Médicale, Pavillon Lefebvre, CHU Purpan
Place du Dr Baylac
FR–31059 Toulouse Cedex 9 (France)
E-Mail chassaing.n@chu-toulouse.fr

Fig. 1. Photographs and X-rays of otocephalic case 1 (**A–C**), case 2 (**D–F**), case 3 (**G–I**), and case 4 (**K–M**). Cardinal features of ODC include: severe micrognathia (cases 2 and 3) or agnathia (cases 1 and 4), microstomia (present in all 4 cases) and low set ears (present in all 4 cases) with sometimes anteromedial position (melotia, cases 1 and 4). All 4 patients have downslanting palpebral fissures.

Here, we report 4 cases with ODC, of which one was described previously [Kauvar et al., 2010]. We searched for mutations in the *OTX2* and *PRRX1* genes and identified *OTX2* mutations in 2 cases. The clinical and molecular results of our 4 cases are described and compared to other reports.

Patients and Methods

Cases

Case 1

This boy was the second child of healthy, nonconsanguineous parents (father 39, mother 36 years old). The pregnancy was uneventful until 28 weeks of gestation, when an amniocentesis was performed because of an unexplained polyhydramnios. The karyotype was normal: 46,XY. The boy was born at 30 weeks of gestation. At birth, the absence of the mandible resulted in an airway obstruction causing an immediate respiratory distress. Intubation was impossible because of a severe microstomia. He died within the first hour of life. The boy weighed 1,505 g (40th percentile) with a length of 41.5 cm (50th percentile) and head circumference of 29.5 cm (60th percentile). He had a severe malformation of the face, including agenesis of the mandible, microstomia and persistent buccopharyngeal membrane (fig. 1A–C). The ears were dysmorphic and anterocaudally positioned. On external inspection, the eyes were normal, and besides mild club feet, no other malformations were noted. No aberrations of the central nervous system were found on macroscopic or microscopic neuropathological examination. Heart, urogenital and intestinal organs were normal. There was no situs abnormality.

Case 2

This female has been reported previously [Kauvar et al., 2010]. She weighed 525 g (10th percentile) with a length of 31 cm (10–50th percentile) and a head circumference of 19.5 cm (3rd–10th percentile) at almost 24 weeks of gestation after an, until then, uncomplicated pregnancy (mother was 17 years old). She died during delivery and had extreme micrognathia with microstomia but a normal position of the ears with overfolded helices, downslanting palpebral fissures and camptodactyly of the fourth and fifth digits. Postmortem X-rays showed extreme micrognathia (fig. 1D–F) and 13 ribs bilaterally. Head and brain MRI showed absence of the mandible, probable choanal atresia and signs of semilobar holoprosencephaly (no central sulcus, dorsally fused ventricles, absent falx cerebri). A full-body MRI showed small kidneys and a hypoplastic spleen, but no situs abnormality. No abnormalities of the eyes were noted. The karyotype was normal: 46,XX. The parents were examined physically for signs of the holoprosencephaly spectrum, but showed no hypotelorism, midface hypoplasia, single central incisor, anosmia, or micrognathia.

Case 3

She was the first child of healthy, nonconsanguineous parents. The family history was unremarkable. A routine ultrasound at a gestational age of 25 weeks revealed a polyhydramnios. An amniocentesis was performed showing a normal 46,XX karyotype. An additional ultrasound showed severe microretrognathia and ear abnormalities. She was born at 26 weeks and 2 days of gestation and died within 90 min of birth due to severe respiratory failure. She weighed 800 g (50th percentile) and had a length of 31.5 cm (20th percentile) and a head circumference of 24.5 cm (60th percentile). Severe micrognathia due to a hypoplastic mandibulum, low set dysmorphic ears, a skin tag at the left ear, and microstomia were observed (fig. 1G–I). Eyes, thorax, abdomen, genitalia, and extremities were normal. Internal organs were normal apart from a relatively high weight of heart and adrenals. No situs inversus was noticed. An X-ray revealed fusion of some ribs and a hemivertebra. Neuropathology revealed a macroscopically and microscopically normal cerebrum and cerebellum.

Case 4

The pregnancy of this male fetus was terminated at 16 weeks gestation because of agnathia associated with bilateral microphthalmia. The mother had isolated severe unilateral microphthal-

mia and was known to have a nonsense mutation (p.Arg97*) in the *OTX2* gene. She had already undergone a pregnancy interruption at 22 weeks gestation for unilateral microphthalmia without signs of mandibular malformation. Her father and her paternal grandmother were also affected by isolated unilateral microphthalmia. The male fetus presented with agnathia, astomia and aglossia, and had low, posteriorly rotated, paramedian and convergent ears. The pharyngeal floor was absent. He had bilateral microphthalmia with downslanted palpebral fissures (fig. 1K–M). The optic chiasma and pituitary gland could not be found. The abdominal and thoracic organs were normal, and there was no situs abnormality. X-rays confirmed the absence of the mandibular bone. The petrosal bone appeared smooth, and the semicircular canals were not well-shaped, but the cochlea was normal. Abnormalities of the extremities including brachymesophalangy of the fifth finger and bilateral talus valgus were present.

Molecular Screening

Informed consent for molecular analysis was obtained for each case. Genetic investigations included array-CGH (Agilent 105K) and direct sequencing of exons and flanking regions of the *PRRX1* and *OTX2* genes using previously published primer pairs [Chassaing et al., 2012]. Sequence variations were numbered considering the adenine of the ATG initiation codon as the first nucleotide (*OTX2* GenBank accession NM_021728.2).

Results

Array-CGH Analysis

Case 1 had an approximately 400-kb deletion in 14q23.1 including the whole *OTX2* gene. The proximal breakpoint was located between 56,184,175 and 56,268,038 and the distal breakpoint between 56,661,990 and 56,699,192 (oligo positions given in NCBI build 36.1/hg18 assembly). No other genes were included in the deletion. Parental analysis showed that this deletion had appeared de novo. Array-CGH revealed no non-polymorphic rearrangements for cases 2, 3 and 4.

Direct Sequencing of the PRRX1 Gene

No mutations were found in the *PRRX1* gene in our 4 cases.

Direct Sequencing of the OTX2 Gene

No additional mutations were identified in the *OTX2* gene in case 1 and no mutations were detected in cases 2 and 3. Case 4 had inherited the nonsense mutation c.289C>T (p.Arg97*) from his mother, who suffered from unilateral severe microphthalmia. He also carried a heterozygous synonymous variation c.525C>G (p.(=)) inherited from his asymptomatic father.

Discussion

The genetic basis of otocephaly is still largely unclear. To date, mutations in only 2 genes, *OTX2* and *PRRX1*, have been identified in a small number of ODC cases [Celik et al., 2012; Chassaing et al., 2012]. The most likely explanation for this is that only a small proportion of the causative genes have been identified as yet. In our small case cohort, we confirmed the role of *OTX2* in ODC and the broad phenotypic variability seen in familial *OTX2* mutations.

The first otocephalic gene described in humans was *PRRX1*, which has been involved in 3 cases reported to date. A candidate gene approach identified a heterozygous missense mutation (p.Phe113Ser) in a 30-week fetus with ODC [Sergi and Kamnasaran, 2011]. The *PRRX1* gene also appeared to be responsible for an autosomal recessive form of otocephaly. An infant born to consanguineous parents carried a nonpolymorphic *PRRX1* missense mutation (p.Ala231Pro) inherited from both parents [Celik et al., 2012]. Functional studies indicated that both missense mutations decrease the ability of the mutant protein to regulate the tenascin-C gene promoter, and as a consequence, they were considered deleterious. The finding of *PRRX1* de novo frameshift mutations (c.267delA, c.266_269dupAAAA) in 2 unrelated families confirmed its role in autosomal dominant otocephaly [Donnelly et al., 2012; Dasouki et al., 2013]. However, mutations in this gene may be involved in fewer than 15% of ODC cases [Celik et al., 2012]; in the 4 cases reported here, no *PRRX1* mutations were identified.

The second otocephalic gene identified in humans is *OTX2*. *OTX2* mutations were firstly described in cases affected by microphthalmia or anophtalmia [Ragge et al., 2005], associated with a variable ocular phenotype and incomplete penetrance. More recently, we extended the phenotype associated with an *OTX2* mutation to otocephaly [Chassaing et al., 2012]. *OTX2* is the vertebrate homologue of the gene orthodenticle *(otd)* identified in drosophila as one of the major genes controlling the development of the head [Simeone et al., 1993]. In mice, the *Otx2* gene is expressed in the mesencephalic neural crest cells which are distributed to the developing mandibular region and rostral brain region [Kimura et al., 1997]. Homozygous *Otx2* mutant mice displayed early developmental failure and total absence of the structures corresponding to the anterior (rostral) part of the head [Matsuo et al., 1995]. Heterozygous *Otx2* mutants were found to display ODC phenotypes in variable proportions depending on the genetic background of the mice, suggest-

ing a role of a modifier gene [Matsuo et al., 1995]. These mutants also inconstantly displayed anophthalmia and holoprosencephaly.

Here, we report 2 additional *OTX2*-mutation ODC cases. The phenotype of *OTX2*-mutated cases seems to be indistinguishable from that of nonmutated ODC cases. Particularly eye involvement, which was the first phenotype associated with *OTX2* mutations, is absent in 2 out of the 4 ODC cases so far reported to be due to an *OTX2* mutation. We show that such mutations in ODC cases not only occur de novo (case 1 and Chassaing et al. [2012]) but that they can also be inherited from a microphthalmic parent (case 4 and Chassaing et al. [2012]). This has serious implications for the counseling of carriers of *OTX2* mutations. The extreme intrafamilial phenotypic variability has already been reported [Chassaing et al., 2012] and argues against any genotype/phenotype correlation. All the *OTX2* mutations reported so far in otocephalic cases are assumed to lead to complete loss-of-function of the protein or absence of protein production (whole gene deletion, premature nonsense or frame shift mutations), but mutations with a similar effect have also been described in microphthalmic cases [reviewed in Chassaing et al., 2012]. The hypothesis of modifier genes was proposed to explain this extreme variability in expression, even within families. In vivo modeling experiments in zebrafish demonstrated that *otx2* can interact genetically with 3 genes (*pgap1*, *prrx1* and *msx1*) which when suppressed in concert with *otx2* lead to exacerbated craniofacial defects far exceeding the defects that result from *otx2* suppression alone. This suggests that the combinatorial effect of additional molecular lesions in the genome may explain the phenotypic variability associated with *OTX2* mutations [Chassaing et al., 2012]. However, which modifier genes are implicated in humans is unknown. Case 4, who was unique for his otocephaly in a 4-generation pedigree of autosomal dominant microphthalmia, inherited a synonymous *OTX2* variation from his healthy father, in addition to the nonsense *OTX2* mutation from his affected mother. Since the father had no abnormalities on ocular examination, it is unlikely that the silent *OTX2* variation explains the intrafamilial phenotypic variability between the fetus and his affected relatives.

Finally, the genetic cause remains unidentified in most cases of ODC. This argues for its broad genetic heterogeneity. Candidate gene approaches previously failed to identify any other genes. Further screening of cases without mutations in the *OTX2* and *PRRX1* genes and using next generation sequencing should help to decipher the molecular basis of this severe developmental defect.

Acknowledgements

The authors would like to thank the families for their participation and the following physicians for their assistance: Tania Attie-Bitach, Ton van Essen and Bert Visser (pathologist).

This work was supported by grants from the Clinical Research Hospital Program from the French Ministry of Health (PHRC 09 109 01) and from Retina France.

References

Celik T, Simsek PO, Sozen T, Ozyuncu O, Utine GE, et al: *PRRX1* is mutated in an otocephalic newborn infant conceived by consanguineous parents. Clin Genet 81:294–297 (2012).

Chassaing N, Sorrentino S, Davis EE, Martin-Coignard D, Iacovelli A, et al: *OTX2* mutations contribute to the otocephaly-dysgnathia complex. J Med Genet 49:373–379 (2012).

Dasouki M, Andrews B, Parimi P, Kamnasaran D: Recurrent agnathia-otocephaly caused by DNA replication slippage in *PRRX1*. Am J Med Genet A 161:803–808 (2013).

Donnelly M, Todd E, Wheeler M, Winn VD, Kamnasaran D: Prenatal diagnosis and identification of heterozygous frameshift mutation in *PRRX1* in an infant with agnathia-otocephaly. Prenat Diagn 32:903–905 (2012).

Gekas J, Li B, Kamnasaran D: Current perspectives on the etiology of agnathia-otocephaly. Eur J Med Genet 53:358–366 (2010).

Kauvar EF, Solomon BD, Curry CJ, van Essen AJ, Janssen N, et al: Holoprosencephaly and agnathia spectrum: presentation of two new patients and review of the literature. Am J Med Genet C Semin Med Genet 154C:158–169 (2010).

Kimura C, Takeda N, Suzuki M, Oshimura M, Aizawa S, Matsuo I: Cis-acting elements conserved between mouse and pufferfish *Otx2* genes govern the expression in mesencephalic neural crest cells. Development 124:3929–3941 (1997).

Matsuo I, Kuratani S, Kimura C, Takeda N, Aizawa S: Mouse Otx2 functions in the formation and patterning of rostral head. Genes Dev 9:2646–2658 (1995).

Ragge NK, Brown AG, Poloschek CM, Lorenz B, Henderson RA, et al: Heterozygous mutations of *OTX2* cause severe ocular malformations. Am J Hum Genet 76:1008–1022 (2005).

Sergi C, Kamnasaran D: *PRRX1* is mutated in a fetus with agnathia-otocephaly. Clin Genet 79:293–295 (2011).

Simeone A, Acampora D, Mallamaci A, Stornaiuolo A, D'Apice MR, et al: A vertebrate gene related to orthodenticle contains a homeodomain of the bicoid class and demarcates anterior neuroectoderm in the gastrulating mouse embryo. EMBO J 12:2735–2747 (1993).

III-2 : Analyse des phénotypes liés aux mutations du gène *STRA6*

Introduction

Des mutations du gène *STRA6* ont été identifiées initialement dans des familles dans lesquelles des patients étaient atteints de syndrome de Matthew-Wood. Il s'agit d'un syndrome polymalformatif associant une atteinte oculaire a type d'AM et un spectre malformatif impliquant en particulier le cœur, les poumons et le diaphragme. Ce syndrome est également appeler spectre PDAC (pour Pulmonary, Diaphragmatic, Anophthalmia, Cardiac). Nous avons pu identifier des mutations délétères du gène *STRA6* dans une famille où trois patients étaient atteints d'AM. Deux présentaient une association malformative s'intégrant dans le cadre du syndrome de Matthew-Wood et un présentait une microphtalmie sévère bilatérale associée à une déficience intellectuelle et une spina bifida L5-S1. Nous avions alors suggéré que le spectre phénotypique pouvait être plus large que l'atteinte polymalformative rapportée initialement. Plusieurs patients avec des atteintes oculaires isolées ont d'ailleurs été rapportés secondairement, et nous avons spécifiquement entrepris de déterminer le spectre phénotypique lié aux mutations du gène *STRA6*.

Méthodes et Résultats

Les travaux réalisés pour caractériser plus finement les conséquences cliniques secondaires à la présence de mutations du gène *STRA6* sont exposés dans ces trois articles :

- Article n°6

Chassaing, N *et al*. (2012). "Phenotypic spectrum of *STRA6* mutations: from Matthew-Wood syndrome to non-lethal anophthalmia." Hum Mutat 30(5): E673-81.

- Article n°7

Chassaing, N *et al*. (2013). "Mutation analysis of the *STRA6* gene in isolated and non-isolated anophthalmia/microphthalmia." Clin Genet 83(3): 244-50.

- Article n°8

Plaisancie, J. and Chassaing, N. (2013). "Microphthalmia 9 (PDAC)." Inborn Errors of Development. The molecular basis of clinical disorders of morphogenesis. Third edition.

Dans le premier article, nous décrivons les données cliniques et moléculaires de sept patients chez qui nous avons identifié des mutations du gène *STRA6*. Dans cet article, nous décrivions le premier patient porteur d'une atteinte oculaire sans autre signe cardinal du syndrome PDAC. A partir de cette observation, secondairement corrélée par d'autres publications, nous avons initié en collaboration avec le Dr Nicola Ragge (Oxford, UK) la recherche de mutation du gène *STRA6* dans une cohorte de 28 patients avec AM isolée ou associée à des éléments du spectre PDAC. Enfin, dans un troisième manuscrit, nous reprenons l'ensemble des données concernant le gène *STRA6* et les phénotypes associés.

Conclusion

Notre travail a permis de montrer la variabilité d'expression clinique avec la possibilité d'atteintes oculaires sans les autres éléments issus de l'acronyme PDAC. Nous avons également soulignés la fréquence importante de signes non inclus dans l'acronyme PDAC (tels que les atteintes du système digestif, du système rénal ou des organes génitaux externes). Enfin sur le plan moléculaire, nous avons montré l'absence de corrélation claire phénotype/génotype. Toutes ces informations sont importantes pour la prise en charge des patients et de leurs familles.

ARTICLE 6

Phenotypic spectrum of *STRA6* mutations:

from Matthew-Wood syndrome to non-lethal anophthalmia

Human Mutation

2009-30(5):E673-81

N. Chassaing, C. Golzio, S. Odent, L. Lequeux, A. Vigouroux, J. Martinovic-Bouriel, F. D. Tiziano, L. Masini, F. Piro, G. Maragliano, A. L. Delezoide, T. Attie-Bitach, S. Manouvrier-Hanu, H. C. Etchevers and P. Calvas

---

Dans le cadre du recrutement de patients AM, nous avons eu l'occasion de recenser des patients dont la présentation clinique pouvait correspondre au spectre du syndrome de Matthew-Wood. Nous avons recherché des mutations du gène, *STRA6*, qui venait d'être impliqué chez une partie des patients atteints de ce syndrome [168, 169]. Des mutations délétères ont pu être identifiées dans 4 familles différentes comportant au total 7 sujets atteints. Nous décrivons dans cet article les premiers patients adultes et les premières présentations cliniques "modérées" liées aux mutations du gène *STRA6*. Nous proposons également un lien entre les mutations de *STRA6* et le spina bifida observé chez un de nos patients. Cette étude nous a permis d'augmenter la connaissance du phénotype lié aux mutations du gène *STRA6* en apportant la description de 7 patients à un total de 14 patients précédemment décrits. De plus six nouvelles mutations sont venues préciser les atteintes liées aux 11 mutations précédemment rapportées.

HUMAN MUTATION Mutation in Brief #1066, 30:E673-681 (2009) Online

MUTATION IN BRIEF

HUMAN MUTATION

Phenotypic Spectrum of *STRA6* Mutations: from Matthew-Wood Syndrome to Non-lethal Anophthalmia

Nicolas Chassaing[1,2,3], Christelle Golzio[4,5], Sylvie Odent[6], Léopoldine Lequeux[3], Adeline Vigouroux[3], Jelena Martinovic-Bouriel[7], Francesco Danilo Tiziano[8], Lucia Masini[9], Francesca Piro[10], Giovanna Maragliano[11], Anne-Lise Delezoide[12], Tania Attié-Bitach[4,5,7], Sylvie Manouvrier-Hanu[13], Heather C. Etchevers[1,4], and Patrick Calvas[1,2,3]*

[1] *INSERM, U563, Centre de Physiopathologie de Toulouse Purpan, Toulouse, 31300 France;* [2] *Université Toulouse III Paul-Sabatier, Toulouse, 31400 France;* [3] *CHU Toulouse, Hôpital Purpan, Service de Génétique Médicale, Toulouse, 31300 France;* [4] *INSERM, U781, Hôpital Necker-Enfants Malades, Paris Cedex 15, 75743 France;* [5] *Université Paris Descartes, Hôpital Necker-Enfants Malades, Paris, 75743 France;* [6] *CHU Rennes, Hôpital Sud, Service de Génétique Médicale, Rennes, 35203 France;* [7] *Département de Génétique, Hôpital Necker-Enfants Malades, Paris Cedex 15, 75743 France*
[8] *Institute of Medical Genetics, Catholic University, Rome, Italy;* [9] *Institute of Obstetrics and Gynecology, Catholic University, Rome, Italy;* [10] *Operative Unit of Pathology, S. Giovanni Hospital, Rome, Italy;* [11] *Complex Unit of Neonatology, S. Giovanni Hospital, Rome, Italy;* [12] *GHU Nord, Hôpital Robert Debré, Service de Biologie du Développement, Paris Cedex 19, 75935 France;* [13] *CHRU Lille, Hôpital Jeanne de Flandre, Service de Génétique Clinique, Lille Cedex, 59037 France*

*Correspondence to Pr Patrick Calvas, Service de Génétique Médicale, Pavillon Lefebvre, CHU Purpan, Place du Dr Baylac, 31059 Toulouse Cedex 9, France.
Tel.: +33 5 61 77 90 79; fax: +33 5 62 74 45 58.
E-mail : calvas.p@chu-toulouse.fr

Communicated by Mark H. Paalman

ABSTRACT: Matthew-Wood, Spear, PDAC or MCOPS9 syndrome are alternative names used to refer to combinations of microphthalmia/anophthalmia, malformative cardiac defects, pulmonary dysgenesis, and diaphragmatic hernia. Recently, mutations in *STRA6*, encoding a membrane receptor for vitamin A-bearing plasma retinol binding protein, have been identified in such patients. We performed *STRA6* molecular analysis in three fetuses and one child diagnosed with Matthew-Wood syndrome and in three siblings where two adult living brothers are affected with combinations of clinical anophthalmia, tetralogy of Fallot, and mental retardation. Among these patients, six novel mutations were identified, bringing the current total of known *STRA6* mutations to seventeen. We extensively reviewed clinical data pertaining to all twenty-one reported patients with *STRA6* mutations (the seven of this report and fourteen described elsewhere) and discuss additional features that may be part of the syndrome. The clinical spectrum associated with STRA6 deficiency is even more variable than initially described. ©2009 Wiley-Liss, Inc.

KEY WORDS: *STRA6*, anophthalmia, Matthew-Wood syndrome, PDAC syndrome, MCOPS9

Received 11 December 2008; accepted revised manuscript 24 February 2009

DOI: 10.1002/humu.21023

INTRODUCTION

Variable combinations of microphthalmia/anophthalmia, pulmonary agenesis/dysplasia, diaphragmatic hernia and malformative cardiac defects have been infrequently reported over the last three decades (Ostor et al., 1978; Spear et al., 1987; Smith et al., 1994; Seller et al., 1996; Berkenstadt et al., 1999; Priolo et al., 2004; Lee et al., 2006; Li and Wei, 2006; Chitayat et al., 2007; Golzio et al., 2007; Pasutto et al., 2007). Such associations have been called Matthew-Wood or Spear syndrome, while Chitayat et al. (2007) devised the acronym PDAC (Pulmonary hypoplasia/agenesis, Diaphragmatic hernia/eventration, Anophthalmia/microphthalmia and Cardiac Defect), and the Mendelian Inheritance in Man database has adopted the term MCOPS9 for "syndromic microphthalmia 9" (MIM# 601186). Recently, mutations in *STRA6* (MIM# 610745), encoding a membrane receptor for the vitamin A-bearing plasma retinol binding protein, have been found in patients with malformations in the PDAC spectrum (Golzio et al., 2007; Pasutto et al., 2007; White et al., 2008; West et al., 2009).

We report herein novel *STRA6* mutations in three fetuses and one child diagnosed with Matthew-Wood syndrome, and in three siblings where two adult living brothers are affected with combinations of clinical anophthalmia, tetralogy of Fallot, and mental retardation. This is the first description of adult patients bearing *STRA6* mutations. These additional cases emphasize that the clinical spectrum associated with *STRA6* mutations is extremely variable.

PATIENTS AND METHODS

Patients

Case 1

This male fetus from healthy and unrelated parents was delivered at 23 weeks of gestation after an ultrasound scan documented bilateral diaphragmatic hernia, anophthalmia and cardiopathy. Autopsy confirmed the presence of bilateral severe microphthalmia (Fig 1A), bilateral diaphragmatic hernia, and a complex heart malformation (hypoplastic left heart syndrome with common atrium and dextroposition of the aorta). The lungs were hypoplastic and dysplastic. The karyotype was 46, XY.

Case 2

This patient has previously been described (Chitayat et al., 2007; patient 7). Briefly, she was the fifth child of consanguineous parents, born at term after a normal pregnancy, with normal growth parameters. She displayed an association of bilateral anophthalmia (Fig 1B), heart malformation, subglottic laryngeal stenosis, bilateral unilobar lungs, hypoplastic left kidney and right vesico-ureteral reflux, supernumerary spleen and hypoplastic uterus. Her karyotype was 46, XX. She died at 19 months post-operatively for an unknown reason, after surgery was performed to expand ocular orbits.

Family 3 (Cases 3-1, 3-2, 3-3)

Case 3-1:

A 40 year old patient was referred after his healthy sister came in for genetic counseling. He is the first child of healthy and unrelated parents. He has moderate mental retardation associated with bilateral anophthalmia and tetralogy of Fallot. Facial dysmorphy includes very short palpebral fissures and closed eyelids, a thin nasal bridge and broad nasal tip (Fig 1C). The hands are small and broad. His height is 160 cm (-2.25 SD) and his karyotype is 46, XY.

Case 3-2:

A sister of case 3-1 died in the first days of life from a tetralogy of Fallot. She reportedly had bilateral clinical anophthalmia but did not undergo autopsy.

Case 3-3:

The adult brother of cases 3-1 and 3-2 is more severely mentally retarded than case 3-1, associated with autistic features. Cerebral CT scan demonstrates small residual ocular structures and presence of optic nerves, thus indicating an extreme bilateral microphthalmia. Cardiac examination shows no malformations. Radiological findings show decreased bone mineral density and a spina bifida occulta at L5-S1.

Family 4 (cases 4-1 and 4-2)

Case 4-1:

This was the third child of consanguineous parents. At 26 weeks of pregnancy, micro/anophthalmia, congenital heart disease and diaphragmatic hernia were diagnosed by ultrasound. Karyotype analysis was performed fetal blood sample (46,XY). At 38 weeks, an elective cesarean section was performed. The child died soon after birth due to respiratory insufficiency. At autopsy, the following observations were made: anophthalmia (absent globes but presence of optic nerves), left diaphragmatic hernia with partial herniation of stomach into thorax, a complex congenital heart malformation characterized by truncus arteriosus (absence of truncal septum, single valvular orifice and short common tract). Liver, pancreas, and gut were normal both macroscopically and histologically.

Case 4-2:

Brother of case 4-1. At 26 weeks of gestation, ultrasound revealed suspicion of anophthalmia, hypoplastic left lung and complex congenital heart disease (left rotation of cardiac axis, and thickened wall of the right heart), suggesting the recurrence of a clinical phenotype strikingly similar to the previous pregnancy. The child died soon after birth, again due to respiratory insufficiency. Clinical anophthalmia (Fig 1D) and hypoplastic left lung was confirmed. Echocardiography showed left rotation of the cardiac axis secondary to lung hypoplasia, but without heart malformation.

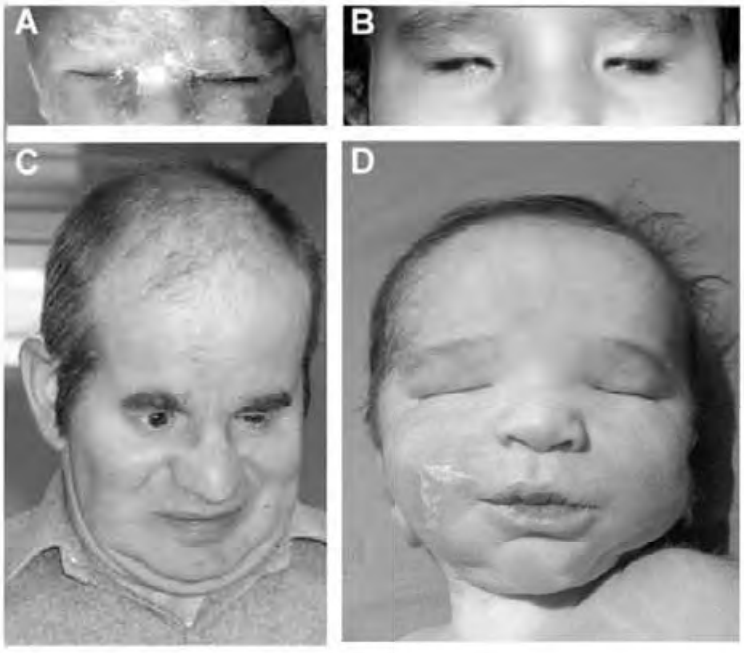

Figure 1. Representative oculofacial phenotypes. A: Case 1 had short palpebral fissures reflecting bilateral severe microphthalmia. **B**: Case 2 presented deep-set orbits, narrow palpebral fissures associated with anophthalmia and wide, diffuse implantation of eyebrows. **C:** Case 3-1 has mild facial dysmorphy with a broad nasal tip. This patient has orbital implants. **D**: Case 4-2 also had a broad nasal bridge and the deep-set orbits associated with clinical anophthalmia.

STRA6 molecular analysis

After informed consent for inclusion in the study was obtained from the parents, DNA was isolated by standard procedures from paraffin-embedded blocks of case 1, from frozen tissue samples of case 2, and from peripheral blood of cases 3-1, 3-3, 4-2 and their unaffected parents and siblings. *STRA6* noncoding and coding exons and exon-intron junctions were amplified by PCR using previously published primers (Golzio et al., 2007).

PCR fragments were subsequently purified with QIAquick Gel Extraction kits (QIAGEN SA France), and sequenced using the Big Dye DNA sequencing kit (Applied Biosystems, UK). Reactions were analyzed in an ABI3100 sequencer (Applied Biosystems, UK).

A sequence variant was considered as disease-causing when: (1) the variant cosegregated with the disease phenotype; *and* (2a) the sequence variant resulted in the prediction of a stop codon, or was predicted to lead to splice-site alteration (BDGP splice site prediction software); or (2b) the substitution involved an amino acid conserved between three vertebrate subclasses (ClustalW software) or (2c) the substitution was predicted to be functionally damaging (PolyPhen software); *and* (3) the sequence variant was absent from a panel of 200 chromosomes from unaffected, unrelated individuals.

Sequence variations were numbered based on GenBank accession NM_022369.3. Nucleotide numbering reflects cDNA numbering with +1 corresponding to the A of the ATG translation initiation codon in the reference sequence, according to journal guidelines (www.hgvs.org/mutnomen). The initiation codon is codon 1.

Table 1. PDAC/MCOPS9 features in *STRA6* mutated patients

		Nucleotide variation	Protein alteration	Lung	Diaphragm	Eyes	Heart	Other
This report	1	c.1090+1G>A c.859C>T	abnormal splicing p.Gln287X	+	+	+	+	-
	2	c.1662delG c.1662delG	p.Arg555GlufsX16 p.Arg555GlufsX16	+	-	+	+	Subglottic laryngeal stenosis Hypoplastic left kidney Right vesico-ureteral reflux Supernumerary spleen Hypoplastic uterus
	3-1	c.1313A>G c.1913G>C	p.Gln438Arg p.Arg638Pro	-	-	+	+	Mental retardation
	3-2	c.1313A>G c.1913G>C	p.Gln438Arg* p.Arg638Pro*	-	-	+	+	-
	3-3	c.1313A>G c.1913G>C	p.Gln438Arg p.Arg638Pro	-	-	+	-	Mental retardation Short stature Spina bifida occulta
	4-1	c.1329delC c.1329delC	p.Leu444TrpfsX34* p.Leu444TrpfsX34*	-	+	+	+	-
	4-2	c.1329delC c.1329delC	p.Leu444TrpfsX34 p.Leu444TrpfsX34	+	-	+	-	-

		Nucleotide variation	Protein alteration	Lung	Diaphragm	Eyes	Heart	Other
Pasutto *et al.* 2007	5	c.878C>T c.878C>T	p.Pro293Leu p.Pro293Leu	+	-	+	+	Ectopic pelvic kidney
	6	c.878C>T c.878C>T	p.Pro293Leu* p.Pro293Leu*	-	-	+	+	-
	7	c.145-147delC c.145-147delC	p.Gly50AlafsX22 p.Gly50AlafsX22	-	+	+	+	Mental retardation Short stature
	8	c.145-147delC c.145-147delC	p.Gly50AlafsX22 p.Gly50AlafsX22	-	+	+	-	-
	9	c.1963C>T c.1963C>T	p.Arg655Cys p.Arg655Cys	+	+	+	-	Hypotonia Failure to thrive
	10	c.1963C>T c.1963C>T	p.Arg655Cys* p.Arg655Cys*	-	-	+	+	-
	11	c.1931C>T c.1931C>T	p.Thr644Met p.Thr644Met	+	+	+	-	Hydronephrosis
	12	c.1931C>T c.1931C>T	p.Thr644Met* p.Thr644Met*	+	-	?	+	Horseshoe kidney
	13	c.1931C>T c.1931C>T	p.Thr644Met* p.Thr644Met*	+	-	+	+	
	14	c.269C>T c.961A>C	p.Pro90Leu p.Thr321Pro	+	+	+	+	Hypoplasic kidneys Bicornuate uterus
Golzio *et al.* 2007	15	c.50_52delACT insCC c.50_52delACT insCC	p.Asp17AlafsX55 p.Asp17AlafsX55	+	+	+	-	Annular pancreas Duodenal stenosis Intra-uterine growth retardation
	16	c.527_528insG c.527_528insG	p.Gly176GlyfsX59 p.Gly176GlyfsX59	+	+	+	+	Multilobed spleen Duodenal stenosis Pancreatic agenesis Intra-uterine growth retardation
White *et al.* 2008	17	c.650G>A c.1774C>T	p.Gly217Glu p.Gln592X	-	-	+	-	Duplicated kidney collecting system
West *et al.* 2009	18	c.31_32dupCC c.69G>A	p.Gly13ProfsX72 p.Trp23X	+	+	+	+	Intra-uterine growth retardation Cryptorchidism Bilateral inguinal hernias Thin corpus callosum
Total (%)				12/21 (57)	10/21 (48)	20/20 (100)	14/21 (67)	

+ : presence ; - : absence ; ?: unknown ;

* These patients had no molecular analysis but their genotype was deduced from that of an affected sib.

Sequence variations were numbered based on GenBank accession NM_022369.3, with +1 corresponding to the A of ATG translation initiation codon.

RESULTS AND DISCUSSION

STRA6 molecular analysis was performed in cases 1, 2, 3-1, 3-3, and 4-2. Case 1 was compound heterozygous for a splicing mutation (c.1090+1G>A) and a stop codon (c 859C>T; p.Gln287X), both leading to the prediction of premature termination of transcription. Case 2 was homozygous for the mutation c.1662delG (p.Arg555GlufsX16), with a predicted premature stop codon. Case 3-1, like case 3-3, was compound heterozygous for two missense mutations, c.1313A>G (p.Gln438Arg) and c.1913G>C (p.Arg638Pro). Mutation p.Arg638Pro was inherited from the mother and p.Gln438Arg was inherited from the father. Both mutations involved a conserved amino acid (Figure 2), and were predicted *in silico* to be damaging (Polyphen software). Case 4-2, was homozygous for the mutation c.1329delC (p.Leu444TrpfsX34) leading to a premature termination of the translation. The positions of *STRA6* mutations described to date are represented on Figure 3.

Figure 2: Alignment of part of human, murine, and avian STRA6 proteins, showing conservation of glutamine 438 and arginine 638 (shaded) in these species.

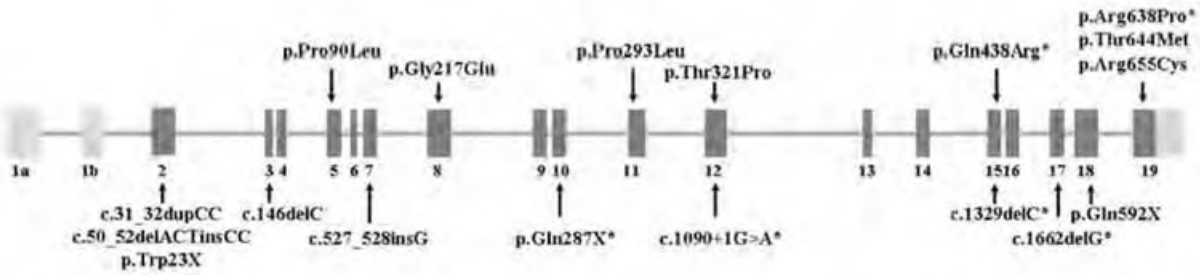

Figure 3: Locations of the different mutations identified to date. Missense mutations are positioned above the representation of *STRA6* gene, while nonsense and frameshift mutations are positioned underneath. Novel mutations identified in this study are indicated with an asterisk (*).

To date, no correlations between the nature of a *STRA6* mutation and phenotypic severity have been found. Patients with missense mutations have had severe phenotypes, whereas some patients with truncating mutations have had milder clinical involvement (Golzio et al., 2007; Pasutto et al., 2007). In previously reported families, there was little intrafamilial variation in severity (Chitayat et al., 2007; Pasutto et al., 2007). Likewise, in the first family reported here, all three affected siblings had bilateral severe microphthalmia, while none was described having diaphragmatic or lung involvement. However, case 3-2 died in the first days of life in the 1970s without further investigation, and a lung defect or diaphragmatic hernia can not be ruled out. In addition, patients 3-1 and 3-2 had a tetralogy of Fallot while patient 3-3 had no cardiac malformation but rather a neural tube closure defect, not previously observed in association with PDAC syndrome.

Patients 3-1 and 3-3 are the first adult patients described with *STRA6* mutations, although other mutated children have already been reported (Pasutto et al., 2007; White et al., 2008). It is interesting to note that apart from clinical anophthalmia, none of the other principal features of PDAC syndrome (diaphragmatic, pulmonary or

cardiac involvement) is systematically present in those patients with *STRA6* mutations currently reported. Including these seven cases, mutations in *STRA6* have been observed in 21 phenotypically diverse patients sharing features of the MCOPS9 syndrome (Golzio et al., 2007; Pasutto et al., 2007; White et al., 2008; West et al., 2009). Their clinical presentation is summarized in Table 1. Phenotypic variability could be related to vitamin A metabolic variability (from absorption to degradation) in either fetuses or their pregnant mothers.

Bilateral microphthalmia/anophthalmia was constant and cardiopathy frequent (14/21; 67 %); pulmonary and/or diaphragmatic involvement were present in about half of the patients. Moreover, additional features appear to be associated with *STRA6* mutations, such as renal abnormalities (6/21), intra-uterine growth retardation (3/21), uterine malformations (2/21), and spleen and/or pancreatic malformations with attendant duodenal atresia (2/21) (Martinovic-Bouriel et al., 2007; White et al., 2008; West et al., 2009). Interestingly, mental retardation appears to be a constant finding in living patients.

Considering this phenotypic variability, it remains difficult to conclude whether Matthew-Wood/Spear/PDAC is a genetically homogeneous syndrome or an association of distinct syndromes overlapping in their clinical presentation. Negative molecular analysis for *STRA6* mutations in some PDAC patients suggests that this spectrum of anomalies is probably genetically heterogeneous, even though *STRA6* screening may ignore some mutations (such as exonic rearrangements, splicing mutations distant from the coding sequence, or mutations in regulatory sequences) (Chitayat et al., 2007; Golzio et al., 2007; Pasutto et al., 2007). STRA6 was recently identified as the cell membrane receptor for plasma retinol binding protein, which transfers circulating vitamin A from the blood into target cells (Kawaguchi et al., 2007). All *STRA6* mutations associated with human disease to date have been shown to largely abolish vitamin A uptake activity (Kawaguchi et al., 2008). It therefore remains likely that other genes implicated in the control of vitamin A intracellular levels during embryonic development are causative in those MCOPS9 associations not linked to *STRA6* mutations. The vitamin A signalling pathway directly regulates the levels of over 500 target proteins (Blomhoff and Blomhoff, 2006) and its own metabolism, while imperfectly understood, involves dozens of intracellular enzymes.

Extensive data from teratogenic and genetic animal models, as well as from Donnai-Barrow syndrome (MIM# 222448) patients with *LRP2* mutations, confirm the important role of vitamin A in human diaphragm and lung development (Kluth et al., 1990; Kantarci et al., 2007). Case 3.3, with a minor form of spina bifida, has the first reported association of *STRA6* mutations with a neural tube closure defect, which is a result of vitamin A metabolite deficiency in mouse models (Kastner et al., 1995). Splenic, pancreatic, intestinal and urogenital malformations sometimes observed in Matthew-Wood patients, as well as the conotruncal nature of the cardiac defects, are also effects of lower perceived retinoid levels in the primordia of these organs in embryonic mice (Kastner et al., 1995).

In conclusion, we report herein five new patients with MCOPS9 syndrome caused by *STRA6* mutations. These data contribute to an expanding database of *STRA6* mutations and to the delineation of the phenotypic variability in patients with such mutations. Further molecular studies on Matthew-Wood/Spear/PDAC/MCOPS9 patients may identify mutations in other genes implicated in the retinoic acid signaling pathway.

ACKNOWLEDGMENTS

The authors thank Drs. Férechté Encha-Razavi, Louise Devisme and Michel Vekemans for their advice and Chantal Esculpavit and Sophie Audollent for their technical assistance. Patient recognizable photos were reproduced with permission from the families, to whom the authors express their gratitude for their participation.

REFERENCES

Berkenstadt M, Lev D, Achiron R, Rosner M, Barkai G. 1999. Pulmonary agenesis, microphthalmia, and diaphragmatic defect (PMD): new syndrome or association? Am J Med Genet 86(1):6-8.

Blomhoff R, Blomhoff HK. 2006. Overview of retinoid metabolism and function. J Neurobiol 66(7):606-30.

Chitayat D, Sroka H, Keating S, Colby RS, Ryan G, Toi A, Blaser S, Viero S, Devisme L, Boute-Benejean O, Manouvrier-Hanu S, Mortier G, Loeys B, Rauch A, Bitoun P. 2007. The PDAC syndrome (pulmonary hypoplasia/agenesis, diaphragmatic hernia/eventration, anophthalmia/microphthalmia, and cardiac defect) (Spear syndrome, Matthew-Wood syndrome): report of eight cases including a living child and further evidence for autosomal recessive inheritance. Am J Med Genet A 143(12):1268-81.

Golzio C, Martinovic-Bouriel J, Thomas S, Mougou-Zrelli S, Grattagliano-Bessieres B, Bonniere M, Delahaye S, Munnich A, Encha-Razavi F, Lyonnet S, Vekemans M, Attie-Bitach T etchevers HC. 2007. Matthew-Wood syndrome is caused by truncating mutations in the retinol-binding protein receptor gene STRA6. Am J Hum Genet 80(6):1179-87.

Kantarci S, Al-Gazali L, Hill RS, Donnai D, Black GC, Bieth E, Chassaing N, Lacombe D, Devriendt K, Teebi A, Loscertales M, Robson C, Liu T, Maclaughlin DT, Noonan KM, Russell MK, Walsh CA, Donahoe PK, Pober BR. 2007. Mutations in LRP2, which encodes the multiligand receptor megalin, cause Donnai-Barrow and facio-oculo-acoustico-renal syndromes. Nat Genet 39(8):957-9.

Kastner P, Mark M, Chambon P. 1995. Nonsteroid nuclear receptors: what are genetic studies telling us about their role in real life? Cell 83(6):859-69.

Kawaguchi R, Yu J, Honda J, Hu J, Whitelegge J, Ping P, Wiita P, Bok D, Sun H. 2007. A membrane receptor for retinol binding protein mediates cellular uptake of vitamin A. Science 315(5813):820-5.

Kawaguchi R, Yu J, Wiita P, Honda J, Sun H. 2008. An Essential Ligand-binding Domain in the Membrane Receptor for Retinol-binding Protein Revealed by Large-scale Mutagenesis and a Human Polymorphism. J Biol Chem 283(22):15160-8.

Kluth D, Kangah R, Reich P, Tenbrinck R, Tibboel D, Lambrecht W. 1990. Nitrofen-induced diaphragmatic hernias in rats: an animal model. J Pediatr Surg 25(8):850-4.

Lee SYR, Shiu YK, Ng WF, Chow CB. 2006. Another patient with pulmonary hypoplasia, microphthalmia and diaphragmatic hernia. Clin Dysmorphol 15(1):43-4.

Li L, Wei J. 2006. A newborn with anophthalmia and pulmonary hypoplasia (the Matthew-Wood syndrome). Am J Med Genet A 140(14):1564-6.

Martinovic-Bouriel J, Bernabe-Dupont C, Golzio C, Grattagliano-Bessieres B, Malan V, Bonniere M, Esculpavit C, Fallet-Bianco C, Mirlesse V, Le Bidois J, Aubry MC, Vekemans M, Morichon N etchevers H, Attie-Bitach T, Encha-Razavi F, Benachi A. 2007. Matthew-Wood syndrome: report of two new cases supporting autosomal recessive inheritance and exclusion of FGF10 and FGFR2. Am J Med Genet A 143(3):219-28.

Ostor AG, Stillwell R, Fortune DW. 1978. Bilateral pulmonary agenesis. Pathology 10(3):243-8.

Pasutto F, Sticht H, Hammersen G, Gillessen-Kaesbach G, Fitzpatrick DR, Nurnberg G, Brasch F, Schirmer-Zimmermann H, Tolmie JL, Chitayat D, Houge G, Fernandez-Martinez L, Keating S, Mortier G, Hennekam RC, von der Wense A, Slavotinek A, Meinecke P, Bitoun P, Becker C, Nurnberg P, Reis A, Rauch A. 2007. Mutations in STRA6 cause a broad spectrum of malformations including anophthalmia, congenital heart defects, diaphragmatic hernia, alveolar capillary dysplasia, lung hypoplasia, and mental retardation. Am J Hum Genet 80(3):550-60.

Priolo M, Casile G, Lagana C. 2004. Pulmonary agenesis/hypoplasia, microphthalmia, and diaphragmatic defects: report of an additional case. Clin Dysmorphol 13(1):45-6.

Seller MJ, Davis TB, Fear CN, Flinter FA, Ellis I, Gibson AG. 1996. Two sibs with anophthalmia and pulmonary hypoplasia (the Matthew-Wood syndrome). Am J Med Genet 62(3):227-29.

Smith SA, Martin KE, Dodd KL, Young ID. 1994. Severe microphthalmia, diaphragmatic hernia and Fallot's tetralogy associated with a chromosome 1;15 translocation. Clin Dysmorphol 3(4):287-91

Spear GS, Yetur P, Beyerlein RA. 1987. Bilateral pulmonary agenesis and microphthalmia. Am J Med Genet Suppl 3:379-82.

West B, Bove KE, Slavotinek AM. 2009. Two novel STRA6 mutations in a patient with anophthalmia and diaphragmatic eventration. Am J Med Genet A.

White T, Lu T, Metlapally R, Katowitz J, Kherani F, Wang TY, Tran-Viet KN, Young TL. 2008. Identification of STRA6 and SKI sequence variants in patients with anophthalmia/microphthalmia. Mol Vis 14:2458-65.

ARTICLE 7

Mutation analysis of the *STRA6* gene in isolated and non-isolated anophthalmia/microphthalmia

Clinical Genetics

2013-83(3): 244-50

N. Chassaing*, N. Ragge*, A. Kariminejad, A. Buffet, S. Ghaderi-Sohi, J. Martinovic and P. Calvas

---

Compte tenu de la variabilité phénotypique observée chez les patients que nous avons décrits, et ceux de la littérature, nous avons essayé de déterminer les critères diagnostiques pouvant orienter l'indication de l'analyse moléculaire du gène *STRA6*. Pour cela, nous avons, en collaboration avec le Dr Nicola Ragge, recherché des mutations du gène *STRA6* chez 28 patients avec des présentations cliniques variées. Sept avaient une AM isolée, 14 une AM associée à un autre critère de l'acronyme PDAC, 3 présentaient un spectre PDAC complet et 7 une AM associée à d'autres malformations. Nous avons identifié des mutations chez deux patients. Un patient avec un tableau complet de syndrome de Matthew-Wood était homozygote pour une mutation d'épissage. L'autre, présentait l'association d'une microphtalmie bilatérale, d'une tétralogie de Fallot et d'une hypoplasie rénale. Chez ce dernier nous avons identifié deux mutations hétérozygotes composites, une mutation faux sens et une délétion emportant une partie de l'exon 15 et les exons 16 à 18. Cet article nous a permis de confirmer l'hétérogénéité clinique du syndrome de Matthew-Wood, puisque aucune mutation du gène *STRA6* n'a été retrouvée chez deux des trois patients avec un tableau complet. Les résultats suggèrent également que la probabilité de trouver des mutations du gène *STRA6* est plus importante dans les AM associées aux malformations du spectre PDAC que dans les AM isolées. Ils ne permettent cependant pas de définir de critères diagnostiques de ce syndrome.

CLINICAL GENETICS An International Journal of Genetics, Molecular and Personalized Medicine

Clin Genet 2013: 83: 244–250
Printed in Singapore. All rights reserved

Published by Blackwell Publishing Ltd
CLINICAL GENETICS
doi: 10.1111/j.1399-0004.2012.01904.x

Short Report

Mutation analysis of the *STRA6* gene in isolated and non-isolated anophthalmia/microphthalmia

Chassaing N, Ragge N, Kariminejad A, Buffet A, Ghaderi-Sohi S, Martinovic J, Calvas P. Mutation analysis of the *STRA6* gene in isolated and non-isolated anophthalmia/microphthalmia.
Clin Genet 2013: 83: 244–250. © John Wiley & Sons A/S. Published by Blackwell Publishing Ltd, 2012

PDAC syndrome [Pulmonary hypoplasia/agenesis, Diaphragmatic hernia/eventration, Anophthalmia/microphthalmia (A/M) and Cardiac Defect] is a condition associated with recessive mutations in the *STRA6* gene in some of these patients. Recently, cases with isolated anophthalmia have been associated with *STRA6* mutations. To determine the minimal findings associated with *STRA6* mutations, we performed mutation analysis of the *STRA6* gene in 28 cases with anophthalmia. In 7 of the cases the anophthalmia was isolated, in 14 cases it was associated with one of the major features included in PDAC and 7 had other abnormalities. Mutations were identified in two individuals: one with bilateral anophthalmia and some features included in PDAC, who was a compound heterozygote for a missense mutation and a large intragenic deletion, and the second case with all the major features of PDAC and who had a homozygous splicing mutation. This study suggests that *STRA6* mutations are more likely to be identified in individuals with A/M and other abnormalities included in the PDAC spectrum, rather than in isolated A/M cases.

Conflict of interest

Nothing to declare.

N Chassaing[a,b*], N Ragge[c,d*], A Kariminejad[e], A Buffet[a], S Ghaderi-Sohi[e], J Martinovic[f] and P Calvas[a,b]

[a]Department of Medical Genetics, CHU Toulouse, Purpan Hospital, 31059 Toulouse, France, [b]EA-4555, Toulouse III Paul-Sabatier University, 31000 Toulouse, France, [c]Wessex Regional Genetics Service, Princess Anne Hospital, Southampton, Hampshire, SO16 5YA UK, [d]School of Life Sciences, Oxford Brookes University, Oxford, OX3 0BP UK, [e]Kariminejad Najmabadi Pathology and Genetic Center, Tehran, 14667 Iran, and [f]Department of Fetal Pathology, Antoine Beclere Hospital, 92141 Clamart, France

*These authors contributed equally to this work.

Key words: anophthalmia – cryptophthalmos – Matthew–Wood – MCOPS9 – microphthalmia – PDAC – *STRA6*

Corresponding author: Dr Nicolas Chassaing, Service de Génétique Médicale, Pavillon Lefebvre, CHU Purpan, Place du Dr Baylac, 31059 Toulouse Cedex 9, France.
Tel.: +33 5 61 77 90 55;
fax: +33 5 62 74 45 58;
e-mail: chassaing.n@chu-toulouse.fr

Received 29 November 2011, revised and accepted for publication 25 May 2012

The acronym PDAC [Pulmonary hypoplasia/agenesis, Diaphragmatic hernia/eventration, Anophthalmia/microphthalmia (A/M) and Cardiac Defect] was introduced by Chitayat et al. (1) to reflect the major components of the syndrome previously reported as Matthew–Wood or Spear syndrome [MCOPS9 (MIM 601186)]. Mutations in *STRA6* (STimulated by Retinoic Acid gene 6) (MIM 610745), which encodes a membrane receptor for the vitamin A-bearing plasma retinol-binding protein (2), have been identified in

23 patients with PDAC malformations (3–9). It has been shown that the clinical spectrum associated with mutations in the *STRA6* gene is more variable than initially described, ranging from PDAC to isolated anophthalmia (3, 8, 10). It has therefore been suggested that mutation analysis in the *STRA6* gene should be performed in individuals with isolated anophthalmia (6, 8, 10). To determine minimal phenotypic criteria associated with *STRA6* mutations (6), we performed mutation analysis of the *STRA6* gene in a cohort of 28 patients with isolated and non-isolated A/M.

Patients and methods

Patients

After obtaining informed consent, we performed *STRA6* molecular analysis in 28 individuals; 7 had isolated anophthalmia and 21 had A/M associated with other malformations. Among the latter, three had all the major features of the PDAC spectrum (pulmonary, diaphragmatic, ocular and cardiac involvement), 14 had A/M with at least one other major PDAC feature, and 4 had A/M with other anomalies. The clinical data are summarized in Table 1; the phenotypes of the two individuals with *STRA6* mutations are described below.

Case 10

A male child was born at 40 weeks, 5 days' gestation to healthy non-consanguineous parents of Caucasian descent. His birth weight was 3.1 kg (9–25th centile), length 51.5 cm (9–25th centile), and head circumference 34 cm (25th centile). Detailed fetal ultrasound at 18 weeks' gestation showed tetralogy of Fallot. Physical examination after delivery showed bilateral microphthalmia and echocardiography confirmed the tetralogy of Fallot and also showed total anomalous pulmonary venous drainage. The cardiac anomalies were both corrected at 5 months of age. Abdominal ultrasound showed bilateral small kidneys with a single cyst on the left kidney. His karyotype was normal and male (46, XY). Detailed family history revealed that his paternal grandfather had congenital cataract, surgically removed at 5 years of age and was visually impaired, and his paternal grandmother had unilateral iris coloboma.

His motor development was normal for a visually impaired child. His speech, although initially delayed was normal by 2 years of age. Assessment at 2.3 years of age showed that his height was 83.5 cm (2nd–9th centile), weight 10.45 kg (2nd centile), and head circumference 46.5 cm (0.4th centile). He was wearing bilateral ocular prostheses and had a left inguinal hernia. At age 2.5 years he was diagnosed with mild renal insufficiency.

Case 22

The case was a 17-week-old male fetus. His parents were healthy, consanguineous and of Iranian descent and he was the product of the couple's second pregnancy. The couple's first pregnancy resulted in a neonatal death of a daughter who was born at term and was found to have multiple congenital abnormalities, including bilateral anophthalmia, cryptophthalmos, left pre-axial polydactyly of the hand, bilateral lung agenesis, and a small heart with a ventricular septal defect. Unfortunately, neither photograph nor DNA sample was obtained.

The pregnancy with case 22 was complicated, with ultrasound demonstrating multiple abnormalities of the fetus, including bilateral elevation of diaphragm, severely hypoplastic lungs and a small, left-rotated heart and an enlarged and elevated liver. The findings were discussed with the parents who decided to terminate the pregnancy. Autopsy was consented and showed bilateral diaphragmatic eventration, bilateral lung agenesis, hypoplastic left atrium and hypoplastic pulmonary arteries. The weight of the liver and heart was within the normal range. In addition, the fetus had bilateral anophthalmia (Fig. 1b), and polysplenia.

STRA6 molecular analysis

Direct sequencing

DNA was isolated from peripheral blood or from paraffin-embedded tissue. *STRA6* exons and exon–intron junctions were sequenced as previously described (3).

QMPSF analysis

To confirm the heterozygous exonic deletion detected in patient 10 (see Results section), we used a quantitative multiplex polymerase chain reaction (PCR) amplification of short fluorescent fragments (QMPSF) technique. Primer pairs for amplifying *STRA6* exons 16, 18 and 19 and two control exons were used to construct two multiplex PCR sets. All primers carried a 10 nucleotide sequence extension at their 5′ end as previously described. The forward primers were 5′-labeled with the 6-FAM fluorochrome (PCR conditions and primer sequences are available on request). DNA fragments generated by QMPSF were separated on an ABI 3100 sequencer (Applied Biosystems, Warrington, UK), and the fluorescence profiles were analyzed with Genemapper v3.1 software (Applied Biosystems).

Characterization of the deletion breakpoint

QMPSF identified deletion of at least exons 16–18. We performed long-range PCR using the Expand Long Template PCR kit (Roche Diagnostics, Meylan, France) with *STRA6* primers 14-forward and 19-reverse. The deleted long-range PCR fragment was purified on 1% agarose gel, sequenced, and compared to the *STRA6* reference genomic sequence (GenBank accession number NM_022369.3).

Results

Direct sequencing

We identified two patients with pathogenic mutations; molecular analysis of the 26 remaining patients detected

Table 1. Phenotype of patients included in this study

Patient	Family history	Consanguinity	*STRA6* Mutation	Lung	Diaphragm	Eyes	Heart	Other
1	–	–	–	–	–	Bilateral anophthalmia	–	–
2	Maternal great-grandfather with unilateral anophthalmia	–	–	–	–	Bilateral anophthalmia	–	–
3	–	–	–	–	–	Bilateral anophthalmia	–	–
4	–	–	–	–	–	Bilateral anophthalmia	–	–
5	–	–	–	–	–	Bilateral anophthalmia	–	–
6	Sister with similar phenotype	–	–	–	–	Bilateral anophthalmia	–	Cleft palate Deafness
7	–	–	–	–	–	Right microphthalmia Left microphthalmia	Double outlet right ventricle	Hydrocephalus
8	–	–	–	–	Diaphragmatic hernia	Unilateral microphthalmia	–	Delleman syndrome
9	–	–	–	–	–	Bilateral anophthalmia	–	Kidney dysplasia
10	Paternal grandfather with congenital cataract Paternal grandmother with unilateral pupil defect	–	c.1120T>C [p.Cys374Arg] c.1343_1841+51delinsT	–	–	Bilateral anophthalmia	Tetralogy of Fallot	Left inguinal hernia Short stature Small kidneys with single cyst Renal failure
11	–	+	–	–	–	Unilateral colobomatous microphthalmia	Truncus arteriosus	–
12	Maternal niece with blindness	+	–	–	–	Bilateral anophthalmia	Moderate pulmonary and supravalvular pulmonary stenosis. Atrio-ventricular septum defect	–
13	–	+	–	–	–	Unilateral anophthalmia	–	–

Table 1. Continued

Patient	Family history	Consanguinity	*STRA6* Mutation	Lung	Diaphragm	Eyes	Heart	Other
14	Brother with Joubert syndrome	+	–	–	–	Bilateral anophthalmia	–	–
15	–	+	–	–	–	Unilateral anophthalmia	–	Corpus callosal hypoplasia
16	–	–	–	Bronchiectasis	–	Unilateral anophthalmia	Complex heart malformation	Undescended testes Umbilical and inguinal hernias Polydactyly
17	–	–	–	–	–	Unilateral anophthalmia	Complete atrio-ventricular septum defect Pulmonary atresia Hypoplastic right ventricle	Bilateral cleft lip and palate Kyphoscoliosis Craniosynostosis
18	–	–	–	–	–	Bilateral anophthalmia	Coarctation of the aorta Pulmonary atresia	Severe unilateral hearing loss
19	–	–	–	Bilateral lung agenesis	Bilateral diaphragmatic eventration	Bilateral microphthalmia	Atrial septal defect	Choanal atresia Laryngotracheal agenesia Bilateral renal hypoplasia
20	Sibling with tetralogy of Fallot and bilobar right lung	–	–	–	–	Bilateral anophthalmia	–	Anterior pituitary agenesis Right carotid artery agenesis Bladder outlet obstruction
21	–	–	–	–	Left diaphragmatic hernia	Bilateral microphthalmia	–	Left renal agenesis and Right multicystic kidney
22	Sibling with bilateral anophthalmia polydactyly, bilateral lung agenesis, and enlarged liver	+	c.1521-1G>A homozygous	Bilateral lung agenesis	Bilateral diaphragmatic eventration	Bilateral anophthalmia	Dilated ductus arteriosus Left atrium hypoplasia	Enlarged liver Hypoplastic spleen Polysplenia
23	Sibling with Matthew–Wood syndrome	+	–	Bilateral lung agenesis	Diaphragmatic hernia	Bilateral anophthalmia	Complex heart malformation	Pelvic kidney

Table 1. Continued

Patient	Family history	Consanguinity	*STRA6* Mutation	Lung	Diaphragm	Eyes	Heart	Other
24	–	–	–	–	Left diaphragmatic eventration	Bilateral microphthalmia	–	–
25	–	–	–	Bilateral lung hypoplasia	Left diaphragmatic eventration	Bilateral microphthalmia	–	Uterine duplication
26	–	–	–	Bilateral lung agenesis	–	Bilateral microphthalmia with retinal dysplasia	–	Bilateral renal dysplasia
27	–	–	–	Unilobar left lung Pulmonary dysplasia	–	Bilateral microphthalmia	Complex heart malformation	Cystic right kidney Hypoplastic semicircular canals
28	–	–	–	–	–	Bilateral microphthalmia	Atrial septal defect	Pelvicaliceal dilatation Chin fibrochondroma

+, present; –, absent.

Fig. 1. *STRA6* patients. (**a**) Facial photograph of individual 10 as an infant demonstrating bilateral anophthalmia. (**b**) Facial photograph of case 22.

only known single-nucleotide polymorphisms (SNPs). In case 22, who had PDAC complex, a homozygous splicing mutation in intron 16 (c.1521-1G>A) was identified. Both asymptomatic parents were heterozygous for this mutation. In patient 10, who had bilateral anophthalmia, cardiac and renal involvement, we identified a heterozygous missense mutation c.1120T>C in exon 13 (p.Cys374Arg), also present in the mother and maternal grandfather who were phenotypically normal. Using an informative SNP, c.1685-24T>C (rs12913041), located in intron 17, it was clear that a deletion of the paternal allele may have occurred. QMPSF analysis confirmed a heterozygous deletion involving at least exons 16 and 18, but not exon 19 (Fig. 2a).

Characterization of the deletion breakpoint

Sequencing of the fragment amplified by long range PCR revealed that the deletion extended from the middle of exon 15 into intron 18 (c.1343_1841+51delinsT,

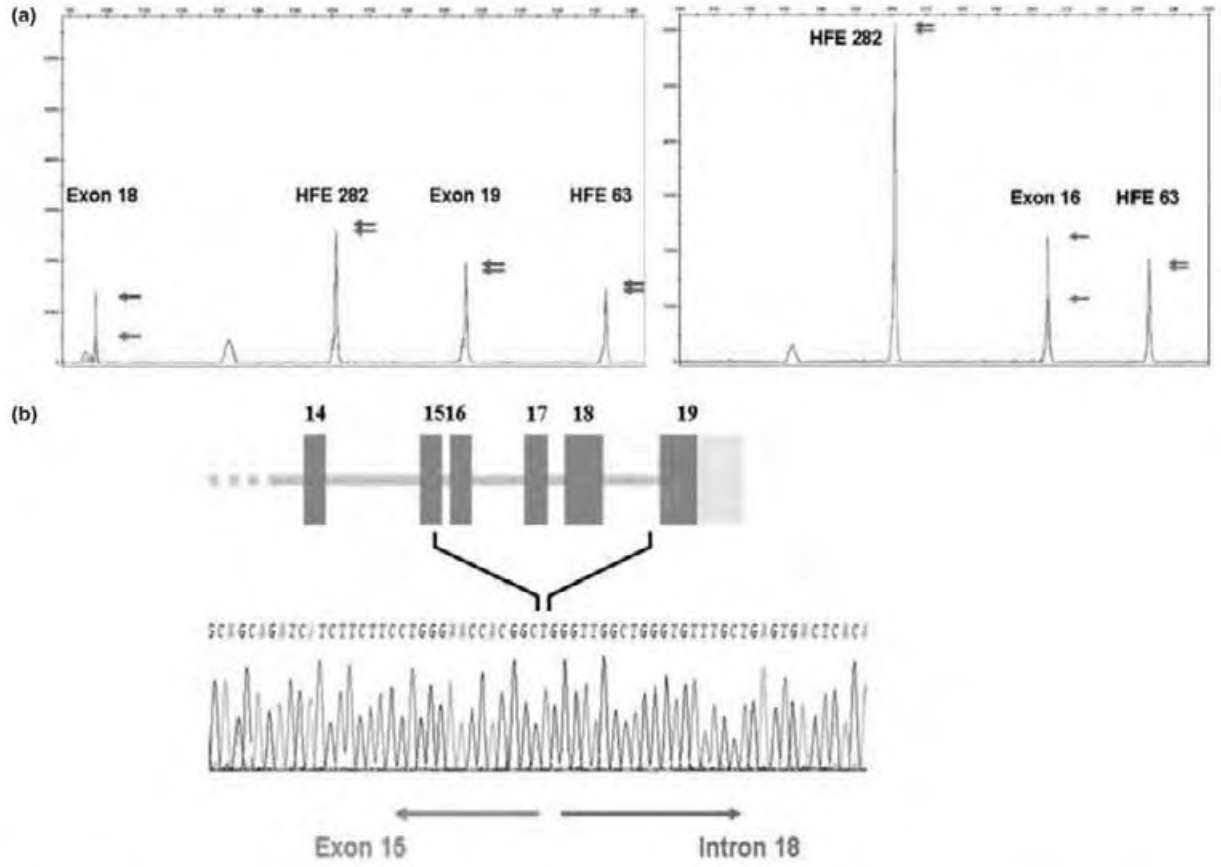

Fig. 2. Illustration of the *STRA6* exon 15 to intron 18 deletion in case 10. (**a**) Quantitative multiplex polymerase chain reaction (PCR) amplification of short fluorescent fragments (QMPSF) results demonstrating deletion of *STRA6* exons 16 and 18. Amplification profiles of case 10 (in red), and normal control (in blue) are superimposed; with the intensity of each peak indicated by an arrow: patient (red), control (blue). Normalization fluorescent profiles are shown, using the control amplicons (HFE282 and HFE63). The heterozygous deletion of *STRA6* exons 16 and 18 is shown by the halving of the intensity of the *STRA6* exon 16 and 18 peaks. Note that there is no reduction in exon 19 peak intensity which is not deleted in this patient. (**b**) Delineation of the extent of the deletion by direct sequencing of the fragment breakpoints after amplification by long range polymerase chain reaction.

Fig. 2b). This deletion was present in the healthy father and the paternal grandfather who had congenital cataract.

Discussion

Although mutations in the *STRA6* gene were initially identified in individuals with complete features of PDAC, recently *STRA6* mutations have been identified in individuals with isolated M/A (8, 10) as well as cases with microphthalmia, neural tube defect (3); bilateral anophthalmia, duplicated renal collecting system (8); bilateral anophthalmia and tetralogy of Fallot (3, 6). Segel et al. (6) suggested that all patients with isolated anophthalmia should have mutation analysis of the *STRA6* gene. To define the spectrum of clinical manifestations associated with *STRA6* mutations, we performed mutation analysis of the *STRA6* gene in a cohort of 28 patients: 7 with isolated anophthalmia and 21 with A/M associated with other abnormalities. We identified *STRA6* mutations in two cases with A/M and anomalies included in the PDAC phenotype, but not in any cases with isolated anophthalmia.

To date, ocular involvement has featured in all *STRA6* mutated patients, perhaps reflecting a greater sensitivity of the developing eye to reduced levels of STRA6. However, this finding may also reflect a bias of ascertainment. Other major features of PDAC variably present in individuals with *STRA6* mutations, are cardiac, lung and diaphragmatic involvement with a frequency of 55% (21/38), 39% (15/38) and 29% (11/38), respectively (this study and 3–10). Additional features include anomalies of the kidney (9/38), spleen (4/38), uterus (3/13 females), and pancreas with accompanying duodenal atresia (2/38), intrauterine growth retardation (3/38), and inguinal hernia (3/38) (this study and 3–10). Cognitive impairment has been documented in some of the living patients (3/16) (3, 5). Some dysmorphic features, such as 'bushy' eyebrows, hypoplastic nipples and hypoplastic toenails have been described. Other, less frequent findings, are thymic hypoplasia, subglottic laryngeal stenosis, cleft palate, pulmonary capillary dysplasia, a thin or absent corpus callosum, arhinencephaly and Dandy–Walker malformation (11). Polydactyly, a finding present in patient 22's sister has not previously been reported in association with *STRA6*

mutations, and may be a rare additional feature. Many of these features reflect the important role that the Vitamin A pathway has in L–R axis determination, and in interactions with limb and face morphogens, such as sonic hedgehog (12).

There is no clear genotype/phenotype association with *STRA6* mutations. Some patients with two missense mutations in *STRA6* exhibited multiple major anomalies of the PDAC spectrum and died shortly after birth (5) while one patient with two frameshift mutations was alive at the age of 14 years (5). It has been suggested that compound heterozygosity for missense mutations may explain milder phenotype (6). However, one patient who was a compound heterozygote for two missense mutations had a severe clinical presentation (5). Of note, the majority of patients (15/17) with milder phenotypes (i.e. with only one or two major features of the PDAC spectrum) reported so far harbor one (8, 9) or two missense mutations (this report and 3, 5, 6). Two patients with frameshifting *STRA6* mutations have been described with only two major features of the PDAC spectrum (anophthalmia and diaphragmatic hernia in one, and anophthalmia with lung hypoplasia in the other). Both cases were fetuses following pregnancy terminations at 23 and 26 weeks' gestation with limited postmortem examination. It is thus difficult to exclude the existence of other major anomalies (3, 5). Inter- and intra-familial clinical variability has also been described (3, 5, 10). Thus genetic background, as well as stochastic effects are likely to influence the phenotypic severity.

Our findings raise the possibility that heterozygosity for the *STRA6* gene mutation may be associated with ocular abnormalities. Although the parents of patient 22, and the parents and maternal grandfather of patient 10 who were heterozygous for an *STRA6* mutation, had normal eyes, the paternal grandfather, who shared the c.1343_1841+51delinsT change, had congenital cataract. Two further individuals, heterozygous for an *STRA6* mutation with eye involvement have been reported: one had bilateral coloboma of the retina and iris (4), while the other had a right optic disc coloboma, left iris coloboma and left microphthalmia (9). It has been shown that *STRA6* is expressed in the anterior part of the embryonic lens (13) and thus heterozygosity for an *STRA6* mutation may have contributed to these ocular abnormalities.

STRA6 gene mutations have not been found in all cases with PDAC syndrome (1, 5). It is possible that some types of *STRA6* mutations (such as exonic rearrangements, splicing mutations distant from the coding sequence, or mutations in regulatory sequences) may have been missed by the molecular analysis strategies used so far. However, since *STRA6* is part of a complex vitamin A – retinol binding protein pathway (2), disruption of other genes in this pathway may cause a PDAC phenotype.

In conclusion, our findings emphasize the phenotypic variability associated with *STRA6* mutations, and underline the difficulty in defining precise clinical criteria that could be useful when considering *STRA6* molecular analysis. To date, *STRA6* mutation analysis have been found in cases with least ocular abnormalities. To further delineate the clinical manifestations associated with *STRA6* mutations it would be worthwhile screening cohorts of patients with other major features included in PDAC, such as isolated diaphragmatic hernia or eventration to determine the spectrum of anomalies associated with this gene mutation.

Acknowledgements

The authors would like to thank the families for their participation and the following physicians and scientists for their assistance: Christine Peres, Danny Morrison, Sabine Sigaudy, Didier Lacombe, Sylvie Odent, Bruno Delobel, Sylvie Manouvrier, Delphine Dupin-Deguine, Martine Sinico, Marie Gonzales, François Cartault, Anne Froute, Christine Francannet, Laurent Gavard. This work was supported by grants from the Clinical Research Hospital Program from the French Ministry of Health (PHRC 09 109 01), Retina France, and from National Institutes of Health (5 R01 DE13849 and -09S1). N. R. was supported by a Senior Surgical Scientist Award from the Academy of Medical Sciences/Health Foundation.

References

1. Chitayat D, Sroka H, Keating S et al. The PDAC syndrome (pulmonary hypoplasia/agenesis, diaphragmatic hernia/eventration, anophthalmia/microphthalmia, and cardiac defect) (Spear syndrome, Matthew–Wood syndrome): report of eight cases including a living child and further evidence for autosomal recessive inheritance. Am J Med Genet A 2007: 143A: 1268–1281.
2. Kawaguchi R, Yu J, Honda J et al. A membrane receptor for retinol binding protein mediates cellular uptake of vitamin A. Science 2007: 315: 820–825.
3. Chassaing N, Golzio C, Odent S et al. Phenotypic spectrum of STRA6 mutations: from Matthew–Wood syndrome to non-lethal anophthalmia. Hum Mutat 2009: 30: E673–E681.
4. Golzio C, Martinovic-Bouriel J, Thomas S et al. Matthew–Wood syndrome is caused by truncating mutations in the retinol-binding protein receptor gene STRA6. Am J Hum Genet 2007: 80: 1179–1187.
5. Pasutto F, Sticht H, Hammersen G et al. Mutations in STRA6 cause a broad spectrum of malformations including anophthalmia, congenital heart defects, diaphragmatic hernia, alveolar capillary dysplasia, lung hypoplasia, and mental retardation. Am J Hum Genet 2007: 80: 550–560.
6. Segel R, Levy-Lahad E, Pasutto F et al. Pulmonary hypoplasia-diaphragmatic hernia-anophthalmia-cardiac defect (PDAC) syndrome due to STRA6 mutations – what are the minimal criteria? Am J Med Genet A 2009: 149A: 2457–2463.
7. West B, Bove KE, Slavotinek AM. Two novel STRA6 mutations in a patient with anophthalmia and diaphragmatic eventration. Am J Med Genet A 2009: 149A: 539–542.
8. White T, Lu T, Metlapally R et al. Identification of STRA6 and SKI sequence variants in patients with anophthalmia/microphthalmia. Mol Vis 2008: 14: 2458–2465.
9. Ng W, Pasutto F, Bardakjian T et al. A puzzle over several decades: eye anomalies with FRAS1 and STRA6 mutations in the same family. Clin Genet 2012. DOI: 10.1111/j.1399-0004.2012.01851.x.
10. Casey J, Kawaguchi R, Morrissey M et al. First implication of STRA6 mutations in isolated anophthalmia, microphthalmia, and coloboma: a new dimension to the STRA6 phenotype. Hum Mutat 2011: 32: 1417–1426. DOI: 10.1002/humu.21590.
11. Slavotinek AM. Eye development genes and known syndromes. Mol Genet Metab 2011: 104: 448–456.
12. Niederreither K, Dolle P. Retinoic acid in development: towards an integrated view. Nat Rev Genet 2008: 9: 541–553.
13. Bouillet P, Sapin V, Chazaud C et al. Developmental expression pattern of Stra6, a retinoic acid-responsive gene encoding a new type of membrane protein. Mech Dev 1997: 63: 173–186.

ARTICLE 8

Microphthalmia 9 (PDAC)

Inborn Errors of Development.

The molecular basis of clinical disorders of morphogenesis

Third Edition

J. Plaisancie and **N. Chassaing**

Dans ce chapitre de livre, nous avons fait une revue de la littérature sur les aspects phénotypiques liés aux mutations du gène *STRA6*, les critères diagnostiques et les diagnostiques différentiels. Nous reprenons l'historique de l'identification de ce gène, les aspects moléculaires et le rôle de *STRA6* et de la vitamine A dans le développement embryonnaire.

Inborn Errors of Development

The molecular basis of clinical disorders of morphogenesis

"Microphthalmia 9 (PDAC)"

Julie PLAISANCIE[1], MD & Nicolas CHASSAING[1*], MD

Service de Génétique Médicale, Hôpital Purpan, CHU Toulouse ; and Université Toulouse III, EA-4555, Toulouse, France.

***chassaing.n@chu-toulouse.fr**

a. Chapter summary

Microphthalmia is defined as a globe with a total axial length that is at least two standard deviations below the mean for age. The classification of microphthalmia is based upon the severity of axial length reduction and the anatomic appearance of the ocular globe. The most severe form of this eye defect is anophthalmia which refers to the complete absence of the globe (in the presence of ocular adnexa). The prevalence of this congenital eye defect has been estimated between 3 and 30 per 100,000 births (Verma and Fitzpatrick 2007). Microphthalmia can be isolated (simple or severe microphthalmia also known as clinical anophthalmia) or be complex in the presence of other kinds of eye defects (coloboma, anterior and posterior eye segment dysgenesis). It can also occur in a syndromic form with various extra-ocular malformations (52 to 95 % of cases (Shah et al., 2012)). Learning difficulties are described in about one fifth of cases with microphthalmia/anophthalmia and/or coloboma (Morrison et al., 2002). Many genes that are known to play a crucial role in ocular development have been implicated in isolated and syndromic forms of anophthalmia/microphthalmia and all patterns of inheritance have been reported.

Among syndromic forms of microphthalmia, a recurrent association of microphthalmia/anophthalmia and various anomalies of lung, diaphragm, and heart has been described. The first combination of pulmonary agenesis, microphthalmia, ventricular septal defect and diaphragmatic defect was reported by Spear *et al.* in 1987 (Spear et al., 1987). Seller *et al.*, in 1996, reported the first sibs with this association and called it Matthew-Wood syndrome as requested by the family (Seller et al., 1996). More recently, the acronym PDAC was introduced to reflect the major components of the syndrome (Pulmonary agenesis or hypoplasia, Diaphragmatic hernia or eventration, Anophthalmia/microphthalmia and Cardiac defects) (Chitayat et al., 2007). The term MCOPS9 was adopted by the Mendelian Inheritance in Man database for "syndromic

microphthalmia 9" (MIM#601186). Mutations in the *STRA6* gene (MIM*610745) were firstly shown to be responsible for this syndromic form of microphthalmia (Pasutto et al., 2007) and then for isolated forms of microphthalmia (Casey et al., 2011). *STRA6* encodes a membrane receptor for vitamin A-bearing plasma retinol binding protein and is involved in vitamin A metabolism, a pathway long recognized for its involvement in eye development (Hyatt and Dowling 1997). *STRA6*-related eye disorders are inherited in an autosomal recessive manner.

b. Gene description

MCOPS9 was presumed to be inherited in an autosomal recessive manner after two affected sibs from unaffected parents were described by Seller *et al.* in 1996 (Seller et al., 1996).

The *STRA6* gene was demonstrated by Pasutto *et al.* (2007) to be implicated in PDAC syndrome after using a positional cloning strategy: they performed homozygosity mapping on two consanguineous Turkish families with a similar phenotype including clinical anophthalmia and variable malformations of the lungs, the heart and the diaphragm (Pasutto et al., 2007). Using parametric and nonparametric linkage analysis of both families together, they identified a common locus in the 15q23-25.1region with a Lod-score of 4.8. The *STRA6* gene, included in this critical locus spanning 12 Mb, appeared as a candidate gene because of its involvement in vitamin A pathway, long known for its critical implication in eye development. They identified a homozygous nucleotide deletion in the first family and a homozygous missense mutation in the second one (Pasutto et al., 2007). Although *STRA6* was originally found to be a retinoic acid-stimulated gene in cancer cell lines, it was the first involvement of a gene from the STRA (stimulated by retinoic acid) group in a human phenotype.

STRA6 is located on the long arm of chromosome 15 in the 15q24.1 region and spans a total length of 29.57 kb. The coding region comprises 18 exons resulting in a transcript length of 2,800 bps encoding a protein of 667 residues.

This gene is expressed during embryonic development and in the adult brain, spleen, kidney, female genital tract and testis (and at lower quantities in heart and lung) (Kawaguchi et al., 2007).

c. Clinical summary

The clinical presentation of MCOPS9 most often consists of a variable combination of congenital defects. The clinical description of the 39 reported mutation-positive patients is summarized in Table I. Four main anomalies were associated with *STRA6* mutations, involving the eyes, the heart, the lungs and the cardiovascular system, grouped under the acronym PDAC. The phenotype is also associated with other more or less frequent findings.

Pulmonary anomalies

Developmental lung defects may be unilateral or bilateral and range from pulmonary agenesis or pulmonary hypoplasia to lobation defect. Alveolar capillary dysplasia has also been reported. Primary pulmonary agenesis or hypoplasia is a rare and mostly sporadic malformation (Seller et al., 1996). Around 40% of patients with MCOPS9 and identified *STRA6* mutations have a developmental lung defect. Lungs abnormalities are primary defects, and may be present even when there is no diaphragmatic hernia.

Diaphragmatic defects

These consist of unilateral or bilateral diaphragmatic hernia or eventration and are identified in about 30% of *STRA6* mutated patients.

Anophthalmia/microphthalmia

Different degrees of axial length reduction of the globe can be present, mostly affecting both eyes. Unilateral microphthalmia/anophthalmia has been described but was associated with contralateral eye defects such as coloboma (Casey et al., 2011). Microphthalmia is classically severe (clinical anophthalmia) and bilateral.

Microphthalmia/anophthalmia seems to be a constant feature of this syndrome, affecting not only the index patients but also all affected relatives (thus avoiding recruitment bias).

Cardiac defects

This organ defect is the second most common abnormality described in association with MCOPS9. More than one *STRA6* mutated patient in two is affected by cardiovascular anomalies. Various heart defects have been described: atrial septal defect, persistent ductus arteriosus, truncus arteriosus communis, atresia of pulmonary artery, right aortic arch, coarctation of aorta, tetralogy of Fallot, and pulmonic valve stenosis. Conotruncal defects seem to be overrepresented, and tetralogy of Fallot is the most frequent malformation observed, corresponding to more than one quarter (6/21, 29%) of heart involvement.

Other frequent features

Abnormalities in other systems have been described in around 50% of patients with MCOPS9. Three systems are most commonly implicated, and may represent additional major features of the syndrome:

-the renal system is involved in about one quarter of patients and various malformations have been described such as pelvic kidney, horseshoe kidney, hydronephrosis and renal hypoplasia.

-the digestive system (inguinal hernia, duodenal stenosis, pancreatic and splenic malformations), are present in one quarter of the mutated patients.

-the genital system is involved in 15% of patients and the reported malformations consist of bicornuate uterus, uterine hypoplasia and cryptorchidism.

Less frequent findings

Intrauterine growth retardation, thymic hypoplasia, subglottic laryngeal stenosis, cleft palate, a thin or absent corpus callosum, arhinencephaly, Dandy–Walker malformation,

spina bifida, hypoplastic nipples, hypoplastic toenails and polydactyly have all been described in association with MCOPS9 (Chassaing et al., 2009; Chassaing et al., 2012; Segel et al., 2009; Slavotinek 2011; West et al., 2009).

Facial dysmorphism has also been described frequently and consists of an unusual trichoglyphic pattern of the eyebrows, large and low set ears, wide nasal bridge and micrognathia (Fig.1).

MCOPS9 is generally a severe malformation syndrome either leading to the termination of the pregnancy after fetal ultrasound findings or lethality in the first years of life. For this reason it is difficult to gather significant data about all of the features of the syndrome, and in particular about the intellectual consequences. Few patients with PDAC spectrum were described alive after the first year of life (Chassaing et al., 2009; Chassaing et al., 2012; Pasutto et al., 2007; Segel et al., 2009; White et al., 2008) and the oldest patient described was 40 years old (Chassaing et al., 2009) at diagnosis. Only 3 of the 7 living patients presenting with the PDAC spectrum had intellectual deficiency (moderate to profound). Patients reported by Casey *et al.* in 2011 (Casey et al., 2011), who have isolated microphthalmia, have no cognitive impairment.

MCOPS9 is inherited in an autosomal recessive manner. Interestingly, ocular anomalies have been described in some individuals heterozygous for a *STRA6* mutation : one had congenital cataracts (Chassaing et al., 2012), one had bilateral coloboma of the retina and iris (Golzio et al., 2007), and one had a right optic disc coloboma, left iris coloboma and left microphthalmia (Ng et al., 2012). These three symptomatic heterozygotes had heterozygous truncating mutations (frameshift or nonsense mutations) (Chassaing et al., 2012; Golzio et al., 2007; Ng et al., 2012). Although most heterozygotes have no ocular phenotype, these findings raise the possibility that the heterozygosity for the *STRA6* gene mutation may rarely be associated with ocular abnormalities.

d. Molecular genetics

A variety of mutations have been found in the *STRA6* gene: the majority of mutations

described to date correspond to point mutations (missense, nonsense and splice mutations, small insertions and deletions) while one exonic deletion has been reported. Currently, twenty-five different mutations in the *STRA6* gene have been found in patients with MCOPS9 (Fig. 2).

It is obviously possible that some types of *STRA6* mutations (such as exonic rearrangements, splicing mutations distant from the coding sequence, or mutations in regulatory sequences) may have been missed by the molecular analysis strategies used. However, since *STRA6* is part of a complex vitamin A – retinol binding protein pathway, disruption of other genes in this pathway may cause a PDAC phenotype.

All *STRA6* pathogenic mutations identified in patients with the PDAC spectrum result in apparent loss of function. In order to better delineate the impact of identified mutations on the STRA6 function, Kawaguchi *et al.* (2008) performed functional analyses on various mutations : the frameshift mutation (c.146delC [p.Gly50Alafs*22]) and five missense mutations (p.Pro90Leu, p.Pro293Leu, p.Thr321Pro, p.Thr644Met and p.Arg655Cys) (Kawaguchi et al., 2008). These studies showed a complete absence of the expression of the *STRA6* mutant as a result of the frameshift mutation, whereas conservation of expression for the mutants with missense mutations was found. It has subsequently been demonstrated that four of the five missense mutations prevent normal cell surface expression of the STRA6 protein, probably by misfolding of the mutant protein (Kawaguchi et al., 2008).

e. Diagnosis

Clinical spectrum

MCOPS9 is a rare polymalformation condition associated with recessive mutations in the *STRA6* gene in some patients. The clinical spectrum associated with *STRA6* mutations is extremely variable between patients, but also within families (Casey et al., 2011; Chassaing et al., 2009; Pasutto et al., 2007). Although mutations in the *STRA6* gene were initially identified in individuals with the full spectrum of features of PDAC, recently *STRA6*

mutations have been identified in individuals with microphthalmia and only one additional feature as well as in isolated microphthalmia/anophthalmia. Of note, all of the *STRA6* mutated patients had microphthalmia/anophthalmia.

The *STRA6*-related phenotype is associated with a heart defect in half of cases and with lung and diaphragmatic defects in almost 40% and 30% of cases respectively. Half of mutated patients have other various anomalies and the renal, digestive and genital systems are also frequently involved in *STRA6*-related disorders (25%, 23%, and 15% respectively).

Genotype/Phenotype correlation

There is no clear genotype/phenotype correlation with *STRA6* mutations. Some patients with two missense mutations in *STRA6* exhibited multiple major anomalies of the PDAC spectrum and died shortly after birth (Pasutto et al., 2007) while one patient with two frameshift mutations was alive at the age of 14 years (Pasutto et al., 2007). It has been suggested that the compound heterozygosity for missense mutations may explain milder phenotypes (Segel et al., 2009). However, one patient who was a compound heterozygote for two missense mutations had a severe clinical presentation (Pasutto et al., 2007). Of note, the majority of patients (15/17) with milder phenotypes (i.e. with only one or two major components of the PDAC acronym) reported so far harbor one (Chassaing et al., 2012; Ng et al., 2012; White et al., 2008) or two missense mutations (Chassaing et al., 2009; Pasutto et al., 2007; Segel et al., 2009). Two patients with frameshift *STRA6* mutations have been described with only two major features of the PDAC spectrum (anophthalmia and diaphragmatic hernia in one, and anophthalmia with lung hypoplasia in the other) (Chassaing et al., 2009; Pasutto et al., 2007). Both cases were fetuses; termination of pregnancy had been carried out at 23 and 26 weeks' gestation with limited postmortem examination. It is thus difficult to exclude the existence of other major anomalies. Modifier genes, environmental variations, and stochastic effects are likely to influence the phenotypic severity.

Diagnostic criteria

The establishment of criteria for the diagnosis of MCOPS9 has been discussed by many authors. Mutations in the *STRA6* gene could explain about one half of the MCOPS9 cases when at least two features among the four previously reported as the major components of the PDAC acronym are present. Indeed, mutations in the *STRA6* gene were identified in 15 out of 24 patients (62%) presenting with involvement of at least 3 out of the Pulmonary, Diaphragmatic, Anophthalmia, and Cardiac components of the PDAC syndrome (Chassaing et al., 2009; Chassaing et al., 2012; Golzio et al., 2007; Ng et al., 2012; Pasutto et al., 2007; West et al., 2009; White et al., 2008). The *STRA6* mutation detection rate is only slightly decreased in patients with only two PDAC components; *STRA6* mutations were identified in 11 among the 24 patients (46%) with two criteria. In addition, *STRA6* mutations were identified in three patients with microphthalmia/anophthalmia and one additional feature which was not previously considered as a major feature of the PDAC spectrum: duplicated renal collecting system (White et al., 2008), neural tube defect (Chassaing et al., 2009), and dysplastic right kidney (Casey et al., 2011).

To date, ocular involvement appears to be a constant feature of the phenotype associated with *STRA6* mutations. Indeed, all patients described with a *STRA6* mutation have microphthalmia/anophthalmia. Incidentally, Segel *et al.* suggested that all patients with isolated anophthalmia should have mutation analysis of the *STRA6* gene (Segel et al., 2009). Eighteen patients with isolated microphthalmia/anophthalmia were screened for *STRA6* mutations in two different cohorts, but no mutation was identified (Chassaing et al., 2012; White et al., 2008). However, using a next generation sequencing approach, Casey et al. identified the same homozygous missense *STRA6* mutation in 10 patients from two families from an Irish Traveller population with isolated microphthalmia/anophthalmia (Casey et al., 2011).Thus, even unusual, isolated microphthalmia/anophthalmia could reflect the presence of *STRA6* mutations.

All together, these data underline the difficulty in establishing criteria to predict the presence of *STRA6* involvement given the extreme phenotypic variability associated with these mutations. However, three kinds of criteria could be defined, based upon their frequency in this multisystemic disorder. Microphthalmia/anophthalmia could be defined as a primary criterion because it appears as a constant feature of this syndrome to date and it could be also the unique feature of this syndrome. Secondary criteria would consist of pulmonary, diaphragmatic, and cardiac anomalies because of their frequency of involvement in this multisystemic disorder and because their presence seems to increase the probability of finding mutations in the *STRA6* gene. In addition, renal, digestive and genital malformations seem to be frequent findings and should also be considered as secondary criteria related to *STRA6* mutations. Tertiary criteria could be the less frequent findings observed in a few patients.

Differential diagnosis

6 conditions with the four components of the PDAC acronym are retrieved by the *London medical Database*: Fryns syndrome, Goldenhar syndrome, Ivemark syndrome, mosaic trisomy 16, Pallister-Killian syndrome and Matthew-Wood syndrome. The combination of 3 out of these 4 features retrieves 51 different syndromes (including 33 with microphthalmia/anophthalmia). The combination of 2 out of these 4 features retrieves 231 different syndromes (including 112 with microphthalmia/anophthalmia).

The diagnosis of MCOPS9 is thus evident in the presence of the four main clinical features (as it can be easily differentiated from the 5 other differential diagnoses), and the molecular analysis of the *STRA6* gene allows confirmation in about half of the patients. The diagnosis is more challenging in patients displaying incomplete phenotypes.

f. Molecular pathogenesis

STRA6 and vitamin A

STRA6 belongs to the STRA (stimulated by retinoic acid) gene family. It encodes a 667-

amino-acid peptide which mediates vitamin A uptake in target organs. The synthesis of STRA6 is up-regulated by a high plasma level of vitamin A loaded-retinol-binding protein (holo-RBP) produced by the liver. STRA6 protein was found to be preferentially expressed at the cell surface of organs distant from the liver including: eye, brain, spleen, kidney, female genital tract and testis (and at lower quantities in heart and lung) (Kawaguchi et al., 2007). STRA6 is a multitransmembrane domain protein (nine transmembrane helices) with an extracellular high affinity binding domain to plasma RPB (Kawaguchi et al., 2008; Kawaguchi et al., 2008). This protein has also two other specific functional sites in the C terminus region (intracellular): a SH2-binding motif and a phosphorylation site (signal transduction). STRA6 is involved in vitamin A (retinol) uptake given its role as a specific receptor of RBP. Retinol is transported in the plasma by the RPB and then is transferred into the cell cytoplasm after interaction with STRA6. Retinol is then transformed, after several enzymatic reactions into retinol derivatives (retinoids). Generated retinoic acid acts within the nucleus as a ligand for nuclear receptors that directly regulate transcriptional activity of multiple developmental target genes (Niederreither and Dolle 2008). STRA6 also catalyzes the loading of free retinol into apo-RBP, which can cause retinol efflux (Kawaguchi et al., 2011). Recently, Kawaguchi *et al.*, showed that, if STRA6 encounters both holo-RBP and apo-RBP, holo-RBP blocks STRA6-mediated retinol efflux by competing with apo-RBP's binding to STRA6 and by counteracting retinol efflux with influx (Kawaguchi et al., 2012). They also demonstrated that STRA6 catalyzes efficient retinol exchange between intracellular cellular retinol binding protein I (CRBP-I) and extracellular RBP, even in the presence of holo-RBP. STRA6's retinol exchange activity may serve to refresh the intracellular retinoid pool.

STRA6 mutations identified in MCOPS9 patients lead to the absence of the STRA6 expression or prevent cell surface expression of STRA6 by misfolding (Kawaguchi et al., 2008). Thus, these *STRA6* alterations are thought to disturb the normal vitamin A cell metabolism, leading to the malformations observed in MCOPS9 patients.

Animal models

Isken *et al.* (2008) used the zebrafish model to analyze Stra6 function (Isken et al., 2008). Morphants injected with Stra6 antisense morpholino oligonucleotides developed microphthalmia, had a curved body axis and showed cardiac edema. Cross-sections through the eyes of 4 dpf larvae confirmed microphthalmia but revealed distinct retinal cell layers with normal stratification. Furthermore, morphants displayed cardiac edema along with dysmorphic heart chambers. Morphants also exhibited an altered morphology of the craniofacial skeleton. The first and second arches were malformed, and the branchial arches were absent.

Using a retinoic acid (RA) synthesis inhibitor in zebrafish embryos, Casey *et al.* (2011) modeled different levels of RA and observed dose-dependent microphthalmia. The inhibitor produced developmental eye defects ranging from mild to severe microphthalmia as well as retinal pigment epithelium coloboma. Heart morphogenesis defects were also present (Casey et al., 2011).

In a mouse model, Ruiz *et al.* (2012) showed that stra6 -/- null mice had a reduction in thickness of the neurosensory retina due to shortening of the rod outer and inner segments (Ruiz et al., 2012). In addition, there was a reduction in cone photoreceptor cell number and cone b-wave amplitude. A typical hallmark in stra6 -/- null eyes was the presence of a persistent primary hypertrophic vitreous, an optically dense vascularized structure located in the vitreous humor between the posterior surface of the lens and neurosensory retina. Despite full disruption of the stra6 gene, these mice had ocular anomalies with impaired visual responses but otherwise were phenotypically normal.

These data underline the inter-species phenotypic variability with *STRA6* inactivation. In addition, it appears that the zebrafish is a more appropriate model to study STRA6 and vitamin A signaling pathway in order to recapitulate part of the human phenotype.

Conclusion

Mutations in the *STRA6* gene result in a spectrum of malformations, from isolated microphthalmia to a severe malformation syndrome affecting many different systems (ocular, cardiac, pulmonary, diaphragmatic, renal, digestive and genital). To date, no phenotype-genotype correlation has been established. Given the extreme phenotypic variability, it is difficult to establish criteria predicting the presence of *STRA6* mutations. In addition, mutations in the *STRA6* gene are identified in only half of patients with a clear diagnosis of MCOPS9 syndrome, implying that this is a genetically heterogeneous condition.

g. References

Casey J, Kawaguchi R, Morrissey M, Sun H, McGettigan P, Nielsen JE, Conroy J, Regan R, Kenny E, Cormican P, Morris DW, Tormey P, Ni Chroinin M, Kennedy BN, Lynch S, Green A, Ennis S. 2011. First implication of STRA6 mutations in isolated anophthalmia, microphthalmia, and coloboma: A new dimension to the STRA6 phenotype. Hum Mutat.

Chassaing N, Golzio C, Odent S, Lequeux L, Vigouroux A, Martinovic-Bouriel J, Tiziano FD, Masini L, Piro F, Maragliano G, Delezoide AL, Attie-Bitach T, Manouvrier-Hanu S, Etchevers HC, Calvas P. 2009. Phenotypic spectrum of STRA6 mutations: from Matthew-Wood syndrome to non-lethal anophthalmia. Hum Mutat 30:E673-681.

Chassaing N, Ragge N, Kariminejad A, Buffet A, Ghaderi-Sohi S, Martinovic J, Calvas P. 2012. Mutation analysis of the STRA6 gene in isolated and non-isolated anophthalmia/microphthalmia. Clin Genet 9999.

Chitayat D, Sroka H, Keating S, Colby RS, Ryan G, Toi A, Blaser S, Viero S, Devisme L, Boute-Benejean O, Manouvrier-Hanu S, Mortier G, Loeys B, Rauch A, Bitoun P. 2007. The PDAC syndrome (pulmonary hypoplasia/agenesis, diaphragmatic hernia/eventration, anophthalmia/microphthalmia, and cardiac defect) (Spear syndrome, Matthew-Wood syndrome): report of eight cases including a living child and further evidence for autosomal recessive inheritance. Am J Med Genet A 143A:1268-1281.

Golzio C, Martinovic-Bouriel J, Thomas S, Mougou-Zrelli S, Grattagliano-Bessieres B, Bonniere M, Delahaye S, Munnich A, Encha-Razavi F, Lyonnet S, Vekemans M, Attie-Bitach T, Etchevers HC. 2007. Matthew-Wood syndrome is caused by truncating mutations in the retinol-binding protein receptor gene STRA6. Am J Hum Genet 80:1179-1187.

Hyatt GA, Dowling JE. 1997. Retinoic acid. A key molecule for eye and photoreceptor development. Invest Ophthalmol Vis Sci 38:1471-1475.

Isken A, Golczak M, Oberhauser V, Hunzelmann S, Driever W, Imanishi Y, Palczewski K, von Lintig J. 2008. RBP4 disrupts vitamin A uptake homeostasis in a STRA6-deficient animal model for Matthew-Wood syndrome. Cell Metab 7:258-268.

Kawaguchi R, Yu J, Honda J, Hu J, Whitelegge J, Ping P, Wiita P, Bok D, Sun H. 2007. A membrane receptor for retinol binding protein mediates cellular uptake of vitamin A. Science 315:820-825.

Kawaguchi R, Yu J, Ter-Stepanian M, Zhong M, Cheng G, Yuan Q, Jin M, Travis GH, Ong D, Sun H. 2011. Receptor-mediated cellular uptake mechanism that couples to intracellular storage. ACS Chem Biol 6:1041-1051.

Kawaguchi R, Yu J, Wiita P, Honda J, Sun H. 2008. An essential ligand-binding domain in the membrane receptor for retinol-binding protein revealed by large-scale mutagenesis and a human polymorphism. J Biol Chem 283:15160-15168.

Kawaguchi R, Yu J, Wiita P, Ter-Stepanian M, Sun H. 2008. Mapping the membrane topology and extracellular ligand binding domains of the retinol binding protein receptor. Biochemistry 47:5387-5395.

Kawaguchi R, Zhong M, Kassai M, Ter-Stepanian M, Sun H. 2012. STRA6-Catalyzed Vitamin A Influx, Efflux, and Exchange. J Membr Biol 245:731-745.

Morrison D, FitzPatrick D, Hanson I, Williamson K, van Heyningen V, Fleck B, Jones I, Chalmers J, Campbell H. 2002. National study of microphthalmia, anophthalmia, and coloboma (MAC) in Scotland: investigation of genetic aetiology. J Med Genet 39:16-22.

Ng W, Pasutto F, Bardakjian T, Wilson M, Watson G, Schneider A, Mackey D, Grigg J, Zenker M, Jamieson R. 2012. A puzzle over several decades: eye anomalies with FRAS1 and STRA6 mutations in the same family. Clin Genet.

Niederreither K, Dolle P. 2008. Retinoic acid in development: towards an integrated view. Nat Rev Genet 9:541-553.

Pasutto F, Sticht H, Hammersen G, Gillessen-Kaesbach G, Fitzpatrick DR, Nurnberg G, Brasch F, Schirmer-Zimmermann H, Tolmie JL, Chitayat D, Houge G, Fernandez-Martinez L, Keating S, Mortier G, Hennekam RC, von der Wense A, Slavotinek A, Meinecke P, Bitoun P, Becker C, Nurnberg P, Reis A, Rauch A. 2007. Mutations in STRA6 cause a broad spectrum of malformations including anophthalmia, congenital heart defects, diaphragmatic hernia, alveolar capillary dysplasia, lung hypoplasia, and mental retardation. Am J Hum Genet 80:550-560.

Ruiz A, Mark M, Jacobs H, Klopfenstein M, Hu J, Lloyd M, Habib S, Tosha C, Radu RA, Ghyselinck NB, Nusinowitz S, Bok D. 2012. Retinoid content, visual responses, and ocular morphology are compromised in the retinas of mice lacking the retinol-binding protein receptor, STRA6. Invest Ophthalmol Vis Sci 53:3027-3039.

Segel R, Levy-Lahad E, Pasutto F, Picard E, Rauch A, Alterescu G, Schimmel MS. 2009. Pulmonary hypoplasia-diaphragmatic hernia-anophthalmia-cardiac defect (PDAC) syndrome due to STRA6 mutations--what are the minimal criteria? Am J Med Genet A 149A:2457-2463.

Seller MJ, Davis TB, Fear CN, Flinter FA, Ellis I, Gibson AG. 1996. Two sibs with anophthalmia and pulmonary hypoplasia (the Matthew-Wood syndrome). Am J Med Genet 62:227-229.

Shah SP, Taylor AE, Sowden JC, Ragge N, Russell-Eggitt I, Rahi JS, Gilbert CE. 2012. Anophthalmos, microphthalmos, and Coloboma in the United kingdom: clinical

features, results of investigations, and early management. Ophthalmology 119:362-368.

Slavotinek AM. 2011. Eye development genes and known syndromes. Mol Genet Metab 104:448-456.

Spear GS, Yetur P, Beyerlein RA. 1987. Bilateral pulmonary agenesis and microphthalmia. Am J Med Genet Suppl 3:379-382.

Verma AS, Fitzpatrick DR. 2007. Anophthalmia and microphthalmia. Orphanet J Rare Dis 2:47.

West B, Bove KE, Slavotinek AM. 2009. Two novel STRA6 mutations in a patient with anophthalmia and diaphragmatic eventration. Am J Med Genet A 149A:539-542.

White T, Lu T, Metlapally R, Katowitz J, Kherani F, Wang TY, Tran-Viet KN, Young TL. 2008. Identification of STRA6 and SKI sequence variants in patients with anophthalmia/microphthalmia. Mol Vis 14:2458-2465.

Table I: MCOPS9 features in *STRA6* mutated patients

	Nucleotide variation	Protein alteration	Lung	Diaphragm	Eye	Heart	Renal system	Digestive system	Genital system	Other
Pasutto *et al.* 2007	c.878C>T c.878C>T	p.Pro293Leu p.Pro293Leu	+	-	+	+	+	-	-	Developmental delay
	c.878C>T* c.878C>T*	p.Pro293Leu p.Pro293Leu	-	-	+	+				
	c.146delC c.146delC	p.Gly50Alafs*22 p.Gly50Alafs*22	-	+	+	+	-	-	-	Alive at 14 years, intellectual deficiency, short stature
	c.146delC c.146delC	p.Gly50Alafs*22 p.Gly50Alafs*22	-	+	+	-	-	-	-	
	c.1963C>T c.1963C>T	p.Arg655Cys p.Arg655Cys	+	+	+	-	-	+	-	Hypotonia, failure to thrive
	c.1963C>T* c.1963C>T*	p.Arg655Cys p.Arg655Cys	-	-	+	+	-	-	-	short stature
	c.1931C>T c.1931C>T	p.Thr644Met p.Thr644Met	+	+	+	-	+	-	-	
	c.1931C>T* c.1931C>T*	p.Thr644Met p.Thr644Met	+	-	?	+	+	-	+	
	c.1931C>T* c.1931C>T*	p.Thr644Met p.Thr644Met	+	-	+	+	-	-	+	
	c.269C>T c.961A>C	p.Pro90Leu p.Thr321Pro	+	+	+	+	+	+	+	
Golzio *et al.* 2007	c.50_52delACTinsCC c.50_52delACTinsCC	p.Asp17Alafs*55 p.Asp17Alafs*55	+	+	+	+	-	+	-	Intra-uterine growth retardation, mild dysmorphism
	c.527_528insG c.527_528insG	p.Gly176Glyfs*59 p.Gly176Glyfs*59	+	+	+	+	-	+	-	Intra-uterine growth retardation, mild dysmorphism
White *et al.* 2008	c.650G>A c.1774C>T	p.Gly217Glu p.Gln592*	-		+	-	+	-	-	
West *et al.* 2009	c.31_32dupCC c.69G>A	p.Gly13Profs*72 p.Trp23*	+	+	+	+	+,	+	+	Intra-uterine growth retardation, thin corpus callosum, mild dysmorphism
Chassaing *et al.* 2009	c.1090+1G>A c.859C>T	Splice mutation p.Gln287*	+	+	+	+	-	-	-	
	c.1662delG c.1662delG	p.Arg555Glufs*16 p.Arg555Glufs*16	+	-	+	+	+	+	+	Subglottic laryngeal stenosis
	c.1313A>G c.1913G>C	p.Gln438Arg p.Arg638Pro	-	-	+	+	-	-	-	Intellectual deficiency

	c.1313A>G* c.1913G>C*	p.Gln438Arg p.Arg638Pro	-	-	+	+	-	-	-	
	c.1313A>G c.1913G>C	p.Gln438Arg p.Arg638Pro	-	-	+	-	-	-	-	Intellectual deficiency, Short stature, Spina bifida occulta
	c.1329delC* c.1329delC*	p.Leu444Trpfs*34 p.Leu444Trpfs*34	-	+	+	+	-	-	-	
	c.1329delC c.1329delC	p.Leu444Trpfs*34 p.Leu444Trpfs*34	+	-	+	-	-	-	-	
Segel *et al.* 2009	c.1678G>C c.1964G>A	p.Asp560His p.Arg655His	-	-	+	+	-	-	-	
Casey *et al.* 2011	c.910_911delinsAA c.910_911delinsAA (pedigree 1)	p.Gly304Lys p.Gly304Lys	9 -	9 -	9 +	9 -	9 -	9-	9-	
	c.910_911delinsAA c.910_911delinsAA (pedigree 2)	p.Gly304Lys p.Gly304Lys	-	-	+	-	+	-	-	
	c.910_911delinsAA c.910_911delinsAA (pedigree 3)	p.Gly304Lys p.Gly304Lys	-	-	+	-	-	+	+	
	c.910_911delinsAA c.910_911delinsAA (pedigree 3)	p.Gly304Lys p.Gly304Lys	-	-	+	+	+	+	+	
Chassaing *et al.* 2012	c.1120T>C c.1343_1841+51delinsT	p.Cys374Arg large deletion	-	-	+	+	+	+	-	Short stature
	c.1521-1G>A c.1521-1G>A	Splice mutation Splice mutation	+	+	+	+	-	+	-	
	c.1521-1G>A* c.1521-1G>A*	Splice mutation Splice mutation	+	-	+	-	-	-	-	Polydactyly
Ng *et al.* 2012	c.52_53insGACT c.1931C>T	p.Tyr18* p.Thr644Met	+	-	+	-	-	-	-	
	c.52_53insGACT c.1931C>T	p.Tyr18* p.Thr644Met	-	-	+	+	-	-	-	
Total (%)			15/39 38%	11/39 28%	38/38 100%	21/39 54%	10/39 25%	9/39 23%	6/39 15%	

Figure 1: Representative oculofacial phenotypes at different ages.

(a) a fetus at 23 weeks of gestation, note short palpebral fissures reflecting bilateral severe microphthalmia ; **(b)** a patient aged three days, note broad nasal bridge and the deep-set orbits associated with clinical anophthalmia ; **(c)** a patient at age 2 years, note bilateral anophthalmia ; **(d)** a patient aged 40 years, note mild facial dysmorphy with a broad nasal tip. This patient has orbital implants.

Reproduced with kind permission from articles published in *Human Mutation* (Chassaing *et al.*, 2009) and *Clinical Genetics* (Chassaing *et al.*, 2012).

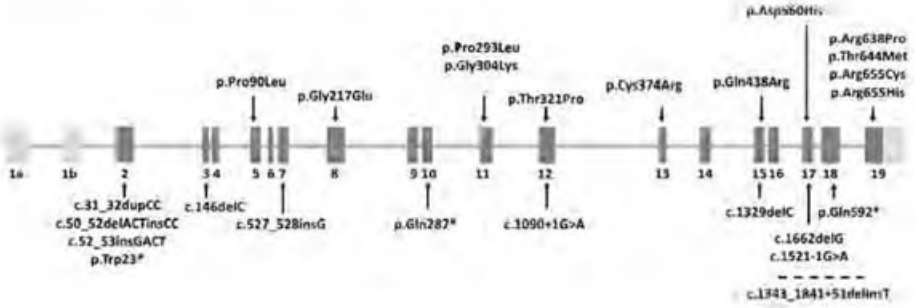

Figure 2: Locations of the 25 mutations identified to date in the *STRA6* gene. Missense mutations are positioned above the representation of the *STRA6* gene, while nonsense and frameshift mutations are positioned underneath.

CHAPITRE IV

RECHERCHE DE NOUVEAUX GENES D'AM

Introduction

Les résultats obtenus dans notre grande cohorte de patients sont concordants avec les données de la littérature et montrent qu'aucune mutation n'est identifiée dans les gènes connus chez près de trois quarts des patients AM. L'explication la plus probable est que seule une petite partie des gènes impliqués dans l'AM est actuellement identifiée.

Face à l'hétérogénéité génétique déjà mise en évidence, d'autres gènes d'AM restent à identifier. Nous avons donc utilisé plusieurs approches pour découvrir de nouveaux gènes d'AM :

- une approche régions et gènes candidats,

- une recherche de micro-réarrangement chromosomique par CGH-array,

- une approche plus fondamentale visant à identifier les cibles des facteurs de transcription déjà impliqués dans les AM (SOX2, OTX2, RAX et PAX6). L'hypothèse étant que les gènes régulés par ces facteurs de transcription, dont le rôle est majeur au cours du développement oculaire embryonnaire, seraient de bons candidats pour être eux-mêmes impliqués dans les AM.

Enfin, le développement des techniques de séquençage haut débit au cours de ma thèse a totalement modifié les approches de recherche de gènes d'AM. Ces techniques ont donc été mises à profit pour analyser un grand nombre de gènes candidats identifiés par les approches citées plus haut. Ces techniques ont également été utilisées dans de nouveaux projets de recherche visant à étudier l'ensemble des parties codantes du génome des patients ("whole exome sequencing"). Les premiers résultats de ces études non ciblées seront évoqués dans le volet "perspectives".

IV-1 : Approche gène candidats

Introduction

L'approche par gène candidat a été très utilisée avant la révolution du séquençage haut débit. Les gènes candidats étant :

- soit des "candidats positionnels" localisés dans une région génomique liée à la pathologie après analyse de liaison ou après identification de remaniement chromosomique par cytogénétique classique ou moléculaire (cf. chapitre suivant),
- soit des "candidats fonctionnels" : la structure d'une protéine codée par un gène, sa fonction supposée, les connaissances sur la famille de protéines à laquelle elle appartient, son patron d'expression au cours du développement, des modèles animaux, sont autant d'arguments qui peuvent pointer un gène et en faire un candidat fonctionnel pour une pathologie donnée.

Cette approche par gènes candidats fonctionnels a permis d'identifier de nombreux gènes d'AM comme *OTX2*[47], *RAX*[57], *VAX1*[109] et *BMP7*[102] par exemple.

Méthodes et Résultats

Nous avons séquencé trois gènes candidats (*SOX1*, *SOX21* et *LHX2*) chez des patients atteints d'AM sans mutation identifiée dans les gènes connus d'AM.

SOX1 et SOX21 sont deux protéines structurellement très proches de SOX2. De plus les gènes *SOX1* et *SOX21* sont localisés sur le chromosome 13, dans la région 13q3, région dont on sait que la délétion peut se traduire phénotypiquement par des AM[170]. Ces gènes étaient donc des candidats fonctionnels de par leur appartenance au même groupe de protéines que SOX2, le groupe des protéines SOXB (comprenant SOX1, SOX2, SOX3, SOX14 et SOX21). Ils étaient de plus des candidats positionnels du fait de leur localisation génomique dans une région chromosomique dont la délétion est parfois associée à des AM. 70 patients, extraits de la cohorte des AM, sans mutation identifiée dans les gènes connus, ont été séquencés pour ces deux gènes sans qu'aucune mutation causale n'ait été identifiée.

LHX2 (LIM homeobox 2) était un autre des gènes candidats aux AM. En effet, l'inactivation de l'expression de *Lhx2* dans le modèle murin provoque une anophtalmie[171]. De plus, il a été montré qu'au cours du développement oculaire, Lhx2 régulait le niveau d'expression ou la localisation de l'expression génique de nombreux gènes clés du développement oculaires et eux-mêmes déjà

impliqués dans l'AM (*Rax*, *Vsx2*/*Chx10*, *Sox2*, et *Otx2*)[172]. Ce gène a été étudié chez 70 patients AM. Les résultats de cette étude sont décrits dans l'article suivant:

- Article n°9

Desmaison, A *et al*. (2010). "Mutations in the *LHX2* gene are not a frequent cause of micro/anophthalmia." Mol Vis 16: 2847-9.

De plus, nous avons recherché des mutations dans une région candidate. Cette région est une région régulatrice du gène *RAX* située à 2kb en amont du gène. Il a été montré qu'une courte séquence de 35 bp de cette région contenait des séquences de fixation des facteurs de transcription SOX2 et OTX2, permettant ainsi la régulation de l'expression du gène *RAX*[173]. Nous avons émis l'hypothèse que des mutations de cette région régulant l'expression du gène *RAX* (impliqué dans l'AM) via les facteurs de transcription SOX2 et OTX2 (eux même impliqués dans l'AM), pourraient également entrainer des malformations oculaires et expliquer la présence d'AM chez certains patients par ailleurs dépourvu de mutation identifiée dans les gènes connus. Aucune anomalie n'a été identifiée chez 51 patients AM dans cette région candidate. Les résultats de cette étude sont décrits dans l'article suivant:

- Article n°10

Chassaing, N *et al*. (2009). "Mutations in the newly identified *RAX* regulatory sequence are not a frequent cause of micro/anophthalmia." Genet Test Mol Biomarkers 13(3): 289-90.

Conclusion

Notre approche par gène candidat a permis d'identifier un variant dans le gène *LHX2*, pour lequel il n'a pas été possible de conclure formellement sur son lien avec le phénotype oculaire présenté par le patient. L'analyse moléculaire des gènes *SOX1* et *SOX21,* ainsi que de la région régulatrice de *RAX* n'a pas permis d'identifier de mutation délétère.

ARTICLE 9

Mutations in the *LHX2* gene are not a frequent cause of micro/anophthalmia

Molecular Vision

2010-16: 2847-9

Desmaison, A. Vigouroux, C. Rieubland, C. Peres, P. Calvas and **N. Chassaing**

Dans cet article, nous décrivons la recherche de mutation dans un gène candidat par la fonction à la genèse d'AM. L'analyse a été conduite chez 70 patients atteints d'AM, chez qui aucune mutation n'avait pu être identifiée par l'analyse préalable des sept gènes couramment testés responsables d'AM. Le gène *LHX2* nous paraissait être un bon candidat compte tenu de l'existence d'une anophtalmie chez les souris KO pour ce gène. De plus, il avait également été montré que ce gène avait pour fonction de réguler le niveau et le patron d'expression de nombreux gènes eux-mêmes connus pour intervenir au cours du développement oculaire. Deux variations faux-sens hétérozygotes ont été identifiées : l'une, p.Pro259Gln, touchait un acide aminé non conservé et était prédite comme bénigne par les outils *in silico* ; l'autre, p.Pro43Arg, touchait un acide aminé conservé et était prédite par les outils *in silico* pour être probablement délétère. Pour cette dernière cependant, l'analyse familiale a montré que cette variation était héritée du père asymptomatique. Il n'a donc pas été possible de conclure entre trois hypothèses sur cette variation faux-sens :

- variation sans lien avec le phénotype oculaire
- mutation dominante avec pénétrance incomplète
- mutation récessive causale, avec chez ce même patient une mutation héritée de la mère non identifiée (remaniement exonique, mutation située dans un intron ou une séquence régulatrice…)

Molecular Vision 2010; 16:2847-2849 <http://www.molvis.org/molvis/v16/a305>
Received 14 September 2010 | Accepted 15 December 2010 | Published 18 December 2010

Mutations in the *LHX2* gene are not a frequent cause of micro/anophthalmia

Annaïck Desmaison,[1] Adeline Vigouroux,[1,2,3] Claudine Rieubland,[4] Christine Peres,[1] Patrick Calvas,[1,2,3] Nicolas Chassaing[1,2,3]

[1]INSERM, U563, Centre de Physiopathologie de Toulouse Purpan, Toulouse, France; [2]CHU Toulouse, Hôpital Purpan, Service de Génétique Médicale, Toulouse, France; [3]Université Toulouse III Paul-Sabatier, Toulouse, France; [4]Division of Medical Genetics, Centre Hospitalier Universitaire Vaudois, Lausanne, Switzerland

Purpose: Microphthalmia and anophthalmia are at the severe end of the spectrum of abnormalities in ocular development. A few genes (orthodenticle homeobox 2 [*OTX2*], retina and anterior neural fold homeobox [*RAX*], SRY-box 2 [*SOX2*], CEH10 homeodomain-containing homolog [*CHX10*], and growth differentiation factor 6 [*GDF6*]) have been implicated mainly in isolated micro/anophthalmia but causative mutations of these genes explain less than a quarter of these developmental defects. The essential role of the LIM homeobox 2 (LHX2) transcription factor in early eye development has recently been documented. We postulated that mutations in this gene could lead to micro/anophthalmia, and thus performed molecular screening of its sequence in patients having micro/anophthalmia.

Methods: Seventy patients having non-syndromic forms of colobomatous microphthalmia (n=25), isolated microphthalmia (n=18), or anophthalmia (n=17), and syndromic forms of micro/anophthalmia (n=10) were included in this study after negative molecular screening for *OTX2*, *RAX*, *SOX2*, and *CHX10* mutations. Mutation screening of *LHX2* was performed by direct sequencing of the coding sequences and intron/exon boundaries.

Results: Two heterozygous variants of unknown significance (c.128C>G [p.Pro43Arg]; c.776C>A [p.Pro259Gln]) were identified in *LHX2* among the 70 patients. These variations were not identified in a panel of 100 control patients of mixed origins. The variation c.776C>A (p.Pro259Gln) was considered as non pathogenic by in silico analysis, while the variation c.128C>G (p.Pro43Arg) considered as deleterious by in silico analysis and was inherited from the asymptomatic father.

Conclusions: Mutations in *LHX2* do not represent a frequent cause of micro/anophthalmia.

Microphthalmia and anophthalmia are at the severe end of the spectrum of abnormalities in ocular development. The combined occurrence rate for these two malformations is estimated between 3 and 30 per 100,000 births [1]. Mutations in several genes have been found in syndromic and non-syndromic anophthalmia. Heterozygous mutations in SRY-box 2 (*SOX2*) account for approximately 10% of anophthalmias [2,3]. Growth differentiation factor 6 (*GDF6*) mutations may account for up to 8% of micro/anophthalmia [4,5]. Other genes have been identified as causing isolated anophthalmia or microphthalmia in humans (orthodenticle homeobox 2 [*OTX2*], retina and anterior neural fold homeobox [*RAX*], and CEH10 homeodomain-containing homolog [*CHX10*]) [1,3,6-8]. These latter are implicated in a very small proportion of affected individuals, implying wide genetic heterogeneity to match the phenotypic variability.

The LIM homeobox 2 (LHX2) transcription factor has been shown to be essential for mammalian eye development and mice deficient in functional Lhx2 protein have been shown to display anophthalmia [9]. More recent studies on mouse models have demonstrated that, during eye development, Lhx2 regulates levels and/or expression patterns of Rax, Chx10, Sox2, and Otx2 [10,11], themselves involved in human micro/anophthalmia.

We hypothesize that mutations in *LHX2* could lead to severe eye developmental disorders including micro/anophthalmia. We thus performed molecular analysis in 70 micro/anophthalmia patients for whom previous molecular analysis of genes implicated in isolated micro/anophthalmia (*SOX2*, *OTX2*, *RAX*, and *CHX10*) failed to identify any causative mutation.

METHODS

Patients: Seventy patients having non-syndromic forms of colobomatous microphthalmia (n=25), isolated microphthalmia (n=18), or anophthalmia (n=17), or syndromic forms of micro/anophthalmia (n=10) were included in this study. Their informed consent was obtained beforehand, according to French law. Micro/anophthalmia was considered as syndromic when the patient presents at least one other non ocular malformation (in our patients, associated malformations were intestinal atresia multiple, corpus callosum agenesis, heart malformation, deafness, Dandy Walker malformation, labiopalatal cleft, sexual ambiguity,

Correspondence to: Dr. Nicolas Chassaing, Service de Génétique Médicale, Pavillon Lefebvre, CHU Purpan, Place du Dr Baylac, 31059 Toulouse Cedex 9, France; Phone: +33 5 61 77 90 55; FAX: +33 5 62 74 45 58; email: chassaing.n@chu-toulouse.fr

Table 1. Primers used for *LHX2* molecular analysis.

Exon	Forward primer	Reverse primer	Product length (bp)
1	TGAGGCGGGGGGCAAGCCCT	GGAGCCACCGGCCTTGCATT	333
2	ATGTCCTGGCAGCCCCCTCC	GCCAAACTGTAAGACTGTGCCTG	404
3	CCGTGTGTTCCCACAGCCCC	CCGTCGAGGCCGCACACTTT	505
4	TGGGTGGGGCGAGTGTGGAT	GTCCTTCCAAGGCCCACGGC	369
5	CTCACCAGCCCTTCCCTGTC	ATGTGGTTAGTTAGTTGCTC	445

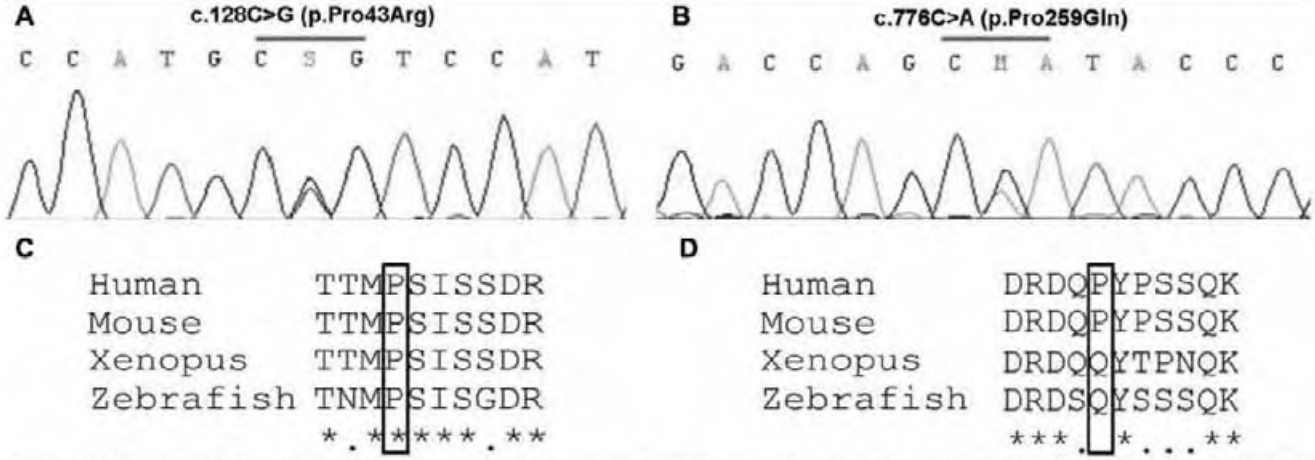

Figure 1. Missense variations identified in this cohort, and conservation of involved amino-acid among species. Electropherograms showing the c.128C>G (p.Pro43Arg: **A**) and the c.776C>A (p.Pro259Gln: **B**) *LHX2* variations. Alignment of part of LHX2 proteins from human, mouse, *Xenopus* and zebrafish, showing conservation of proline 43 (**C**, boxed) in these species, and absence of proline 259 conservation (**D**, boxed), which is replaced by a glutamine in *Xenopus* and zebrafish.

hypospadias, arthrogryposis, and choanal atresia). All patients included had undergone molecular analysis of *SOX2*, *OTX2*, *RAX*, *CHX10*. Direct sequencing of the coding regions and exon/intron boundaries and exclusion of exonic rearrangement by Quantitative Multiplex PCR of Short fluorescent Fragments (QMPSF) of these genes failed to identify any causative mutation in these patients.

Techniques: The 5 exons of the *LHX2* gene were amplified by PCR using primers deduced from the *LHX2* genomic sequence. Primer pairs and PCR conditions used are summarized in Table 1. Products were amplified in 25 µl reactions containing 50 ng genomic DNA, 1× PCR buffer, 0.2 mM dNTPs, 2 mM $MgCl_2$, 100 nM forward primer, 100 nM reverse primer, and 1 U of Taq polymerase. Betaine (1 M) was added in PCR mix for exons 1 and 2. All PCR reactions were performed with a 5 min 95 °C denaturing step, followed by 14 cycles of 95 °C for 30 s, annealing temperature for 30 s (70 °C to 62 °C, −0.5 °C/cycle) and 72 °C for 45 s, followed by 20 cycles of 95 °C for 30 s, 62 °C for 30 s, and 72 °C for 45 s with a final elongation step of 72 °C for 7 min. PCR amplifications were subsequently purified using QIAquick Gel Extraction kit (QIAGEN SA, Courtaboeuf, France), and both forward and reverse strands were sequenced using Big Dye DNA sequencing kit (Applied Biosystems, Warrington, UK). Reactions were analyzed in an ABI3100 sequencer (Applied Biosystems). Sequence variations were numbered with the adenine of the ATG initiation codon as the first nucleotide (the *LHX2* GenBank accession number was NM_004789.3).

RESULTS AND DISCUSSION

LHX2 encodes the transcription factor LHX2 which is highly conserved across species [12] and has recently been demonstrated to play a critical role in eye development [10, 11]. LHX2 is required to induce or maintain expression of genes required at the early optic vesicle stage for regionalization, establishment of retinal dorsoventral polarity, retinal progenitor cell properties, and lens specification [11]. LHX2 has thus been proposed to link the multiple pathways needed for transition of the optic vesicle to the optic cup [11]. Mice lacking *Lhx2* expression display anophthalmia, and this transcription factor has been involved in regulation of expression levels and/or expression patterns of genes already involved in micro/anophthalmia (*SOX2*,*RAX*,*CHX10*, and *OTX2*) during eye development [10,11]. We hypothesized that mutations in *LHX2* may be involved in human micro/anophthalmia, and thus molecular screening of this gene in 70 micro/anophthalmic patients was performed.

Molecular analysis allowed identification of three sequence variations. We observed presence of the described

SNP c.783G>C (p.Pro261Pro) either in a heterozygous or homozygous state in 42 out of 70 patients. In addition, two variants of unknown significance were identified. The heterozygous c.128C>G (p.Pro43Arg; Figure 1A) was identified in an anophthalmic patient originating from Libya for whom no other sequence variation was found. Pro43 amino-acid is conserved among species (Figure 1C) and is located closely to the conserved LIM domain 1 of the protein. This variation was not identified in a panel of 200 control chromosomes of mixed geographical origins (Caucasian, African, and Asian), and was considered as probably damaging by in silico analysis (PolyPhen and SIFT software). However, familial study has shown that this variation was inherited from his father who harbors a normal ocular examination. Thus, this heterozygous variation may be non-pathogenic, even if dominant inheritance with incomplete penetrance can not be totally ruled out. We cannot also exclude presence of an undetected maternally inherited mutation (e.g located in intronic or promoter region sequences, or an exonic rearrangement) fitting with an autosomal recessive inheritance. In a French patient with colobomatous microphthalmia, we identified the heterozygous variation c.776C>A (p.Pro259Gln; Figure 1B). This variation was not identified in a panel of 200 chromosomes from Caucasian controls. No sample was available for his parents, and familial segregation study was not possible. Additionally, there are arguments against the implication of this variation in the patient's ocular phenotype. First, Pro259 is not a conserved amino-acid among species (Figure 1D), and a glutamine is present at this position in several distant species including *Xenopus*, Chicken, and Fugu Fish [12]. Second, this variation was considered as non damaging by in silico analysis (PolyPhen and SIFT software). Thus, we consider this variant as probably non deleterious. Molecular analysis failed to identify any other sequence variation in the remaining 68 patients included in this study.

In conclusion, although mutations in *LIIX2* may nevertheless be implicated in some micro/anophthalmia patients, our results suggest that such sequence variations are not a frequent cause of micro/anophthalmia. Molecular basis of these ocular malformations remains still poorly understood and further work remains to be achieved to identify new micro/anophthalmia genes.

ACKNOWLEDGMENTS

This work was supported by a grant from the Clinical Research Hospital Program from the French Ministry of Health (PHRC 09 109 01) and by Retina France. The authors are grateful to Jacqueline Butterworth for help in preparing the manuscript.

REFERENCES

1. Verma AS, Fitzpatrick DR. Anophthalmia and microphthalmia. Orphanet J Rare Dis 2007; 2:47. [PMID: 18039390]
2. Fantes J, Ragge NK, Lynch SA, McGill NI, Collin JR, Howard-Peebles PN, Hayward C, Vivian AJ, Williamson K, van Heyningen V, FitzPatrick DR. Mutations in SOX2 cause anophthalmia. Nat Genet 2003; 33:461-3. [PMID: 12612584]
3. Ragge NK, Lorenz B, Schneider A, Bushby K, de Sanctis L, de Sanctis U, Salt A, Collin JR, Vivian AJ, Free SL, Thompson P, Williamson KA, Sisodiya SM, van Heyningen V, Fitzpatrick DR. SOX2 anophthalmia syndrome. Am J Med Genet A 2005; 135:1-7. [PMID: 15812812]
4. Asai-Coakwell M, French CR, Berry KM, Ye M, Koss R, Somerville M, Mueller R, van Heyningen V, Waskiewicz AJ, Lehmann OJ. GDF6, a novel locus for a spectrum of ocular developmental anomalies. Am J Hum Genet 2007; 80:306-15. [PMID: 17236135]
5. Gonzalez-Rodriguez J, Pelcastre EL, Tovilla-Canales JL, Garcia-Ortiz JE, Amato-Almanza M, Villanueva-Mendoza C, Espinosa-Mattar Z, Zenteno JC. Mutational screening of CHX10, GDF6, OTX2, RAX and SOX2 genes in 50 unrelated microphthalmia-anophthalmia-coloboma (MAC) spectrum cases. Br J Ophthalmol 2010; 94:1100-4. [PMID: 20494911]
6. Faiyaz-Ul-Haque M, Zaidi SH, Al-Mureikhi MS, Peltekova I, Tsui LC, Teebi AS. Mutations in the CHX10 gene in non-syndromic microphthalmia/anophthalmia patients from Qatar. Clin Genet 2007; 72:164-6. [PMID: 17661825]
7. Lequeux L, Rio M, Vigouroux A, Titeux M, Etchevers H, Malecaze F, Chassaing N, Calvas P. Confirmation of RAX gene involvement in human anophthalmia. Clin Genet 2008; 74:392-5. [PMID: 18783408]
8. Wyatt A, Bakrania P, Bunyan DJ, Osborne RJ, Crolla JA, Salt A, Ayuso C, Newbury-Ecob R, Abou-Rayyah Y, Collin JR, Robinson D, Ragge N. Novel heterozygous OTX2 mutations and whole gene deletions in anophthalmia, microphthalmia and coloboma. Hum Mutat 2008; 29:E278-83. [PMID: 18781617]
9. Porter FD, Drago J, Xu Y, Cheema SS, Wassif C, Huang SP, Lee E, Grinberg A, Massalas JS, Bodine D, Alt F, Westphal H. Lhx2, a LIM homeobox gene, is required for eye, forebrain, and definitive erythrocyte development. Development 1997; 124:2935-44. [PMID: 9247336]
10. Tétreault N, Champagne MP, Bernier G. The LIM homeobox transcription factor Lhx2 is required to specify the retina field and synergistically cooperates with Pax6 for Six6 trans-activation. Dev Biol 2009; 327:541-50. [PMID: 19146846]
11. Yun S, Saijoh Y, Hirokawa KE, Kopinke D, Murtaugh LC, Monuki ES, Levine EM. Lhx2 links the intrinsic and extrinsic factors that control optic cup formation. Development 2009; 136:3895-906. [PMID: 19906857]
12. Viczian AS, Bang AG, Harris WA, Zuber ME. Expression of Xenopus laevis Lhx2 during eye development and evidence for divergent expression among vertebrates. Dev Dyn 2006; 235:1133-41. [PMID: 16470628]

The print version of this article was created on 15 December 2010. This reflects all typographical corrections and errata to the article through that date. Details of any changes may be found in the online version of the article.

ARTICLE 10

Mutations in the newly identified *RAX* regulatory sequence are not a frequent cause of micro/anophthalmia

Genetic Testing and Molecular Biomarkers

2009-13(3): 289-90

N. Chassaing, A. Vigouroux and P. Calvas

Cet article rapporte la recherche de mutation dans une séquence régulatrice du gène *RAX*. Cette séquence régulatrice était doublement intéressante car elle permet la régulation d'expression d'un gène d'AM (*RAX*) par des facteurs de transcription impliqués dans l'AM (SOX2 et OTX2). Nous y décrivons la recherche de mutation chez 51 patients atteints d'AM, chez qui aucune mutation n'avait pu être préalablement identifiée par l'analyse des sept gènes systématiquement testés chez les sujets souffrant d'AM. Deux variations de séquences non représentées dans les bases de données ont été identifiées à proximité de la séquence critique de 35 pb de fixation des facteurs de transcription. Ces deux variations ont cependant été retrouvées chez 2 % et 5 % des contrôles, rendant très improbable leur implication dans les phénotypes oculaires de ces patients. Aucune autre variation de séquence n'a été retrouvée.

GENETIC TESTING AND MOLECULAR BIOMARKERS
Volume 13, Number 3, 2009

Pp. 289–290
DOI: 10.1089/gtmb.2008.0143

Letters to the Editor

Mutations in the Newly Identified *RAX* Regulatory Sequence Are Not a Frequent Cause of Micro/Anophthalmia

Nicolas Chassaing,[1–3] Adeline Vigouroux,[1,2] and Patrick Calvas[1–3]

Aim: Microphthalmia and anophthalmia are at the severe end of the spectrum of abnormalities in ocular development. A few genes (*SOX2*, *OTX2*, *RAX*, and *CHX10*) have been implicated in isolated micro/anophthalmia, but causative mutations of these genes explain less than a quarter of these developmental defects. A specifically conserved SOX2/OTX2-mediated *RAX* expression regulatory sequence has recently been identified. We postulated that mutations in this sequence could lead to micro/anophthalmia, and thus we performed molecular screening of this regulatory element in patients suffering from micro/anophthalmia. *Methods*: Fifty-one patients suffering from nonsyndromic microphthalmia ($n = 40$) or anophthalmia ($n = 11$) were included in this study after negative molecular screening for *SOX2*, *OTX2*, *RAX*, and *CHX10* mutations. Mutation screening of the *RAX* regulatory sequence was performed by direct sequencing for these patients. *Results*: No mutations were identified in the highly conserved *RAX* regulatory sequence in any of the 51 patients. *Conclusions*: Mutations in the newly identified *RAX* regulatory sequence do not represent a frequent cause of nonsyndromic micro/anophthalmia.

Introduction

Microphthalmia and anophthalmia are at the severe end of the spectrum of abnormalities in ocular development. The combined occurrence rate for these two malformations is 1/10,000 births (Morrison *et al.*, 2002; Lowry *et al.*, 2005). Mutations in several genes have been isolated in syndromic and nonsyndromic anophthalmia. Heterozygous mutations in *SOX2* account for approximately 10% of anophthalmia (Fantes *et al.*, 2003; Ragge *et al.*, 2005). Other genes have been identified to cause isolated anophthalmia or extreme microphthalmia in humans (*OTX2*, *RAX*, and *CHX10*) (Verma and Fitzpatrick, 2007). The latter are implicated in a very small proportion of affected individuals, implying wide genetic heterogeneity to match the phenotypic variability.

The *RAX* homeobox gene is essential for vertebrate eye development. In humans, the role of *RAX* in eye formation is clearly supported by the identification of truncating and missense mutations in patients with anophthalmia (Voronina *et al.*, 2004; Lequeux *et al.*, 2008). Recently, Danno *et al.*, (2008) identified a specific 35-nucleotide conserved regulatory sequence located 2 kb upstream of the promotor. They showed that OTX2 and SOX2, two proteins, also directly implicated in micro/anophthalmia, bind this conserved sequence, and act as direct upstream regulators of *RAX* expression (Danno *et al.*, 2008). We hypothesize that mutations in this regulatory sequence could disturb the early embryologic process of eye formation, and consequently lead to micro/anophthalmia. Molecular analysis was therefore performed in 51 nonsyndromic micro/anophthalmia patients for whom previous molecular analysis of genes implicated in isolated micro/anophthalmia (*SOX2*, *OTX2*, *RAX*, and *CHX10*) had failed to identify any causative mutation.

Patients and Methods

Patients

Fifty-one patients suffering from nonsyndromic microphthalmia ($n = 40$) or anophthalmia ($n = 11$) were included in this study after their informed consent was obtained according to French law. All had undergone molecular analysis of *SOX2*, *OTX2*, *RAX*, and *CHX10* genes without any causative mutation identified.

Methods

The 35-nucleotide conserved *RAX* regulatory sequence (1-3117 to 1-3084) was amplified by PCR using a set of primers deduced from the *RAX* 5′ genomic sequence (forward:

[1]INSERM, U563, Centre de Physiopathologie de Toulouse Purpan, Toulouse, France.
[2]CHU Toulouse, Hôpital Purpan, Service de Génétique Médicale, Toulouse, France.
[3]Université Toulouse III Paul-Sabatier, Toulouse, France.

CCAGGCTCCTTACTGTTGCT; reverse: GCTTCCTTTGTG CAGGACAT), corresponding to amplification of a 243-bp fragment. The PCR-amplified strands were subsequently purified with QIAquick Gel Extraction kit (Qiagen SA, Courtaboeuf, France), and both strands were sequenced using Big Dye DNA sequencing kit (Applied Biosystems, Courtaboeuf, France). Reactions were analyzed in an ABI3100 sequencer (Applied Biosystems).

Results and Discussion

To date, *RAX* mutations explain only a minority of micro/anophthalmia cases. However, because only the coding sequences have been studied previously, the possibility of recurrent mutations in regulatory sequences could not be ruled out.

The recently described *RAX* regulatory sequence was a good candidate region for mutations in micro/anophthalmia, as OTX2, SOX2 (two proteins that bind this sequence and then regulate *RAX* expression), and RAX proteins expressed in early eye development and mutations of genes encoding these three proteins lead to micro/anophthalmia (Verma and Fitzpatrick, 2007; Danno *et al*., 2008). The *RAX* regulatory sequence is highly conserved among species (Danno *et al*., 2008), and mutations in this sequence would probably impair SOX2 and OTX2 DNA pairing and thus *RAX* expression. Molecular analysis allows to identify two not previously described heterozygous single-nucleotide polymorphisms (1-3058C > T and 1-3046G > A) located near the highly conserved regulatory sequence in, respectively, one and two patients. However, these variations were also found, respectively, in 2% and 5% of a control population of 50 individuals and, hence, could be considered as nonpathogenic variations. Molecular analysis failed to identify any sequence variation of the *RAX* 35-nucleotide conserved regulatory element in the 51 patients included in this study.

In conclusion, although mutations in this sequence may nevertheless be implicated in some micro/anophthalmia patients, our results suggest that such sequence variations are not a frequent cause of micro/anophthalmia. Molecular basis of these ocular malformations remains still poorly understood, and further work remains to be done to identify new micro/anophthalmia genes.

Disclosure Statement

No competing financial interests exist.

References

Danno H, Michiue T, Hitachi K, *et al*. (2008) Molecular links among the causative genes for ocular malformation: Otx2 and Sox2 coregulate Rax expression. Proc Natl Acad Sci USA 105:5408–5413.

Fantes J, Ragge NK, Lynch SA, *et al*. (2003) Mutations in SOX2 cause anophthalmia. Nat Genet 33:461–463.

Lequeux L, Rio M, Vigouroux A, *et al*. (2008) Confirmation of RAX gene involvement in human anophthalmia. Clin Genet 74:392–395.

Lowry RB, Kohut R, Sibbald B, Rouleau J (2005) Anophthalmia and microphthalmia in the Alberta congenital anomalies surveillance system. Can J Ophthalmol 40:38–44.

Morrison D, Fitz Patrick D, Hanson I, *et al*. (2002) National study of microphthalmia, anophthalmia, and coloboma (MAC) in Scotland: investigation of genetic aetiology. J Med Genet 39:16–22.

Ragge NK, Lorenz B, Schneider A, *et al*. (2005) SOX2 anophthalmia syndrome. Am J Med Genet A 135:1–7.

Verma AS, Fitzpatrick DR (2007) Anophthalmia and microphthalmia. Orphanet J Rare Dis 2:47.

Voronina VA, Kozhemyakina EA, O'Kernick CM, *et al*. (2004) Mutations in the human RAX homeobox gene in a patient with anophthalmia and sclerocornea. Hum Mol Genet 13:315–322.

Address reprint requests to:
Patrick Calvas, M.D., Ph.D.
Service de Génétique Médicale
Pavillon Lefebvre
CHU Purpan
Place du Dr Baylac
31059 Toulouse Cedex 9
France

E-mail: calvas.p@chu-toulouse.fr

IV-2 : Approche CGH-array

Introduction

Des anomalies chromosomiques détectées par les techniques de cytogénétique conventionnelle sont identifiées chez 7,7 à 10 % des patients avec AM [24, 26]. Il s'agit essentiellement de trisomie 13 ou 18, ou l'atteinte oculaire n'est pas au premier plan. La CGH-array est un outil de cytogénétique moléculaire permettant de détecter des remaniements chromosomiques non visibles sur un caryotype standard. Cette technique a démontré son intérêt pour identifier des délétions/duplications cryptiques, et ainsi identifier les bases moléculaires de nombreux syndromes. L'approche par gènes candidats positionnels (candidats positionnels sur les données de cytogénétique) a permis d'identifier différents gènes d'AM (*SOX2*, *BMP4*, *TMX3*….)[4, 99, 174]. Quand des remaniements chromosomiques sont détectés par la cytogénétique conventionnelle (caryotype) ou la cytogénétique moléculaire (CGH-array) chez des patients avec AM, il est logique de faire l'hypothèse que le gène en cause dans leur anomalie du développement oculaire pourrait être situé au niveau du remaniement. En connaissant le(s) gène(s) situé(s) au niveau de la délétion, de la duplication ou de la translocation, il est possible de chercher des arguments fonctionnels permettant de suspecter un rôle à chacun de ces gènes dans la genèse de l'AM (famille de protéine, patron d'expression, modèles animaux etc…). La seconde étape consiste ensuite à rechercher des mutations ponctuelles de ces gènes candidats chez des patients atteints d'AM.

Pour des raisons pratiques (quantité d'ADN pour certains patients, ancienneté de l'ADN pour d'autres, résolution de la technique de CGH-array dans notre laboratoire au moment du projet, CGH-array faites dans un cadre diagnostic, budget…), nous n'avons pas réalisé de recherche systématique de micro-réarrangements chromosomiques dans la cohorte de patients étudiés. Nous avons, par contre, participé au travail de thèse d'Université du Dr. Andrée Delahaye qui a testé par CGH-array 65 patients présentant une anomalie du développement oculaire d'allure syndromique (associée à une déficience intellectuelle et/ou des malformations d'organes).

Méthodes et Résultats

En plus de la validation par la technique de CGH-array des 8 délétions identifiées dans notre laboratoire par QMPSF (5 *SOX2*, 2 *OTX2* et 1 *RAX*, cf. chapitre "analyse moléculaire des gènes connus"), la CGH-array a permis d'identifier 4 remaniements chromosomiques dont le caractère causal est discuté dans l'article ci-dessous (patients 10, 11, 12, et 14) :

- Article n°11

Delahaye, A *et al*. (2012). "Genomic imbalances detected by array-CGH in patients with syndromal ocular developmental anomalies." Eur J Hum Genet 20(5): 527-33.

Conclusion

La CGH-array est une technique à considérer dans le but d'identifier de nouveaux gènes responsables de maladies. Pour des raisons pratiques et budgétaires, nous n'avons pas réalisé cette analyse de manière systématique, mais avons pu participer au travail du Dr Delahaye focalisé sur cette technique dans les anomalies du développement oculaire. Cette collaboration, a également abouti à caractériser finement les délétions des gènes *SOX2*, *OTX2* et *RAX* identifiées par la QMPSF dans un cadre diagnostique. Enfin, les régions désignées par ces remaniements ont permis de considérer les gènes impliqués comme des gènes candidats aux anomalies du développement oculaire. Ces gènes candidats par la position ont ainsi été analysés pour les approches de séquençage à haut débit citées plus loin. (cf. chapitre "séquençage haut débit des gènes candidats").

ARTICLE 11

Genomic imbalances detected by array-CGH in patients with syndromal ocular developmental anomalies

European Journal of Human Genetics

2012-20(5): 527-33

A. Delahaye, P. Bitoun, S. Drunat, M. Gerard-Blanluet, **N. Chassaing**, A. Toutain, A. Verloes, F. Gatelais, M. Legendre, L. Faivre, S. Passemard, A. Aboura, S. Kaltenbach, S. Quentin, C. Dupont, A. C. Tabet, S. Amselem, J. Elion, P. Gressens, E. Pipiras and B. Benzacken

---

65 patients atteints d'anomalies malformatives oculaires associées à une déficience intellectuelle et/ou d'autres malformations ont été analysés par la technique de CGH-array 105 ou 180K. 14 remaniements ont été identifiés chez ces patients. Pour 10 d'entre eux, il existe des arguments pour établir un lien de causalité entre le remaniement identifié et l'atteinte oculaire. Pour quatre de ces remaniements le lien avec l'atteinte oculaire a été considéré improbable. Parmi les 10 remaniements considérés comme potentiellement causaux, 4 impliquent des gènes dont le rôle dans le développement oculaire était déjà connu (2 délétions d'*OTX2* et 2 de *FOXC1*). Les 6 autres remaniements permettent de pointer de nouveaux candidats à la genèse d'anomalies du développement embryonnaire de l'œil.

European Journal of Human Genetics (2012) 20, 527–533

www.nature.com/ejhg

ARTICLE

Genomic imbalances detected by array-CGH in patients with syndromal ocular developmental anomalies

Andrée Delahaye*[,1,2,3,15], Pierre Bitoun[4,15], Séverine Drunat[5], Marion Gérard-Blanluet[5], Nicolas Chassaing[6], Annick Toutain[7], Alain Verloes[3,5,8], Frédérique Gatelais[9], Marie Legendre[10], Laurence Faivre[11], Sandrine Passemard[3,5,8], Azzedine Aboura[5], Sophie Kaltenbach[5,12], Samuel Quentin[13], Céline Dupont[1,5], Anne-Claude Tabet[5], Serge Amselem[9], Jacques Elion[3,5,8,14], Pierre Gressens[3,8], Eva Pipiras[1,2,3,16] and Brigitte Benzacken[1,2,3,5,16]

In 65 patients, who had unexplained ocular developmental anomalies (ODAs) with at least one other birth defect and/or intellectual disability, we performed oligonucleotide comparative genome hybridisation-based microarray analysis (array-CGH; 105A or 180K, Agilent Technologies). In four patients, array-CGH identified clinically relevant deletions encompassing a gene known to be involved in ocular development (*FOXC1* or *OTX2*). In four other patients, we found three pathogenic deletions not classically associated with abnormal ocular morphogenesis, namely, del(17)(p13.3p13.3), del(10)(p14p15.3), and del(16)(p11.2p11.2). We also detected copy number variations of uncertain pathogenicity in two other patients. Rearranged segments ranged in size from 0.04 to 5.68 Mb. These results show that array-CGH provides a high diagnostic yield (15%) in patients with syndromal ODAs and can identify previously unknown chromosomal regions associated with these conditions. In addition to their importance for diagnosis and genetic counselling, these data may help identify genes involved in ocular development.
European Journal of Human Genetics (2012) **20,** 527–533; doi:10.1038/ejhg.2011.233; published online 11 January 2012

Keywords: ocular developmental anomaly; array-CGH; *OTX2*; *FOXC1*; 16p11.2 deletion; *YWHAE*

INTRODUCTION

Ocular developmental anomalies (ODAs) are severe structural defects of the eye caused by disruption of the complex process of ocular morphogenesis during early gestation.[1] ODAs occur in about 1 in 3000 to 4000 neonates and have been estimated to account for at least 25% of cases of childhood visual impairment worldwide.[2,3] ODAs include anophthalmia, microphthalmia, coloboma (failure of the optic fissure to close), congenital cataract (opacity of the lens fibres), and dysgenesis of the anterior segment (iris and cornea). These anomalies can occur separately or in combination and can be accompanied with other birth defects and/or with intellectual disability. The broad clinical spectrum of syndromal ODAs reflects the complexity of the pathways involved in ocular development. Many genes are known to be involved in ocular development, including several genes initially identified in chromosomal rearrangements.[4]

Chromosomal abnormalities are found in 7.7 to 10% of neonates with ocular anomalies and other birth defects.[5,6] The introduction of microarray technology has shown a very high rate of rearrangements undetectable with standard or high-resolution karyotyping. Submicroscopic copy number variations (CNVs) account for a substantial proportion of normal and pathogenic genetic variation in humans.[7] Few studies have specifically addressed the role for submicroscopic chromosomal imbalances in ODAs. In a case–series study of 32 patients with non-syndromal anophthalmia, microphthalmia, or coloboma, a single causal deletion was found, suggesting a limited causal role for CNVs in non-syndromal ODAs.[8] Another study found pathogenic CNVs in 5 (13%) of 37 patients with ocular birth defects.[9]

The objective of this study was to determine the prevalence of genomic imbalances identified using comparative genomic hybridisation-based microarray analysis (array-CGH) in patients with syndromal ODAs.

PATIENTS AND METHODS

Informed consent to participation was obtained from all patients and/or parents before study inclusion. Parents also gave informed consent for their own tests.

PATIENTS

A total of 65 unrelated patients (42 males and 23 females) were included. They were born to non-consanguineous parents and had unexplained syndromal ODAs with normal karyotypes. All patients were examined by experienced ophthalmologists and clinical

[1]AP-HP, Hôpital Jean Verdier, Service d'Histologie, Embryologie, et Cytogénétique, Bondy, France; [2]Université Paris-Nord, Paris 13, UFR SMBH, Bobigny, France; [3]Inserm, U676, Paris, France; [4]AP-HP, Hôpital Jean Verdier, Consultations de génétique médicale, Service de Pédiatrie, Bondy, France; [5]AP-HP, Hôpital Robert Debré, Département de Génétique, Paris, France; [6]CHU Toulouse, Hôpital Purpan, Service de Génétique Médicale, Toulouse, France; [7]CHU de Tours, Hôpital Bretonneau, Département de Génétique, Tours, France; [8]Université Paris Diderot, Faculté de Médecine, Paris, France; [9]CHU d'Angers, Service d'endocrinologie diabétologie pédiatrique, Angers, France; [10]Inserm, U933, Université Paris 6, AP-HP, Hôpital Armand-Trousseau, Paris, France; [11]CHU de Dijon, Centre de Génétique, Dijon, France; [12]AP-HP, Hôpital Necker-Enfants-Malades, Service de Cytogénétique, Université Paris Descartes, Paris, France; [13]AP-HP, Hôpital Saint-Louis, Plateforme génomique, Institut Universitaire d'Hématologie, Paris, France; [14]Inserm, U763, Paris, France
*Correspondence: Dr A Delahaye, AP-HP, Hôpital Jean Verdier, Service d'Histologie, Embryologie, et Cytogénétique, Avenue du 14 Juillet, 93140 Bondy, France. Tel: +33 148 026674; Fax: +33 148 026737; E-mail: andree.delahaye@jvr.aphp.fr
[15]These authors contributed equally to this work.
[16]These authors contributed equally to this work.
Received 15 June 2011; revised 11 November 2011; accepted 15 November 2011; published online 11 January 2012

geneticists, and had negative routine diagnostic work-up results. There were 38 patients with micro-anophthalmia and coloboma, 7 with optic nerve hypoplasia, 2 with aniridia, 8 with anterior segment anomalies, 8 with congenital cataract, and 2 with other ocular defects (Duane syndrome and buphthalmos, respectively). Only patients with intellectual disability and/or at least one extraocular birth defect were included. Individual patient characteristics are reported in Supplementary Table 1.

Array-CGH

Blood samples were obtained from the study patients and, when possible, from their parents. Genomic DNA was isolated from blood samples using standard protocols. Oligonucleotide array-CGH was performed using the Human Genome CGH Microarray Kit 105A or SurePrint G3 Human CGH Microarray Kit, 4×180K (Agilent Technologies, Santa Clara, CA, USA). In the 105A kit, the arrays include a total of 105 750 probes, with an overall median probe spacing of 22 kb, and in the 180K kit a total of 180 880 probes, with an overall median probe spacing of 13 kb. Experiments were performed according to the standard Agilent protocol (Agilent Oligonucleotide Array-Based CGH for Genomic DNA Analysis, version 6.3). Commercially available genomic DNA (Promega, Madison, WI, USA) was used as the control. Hybridised slides were scanned with a microarray scanner (G2505B SureScan High-Resolution Technology Agilent), and the image data were extracted and converted to text files using Agilent Feature Extraction software. The data were graphed and analysed using Agilent CGH Analytics software (statistical algorithm: ADM-2; sensitivity threshold: 6.1). Only gains or losses that encompassed at least three consecutive oligomers on the array were considered. CNVs previously identified in unaffected individuals according to the Database of Genomic Variants (http://projects.tcag.ca/variation/) were excluded. The validation method was chosen based on the imbalance type (deletion or duplication), size, and sample availability (DNA and/or metaphase spreads). Then, the clinical relevance of observed chromosomal aberrations was estimated according to data found in the scientific literature and databases for each of the regions and genes involved, using the DECIPHER database (http://www.sanger.ac.uk/PostGenomics/decipher/) for known microdeletion and microduplication syndromes and the Online Mendelian Inheritance in Man (OMIM, www.ncbi.nlm.nih.gov/Omim/getmorbid.cgi) for known disease-causing genes, gene functions, and inheritance patterns. Whenever possible, to discriminate between *de novo* and inherited anomalies, the parents were tested using fluorescence *in situ* hybridisation (FISH), multiplex ligation-dependent probe amplification (MLPA), or real-time quantitative PCR technology (qPCR). When there was a family history of ODA or X-linked anomaly, additional family members were studied to evaluate the familial segregation of the inherited anomalies. DNA copy alterations were considered possibly pathogenic when they involved regions known to be associated with microdeletion or microduplication syndromes, involved known dosage-sensitive genes, involved known eye development genes, consisted in *de novo* imbalances, or exhibited a pattern of family segregation consistent with pathogenicity.

Fluorescence *in situ* hybridisation

FISH was performed using standard protocols with commercially available probes. BAC clones from the RPCI human BAC library were selected in the chromosomal region of interest using the UCSC Genome Browser (http://genome.cse.ucsc.edu). DNA was labelled with Spectrum GreenTM-11-dUTP or Spectrum OrangeTM-11-dUTP (Vysis, Downers Grove, IL, USA) by nick translation, using a commercial kit (Roche Diagnostics GMBH; http://www.rochediagnostics.com) according to the manufacturer's instructions. All BAC clones used for confirmation are described in the online Supplementary Information file (Supplementary Table 2).

Multiplex ligation-dependent probe amplification

The microdeletion syndrome-specific MLPA kit SALSA P297-B1 was used with MRC-Holland reagents (MRC-Holland, Amsterdam, the Netherlands) according to the manufacturer's protocol. Amplification products were analysed using capillary electrophoresis in the DNA Analyser 3130XL and GeneMapper software v3.7 (Applied Biosystems, Life Technologies, Carlsbad, CA, USA). This kit contains probes targeting the 16p11.2 region (*MAZ*, *MVP*, *HIRIP3*, *DOC2A*, and *MAPK3* genes).

Real-time qPCR

Real-time qPCR was performed on a StepOnePlus Real-Time PCR System (Applied Biosystems, Life Technologies) with fluorescent SYBR Green dye (Power SYBR green PCR master mix, Applied Biosystems, Life Technologies). Gene-specific primers for the target gene and endogenous control genes (*F9* and *PTEN*) were designed using Primer Express Software (Applied Biosystems, Life Technologies). The BLAST program from the NCBI browser (http://www.ncbi.nlm.nih.gov/BLAST) was used for *in silico* specificity analysis. Amplification efficiencies were calculated based upon the generation of standard curves using serial dilutions of genomic DNA. Assays with amplification efficiencies between 85 and 120% were considered acceptable. Each sample was run in triplicate for target gene quantification compared with endogenous control genes. Data were processed using the StepOne software v.2 (Applied Biosystems, Life Technologies), with the comparative ΔΔ threshold cycle-number method.[10] All the primers and probes used for qPCR are described in the online Supplementary Information file (Supplementary Table 2).

Microsatellite analysis

Microsatellites were selected from UCSC Genome Browser microsatellites or simple repeat tracks, and primers were designed using the NCBI Primer-BLAST program. For a single reaction, a master mix of 2.5 μl 10× PCR buffer with 25 mM MgCl2, 1 μl 5 mM dNTP, 0.125 μl AmpliTaq Gold enzyme (Applied Biosystems, Life Technologies), 0.25 μl 20 pM primers (forward and reverse), and 16 375 μl sterile H2O was prepared. A volume of 1 μl DNA (50 ng/μl) was added to each reaction. The PCR reaction was run in Eppendorf Thermocyclers (Eppendorf, Hamburg, Germany) using the following conditions: hot start at 95 °C for 10 min, 95 °C for 10 s, 50 °C for 10 s for 36 cycles, followed by a final extension step at 72 °C for 4 min. Samples were analysed on an ABI 3730 XL DNA sequencing analyser and processed using GeneMapper 3.7 software (Applied Biosystems, Life Technologies).

RESULTS

Molecular karyotyping

Array-CGH identified 15 DNA CNVs involving segments larger than 100 kb in 14 patients (Table 1). These alterations were consistently confirmed by FISH, MLPA, or qPCR. The altered segments ranged in size from 0.04 to 5.68 Mb (Figure 1). In four patients, we identified clinically relevant deletions encompassing a gene known to be involved in ocular development (*FOXC1* or *OTX2*; Table 1, patient no. 1–4). In four other patients, three pathogenic deletions not classically associated with ODAs were found, namely, del(10)(p14p15.3), del(17)(13.3p13.3), and del(16)(p11.2p11.2) (Table 1, patient no. 5–8). Microsatellite analyses showed that the deletions were *de novo* and paternally derived for patient no. 1, 2, and 5, and *de novo*

Table 1 DNA copy alterations identified using array-CGH

Patient	*Imbalance*	*Size (Mb)*	*ISCN description*[a]	*Inheritance*	*Major genes involved*	*DECIPHER patient*
Possibly pathogenic chromosomal anomalies						
Patient 1	Del	5.68	6p25.1p25.3(107,883-5,684,125)x1	Pat (dn)	***FOXC1***	PAR251592
Patient 2	Del	1.95	6p25.2p25.3(477,352-2,472,573)x1	Pat (dn)	***FOXC1***	PAR251563
Patient 3	Del	0.61	4q34q34(176,398,264-177,004,339)x1	Pat (inh)	*GPM6A*	PAR251586
	Del	2.25	14q22.2q23.1(54,287,767-56,543,234)x1	Mat (inh)	***OTX2***, *GCH1*	
Patient 4	Del	0.04	11p15.4p15.4(3,765,195-3,809,332)x1	U	*RHOG*	PAR254661
	Del	0.11	14q23.1q23.1(56,326,564-56,433,789)x1		***OTX2***	
Patient 5	Del	5.55	10p14p15.3(2,911,242-8,457,638)x1	Pat (dn)	*AKR1C2, GATA3*	PAR251587
Patient 6	Del	0.5	17p13.3p13.3(1,105,199-1,605,301)x1	U	*YWHAE*	PAR251562
Patient 7	Del	0.6	16p11.2p11.2(29,500,084-30,106,254)x1	Mat (dn)	*SEZ6L2*	PAR251593
Patient 8	Del	0.55	16p11.2p11.2(29,560,300-30,106,254)x1	Non-mat	*SEZ6L2*	PAR256688
Patient 9	Dup	0.18	11p15.4p15.4(7,283,552-7,466,165)x3	Pat (inh)	*SYT9, OLFML1*	PAR251548
Patient 10	Del	0.36	20p12.1p12.1(15,003,653-15,360,378)x1	U	*MACROD2*	PAR251588
Probably non-pathogenic variant						
Patient 11	Del	0.41	Xq25q25(127,268,216-127,679,006)x1	Mat (inh)	Pseudogenes	PAR251582
Patient 12	Del	0.77	2q23.3q23.3(153,511,511-154,277,644)x1	Mat (inh)	*RPRM*	PAR251584
Patient 13	Dup	0.2	6p11.2p11.2(27,767,070-27,969,040)x3	Mat (inh)	*tRNA* genes, histone gene cluster	PAR251546
Patient 14	Del	0.2	8p23.2p23.3(3,079,016-3,276,030)x1	Pat (inh)	*CSMD1*	PAR251596

Abbreviations: Del, deletion; dn, *de novo*; Dup, duplication; inh, inherited; ISCN, International System for Human Cytogenetic Nomenclature (2009); mat, maternal; pat, paternal; U, unavailable.
[a]On NCBI human genome Build 36 (UCSC hg18).
Bold denotes gene known to be involved in ocular development.

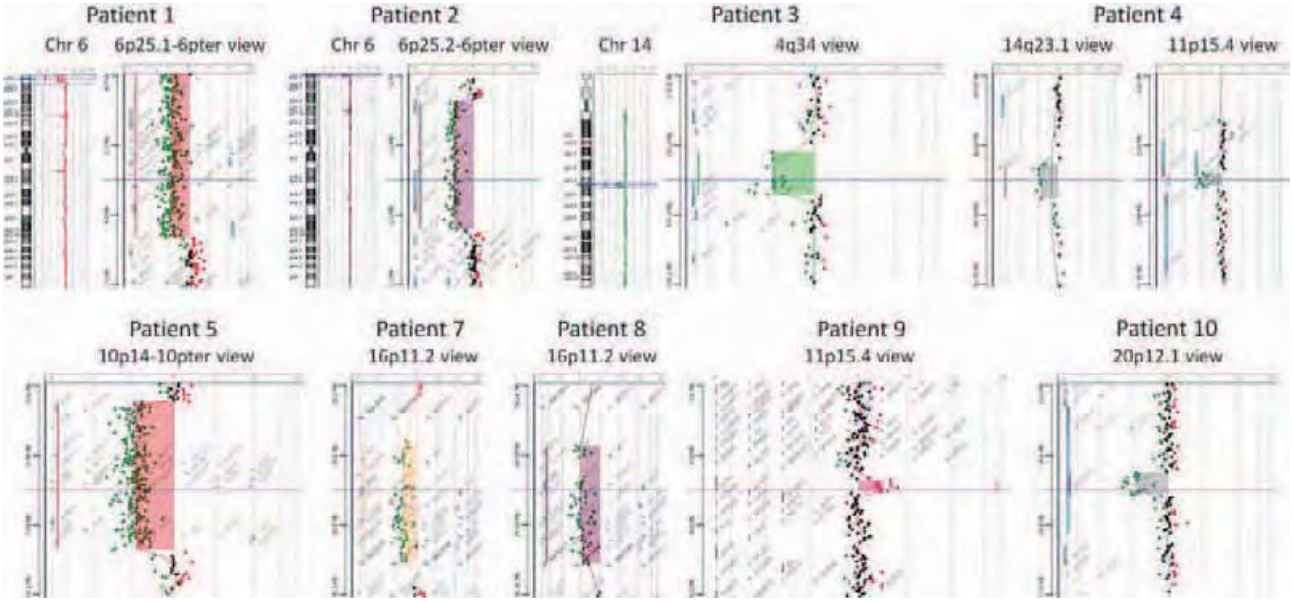

Figure 1 Possibly pathogenic chromosomal anomalies identified in patients with syndromal ODAs. Chromosome views and/or gene views of the affected chromosome or chromosome band produced by the Agilent CGH Analytics software and showing the aberrant region, which is highlighted in colour. On gene views, the dots correspond to the array targets, arranged on the *y* axis according to their genomic position and on the *x* axis according to their log2 intensity ratio value.

and maternally derived for patient no. 7. In patient no. 9, the inherited 11p15.4 duplication involving genes not known to be associated with disease was interpreted as possibly pathogenic because the pattern of family segregation suggested an autosomal dominant defect with incomplete penetrance and variable expressivity (Figure 2, Family A). In patient no. 10, we provisionally classified the 360-kb 20p12.1 deletion as possibly pathogenic, although no known disease-associated gene, microdeletion, or microduplication syndrome was found. We are seeking to obtain samples from the parents and sisters to clarify the clinical significance of this deletion. In a male patient (patient no. 11) with an Xq25 deletion involving genes not known to be associated with disease and inherited from a healthy mother, the family study identified this Xq25 deletion in an asymptomatic maternal uncle and was therefore probably a non-pathogenic variant (Figure 2, family B, and Table 1). In three patients (patient no. 12, 13, and 14), DNA copy alterations were inherited from a phenotypically normal parent with no family history of ODA and were interpreted as likely non-pathogenic variants (Table 1). All 14 patients have been submitted for registration in the DECIPHER database (http://www.sanger.ac.uk/PostGenomics/decipher/).

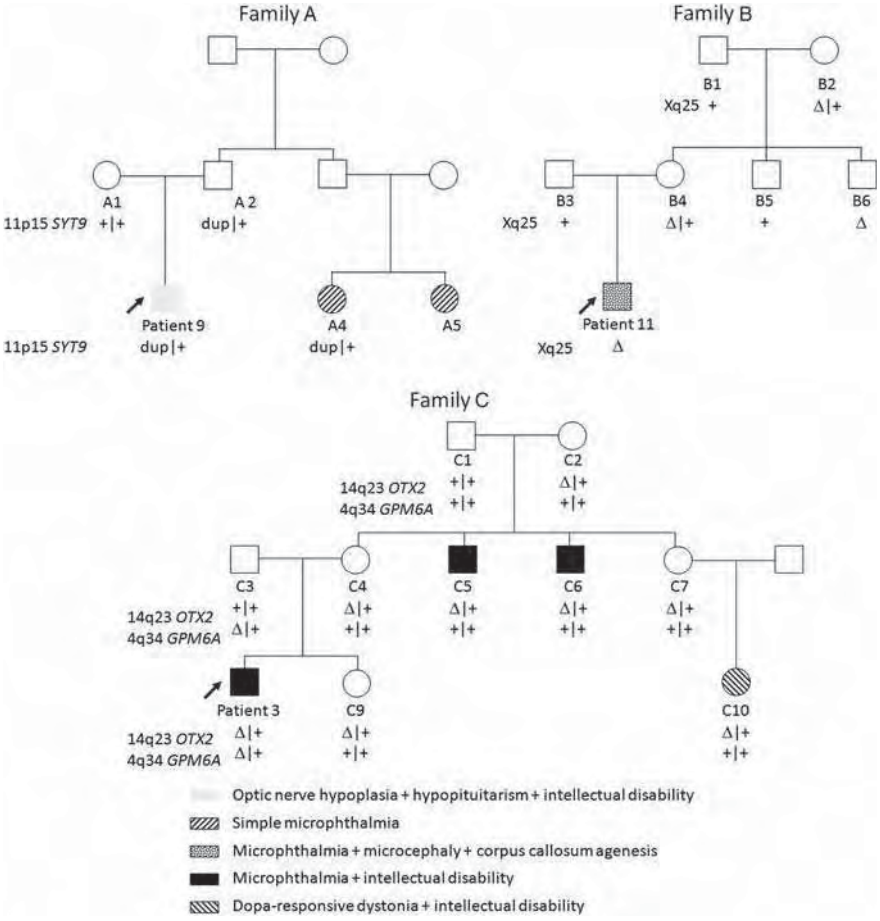

Figure 2 Family segregation of possibly pathogenic chromosomal anomalies. Family studies were performed for patient no. 9 (family A), 11 (family B), and 3 (family C). In family A, segregation of the 11p15 duplication was consistent with an autosomal dominant disorder with incomplete penetrance and variable expression. In family B, the Xq25 deletion was present in an asymptomatic maternal uncle, suggesting that it was a non-pathogenic variant devoid of clinical significance. Family C demonstrates the incomplete penetrance and variable expressivity of phenotypes associated with *OTX2* defects. The additional paternally inherited imbalance in patient no. 3 suggests that *GPM6A* haploinsufficiency may modify the phenotype associated with *OTX2* defects. dup, duplication; Δ, deletion; +, wild type.

Clinical data of patients with clinically relevant chromosomal abnormalities

Patient no. 1. This girl with a 6p25 deletion encompassing the *FOXC1* gene was referred to a clinical geneticist at 1 month of age for dilated cardiomyopathy and facial dysmorphism. She was the first and only child of healthy non-consanguineous parents. The pregnancy was uneventful. She was born at 39 weeks of gestation after a normal vaginal delivery. At birth, she had normal values for weight (2845 g), length (47.5 cm), and occipitofrontal circumference (34 cm). Dysmorphic features included a prominent forehead, hypertelorism, down-slanting palpebral fissures, a broad nasal bridge, and ocular proptosis. The combination of dilated cardiomyopathy and facial dysmorphism prompted further investigations. The conventional cytogenetic analysis was normal. The ophthalmologist found bilateral Axenfeld's anomaly with iridocorneal adhesions and corectopia of the right eye. Magnetic resonance imaging (MRI) of the brain showed a short corpus callosum and mega cisterna magna. During follow-up, mild motor delay developed and the cardiomyopathy remained stable. At last follow-up, she was 2 years of age and unable to walk alone; her weight was 10.2 kg (−1.5 SD), her height 81 cm (−1 SD), and her OFC 46 cm (−1 SD).

Patient no. 2. This 27-year-old man with a 6p25 deletion encompassing the *FOXC1* gene was born to non-consanguineous parents. He had Rieger syndrome with low vision and bilateral Rieger ocular anomaly (iris hypoplasia, iridocorneal adhesions, and posterior embryotoxon) complicated by bilateral glaucoma. Other abnormalities were hypotrophy, hypodontia, and autistic spectrum disorder. Cerebral MRI could not be performed.

Patient no. 3. This 24-year-old male belonging to family C (Figure 2) and his two maternal uncles (C5 and C6) had various combinations of colobomatous microphthalmia, palate anomalies, facial dysmorphism, renal malformation, microcephaly, and intellectual disability. They had a 14q23 deletion encompassing the *OTX2* gene. The carrier females had mild features (strabismus, nystagmus, low-normal intelligence, and speech problems), except one (C7), who was asymptomatic. Cousin C10 had developmental delay, strabismus, marked scoliosis, mild dysmorphism, and dopa-responsive dystonia. No other family members carrying the deletion had neurological symptoms suggesting dystonia.

Patient no. 4. This 14 year-old girl with a 14q23 deletion encompassing the *OTX2* gene was the first of two children of healthy

non-consanguineous parents. There was no family history of ODA. She was born at full term after a normal vaginal delivery. Her birth weight (2400 g) and length (46 cm) were at −2 SD (third percentile). She had severe bilateral microphthalmia, facial dysmorphism (prominent forehead and depressed nasal bridge), and developmental delay. When she was 4 years old, her weight was 10 kg (−3 SD), her height was 87 cm (−3.5 SD), and her skeletal bone age was 2 years. Investigations showed growth hormone deficiency and she was started on growth hormone replacement therapy. Brain MRI showed anterior pituitary hypoplasia and an ectopic posterior pituitary gland. At 10 years of age, after more than 5 years of growth hormone treatment, her weight was 21 kg (−2 SD) and her height 124 cm (−2 SD).

Patient no. 5. This 9-year-old boy with 10p14p15 deletion was the first and only child of healthy non-consanguineous parents. He was born at full term after a normal vaginal delivery, with growth parameters at −2 SD: weight 2380 g (fifth percentile); length 45 cm (third percentile), and OFC 32 cm (fifth percentile). He had multiple birth defects consisting of choanal atresia, bilateral coloboma of the iris, malrotation of the midgut, grade III vesicoureteral reflux, facial dysmorphism (blepharophimosis with down-slanting palpebral fissures), and microcephaly (OFC at −4 SD). During follow-up, epilepsy and developmental delay were diagnosed, followed by bilateral hearing impairment and hypoparathyroidism.

Patient no. 6. This 9-year-old boy previously described by Schiff *et al*[11] as patient D had a 17p13.3. deletion. He was the second child of healthy non-consanguineous parents. He had prenatal-onset growth retardation, bilateral chorioretinal coloboma with lens coloboma and right microcornea, developmental delay, and facial dysmorphism (large face, hypertelorism, down-slanting palpebral fissures, ptosis, short nose, pointed chin, and everted lower lip). Multidrug-resistant epilepsy developed during follow-up.

Patient no. 7. This 4-year-old girl with a 16p11.2 deletion had septo-optic dysplasia, with pituitary deficiency and intellectual disability. The ophthalmological examination was abnormal, with colobomatous microphthalmia of the left eye, persistent hyperplastic primary vitreous, and cataract of right eye. Brain MRI showed agenesis of the septum pellucidum and olfactory bulb and hypoplasia of the optic tract.

Patient no. 8. This 6-year-old boy with a 16p11.2 deletion was the second of two children of healthy non-consanguineous parents. There was no family history of ODA. He was born at full term after a normal vaginal delivery, with growth parameters at −2 SD: weight 2735 g (5–10th percentile); length 48 cm (10th percentile); and OFC 33 cm (10th percentile). Congenital nasolacrimal duct obstruction was repaired surgically. Chorioretinal coloboma with microcornea was found in the left eye; the right eye was normal. During follow-up, mild psychomotor delay with a speech defect developed. Brain MRI was not performed.

Patient no. 9. This 10-year-old boy with a 11p15.4 duplication was the first and only child of healthy non-consanguineous parents and belonged to family A (Figure 2). He had optic nerve hypoplasia, growth hormone and TSH deficiency, sleep disorder, and intellectual disability. Brain MRI showed anterior pituitary hypoplasia and ectopia of the posterior pituitary gland without other septal anomalies. His two paternal female cousins had simple microphthalmia.

Patient no. 10. This girl with a 20p12.1 deletion was the first-born child of healthy non-consanguineous parents. Abnormalities at birth consisted of bilateral anophthalmia, cleft lip and palate, deafness, and bilateral inguinal hernia. Her psychomotor development and stature were normal. She had a sister with unilateral microphthalmia and cleft lip and palate.

DISCUSSION

Using whole-genome array-CGH, we found 10 potentially pathogenic chromosome imbalances among 65 patients with ODAs. This diagnostic yield of 15% is consistent with the findings from oligonucleotide-based array studies in patients with unexplained intellectual disability or developmental delay.[12,13] Our study's arrays resolutions are theoretically lower than those used in the two previous array-CGH studies of patients with ODA.[8,9] However, our diagnostic yield is similar or better. This is certainly explained by differences in the inclusion criteria; unlike us, these two studies included patients with isolated ODAs.

The chromosomal abnormalities identified in patient no. 1–8 were considered causal. In four patients (no. 1–4), we found deletions encompassing a gene known to be involved in ocular development (*FOXC1* or *OTX2*), in keeping with an earlier study.[9] Adding our patients to those of this previous study, 8% of patients with ODAs had deletions encompassing *OTX2* (n=3), *FOXC1* (n=3), *COH1* (n=1), or *PAX6* (n=1). *FOXC1* alterations (mutations or 6p25.3 deletions/duplications) are involved in Axenfeld–Rieger anomaly or syndrome (MIM 601090, 602482, and 601631) and were recently shown to cause cerebellar vermis hypoplasia and to contribute to the Dandy–Walker continuum.[14] *OTX2* deletions and heterozygous mutations cause syndromal micro-anophthalmia (MIM 600037 and 610125)[15] and developmental anomalies of the pituitary gland,[16] and *OTX2* mutations can cause septo-optic dysplasia.[17] Family C and several previously described families were reported with *OTX2* alterations in patients presenting micro-anophthalmia and/or pituitary deficiency but inherited from an asymptomatic parent,[9,16,18,19] suggesting the incomplete penetrance of *OTX2*-associated phenotypes. Therefore, a CNV encompassing *OTX2* transmitted by an unaffected parent can be pathogenic for his child. Intrafamilial heterogeneity of *OTX2* defects may be explained, in some cases, by an additional imbalance. The *GPM6A* gene included in the paternally inherited 610-kb deletion at 4q34 of our patient no. 3 and the *RHOG* gene in the 11p15 deletion of patient no. 4 have both been implicated in neurite outgrowth.[20,21] RHO–ROCK signalling is involved in regulating the microfilament system, which is a key regulator of epithelial morphogenesis[22] and controls the early phases of optic cup morphogenesis.[23] These data support a role for *RHOG* in ODAs. We therefore suggest that *RHOG* haploinsufficiency may modulate the *OTX2*-related phenotype of patient no. 4.

Patient no. 5 and no. 6 carry pathogenic deletions that are not classically associated with ODAs. In both patients, the extraocular phenotype is consistent with the deletion. Their ODA could be related to a separate unknown cause or explained by the incomplete penetrance of an unknown ocular developmental gene included in their deletion. In patient no. 5, the deletion includes *GATA3*, which is involved in the HDR syndrome (hypoparathyroidism, deafness, and renal dysplasia syndrome, MIM 146255), and the phenotype is consistent with HDR syndrome. The additional anomalies are possibly due to the other genes included in the large 10p14p15 deletion in this patient. In keeping with earlier data,[11,24] ocular coloboma was a feature in our patient no. 6, pointing to a critical 0.67-Mb region for coloboma, with incomplete penetrance.

CNVs associated with partially penetrant phenotypes raise challenges, as seen also in our patient no. 7 and 8, who had a 16p11.2 deletion. The 16p11.2 deletion syndrome (OMIM 611913) has been

described in at least 100 individuals. The common deleted or duplicated region is 555 kb in length and is flanked by two low copy repeats of about 147 kb, suggesting that its pathogenic effects may be mediated by non-allelic homologous recombination. Recurrent microdeletions and microduplications at 16p11.2 have been shown to confer susceptibility to autistic spectrum disorder and have been identified in up to 1% of patients with this diagnosis.[25] The 16p11.2 deletion frequently co-segregates with severe early-onset obesity.[26,27] ODA is not a common feature of 16p11.2 deletions. In a neonate with multiple anomalies, including right ocular coloboma and chorioretinitis, array-CGH detected a 16p11.2 deletion on the G-banded karyotype; the size of the deletion was not estimated, and the break points were not reported.[28] More recently, microphthalmia and optic nerve coloboma were reported in a patient with a *de novo* 16p11.2 microdeletion.[29] Our finding of a 16p11.2 deletion in two patients with ODAs supports a causal link between 16p11.2 haploinsufficiency and low-penetrance coloboma. A less likely hypothesis is that of an autosomal recessive disorder with loss of one of the alleles, allowing the mutation-carrying allele to cause the ODA. In this chromosomal region, *SEZ6L2* may be involved in ocular development, as it is expressed in the forebrain during development[30] as well as in the eye (BioGPS, http://biogps.gnf.org/; GeneHub-GEPIS, http://www.cgl.ucsf.edu/Research/genentech/genehub-gepis/genehub-gepis-search.html). Further studies are needed to evaluate the potential role for *SEZ6L2* or another 16p11.2 gene in ocular development.

The clinical relevance of the CNV detected by array-CGH was unclear in two of our patients. Criteria for pathogenic CNVs, as opposed to non-pathogenic CNVs, have been suggested (see Table 1 of Lee *et al*[31]). Nevertheless, it may be difficult to draw a definitive conclusion,[7,32] most notably when samples cannot be obtained from both parents (and, in some cases, other family members). Unavailability of family samples is probably the greatest challenge raised by the use of array-CGH as a routine diagnostic tool. In our patient no. 10, the absence of family samples hindered our ability to interpret the 360-kb deletion at 20p12.1 in exon 6 and intron 6 of *MACROD2*. This deletion is not registered among the non-pathogenic CNVs in the DGV database. The function of *MACROD2* (previously *c20orf133*) is unknown. Genome-wide association studies found significant associations of *MACROD2* single-nucleotide polymorphisms with autistic spectrum disorder,[33] brain infarction,[34] and brain volume in multiple sclerosis.[35] The 360-kb deletion is located close to a hotspot of *de novo* and inherited CNVs with variable and non-recurrent break points, involving exon 5 and/or intron 5 of *MACROD2*. CNVs of this hotspot were found in control individuals in the DGV database and in individuals with schizophrenia,[36] holoprosencephaly,[37] and Kabuki syndrome,[38,39] suggesting limited or absent clinical relevance.[40] The phenotype in patient no. 10 does not resemble Kabuki syndrome. These facts argue against a role for *MACROD2* in ODAs.

The clinical relevance of the 11p15 microduplication detected in patient no. 9 is uncertain. This 180-kb duplication partially encompasses two genes, *SYT9* (OMIM 613528) and *OLFML1*. Confirmation using qPCR cannot distinguish a tandem/inverted duplication from an insertion at a distance. The *SYT9* gene is specifically expressed in the mouse brain and may have a role in calcium-sensitive synaptic neurotransmitter release,[41] but neither *SYT9* nor *OLFLM1* is known to be associated with clinical disease. The 11p15 duplication was also found in a cousin of patient no. 9 who has a different ODA. Microanophthalmia, optic nerve hypoplasia, and hypopituitarism belong to the growing spectrum of anomalies known to occur in septo-optic dysplasia.[17] The pattern of family segregation is consistent with an autosomal dominant defect with incomplete penetrance and variable expression. In the absence of similar cases, we can suggest, but not confirm, that this variant is pathogenic.

In our study, two-thirds of the patients were males, in keeping with the known male predominance among patients with ODA (and intellectual disability). No pathogenic CNVs were found in the X chromosome in our study or in earlier work. Therefore, the male preponderance can probably not be ascribed to genomic rearrangements involving developmental genes on the X chromosome. However, we cannot rule out inadequate distribution of oligonucleotide probes on the X chromosome.

In conclusion, our results emphasise the benefits of whole-genome array-CGH for the diagnosis of ODA syndromes. Detecting the genetic defect has important consequences for genetic counselling of the families and follow-up of the patients. Detailed molecular analysis of the rearranged regions may help to identify the genes involved in ocular development.

CONFLICT OF INTEREST

The authors declare no conflict of interest.

ACKNOWLEDGEMENTS

We thank the patients and their families who participated in this study and the medical staff involved in the diagnosis of syndromal ocular development anomalies.

1 Fitzpatrick DR, van Heyningen V: Developmental eye disorders. *Curr Opin Genet Dev* 2005; **15**: 348–353.
2 Hornby SJ, Gilbert CE, Rahi JK *et al*: Regional variation in blindness in children due to microphthalmos, anophthalmos and coloboma. *Ophthalmic Epidemiol* 2000; **7**: 127–138.
3 Morrison D, FitzPatrick D, Hanson I *et al*: National study of microphthalmia, anophthalmia, and coloboma (MAC) in Scotland: investigation of genetic aetiology. *J Med Genet* 2002; **39**: 16–22.
4 Mihelec M, St Heaps L, Flaherty M *et al*: Chromosomal rearrangements and novel genes in disorders of eye development, cataract and glaucoma. *Twin Res Hum Genet* 2008; **11**: 412–421.
5 Kallen B, Tornqvist K: The epidemiology of anophthalmia and microphthalmia in Sweden. *Eur J Epidemiol* 2005; **20**: 345–350.
6 Stoll C, Alembik Y, Dott B, Roth MP: Congenital eye malformations in 212,479 consecutive births. *Ann Genet* 1997; **40**: 122–128.
7 Lee C, Scherer SW: The clinical context of copy number variation in the human genome. *Expert Rev Mol Med* 2010; **12**: e8.
8 Raca G, Jackson CA, Kucinskas L *et al*: Array comparative genomic hybridization analysis in patients with anophthalmia, microphthalmia, and coloboma. *Genet Med* 2011; **13**: 437–442.
9 Balikova I, de Ravel T, Ayuso C *et al*: High frequency of submicroscopic chromosomal deletions in patients with idiopathic congenital eye malformations. *Am J Ophthalmol* 2011; **151**: 1087–1094, e1045.
10 Winer J, Jung CK, Shackel I, Williams PM: Development and validation of real-time quantitative reverse transcriptase-polymerase chain reaction for monitoring gene expression in cardiac myocytes *in vitro*. *Anal Biochem* 1999; **270**: 41–49.
11 Schiff M, Delahaye A, Andrieux J *et al*: Further delineation of the 17p13.3 microdeletion involving YWHAE but distal to PAFAH1B1: four additional patients. *Eur J Med Genet* 2010; **53**: 303–308.
12 Koolen DA, Pfundt R, de Leeuw N *et al*: Genomic microarrays in mental retardation: a practical workflow for diagnostic applications. *Hum Mutat* 2009; **30**: 283–292.
13 Xiang B, Zhu H, Shen Y *et al*: Genome-wide oligonucleotide array comparative genomic hybridization for etiological diagnosis of mental retardation: a multicenter experience of 1499 clinical cases. *J Mol Diagn* 2010; **12**: 204–212.
14 Aldinger KA, Lehmann OJ, Hudgins L *et al*: FOXC1 is required for normal cerebellar development and is a major contributor to chromosome 6p25.3 Dandy-Walker malformation. *Nat Genet* 2009; **41**: 1037–1042.
15 Nolen LD, Amor D, Haywood A *et al*: Deletion at 14q22-23 indicates a contiguous gene syndrome comprising anophthalmia, pituitary hypoplasia, and ear anomalies. *Am J Med Genet A* 2006; **140**: 1711–1718.
16 Dateki S, Kosaka K, Hasegawa K *et al*: Heterozygous orthodenticle homeobox 2 mutations are associated with variable pituitary phenotype. *J Clin Endocrinol Metab* 2010; **95**: 756–764.
17 McCabe MJ, Alatzoglou KS, Dattani MT: Septo-optic dysplasia and other midline defects: the role of transcription factors: HESX1 and beyond. *Best Pract Res Clin Endocrinol Metab* 2011; **25**: 115–124.

18 Ragge NK, Brown AG, Poloschek CM *et al*: Heterozygous mutations of OTX2 cause severe ocular malformations. *Am J Hum Genet* 2005; **76**: 1008–1022.
19 Schilter KF, Schneider A, Bardakjian T *et al*: OTX2 microphthalmia syndrome: four novel mutations and delineation of a phenotype. *Clin Genet* 2011; **79**: 158–168.
20 Alfonso J, Fernandez ME, Cooper B, Flugge G, Frasch AC: The stress-regulated protein M6a is a key modulator for neurite outgrowth and filopodium/spine formation. *Proc Natl Acad Sci USA* 2005; **102**: 17196–17201.
21 Katoh H, Negishi M: RhoG activates Rac1 by direct interaction with the Dock180-binding protein Elmo. *Nature* 2003; **424**: 461–464.
22 Sawyer JM, Harrell JR, Shemer G, Sullivan-Brown J, Roh-Johnson M, Goldstein B: Apical constriction: a cell shape change that can drive morphogenesis. *Dev Biol* 2010; **341**: 5–19.
23 Eiraku M, Takata N, Ishibashi H *et al*: Self-organizing optic-cup morphogenesis in three-dimensional culture. *Nature* 2011; **472**: 51–56.
24 Nagamani SC, Zhang F, Shchelochkov OA *et al*: Microdeletions including YWHAE in the Miller-Dieker syndrome region on chromosome 17p13.3 result in facial dysmorphisms, growth restriction, and cognitive impairment. *J Med Genet* 2009; **46**: 825–833.
25 Fernandez BA, Roberts W, Chung B *et al*: Phenotypic spectrum associated with *de novo* and inherited deletions and duplications at 16p11.2 in individuals ascertained for diagnosis of autism spectrum disorder. *J Med Genet* 2010; **47**: 195–203.
26 Bochukova EG, Huang N, Keogh J *et al*: Large, rare chromosomal deletions associated with severe early-onset obesity. *Nature* 2010; **463**: 666–670.
27 Walters RG, Jacquemont S, Valsesia A *et al*: A new highly penetrant form of obesity due to deletions on chromosome 16p11.2. *Nature* 2010; **463**: 671–675.
28 Hernando C, Plaja A, Rigola MA *et al*: Comparative genomic hybridisation shows a partial *de novo* deletion 16p11.2 in a neonate with multiple congenital malformations. *J Med Genet* 2002; **39**: E24.
29 Bardakjian TM, Kwok S, Slavotinek AM, Schneider AS: Clinical report of microphthalmia and optic nerve coloboma associated with a *de novo* microdeletion of chromosome 16p11.2. *Am J Med Genet A* 2010; **152A**: 3120–3123.
30 Kumar RA, Marshall CR, Badner JA *et al*: Association and mutation analyses of 16p11.2 autism candidate genes. *PLoS One* 2009; **4**: e4582.
31 Lee C, Iafrate AJ, Brothman AR: Copy number variations and clinical cytogenetic diagnosis of constitutional disorders. *Nat Genet* 2007; **39**: S48–S54.
32 Rodriguez-Revenga L, Mila M, Rosenberg C, Lamb A, Lee C: Structural variation in the human genome: the impact of copy number variants on clinical diagnosis. *Genet Med* 2007; **9**: 600–606.
33 Anney R, Klei L, Pinto D *et al*: A genome-wide scan for common alleles affecting risk for autism. *Hum Mol Genet* 2010; **19**: 4072–4082.
34 Debette S, Bis JC, Fornage M *et al*: Genome-wide association studies of MRI-defined brain infarcts: meta-analysis from the CHARGE Consortium. *Stroke* 2010; **41**: 210–217.
35 Baranzini SE, Wang J, Gibson RA *et al*: Genome-wide association analysis of susceptibility and clinical phenotype in multiple sclerosis. *Hum Mol Genet* 2009; **18**: 767–778.
36 Xu B, Woodroffe A, Rodriguez-Murillo L *et al*: Elucidating the genetic architecture of familial schizophrenia using rare copy number variant and linkage scans. *Proc Natl Acad Sci USA* 2009; **106**: 16746–16751.
37 Bendavid C, Rochard L, Dubourg C *et al*: Array-CGH analysis indicates a high prevalence of genomic rearrangements in holoprosencephaly: an updated map of candidate loci. *Hum Mutat* 2009; **30**: 1175–1182.
38 Maas NM, Van de Putte T, Melotte C *et al*: The C20orf133 gene is disrupted in a patient with Kabuki syndrome. *J Med Genet* 2007; **44**: 562–569.
39 Kuniba H, Yoshiura K, Kondoh T *et al*: Molecular karyotyping in 17 patients and mutation screening in 41 patients with Kabuki syndrome. *J Hum Genet* 2009; **54**: 304–309.
40 Bradley WE, Raelson JV, Dubois DY *et al*: Hotspots of large rare deletions in the human genome. *PLoS One* 2010; **5**: e9401.
41 Xu J, Mashimo T, Sudhof TC: Synaptotagmin-1, -2, and -9: Ca(2+) sensors for fast release that specify distinct presynaptic properties in subsets of neurons. *Neuron* 2007; **54**: 567–581.

Supplementary Information accompanies the paper on European Journal of Human Genetics website (http://www.nature.com/ejhg)

IV-3 : Approche expérimentale

Introduction au chapitre

Pour identifier de nouveaux gènes d'AM, nous avions émis l'hypothèse que ces nouveaux gènes pourraient être des gènes régulés par les facteurs de transcription (FT) déjà connus comme responsables d'AM et exprimés précocement dans le développement oculaire. L'analyse des gènes régulés par les facteurs de transcription déjà impliqués dans les AM, de leur fonction et de leur cartographie d'expression spatiale et temporelle constitue une étape clef de la compréhension des mécanismes moléculaires impliqués dans le développement oculaire normal[175], et de l'identification de nouveaux gènes impliqués dans les défauts du développement oculaire. Nous avons tenté d'identifier par l'approche expérimentale exposée ici les gènes régulés par les FTs SOX2, OTX2, PAX6 et RAX dont l'importante contribution au développement oculaire a été démontrée à maintes reprises (voir chapitre "introduction aux facteurs de transcription étudiés")

Pour identifier les gènes cibles de ces 4 FTs, nous avons mené en parallèle des analyses transcriptomiques et une approche par immunoprécipitation de chromatine.

Pour ces expériences, nous avons travaillé à partir de cellules souches embryonnaires établies en lignée (CCE), génétiquement modifiées (surexprimant le gène *Rax*, CCE-Rx). La surexpression de *Rax* permet leur différenciation en cellules rétiniennes[176]. Cette lignée nous a été transmise par le Pr. S. Watanabe (Kobe, Japon). Son équipe avait pu montrer qu'en introduisant une cassette d'expression du gène *Rax* dans des cellules souches embryonnaires d'origine murine (CCE), ces cellules conservaient leur caractère indifférencié et continuaient à proliférer en présence de LIF (Leukemia Inhibitoring Factor), comme les cellules CCE non modifiées. Par contre, la surexpression exogène de *Rax* leur conférait la possibilité de migrer dans des explants rétiniens et de s'intégrer dans ceux-ci, contrairement aux cellules mères non modifiées. Les CCE-Rx s'intégraient alors principalement dans la couche ganglionnaire, étaient capable de se connecter avec les cellules rétiniennes et d'approcher les capacités électrophysiologies de ces cellules.

Ces données montrent que la surexpression du gène *Rax* dans ces cellules souches embryonnaires, leur confère, dans des conditions spécifiques, une plus grande capacité à se différencier en cellules rétiniennes. Ce modèle cellulaire de cellules souches embryonnaires "orientées" vers une différentiation rétinienne, nous a paru un modèle cellulaire propice à rechercher les cibles des FTs étudiés au cours du développement oculaire.

IV-3-A : Transcriptomique

Introduction

Dans une première approche, la recherche des cibles des FTs Sox2, Otx2, Rax et Pax6, a été conduite à l'aide des analyses transcriptomiques des cellules CCE-Rx après inhibition ou surexpression de ces FTs.

Méthodes et Résultats

- Culture Cellulaire

Les CCE-Rx indifférenciées sont cultivées dans des boîtes de culture de 10cm de diamètre revêtues de gélatine (Biocoat) dans 6 ml de milieu DMEM supplémenté avec 15% de sérum de veau fœtal, 100 uM 2-mercaptoéthanol, 10 ng / ml LIF, 2 mM glutamine et 100 uM MEM non-acides aminés essentiels. Les cellules CCE sont maintenues dans un incubateur humidifié à 37 °C et 5% de CO_2 dans l'air. Le milieu de culture a été changé tous les jours. Les CCE-Rx indifférenciées sont adhérentes et sont passées toutes les 48H.

Pour la formation de corps embryoïdes (cellules en cours de différenciation), les CCE-Rx sont cultivées en suspension dans des boîtes de Pétri en plastique non adhérent de 6 cm de diamètre avec 4 ml de milieu de culture. Le milieu de culture diffère de celui des cellules indifférenciées : la concentration de SVF est de 10 %, et il n'y a pas de LIF (leukemia Inhibitoring Factor). Les cellules poussent en suspension et forment des agrégats cellulaires, les corps embryoïdes.

- Transfection

Le protocole de transfection a été adapté du protocole de transfection décrit pour ces cellules[177]. Les cellules CCE-Rx indifférenciées adhérentes sont détachées par trypsinisation et 1.2 10^6 cellules sont ensemencées dans une boîte non adhérente de 6 cm. Pour la transfection, il n'y a pas d'antibiotiques dans le milieu. La transfection utilise de l'Effectene et permet une efficacité de transfection importante (Fig. 26).

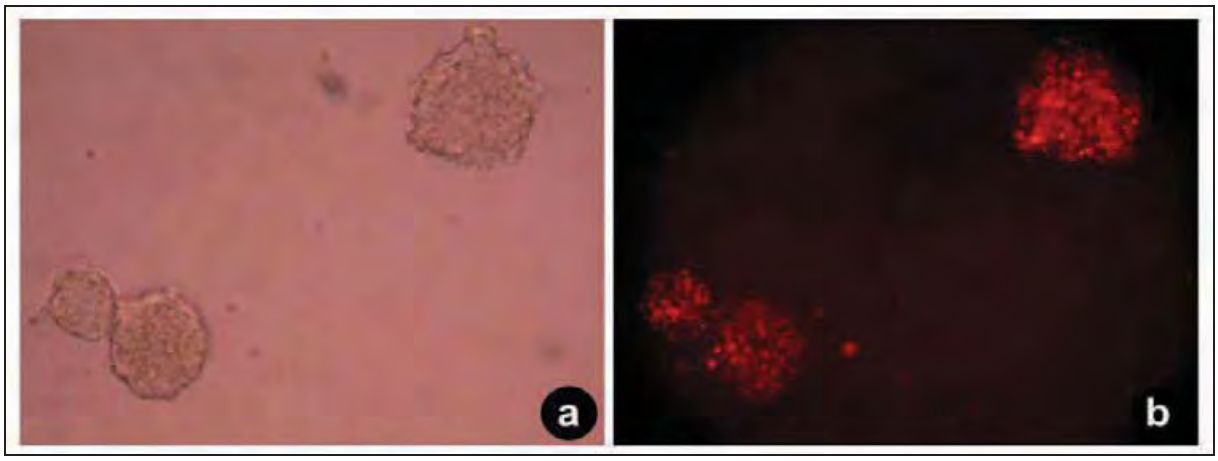

Figure 26: Efficacité de transfection des corps embryoïdes

(**a**) Aspect des corps embryoïdes en culture 48H après mise en culture des CCE-Rx. (**b**) L'efficacité de la transfection a été analysée à l'aide d'un vecteur de transfection dsRED 48H post transfection. La fluorescence rouge signe la bonne efficacité de la transfection et l'expression du vecteur. Tous les corps embryoïdes semblent avoir été efficacement transfectés, même s'il n'est pas possible de définir le taux de cellules transfectées dans chaque corps embryoïde.

Pour les transfections de vecteur d'expression (vecteur d'expression Qiagen pQE-TriSystem) d'OTX2, PAX6, RAX, ou SOX2, 1 µg d'ADN du vecteur était associé à 3.2 µl d'enhancer et 8 µl d'Effectene selon le protocole du fabriquant et ajouté directement au moment de l'ensemencement dans les boîtes de Pétri non adhérentes en vue de la formation de corps embryoïdes. De la même façon, pour les siRNA (Stealth siRNA, Invitrogen), les siRNA à 50nM final (siOtx2, siPax6, siRax) ou 400nM final (siSox2) étaient associés à 2.4 µl d'enhancer et 8 µl d'Effectene selon le protocole du fabriquant et ajoutés directement au moment de l'ensemencement dans les boîtes de Pétri non adhérentes. La quantité de vecteur d'expression ou de siRNA nécessaire a été optimisée pour chaque condition.

- Efficacité des siRNA

Afin d'identifier les meilleures conditions d'inhibition de l'expression des FTs ciblés, 4 siRNA différents ont été testés pour chaque FT. De même, différentes concentrations (de 5 à 400nM final) ont été testées. Les ARN ont été extraits des corps embryoïdes 48H post transfection et ont été analysés par qPCR en prenant comme gènes rapporteurs *Gapdh* et *β-Actine*. Les résultats obtenus ont été comparés à des ARNm extraits de corps embryoïdes transfectées avec un siRNA scramble (Invitrogen, Scramble siRNA, Medium GC). Les résultats obtenus pour les niveaux d'inhibition des 4 FTs étudiés sont représentés figure 27. Il n'a pas été possible d'obtenir une extinction totale de l'expression des FTs compte tenu de leur expression soutenue dans ces cellules (particulièrement *Sox2*) et de la croissance cellulaire importante entre la transfection et les 48H de culture cellulaire en suspension nécessaire à la formation des corps embryoïdes.

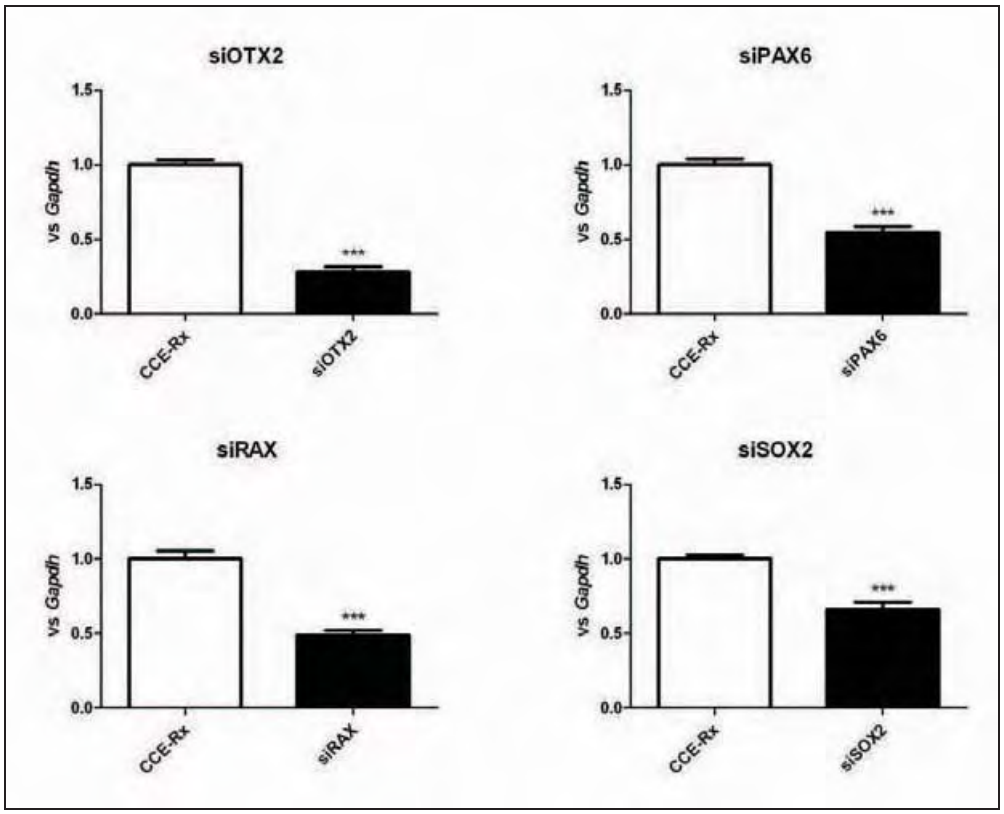

Figure 27: Efficacité des siRNA utilisés pour les analyses transcriptomiques

Le taux d'ARNm résiduel pour les 4 facteurs de transcription d'intérêt a été quantifié par qPCR 48H après transfection des cellules CCE-Rx par les siRNA correspondants. Ces résultats ont été normalisés par rapport à l'expression de *Gapdh*. L'expression résiduelle des facteurs de transcription étudiés est de 28 % pour *Otx2*, 54 % pour *Pax6*, 48 % pour *Rax* et 66 % pour *Sox2*.

Des résultats similaires ont été obtenus en analysant l'expression protéique de ces 4 FTs par western blot 48H après transfection (Fig. 28 et 29).

- Vecteurs de surexpression

Pour analyser l'efficacité des vecteurs de surexpression, nous avons extrait les protéines des cellules CCE-Rx 48H après transfection par un vecteur vide (contrôle) ou par un vecteur d'expression d'un des 4 FTs étudiés. Des analyses par western blot ont été faites soit en utilisant des Anticorps (Ac) spécifiques ciblant les FTs étudiés (Otx2-Abcam ab21990; Pax6-Sigma AV32741; Sox2 R&D MAB2018 et Rax-SantaCruz sc-79028) (Fig. 28), soit en utilisant un Ac primaire dirigé contre le motif poly-histidine (Qiagen) présent sur chaque vecteur d'expression permettant d'étudier l'expression de tous les vecteurs d'expression avec un Ac primaire unique (Fig. 29). Ces analyses ont permis de confirmer l'efficacité des vecteurs d'expression.

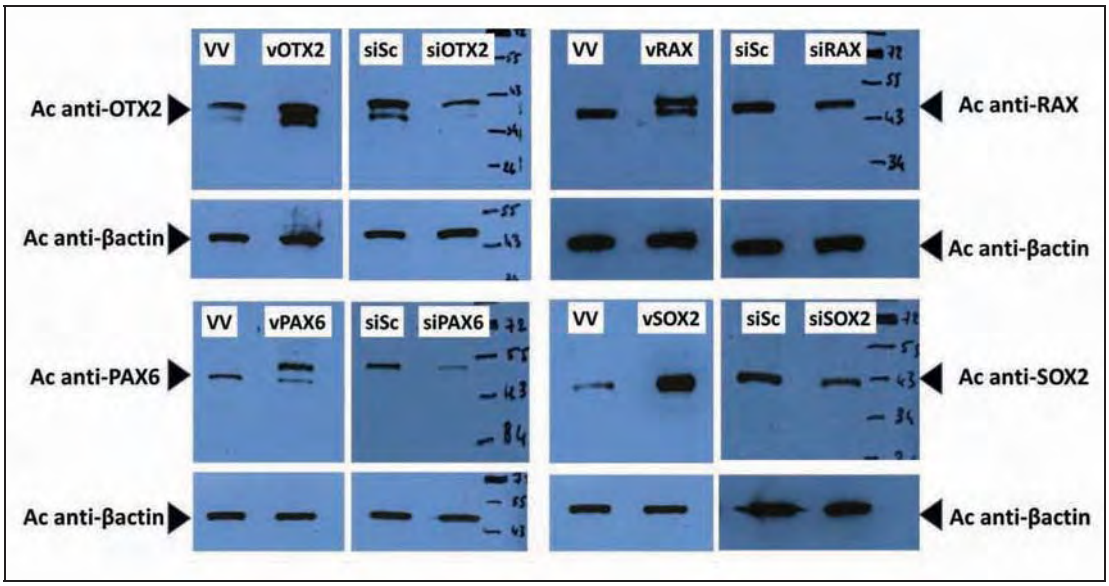

Figure 28: Analyse en western blot de l'efficacité des vecteurs d'expression et des siRNA pour chaque facteur de transcription étudié (Otx2, Pax6, Rax et Sox2)

Les protéines ont été extraites des corps embryoïdes 48H après transfection et l'expression des protéines d'intérêt est étudié après transfection d'un vecteur d'expression spécifique (vFT ; comparée à la transfection d'un vecteur vide (VV)) ou après transfection d'un siRNA spécifique (siFT ; comparée à la transfection d'un siRNA scramble (siSc)). La quantité de la protéine d'intérêt est rapportée à la quantité de protéine totale représentée par la quantité de β-actine. On retrouve une diminution des protéines ciblées lors de l'utilisation des siRNA spécifiques en comparaison du siRNA scramble. Il existe également une surexpression protéique induite par la transfection des vecteurs de surexpression.

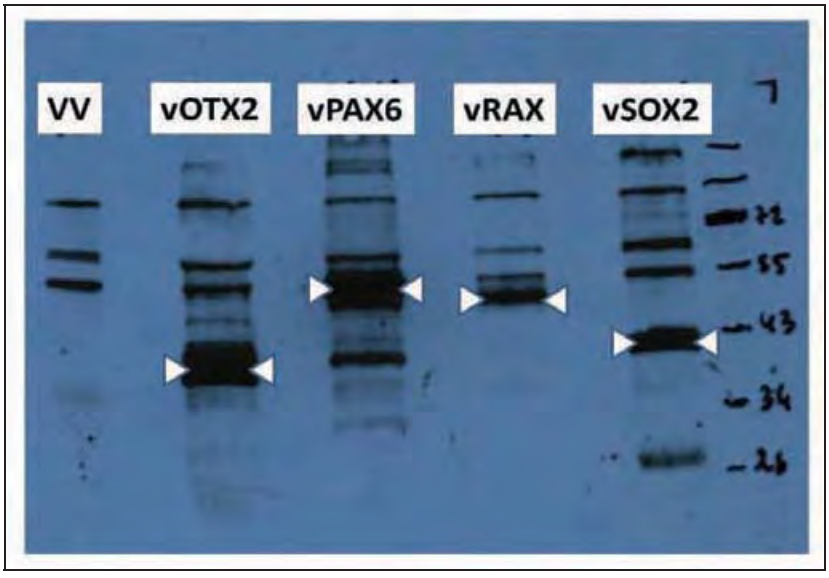

Figure 29: Analyse en western blot de l'efficacité des vecteurs d'expression pour chaque facteur de transcription étudié (Otx2, Pax6, Rax et Sox2) a l'aide d'un Ac anti pentahistidine.

Les protéines ont été extraites des corps embryoïdes 48H après transfection. Les facteurs de transcription étudiés exprimés dans les vecteurs d'expression Qiagen (vFT) ont une extension de 10 histidines en C-terminal permettant leur identification sur western blot grâce à l'utilisation d'un Ac primaire dirigé contre le motif penta-his. La première ligne représente les protéines extraites de cellules CCE-Rx transfectées par un vecteur vide (VV). Les bandes correspondant aux protéines d'intérêt sont marquées par des flèches blanches.

Nous avons ainsi validé la possibilité de moduler (inhibition ou surexpression) l'expression des FTs d'intérêt dans les cellules CCE-Rx. Ce résultat permettait l'analyse des modifications du transcriptome secondairement à chacune de ces modulations.

- Analyses transcriptomiques

48H après transfection par les vecteurs d'expression, ou les siRNA, les ARNm ont été extraits des corps embryoïdes et hybridées sur des puces Affymetrix GeneChip® Mouse Gene 1.0 ST Array couvrant plus de 26000 transcrits. Les conditions étudiées ont été : siSc, siOtx2, siPax6, siRax, siSox2, vecteur vide (VV), vOtx2, vPax6 et vRax. Compte tenu de l'expression basale importante de Sox2, nous ne sommes pas arrivés dans un premier temps à obtenir une surexpression franche de Sox2 et la condition vSox2 n'a donc pas pu être analysée. L'analyse des données a été faite par Sophie Lamarre à la plateforme Biopuce (Génotoul). Brièvement, la qualité des hybridations a été validée et les profils d'expression pour chaque condition ont été analysés après avoir corrigé les bruits de fond et normalisé les données à l'aide des logiciels RMA (version 2.14.2)[178] et R[179]. Les analyses statistiques de différentiel d'expression entre les conditions ont été réalisées avec le pack Limma[180]. Une p-value corrigée par le FDR (False Discovery Rate) a été utilisée pour les analyses de significativité. Un exemple de résultat obtenu est présenté dans la figure 30.

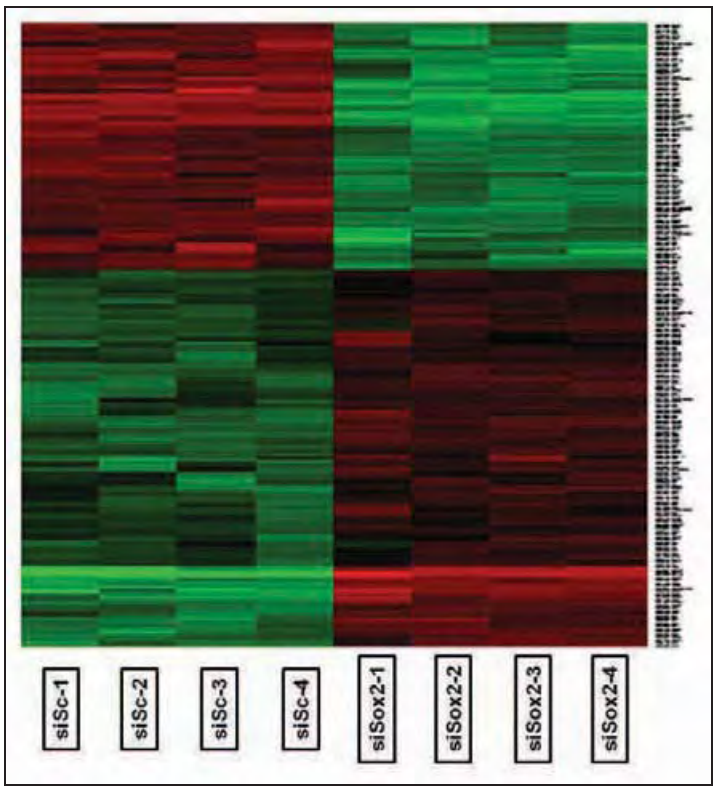

Figure 30: Représentation des gènes différentiellement exprimés entre deux conditions expérimentales.

Le niveau d'expression des gènes différentiellement exprimés entre les deux conditions est visualisable sur ce schéma (HeatMap). Le quadruplicat témoin (siSc) et représenté par les 4 premières colonnes à gauche de la figure, la condition étudiée (siSox2), par les 4 colonnes à droite. Les gènes sous exprimés dans une condition sont représentés en vert, les gènes surexprimés sont représentés en rouge.

- Validation des résultats

Les résultats significatifs obtenus pour les différentes conditions sont donnés sous forme de tableaux dans les annexes. Brièvement, les modifications d'expression entre les différentes conditions étaient plutôt modérées, avec un nombre de gènes dont l'expression était modifiée par rapport au contrôle VV ou siSC (log2-fold change à 0.5, p-value <0.05) variable d'une condition à l'autre : siOtx2 (16), siPax6 (7), siRax (11), siSox2 (230), vOtx2 (21), vPax6 (71) et vRax (57). L'ensemble des gènes avec une expression significativement modifiée (sans tenir compte de la variation du log2-fold change) a été jointe dans les annexes.

Pour valider ces résultats, nous avons sélectionné 25 gènes dont l'expression avait été modifiée dans au moins une condition d'analyse transcriptomique pour contrôler par PCR quantitative (qPCR) les résultats obtenus par l'analyse transcriptomique. Pour couvrir les différentes conditions expérimentales, nous avons sélectionné les gènes *En1, Mmp9, Sema6a, Hhip, Nrp2, Efhd1, Pfn2, Lmo2, Hbegf, Sertad3, Cct2, Nr0b1, Stxbp3b, Fgf15, Dmbx1, Gprc5c, Gbx2, Cds1, Ar, Glt28d2, Cetn2, Car3, Pkia, Sfrp2, Wwtr1*. Nous avons refait des analyses de transfection (n=12) et extraits les ARNm 48H post transfection. L'expression de chaque gène a été normalisée par rapport à l'expression de *Gapdh* et *β-Actine*.

Nous avons pu ainsi confirmer la variation significative de l'expression de 19 gènes dans une condition donnée (*En1, Mmp9, Sema6a, Hhip, Ar, Nrp2, Efhd1, Pfn2, Lmo2, Hbegf, Sertad3, Cct2, Nr0b1, Stxbp3b, Fgf15, Dmbx1, Gprc5c, Gbx2, Cds1*). Les résultats pour 12 d'entre eux sont présentés dans la figure 31. Pour 6 autres gènes (*Glt28d2, Cetn2, Car3, Pkia, Sfrp2, Wwtr1*), en raison de niveaux d'expression trop faibles, ou d'écarts types importants entre les différents échantillons nous n'avons pu confirmer de façon statistiquement significative la variation d'expression de ces gènes.

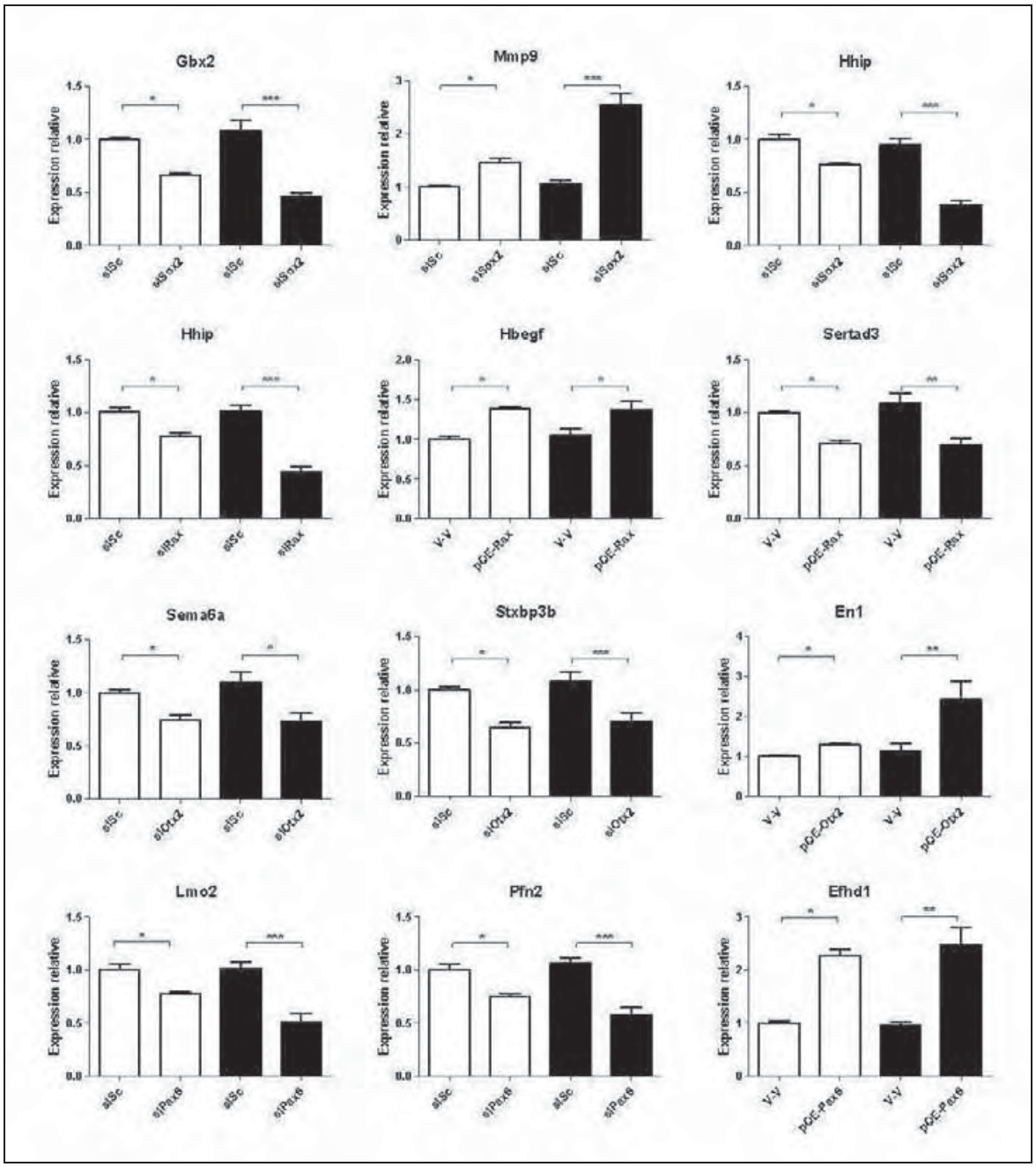

Figure 31: Confirmation par qPCR ciblée des résultats obtenus lors de l'approche transcriptomique.

Les résultats des analyses transcriptomiques (en blanc, n=4) sont comparés avec les résultats des analyses qPCR ciblées (en noir, n=12). Les expressions des gènes étudiés sont rapportées à l'expression du gène *Gapdh*. Des exemples ont été représentés pour les vecteurs de surexpression (pQE-(FT)) ou pour les siRNA (si(FT)). Ces expressions ont été comparées aux niveaux d'expression dans les cellules CCE-Rx après transfection d'un vecteur vide (V-V) ou d'un siRNA scramble (siSc).

- Analyse d'expression tissulaire

L'analyse transcriptomique, a ainsi permis de sélectionner les meilleurs gènes candidats pour être impliqués dans les AM. Ces gènes ont été sélectionnés car, en plus d'être régulés par au moins un

des facteurs de transcription étudiés, ils avaient une expression connue au cours du développement oculaire et/ou cérébral, ou appartenaient à une famille de gènes elle-même impliquée dans le développement oculaire chez l'homme ou l'animal.

L'expression oculaire embryonnaire de certains d'entre eux (*Dmbx1, Gdf2, Aldh1a3, Sfrp2, Sv2c, Plagl1, Fgf15, Cdh20, Stxbp3b, Rrh, Gprc5c, Bhlhe40, Gbx2, Cds1*) a été définie. De l'ARNm a été extrait des ébauches oculaires, du cerveau et des membres de 10 embryons de souris NMRI au stade E.11.5 et la présence de l'expression de ces gènes a été étudiée par RT-PCR/migration dans ces 3 tissus. Tous les gènes candidats sont exprimés dans l'œil. Pour la majorité des gènes, il n'existe pas de spécificité tissulaire car ils sont exprimés dans les 3 tissus (œil, cerveau, membres). Certains gènes présentent une expression plus importante dans l'œil et le cerveau (*Fgf15*, *Cadh20*). *Aldh1a3* présente quant à lui une spécificité oculaire. Un exemple des résultats obtenus est présenté dans la figure 32.

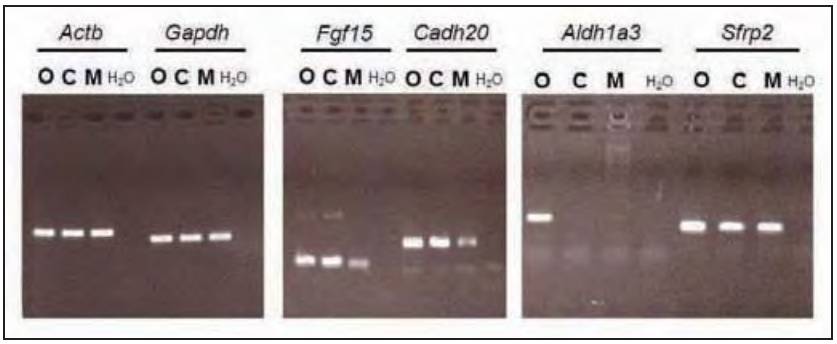

Figure 32: Analyse par RT-PCR de l'expression chez l'embryon de souris à E11.5 des gènes identifiés par l'approche transcriptomique.

Les ARNm ont été extraits à partir des yeux (**O**), du cerveau (**C**) ou des membres (**M**). Des amorces spécifiques permettant l'amplification d'un set de gènes d'intérêt (identifiés lors de l'approche transcriptomique) ont permis d'analyser l'expression de ces gènes dans ces trois tissus. L'amplification de la *β-actine* et de *Gapdh* sert de témoin positif. La majorité des gènes étudiés est exprimée dans les trois tissus (ici l'exemple de *Sfrp2*), certains comme *Fgf15* et *Cadh20* sont plus exprimés dans l'œil et dans le cerveau que dans les membres et, d'autres comme *Aldh1a3* ne sont exprimés que dans l'œil.

Conclusion

L'approche transcriptomique nous a permis d'identifier certains gènes cibles des FTs d'intérêt. Nous avons pu valider les résultats sur 12 nouveaux échantillons par PCR quantitative ciblée. Certains gènes apparaissaient comme de bons candidats à cette étape et nous avons validé leur expression oculaire embryonnaire chez la souris. L'idée initiale était de choisir les meilleurs candidats pour les séquencer dans notre cohorte de patients. L'arrivée du séquençage haut débit a fait évoluer le projet en permettant le séquençage haut débit ciblé de la majorité des gènes candidats identifiés lors de cette étape (voir chapitre "séquençage des gènes candidats").

IV-3-B : Immunoprécipitation de la chromatine

Introduction

Une alternative à la recherche des cibles des FTs SOX2, OTX2, RAX et PAX6, a été développée. Nous avons souhaité utiliser la technique d'immunoprécipitation de chromatine (ChIP). S'agissant d'une méthode plus spécifique et moins communément utilisée que les méthodes présentées précédemment (RT-PCR, qPCR, western blot…), nous nous sommes attachés à détailler le protocole expérimental.

Méthodes et Résultats

- Principe général de la ChIP

Le principe de la fiche est schématisé figure 33.

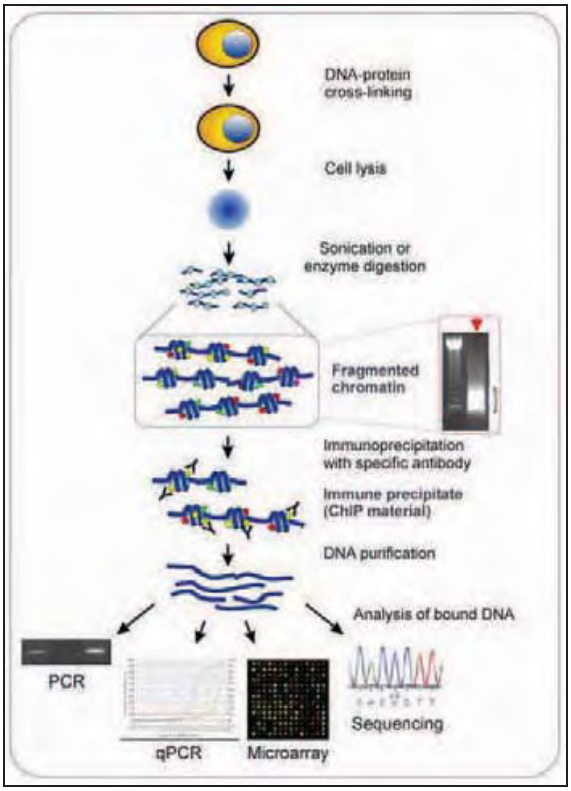

Figure 33: Principe général de la ChIP.

La première étape consiste à lier de manière réversible (en formant des liaisons non covalentes à l'aide de formaldéhyde) les protéines qui sont au contact de l'ADN. Les cellules sont ensuite lysées et les débris cellulaires éliminés. Seul l'ADN et les protéines associées sont récupérés. Cet ADN est fragmenté (par sonication) en fragments de 200 à 400 pb. Une immunoprécipitation de chromatine est alors réalisée à l'aide d'Ac spécifique contre le FT étudié et d'IgG (contrôle négatif). Après cette étape, les molécules d'ADN sont débarrassées des protéines et la chromatine obtenue peut être analysée (par PCR, qPCR, sur puces ou par séquençage).

- Culture cellulaire

Les cellules CCE-Rx sont cultivées comme décrit dans le chapitre précédent. Le protocole de ChIP débute 48H après l'ensemencement en suspension en l'absence de LIF (formation des corps embryoïdes).

- Protocole de ChIP

Pour l'étape de fixation des protéines à l'ADN (crosslinking), 27µl/ml de Formaldéhyde 36% sont ajoutés directement dans le milieu de culture et laissés 10 minutes à température ambiante (TA). La réaction de crosslinking est arrêtée par l'ajout de Glycine 1M (125µl/ml). Les étapes suivantes requièrent l'utilisation de tubes limitant la fixation de l'ADN (tubes Low-Bind) et toujours en présence d'inhibiteurs de protéases. Les cellules sont récupérées par centrifugation (500 rpm 5 minutes à 4°C) puis, lavées dans 10 ml de PBS froid (500 rpm 5 minutes à 4°C). Le culot cellulaire est repris dans 500µl de tampon de lyse SDS dans un tube eppendorff de 1.5 ml. On laisse 20 minutes à TA avant de faire, dans la glace, 6x30sec de sonication à 30% de puissance de l'appareil en laissant une minute entre chaque sonication. On centrifuge à 13000 rpm à 4°C pendant 10 minutes et on récupère le surnageant dans un nouveau tube pour 12x30sec de sonication à 30% de puissance en laissant une minute entre chaque sonication. On centrifuge à 13000 rpm à 4°C pendant 10 minutes et on récupère la majorité du surnageant dans un nouveau tube (on laisse 50 µl dans le tube). On rajoute à ces 50 µl, 500µl de ChIP dilution buffer (Upstate) et on centrifuge à 13000 rpm à 4°C pendant 10 minutes. Le surnageant est couplé au précédent. C'est la chromatine.

50 µl de cette solution de chromatine sont prélevés (Total Input) et l'ADN est nettoyé des protéines (on rajoute 5 % de NaCl 5M, 2µl de protéinase K et on chauffe 5h à 67°C dans un bain sec). L'ADN est purifié sur colonne Qiagen, dosé au Nanodrop™ et 300 ng sont déposés sur gel pour vérifier la sonication. La taille cible est entre 200 et 400 bp (Fig. 34).

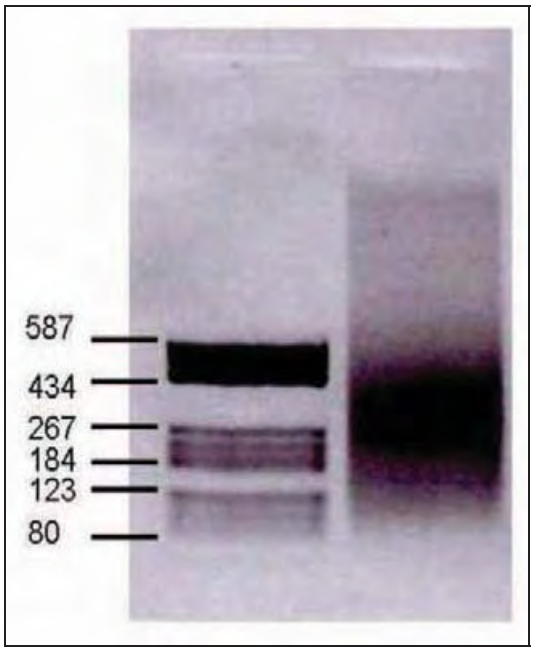

Figure 34: Exemple de résultat de sonication.

La migration sur gel permet d'évaluer l'efficacité de la sonication. Sur cet exemple, le smear de chromatine fragmentée se situe en majorité entre 200 et 400 bp.

Cette étape sur le « Total Input » permet de quantifier la quantité de chromatine récupérée et d'analyser son niveau de fragmentation. Si ces données sont satisfaisantes, on peut passer à l'étape d'immunoprécipitation proprement dite. Pour cela, on prépare 50 µl de billes magnétiques (Dynabeads Prot A ou Prot G en fonction de l'Ac utilisé) avec 10 µg d'Ac spécifique (anti-FT) ou non spécifique en tant que témoin (IgG) et 200 µl de tampon AB Binding (kit Dynabeads) pendant 1h à 4 °C sur rotor à faible vitesse (20 tours/minute). Les Ac utilisés étaient : Ac dirigés contre Otx2 (ab21990-100, abcam), Pax6 (sc-11357, Santa Cruz Biotechnology), Rax (sc-79028, Santa Cruz Biotechnology), Sox2 (sc-17320, Santa Cruz Biotechnology) et IgG (Mouse IgG Millipore PP54). On utilise le rack magnétique pour enlever le surnageant et on rajoute 600 µl de la chromatine obtenue précédemment (20 µg de chromatine idéalement) et on laisse agiter faiblement au rotor (20 tours/minute) pendant la nuit à 4°C. Le lendemain, des complexes billes-Ac/FT-chromatine se sont formés. On met sur les tubes sur le rack magnétique et on enlève le surnageant. Plusieurs lavages de 4 minutes à + 4° C sont fait sur le rotor à 20 tours/minute : 150µl tampon Low Salt (kit Upstate), 150µl tampon High Salt (kit Upstate), 150µl tampon LiCl (kit Upstate), 200µl tampon Tris-EDTA. Entre chaque lavage, les tubes sont mis sur le rack magnétique, et le surnageant est enlevé. Ces lavages permettent d'enlever la chromatine fixée de manière non spécifique aux couples billes/Ac. 200µl de tampon d'élution contenant NaCl et protéinase K sont ensuite ajoutés, et les tubes sont chauffés pendant 5h à 67°C en bain sec. Cette étape permet de dissocier la chromatine des billes magnétiques

et des protéines. Les tubes sont ensuite remis sur le rack magnétique et le surnageant (contenant la chromatine libre) est mis dans un tube propre. Ce surnageant est ensuite purifié sur colonne Qiagen et élué dans 35 µl de tampon d'élution. Les quantités, très faibles, de chromatine sont, à ce stade, souvent indosables. Cet ADN peut ensuite être dilué pour vérifier la spécificité de la chromatine par PCR quantitative. Il peut également être utilisé pour le séquençage haut débit (ChIP-seq).

- Validation de la spécificité des immunoprécipitations.

A partir des immunoprécipités de chromatine, nous avons essayé de reproduire par qPCR des résultats déjà publiés dans la littérature (Fig. 35). Les résultats ont été comparables aux données publiées pour Otx2, Pax6 et Sox2, validant ainsi la qualité de l'approche technologique. Aucun résultat de ChIP sur Rax n'étant disponible dans la littérature, nous ne disposions donc pas de données préliminaires pour valider notre protocole d'immunoprécipitation pour ce gène.

- ChIP-seq

Après validation du protocole de ChIP, les immunoprécipités ont été séquencés par des techniques de haut débit (Otx2, Pax6, Rax, Sox2 et IgG). Ils ont été confiés à la Société Fasteris en Suisse. Le séquençage des 5 librairies a été réalisé sur une machine HiSeq 2000™ (Illumina) et entre 14 et 18 millions de fragments ont été séquencés pour chaque librairie. 95% des lectures ont pu être replacées en séquence unique sur le génome à l'aide du logiciel BWA[181]. La recherche de pics (région supposée de fixation des FT, définie dans l'analyse par les critères suivants : 15 lectures différentes dans une région de 150 paires de bases) a été faite avec le logiciel SeqMonk. 14701 pics ont ainsi été identifiés parmi les 5 librairies. Après lissage avec les résultats obtenus dans la librairie non spécifique IgG, l'analyse montre des résultats spécifiques seulement pour les immunoprécipités d'Otx2 et Sox2. Les résultats pour Pax6 et Rax apparaissent aspécifiques, et les pics identifiés pour ces échantillons correspondent à des séquences de chromatine ouverte sans lien avec l'Ac utilisé et retrouvés également dans l'échantillon IgG. La présence des pics pouvait être visualisée avec le logiciel SeqMonk. Des exemples de pics obtenus dans les échantillons Otx2 et Sox2 sont représentés dans les figures 36 et 37. La localisation génomique des 200 pics les plus importants pour les librairies Otx2 et Sox2 a été ajoutée sous forme de tableau dans les annexes.

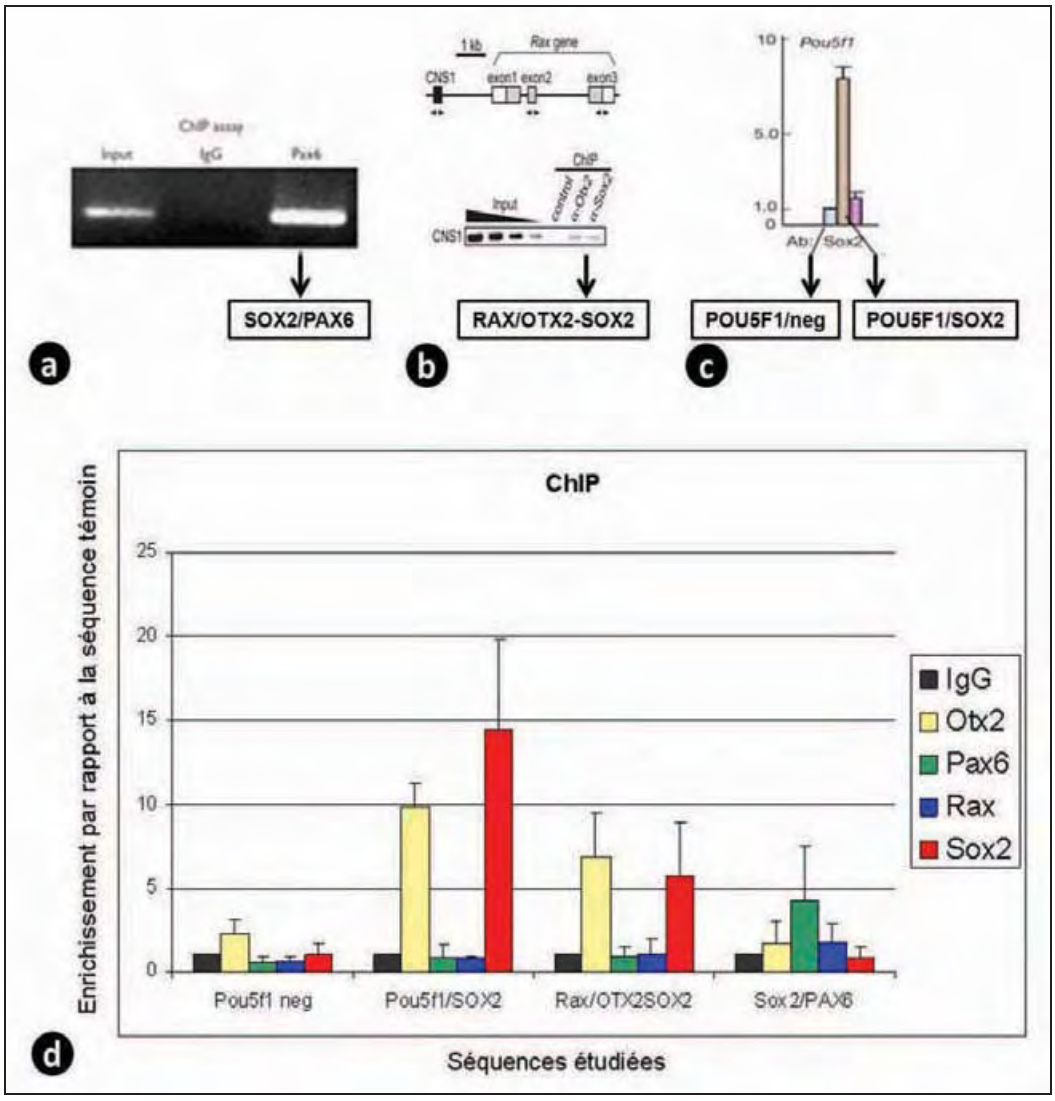

Figure 35: Validation des résultats de ChIP par qPCR ciblée.

(a, **b, c)** Résultats de ChIP de la littérature : **(a)** Fixation de Pax6 sur la séquence de *Sox2* mise en évidence par ChIP-PCR[182]. **(b)** Fixation d'Otx2 et Sox2 sur la séquence CNS1 de *Rax* démontrée par ChIP-PCR[173]. **(c)** qPCR après ChIP[114]: fixation de SOX2 sur la séquence promotrice de *Pou5f1*. En revanche, Sox2 ne se fixe pas sur une région située en 5' à distance de cette région régulatrice (*Pou5f1 neg*). **(d)** Validation du protocole de ChIP par qPCR. qPCR ciblée sur les séquences cibles des FT Sox2, Otx2 et Pax6. Comme démontré en **a**, **b** et **c**, *Pou5f1* est une cible de Sox2 ; *Rax* est une cible pour Otx2 et Sox2 ; *Sox2* est une cible pour Pax6. *Pou5f1 neg* sert de séquence contrôle négative. On compare l'enrichissement de ces régions par rapport à une séquence témoin après immunoprécipitation à l'aide d'Ac dirigés contre Otx2, Pax6, Rax ou Sox2 ou d'un Ac témoin (IgG). Les résultats obtenus à partir de 3 expériences d'immunoprécipitation sont comparables aux résultats précédemment publiés, validant ainsi notre protocole de ChIP.

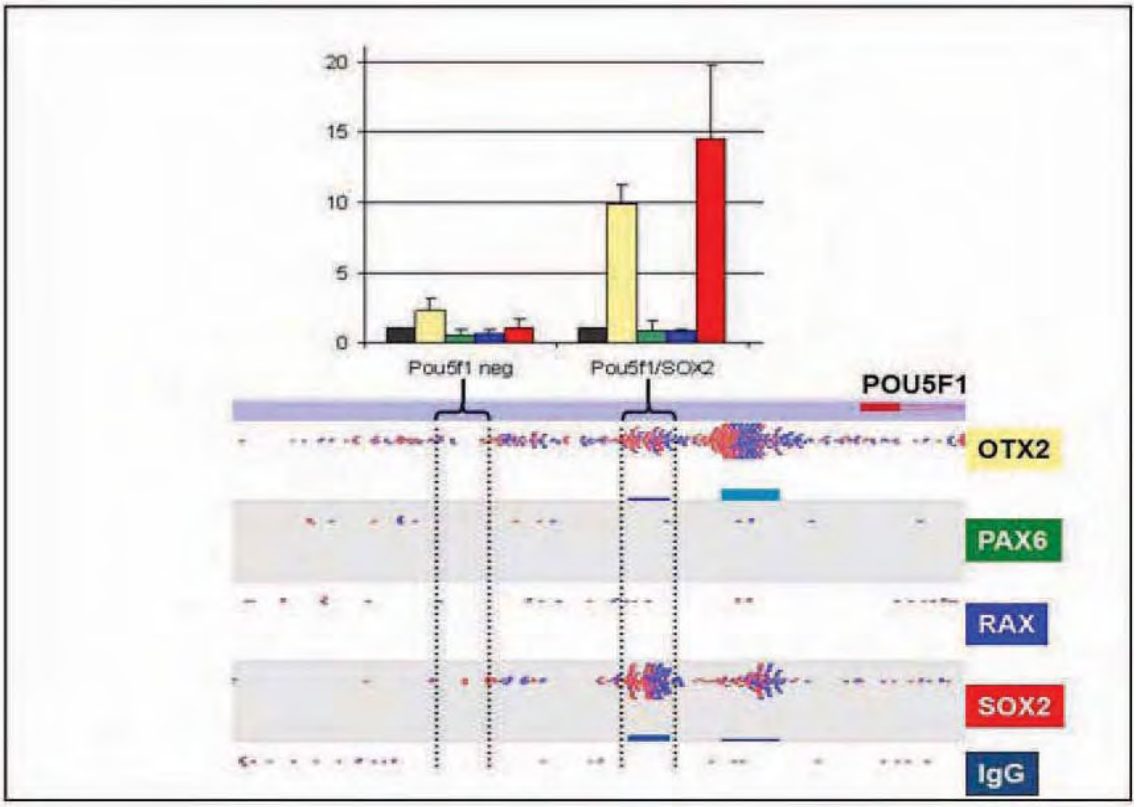

Figure 36: Corrélation entre les résultats de ChIP-qPCR et ChIP-seq.

La partie haute représente les résultats obtenus par ChIP-qPCR (voir figure 35). La partie basse de la figure représente les résultats visualisés à partir du logiciel SeqMonk. Les résultats obtenus pour les 5 échantillons sont représentés avec un code couleur identique à celui de la ChIP-qPCR. Chaque trait représente une séquence lue lors du séquençage haut débit et localisé dans cette région. Les lectures en rouge correspondent au brin sens, et en bleu au brin antisens. La localisation des séquences étudiées par ChIP-qPCR en amont de *Pou5f1* est indiquée sur la fenêtre SeqMonk. Pou5f1 neg correspond à la séquence témoin négative où aucun FT n'est fixé (en qPCR comme en ChIP). La séquence Pou5f1/Sox2 correspond à la séquence précédemment décrite du site de fixation du FT Sox2 en amont de *Pou5f1*. La reconnaissance de cette séquence par Sox2 est confirmée en ChIP-qPCR et en ChIP-seq. Ces deux techniques montrent également que cette séquence est reconnue par le FT Otx2. On note également la présence d'une séquence régulatrice de Pou5f1, ciblée principalement par Otx2, à proximité du gène, et non étudié par qPCR ciblée.

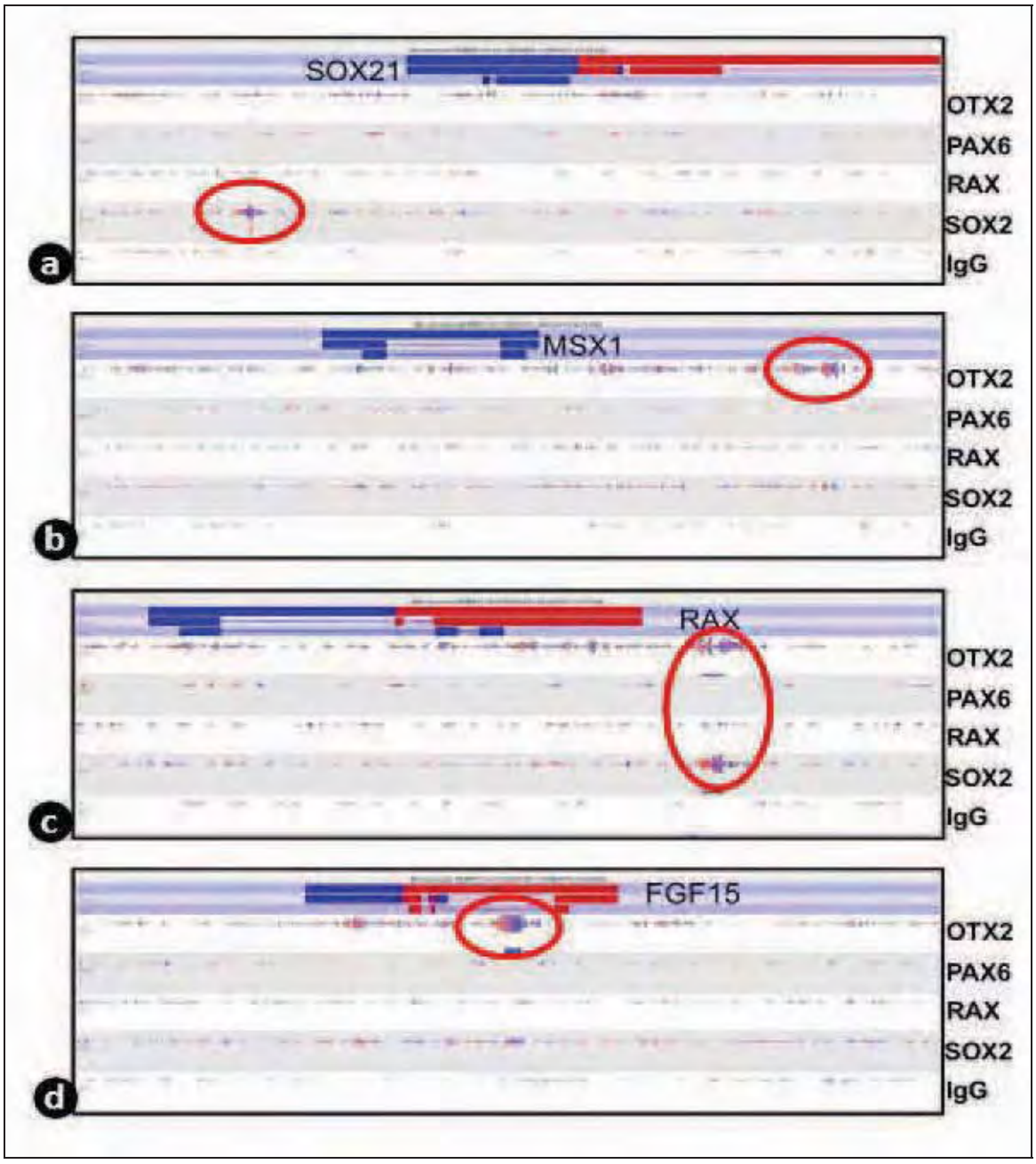

Figure 37: Exemples de pics visualisables avec le logiciel SeqMonk.

Quelques exemples de pics sont montrés, situés à proximité de gènes déjà discuté précédemment dans ce travail. (**a**) *Sox21* (un de nos gènes candidats fonctionnel) est régulé par Sox2. (**b**) Une région en amont du gène *Msx1* (cible d'Otx2 démontrée dans le travail sur l'otocéphalie) est effectivement reconnue par Otx2. (**c**) La séquence régulatrice du gène *RAX* (séquencée comme région candidate d'AM, cf. chapitre "gènes candidats") est bien reconnue par Otx2 et Sox2. (**d**) Enfin, exemple de résultat de ChIP-seq à proximité d'un des gènes identifiés comme régulé par Otx2 dans notre approche transcriptomique (gène *Fgf15*). La ChIP-seq retrouve un site de fixation d'Otx2 dans la région intronique

Les analyses bio-informatiques ont montré que l'on retrouvait majoritairement dans les pics Otx2 et Sox2 les séquences nucléotidiques consensus respectives de fixation de chacun des FT à l'ADN. De plus, ces analyses ont permis de montrer que la majorité des sites de fixation des FTs étaient situés à proximité immédiate (moins de 5 kb) des séquences géniques ou dans les régions introniques.

- ChIP-seq à partir d'yeux d'embryons murins microdisséqués

Nous avons tenté de reproduire les résultats obtenus sur les cultures cellulaires à partir d'yeux microdisséqués d'embryons de souris (stade E11.5). Les yeux de 20 embryons ont été groupés pour obtenir de la chromatine selon un protocole proche de celui décrit pour les CCE-Rx. La chromatine issue de ces yeux embryonnaires a été immunoprécipitée avec les Ac anti Otx2, Pax6, Rax et Sox2 et IgG. La qPCR n'a pas permis de montrer d'enrichissement au niveau des régions étudiées précédemment sur les cellules CCE-Rx. Partant du principe que la fixation à ces sites de régulation d'expression génique pouvait varier au cours du temps, nous avons initié une analyse en ChIP-seq malgré ces résultats préliminaires. Les résultats de la ChIP-seq n'ont pas été probants car le même profil d'enrichissement était visible pour l'immunoprécipitation réalisée avec chaque FT et avec l'IgG, signant ainsi des enrichissements non spécifiques liés à la conformation chromatinienne. La difficulté d'obtention de quantité suffisante de chromatine (étape de lyse des yeux), la présence de nombreux types cellulaires différents dans les structures oculaires, l'expression probablement moindre des facteurs de transcription étudiés que dans nos cultures de cellules souches embryonnaires sont des explications plausibles pour expliquer les difficultés rencontrées à cette étape.

Conclusion

Nous avons pu mettre au point un protocole de ChIP efficace dans notre modèle de corps embryoïdes de CCE-Rx pour les facteurs de transcription Otx2 et Sox2. Nous n'avons par contre pas pu avoir de résultats spécifiques pour Rax et Pax6 ni à partir de culture cellulaire CCE-Rx ni, dans l'œil en développement. Les résultats obtenus pour Otx2 et Sox2 ont permis de valider des résultats déjà exploités (exemples donnés figure 37). Ils nous ont également permis d'apporter des arguments pour l'implication des gènes porteurs de mutation identifiés par séquençage haut débit comme nous allons le voir dans le chapitre suivant.

IV-3-C : Séquençage gènes candidats

Introduction

L'étape ultérieure à l'identification de gènes potentiellement impliqués dans les défauts du développement oculaire consiste à valider leurs implications en pathologie humaine. Nos différentes approches (CGH-array et expérimentales) nous ont permis d'identifier de nombreux gènes candidats positionnels (présent dans un remaniement identifié par CGH) ou fonctionnels (régulés par un ou plusieurs des 4 FTs étudiés). Alors que nous avions initialement envisagé sélectionner les meilleurs gènes candidats (gènes régulés par plusieurs FT étudiés, arguments fonctionnels et/ou positionnels) et les séquencer sur un grand nombre de patients sans mutation retrouvée dans les gènes d'AM connus, la révolution du séquençage haut débit nous a fait modifier notre stratégie et nous avons opter pour le séquençage d'un grand nombre de gènes candidats chez un petit nombre de patients.

Méthodes

- Choix des gènes et méthode de capture

La technologie de séquençage haut débit nous permettait de séquencer simultanément plusieurs centaines de gènes. Un total de 407 gènes candidats ont été sélectionnés sur différents critères. Les premières méthodes de sélection étaient en rapport direct avec le travail réalisé au cours de cette thèse : sélection des gènes localisés au niveau des régions porteuses de microremaniements chromosomiques identifiées par CGH-array (35 gènes candidats positionnels)[28], et sélection des gènes régulés par au moins un des quatre FTs étudiés et ayant une expression oculaire et/ou cérébrale connue (152 gènes). Nous avons par ailleurs rajouté dans notre sélection de gènes candidats, 66 gènes impliqués dans des formes isolées ou syndromiques d'AM chez la souris (MGI, Mouse Genome Informatics), ainsi que 154 gènes décrits dans la littérature pour être impliqués dans le développement oculaire chez les invertébrés et/ou les vertébrés. Pour chacun des gènes sélectionnés, les séquences régulatrices potentielles (région situées dans les 20kb à proximité des gènes ou dans les exons et conservées entre les espèces, Fig. 39) ont aussi été incluses. Nous avons également souhaité inclure dans les régions séquencées, l'ensemble des miRNA et snoRNA. La proportion de gènes candidats sélectionnés par les différentes approches est schématisée sur la figure 38.

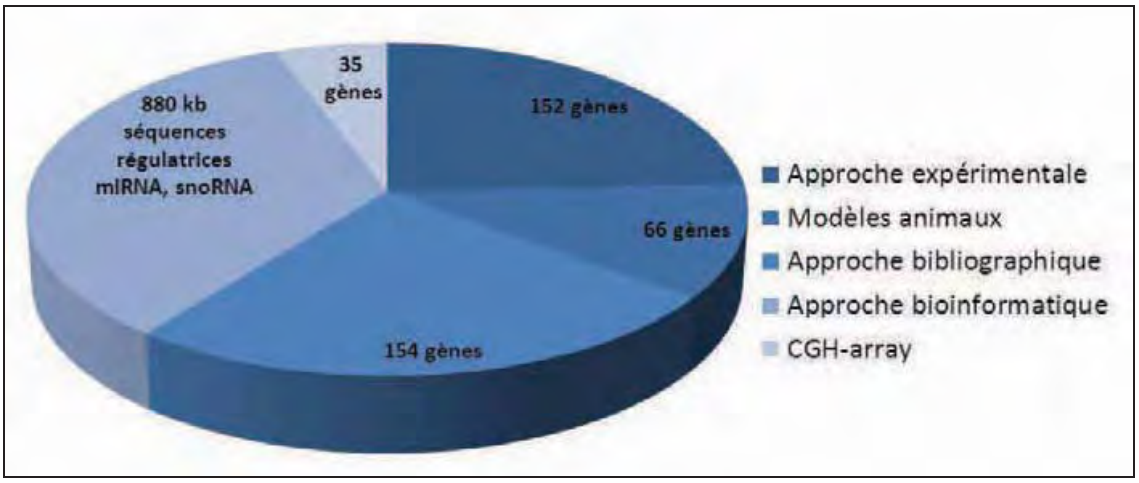

Figure 38: Les différentes approches de sélection des gènes candidats.

- Choix des patients

Pour des raisons de budget, nous avons dû limiter à 22 le nombre de patients chez qui le séquençage des 407 gènes candidats a été réalisé. Deux témoins (mutés dans *VSX2* et *STRA6* respectivement) ont également été séquencés pour confirmer la possibilité de retrouver des mutations connues en utilisant notre stratégie d'analyse. Compte tenu du nombre important de gènes candidats testés, et de leurs effets potentiellement variable sur le développement oculaire, nous avons élargi la sélection de nos patients à un ensemble de malformations oculaires différentes, isolées ou syndromiques. Ainsi, parmi les 22 patients sélectionnés, 10 avait une atteinte oculaire strictement isolée, 4 une atteinte oculaire associée à une déficience intellectuelle et 8 des malformations associées. L'atteinte oculaire était bilatérale chez 20 patients et unilatérale chez 2. Au niveau oculaire, 4 avaient une AM isolée, 6 une AM colobomateuse, 6 une AM complexe (avec autre malformation oculaire) et 6 une dysgénésie du segment antérieur.

Dans les suites de cette analyse, des mutations de 2 gènes (*NOTCH1* et *PTCH1*) ont été recherchées dans une nouvelle cohorte de 48 patients avec AM isolée (n=17), AM complexe (n=9), AM colobomateuse (n=8), et dysgénésie du segment antérieur (n=14).

- Méthode de capture

Pour isoler ces 407 gènes et leurs séquences potentiellement régulatrices, nous avons utilisé un kit de capture SureSelect d'Agilent à façon : 56.059 sondes, couvrant 2.46 Mb, ont été dessinées et synthétisées. Ces sondes permettaient la capture des séquences codantes des gènes et de leurs séquences potentiellement régulatrices (Fig. 39). La capture des régions d'intérêt a été faite selon le protocole spécifique d'Agilent.

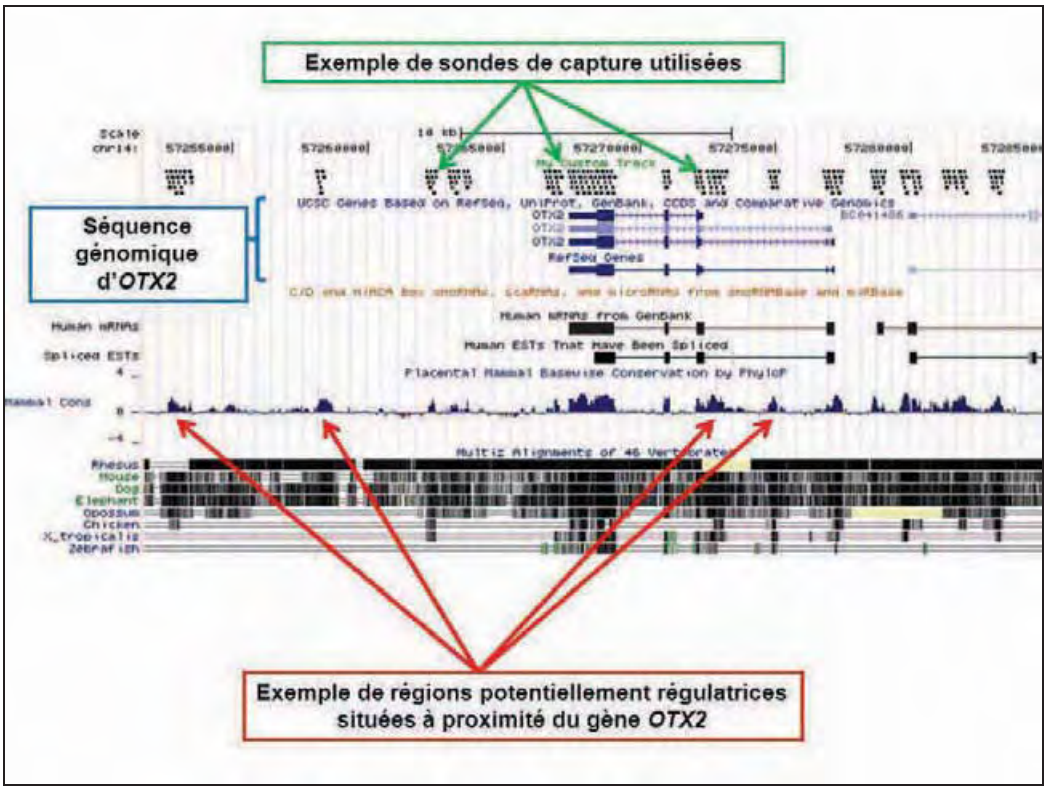

Figure 39: Exemple de sondes utilisées pour la capture du gène *OTX2*.

Représentation du gène *OTX2* dans UCSC Genome Browser. Les séquences exoniques et introniques du gène et les différentes isoformes sont indiquées. Les pics indiqués par les flèches rouges correspondent aux régions génomiques conservées situées dans ou à proximité du gène *OTX2*. Chaque point noir (indiqués par les flèches vertes) correspond à une sonde de capture de 120 nucléotides. Ces sondes ont été définies pour permettre la capture des séquences codantes, des séquences 5' et 3' UTR et des séquences potentiellement régulatrices.

- Méthode de séquençage

Une séquence de reconnaissance spécifique de 6 nucléotides a été ajoutée à chacun des 24 échantillons permettant un multiplexage des échantillons, passés en deux runs de séquence sur un séquenceur Illumina GAIIx avec des lectures en paired-end de 2 fois 75 nucléotides. Les lectures ont ensuite été assemblées et comparée au génome humain (version hg19) avec les logiciels CASAVA1.7 et ELANDv2.

- Méthode de tri des variants

La stratégie de tri des variants a consisté à sélectionner dans l'ordre suivant les variants, 1) répondant aux critères de qualité, 2) absent des bases de données locales et publiques (sbSNP132, 1000 Génomes et HapMap), 3) exonique ou touchant un site consensus d'épissage, 4) mutations à effet délétère prédit (frameshift, non-sens, faux-sens prédites *in silico* comme délétères par le logiciel Polyphen-2), et 5) confirmés par séquençage Sanger.

- Validation par séquençage Sanger des variants identifiés

Pour chaque variant répondant aux 4 premiers critères de sélection, un séquençage Sanger a été réalisé pour confirmer ou non la présence du variant. Une analyse de ségrégation familiale a été réalisée pour les variants confirmés quand les prélèvements parentaux étaient disponibles.

- Séquençage Sanger des deux gènes principaux

Deux gènes d'intérêt (*NOTCH1* et *PTCH1*) sont ressortis de notre première analyse et ces gènes ont été séquencés par séquençage Sanger dans une nouvelle cohorte de 48 patients avec anomalies oculaires.

- Recherche de remaniement

Après avoir montré que nous étions capables de faire des analyses semi-quantitatives en utilisant la variation du nombre de lectures sur l'X entre les femmes et les hommes, nous avons recherché des microremaniements. Pour chacune des 56.059 sondes nous avons fait un rapport entre le nombre de lectures pour un patient donné par rapport à la moyenne des lectures sur les 24 patients analysés (après ajustement avec la profondeur de lecture moyenne de chaque patient). Une région était considérée comme potentiellement délétée quand le rapport (patient/moyenne des patients) était inférieur à 0.6 sur 3 sondes non chevauchantes successives, et potentiellement dupliquée si le rapport était supérieur à 1.4 sur 3 sondes non chevauchantes successives. Pour éviter des faux-positifs, seules ont été analysées les sondes pour lesquelles la profondeur de lecture était supérieure à 20.

Résultats

Les principaux résultats de l'analyse par séquençage haut-débit des 407 gènes candidats sont décrits ci-dessous.

- Qualité du séquençage

La profondeur moyenne de lecture pour les 2,46 Mb étudiés par patient était supérieure à 300X, avec 97 % des régions étudiées avec une couverture supérieure à 10X et 94 % supérieure à 25X.

- Nombre de variants

Environ 2500 variations par patient ont été identifiées Le nombre de variants à chaque étape du filtrage des variants et résumé dans le tableau 3.

Identified variants	Average over 24 samples	Standard Deviation
Total variants	2566	125
High confidence variant calls	2482	126
After exclusion of known variants (dbSNPv132 + HapMap + inhouse)	236	28
After exclusion of non-genic - intronic variants	10	3
After exclusion of synonymous variants	6	2
Predicted damaging	3	1
Validated by Sanger Sequencing	2.5 *(range 0-5)*	1

Tableau 3: Nombre de variants identifiés par séquençage des gènes candidats.

Nombre de variants aux différentes étapes de filtrage.

- Identification de variations dans *PTCH1*

Le résultat principal de cette étude est l'identification de variations répondant aux critères de sélection dans *PTCH1* chez 4 patients (une frameshift et 3 variations faux-sens). Ces variations touchaient principalement des acides aminés conservés au cours d l'évolution (Fig. 40). Une seconde analyse de nos résultats a permis d'identifier deux autres variants rares de *PTCH1* qui avaient été écartées lors de l'étape de filtrage car ils étaient prédit comme probablement non délétères par le logiciel Polyphen-2. Un de ces deux variants supplémentaires a été identifié chez un patient, alors que l'autre a été identifié chez notre contrôle (C2) muté dans le gène *STRA6*.

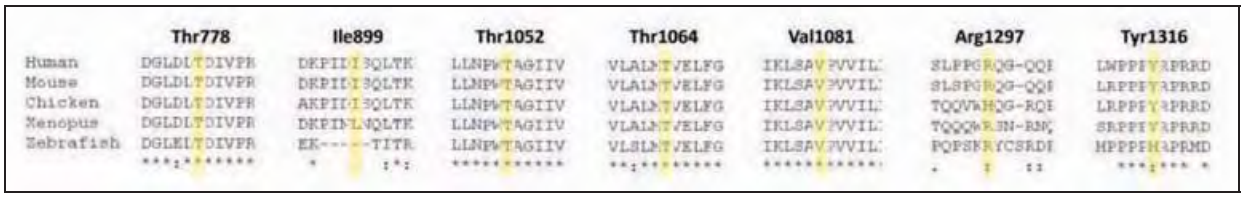

Figure 40: Conservation inter-espèces des acides aminés impliqués dans les mutations faux-sens identifiées chez les patients AM.

L'analyse de ségrégation familiale (Fig. 41) a montré que ces variants été héritées avec une pénétrance largement incomplète.

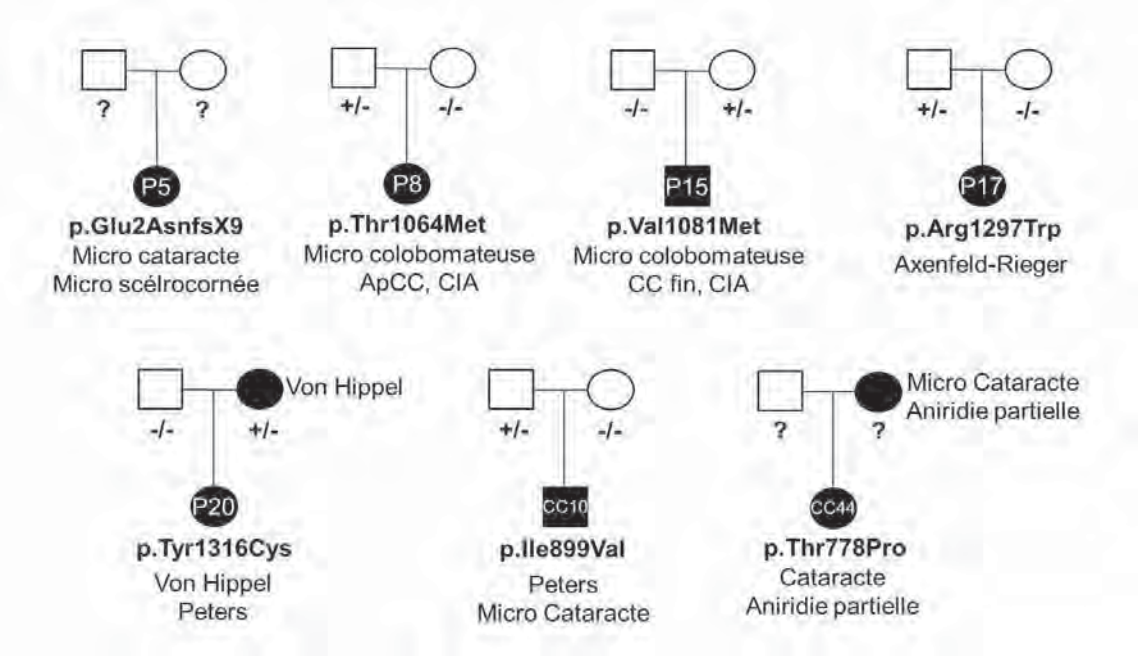

Figure 41: Analyses de ségrégation familiale des variants identifiés dans *PTCH1* chez les patients AM

+/- : présence de la mutation à l'état hétérozygote ; -/- : absence de mutation ; ?: non testé

De nombreux arguments sont en faveur du rôle de PTCH1 dans le développement oculaire (voir article 12). Afin de confirmer le rôle délétère des variants identifiés chez les patients, ils ont été testés sur un modèle de zebrafish par le Dr. Erica E. Davis. Ces analyses ont permis de montrer que ces variants faux sens avaient un effet hypomorphes sur l'activité de PTCH1 contrairement à un polymorphisme fréquent et à la variation faux-sens identifiée chez le contrôle.

PTCH1 apparait donc comme un second gène majeur (10 % des patients) d'anomalies du développement oculaire, avec une variabilité phénotypique importante et une pénétrance incomplète.

Le détail des résultats et la discussion sur les résultats obtenus sont décrits dans l'article en cours de préparation:

- Article n°12

Chassaing et al. "Hypomorphic *PTCH1* mutations lead to phenotypically heterogeneous ocular developmental anomalies." En Préparation

- Autres variants d'intérêts

1) Parmi les patients analysés, nous avons pu identifier chez deux d'entre eux une mutation dans des gènes connus d'anomalies du développement oculaire. Chez un patient avec anophtalmie bilatérale, une mutation faux-sens délétère apparue *de novo* a été identifiée dans le gène *PAX6*. Le phénotype d'anophtalmie isolée n'avait jusqu'ici pas été décrit associé à des mutations hétérozygotes du gène *PAX6*. Chez un patient avec microphtalmie isolée, nous avons mis en évidence dans le gène *STRA6* une hétérozygotie composite pour une mutation faux-sens et une délétion de grande taille (voir plus bas les résultats de la recherche de remaniements).

2) Dans cinq gènes, *FAT4*, *IFT172*, *NOTCH1*, *RPGRIP* et *TSHZ2*, nous avons identifié des variations chez deux patients différents (Tableau 4). Nous nous sommes plus particulièrement intéressés à *NOTCH1*, gène dans lequel deux patients présentaient un variant faux-sens hétérozygote prédit comme délétère, et hérité d'un parent symptomatique dans une famille. La régulation de l'expression de *Notch1* par Sox2 au cours du développement oculaire avait été précédemment démontrée (Fig. 42)[121].

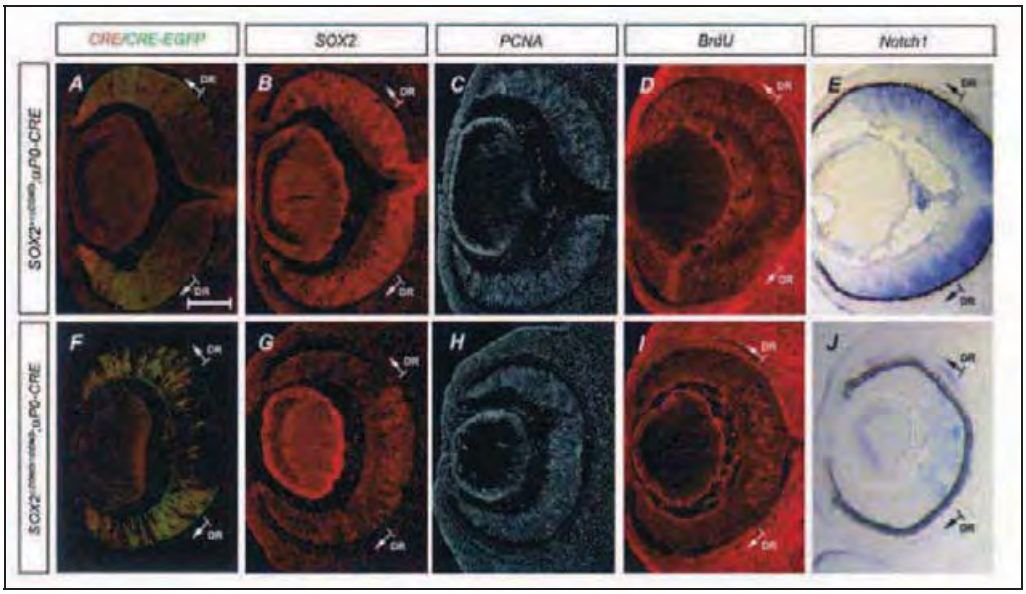

Figure 42: Régulation de l'expression de Notch1 par SOX2 au cours du développement.[1]

Diminution drastique de l'expression de Notch1 (panel de droite) dans la rétine après inactivation spécifique de l'expression de *SOX2* dans la rétine par recombinaison conditionnelle (en bas).

De plus, nos analyses transcriptomiques et en ChIP-seq sur des cellules souches embryonnaires murines surexprimant le gène *Rax* retrouvaient la régulation de l'expression du gène *NOTCH1* par le FT SOX2 (Fig. 43 et 44).

[1] Taranova et al. Genes Dev. 2006

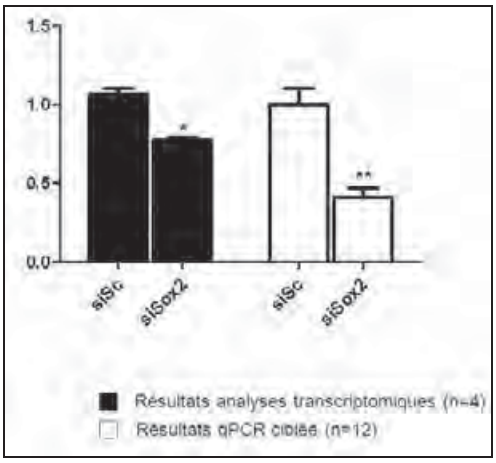

Figure 43: Diminution de l'expression de *Notch1* identifiée lors de l'approche transcriptomique et validée par qPCR ciblée.

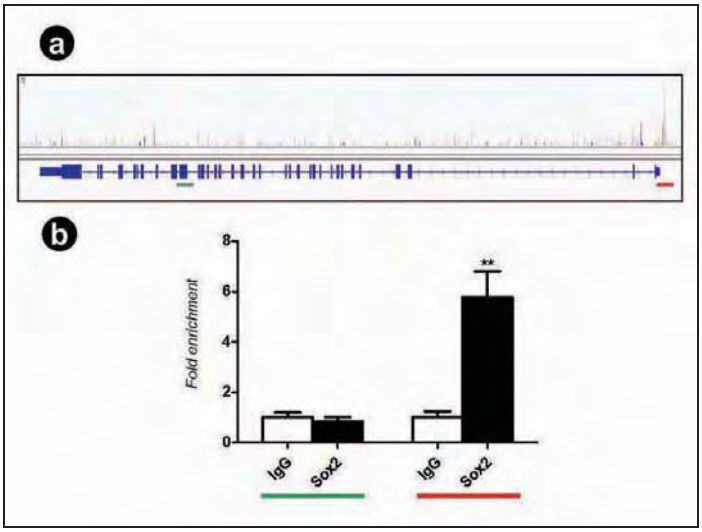

Figure 44: Identification d'un site de fixation du FT Sox2 à proximité immédiate du gène *Notch1*.

Résultats sur IGV de la ChIP-Seq pour Sox2 montrant la présence d'un pic dans la région 5' en amont du gène Notch1 (**a**) et confirmation de ces résultats par ChIP-qPCR sur 5 nouveaux échantillons (**b**). Les séquences étudiées en qPCR, témoin et site de fixation de Sox2 sont indiquées respectivement en vert et en rouge.

Ce faisceau d'arguments (identification de deux variants transmis par des parents symptomatiques, expression oculaire, régulation par SOX2) nous a fait pousser les analyses sur ce gène. 48 patients AM ont été séquencés à la recherche de mutations causales de leur atteinte oculaire. Aucune mutation délétère n'a pu être mise en évidence. De plus, nous avons pu poursuivre les analyses moléculaires dans un des deux familles et montrer que le fils atteint (microphtalmie colobomateuse) d'un de ces

deux patients ne portait pas la variation de *NOTCH1* identifié chez son père. Ce résultat allait à l'encontre d'un lien entre cette variation et le phénotype oculaire.

3) D'autres gènes candidats étaient porteurs de variants potentiellement à l'origine des atteintes oculaires des patients (Tableau 4). Un total de 41 gènes différents était porteur de mutation possiblement pathogènes. Nous nous sommes focalisés sur *NOTCH1* et *PTCH1*, et l'implication de ces différents gènes dans les défauts du développement oculaire reste encore à démontrer.

4) De nombreuses variations ont été identifiées dans les régions potentiellement régulatrices. Les analyses de ségrégation familiale ont montré que ces variations étaient toujours transmises par un des deux parents, et leur implication dans le phénotype oculaire est donc difficile à établir.

Patient	Gene	Transcript	cDNA change	Protein change	Status	Polyphen-2	SIFT	EVS	Inheritance (phenotype)
P1	*PAX6*	ENST00000379115	c.192C>A	p.Asn64Lys	Ht	D (1.000)	D (0)	Abs	*De novo*
P3	*FAT4*	ENST00000394329	c.7960A>C	p.Lys2654Gln	Ht	P (0.477)	T(0.76)	Abs	Pat (Asy)
	MYO1C	ENST00000359786	c.391C>T	p.Arg131Cys	Ht	D (0.959)	T(0.17)	3/13004	Mat (Asy)
	SALL3	ENST00000537592	c.2254G>A	p.Val752Met	Ht	D (0.9555)	-	Abs	Mat (Asy)
	SOX14	ENST00000306087	c.722delA	p.*241Tyrext*?	Ht	-	-	Abs	Mat (Asy)
	TSHZ2	ENST00000371497	c.247T>G	p.Ser83Ala	Ht	D (0.946)	D(0)	4/13006	Pat (Asy)
P4	*FAT1*	ENST00000441802	c.4336G>A	p.Val1446Ile	Ht	D(0.998)	T(0.36)	8/11838	Pat (Asy)
	FAT4	ENST00000394329	c.131A>C	p.Glu44Ala	Ht	P (0.496)	T(0.6)	3/12132	Mat,Pat (Asy)
	DAB1	ENST00000371236	c.1075G>A	p.Gly359Arg	Ht	D (0.987)	T(0.07)	Abs	Pat (Asy)
P5	***PTCH1***	ENST00000375274	c.4delG	p.Glu2Asnfs*9	Ht	-	-	Abs	Unk
	PLXNC1	ENST00000258526	c.3649T>C	p.Cys1217ARg	Ht	D(0.998)	D(0.01)	9/12997	
	IFT172	ENST00000260570	c.3880C>T	p.Arg1294Cys	Ht	D(1.000)	D(0.01	1/13005	
	WNT7A	ENST00000285018	c.232C>T	p.Arg78Cys	Ht	D(1.000)	D(0)	Abs	
P6	*STRA6*	ENST00000395105	c.1735C>G	p.Pro579Ala	Hemi	D (0.999)	T(0.11)	Abs	Mat (Asy)
P7	*CDH1*	ENST00000261769	c.670C>T	p.Arg224Cys	Ht	P (0.837)	D(0)	2/12996	Unk
	CYP26C1	ENST00000285949	c.1243C>G	p.His415Asp	Ht	D (1.000)	D(0)	Abs	
	IFT172	ENST00000260570	c.5133delC	p.Asn1711Asnfs*20	Ht	-	-	Abs	

	VAX2	ENST00000234392	c.398C>T	p.Thr133Ile	Ht	P (0.933)	T(0.33)	Abs	
P8	***PTCH1***	ENST00000331920	c.3191C>T	p.Thr1064Met	Ht	D(1.000)	T(0.1)	2/13006	Pat (Asy)
	SEZ6L2	ENST00000308713	c.323C>T	p.Thr108Ile	Ht	P(0.937)	T(0.22)	Abs	Pat (Asy)
P9	*RPGRIP1*	ENST00000400017	c.2424C>G	p.Cys808Trp	Ht	D (0.999)	D(0)	Abs	Pat (Asy)
P10	*PFKP*	ENST00000381125	c.738_739insG	p.Trp248Alafs*19	Ht	-	-	Abs	Mat (Asy)
	NOTCH4	ENST00000375023	c.2443T>G	p.Cys815Gly	Ht	D(1.000)	D(0)	22/8350	Mat (Asy)
P11	*NR5A2*	ENST00000367362	c.884C>T	p.Thr295Met	Ht	P(0.904)	D(0.02)	11/12995	Unk
	RPGRIP1	ENST00000400017	c.808A>G	p.Ile270Val	Ht	P(0.994)	T(0.11)	6/11846	
P12	*GRASP*	ENST00000293662	c.1084G>A	p.Gly362Ser	Ht	D (0.987)	T(0.43)	56/11118	Mat (Asy)
	NOTCH1	ENST00000277541	c.2434G>A	p.Gly812Arg	Ht	D (1.000)	D(0.05)	7/12560	Pat (Asy)
P13	*MITF*	ENST00000352241	c.738G>A	p.Asp246Asn	Ht	P(0.858)	T(0.45)	Abs	Mat (Asy)
	EFHD1	ENST00000264059	c.155C>T	p.Thr82Met	Ht	D(0.945)	T(0.06)	1/12893	Mat (Asy)
P14	*NOTCH1*	ENST00000277541	c.67G>T	p.Arg23Leu	Ht	P(0.689)	T(0.38)	Abs	Mat (Sy)
	ARR3	ENST00000307959	c.1052C>T	p.Pro351Leu	Hemi	D(0.945)	T(1)	Abs	Mat (Sy)
P15	*FGFR3*	ENST00000260795	c.1879G>A	p.Glu627Lys	Ht	D(0.990)	D(0)	Abs	Pat (Asy)
	PTCH1	ENST00000331920	c.3241G>A	p.Val1081Met	Ht	D(0.991)	D(0.02)	1/13006	
	SULF1	ENST00000458141	c.529G>A	p.Gly177Ser	Ht	D(1.000)	D(0)	Abs	
	CHRD	ENST00000204604	c.1370C>G	Thr457Ser	Ht	D(0.999)	T(0.1)	6/13000	
P17	*CHST5*	ENST00000336257	c.737T>C	p.Ile246Thr	Ht	D (0.998)	T(0.06)	Abs	Mat (Asy)
	DACT1	ENST00000335867	c.2010G>C	p.Lys670Asn	Ht	P (0.868)	T(0.32)	Abs	Mat (Asy)
	FRAS1	ENST00000264895	c.3700G>A	p. Ala1234Thr	Ht	P(0.611)	T(0.29)	2/12336	Pat (Asy)
P18	*DICER1*	ENST00000343455	c.2191G>A	p.Gln731Lys	Ht	P(0.950)	T(0.52)	Abs	Unk
	MAP3K1	ENST00000399503	c.1420A>G	p.Ile474Val	Ht	P(0.540)	T(0.19)	Abs	
	GLI2	ENST00000361492	c.1859C>T	p.Thr620Met	Ht	P(0.832)	T(0.09)	11/12995	
P19	*KIF21A*	ENST00000395670	c.2287G>A	p.Val763Met	Ht	D(0.998)	D(0.01)	Abs	Pat (Asy)
	GLIS3	ENST00000381971	c.2710G>C	p.Gly904Arg	Ht	D(1.000)	D(0)	6/13000	Pat (Asy)
P20	***PTCH1***	ENST00000331920	c.3947A>G	p.Tyr1316Cys	Ht	D(0.983)	T(0.07)	9/12499	Mat (Sy)
	FREM1	ENST00000380880	c.1493G>A	Arg498Gln	Ht	D(1.000)	T(0.43)	9/12453	Mat (Sy)
P21	*ADAM17*	ENST00000310823	c.847C>T	p.Arg283Cys	Ht	D (1.000)	T(0.08)	Abs	Pat (sy)
	SFRP2	ENST00000274063	c.628A>G	p.Asn209Gly	Ht	P (0.918)	T(0.24)	Abs	Pat (sy)

	TSHZ2	ENST00000371497	c.1289A>T	p.Gln430Leu	Ht	P (0.958)	D(0.01)	Abs	Mat (Asy)
P22	*PITRM1*	ENST00000380989	c.2423A>G	p.Lys808Arg	Ht	P (0.708)	T(0.48)	Abs	Pat (Asy)
	PRPF8	ENST00000304992	c.3527C>T	p.Ser1176Phe	Ht	D (0.999)	D(0)	Abs	Mat (Asy)
	RARG	ENST00000425354	c.245C>T	p.Pro82Leu	Ht	D (0.999)	D(0.02)	Abs	Pat (Asy)
	EPHB2	ENST00000400191	c.787G>A	p.Val263Ile	Ht	P(0.882)	T(0.24)	2/13004	Pat (Asy)
C1*	*FRAS1*	ENST00000264895	c.9364C>T	p.Arg3122Trp	Ht	D (1.000)	D(0)	Abs	Pat (Asy)
	VSX2	ENST00000261980	c.71_72insG	p.Ala25Argfs*101	Ht	-	-	Abs	Pat (Asy)
	VSX2	ENST00000261980	c.667G>A	p.Gly223Arg	Ht	D (1.000)	T(0.14)	Abs	Mat (Asy)
	NDST2	ENST00000309979	c.25C>T	p.Arg9Cys	Ht	D(1.000)	D(0)	4/13002	Pat (Asy)
	NDST2	ENST00000309979	c.199C>T	p.Arg67Trp	Ht	D(0.990)	T(0.18)	1/12989	Mat (Asy)
C2*	*STRA6*	ENST00000395105	c.1313A>G	p.Gln438Arg	Ht	D (1.000)	D(0.05)	Abs	Pat (Asy)
	STRA6	ENST00000395105	c.1913G>C	p.Arg638Pro	Ht	D (1.000)	D(0)	1/12990	Mat (Asy)

Tableau 4: Variations retenues après filtrage des variants identifiés chez les 22 patients (P1 à P22) et les deux contrôles (C1 et C2)

- Résultats de la recherche de remaniements

Pour rechercher la présence de remaniements exoniques et/ou géniques, nous avons comparé la profondeur de lecture donnée pour chaque sonde de capture entre chaque patient et la moyenne des patients. Seules les sondes de capture ayant une profondeur minimum de 20 lectures ont été étudiées. Cette approche n'ayant pas été rapportée précédemment, nous avons souhaité en étudier la faisabilité en regardant le ratio (patient)/(moyenne des patients) pour les sondes de capture situées sur le chromosome X. Le résultat attendu (et obtenu) était d'avoir un ratio deux fois plus important pour les femmes (46,XX) que pour les hommes (46, XY). Une des patientes avait un caryotype 47, XXX (triploX) ce qui a pu être visualisé par notre approche (Fig. 45). Cette première approche a démontré la possibilité de rechercher des modifications du nombre de copies sur l'ensemble des sondes de capture situées sur les autosomes.

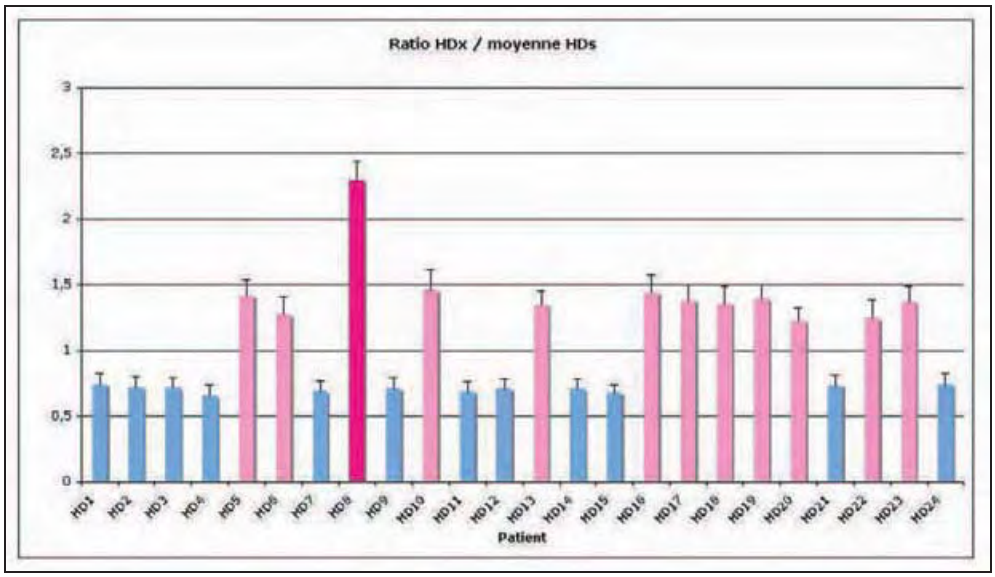

Figure 45: Confirmation de la possibilité d'étudier le nombre de copie par analyse de la profondeur de lecture.

Le ratio entre le nombre de lecture pour une sonde de capture donnée entre chaque patient (HDx) et la moyenne des patients (moyenne HDs) a été calculé pour les 1400 sondes de capture localisées sur l'X ayant > 20 lectures. Est représenté sur cette figure, la moyenne des ratios pour chaque patient. On voit que les patients de sexe féminin (en rose clair) ont une moyenne des ratios deux fois supérieure à celle des garçons (en bleu). La patiente porteuse d'un triploX est représentée en rose foncée et à une moyenne des ratios trois fois supérieure à celle des garçons.

La recherche de variation du nombre de copies a pu être réalisée sur 53231 des sondes de lecture (soit 95 % des sondes avec une profondeur de lecture >20). Les remaniements ont été retenus selon le critère d'un ratio < 0.6 (délétion) ou > 1.4 (duplication) pour 3 sondes consécutives non chevauchantes. 4 remaniements ont pu être identifiés par cette technique : une délétion hétérozygote du gène *STRA6*, une duplication du gène *VSX2*, une duplication partielle du gène *FAT1* et une délétion sur le chromosome 13 correspondant à un CNV connu (Fig. 46). Les délétions des trois remaniements probablement en cause dans le phénotype oculaire ont été faites par QMPSF (délétion de *STRA6* chez le patient 6 [HD6]) ou par CGH array (duplication de *FAT1* chez le patient 10 [HD10] et duplication de *VSX2* chez le patient 14 [HD14]) (Fig. 47). Le patient 6 est hétérozygote composite pour la délétion de *STRA6* et une mutation ponctuelle. L'analyse parentale n'a pas pu être réalisée pour la duplication partielle du gène *FAT1* chez le patient 10. *FAT1* code pour une protocadhérine qui lorsqu'elle est inactivée chez les souris (KO) entraine des anophtalmies chez 40 % des embryons de souris[183]. L'analyse familiale de la duplication du gène *VSX2* a montré que cette duplication était apparue *de novo* chez la mère du patient 14 elle-même pauci-symptomatique (Fig.

47). Il existe donc des arguments pour penser que ces trois remaniements sont impliqués dans le phénotype oculaire des patients. Ces résultats, confirmés par des approches plus classique de recherche d'anomalie du nombre de copies montrent la faisabilité de la recherche de tels remaniements à partir des données de séquençage haut débit.

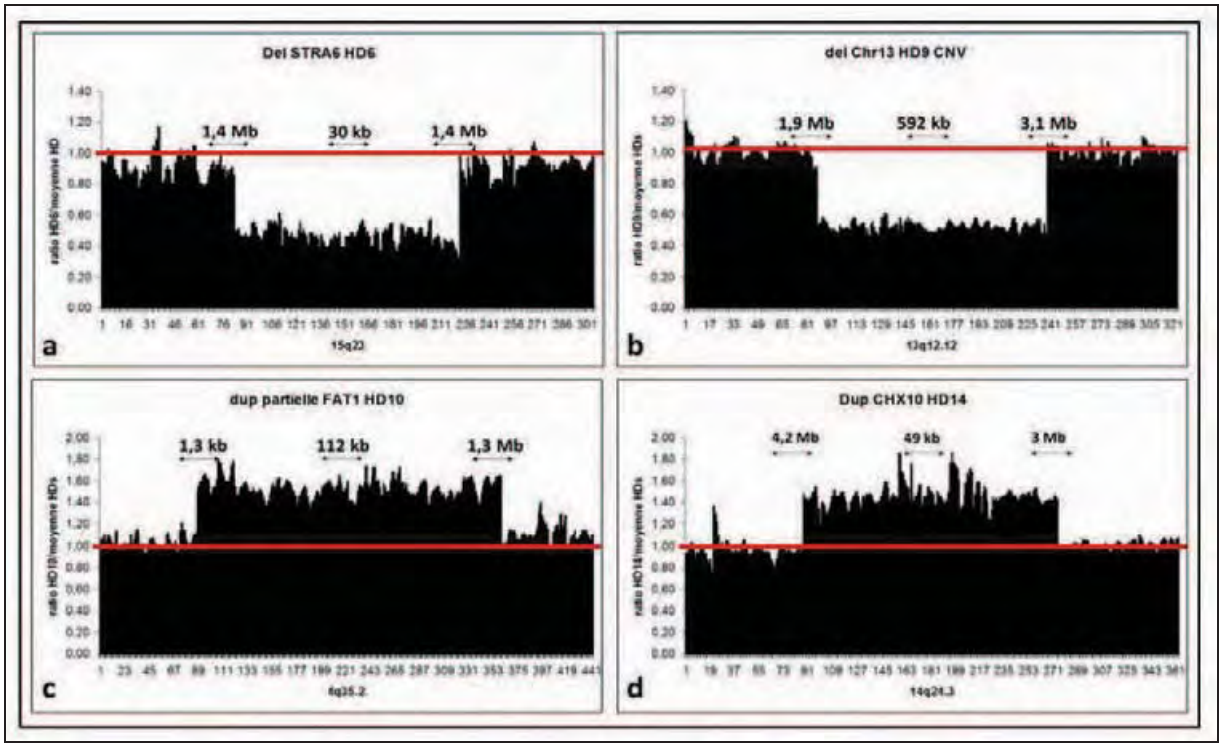

Figure 46: Résultats de la recherche de microremaniements chromosomiques par l'analyse du nombre de lectures en séquençage haut débit.

Pour chaque sonde de capture, le nombre de lecture d'un patient a été rapporté à la moyenne des 24 patients. Un rapport de 1 en abscisse (indiqué par un trait rouge) est normal, alors qu'une délétion est marquée par un rapport à 0,5 (**a**,**b**) et une duplication un rapport à 1,5 (**c**,**d**). En ordonnée, sont indiqués le nombre de sonde de capture étudiés : par exemple pour *STRA6*, 150 sondes successives apparaissent délétées (**a**). La taille minimale de la délétion/duplication est indiquée au milieu de chaque figure et la distance d'incertitude sont indiqués de part et d'autre (distance entre la première sonde délétée/dupliquée et la sonde suivante non remaniée). Le patient 6 a une délétion hétérozygote du gène *STRA6* (**a**), le patient 9 un CNV polymorphique au niveau du bras long du chromosome 13 (**b**), le patient 10 a une duplication partielle du gène *FAT1* (**c**), et le patient 14 a une duplication du gène *CHX10/VSX2* (**d**).

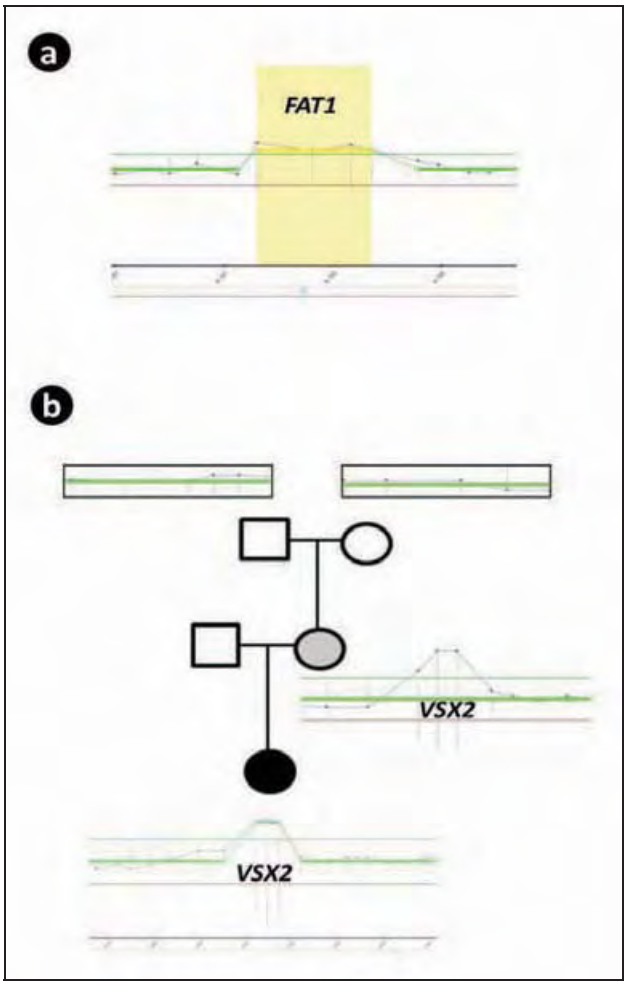

Figure 47: Confirmation par CGH-array 44K des duplications identifiées par le séquençage haut débit.

(**a**) Confirmation de la présence d'une duplication de 345 kb impliquant le gène *FAT1* chez le patient 10. (**b**) Confirmation de la présence d'une duplication de 74 kb impliquant le gène *VSX2* chez le patient 14. Cette duplication est héritée de la mère pauci-symptomatique (large excavation papillaire). L'analyse de ségrégation familiale montre que la duplication est apparue *de novo* chez la mère du patient 14 (**b**).

Conclusion

Le séquençage de 407 gènes candidats dans une cohorte de 22 patients atteints d'anomalies du développement embryonnaire de l'œil nous a permis d'identifier l'implication d'un deuxième gène majeur dans ces malformations. Nous avons ainsi pu démontrer que la présence de variations hypomorphes du gène *PTCH1* étaient retrouvées chez près de 10 % des patients atteints de ces défauts du développement. Notre analyse nous a également permis d'identifier d'autres gènes intéressants dont le caractère causal dans ces malformations reste à démontrer. Enfin, nous avons pu par cette approche originale étudier les séquences régulatrices supposées de ces gènes et mettre au point un algorithme permettant de rechercher des anomalies de nombre de copie à partir des profondeurs de lecture observées.

ARTICLE 12

Targeted resequencing identifies *PTCH1* as a major contributor to ocular developmental anomalies and extends the SOX2 regulatory network

Soumis

N. Chassaing*, E. E. Davis*, A. Causse, V. David, A. Desmaison, A. R. Niederriter, S. Lamarre, C. Vincent-Delorme, L. Pasquier, C. Coubes, D. Lacombe, M. Rossi, J.-L. Dufier, H. Dollfus, J. Kaplan, N. Katsanis, H. C. Etchevers, S. Faguer and P. Calvas

---

Nous décrivons dans cet article l'identification de mutations hypomorphes chez 10 % des patients (7/70) atteints d'anomalies embryonnaires du développement de l'œil (dysgénésies du segment antérieur ou AM). Des mutations de ce gène ont été identifiées par séquençage haut débit ciblé sur 407 gènes candidats. Nous avons pu montrer que ces mutations avaient un pénétrance incomplète et pouvaient être héritées de parents asymptomatiques. Nous avons cependant confirmé le caractère délétère (variations hypomorphes) de ces variations sur l'activité de ptch1 dans un modèle de poisson zèbre. Nous avons également montré que l'expression de *Ptch1* était régulée par Sox2 et qu'elle était importante au cours du développement oculaire.

Ces résultats s'intègrent avec les données connues sur la voie SHH (et PTCH1 qui en est un régulateur) dans le développement de l'œil dans plusieurs modèles. Chez l'homme, des mutations de *PTCH1* ont été décrites dans le syndrome de Gorlin et l'holoprosencéphalie. Ces deux syndromes sont associés à des malformations oculaires et notamment des AM. Chez le poisson des cavernes dont l'œil involue au cours du développement, il a été montré une surexpression et un patron d'expression étendu du gène *shh* comparativement au poisson des surfaces (appartenant à la même espèce de poisson, *Astyanax mexicanus*) qui a des yeux se développant normalement.

L’ensemble de ces résultats (fréquence des variants hypomorphes chez nos patients, régulation de l’expression de *Ptch1* par Sox2, expression oculaire embryonnaire de Ptch1, phénotype oculaires dans le syndrome de Gorlin et l’holoprosencéphalie, modèle du poisson des cavernes) vont dans le sens d’une implication forte de la voie SHH dans le développement oculaire et ouvres de nouvelles perspectives physiopathologiques pour les anomalies du développement de l’œil.

Les autres résultats évoqués dans cet article ont été discutés plus en détail dans ce sous-chapitre du "séquençage haut-débit des gènes candidats".

Targeted resequencing identifies *PTCH1* as a major contributor to ocular developmental anomalies and extends the SOX2 regulatory network

Nicolas Chassaing[1,2,21*], Erica E. Davis[3,4,21], Alexandre Causse[2,5], Véronique David[6,7], Annaïck Desmaison[2], Adrienne R. Niederriter[3], Sophie Lamarre[8,9], Catherine Vincent-Delorme[10], Laurent Pasquier[11], Christine Coubes[12], Didier Lacombe[13,14], Massimiliano Rossi[15], Jean-Louis Dufier[16], Helene Dollfus[17], Josseline Kaplan[18], Nicholas Katsanis[3,4], Heather C. Etchevers[2,19], Stanislas Faguer[20], Patrick Calvas[1,2].

[1]CHU Toulouse, Service de Génétique Médicale, Hôpital Purpan, 31059 Toulouse, France;

[2] Université Paul-Sabatier Toulouse III, EA-4555, 31000 Toulouse, France;

[3]Center for Human Disease Modeling, Duke University Medical Center, Durham, North Carolina, USA;

[4]Department of Pediatrics and Department of Cell Biology, Duke University Medical Center, Durham, North Carolina, USA;

[5] CHU Toulouse, Service d'Ophtalmologie, Hôpital Purpan, 31059 Toulouse, France;

[6]Institut de Génétique et Développement, CNRS UMR6290, Université de Rennes 1, IFR140 GFAS, Faculté de Médecine, 35043 Rennes, France ;

[7]Laboratoire de Génétique Moléculaire, CHU Pontchaillou, 35043 Rennes Cedex, France ;

[8]INRA, UMR792, Ingénierie des Systèmes Biologiques et des Procédés, Toulouse, France ;

[9]Plateforme Biopuces de la Génopole de Toulouse Midi Pyrénées, INSA/DGBA 135, Toulouse, France ;

[10]Service de Génétique Médicale, Hôpital Jeanne de Flandre, 59037 Lille, France ;

[11] Service de Génétique clinique, Hôpital Sud, 35200 Rennes, France;

[12]Service de Génétique Médicale, Hôpital Arnaud de Villeneuve, 34295 Montpellier, France ;

[13]Service de Génétique Médicale, Hôpital Pellegrin, 33076 Bordeaux Cedex, France ;

[14]Université Bordeaux Segalen, Laboratoire MRGM, 33076 Bordeaux, France ;

[15]Service de Cytogénétique Constitutionnelle, Hospices Civils de Lyon, Groupement Hospitalier Est, 69677 Bron, France

[16]Service d'Ophtalmologie, Hôpital Necker enfants Malades, 75015 Paris, France ;

[17]Service de Génétique Médicale, Hôpitaux Universitaires de Strasbourg, 67091 Strasbourg, France ;

[18]INSERM U781 & Department of Genetics, Paris Descartes University, 75015 Paris, France;

[19]INSERM, U910, Université de la Méditerranée Faculté de Médecine, 13385, Marseille, France;

[20]INSERM unit 1048, I2MC, Team 12, 31432 Toulouse, France

[21]These authors contributed equally to this work

***Correspondence**: Dr Nicolas Chassaing, Service de Génétique Médicale, Pavillon Lefebvre, CHU Purpan, Place du Dr Baylac, 31059 Toulouse Cedex 9, France.

Tel.: +33 5 61 77 90 55; fax: +33 5 62 74 45 58.

e-mail : chassaing.n@chu-toulouse.fr

Ocular developmental anomalies (ODA) such as Anophthalmia/Microphthalmia (AM) or anterior segment dysgenesis (ASD) have an estimated combined incidence of 3.7 in 10.000 births[1]. Mutations in *SOX2* are the most frequent contributors to severe ODA[2], yet account for a minority of the genetic drivers[3]. To identify novel ODA loci, we conducted targeted high-throughput sequencing of 407 candidate genes in an initial cohort of 22 sporadic ODA patients. Patched 1 (*PTCH1*), an inhibitor of sonic hedgehog (SHH) signaling, harbored an enrichment of rare heterozygous variants in comparison to either controls, or to the other candidate genes (four missense and one frameshift), and targeted resequencing of *PTCH1* in a second cohort of 48 ODA patients identified two additional rare nonsynonymous changes. Consistent with a role of PTCH1 in ODA, functional analysis in a zebrafish *in vivo* complementation model showed that all six patient missense mutations affect SHH signaling. Finally, through transcriptomic and ChIP analyses, we show that SOX2 binds to an intronic domain of the *PTCH1* locus to regulate *PTCH1* expression. Together, these results identify the SHH signaling pathway as a novel effector of SOX2 activity during human ocular development, and demonstrate that *PTCH1* contributes mutations to as much as 10% of ODA.

ODA are underscored by extensive genetic heterogeneity, phenotypic variability, and non-penetrance, all of which render them largely intractable for traditional family-based genetic approaches. We selected 407 candidate genes (**Supplementary Table 1**) involved in ocular development for targeted exon liquid capture followed by massively parallel sequencing. We screened 22 unrelated individuals with ODA and mutation negative for *SOX2*, *OTX2, RAX* andVSX2; and two positive control individuals (with known mutations in either *STRA6* or in *VSX2*). These affected individuals had isolated ASD (n=6); or AM that was isolated (n=4), associated with ASD (n=6), or coincident with coloboma (n=6) (**Supplementary Table 2**). We identified ~ 2,500 variants in each patient; after stringent bioinformatic filtering that focused exclusively on alleles that were a) absent from dbSNP132, HapMap and our in-house exomes; and b) predicted *in silico* to be deleterious (**Supplementary Table 3**), we observed 0-5 variants per individual in a total of 46 loci. These genes harbored variation in the following locus-wide distribution: >1 variant/gene in 10 genes (**Fig. 1a; Supplementary Tables 4, 5);** 1 variant/gene in 36 genes; the remaining 361 genes were bereft of rare functional variants predicted to be deleterious (**Supplementary Table 4,** discussed in the **Supplementary Note**).

Among these 46 loci, *PTCH1* carried the greatest mutational burden, and was the most significantly enriched for rare putative pathogenic variants in the initial ODA cohort in comparison to 13,006 control chromosomes in the Exome Variant Server (EVS; p<0.0001; **Fig. 1a,b; Table 1**), and remained nominally significant after correction for the 407 target gene set (p=0.04). Notably, the only other genes harboring an enrichment of rare variants predicted to be pathogenic in the ODA cohort were *VSX2* and *STRA6,* both of which have been identified previously as rare ODA contributors[4,5] and were mutated in the positive control individuals C1 and C2, respectively (p<0.01 vs. 13,006 EVS chromosomes; **Fig. 1a; Supplementary Table 5**).

Four individuals harbored rare *PTCH1* heterozygous changes predicted to be deleterious (**Fig. 1b; Table 1**). One patient with microphthalmia with cataract and sclerocornea (P5) had a frameshifting deletion (c.4delG, p.Glu2Asnfs*9) in exon 1 of *PTCH1* isoform NP_001077072. Individual P17, presenting with a bilateral Axenfeld-Rieger malformation, had a c.3889C>T (p.Arg1297Trp). Two additional unrelated patients with colobomatous microphthalmia, corpus callosum abnormality, and

atrial septal defects (P8 and P15) harbored c.3191C>T (p.Thr1064Met) and c.3241G>A (p.Val1081Met) changes. With the exception of P5, for whom we were unable to perform segregation analysis, we determined that each of these three *PTCH1* mutations was inherited from an asymptomatic parent (**Table 1** and **Supplementary Table 4**), consistent with incomplete penetrance.

Because of the significant enrichment of *PTCH1* variants in our first-pass filtering strategy, and cognizant of the imperfect sensitivity and specificity of prediction algorithms, we returned to the set of rare variants remaining prior to *in silico* predictions. We found two additional heterozygous rare *PTCH1* missense variants filtered out initially because they were considered benign by PolyPhen-2. Patient P20, affected with a bilateral Peters anomaly, harbored a heterozygous p.Tyr1316Cys change that was inherited from her symptomatic mother. Additionally, we identified a heterozygous p.Asp436Asn change in the control sample C2 (**Fig. 1b, Table 1**).

The significant enrichment of mutational burden in the 24 cases compared to 6500 EVS controls ($p<0.001$), and *in silico* prediction evidence were suggestive but not conclusive with regard to the deleterious effect of the *PTCH1* missense variants identified in the ODA cohort. Moreover, the observed incomplete penetrance posed interpretive challenges. Therefore, we evaluated the effect of all discovered alleles *in vivo*. Ptch1 is a transmembrane dependence receptor which functions with Shh as part of a dosage sensitive pathway resulting in activation of downstream target genes, including the Smoothened (smo) co-receptor, Ptch1 itself, and Gli transcription factors[6]. Shh signaling is a key regulator of somite patterning[7], and the *ptch1*^{tj222} (*leprechaun*) zebrafish mutant, harboring a p.Tyr590* mutation, has a visibly more obtuse angle of the somitic chevron compared to wild type (WT) embryos[8]. We have shown previously that *in vivo* complementation studies of human mutations in Shh effector molecules using somite defects as a phenotypic readout are a robust assay to determine allele pathogenicity[9]. We therefore employed this strategy to test the ability of human mRNAs harboring the ODA *PTCH1* missense mutations to rescue the *ptch1* MO-induced somite angle defects in comparison to that of WT.

Using a previously validated morpholino antisense oligonucleotide (MO)[10], we recapitulated the highly penetrant somite phenotype in WT embryos injected with 12 ng *ptch1* MO (81.5° degrees vs. 107° degrees for control vs. MO; $p<0.0001$; **Fig. 2, Supplementary Table 6**). Importantly, co-injection 100 pg of capped human *PTCH1* WT mRNA resulted in a significant amelioration of the somite defect (85.9° vs. 107° for WT rescue vs. MO; $p<0.0001$). In addition to the five missense (p.Asp436Asn, p.The1064Met, p.Val1081Met, p.Arg1297Trp, p.Tyr1316Cys) mutations identified among the 22 patients and 2 control ODA individuals, we also evaluated the effect of human *PTCH1* mRNA carrying the known pathogenic missense p.Thr1052Met change, associated previously with an holoprosencephaly (HPE)-like phenotype (including bilateral microphthalmia) and normal MRI[11] or with alobar HPE[12]. As a negative control for the assay, we also evaluated a nonsynonymous change found commonly in population controls, p.Pro1315Leu. In contrast to the significant rescue of the morphant phenotype resulting from co-injection of either WT mRNA or the negative control mRNA (p.Pro1315Leu), the morphant somite angle defect was partially rescued for each allele identified in our ODA cohort (mean somite angle ranging from 91.3° to 94.5°; $p<0.0001$ for each co-injection vs. MO) but remained significantly worse than WT rescue ($p<0.0001$ for each co-injection vs. WT rescue). We observed similar results for the p.Thr1052Met change (associated with HPE) (**Fig. 2, Supplementary Table 6**). Notably, co-injection of *ptch1* MO with the mRNA bearing the p.Asp436Asn

change identified in control C2 showed phenotypic rescue similar to that of the WT and negative control mRNAs, demonstrating that this change is benign. Injection of WT or mutant mRNA in the absence of MO resulted in no significant defects, arguing in favor of a loss-of-function rather than a dominant-negative effect. Together, these results provided *in vivo* evidence that all rare missense variants identified in our ODA discovery cohort, as well as the mutation associated with HPE, have a hypomorphic effect on PTCH1 protein activity (**Supplementary Table 6**), while the common variant p.Pro1315Leu and the p.Asp436Asn change identified in a control patient had no detectable effect on protein function.

Given these observations, we conducted bidirectional Sanger sequencing of the coding regions of *PTCH1* in an independent cohort of 48 samples with ODA. We identified two additional rare heterozygous *PTCH1* missense variants: p.Ile899Val in a patient with bilateral Peters anomaly, and p.Thr778Pro in an autosomal dominant AM-ASD family, each of which was absent from EVS (**Fig. 1b, Table 1** and **Supplementary Table 4**). An *in vivo* functional assay of each of the two additional variants demonstrated that, similar to the alleles found in our original cohort, both changes resulted in partial loss of PTCH1 function (mean somite angle 90.0° and 94.7° for p.Thr778Pro and p.Ile899Val respectively; $p<0.0001$ for each MO plus mutant mRNA co-injection versus either MO alone or WT rescue; **Fig. 2; Supplementary Table 6**). Combined, we identified a total of seven rare heterozygous *PTCH1* variants (six missense and one frameshifting) in a total of seventy individuals with ODA (10%; **Fig. 1b**).

Pursuant to the elevated incidence of ODA patients with pathogenic *PTCH1* variants, we wondered if this locus might be linked mechanistically to SOX2, as observed previously for other genes implicated in disorders of ocular development[13,14]. We first asked whether *Ptch1* might be regulated transcriptionally by SOX2. First, using RNA *in situ* hybridization, we found that robust embryonic *Ptch1* expression in the neural retina and lens persists to later stages in the adult mouse (**Fig. 3**) as observed in humans[15], and overlaps the known expression pattern of *Sox2*[16]. Using a physiologically relevant CCE-Rx model[17], we suppressed *Sox2* and tested the abundance of *Ptch1* message; in biological triplicate experiments, we found that *Ptch1* is upregulated significantly upon *Sox2* suppression ($p<0.001$; **Fig. 4a**), suggesting that the *Ptch1* locus might be under the transcriptional regulation of SOX2. We therefore performed chromatin immunoprecipitation (ChIP)-seq on CCE-Rx cells using an antibody against Sox2; we identified a peak in intron 15 of *Ptch1*, which was confirmed using targeted ChIP-qPCR on five independent samples. Importantly, amplification of the *Ptch1* exon 20 negative region was equivalent when precipitated with either non-specific IgG or Sox2 antibody, while amplification of the intron 15 region showed greater than five-fold enrichment in chromatin immunoprecipitated by the Sox2-specific antibody ($p<0.01$; **Fig. 4b-c**). Together, these data suggest that *PTCH1* expression is regulated directly by SOX2.

The SHH signaling pathway is associated strongly with ocular development in models ranging from insects to mammals that reflect ~ 600 million years of selection[15,18-22]. The *ptch1* zebrafish mutant displays an incompletely penetrant lens malformation phenotype that can be recapitulated with *ptch1* MO injection only at high doses[8]. In addition, an ENU mutagenesis screen in zebrafish for visual system mutants identified a splice-acceptor site mutation in *ptch2* that results in ocular colobomas[23], and *ptch1;ptch2* double mutants have a severe ocular phenotype with absent lens development at 24 hpf and completely absent eyes at 48 hpf[10], phenocopying AM. Eye defects in *ptch1*^{tj222} mutants could be suppressed by pharmacologically inhibiting the Hedgehog pathway with cyclopamine,

providing evidence in support of a direct involvement of SHH signaling in the manifestation of the phenotype. Last, optic morphogenesis and gene expression patterns have been compared in blind cavefish and sighted surface fish embryos, both morphological variants of the same *Astyanax mexicanus* species[24]. In contrast to surface fish embryos, cavefish embryos develop small eye primordia, which later arrest in development, degenerate and sink into the orbits, recapitulating human secondary anophthalmia. An expansion of the shh signaling domain in the presumptive ocular neuroepithelium resulted in hyperactivation of downstream genes, lens apoptosis and arrested eye growth and development in cavefish embryos[24]. These features could be mimicked in surface fish by shh overexpression, and eye development was restored partially in cavefish embryos by using cyclopamine[24]. In humans, *PTCH1* mutations have been associated previously with basal cell nevus syndrome (BCNS; MIM#109400) and with holoprosencephaly (HPE7; MIM#610828). Of note, ODA such as AM or ASD are part of both the BCNS[25] and HPE[26] phenotypes.

Despite the demonstrated functional consequences of *PTCH1* variants on SHH signaling, the wide phenotypic spectrum within our ODA cohort, coupled to the incomplete penetrance observed among families, suggests that additional factors contribute to the phenotype. Such factors may include the other 45 genes harboring rare variants in the initial cohort of 22 ODA samples. However, their rarity in cases and undetectable enrichment of variation in comparison to controls suggests that their contribution will be modest; increased sample numbers and robust experimental models to test epistasis are required to demonstrate their involvement, if any, in ODA.

In summary, high-throughput sequencing of candidate genes in ODA identified *PTCH1* as a significant contributor to congenital ocular malformations (10% in our cohort), placing it similar to its transcriptional regulator, SOX2, in terms of genetic burden to this phenotypic category[2]. Importantly, this study highlights the importance of a multifaceted approach towards identifying genetic contributors to traits such as ODA that are hallmarked by incomplete penetrance and genetic heterogeneity, especially when the cohort size is modest due to low disease frequency in the population. This study exemplifies how together, a combined candidate gene sequencing approach, *in vivo* functional assessment of allele pathogenicity, and placement to a known disease gene network provides robust interpretive data that would not have been possible to achieve through genetic studies alone.

METHODS

Methods and any associated references are available in the online version of the paper.

ACKNOWLEDGMENTS

The authors thank the families, Christine Peres, Beatrice Atlan, and Jason Willer for their technical assistance. The authors are grateful to the following physicians: C. Baumann, M. Mathieu-Dramard, B. Duban-Bedu, C. Francannet, P. Jalbert, S. Julia, B. Leheup, S. Lyonnet, S. Mercier, M. Privat, P. Ribaï, and A. Toutain. This work was supported by grants from the Clinical Research Hospital Program from the French Ministry of Health (PHRC 09 109 01) and from Retina France.

AUTHOR CONTRIBUTIONS

N.C., E.E.D, H.C.E., S.F., and P.C. designed and directed the study. N.C., E.E.D, N.K., H.C.E., S.F., and P.C. wrote the manuscript. C.V-D., L.P., C.C., D.L., M.R., J-L.D., H.D., and J.K. collected samples and provided the subjects' clinical information. N.C., A.C., V.D., A.D., and S.L. performed ChIP and transcriptomic analyses and confirmation of NGS results. H.C.E performed HIS analyses. V.D. performed *PTCH1* molecular screening. E.E.D, A.R.N, and N.K. performed zebrafish studies.

COMPETING FINANCIAL INTERESTS

The authors declare no competing financial interests

Figure 1: PTCH1 has a significantly enriched mutational burden in ODA.

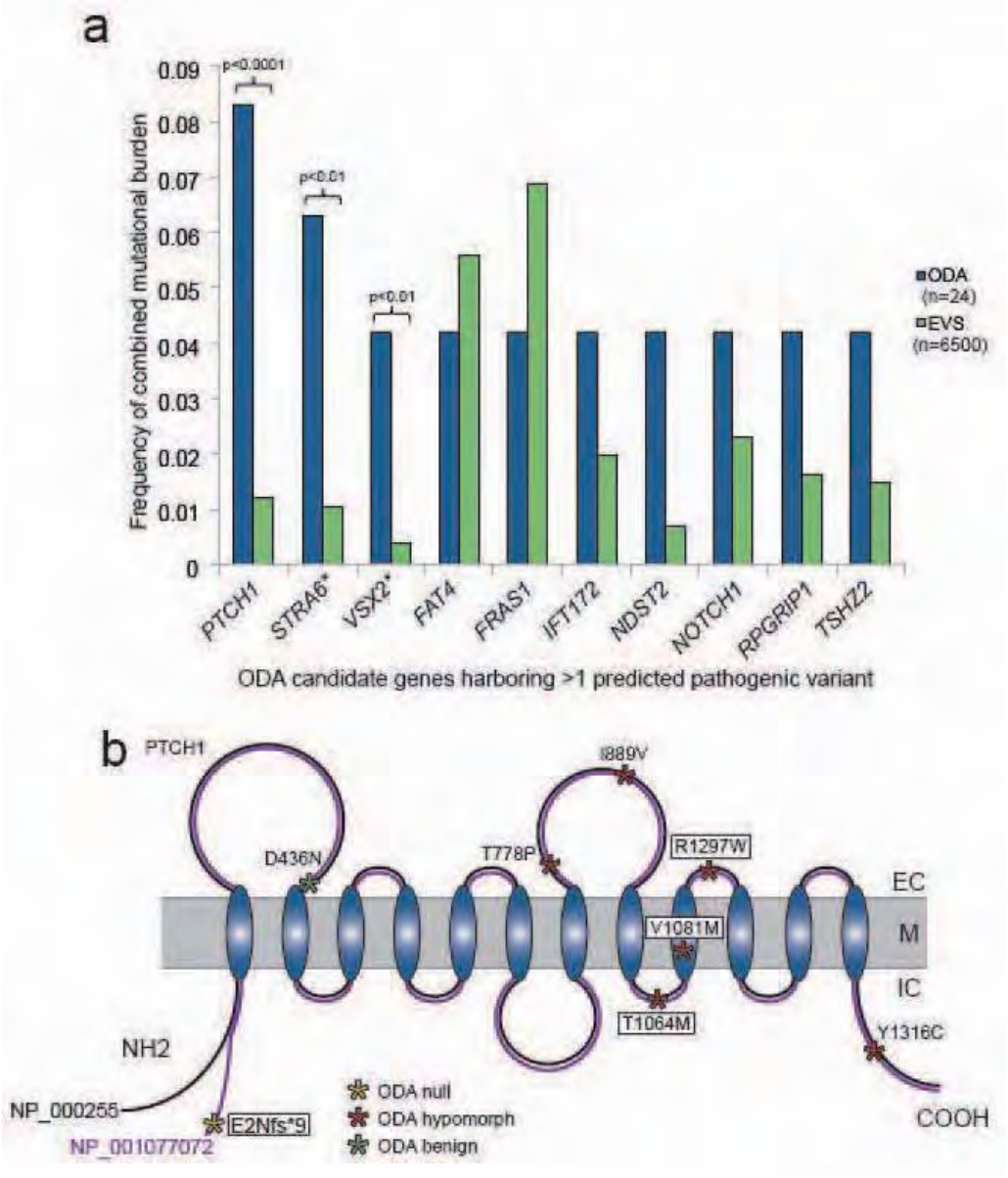

(**a**) Mutational burden for all genes harboring >1 rare predicted pathogenic variants in the initial cohort of ocular developmental anomalies (ODA) compared to healthy control individuals from the Exome Variant Server (EVS). Frequency of combined mutational burden is shown for the ten genes harboring multiple rare (<1% alternate allele frequency) functional variants (frameshift, nonsense and splicing variants were considered as damaging; missense variants were classified as damaging or not based on PolyPhen-2) in ODA cases (n=22 unknown + 2 positive controls) vs. Exome Variant Server (EVS) controls (n=6,500). P-values are indicated for the only three genes with a significant enrichment in cases versus controls (chi squared test). **STRA6* and *VSX2* are previously identified causal genes in the positive control ODA samples. (**b**) Schematic representation of the PTCH1 receptor with its extra-cellular (EC), transmembrane (M), and intra-cellular domains (IC). The positions of the *PTCH1* mutations identified in ODA are represented with asterisks, with the color indicating variant pathogenicity. The four variants enclosed with boxes were identified in the initial discovery cohort. p.E2Nfs*9 is specific to isoform NP_001077072 (purple), which is identical to NP_000255 (black) except for an alternate 66 amino acid region at the N-terminus.

Figure 2: *PTCH1* variants identified in ODA patients are pathogenic.

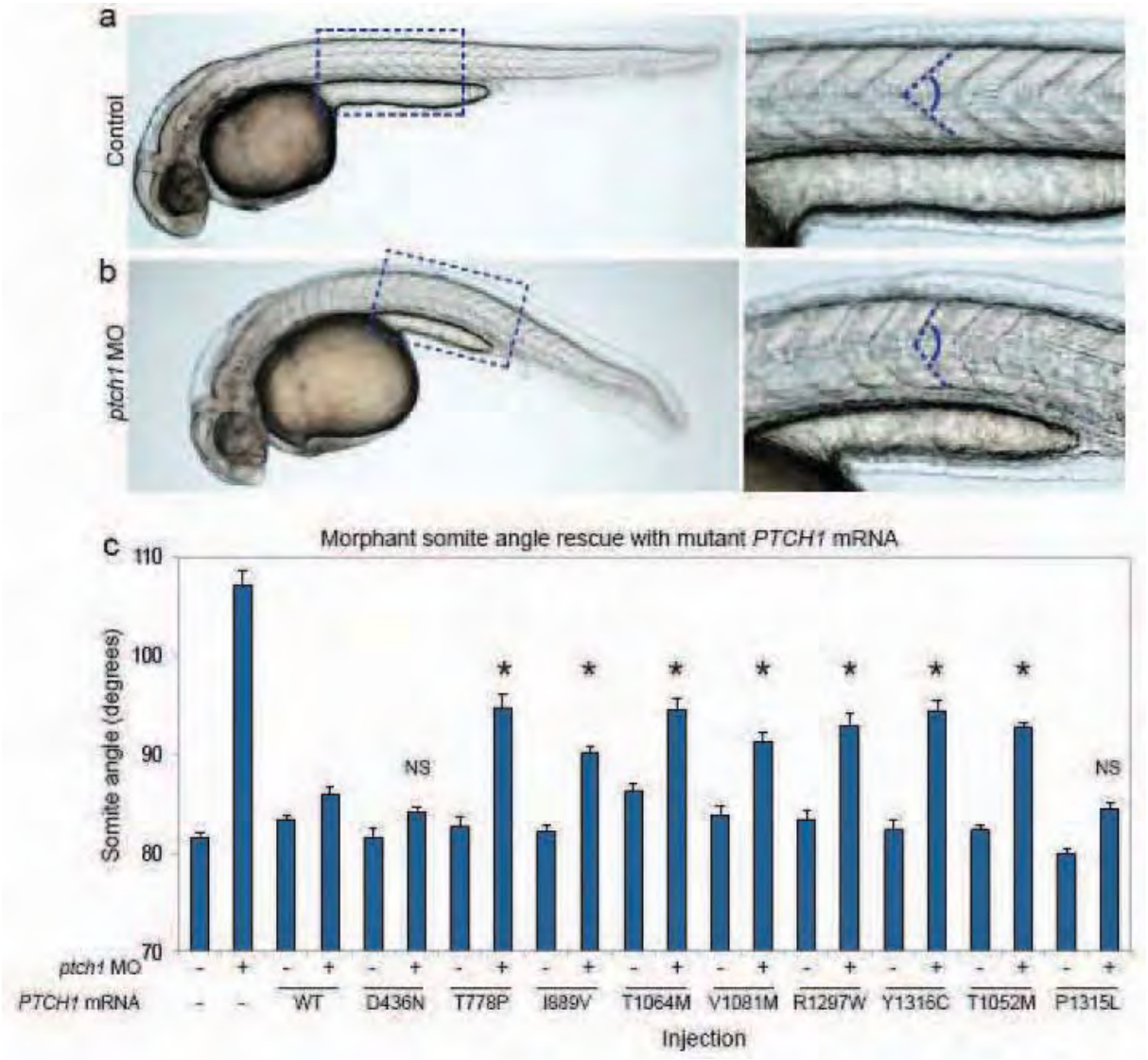

(**a**, **b**) Representative lateral images of uninjected control and *ptch1* MO-injected live embryos taken at 36 hours post fertilization (hpf); dashed boxes are enlarged in the insets (right). Magnified panels show chevron-shaped somites (controls) and abnormal-shaped somites (morphants), caused by aberrant Hedgehog signaling in the zebrafish myotome. Dashed blue lines indicate measurement position (at the midpoint between the proximal hindgut and the anus) used for phenotypic scoring of embryo batches. (**c**) All six nonsynonymous *PTCH1* variants identified in ODA cases were hypomorphic as indicated by the partial, but not complete, ability of mutant mRNA to rescue the *ptch1* MO-induced somite angle defects. *PTCH1* p.Thr1052Met, a rare variant (minor allele frequency in controls 0.001; n=13,006 chromosomes (EVS)), reported previously in HPE is also hypomorphic. Rescue with a common PTCH1 p.Pro1315Leu encoding variant (rs357564; present in homozygosity in 8% of controls; n=12,568 chromosomes in EVS) was not significantly (NS) different from wild-type (WT), providing support for the specificity of the assay. The missense variant p.Asp436Asn identified in the ODA control C2 was benign in this assay. We measured 48-52 embryos per injection batch with blind scoring. Asterisks indicate statistical differences between mutant and WT rescue ($p<0.0001$; Student's t-test). Error bars, s.e.m. See **Supplementary Table 6** for somite measurement data.

Figure 3: *Ptch1* transcripts are present in periocular mesenchyme and the neural retina throughout eye morphogenesis and into postnatal life.

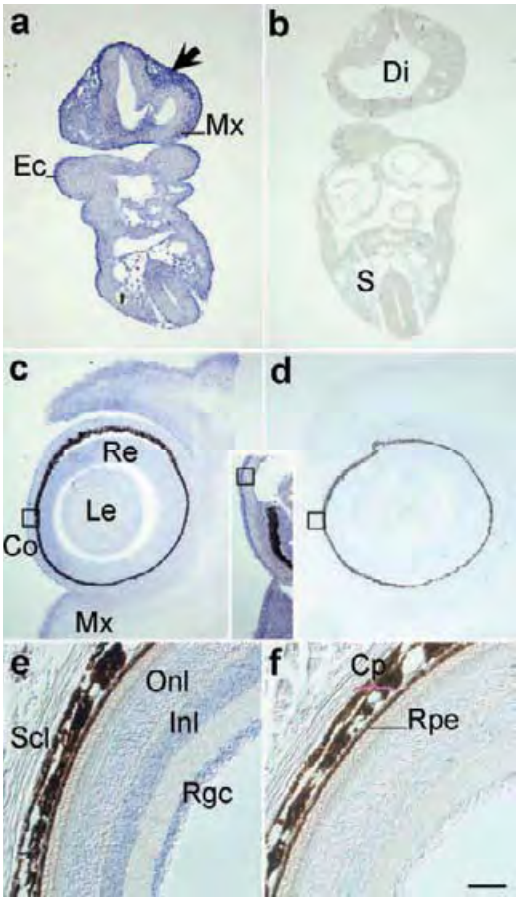

(**a**) On embryonic day (E)9.5 in mouse embryos, *Ptch1* is expressed in cephalic mesectoderm of neural crest origin in the head (arrow) and maxillary arch (Mx); in the basal diencephalon (Di) and basal neural tube at trunk levels, and in the somitic sclerotome (S). Ectodermal expression is constant at all embryonic stages examined (Ec). By E11.5, the distal diencephalic infundibulum transcribes *Ptch1* (not shown) as does the subectodermal mesenchyme of the future eyelids and palate. (**c**) Mesenchymal *Ptch1* expression continues at E13.5; the lateral neural retina (Re) and differentiated outer cells of the lens (Le) begin to also transcribe *Ptch1*, which continues throughout these structures at E15.5 (inset). By this stage, initially generalized expression in the developing cornea (Co, box) has become restricted to the epithelium. Scale bar **a**-**d**, 400 µm. (**e**) In adult mouse eyes at postnatal day 50, transcripts are found within the outer and inner nuclear layers (Onl, Inl), corresponding to photoreceptor and Müller cell bodies, and within the retinal ganglion cell layer (Rgc), testifying to a postnatal role in retinal maintenance. Rpe, retinal pigmented epithelium; Cp; choroid plexus. Transcripts not observed within the stroma of the anterior chamber or the sclera (Scl). Scale bar **e**,**f**, 200 µm. Hybridization with a sense-oriented *Ptch1* probe as negative control in **b**, **d**, **f**.

Figure 4: SOX2 regulates *PTCH1* expression directly

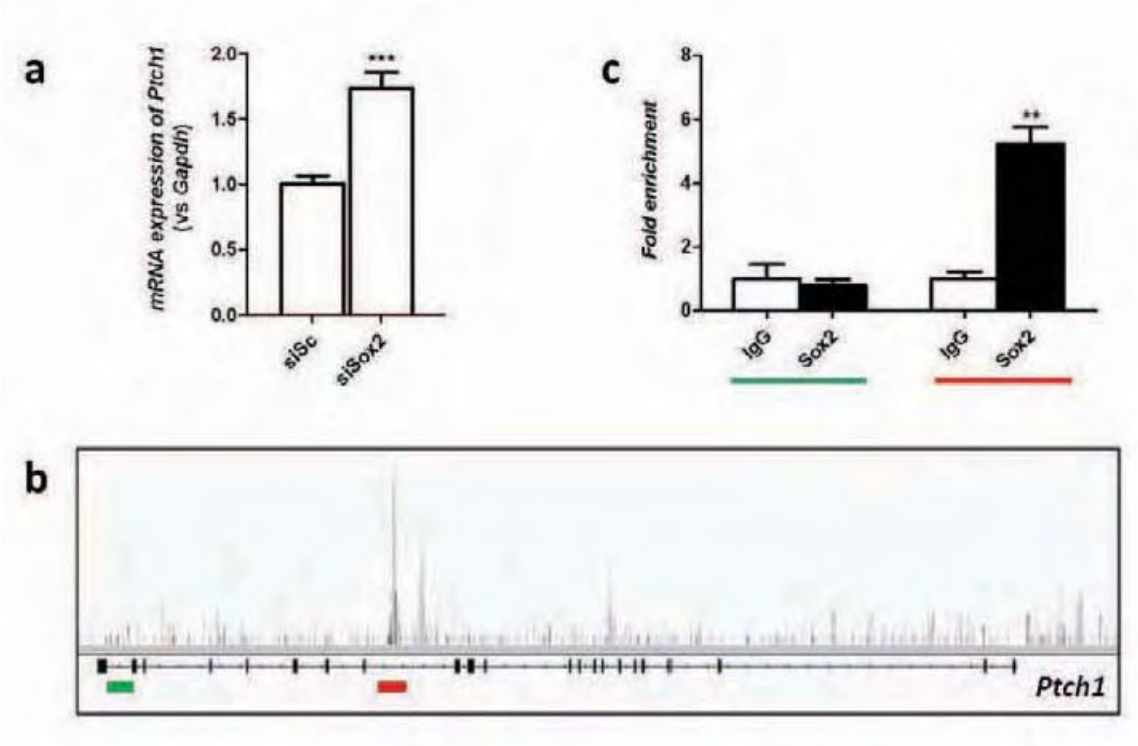

(**a**) Targeted quantitative PCR after transfection of CCE-RX cells with a scrambled siRNA (siSc, n=9) or a siRNA targeting *Sox2* (siSox2, n=9). This experiment showed that decreased expression of *Sox2* leads to increased expression of *Ptch1* (**b**) Results of ChIP-seq performed on CCE-RX cells using an antibody against SOX2. The *Ptch1* gene structure is represented underneath the DNA fragments sequenced after ChIP, with higher peaks corresponding to more enrichment. A peak was identified in intron 15 of *Ptch1* (underlined in red), while an example of an unenriched region is shown in intron 22 (underlined in green). (**c**) Results obtained by ChIP-seq were confirmed using targeted ChIP-qPCR on 5 independent samples. Amplification of the exon 20 negative region (in green) was equivalent whether using non-specific IgG or a SOX2 antibody, while amplification of the intron 15 region (in red) showed greater than five-fold enrichment in chromatin immunoprecipitated by the SOX2-specific antibody. (**a, c**) Asterisks indicate statistical differences between the different conditions rescue (**: $p<0.01$, ***: $p<0.001$; Mann-Whitney U-test). Error bars, s.e.m.

Table 1 : *PTCH1* variants identified in ODA patients and/or studied *in vivo* using zebrafish experiments

Patient	Transcript ID	cDNA Variation	Protein Variation	Inheritance	GERP score	Grantham score	Polyphen2 Hum-Div	Polyphen2 Hum-Var	SIFT	EVS	Protein Location	Zebrafish studies
P5	ENST00000375274	c.4delG	p.Glu2Asnfs*9	Unk	-		-	-	-	Abs	-	-
P8	ENST00000331920	c.3191C>T	p.Thr1064Met	Asy Fa	5.61	81	D(1.00)	D(0.990)	T(0.1)	2/13006	TM	Hypomorphic
P15	ENST00000331920	c.3241G>A	p.Val1081Met	Asy Mo	5.32	21	D(0.991)	P(0.782)	D(0.02)	1/13006	EC	Hypomorphic
P17	ENST00000331920	c.3889C>T	p.Arg1297Trp	Asy Fa	2.75	101	B(0)	B(0)	T(0.07)	1/12914	IC	Hypomorphic
P20	ENST00000331920	c.3947A>G	p.Tyr1316Cys	Sy Mo	4.92	194	D(0.983)	P(0.541)	T(0.07)	9/12499	IC	Hypomorphic
C2	ENST00000331920	c.1306G>A	p.Asp436Asn	-	5.63	23	P(0.115)	P(0.066)	T(0.98)	Abs	EC	Benign
CC-44	ENST00000331920	c.2332A>C	p.Thr778Pro	Unk	5.73	38	D(0.999)	D(0.990)	T(0.18)	Abs	EC	Hypomorphic
CC-10	ENST00000331920	c.2695A>G	p.Ile899Val	Asy Fa	3.49	29	B(0.03)	B(0.071)	T(0.5)	Abs	EC	Hypomorphic
HPE[12]	ENST00000331920	c.3143C>T	p.Thr1052Met	Asy Fa	5.87	81	D(0.951)	P(0.608)	D(0.02)	15/13006	IC	Hypomorphic
rs357564	ENST00000331920	c.3944C>T	p.Pro1315Leu	-	4.83	98	D(0.906)	B(0.444)	T(0.22)	3761/12568	IC	Benign

P: patient; C: control; CC: confirmation cohort; HPE: holoprosencephaly

Unk: unknown; Fa: father; Mo: mother; Asy: asymptomatic; Sy: symptomatic; Abs: absent; - : not available

The Genomic Evolutionary Rate Profiling (GERP) score ranges from -12.3 to 6.17, with 6.17 being the most conserved.

D: probably damaging; P: possible damaging, B: probably benign; T: tolerated

TM: transmenbrane domain; EC: extra-cellular domain; IC: c intra-cellular domain

Grantham scores, which categorize codon replacements into classes of increasing chemical dissimilarity, were designated conservative (0-50), moderately conservative (51-100), moderately radical (101-150), or radical (≥151)[27].

SUPPLEMENTARY NOTE

Screening of the 407 candidate genes identified between zero and five variants predicted to be damaging among the 22 patients and 2 controls included in this study (**Supplementary Table 4**).

We identified the previously discovered mutations from the positive control ODA samples (C1 and C2; **Supplementary Table 4**).

In six patients, *PTCH1* variants were identified (see **Main Text**).

In two patients among the discovery cohort of 22 patients (P1 and P6), we identified mutations in genes previously implicated in human ocular developmental anomalies (ODA). P1 harbored a *de novo* heterozygous variant encoding p.Asn64Lys. Asn64 is located in the highly conserved paired domain of *PAX6*. Interestingly, an ENU-induced microphthalmic mouse mutant was shown to bear the same *PAX6* missense mutation (p.Asn64Lys), demonstrating its probable deleterious effect[28]. Heterozygous *PAX6* mutations are associated with ASD (frequently aniridia). P1 displayed bilateral anophthalmia, and this is the first description of a heterozygous *PAX6* mutation in anophthalmia. Mutation filtering of P6 identified a homozygous *STRA6* missense mutation (p.Pro579Ala). This variant altered a conserved amino acid, and was predicted to be probably damaging by Polyphen-2 software (score 0.999). When we performed familial segregation analysis of this mutation, we demonstrated that P6 was compound heterozygous for the p.Pro579Ala mutation and a *STRA6* deletion inherited from the father. P6 displayed bilateral microphthalmia with colobomatous cyst, developmental delay, short stature (-2 SD) and left duplicated pyelocaliceal system. *STRA6* mutations were first reported to be involved in syndromic anophthalmia (MCOPS9, Matthew-Wood syndrome), and subsequently the associated phenotype was extended to isolated microphthalmia[4].

In each of five genes (*FAT4*, *IFT172*, *NOTCH1*, *RPGRIP1* and *TSHZ2*) we identified two ODA patients with a heterozygous missense variant (see **Fig. 1**). P4, born from healthy consanguineous parents bears a heterozygous p.Glu44Ala missense variant in *FAT4*. Molecular analysis of the asymptomatic parents showed that they were both heterozygous for this variation. The other heterozygous *FAT4* missense variant (P3, p.Lys2654Gln) was inherited from an asymptomatic parent. In mice, *Fat4* expression has been shown to be regulated directly by PAX6 during lens formation, and it has been suggested that *Fat4* may be implicated in lens morphogenesis because of its role in planar cell polarity[29]. More recently, FAT4 mutations have been associated in humans with Van Maldergem syndrome, an autosomal-recessive multiple malformation syndrome affecting brain but not eyes[30]. Since *FAT4* missense variant identified in our ODA patients were inherited from asymptomatic parents, we suspect that these changes are unlikely to cause the ocular defects, although we cannot exclude the possibility of incomplete penetrance, oligogenic inheritance or recessive inheritance with an unidentified second mutation.

Patients P5 and P7 were both heterozygous for a variant in *IFT172* (p.Arg1294Cys and p.Asn1711Asnfs*20). Parental segregation analysis of these two variations was unavailable. *IFT172* has been recently implicated in a mouse model of VACTERL-H association. The authors demonstrated that IFT172 was required for ciliogenesis and Hedgehog (Hh) signaling. None of the studied mice display ocular involvement[31] which is not in favor of implication of P5 and P7 variants in the ODA phenotype.

Two patients also bear heterozygous *NOTCH1* missense variants: P14 harbors the heterozygous p.Arg23Leu encoding change inherited from a paucisymptomatic mother (increased papillary excavation), while P12 has a heterozygous p.Gly812Arg missense variation inherited from his father, who had glaucoma. *NOTCH1* expression has been demonstrated to be regulated by SOX2, and an implication of NOTCH1 in lens development has been reported[32,33]. Familial segregation of the p.Gly812Arg variant showed that P12's son, who also had colobomatous microphthalmia, did not share the p.Gly812Arg variant. This last result argues against implication of this missense variation in the ODA phenotypes.

Two patients P9 and P11 were heterozygous for *RPGRIP* changes (p.Cys808Trp and p.Ile270Val respectively). Parental analysis shows that P9 variation was inherited from the asymptomatic father. Recessive *RPGRIP* mutations have previously been associated with Leber congenital amaurosis[34], and thus, these heterozygous changes are unlikely to cause ODA.

Finally, two heterozygous variants of *TSHZ2* were identified among the 22 patients: P3 was heterozygous for a p.Ser83Ala variant inherited from an asymptomatic father; P21 was heterozygous for a p.Gln430Leu variant, inherited from an asymptomatic mother. Targeted expression of the *tsh* gene in Drosophila can cause ectopic eye development in non-eye tissues, while in mice, *Tsh* genes have been demonstrated to regulate the activity and/or expression of genes involved in formation of the fly eye[35]. The heterozygous missense changes identified in P3 and P21 were each inherited from an asymptomatic parent. As these variants were inherited, we posit that these *TSHZ2* variants are unlikely to cause the ocular defects, even if they may participate in the ocular phenotype.

In addition to those discussed above, other heterozygous variants predicted to be deleterious were identified in 35 different genes among the 22 patients. Among these, some genes are of particular interest: *VAX2* and *SOX14* are paralogs of genes already involved in ODA (*VAX1* and *SOX2* respectively); *CYP26C1, PITRM1*, *PFKP*, *PRPF8*, and *MYO1C* were found to be deleted in ODA patients by array-CGH and were thus considered as candidate genes[36,37]; and finally, four genes have been implicated in microphthalmia in mouse models (*ADAM17*, *MITF*, and *SULF1*). Further information about these variants is summarized in **Supplementary Table 4**. Whether these variants participate in the human ocular developmental anomalies remain unclear, and would require further functional studies.

ONLINE METHODS

Candidate gene selection

We selected 407 candidate genes based on lines of evidence for putative involvement in ODA (**Supplementary Table 1**). Based on data in the literature, these genes were related to normal or abnormal ocular development in vertebrates and/or invertebrates.

Patients

70 ODA patients (22 in the discovery cohort, 48 in the replication cohort), and two positive controls with known mutations were enrolled in this study. Informed consent was obtained from each participant, which adhered to the tenets of the Declaration of Helsinki and was approved by the local Ethics Committee (CPP Sud-Ouest et Outre-Mer II). Ocular phenotypes of the 22 patients included in the first cohort were isolated ASD (n=6), isolated AM (n=4), AM with ASD (n=6), or AM with coloboma (n=6) (reviewed in **Supplementary Table 2**). Ocular phenotypes of the 48 patients included in the second cohort were isolated ASD (n=14), isolated AM (n=17), AM with ASD (n=9), or AM with coloboma (n=8).

Targeted enrichment and high throughput DNA sequencing

A custom-made SureSelect oligonucleotide probe library was designed to capture the exons of 407 candidate genes (**Supplementary Table 1**). The probe library also aimed to capture 880 kb of potential regulatory sequences (i.e. non coding region located within 20 kb of the 407 genes and conserved among species). A total of 56,059 probes, covering 2.46 Mb, were designed and synthesized. Sequence capture, enrichment, and elution were performed according to the manufacturer's instructions (SureSelect, Agilent). Each eluted-enriched DNA sample was then sequenced on an Illumina GAIIx as paired-end 75 bp reads (Integragen). Sequence reads were aligned to the reference human genome (UCSC hg19) using commercially available software (CASAVA1.7, Illumina) and the ELANDv2 alignment algorithm. The mean coverage was 325X with 96.9% of the targeted sequences over 10X and 93.4% over 25X.

Filtering strategy

All variants reported were filtered to ensure an optimal prioritization of candidate mutations (**Supplementary Table 3**). We first filtered out variants that did not meet the quality criteria (array confidence <0.3, sequence read depth <10 and sequence base quality <10). We then filtered out all variants present in the local, in-house exome sequencing database as well as in dbSNP132, 1000 Genomes Project, and the HapMap Project databases. Only exonic and splice-site variants were retained; we removed synonymous variants and variants predicted to be benign by the Polyphen-2

software. The presence of the final selected variants was confirmed by Sanger sequencing. Primers were designed to surround the candidate mutations, and are available upon request.

Mutational burden analysis

We determined the mutational burden for the ten genes identified in the targeted resequencing of ODA samples harboring multiple rare (<1% alternate allele frequency) functional variants (frameshift, nonsense and splicing variants were considered as damaging; missense variants were classified as damaging or not based on PolyPhen-2) in ODA cases (n=22 unknown + 2 positive controls) vs. Exome Variant Server (EVS) controls (n=6,500). EVS was accessed in November 2013 and a chi-squared test was used for comparisons.

***PTCH1* molecular screening**

To support further the involvement of *PTCH1* lesions in ODA, we screened this locus in a new cohort of 48 patients by direct bidirectional Sanger sequencing. Primers used to amplify the 23 coding exons and intron-exon splice junctions are listed in **Supplementary Table 7**.

Zebrafish embryo microinjection and manipulation

We obtained a previously published[8] morpholino antisense oligonucleotide (MO; GeneTools) targeting the splice donor site of *ptch1* exon 3; 1 nl of the indicated cocktail was injected into wild-type (WT) zebrafish embryos at the one-to-four-cell stage (n=48-52 embryos/injection, repeated at least twice; with masked scoring).

Embryos were reared at 28.5° C and imaged live at 36 hours post fertilization (hpf). To generate human *PTCH1* WT and mutant mRNA, we first obtained a full-length open reading frame (ORF) construct (clone ID: 100016192; OpenBiosystems). We generated a stop codon, and subsequently introduced additional nonsynonymous changes using site-directed mutagenesis (QuikChange; Agilent). We then transferred sequenced-confirmed *PTCH1* ORFs into the pCS2+ plasmid (LR clonase II; Life Technologies), linearized with NotI, and performed *in vitro* transcription with the SP6 mMessage mMachine kit (Ambion). For rescue experiments, 12 ng MO and 100 pg of *PTCH1* mRNA were injected respectively. Live embryo imaging of lateral views was conducted on a Nikon AZ100 microscope at 6x magnification facilitated by NIS Elements software. Somite angle measurements were recorded from the resulting images using ImageJ software.

Chromatin Immunoprecipitation (ChIP)

We performed quantitative ChIP-seq in murine stem cells genetically modified to overexpress *Rax* (retina and anterior neural fold homeobox) (CCE-Rx cells, a kind gift from Pr. S. Watanabe)[17]. These cells have the ability to differentiate into retinal ganglion cells, were cultured using the standard procedures[17]. $2x10^6$ resuspended CCE-Rx cells were cultured in LIF-free medium on 10-cm bacterial

plates. 48 hours later, CCE-Rx embryoid bodies were treated with formaldehyde for 10 minutes, chromatin was prepared, and ChIP was performed according to the Upstate (Millipore) protocol, using 10 µg of anti-Sox2 antibody (Santa Cruz Biotechnology, sc-17320) or mouse IgG (Millipore, PP54) as a control. ChIP-seq libraries were prepared and sequenced using the standard Illumina protocol. Peaks were called with SeqMonk using the contig generator function. Inside intron 15 of *Ptch1*, a peak was identified in the Sox2-immunoprecipitated sample. The online Jaspar database confirmed the presence of a putative Sox2 binding site within the peak sequence. Amplicons corresponding to the *Ptch1* intron 15 Sox2 ChIP-seq peak and to a region not predicted to bind Sox2 in intron 22 (see **Supplementary Table 7** for primers) were selected for validation. These amplicons were tested in 5 independent samples immunoprecipitated either with Sox2 or mouse IgG antibodies.

Quantitative RT-PCR

Quantitative PCR analysis was performed in CCE-Rx cells to confirm *Ptch1* regulation by Sox2. CCE-Rx cells were cultured using the standard procedures[17] and transfected as previously described[38] either with an siRNA targeting *Sox2* mRNA or with a scrambled siRNA (Invitrogen, Stealth™ siRNA MSS277200 and Negative Control Medium GC respectively). Quantitative real-time PCR analyses on complementary DNA transcribed from total RNA showed that the remaining *Sox2* expression was 50% at 24 hours post transfection and 75% at 48 hours post transfection. 48 hours after transfection of either the siSOX2 (n=9) or the siScramble (n=9), total RNA was isolated using the GenElute Mammalian Total RNA Miniprep kit (Sigma-Aldrich). Samples were used to analyze *Ptch1* expression levels in the siSOX2 samples compared to controls (**Supplementary Table 7** for primers).

***In situ* hybridization**

In situ hybridization was carried out on paraffin sections using a murine *Ptch1* probe [39] according to standard protocols[40].

SUPPLEMENTARY TABLES

Supplementary Table 1: List of the 407 candidate genes
Supplementary Table 2: Phenotypes of ODA patients
Supplementary Table 3: Variant prioritization
Supplementary Table 4: Final prioritized variants in patients with ODA
Supplementary Table 5: Mutational burden of rare functional variants in ODA cases versus EVS controls.
Supplementary Table 6: Somite angle measurements for PTCH1 *in vivo* complementation assays.
Supplementary Table 7: Primers used for qPCR and *PTCH1* mutational analysis

URLs

1000 Genomes Project (http://www.1000genomes.org/)
HapMap Project (http://hapmap.ncbi.nlm.nih.gov/)
dbSNP (http://www.ncbi.nlm.nih.gov/projects/SNP/)
Exome Variant Server (http://evs.gs.washington.edu/EVS/)
Polyphen-2 (http://genetics.bwh.harvard.edu/pph2/)
SIFT (http://sift.jcvi.org/)
Jaspar (http://jaspar.genereg.net/)
HGMD (http://www.hgmd.cf.ac.uk/ac/index.php)

REFERENCES

1. Bermejo, E. & Martinez-Frias, M.L. Congenital eye malformations: clinical-epidemiological analysis of 1,124,654 consecutive births in Spain. *Am J Med Genet* **75**, 497-504 (1998).
2. Fantes, J. et al. Mutations in SOX2 cause anophthalmia. *Nat Genet* **33**, 461-3 (2003).
3. Verma, A.S. & Fitzpatrick, D.R. Anophthalmia and microphthalmia. *Orphanet J Rare Dis* **2**, 47 (2007).
4. Chassaing, N. et al. Phenotypic spectrum of STRA6 mutations: from Matthew-Wood syndrome to non-lethal anophthalmia. *Hum Mutat* **30**, E673-81 (2009).
5. Ferda Percin, E. et al. Human microphthalmia associated with mutations in the retinal homeobox gene CHX10. *Nat Genet* **25**, 397-401 (2000).
6. Villavicencio, E.H., Walterhouse, D.O. & Iannaccone, P.M. The sonic hedgehog-patched-gli pathway in human development and disease. *Am J Hum Genet* **67**, 1047-54 (2000).
7. Bumcrot, D.A. & McMahon, A.P. Somite differentiation. Sonic signals somites. *Curr Biol* **5**, 612-4 (1995).
8. Koudijs, M.J. et al. The zebrafish mutants dre, uki, and lep encode negative regulators of the hedgehog signaling pathway. *PLoS Genet* **1**, e19 (2005).
9. Putoux, A. et al. KIF7 mutations cause fetal hydrolethalus and acrocallosal syndromes. *Nat Genet* **43**, 601-6 (2011).
10. Koudijs, M.J., den Broeder, M.J., Groot, E. & van Eeden, F.J. Genetic analysis of the two zebrafish patched homologues identifies novel roles for the hedgehog signaling pathway. *BMC Dev Biol* **8**, 15 (2008).
11. Ribeiro, L.A., Murray, J.C. & Richieri-Costa, A. PTCH mutations in four Brazilian patients with holoprosencephaly and in one with holoprosencephaly-like features and normal MRI. *Am J Med Genet A* **140**, 2584-6 (2006).
12. Ming, J.E. et al. Mutations in PATCHED-1, the receptor for SONIC HEDGEHOG, are associated with holoprosencephaly. *Hum Genet* **110**, 297-301 (2002).
13. Danno, H. et al. Molecular links among the causative genes for ocular malformation: Otx2 and Sox2 coregulate Rax expression. *Proc Natl Acad Sci U S A* **105**, 5408-13 (2008).
14. Kamachi, Y., Uchikawa, M., Tanouchi, A., Sekido, R. & Kondoh, H. Pax6 and SOX2 form a co-DNA-binding partner complex that regulates initiation of lens development. *Genes Dev* **15**, 1272-86 (2001).
15. Bakrania, P. et al. Mutations in BMP4 cause eye, brain, and digit developmental anomalies: overlap between the BMP4 and hedgehog signaling pathways. *Am J Hum Genet* **82**, 304-19 (2008).
16. Hever, A.M., Williamson, K.A. & van Heyningen, V. Developmental malformations of the eye: the role of PAX6, SOX2 and OTX2. *Clin Genet* **69**, 459-70 (2006).
17. Tabata, Y. et al. Specification of the retinal fate of mouse embryonic stem cells by ectopic expression of Rx/rax, a homeobox gene. *Mol Cell Biol* **24**, 4513-21 (2004).
18. Chiang, C. et al. Cyclopia and defective axial patterning in mice lacking Sonic hedgehog gene function. *Nature* **383**, 407-13 (1996).
19. Christiansen, A.E., Ding, T. & Bergmann, A. Ligand-independent activation of the Hedgehog pathway displays non-cell autonomous proliferation during eye development in Drosophila. *Mech Dev* **129**, 98-108 (2012).
20. Macdonald, R. et al. Midline signalling is required for Pax gene regulation and patterning of the eyes. *Development* **121**, 3267-78 (1995).
21. Nasrallah, I. & Golden, J.A. Brain, eye, and face defects as a result of ectopic localization of Sonic hedgehog protein in the developing rostral neural tube. *Teratology* **64**, 107-13 (2001).
22. Takabatake, Y., Takabatake, T., Sasagawa, S. & Takeshima, K. Conserved expression control and shared activity between cognate T-box genes Tbx2 and Tbx3 in connection with Sonic hedgehog signaling during Xenopus eye development. *Dev Growth Differ* **44**, 257-71 (2002).

23. Lee, J. et al. An ENU mutagenesis screen in zebrafish for visual system mutants identifies a novel splice-acceptor site mutation in patched2 that results in Colobomas. *Invest Ophthalmol Vis Sci* **53**, 8214-21 (2013).
24. Yamamoto, Y., Stock, D.W. & Jeffery, W.R. Hedgehog signalling controls eye degeneration in blind cavefish. *Nature* **431**, 844-7 (2004).
25. Bree, A.F. & Shah, M.R. Consensus statement from the first international colloquium on basal cell nevus syndrome (BCNS). *Am J Med Genet A* **155A**, 2091-7 (2011).
26. Pineda-Alvarez, D.E. et al. A broad range of ophthalmologic anomalies is part of the holoprosencephaly spectrum. *Am J Med Genet A* **155A**, 2713-20 (2011).
27. Li, W.H., Wu, C.I. & Luo, C.C. Nonrandomness of point mutation as reflected in nucleotide substitutions in pseudogenes and its evolutionary implications. *J Mol Evol* **21**, 58-71 (1984).
28. Ramaesh, T. et al. Histopathological characterisation of effects of the mouse Pax6(Leca4) missense mutation on eye development. *Exp Eye Res* **89**, 263-73 (2009).
29. Xie, Q. et al. Pax6 interactions with chromatin and identification of its novel direct target genes in lens and forebrain. *PLoS One* **8**, e54507 (2013).
30. Cappello, S. et al. Mutations in genes encoding the cadherin receptor-ligand pair DCHS1 and FAT4 disrupt cerebral cortical development. *Nat Genet* **45**, 1300-8 (2013).
31. Friedland-Little, J.M. et al. A novel murine allele of Intraflagellar Transport Protein 172 causes a syndrome including VACTERL-like features with hydrocephalus. *Hum Mol Genet* **20**, 3725-37 (2011).
32. Rowan, S. et al. Notch signaling regulates growth and differentiation in the mammalian lens. *Dev Biol* **321**, 111-22 (2008).
33. Taranova, O.V. et al. SOX2 is a dose-dependent regulator of retinal neural progenitor competence. *Genes Dev* **20**, 1187-202 (2006).
34. Dryja, T.P. et al. Null RPGRIP1 alleles in patients with Leber congenital amaurosis. *Am J Hum Genet* **68**, 1295-8 (2001).
35. Manfroid, I., Caubit, X., Kerridge, S. & Fasano, L. Three putative murine Teashirt orthologues specify trunk structures in Drosophila in the same way as the Drosophila teashirt gene. *Development* **131**, 1065-73 (2004).
36. Delahaye, A. et al. Genomic imbalances detected by array-CGH in patients with syndromal ocular developmental anomalies. *Eur J Hum Genet* **20**, 527-33 (2012).
37. Meire, F. et al. Nonsyndromic bilateral and unilateral optic nerve aplasia: first familial occurrence and potential implication of CYP26A1 and CYP26C1 genes. *Mol Vis* **17**, 2072-9 (2011).
38. Ko, B.S., Chang, T.C., Shyue, S.K., Chen, Y.C. & Liou, J.Y. An efficient transfection method for mouse embryonic stem cells. *Gene Ther* **16**, 154-8 (2009).
39. Goodrich, L.V., Johnson, R.L., Milenkovic, L., McMahon, J.A. & Scott, M.P. Conservation of the hedgehog/patched signaling pathway from flies to mice: induction of a mouse patched gene by Hedgehog. *Genes Dev* **10**, 301-12 (1996).
40. Chotteau-Lelievre, A., Dolle, P. & Gofflot, F. Expression analysis of murine genes using in situ hybridization with radioactive and nonradioactively labeled RNA probes. *Methods Mol Biol* **326**, 61-87 (2006).

Supplementary Table 1 : List of the 407 candidate genes

gene	approved_name	previous_symbols	accession_numbers	refseq_ids	synonyms	chromosome
ACVR1	activin A receptor, type I	ACVRLK2		NM_001105	SKR1, ALK2, ACVR1A	2q23-q24
ACVR1C	activin A receptor, type IC		BC022530	NM_145259	ALK7, ACVRLK7	2q24.2
ADAM17	ADAM metallopeptidase domain 17	TACE	U69611		cSVP, CD156B	2p25
ADAM23	ADAM metallopeptidase domain 23		AB009672	NM_003812	MDC3	2q33
ADH1A	alcohol dehydrogenase 1A (class I), alpha polypeptide	ADH1	M12963	NM_000667		4q23
AES	amino-terminal enhancer of split		GRG5, TLE5	NM_198969	AK094591	19p13.3
ALCAM	activated leukocyte cell adhesion molecule		AK054632	NM_001627	CD166, MEMD	3q13.1
ALDH1A1	aldehyde dehydrogenase 1 family, member A1	PUMB1, ALDH1	K03000		RALDH1	9q21.13
ALDH1A2	aldehyde dehydrogenase 1 family, member A2		AB015228		RALDH2	15q21.2
ALDH1A3	aldehyde dehydrogenase 1 family, member A3	ALDH6	U07919		RALDH3	15q26
ALDOA	aldolase A, fructose-bisphosphate		X05236	NM_000034		16p11.2
ALK	anaplastic lymphoma receptor tyrosine kinase		D45915	NM_004304	CD246	2p23
ALX4	ALX homeobox 4	PFM2	AF294629		FPP, PFM, KIAA1788	11p11.2
AP3B1	adaptor-related protein complex 3, beta 1 subunit		U81504		ADTB3A, HPS2	5q14.1
APBB1IP	amyloid beta (A4) precursor protein-binding, family B, member 1 interacting prote		AB085852	NM_019043	INAG1, RIAM	10p12.1
APLN	apelin		AF179680	NM_017413	apelin, XNPEP2	Xq25
ARNTL	aryl hydrocarbon receptor nuclear translocator-like		D89722	NM_001178	MOP3, JAP3, BMAL1, PAS	11p15
ARR3	arrestin 3, retinal (X-arrestin)			NM_004312	ARRX	Xq
ASCL1	achaete-scute complex homolog 1 (Drosophila)		L08424		ASH1, HASH1, bHLHa46	12q22-q23
ATN1	atrophin 1	D12S755E, DRPLA	U23851	NM_001940	B37	12p
ATOH1	atonal homolog 1 (Drosophila)		U61148	NM_005172	HATH1, MATH-1, Math1,	4q22
ATOH7	atonal homolog 7 (Drosophila)		AF418922		Math5, bHLHa13	10q22.2
ATOH8	atonal homolog 8 (Drosophila)		AK074681	NM_032827	HATH6, FLJ14708, bHLHa	2p11.2
ATP5C1	ATP synthase, H+ transporting, mitochondrial F1 comple	ATP5CL1, ATP5C	D16561	NM_005174		10p14
AXIN1	axin 1		AF009674		PPP1R49	16p13.3
AXIN2	axin 2		AF078165	NM_004655	MGC126582, DKFZp781B	17q23-q24
B3GALTL	beta 1,3-galactosyltransferase-like		AB101481	NM_194318	B3GTL, B3Glc-T	13q12.3
BARHL2	BarH-like homeobox 2		AJ251753			1p22.2
BCOR	BCL6 corepressor		AF317391	NM_017745	FLJ20285, KIAA1575	Xp11.4
BEST1	bestrophin 1	VMD2	AF057170	NM_004183	BMD, BEST	11q12
BHLHA9	basic helix-loop-helix family, member a9			XM_001125971	bHLHa9, BHLHF42	17p13.3
BHLHE22	basic helix-loop-helix family, member e22	TNRC20, BHLHB5	CAGL85, Beta3, bHLHe22	NM_152414	U80755	8q12.1
BHLHE40	basic helix-loop-helix family, member e40	STRA13, BHLHB2	AB004066	NM_003670	DEC1, bHLHe40	3p26
BMI1	BMI1 polycomb ring finger oncogene	PCGF4	BC011652	NM_005180	RNF51	10p13
BMP2	bone morphogenetic protein 2	BMP2A				20p12
BMP4	bone morphogenetic protein 4	BMP2B	AF035427	NM_001202		14q22-q23
BMP7	bone morphogenetic protein 7				OP-1	20q13
BMPR1A	bone morphogenetic protein receptor, type IA	ACVRLK3	BC028383	NM_004329	ALK3, CD292	10q22.3

BMPR1B	bone morphogenetic protein receptor, type IB		D89675	NM_001203	ALK6, CDw293	4q23-q24	
CASP3	caspase 3, apoptosis-related cysteine peptidase		BC016926	NM_004346	CPP32, CPP32B, Yama, ap	4q34	
CASP6	caspase 6, apoptosis-related cysteine peptidase		U20536	NM_001226	MCH2	4q25	
CASZ1	castor zinc finger 1		AK000328	NM_017766	FLJ20321, ZNF693, castor,	1p36.22	
CDH1	cadherin 1, type 1, E-cadherin (epithelial)	UVO	L08599	NM_004360	uvomorulin, CD324	16q22.1	
CDH2	cadherin 2, type 1, N-cadherin (neuronal)	NCAD	S42303	NM_001792	CDHN, CD325	18q12.1	
CDH20	cadherin 20, type 2		AF217289	NM_031891	CDH7L3, Cdh7	18q21.33	
CDIPT	CDP-diacylglycerol--inositol 3-phosphatidyltransferase		AF014807	NM_006319	PIS1, PIS	16p12.1	
CDS1	CDP-diacylglycerol synthase (phosphatidate cytidylyltransferase) 1		U65887			4q21	
CHD7	chromodomain helicase DNA binding protein 7		AB037837	XM_098762	KIAA1416, FLJ20357, FLJ2	8q12.2	
CHRD	chordin		AF076612	NM_003741		3q27	
CHST15	carbohydrate (N-acetylgalactosamine 4-sulfate 6-O) sulfotransferase 15		AB011170	NM_015892	GALNAC4S-6ST, BRAG, KI/	10q26	
CHST5	carbohydrate (N-acetylglucosamine 6-O) sulfotransferase 5		AF176839	NM_012126	I-GLCNAC-6-ST, FLJ22167	16q23.1	
CNBP	CCHC-type zinc finger, nucleic acid binding protein	DM2, ZNF9	U19765	NM_003418	RNF163, ZCCHC22, CNBP1	3q21	
CPNE5	copine V		H09181	NM_020939	CPN5, COPN5, KIAA1599	6p21.2	
CRABP2	cellular retinoic acid binding protein 2		BC001109	NM_001878	CRABP-II	1q21.3	
CRK	v-crk sarcoma virus CT10 oncogene homolog (avian)		D10656	NM_016823		17p13	
CRMP1	collapsin response mediator protein 1		D78012	NM_001313	DRP-1, DPYSL1	4p16.1	
CRX	cone-rod homeobox	CORD2	AF024711	NM_000554	CRD, LCA7, OTX3	19q13.3	
CRYAA	crystallin, alpha A	CRYA1			HSPB4	21q22.3	
CRYAB	crystallin, alpha B	CRYA2			HSPB5	11q22.3-q23.1	
CRYBB2	crystallin, beta B2	CCA2, CRYB2A, CRYB2		NM_000496		22q11.23	
CRYGA	crystallin, gamma A	CRYG1		NM_014617	CRYG5, CRY-g-A	2q33-q35	
CRYGB	crystallin, gamma B	CRYG2		NM_005210		2q33-q35	
CRYGD	crystallin, gamma D	CRYG4		NM_006891		2q33-q35	
CRYGS	crystallin, gamma S	CRYG8		NM_017541			3
CSMD1	CUB and Sushi multiple domains 1			NM_033225	KIAA1890, PPP1R24	8p23.2	
CSNK1E	casein kinase 1, epsilon			NM_001894	HCKIE, CKIE, CKIepsilon	22q13.1	
CSPG5	chondroitin sulfate proteoglycan 5 (neuroglycan C)		AF059274	NM_006574	NGC	3p21.3	
CTNNBIP1	catenin, beta interacting protein 1		AB021262	NM_020248	ICAT, MGC15093	1pter-p36.31	
CYP1B1	cytochrome P450, family 1, subfamily B, polypeptide 1	GLC3A	U56438	NM_000104	CP1B	2p22.2	
CYP26A1	cytochrome P450, family 26, subfamily A, polypeptide 1		AF005418		P450RAI, CP26, CYP26, P4	10q23-q24	
CYP26B1	cytochrome P450, family 26, subfamily B, polypeptide 1			NM_019885	P450RAI-2	2p12	
CYP26C1	cytochrome P450, family 26, subfamily C, polypeptide 1			NM_183374		10q23.33	
DAAM1	dishevelled associated activator of morphogenesis 1		AB014566	NM_014992	KIAA0666	14q22.3	
DAB1	disabled homolog 1 (Drosophila)		BC067445	NM_021080		1p32-p31	
DACH1	dachshund homolog 1 (Drosophila)	DACH	AJ005670	NM_004392		13q22	
DACH2	dachshund homolog 2 (Drosophila)		AF428101	NM_053281		Xq21.3	
DACT1	dapper, antagonist of beta-catenin, homolog 1 (Xenopus laevis)		AF251079	NM_016651	DAPPER1, THYEX3, HDPR1	14q22.3	
DBX1	developing brain homeobox 1			NM_001029865		11p15.1	
DECR1	2,4-dienoyl CoA reductase 1, mitochondrial	DECR	L26050		SDR18C1	8q21.3	
DECR2	2,4-dienoyl CoA reductase 2, peroxisomal		AJ293009	NM_020664	PDCR, SDR17C1	16p13.3	

DICER1	dicer 1, ribonuclease type III		Dicer, KIAA0928, K12H4.8-LIKE, HERNA		AB028449	14q32.2
DIXDC1	DIX domain containing 1		AB051522		KIAA1735	11q23.1
DKK1	dickkopf 1 homolog (Xenopus laevis)				SK, DKK-1	10q11.2
DKK2	dickkopf 2 homolog (Xenopus laevis)		AB033208			4q25
DKK3	dickkopf 3 homolog (Xenopus laevis)		AF177396	NM_013253	REIC, RIG	11p15.3
DMBX1	diencephalon/mesencephalon homeobox 1	OTX3	AB037699		PAXB	1p34.1
EBF1	early B-cell factor 1	EBF	AF208502	NM_024007	OLF1	5q34
EFHD1	EF-hand domain family, member D1			NM_025202	FLJ13612	2q37.1
EFNB1	ephrin-B1	EPLG2, CFNS	U09303	NM_004429	LERK2, Elk-L	Xq12
EFNB2	ephrin-B2	EPLG5	L38734	NM_004093	LERK5, Htk-L, HTKL, MGC1	13q33
EGR1	early growth response 1		M62829	NM_001964	TIS8, G0S30, NGFI-A, KRO	5q23-q31
EHD1	EH-domain containing 1	PAST1	AF099011	NM_006795	H-PAST, HPAST1, FLJ4262	11q13
EIF2AK3	eukaryotic translation initiation factor 2-alpha kinase 3		AF110146	NM_004836	PEK, PERK	2p12
ELF3	E74-like factor 3 (ets domain transcription factor, epithe	ESX	AF016295	NM_004433	EPR-1, ESE-1, ERT	1q32.2
EMX1	empty spiracles homeobox 1		X68879			2p13.2
EMX2	empty spiracles homeobox 2		AF301598	NM_004098		10q26.11
EN1	engrailed homeobox 1		L12699			2q14.2
EN2	engrailed homeobox 2			NM_001427		7q36.2
ENO2	enolase 2 (gamma, neuronal)		M22349			12p13
EOMES	eomesodermin		BC025363	NM_005442	TBR2	3p24.1
EPHB2	EPH receptor B2	DRT, ERK, EPHT3	AF025304	NM_017449	Hek5, Tyro5	1p36.1-p35
ETV1	ets variant 1			NM_004956	ER81	7p22
ETV6	ets variant 6		BC043399	NM_001987	TEL	12p13
EVX1	even-skipped homeobox 1					7p15.2
EXT1	exostosin 1	LGCR, LGS	S79639		ttv	8q24.11
EYA1	eyes absent homolog 1 (Drosophila)	BOR	AJ000098	NM_000503, NM_172060		8q13.3
FAM208B	family with sequence similarity 208, member B	C10orf18	FLJ20360, bA318E3.2, KIAA2(	NM_017782	BX649177	10p15.1
FAT1	FAT tumor suppressor homolog 1 (Drosophila)	FAT	X87241	NM_005245	CDHF7, CDHR8	4q35.2
FAT4	FAT tumor suppressor homolog 4 (Drosophila)		AY356402	NM_024582	CDHF14, FAT-J, CDHR11	4q28.1
FBXO18	F-box protein, helicase, 18		AK095343	NM_032807	FBH1, FLJ14590, Fbx18	10p15.1
FGF1	fibroblast growth factor 1 (acidic)	FGFA	X59065	NM_000800	AFGF, ECGF, ECGFA, ECGF	5q31.3-q33.2
FGF10	fibroblast growth factor 10			NM_004465		5p13-p12
FGF17	fibroblast growth factor 17		AB009249	NM_003867	FGF-13	8p21.3
FGF18	fibroblast growth factor 18		AB007422	NM_033649, NM_00	FGF-18, ZFGF5	5q34
FGF19	fibroblast growth factor 19		AB018122	NM_005117		11q13.1
FGF2	fibroblast growth factor 2 (basic)	FGFB	J04513	NM_002006		4q26
FGF8	fibroblast growth factor 8 (androgen-induced)		D38752	NM_006119, NM_03	AIGF	10q25-q26
FGF9	fibroblast growth factor 9 (glia-activating factor)		D14838			13q11-q12
FGFBP1	fibroblast growth factor binding protein 1		M60047	NM_005130	HBP17, FGFBP	4p15.32
FGFR1	fibroblast growth factor receptor 1	FLT2, KAL2	M34185		H2, H3, H4, H5, CEK, FLG,	8p12
FGFR2	fibroblast growth factor receptor 2	KGFR, BEK, CFD1, JWS	AK026508	NM_022976, NM_00	CEK3, TK14, TK25, ECT1, K	10q25.3-q26
FGFR3	fibroblast growth factor receptor 3	ACH	M64347	NM_000142	CEK2, JTK4, CD333	4p16.3

FIGN	fidgetin		AK001267	NM_018086		2q24
FKBP8	FK506 binding protein 8, 38kDa		L37033	NM_012181	FKBP38, FKBPr38	19p12
FMR1	fragile X mental retardation 1	POF1, POF	X69962	NM_002024	FMRP, FRAXA, MGC87458	Xq27.3
FOXC1	forkhead box C1	FKHL7, IRID1	AF048693		FREAC3, ARA, IGDA, IHG1	6p25
FOXC2	forkhead box C2 (MFH-1, mesenchyme forkhead 1)	FKHL14	Y08223	NM_005251	MFH-1	16q24.1
FOXD1	forkhead box D1	FKHL8	U59831	NM_004472	FREAC4	5q12-q13
FOXE3	forkhead box E3	FKHL12	AF275722	NM_012186	FREAC8	1p32
FOXF1	forkhead box F1	FKHL5	U13219	NM_001451	FREAC1	16q24
FOXG1	forkhead box G1	FKHL2, FOXG1B, FKHL4, FKH2, FKHL1, FOXG1C, FKHL3, FOXG1A			HFK2, QIN, BF1, HFK1, HFI	14q11-q13
FOXI3	forkhead box I3		BN001221, BN001222	NM_001135649		2p11.2
FOXK1	forkhead box K1		BK004104		IMAGE:5164497	7p22
FOXL1	forkhead box L1	FKHL11	AF315075	NM_005250	FREAC7, FKH6	16q24
FOXM1	forkhead box M1	FKHL16	Y12773	NM_021953	HFH-11, trident, HNF-3, IN	12p13
FOXN2	forkhead box N2	HTLF		NM_002158		2p22-p16
FOXN3	forkhead box N3	C14orf116, CHES1		NM_005197		14q24.3-q31
FOXN4	forkhead box N4		AF425596	XM_062735		12q24.12
FOXO3	forkhead box O3	FKHRL1, FOXO3A	AF032886		AF6q21, FOXO2	6q21
FOXP1	forkhead box P1		AF146696	NM_032682	QRF1, 12CC4, HSPC215, h	3p14.1
FOXP2	forkhead box P2	TNRC10, SPCH1	U80741	NM_014491	CAGH44	7q31
FOXP4	forkhead box P4		AB080747	NM_138457	FLJ40908	6p21.1
FOXS1	forkhead box S1	FKHL18	AF042831	NM_004118	FREAC10	20q11.1-q11.2
FRAS1	Fraser syndrome 1		AB040933		FLJ22031, FLJ14927, KIAA	4q21
FREM1	FRAS1 related extracellular matrix 1	C9orf154	AK058190	NM_144966	FLJ25461, C9orf145, C9or	9p22.3
FREM2	FRAS1 related extracellular matrix protein 2		BX538150	NM_207361	DKFZp686J0811	13q13.3
FRS2	fibroblast growth factor receptor substrate 2		AF036717	NM_006654	SNT-1, FRS2alpha, SNT1, F	12q15
FUZ	fuzzy homolog (Drosophila)		BC016793	NM_025129	FLJ22688, Fy	19q13.33
FZD10	frizzled family receptor 10		AB027464		CD350	12q24.33
FZD2	frizzled family receptor 2		L37882	NM_001466		17q21.1
FZD3	frizzled family receptor 3		AJ272427	NM_145866		8p21
FZD5	frizzled family receptor 5	C2orf31	U43318	NM_003468	HFZ5, DKFZP434E2135	2q33.3
FZD7	frizzled family receptor 7		AB010881	NM_003507	FzE3	2q33
FZD8	frizzled family receptor 8		AB043703	NM_031866		10p11.2
GAS1	growth arrest-specific 1			NM_002048		9q21.3-q22
GATA3	GATA binding protein 3		X55122	NM_001002295	HDR	10p15
GBX2	gastrulation brain homeobox 2		AF118452	NM_001485		2q37.2
GDF11	growth differentiation factor 11		AF100907		BMP-11	12q13.13
GDF2	growth differentiation factor 2		AF156891	NM_016204	BMP-9, BMP9	10q11.22
GDF3	growth differentiation factor 3		AF263538			12p13.1
GDF6	growth differentiation factor 6			NM_001001557	BMP13	8q22.1
GJA1	gap junction protein, alpha 1, 43kDa	ODDD, GJAL	BC026329	NM_000165	CX43, ODD, ODOD, SDTY3	6q22-q23
GJA3	gap junction protein, alpha 3, 46kDa	CZP3	AF075290	NM_021954	CX46	13q12.11
GJA8	gap junction protein, alpha 8, 50kDa	CAE1, CZP1, CAE	U34802	NM_005267	CX50	1q21.1

GJE1	gap junction protein, epsilon 1, 23kDa				CX23	6q24.1
GLI2	GLI family zinc finger 2			NM_005270	THP2, HPE9, THP1	2q14
GLIPR1L1	GLI pathogenesis-related 1 like 1		BC014603	NM_152779	MGC26856	12q21.1
GLIS3	GLIS family zinc finger 3	ZNF515	BC033899	NM_152629	MGC33662	9p24.2
GPC4	glypican 4		AF030186	NM_001448	K-glypican	Xq26.1
GPRC5A	G protein-coupled receptor, family C, group 5, member A	RAI3, GPCR5A	AF095448		RAIG1	12p13-p12.3
GPRC5C	G protein-coupled receptor, family C, group 5, member C		AF207989		RAIG-3	17q25
GRASP	GRP1 (general receptor for phosphoinositides 1)-associated scaffold protein		AC019244			12q13.13
GRIP1	glutamate receptor interacting protein 1		AJ133439			12q13.13
GULP1	GULP, engulfment adaptor PTB domain containing 1		AF191771	NM_016315	CED6, CED-6, GULP	2q32.3-q33
HCCS	holocytochrome c synthase				CCHL	Xp22
HES1	hairy and enhancer of split 1, (Drosophila)	HRY	L19314		FLJ20408, HES-1, Hes1, bH	3q28-q29
HES2	hairy and enhancer of split 2 (Drosophila)		AL031848	NM_019089	bHLHb40	1p36.31
HES5	hairy and enhancer of split 5 (Drosophila)		AL139246		bHLHb38	1p36
HESX1	HESX homeobox 1		AF059734		RPX, ANF	3p14.3
HEY2	hairy/enhancer-of-split related with YRPW motif 2		AJ249545		bHLHb32, HERP1	6q
HHEX	hematopoietically expressed homeobox	PRHX	Z21533		HEX, HOX11L-PEN	10q23.33
HHIP	hedgehog interacting protein		AK024645		HIP, FLJ20992	4q31.21-q31.3
HIC1	hypermethylated in cancer 1			NM_006497	ZBTB29, ZNF901	17p13.3
HMBOX1	homeobox containing 1		AY522342	NM_024567	HNF1LA, PBHNF, FLJ2161(	8p12
HMGA1	high mobility group AT-hook 1	HMGIY	AF176039	NM_145899		6p21
HMGA2	high mobility group AT-hook 2	HMGIC	U28754	NM_003483	BABL, LIPO	12q15
HMX1	H6 family homeobox 1		M99587	NM_018942	H6, NKX5-3	4p16.1
HOXA1	homeobox A1	HOX1F, HOX1				7p15.2
HRAS	v-Ha-ras Harvey rat sarcoma viral oncogene homolog	HRAS1		NM_176795	AJ437024	11p15.5
ID3	inhibitor of DNA binding 3, dominant negative helix-loop-helix protein		X69111	NM_002167	HEIR-1, bHLHb25	1p36.13-p36.12
ID4	inhibitor of DNA binding 4, dominant negative helix-loop-helix protein		U16153	NM_001546	bHLHb27	6p22.3
IFITM1	interferon induced transmembrane protein 1	IFI17	J04164	NM_003641	9-27, CD225	11p15.5
IFT172	intraflagellar transport 172 homolog (Chlamydomonas)		AB033005	NM_015662	SLB, wim, osm-1	2p23.3
IGDCC3	immunoglobulin superfamily, DCC subclass, member 3	PUNC	AF063936	NM_004884	HsT18880	15q22.3-q23
IGSF11	immunoglobulin superfamily, member 11		AB079879		BT-IgSF, MGC35227, Igsf1	3q21.2
INPP5E	inositol polyphosphate-5-phosphatase, 72 kDa	JBTS1	AF187891	NM_019892	PPI5PIV, CORS1	9q34.3
INSM1	insulinoma-associated 1			NM_002196	IA-1	20p11.2
IRX3	iroquois homeobox 3		U90308		IRX-1	16q12.2
ITGA3	integrin, alpha 3 (antigen CD49C, alpha 3 subunit of VLA-	MSK18	M59911	NM_005501	CD49c, VLA3a, VCA-2, GAI	17q21.33
JAG1	jagged 1	AGS, JAGL1	U61276	NM_000214	AHD, AWS, HJ1, CD339	20p12.1-p11.23
JMJD6	jumonji domain containing 6	PTDSR	AB011157	NM_015167	PTDSR1, KIAA0585	17q25
KIAA1586	KIAA1586		AB046806	XM_166451		6p12.1
KIF21A	kinesin family member 21A	FEOM1	AK000059	NM_017641	FLJ20052	12q12
KLF6	Kruppel-like factor 6	BCD1, ST12, COPEB	U51869		CPBP, GBF, Zf9, PAC1	10p15
LEF1	lymphoid enhancer-binding factor 1				TCF1ALPHA, TCF10, TCF7L	4q23-q25
LEFTY1	left-right determination factor 1	LEFTB	AF081507	NM_020997	LEFTYB	1q42.1

LEFTY2	left-right determination factor 2	TGFB4, EBAF	U81523	NM_003240	LEFTA, LEFTYA	1q42.1
LEPREL1	leprecan-like 1			NM_018192	FLJ10718, MLAT4, P3H2	3q29
LGR5	leucine-rich repeat containing G protein-coupled recept	GPR67, GPR49	AF062006	NM_003667	HG38, FEX	12q22-q23
LHX2	LIM homeobox 2		U11701		LH-2, hLhx2	9q33.3
LIM2	lens intrinsic membrane protein 2, 19kDa			NM_030657	MP19, MP17	19q13.4
LIX1	Lix1 homolog (chicken)	C5orf11		NM_153234		5q15
LMO2	LIM domain only 2 (rhombotin-like 1)	RBTNL1	X61118	NM_005574	TTG2, RHOM2, RBTN2	11p13
LRP5	low density lipoprotein receptor-related protein 5	LRP7, OPPG, EVR1	AF064548	NM_002335	LR3, BMND1, HBM, OPS	11q13.4
LRP6	low density lipoprotein receptor-related protein 6		AF074264			12p13.2
LRRTM4	leucine rich repeat transmembrane neuronal 4		AK122612	NM_024993	FLJ12568	2p12
MAB21L1	mab-21-like 1 (C. elegans)		BC028170	NM_005584	CAGR1	13q13.3
MAB21L2	mab-21-like 2 (C. elegans)		AF155219	NM_006439		4q31
MACROD2	MACRO domain containing 2	C20orf133	BC101218	NM_080676	dJ631M13.5	20p12.1
MAF	v-maf musculoaponeurotic fibrosarcoma oncogene homolog (avian)				c-MAF	16q22-q23
MAP3K1	mitogen-activated protein kinase kinase kinase 1, E3 ubi	MEKK1	U29671, AF042838	XM_042066	MEKK, MAPKKK1	5q11.2
MAPK1	mitogen-activated protein kinase 1	PRKM2, PRKM1	ERK, ERK2, p41mapk, MAPK2		M84489	22q11.2
MARCKSL1	MARCKS-like 1	MLP	AF031640	NM_023009	F52, MacMARCKS, MLP1	1p35.1
MEGF9	multiple EGF-like-domains 9	EGFL5	AB011542	NM_001080497		9q32-q33.3
MEIS1	Meis homeobox 1			NM_002398		2p14
MEIS2	Meis homeobox 2		AF017418	NM_170677	MRG1, HsT18361	15q14
MEIS3	Meis homeobox 3		BC025404	XM_085929	MRG2, DKFZp547H236	19q13.32
MFRP	membrane frizzled-related protein		AB055505	NM_031433	FLJ30570, rd6, NNO2, C1C	11q23.1
MIP	major intrinsic protein of lens fiber			NM_012064	MP26, LIM1, AQP0	12q13
MITF	microphthalmia-associated transcription factor	WS2A, WS2		NM_198159	MI, bHLHe32	3p14.1-p12.3
MMP9	matrix metallopeptidase 9 (gelatinase B, 92kDa gelatina	CLG4B				20q12-q13
MSI1	musashi homolog 1 (Drosophila)		AB012851	NM_002442		12q24
MSX2	msh homeobox 2	PFM1	D26145		CRS2, FPP, HOX8, MSH, PF	5q35.2
MVP	major vault protein		X79882	NM_005115	LRP, VAULT1	16p11.2
MYO1C	myosin IC		X98507		myr2	17p13.3
NAT2	N-acetyltransferase 2 (arylamine N-acetyltransferase)	AAC2	D90042	NM_000015		8p22
NDST1	N-deacetylase/N-sulfotransferase (heparan glucosaminy	HSST	U18918	NM_001543	NST1	5q33.1
NDST2	N-deacetylase/N-sulfotransferase (heparan glucosaminyl)	2	U36601	NM_003635	NST2, HSST2	10q22
NDST3	N-deacetylase/N-sulfotransferase (heparan glucosaminyl)	3	AF074924	NM_004784	HSST3	4q26
NET1	neuroepithelial cell transforming 1		AJ010046	NM_005863	ARHGEF8, NET1A	10p15
NEUROD1	neuronal differentiation 1	NEUROD	U50823	NM_002500	BETA2, BHF-1, NeuroD, bH	2q32
NEUROG2	neurogenin 2		AF303002	NM_024019	Atoh4, Math4A, ngn-2, bH	4q25
NGFR	nerve growth factor receptor		M14764		TNFRSF16, CD271, p75NT	17q21-q22
NKX2-8	NK2 homeobox 8	NKX2H			NKX2.8, Nkx2-9	14q13.3
NLK	nemo-like kinase		AF197898	NM_016231		17q11.2
NNAT	neuronatin			NM_005386	Peg5	20q11.2-q12
NOG	noggin	SYNS1, SYM1	U31202	NM_005450		17q22
NOTCH1	notch 1	TAN1	AF308602	NM_017617		9q34.3

NOTCH4	notch 4	INT3				6p21.3
NPM1	nucleophosmin (nucleolar phosphoprotein B23, numatrin)		M26697	NM_002520	B23, NPM	5q35.1
NPTX2	neuronal pentraxin II			NM_002523		7q21.3-q22.1
NR0B1	nuclear receptor subfamily 0, group B, member 1	AHC, DSS	S74720	NM_000475	DAX1, AHCH	Xp21.3
NR2E1	nuclear receptor subfamily 2, group E, member 1	TLX	Y13276		TLL, XTLL	6q21
NR2E3	nuclear receptor subfamily 2, group E, member 3				PNR, rd7, RP37	15q24
NR2F1	nuclear receptor subfamily 2, group F, member 1	ERBAL3, TFCOUP1	BC004154	NM_005654	EAR-3, COUP-TFI, TCFCOU	5q14
NR2F2	nuclear receptor subfamily 2, group F, member 2	ARP1, TFCOUP2	M64497		COUP-TFII, COUPTFB, SVP	15q26
NR4A1	nuclear receptor subfamily 4, group A, member 1	HMR, GFRP1	L13740		TR3, N10, NAK-1, NGFIB, I	12q13
NR5A2	nuclear receptor subfamily 5, group A, member 2	FTF	U93553		FTZ-F1beta, hB1F, LRH-1,	1q32.11
NRP2	neuropilin 2		AF016098		VEGF165R2	2q33.3
NRXN1	neurexin 1		AB011150		KIAA0578, Hs.22998	2p16.3
NRXN2	neurexin 2			NM_015080		11q13
NTN1	netrin 1		U75586		NTN1L	17p13-p12
NUDT11	nudix (nucleoside diphosphate linked moiety X)-type motif 11		AK001490		DIPP3b, FLJ10628, hDIPP3	Xp11.22-p11.1
OFCC1	orofacial cleft 1 candidate 1		AF548113	NM_153003	MRDS1	6p24.3
OLFM3	olfactomedin 3		AF397392		NOE3	1p22
OLFML1	olfactomedin-like 1		AY358591	NM_198474	UNQ564	11p15
OLFML2B	olfactomedin-like 2B		BX648975	NM_015441	DKFZP586L151	1q23.1
OLIG1	oligodendrocyte transcription factor 1		AP000109	NM_138983	BHLHB6, bHLHe21	21q22.11
OLIG2	oligodendrocyte lineage transcription factor 2	PRKCBP2, BHLHB1	U48250	NM_005806	RACK17, OLIGO2, bHLHe1	21q22.11
OPTN	optineurin	GLC1E	AF420371	NM_021980	FIP2, HYPL, TFIIIA-INTP, N	10p14
OTX1	orthodenticle homeobox 1					2p15
OTX2	orthodenticle homeobox 2		AF298117	NM_021728.		14q22.3
PAX2	paired box 2					10q24.31
PAX3	paired box 3	WS1			HUP2	2q36.1
PAX6	paired box 6	AN2	AY707088	NM_001604	D11S812E, AN, WAGR	11p13
PAX8	paired box 8		X69699			2q13
PBX4	pre-B-cell leukemia homeobox 4		AJ300182			19p12
PEA15	phosphoprotein enriched in astrocytes 15		Y13736	NM_003768	HMAT1, MAT1, PED, PEA-	1q21.1
PFKP	phosphofructokinase, platelet		AK092597	NM_002627	PFK-C, PFKF	10p15.3-p15.2
PFN2	profilin 2		L10678	NM_002628		3q25.1
PGAP1	post-GPI attachment to proteins 1			NM_024989	FLJ12377, Bst1	2q33.1
PIP	prolactin-induced protein			NM_002652	GCDFP-15, GCDFP15, GPIF	7q32-qter
PITPNA	phosphatidylinositol transfer protein, alpha	PITPN	M73704		VIB1A	17p13.3
PITRM1	pitrilysin metallopeptidase 1		AB029027		MP1, KIAA1104, hMP1, Pr	10p15.2
PITX2	paired-like homeodomain 2	IRID2, IHG2, RIEG, RIEG1,	U69961		IGDS, RS, Brx1, Otlx2, ARP	4q25
PITX3	paired-like homeodomain 3					10q24.32
PKNOX1	PBX/knotted 1 homeobox 1		PREP1			21q22.3
PKNOX2	PBX/knotted 1 homeobox 2		AK023136			11q24.2
PLCE1	phospholipase C, epsilon 1			NM_016341	KIAA1516, PLCE, NPHS3	10q23
PLXDC1	plexin domain containing 1		AF279144	NM_020405	TEM3, TEM7	17q21.1

PLXNC1	plexin C1		AF030339		VESPR, CD232	12q23
PMEL	premelanosome protein	SIL, SILV	AK092881	NM_006928	D12S53E, SI, Pmel17, gp1(	12q13-q14
PORCN	porcupine homolog (Drosophila)		AF317058	NM_022825	MG61, PORC, PPN, por	Xp11.23
POU2F1	POU class 2 homeobox 1	OTF1	BC001664	NM_002697	37165	1q24.2
POU5F1	POU class 5 homeobox 1	OTF3	Z11898	NM_002701	OCT3, Oct4, MGC22487	6p21.33
PPP4C	protein phosphatase 4, catalytic subunit			NM_002720	PP4, PPX	16p11.2
PRMT8	protein arginine methyltransferase 8	HRMT1L3, HRMT1L4	AF263539	NM_019854		12p13.3
PROM1	prominin 1	PROML1, MCDR2, STGD4	AF027208	NM_006017	AC133, CD133, RP41	4p15
PROX1	prospero homeobox 1		U44060	NM_002763		1q41
PRPF8	PRP8 pre-mRNA processing factor 8 homolog (S. cerevisi	RP13	AB007510		PRPC8, Prp8	17p13.3
PRR15	proline rich 15		BC029131	NM_175887		7p15.1
PRSS56	protease, serine, 56			NM_001195129		2q37.1
PTCH1	patched 1	NBCCS, PTCH	AI494442	NM_000264	BCNS	9q22.1-q31
PTCH2	patched 2		AF091501	NM_003738		1p34.1
PTK7	PTK7 protein tyrosine kinase 7		AF447176		CCK4	6p21.1-p12.2
PTPN11	protein tyrosine phosphatase, non-receptor type 11	NS1	D13540		BPTP3, SH-PTP2, SHP-2, P	12q24.1
PYGO2	pygopus homolog 2 (Drosophila)		BC006132	NM_138300		1q22
QPRT	quinolinate phosphoribosyltransferase		D78177	NM_014298	QPRTase	16p11.2
RAB23	RAB23, member RAS oncogene family		AB034244			6p12.1
RAB3GAP1	RAB3 GTPase activating protein subunit 1 (catalytic)		D31886	NM_012233	RAB3GAP, KIAA0066, RAB	2q21.3
RAB3GAP2	RAB3 GTPase activating protein subunit 2 (non-catalytic)		AB020646	NM_012414	RAB3-GAP150, KIAA0839,	1p36.13-p35.3
RAC1	ras-related C3 botulinum toxin substrate 1 (rho family, small GTP binding protein F		AJ132695	NM_018890	TC-25, p21-Rac1, Rac-1	7p22
RARA	retinoic acid receptor, alpha		X06538		RAR, NR1B1	17q21.1
RARB	retinoic acid receptor, beta		Y00291	NM_000965, NM_01	HAP, NR1B2, RRB2	3p24
RARG	retinoic acid receptor, gamma		M57707	NM_000966	RARC, NR1B3	12q13
RAX	retina and anterior neural fold homeobox		AF115392		RX	18q21.31
RBM17	RNA binding motif protein 17		AF083384	NM_032905	SPF45, MGC14439	10p15.1
RBP1	retinol binding protein 1, cellular			NM_002899	CRABP-I, CRBP1, CRBP, RB	3q21-q23
RELA	v-rel reticuloendotheliosis viral oncogene homolog A (av	NFKB3	Z22951	NM_021975	p65	11q13
RGS16	regulator of G-protein signaling 16		U70426	NM_002928	A28-RGS14, RGS-r	1q25-q31
RGS2	regulator of G-protein signaling 2, 24kDa	G0S8	L13463	NM_002923		1q31
RHOA	ras homolog family member A	ARH12, ARHA	BC001360	NM_001664	RhoA, Rho12, RHOH12	3p21.3
RND2	Rho family GTPase 2	ARHN	X95456	NM_005440	Rho7, RhoN	17q21
RPGRIP1	retinitis pigmentosa GTPase regulator interacting protei	RPGRIP	AF227257	NM_020366	RGI1, LCA6	14q11
RPSA	ribosomal protein SA	LAMR1	S37431	NM_002295	LRP, 37LRP, p40, SA	3p21.3
RRH	retinal pigment epithelium-derived rhodopsin homolog		AF012270	NM_006583	peropsin	4q25
RTN4RL1	reticulon 4 receptor-like 1		AF532859	NM_178568	NGRH2, NgR3, DKFZp547J	17p13.3
SALL3	sal-like 3 (Drosophila)		AJ007421	NM_171999	ZNF796	18q23
SCUBE1	signal peptide, CUB domain, EGF-like 1			NM_173050		22q13
SEMA3E	sema domain, immunoglobulin domain (Ig), short basic c	SEMAH	AB002329	NM_012431	M-SemaK, KIAA0331, coll-	7q21.11
SEMA4C	sema domain, immunoglobulin domain (Ig), transmembr	SEMAI	AB051526	NM_017789	Semacl1, Semaf	2q11.2
SEMA6A	sema domain, transmembrane domain (TM), and cytopl	SEMAQ	AB037789	NM_020796	KIAA1368, SEMA6A1, SEM	5q23

SEMA6D	sema domain, transmembrane domain (TM), and cytoplasmic domain, (semaphor		AF389430	NM_024966	KIAA1479, FLJ11598	15q21.1
SERPINF1	serpin peptidase inhibitor, clade F (alpha-2 antiplasmin,	PEDF	M76979	NM_002615	EPC-1, PIG35	17p13.3
SERTAD3	SERTA domain containing 3		AF192529	NM_013368	RBT1	19q13.2
SEZ6L2	seizure related 6 homolog (mouse)-like 2		AY358404	NM_012410	PSK-1, FLJ90517	16p12.1
SFRP1	secreted frizzled-related protein 1		AF017987	NM_003012	SARP2, FRP, FRP-1	8p11.21
SFRP2	secreted frizzled-related protein 2		AF017986		SARP1, SDF-5, FRP-2	4q31.3
SFRP4	secreted frizzled-related protein 4		AF026692	NM_003014	frpHE, FRP-4, FRPHE	7p14.1
SGMS1	sphingomyelin synthase 1	TMEM23	AY280959	NM_147156	MOB, MGC17342, SMS1	10q11.2
SHH	sonic hedgehog	HPE3, HLP3		NM_000193	HHG1, SMMCI, TPT, TPTP!	7q36
SIX1	SIX homeobox 1	DFNA23	X91868			14q23.1
SIX3	SIX homeobox 3	HPE2	AF092047	NM_005413		2p21
SIX6	SIX homeobox 6	OPTX2	AF141651		Six9	14q23.1
SKI	v-ski sarcoma viral oncogene homolog (avian)		X15218	NM_003036		1p36.33
SMAD4	SMAD family member 4	MADH4	U44378	NM_005359	DPC4	18q21.1
SMO	smoothened, frizzled family receptor	SMOH	U84401	NM_005631	FZD11	7q32.1
SMOC1	SPARC related modular calcium binding 1		AJ249900			14q24.1
SOCS2	suppressor of cytokine signaling 2		AF037989		STATI2, SSI2, SOCS-2, SSI-:	12q
SOX1	SRY (sex determining region Y)-box 1			NM_005986		13q34
SOX13	SRY (sex determining region Y)-box 13			NM_005686	Sox-13, ICA12, MGC11721	1q32
SOX14	SRY (sex determining region Y)-box 14		AJ006230	NM_004189	SOX28	3q22-q23
SOX2	SRY (sex determining region Y)-box 2		BC013923	NM_003106		3q26.3-q27
SOX21	SRY (sex determining region Y)-box 21		AF107044	NM_007084	SOX25	13q31-q32
SOX3	SRY (sex determining region Y)-box 3	PHP				Xq27
SOX4	SRY (sex determining region Y)-box 4		AF070669	NM_003107		6p22.3
SOX8	SRY (sex determining region Y)-box 8		AF164104			16p13.3
SOX9	SRY (sex determining region Y)-box 9	CMD1, CMPD1	S74506	NM_000346	SRA1	17q23
SP1	Sp1 transcription factor		J03133			12q13.1
SP3	Sp3 transcription factor		M97191	NM_003111	SPR-2	2q31
SPINK1	serine peptidase inhibitor, Kazal type 1			NM_003122	Spink3, PCTT, PSTI, TATI	5q32
SPOCK3	sparc/osteonectin, cwcv and kazal-like domains proteoglycan (testican) 3		AJ001454		testican-3	4q32.3
SRGAP3	SLIT-ROBO Rho GTPase activating protein 3	SRGAP2	AB007871		KIAA0411, MEGAP, WRP,	3p25.3
ST6GAL2	ST6 beta-galactosamide alpha-2,6-sialyltranferase 2	SIAT2	AB059555	NM_032528	KIAA1877, St6gal2, St6Gal	2q11-q12
STMN2	stathmin-like 2	SCGN10		NM_007029	SCG10	8q21.13
STMN3	stathmin-like 3		AF069709	NM_015894	SCLIP	20q13.3
STRA6	stimulated by retinoic acid gene 6 homolog (mouse)		AF352728		FLJ12541	15q24.1
STX3	syntaxin 3	STX3A	AJ002076	NM_004177		11q12.1
SULF1	sulfatase 1		AB029000	NM_015170	KIAA1077, SULF-1	8q13.1
SULF2	sulfatase 2		AY101176	NM_018837	KIAA1247, HSULF-2, SULF-	20q13.12-q13.13
SUPT5H	suppressor of Ty 5 homolog (S. cerevisiae)		U56402	NM_003169	SPT5H, SPT5, FLJ34157	19q13
SV2C	synaptic vesicle glycoprotein 2C		AB028977			5q13
SYT9	synaptotagmin IX		AK055003	NM_175733		11p15.4
TBX2	T-box 2		AB209378	NM_005994		17q23.2

TBX20	T-box 20		AJ237589	NM_020417		7p14.3
TBX3	T-box 3	UMS	BC025258	NM_016569, NM_00	TBX3-ISO, XHL	12q24.1
TBX5	T-box 5	HOS	U89353	NM_080717		12q24.1
TCF12	transcription factor 12		HEB, HTF4, HsT17266, bHLHb	NM_003205	BC050556	15q21
TCF3	transcription factor 3 (E2A immunoglobulin enhancer binding factors E12/E47)		M65214	NM_003200	E2A, ITF1, MGC129647, M	19p13.3
TFAP2A	transcription factor AP-2 alpha (activating enhancer binc	TFAP2, AP2TF	X52611	NM_003220	AP-2	6pter-p22.3
TFAP2C	transcription factor AP-2 gamma (activating enhancer binding protein 2 gamma)			NM_003222	AP2-GAMMA, ERF1, TFAP	20q13.2
TFE3	transcription factor binding to IGHM enhancer 3		X96717	NM_006521	TFEA, bHLHe33	Xp11.22
THBS1	thrombospondin 1			NM_003246	TSP1, THBS, TSP, THBS-1,	15q15
TIMP3	TIMP metallopeptidase inhibitor 3	SFD		NM_000362		22q12.3
TLE4	transducin-like enhancer of split 4 (E(sp1) homolog, Drosophila)		E(spI), ESG, GRG4	XM_212237	M99439	9q21.32
TMX3	thioredoxin-related transmembrane protein 3	TXNDC10	BX647846	NM_019022	FLJ20793, KIAA1830, PDIA	18q22
TNFRSF19	tumor necrosis factor receptor superfamily, member 19		AB040434	NM_018647	TAJ-alpha, TROY, TAJ, TRA	13q12.11-q12.3
TRPM1	transient receptor potential cation channel, subfamily M	MLSN1	AF071787	NM_002420	LTRPC1	15q13.3
TSHZ1	teashirt zinc finger homeobox 1	SDCCAG33	AF039698	NM_005786	NY-CO-33, TSH1	18q22.3
TSHZ2	teashirt zinc finger homeobox 2	C20orf17, ZNF218	AF230201	NM_173485	ZABC2, OVC10-2, TSH2	20q13.2
TSHZ3	teashirt zinc finger homeobox 3	ZNF537	AL136805	NM_020856	KIAA1474, TSH3	19q13.11
TWSG1	twisted gastrulation homolog 1 (Drosophila)		AA486291		TSG	18p11.3
UNC5A	unc-5 homolog A (C. elegans)		AB075856	XM_030300	KIAA1976, UNC5H1	5q35.3
UNC5B	unc-5 homolog B (C. elegans)		AB096256	NM_170744	UNC5H2, p53RDL1	10q22.2
VAX1	ventral anterior homeobox 1		AK127095	XM_301242		10q26.11
VAX2	ventral anterior homeobox 2		Y17791		DRES93	2p13.3
VSX1	visual system homeobox 1	PPCD	AF176797		PPD	20p11.21
VSX2	visual system homeobox 2	HOX10, CHX10	AC005519	NM_182894	RET1	14q24.3
WNT1	wingless-type MMTV integration site family, member 1	INT1	X03072			12q13
WNT2B	wingless-type MMTV integration site family, member 2B	WNT13	AB045116	NM_004185	XWNT2	1p13
WNT7A	wingless-type MMTV integration site family, member 7A		D83175	NM_004625		3p25
WNT7B	wingless-type MMTV integration site family, member 7B		AF416743	NM_058238		22q13
WNT8B	wingless-type MMTV integration site family, member 8B		X91940	NM_003393		10q24
YWHAE	tyrosine 3-monooxygenase/tryptophan 5-monooxygenase activation protein, epsi		U54778	NM_006761	FLJ45465	17p13.3
ZFP42	zinc finger protein 42 homolog (mouse)		AK056719	NM_174900	REX1, ZNF754	4q35.2
ZIC1	Zic family member 1		D76435	NM_003412	ZIC, ZNF201	3q24
ZIC5	Zic family member 5		AF378304	NM_033132		13q32.2

Supplementary Table 2: Phenotypes of ODA patients

Patient	Gender	Age (years)	Ethnicity	Right Eye	Left Eye	Other	Family History		Consanguinity
							Maternal	Paternal	
P1	M	10	E	Ano	Ano	Microcephaly PMD	-	-	-
P2	M	5	E	Cat	Micro	-	-	-	-
P3	M	9	N-Af	-	Micro Scl	Hypospadias Ectopic Kidney	-	-	-
P4	M	3	E	Micro MicroC Cat Col	Peters	PMD	-	-	+
P5	F	43	S-Am	Micro Cat	Micr Scl	-	Unk	Unk	Unk
P6	F	6	E	Micro Col Cyst	Micro Col Cyst	Short Stature Left duplicated pyelocaliceal system PMD	-	-	-
P7	M	3	N-Af	Micro	Micro	IUGR Sex Amb Arthrogryposis PMD	-	-	-
P8	F	5	E	Micro Col	Micro	IUGR Partial CCA ASD PMD	-	-	-
P9	M	6	E	Micro Scl	Ano	-	-	-	-
P10	F	6	E	Micro	Micro Scl	-	-	-	-
P11	M	5	E	Micro Col Cyst	Micro Col	Pyriform sinus stenosis SMMCI GH deficiency	-	-	-

P12	M	37	E	Micro Col	Micro Col	-	-	-	-
P13	F	9	E	Micro	-	PMD	-	-	-
P14	M	6	E	Micro Col	Micro Col	-	Increased papillary excavation	-	-
P15	M	4	N-Af	Micro Col	Micro Col	CCH ASD	-	-	-
P16	F	5	E	Peters	-	-	-	-	-
P17	F	21	E	A-R	A-R	-	-	-	-
P18	F	14	E	MG	Morning Glory	-	-	-	-
P19	F	5	E	Aniridia	Aniridia	CH PMD	-	-	-
P20	F	5	E	Peters A-R	Peters A-R	-	Unilateral Peters Embryotoxon	-	-
P21	M	3	E	Micro Scl	Micro Scl	PMD	-	Embryotoxon	-
P22	F	10	As	Peters	Peters	PMD	-	-	-
C1*	F	3	N-Af	Micro Cat Col	Micro Cat Col	-	-	-	-
C2*	M	42	E	Ano	Ano	Fallot tetralogy	-	-	-
CC10**	M	12	E	Peters	Peters	-	-	-	+
CC44**	F	19	Af-Am	Micro Cat Partial aniridia	Micro Cat Partial aniridia	-	Micro Cat Partial aniridia	-	-

Ano: anophthalmia; Micro: microphthalmia; MicroC: microcornea; Cat: cataract; Scl: sclerocornea; Col: coloboma; Col Cyst: colobomatous cysts; A-R: Axenfeld-Rieger; MG: Morning Glory

PMD: Psychomotor Delay; IUGR: intra uterine growth retardation; Sex Amb: sexual ambiguity; CCA: corpus callosum agenesis; CCH: corpus callosum hypoplasia; ASD: atrial septal defect; SMMCI: Solitary median maxillary central incisor, CH: cerebellar hypoplasia; Unk: unknown

E: European; N-Af: North African; S-Am: South American; As: Asian; Af-Am: African-American

Patients carrying a *PTCH1* mutation are underlined

*Positive controls with known mutations in *VSX2* (C1) or *STRA6* (C2)

** Replication cohort patients 10 (CC10) and 44 (CC44)

Supplementary Table 3: Variant prioritization

Identified variants	Average over 24 samples	Standard Deviation
Total variants	2566	125
High confidence variant calls	2482	126
After exclusion of known variants (dbSNPv132 + HapMap + in-house)	236	28
After exclusion of non-genic - intronic variants	10	3
After exclusion of synonymous variants	6	2
Predicted damaging	3	1
Validated by Sanger Sequencing	2.5 *(range 0-5)*	1

A custom-made SureSelect oligonucleotide probe library was designed to capture the exons of 407 candidate genes and 880 kb of potential regulatory sequences. The mean coverage was 325X with 96.9% of the targeted sequences over 10X and 93.4 over 25X. Frameshift, nonsense and splicing variants were considered as damaging. Missense variants were classified as damaging or not based on Polyphen-2 software results.

Supplementary Table 4: Final prioritized variants in patients with ODA

Patient	Gene	Transcript	cDNA change	Protein change	Status	Polyphen-2	SIFT	EVS	Inheritance (phenotype)
P1	*PAX6*	ENST00000379115	c.192C>A	p.Asn64Lys	Ht	D (1.000)	D (0)	Abs	*De novo*
P3	*FAT4*	ENST00000394329	c.7960A>C	p.Lys2654Gln	Ht	P (0.477)	T(0.76)	Abs	Pat (Asy)
	MYO1C	ENST00000359786	c.391C>T	p.Arg131Cys	Ht	D (0.959)	T(0.17)	3/13004	Mat (Asy)
	SALL3	ENST00000537592	c.2254G>A	p.Val752Met	Ht	D (0.9555)	-	Abs	Mat (Asy)
	SOX14	ENST00000306087	c.722delA	p.*241Tyrext*?	Ht	-	-	Abs	Mat (Asy)
	TSHZ2	ENST00000371497	c.247T>G	p.Ser83Ala	Ht	D (0.946)	D(0)	4/13006	Pat (Asy)
P4	*FAT1*	ENST00000441802	c.4336G>A	p.Val1446Ile	Ht	D(0.998)	T(0.36)	8/11838	Pat (Asy)
	FAT4	ENST00000394329	c.131A>C	p.Glu44Ala	Ht	P (0.496)	T(0.6)	3/12132	Mat,Pat (Asy)
	DAB1	ENST00000371236	c.1075G>A	p.Gly359Arg	Ht	D (0.987)	T(0.07)	Abs	Pat (Asy)
P5	***PTCH1***	ENST00000375274	c.4delG	p.Glu2Asnfs*9	Ht	-	-	Abs	Unk
	PLXNC1	ENST00000258526	c.3649T>C	p.Cys1217ARg	Ht	D(0.998)	D(0.01)	9/12997	
	IFT172	ENST00000260570	c.3880C>T	p.Arg1294Cys	Ht	D(1.000)	D(0.01	1/13005	
	WNT7A	ENST00000285018	c.232C>T	p.Arg78Cys	Ht	D(1.000)	D(0)	Abs	
P6	*STRA6*	ENST00000395105	c.1735C>G	p.Pro579Ala	Hemi	D (0.999)	T(0.11)	Abs	Mat (Asy)
P7	*CDH1*	ENST00000261769	c.670C>T	p.Arg224Cys	Ht	P (0.837)	D(0)	2/12996	Unk
	CYP26C1	ENST00000285949	c.1243C>G	p.His415Asp	Ht	D (1.000)	D(0)	Abs	
	IFT172	ENST00000260570	c.5133delC	p.Asn1711Asnfs*20	Ht	-	-	Abs	
	VAX2	ENST00000234392	c.398C>T	p.Thr133Ile	Ht	P (0.933)	T(0.33)	Abs	
P8	***PTCH1***	ENST00000331920	c.3191C>T	p.Thr1064Met	Ht	D(1.000)	T(0.1)	2/13006	Pat (Asy)
	SEZ6L2	ENST00000308713	c.323C>T	p.Thr108Ile	Ht	P(0.937)	T(0.22)	Abs	Pat (Asy)
P9	*RPGRIP1*	ENST00000400017	c.2424C>G	p.Cys808Trp	Ht	D (0.999)	D(0)	Abs	Pat (Asy)
P10	*PFKP*	ENST00000381125	c.738_739insG	p.Trp248Alafs*19	Ht	-	-	Abs	Mat (Asy)
	NOTCH4	ENST00000375023	c.2443T>G	p.Cys815Gly	Ht	D(1.000)	D(0)	22/8350	Mat (Asy)
P11	*NR5A2*	ENST00000367362	c.884C>T	p.Thr295Met	Ht	P(0.904)	D(0.02)	11/12995	Unk
	RPGRIP1	ENST00000400017	c.808A>G	p.Ile270Val	Ht	P(0.994)	T(0.11)	6/11846	
P12	*GRASP*	ENST00000293662	c.1084G>A	p.Gly362Ser	Ht	D (0.987)	T(0.43)	56/11118	Mat (Asy)
	NOTCH1	ENST00000277541	c.2434G>A	p.Gly812Arg	Ht	D (1.000)	D(0.05)	7/12560	Pat (Asy)
P13	*MITF*	ENST00000352241	c.738G>A	p.Asp246Asn	Ht	P(0.858)	T(0.45)	Abs	Mat (Asy)
	EFHD1	ENST00000264059	c.155C>T	p.Thr82Met	Ht	D(0.945)	T(0.06)	1/12893	Mat (Asy)

P14	*NOTCH1*	ENST00000277541	c.67G>T	p.Arg23Leu	Ht	P(0.689)	T(0.38)	Abs	Mat (Sy)
	ARR3	ENST00000307959	c.1052C>T	p.Pro351Leu	Hemi	D(0.945)	T(1)	Abs	Mat (Sy)
P15	*FGFR3*	ENST00000260795	c.1879G>A	p.Glu627Lys	Ht	D(0.990)	D(0)	Abs	Pat (Asy)
	PTCH1	ENST00000331920	c.3241G>A	p.Val1081Met	Ht	D(0.991)	D(0.02)	1/13006	
	SULF1	ENST00000458141	c.529G>A	p.Gly177Ser	Ht	D(1.000)	D(0)	Abs	
	CHRD	ENST00000204604	c.1370C>G	Thr457Ser	Ht	D(0.999)	T(0.1)	6/13000	
P17	*CHST5*	ENST00000336257	c.737T>C	p.Ile246Thr	Ht	D (0.998)	T(0.06)	Abs	Mat (Asy)
	DACT1	ENST00000335867	c.2010G>C	p.Lys670Asn	Ht	P (0.868)	T(0.32)	Abs	Mat (Asy)
	FRAS1	ENST00000264895	c.3700G>A	p. Ala1234Thr	Ht	P(0.611)	T(0.29)	2/12336	Pat (Asy)
P18	*DICER1*	ENST00000343455	c.2191G>A	p.Gln731Lys	Ht	P(0.950)	T(0.52)	Abs	Unk
	MAP3K1	ENST00000399503	c.1420A>G	p.Ile474Val	Ht	P(0.540)	T(0.19)	Abs	
	GLI2	ENST00000361492	c.1859C>T	p.Thr620Met	Ht	P(0.832)	T(0.09)	11/12995	
P19	*KIF21A*	ENST00000395670	c.2287G>A	p.Val763Met	Ht	D(0.998)	D(0.01)	Abs	Pat (Asy)
	GLIS3	ENST00000381971	c.2710G>C	p.Gly904Arg	Ht	D(1.000)	D(0)	6/13000	Pat (Asy)
P20	***PTCH1***	ENST00000331920	c.3947A>G	p.Tyr1316Cys	Ht	D(0.983)	T(0.07)	9/12499	Mat (Sy)
	FREM1	ENST00000380880	c.1493G>A	Arg498Gln	Ht	D(1.000)	T(0.43)	9/12453	Mat (Sy)
P21	*ADAM17*	ENST00000310823	c.847C>T	p.Arg283Cys	Ht	D (1.000)	T(0.08)	Abs	Pat (sy)
	SFRP2	ENST00000274063	c.628A>G	p.Asn209Gly	Ht	P (0.918)	T(0.24)	Abs	Pat (sy)
	TSHZ2	ENST00000371497	c.1289A>T	p.Gln430Leu	Ht	P (0.958)	D(0.01)	Abs	Mat (Asy)
P22	*PITRM1*	ENST00000380989	c.2423A>G	p.Lys808Arg	Ht	P (0.708)	T(0.48)	Abs	Pat (Asy)
	PRPF8	ENST00000304992	c.3527C>T	p.Ser1176Phe	Ht	D (0.999)	D(0)	Abs	Mat (Asy)
	RARG	ENST00000425354	c.245C>T	p.Pro82Leu	Ht	D (0.999)	D(0.02)	Abs	Pat (Asy)
	EPHB2	ENST00000400191	c.787G>A	p.Val263Ile	Ht	P(0.882)	T(0.24)	2/13004	Pat (Asy)
C1*	*FRAS1*	ENST00000264895	c.9364C>T	p.Arg3122Trp	Ht	D (1.000)	D(0)	Abs	Pat (Asy)
	VSX2	ENST00000261980	c.71_72insG	p.Ala25Argfs*101	Ht	-	-	Abs	Pat (Asy)
	VSX2	ENST00000261980	c.667G>A	p.Gly223Arg	Ht	D (1.000)	T(0.14)	Abs	Mat (Asy)
	NDST2	ENST00000309979	c.25C>T	p.Arg9Cys	Ht	D(1.000)	D(0)	4/13002	Pat (Asy)
	NDST2	ENST00000309979	c.199C>T	p.Arg67Trp	Ht	D(0.990)	T(0.18)	1/12989	Mat (Asy)
C2*	*STRA6*	ENST00000395105	c.1313A>G	p.Gln438Arg	Ht	D (1.000)	D(0.05)	Abs	Pat (Asy)
	STRA6	ENST00000395105	c.1913G>C	p.Arg638Pro	Ht	D (1.000)	D(0)	1/12990	Mat (Asy)

Ht: heterozygous; Hemi: hemizygous; Abs: absent; Unk: unknown; Pat: paternal; Mat: maternal; Asy: Asymptomatic; Sy: symptomatic
EVS: Exome variant server; Abs: absent; D: probably damaging; P: possibly damaging, B: probably benign; T: tolerated
*Positive controls with known mutations in *VSX2* (C1) or *STRA6* (C2)

Supplementary Table 5: Mutational burden of rare variants (<1% alternate allele frequency; not present in homozygosity) in genes with >1 predicted pathogenic variants (Frameshift, nonsense and splicing variants were considered as damaging; missense variants were classified as damaging or not based on Polyphen-2) in ODA cases (n=22 unknown + 2 positive controls) vs. Exome Variant Server (EVS) controls (n=6,500)

	ODA (n=48 chromosomes)		EVS EA* (n=8600** chromosomes)		EVS AA* (n=4406** chromosomes)		EVS EA+AA (n=13006 chromosomes)		ODA vs. EVS EA+AA
Gene	**Predicted pathogenic alleles**	**Frequency of mutational burden**	**Predicted pathogenic alleles**	**Frequency of mutational burden**	**Predicted pathogenic alleles**	**Frequency of mutational burden**	**Predicted pathogenic alleles**	**Frequency of mutational burden**	**p-value**
PTCH1	4	0.083	88	0.010	69	0.016	157	0.012	<0.0001
*STRA6***	3	0.063	73	0.008	62	0.014	135	0.010	0.0049
*VSX2***	2	0.042	15	0.002	37	0.008	52	0.004	0.0034
FAT4	2	0.042	458	0.053	267	0.061	725	0.056	0.9130
FRAS1	2	0.042	554	0.067	283	0.072	837	0.069	0.6469
IFT172	2	0.042	153	0.018	104	0.024	257	0.020	0.5701
NDST2	2	0.042	55	0.006	35	0.008	90	0.007	0.0446
NOTCH1	2	0.042	189	0.023	98	0.024	287	0.023	0.7092
RPGRIP1	2	0.042	114	0.014	80	0.021	194	0.016	0.4153

* EVS, Exome Variant Server; EA, European American; AA, African American

** Chromosome numbers were adjusted to the average number of calls across the gene if EVS displayed variant call data for <13006 chromosomes. Adjusted numbers- *STRA6* (EA, 8594; AA, 4396); *FRAS1* (EA, 8232; AA, 3918); *NOTCH1* (EA, 8322; AA, 4104); *RPGRIP1* (EA, 8138; AA,3792)

*** *STRA6* and *VSX2* each harbor known causal variants in the two positive control ODA individuals (C1 and C2)

Supplementary Table 6: Somite angle measurements for *PTCH1 in vivo* complementation assays.

Injection	Somite angle Measurements			p-values			Pathogenicity
	n	Mean (°)	S.E.M.	vs. WT RNA	vs. WT rescue	vs. MO	
Controls	49	81.5	0.4	0.0037	<0.0001	<0.0001	
MO	50	107.0	1.6	<0.0001	<0.0001		
WT RNA	49	83.4	0.4				
MO + WT RNA	50	85.9	0.7	0.0041			
D436N RNA	53	81.6	0.8	0.0657		<0.0001	
MO + D436N RNA	50	84.1	0.6		0.0530	<0.0001	Benign
T778P RNA	50	82.6	1.1	0.5122		<0.0001	
MO + T778P RNA	51	94.7	1.3		<0.0001	<0.0001	Hypomorph
I899V RNA	50	82.1	0.7	0.1572		<0.0001	
MO + I899V RNA	50	90.0	0.7		<0.0001	<0.0001	Hypomorph
T1064M RNA	50	86.3	0.8	0.0010		<0.0001	
MO + T1064M RNA	50	94.5	1.0		<0.0001	<0.0001	Hypomorph
V1081M RNA	45	83.9	0.9	0.6107		<0.0001	
MO + V1081M RNA	50	91.3	0.9		<0.0001	<0.0001	Hypomorph
R1297W RNA	49	83.2	1.0	0.8722		<0.0001	
MO + R1297W RNA	50	92.8	1.3		<0.0001	<0.0001	Hypomorph
Y1316C RNA	52	82.4	0.8	0.2986		<0.0001	
MO + Y1316C RNA	52	94.3	1.2		<0.0001	<0.0001	Hypomorph
T1052M* RNA	48	82.3	0.5	0.1121		<0.0001	
MO + T1052M* RNA	49	92.6	0.6		<0.0001	<0.0001	Hypomorph
P1315L RNA**	50	79.9	0.5	<0.0001		<0.0001	
MO + P1315L RNA**	52	84.4	0.7		0.1628	<0.0001	Benign

*Positive control: Associated with holoprosencephaly (HPE)[1]

**Negative control: Common variant (30% minor allele frequency, present in homozygosity in 8% of control individuals in ESP6500).

REFERENCES

1. Ming, J.E. et al. Mutations in PATCHED-1, the receptor for SONIC HEDGEHOG, are associated with holoprosencephaly. Hum Genet 110, 297-301 (2002).

Supplementary Table 7 : Primers used

Quantitative PCR (expression studies)

Gene	Forward primer	Reverse primer
Gapdh	AGGTCGGTGTGAACGGATTTG	GTAGACCATGTAGTTGAGGTCA
Ptch1	TGGGGCCTTCGCTGTGGGAT	ACTCGTCCACCAACTTCCACC

Quantitative PCR (ChIP)

Region	Forward primer	Reverse primer
Gapdh Control	CCATGAGTGGACCCTTCTTT	ATGGCATGGACTGTGGTCTA
Ptch1 Negative Control	CACAGGGAGGTAGGATGGTG	GGATTCACATCCTGGAGGTTT
Ptch1 SOX2 target sequence	AGAGGGGAGAGTTGGAGCAGCC	GTGGTCCCTCTACCCAGGGCC

PTCH1 molecular analysis

Exon	Forward primer	Reverse primer
M13PTCH1-Exon1	TGTAAAACGACGGCCAGTggcgatcccaaagagttaga	CAGGAAACAGCTATGACCcttccgcgaactggatgt
M13PTCH1-Exon2	TGTAAAACGACGGCCAGTcagagtggtccgtcccggag	CAGGAAACAGCTATGACCcctcccttctgcttcgtccc
M13PTCH1-Exon3	TGTAAAACGACGGCCAGTcccaagtggctcagcgtcat	CAGGAAACAGCTATGACCtgctcacacatcagccagtctc
M13PTCH1-Exon4	TGTAAAACGACGGCCAGTcccttcccagaagcagtccaa	GGGCTGCAATACAGAAGAGGcagctgggctgccctgaagt
M13PTCH1-Exon5	TGTAAAACGACGGCCAGTcctttaaccttgtaaac	CAGGAAACAGCTATGACCgcctcgtcttcgaaactacgaacatt
M13PTCH1-Exon6	TGTAAAACGACGGCCAGTggctaatgggaggtgtatggc	CAGGAAACAGCTATGACCtgcagatatgctggaaaggagca
M13PTCH1-Exon7	TGTAAAACGACGGCCAGTgttaggccggctaggtatga	CAGGAAACAGCTATGACCtggctagcgaggataacggttt
M13PTCH1-Exon8	TGTAAAACGACGGCCAGTcccatcaagttccctgaattgca	CAGGAAACAGCTATGACCgcgtcactgagcccggtgtat
M13PTCH1-Exon9	TGTAAAACGACGGCCAGTaggcaaacggcaaatgggaa	CAGGAAACAGCTATGACCactccagcgacaccagccct
M13PTCH1-Exon10	TGTAAAACGACGGCCAGTtacccacttccctgagggcg	CAGGAAACAGCTATGACCttcccatttgccgtttgcct
M13PTCH1-Exon11	TGTAAAACGACGGCCAGTccgagatgcagctcttggga	CAGGAAACAGCTATGACCtgaggttacggaagccctgc
M13PTCH1-Exon12	TGTAAAACGACGGCCAGTcccgaaagccatgcataaagg	CAGGAAACAGCTATGACCggcaggtggctctgtttccc
M13PTCH1-Exon13	TGTAAAACGACGGCCAGTgggaagcagcctctgtccaa	CAGGAAACAGCTATGACCcccaggtttgtgccttatcgg
M13PTCH1-Exon14a	TGTAAAACGACGGCCAGTtcctccatgtggcctcctca	CAGGAAACAGCTATGACCcagtggaggctggagtcgga
M13PTCH1-Exon14b	TGTAAAACGACGGCCAGTcagtggaggctggagtcgga	CAGGAAACAGCTATGACCtcctccatgtggcctcctca
M13PTCH1-Exon15	TGTAAAACGACGGCCAGTttgatctgtcgaagagaaacaggtcc	CAGGAAACAGCTATGACCggctgctgcagaaacagttca
M13PTCH1-Exon16	TGTAAAACGACGGCCAGTttctggtggtaggaacacgcc	CAGGAAACAGCTATGACCgagcagtggctggcagcag
M13PTCH1-Exon17	TGTAAAACGACGGCCAGTgcggtcactaacgtaggagg	CAGGAAACAGCTATGACCtcccaatgtgatagagtgcggg
M13PTCH1-Exon18	TGTAAAACGACGGCCAGTcggacctccgatactagtcgt	CAGGAAACAGCTATGACCccatggacctcaccacctcg
M13PTCH1-Exon19	TGTAAAACGACGGCCAGTtgtcagagggaagggtcgcc	CAGGAAACAGCTATGACCaccctgcactgcctacggct
M13PTCH1-Exon20a	TGTAAAACGACGGCCAGTcgtgggttaacgaaccctgt	CAGGAAACAGCTATGACCtctccttgcacacgcctgct
M13PTCH1-Exon20b	TGTAAAACGACGGCCAGTgtcgttggactagaacacttgtag	CAGGAAACAGCTATGACCcgtcgtggagcagtagcactg
M13PTCH1-Exon21	TGTAAAACGACGGCCAGTaacttacacttgacgccaacct	CAGGAAACAGCTATGACCgaacccgccctctagccctc
M13PTCH1-Exon22	TGTAAAACGACGGCCAGTttatgccgtgtcacgcgtcc	CAGGAAACAGCTATGACCcaaaccacaggaagatggca
M13PTCH1-Exon23a	TGTAAAACGACGGCCAGTcgggtgtaaatacccgtcgtcg	CAGGAAACAGCTATGACCgcgacagtcacggaggcaga
M13PTCH1-Exon23b	TGTAAAACGACGGCCAGTcctgccgttccggtcgtc	CAGGAAACAGCTATGACCgggtccagcgtgggatgt

CHAPITRE V

TRAVAUX COLLABORATIFS

Introduction

Le recrutement du laboratoire au travers du PHRC national, et l'analyse moléculaire de la plupart des gènes connus d'AM nous a permis de constituer une des plus grande cohorte de patients AM ne portant pas de mutation dans les gènes connus (120 patients). Cette cohorte est précieuse pour identifier de nouveaux gènes d'AM. Nous avons donc été sollicités par différentes équipes au niveau national ou international pour collaborer à leurs études.

Méthodes et Résultats

Pour les articles présentées ci-dessous, nous avons été contacté par des équipes ayant identifié un nouveau gène d'AM par CGH-array (*TMX3*) ou séquençage d'exome (*ALDH1A3* et *RARB*). Ces équipes souhaitaient valider leurs résultats sur une cohorte de patient avec un phénotype similaire à celui de leur famille, et chez qui la présence de mutation dans les gènes connus avait été exclue.

Les résultats de ces collaborations sont décrits dans les 3 articles suivants:

- Article n°13

Fares-Taie, L *et al*. (2013). "*ALDH1A3* mutations cause recessive anophthalmia and microphthalmia." Am J Hum Genet 92(2): 265-70.

- Article n°14

Myriam Srour *et al*. (2013) "Recessive and dominant mutations in the retinoic acid receptor beta in cases with microphthalmia and diaphragmatic hernia " Am J Hum Genet 93: 1–8

- Article n°15

Chao, R *et al*. (2010). "A male with unilateral microphthalmia reveals a role for *TMX3* in eye development." PLoS One 5(5): e10565.

Conclusion

Ces collaborations montrent bien que le travail présenté sur la première partie de ma thèse (recherche de mutation dans les gènes connus) est une étape clef à l'identification de nouveaux gènes d'AM. Le travail laborieux consistant à rechercher chez les patients AM des mutations dans les gènes connus présente deux intérêts. D'une part, il permet de déterminer les fréquences d'implication des gènes étudiés, et les phénotypes associés. D'autre part, il permet de constituer une cohorte de patients sans mutation dans les gènes connus qui peut être utilisée pour valider l'implication de gènes nouvellement identifiés par différentes approches.

ARTICLE 13

***ALDH1A3* mutations cause recessive anophthalmia and microphthalmia**

American Journal of Human Genetics

2013-92(2): 265-70

L. Fares-Taie*, S. Gerber*, **N. Chassaing***, J. Clayton-Smith, S. Hanein, E. Silva, M. Serey, V. Serre, X. Gerard, C. Baumann, G. Plessis, B. Demeer, L. Bretillon, C. Bole, P. Nitschke, A. Munnich, S. Lyonnet, P. Calvas, J. Kaplan, N. Ragge and J. M. Rozet

---

Nous avons été contactés par l'équipe des Docteurs Josseline Kaplan et Jean-Michel Rozet pour valider l'implication du gène *ALDH1A3* dont des mutations avaient été identifiées dans une de leur famille consanguine par une combinaison d'homozygosity mapping et d'exome sequencing. Ce gène faisait partie de nos meilleurs gènes candidats après notre approche transcriptomique (expression régulée par PAX6, seul gène à avoir une spécificité d'expression oculaire, voire chapitre correspondant). Il est de plus impliqué dans le métabolisme de l'acide rétinoïque, élément clef au cours du développement oculaire. Dans la famille initiale, il avait été identifié une mutation faux-sens à l'état homozygote. Compte-tenu de ce mode de transmission récessif, nous avons pu inclure 28 patients AM issus de parents apparentés. Ces patients provenaient de notre cohorte de patient Toulousaine (12 patients), et de la cohorte de patient de notre collaboratrice le Dr Nicola Ragge à Oxford que nous avons associé à ce projet (16 patients). Il a pu ainsi être identifié des mutations dans deux familles supplémentaires confirmant ainsi l'implication du gène *ALDH1A3* dans l'AM.

ALDH1A3 Mutations Cause Recessive Anophthalmia and Microphthalmia

Lucas Fares-Taie,[1,15] Sylvie Gerber,[1,15] Nicolas Chassaing,[2,3,15] Jill Clayton-Smith,[4] Sylvain Hanein,[1] Eduardo Silva,[5] Margaux Serey,[1] Valérie Serre,[1,6] Xavier Gérard,[1] Clarisse Baumann,[7] Ghislaine Plessis,[8] Bénédicte Demeer,[9] Lionel Brétillon,[10] Christine Bole,[11] Patrick Nitschke,[12] Arnold Munnich,[1] Stanislas Lyonnet,[1] Patrick Calvas,[2,3] Josseline Kaplan,[1,*] Nicola Ragge,[13,14] and Jean-Michel Rozet[1,*]

Anophthalmia and microphthalmia (A/M) are early-eye-development anomalies resulting in absent or small ocular globes, respectively. A/M anomalies occur in syndromic or nonsyndromic forms. They are genetically heterogeneous, some mutations in some genes being responsible for both anophthalmia and microphthalmia. Using a combination of homozygosity mapping, exome sequencing, and Sanger sequencing, we identified homozygosity for one splice-site and two missense mutations in the gene encoding the A3 isoform of the aldehyde dehydrogenase 1 (*ALDH1A3*) in three consanguineous families segregating A/M with occasional orbital cystic, neurological, and cardiac anomalies. ALDH1A3 is a key enzyme in the formation of a retinoic acid gradient along the dorso-ventral axis during early eye development. Transitory expression of mutant *ALDH1A3* open reading frames showed that both missense mutations reduce the accumulation of the enzyme, potentially leading to altered retinoic acid synthesis. Although the role of retinoic acid signaling in eye development is well established, our findings provide genetic evidence of a direct link between retinoic-acid-synthesis dysfunction and early-eye-development anomalies in humans.

Anophthalmia and microphthalmia (A/M) are rare errors of eye development (with a combined prevalence of 3:100,000 to 30:100,000).[1] Whereas true anophthalmia refers to the histological absence of ocular tissue in the orbit, microphthalmia ranges from extreme cases with only tiny or no visible remnants of globe in the orbit (also called "clinical anophthalmia") to simple microphthalmia with structurally normal small eyes (axial length at least 2 SD below the mean for an individual of that age).[1] A/M may affect one or both eyes. Both errors are associated with systemic anomalies in at least 50% of individuals,[2] a large proportion of such individuals presenting with defined syndromes.[1,3–5] Learning difficulties are described in one-fifth of individuals with A/M and/or coloboma.[6] This frequency is probably higher in individuals with A/M when isolated colobomia cases are excluded. Both genetic and environmental factors contribute to A/M. Monogenic A/M is inherited as autosomal-dominant (AD), autosomal-recessive (AR), or X-linked traits. Both AD and AR forms are characterized by clinical and genetic heterogeneity.[3] To date, mutations in genes critical for normal eye development have been identified in 20%–40% of A/M cases, some genes being involved in simple, complex, and syndromic A/M.[7–10] With the exception of *SOX2* mutations, which underlie 10%–15% of severe A/M cases, mutations in other genes are, individually, uncommon causes of the disease.[3,10–12]

Using a combination of the Affymetrix GeneChip Human Mapping 10K 2.0 Array and microsatellite markers, we performed homozygosity mapping in a multiplex inbred Pakistani pedigree with multiple loops of consanguinity (Figure 1) in whom Sanger sequencing failed to detect mutations in *GDF6* (MIM 601147), *FOXE3* (MIM 601094), *OTX2* (IM 600037), *PAX6* (MIM 607108), *RAX* (MIM 601881), *SOX2* (MIM 184429), and *VSX2* (*CHX10*, [MIM 142993]). Informed consent was obtained from each individual participating in this study, which was approved by Le Comité de Protection des Personnes Ile de France II or by the Cambridgeshire 1 Multicenter Research Ethics Committee (04/Q0104/129). Considering that A/M-causing mutations are rare, we assumed that affected individuals of the two available nuclear families (IV1, IV4, and IV5; Figure 1) were most likely homozygous for the same disease-causing mutation and surrounding SNP markers. This strategy defined three regions with LOD scores ≥ 3 (2p24.2–p24.1, 5.5Mb; 8q24, 0.7Mb; and 15q26.3, 3.8Mb) and one region with a LOD score close to 3 (4p14–p11, 10.1Mb) (Figure 1A). Analysis of highly informative microsatellite markers in each candidate region allowed us to show that an apparent linkage on

[1]INSERM U781 & Department of Genetics, Paris Descartes University, 75015 Paris, France; [2]CHU Toulouse, Service de Génétique Médicale, Hôpital Purpan, 31059 Toulouse, France; [3]Université Paul-Sabatier Toulouse III, EA-4555, 31000 Toulouse, France; [4]Genetic Medicine, Manchester Academic Health Sciences Centre, St Mary's Hospital, Manchester M13 9WL, UK; [5]IBILI, Faculty of Medicine, University of Coimbra, Department of Ophthalmology, Centro Hospitalar Universitário de Coimbra, 3000-548 Coimbra, Portugal; [6]Université Paris Diderot, 75205 Paris Cedex 13, France; [7]Department of Genetics, CHU Robert Debré, 75019 Paris, France; [8]Department of Medical Genetics, CHU de Caen, Hôpital de la Côte de Nacre, 14033 Caen Cedex 9, France; [9]Department of Pediatrics, CHU d'Amiens, Hôpital Nord, 80054 Amiens Cedex 1, France; [10]INRA UMR1324 & CNRS UMR6265, Centre des Sciences du Goût et de l'Alimentation, Université de Bourgogne, 21065 Dijon, France; [11]Genomics Plateform, IMAGINE Foundation and Paris Descartes University, 75015 Paris, France; [12]Bioinformatics Plateform, Paris Descartes University, 75015 Paris, France; [13]Wessex Clinical Genetics Service, University Hospital Southampton, Southampton SO 16 5YA UK; [14]Oxford Brookes University, Oxford OX1 3QX, UK
[15]These authors contributed equally to this work
*Correspondence: josseline.kaplan@inserm.fr (J.K.), jean-michel.rozet@inserm.fr (J.-M.R.)
http://dx.doi.org/10.1016/j.ajhg.2012.12.003.

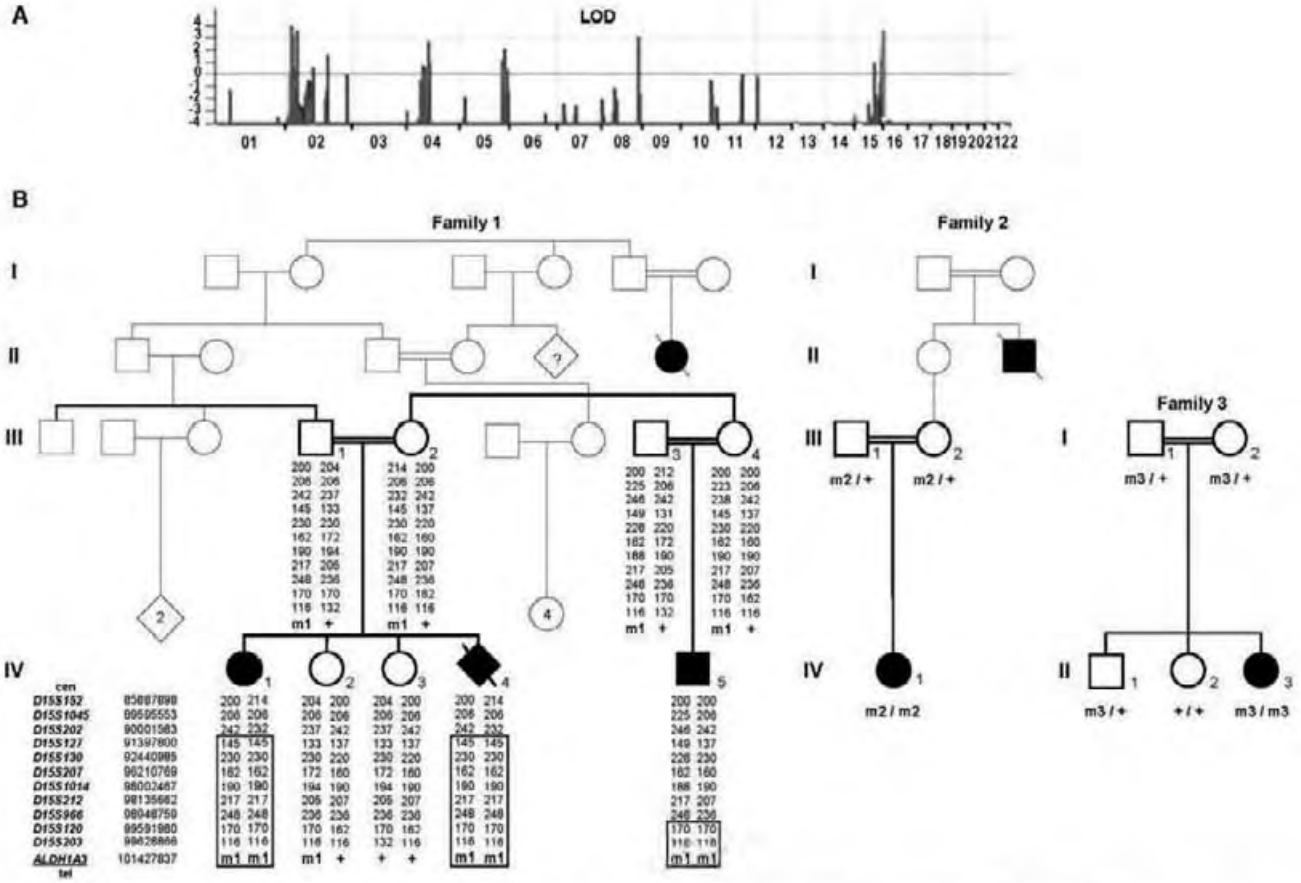

Figure 1. Linkage Analysis, Pedigree, and Segregation Analysis in A/M Families with Homozygous *ALDH1A3* Mutations
(A) Full parametric linkage analysis of family 1 using a combination of Affymetrix GeneChip Human Mapping 10K 2.0 Arrays. Parametric LOD scores were calculated with the MERLIN software program.
(B) Pedigree, haplotype, and/or segregation analyses of *ALDH1A3* mutations in the three A/M families. The positions of microsatellite markers of the 15q26.3 region based on hg19 assembly of the human genome were obtained from the: Human (*Homo sapiens*) Genome Browser Gateway at UCSC. m1, c.265C>T (p.Arg89Cys); m2, c.1477G>C (p.Ala493Pro); m3, c.475+1G>T; +, wild-type allele.

chromosomes 2p24, 8q24, and 4p14–p11 resulted from uninformative SNP markers (data not shown). Conversely, homozygosity for informative markers of the 15q26.3 locus was confirmed (Figure 1B).

The critical interval on 15q26.3 spanned 3.8 Mb and contained 31 genes. To identify the disease-causing mutation, we subjected the DNA of the index case, IV1, to whole-exome sequencing by using the SureSelect^{XT} Human All Exon V3 50 Mb target-enrichment kit (Agilent Technologies, Massy, France) in accordance with the manufacturer's recommendations. Each genomic DNA fragment was sequenced with the use of the paired-end strategy and an average read length of 75 bases (Illumina HISEQ, Illumina, San Diego, CA, USA). Image analysis and base calling were performed with the Illumina Sequence Control Software (SCS) with Real Time Analysis (RTA) version 1.9 and default parameters were used. Sequences were aligned to the human genome reference sequence (hg19 assembly), and SNPs were called on the basis of allele calls and read depth with the use of the CASAVA pipeline (Consensus Assessment of Sequence and Variation 1.8, Illumina). Genetic variation annotation was performed with an in-house pipeline (Plateforme Bioinformatique Paris Descartes, Paris, France).

Considering that A/M-causing mutations are uncommon, we searched for homozygous variants absent in the dbSNP132, Exome Variant Server, 1000 Genomes, and in-house databases or with allelic frequencies <0.01. We found no homozygosity for consensus splice-site changes, nonsense mutations, or insertions or deletions in coding regions upon whole-genome analysis. We subsequently selected nonsynonymous changes predicted to be "damaging" or "possibly damaging" using the Polyphen and SIFT programs available through our in-house analysis pipeline. This led to the selection of 28 variants in 27 genes. The only gene mapping in the 3.8 Mb interval on chromosome 15q26.3, *ALDH1A3* (NM_000693.2 [MIM600463]), harbored a homozygote missense mutation, c.265C>T (p.Arg89Cys) (Table S1, available online). The mutation was confirmed by Sanger sequencing, and familial analysis confirmed the biparental transmission of the mutation and segregation with the disease (Figure 1).

ALDH1A3 encodes a retinaldehyde dehydrogenase (ALDH1A3; also referred to as RALDH1A3, RALDH3, or

ADLH6) involved in retinoic acid synthesis through the oxidation of retinaldehyde. It plays a pivotal role in retinoic acid signaling in eye development.[13–17] Thus, *ALDH1A3* was regarded a strong candidate gene by virtue of both its localization and its function.

We performed Sanger sequencing of all 13 exons and the intron-exon boundaries of *ALDH1A3* (Table S2) in a series of 28 additional A/M index individuals born to consanguineous parents with no mutation in *GDF6*, *FOXE3*, *OTX2*, *PAX6*, *RAX*, *SOX2*, or *VSX2*. We identified homozygous *ALDH1A3* mutations in 2 of 28 simplex individuals (Figure 1). The first simplex individual, a girl born to Turkish parents, harbored a homozygous missense mutation, c.1477G>C (p.Ala493Pro) (IV1, family 2). The second individual, a girl born to Moroccan parents, harbored a homozygous splice-site mutation, c.475+1G>T (II3, family 3). Biparental transmission was confirmed in the two families.

The three mutations were absent in the SNP databases, in the Exome Variant Server, and in 200 control chromosomes. The mutations were analyzed with Alamut Mutation Interpretation software, a decision-support system for mutation interpretation based on Align GVD, Polyphen-2, SIFT, SpliceSiteFinder-like, MaxEntScan, NNSPLICE, and Human Splicing Finder. The c.475+1G>T mutation is predicted to abolish the splice-donor site of intron 4. This is expected to result in an in-frame skipping of exon 5, which contributes to the nicotinamide adenine dinucleotide (NAD) binding pocket (exon 5 codes for residues 159–179; NAD binding pocket: residues 8–135 and 159–170; Protein Data Bank [PDB] 1BXS). The c.265C>T (p.Arg89Cys) mutation affects an amino acid conserved from human to worm and in the ALDH1A1 and ALDH1A2 paralogs. The c.1477G>C (p.Ala493Pro) mutation changes a residue conserved from human to frog. In fish, fly, and *C. elegans*, the p.Ala493 residue is replaced by a leucine or a glycine residue. The replacement of the positively charged p.Arg89 by a cysteine residue and the replacement of p.Ala495 by a proline residue were both predicted to be deleterious by the Alamut Interpretation software.

The three-dimensional structure of the tetrameric human ALDH1A3 (residues 20–511; Figure S1A) was modeled by comparative protein modeling methods and energy minimization with the use of the Swiss-Model program in the automated mode.[18–20] The 2.35 Å coordinate set for the tetrameric sheep liver class 1 aldehyde dehydrogenase with bound NAD (PDB code 1BXS) was used as a template for modeling the human ALDH1A3 protein (71.3% sequence identity). Swiss-PdbViewer 3.7 was used for structural insight into ALDH1A3 substitutions. The p.Arg89 residue is located between two helixes in a conserved loop of the NAD binding domain. Molecular modeling of the wild-type (WT) protein suggests that the p.Arg89 amino acid is involved in the stabilization of the tetramer through its interaction with p.Asn511 residue at a distance of 5 Å in another subunit (Figure S1B). This latter residue is located in a loop connecting the two β sheets of the monomeric oligomerization domain. Thus, the p.Arg89Cys substitution most likely affects the stability of the tetramer. The p.Ala493 residue is located in a small helix between two β sheets involved in the oligomerization domain of the enzyme (Figure S1C). The introduction of a proline at position 493 in the helix is expected to introduce an elbow, leading to an incorrect position of the two β sheets relative to each other and hampering the tetramerization of the enzyme.

Using site-directed mutagenesis (QuikChange II Site-Directed Mutagenesis Kit, Agilent), we introduced the c.265C>T (p.Arg89Cys) and c.1477G>C (p.Ala493Pro) A/M mutations into a pCMV6-entry eukaryote expression vector that encodes the full *ALDH1A3* open reading frame and is fused to c-Myc (Origen, Rockville, MD, USA). We also generated a construct harboring a mutation that affected the p.Trp180 (c.538T>G; p.Trp180Gly) residue. This residue corresponds to the p.Trp168 amino acid, which is directly involved in the fixation of NAD in the sheep ALDH1 and does not interfere with the oligomerization of the protein. Primers used for mutagenesis are shown in Table S3. We assessed the effect of the *ALDH1A3* substitutions on mRNA and protein levels in human embryonic kidney cells (HEK293 cells) transiently cotransfected with WT or mutant *ALDH1A3* constructs, and pCGA-GFP (Addgene, Cambridge, MA, USA) to normalize the data. RT-qPCR using primers specific to the c-Myc tag and the GFP normalizer (Table S4) showed no significant difference in expression between WT and mutant *ALDH1A3* mRNA (Figure S2). Immunoblot analysis revealed that the c-Myc-tagged ALDH1A3 p.Arg89Cys and p.Ala493Pro mutant protein levels were strongly reduced compared to the WT and p.Trp180Gly mutant proteins, suggesting that the p.Arg89Cys and p.Ala493Pro mutant proteins might be unstable and subject to proteasomal degradation, leading to an absence or low level of high-molecular-weight complexes (Figure 2).

Together, our findings suggest that the synthesis of retinoic acid by *ALDH1A3* is impaired in the affected individuals (n = 5) of the three families who consistently presented severe bilateral clinical anophthalmia (extreme microphthalmia with no visible ocular structure). In family 1, the A/M index individual (IV1) was born after full-term normal delivery and was in the 2nd centile for weight (2.59 kg), 3rd centile for length (46.5 cm), and 10th centile for head circumference (33.5 cm). She exhibited small optic nerves and a small optic chiasm upon a cerebral MRI at 1 week of age. Autism was diagnosed at the age of 3 years. She has two healthy sisters. Her mother's last pregnancy before the study was terminated at 23 weeks of gestation after ultrasonography detection of apparent bilateral anophthalmia with normal brain structures (IV4) detected on ultrasonography. Her maternal cousin (IV5) was born at 34 weeks of gestation by Caesarian section and had a birth weight of 2 kg. He had severe bilateral microphthalmia with cysts (a rudimentary globe on the left and a grossly abnormal globe associated with a cyst on the right), moderate pulmonary and supravalvar

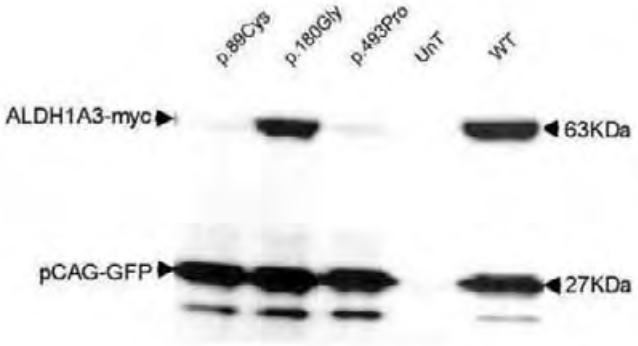

Figure 2. Immunoblot Analysis of Mutant and Wild-Type ALDH1A3 Proteins

HEK293 cells were transfected with pCMV6-Entry-ALDH1A3-WT-cMyc, pCMV6-Entry-ALDH1A3-Arg89CYS-aMyc, pCMV6-Entry-ALDH1A3-Trp180Gly-cMyc, and pCMV6-Entry-ALDH1A3-ALA493PRO-cMyc plasmids, respectively. The pCAG-GFP plasmid was systematically cotransfected with the pCMV6-Entry-ALDH1A3 constructs. Untransfected (UnT) cells served as controls. Total proteins were extracted and run (50 μg) on a NuPAGE 4%–12% Bis-TrisGel (Life Technologies, Cergy Pontoise, France). c-Myc-tagged proteins and GFP were detected with the use of mouse anti-cMyc (1:1,000, Santa Cruz, San Diego, CA, USA) and mouse anti-GFP (1:1,000, Roche, Meylan, France) primary antibodies, respectively, and with rabbit anti-mouse IgG-HRP (2 mg/ml, 1:5,000; Abcam, Paris, France) as a secondary antibody. Immunoblots were revealed with the use of SuperSignalWest Dura Extended Duration Substrate (Thermo Scientific, Courtaboeuf, France) and the Chemidoc XRS+ Imaging System (Bio-Rad, Marnes-la-Coquette, France). Immunoblot images were acquired and analyzed with the Image Lab software 3.0.1 build 18 (Bio-Rad). Transfections and immunoblots were performed in triplicate. The figure shows the result of one experiment. A drastic reduction in the amount of the p.Arg89Cys (p.89Cys) and p.Ala493Pro (p.493Pro) mutant proteins is shown as compared to the wild-type (WT) and p.Trp180Gly (p.180Gly) mutant proteins.

pulmonary stenosis, and a moderately sized atrial septal defect. His growth progressed along the 2nd–9th centile for weight and length and 0.4th centile for head circumference. At the age of 4 years, he has a possible diagnosis of autism. The proband in family 2 (IV1) has left and extreme right microphthalmia. She had no other health problems and displays normal intelligence. A review of the family's medical history revealed that a maternal uncle died at the age of 1 month with bilateral clinical anophthalmia, but we were unable to obtain additional clinical details. Finally, the proband in family 3, who had a homozygous c.475+1G>T mutation was born after a full term and normal delivery and had a birth weight of 3.5 kg (II3; family 3). She presented with severe right microphthalmia and severe left microphthalmia with cyst. An MRI showed dysplastic globes, a hypoplastic chiasm and optic nerves, and a normal remainder of the brain. She had no other health problems and displays normal intelligence.

In the mouse, *Aldh1a3*, along with *Aldh1a1* and *Aldh1a2*, contributes to the synthesis of retinoic acid, which functions as ligand for nuclear receptors that directly regulate gene expression crucial for embryonic eye development.[16,17] *Aldh1a1*, *Aldh1a2*, and *Aldh1a3* are expressed with unique, nonoverlapping, spatiotemporal patterns in embryonic eyes, leading to tissue- and time-restricted retinoic acid synthesis during development.[16,17] ALDH1A3 is a key enzyme in the formation of a retinoic acid gradient along the dorso-ventral axis during early eye development. It is required for the complete invagination of the ventral optic cup and closure of the choroid fissure.[15–17,21,22] It also contributes to correct axonal projections of retinal cells into the brain.[21,22] Interestingly, the phenotype of A/M individuals with *ALDH1A3* mutations is consistent with abnormal closures of the choroid fissure and abnormal optic nerve development. Indeed, evidence of cysts in at least two individuals suggests that globe induction—and probably invagination—is present, whereas closure of the choroid fissure may be lacking. In addition, available MRIs showed hypoplastic optic nerves (n = 2).

In addition to being a key player in the developing sensory neuroepithelia of the eye, in the mouse, *Aldh1a3* plays a role in the development of the nose and ear and in discrete sites within the CNS.[16,17] However, knockout of *Aldh1a3* causes malformations restricted to ocular and nasal regions.[21,22] *Aldh1a3*$^{-/-}$ mutant embryos begin the process of optic cup formation, but they exhibit ventral retina shortening associated with lens rotation and persistence of primary vitreous.[16,21] In addition, the knockout causes choanal atresia, which is responsible for respiratory distress and the death of *Aldh1a3*$^{-/-}$ mutants at birth.[21] Individuals homozygous for *ALDH1A3* mutations had ocular malformations but no nasal defects. Unlike the *Aldh1a3* knockout mouse, the affected individuals of the three families harbor mutations expected to result in the production of mutant proteins. We cannot exclude the possibility that the complete loss of function of both *ALDH1A3* alleles is lethal in humans.

Two out of the four living affected individuals had autism (IV1 and IV5; family 1). The available cerebral MRI of individual IV1 revealed normal cerebellar and cerebral features. Autism and intellectual disability are not infrequent features in individuals affected with A/M.[6] However, given that two A/M individuals had normal intelligence, autism may be unrelated to altered *ALDH1A3* function in the CNS. Similarly, it is difficult to decide whether the cardiac anomalies noted in an individual (IV5, family 1) are caused by *ALDH1A3* mutations. Nevertheless, it is worth remembering that extraocular anomalies are not uncommon in A/M and that environmental or epigenetic factors have been proposed to explain that some genes are involved in variable phenotypes.[12] Additional studies will hopefully allow a more accurate clinical definition of A/M caused by *ALDH1A3* mutations.

In summary, we report that mutations in *ALDH1A3* cause bilateral severe microphthalmia, possibly in association with heart anomalies and autism. Interestingly, the role of retinoic acid synthesis from vitamin A in eye development is well established. Yet, the deciphering of the genetic causes underlying A/M in humans has resulted

in the identification of a number of master control genes for the growth and development of eyes, downstream of retinoic acid signaling. The previous example of a direct link between vitamin A deficiency and severe hereditary developmental eye defect in humans is *STRA6* [MIM 610745], the gene that encodes the membrane receptor for retinol-binding protein, which mediates cellular uptake of vitamin A,[23] and mutations in this gene can cause nonsyndromic and syndromic A/M.[8,9] Our data provide evidence of a direct link between retinoic acid synthesis dysfunction and eye anomalies in humans. Finally, considering that eye defects in mouse *aldh1a* mutants can be rescued by maternal dietary retinoic acid supplementation,[22] this raises the possibility of using this strategy to prevent A/M in conceptus that harbor *ALDH1A3* mutations.

Supplemental Data

Supplemental Data include Supplemental Experimental Procedures, two figures, and four tables and can be found with this article online at http://www.cell.com/AJHG.

Acknowledgments

We are grateful to the families for their participation in the study. We thank A. Martin and L. Harrison for research co-ordination, A. Salt and R. Collin (Moorfields Eye Hospital, London) for clinical support, and D. Robinson (Wessex Regional Genetics Laboratory, Salisbury), N. Graham (Southampton University Hospitals Trust, Southampton), E. Leclerc and B. Leloire (CRB-CHU Biobanque de Picardie, Amiens), and Soraya Sin (Laboratoire d'Oncogénétique, Hôpital René Huguenin-Institut Curie, St Cloud) for technical assistance. This work was supported by grants from Retina France, the Clinical Research Hospital Program of the French Ministry of Health (PHRC 09 109 01), the Academy of Medical Sciences/Health Foundation (NR), VICTA (Visually Impaired Children Taking Action), MACS (Microphthalmia and Anophthalmia Children's Society), and the Hampshire and Isle of Wight Comprehensive Local Research Network.

Received: September 21, 2012
Revised: October 15, 2012
Accepted: December 7, 2012
Published: January 10, 2013

Web Resources

The URLs for data presented herein are as follows:

Plateforme Bioinformatique Paris Descartes (BIPD), http://mendel.necker.fr/polyweb/index.html
Alamut Interpretation Software 2.0, http://alamut.interactive-biosoftware.com
Exome Variant Server, http://evs.gs.washington.edu/EVS
Genome Browser, http://genome.ucsc.edu
Online Mendelian Inheritance in Man (OMIM), http://www.omim.org
Swiss-PdbViewer 3.7, http://www.expasy.org/spdbv
dbSNP, http://www.ncbi.nlm.nih.gov/projects/SNP
1000 Genomes, http://www.1000genomes.org

References

1. Verma, A.S., and Fitzpatrick, D.R. (2007). Anophthalmia and microphthalmia. Orphanet J. Rare Dis. *2*, 47.
2. Tucker, S., Jones, B., and Collin, R. (1996). Systemic anomalies in 77 patients with congenital anophthalmos or microphthalmos. Eye (Lond.) *10*, 310–314.
3. Bardakjian, T.M., and Schneider, A. (2011). The genetics of anophthalmia and microphthalmia. Curr. Opin. Ophthalmol. *22*, 309–313.
4. Slavotinek, A.M. (2011). Eye development genes and known syndromes. Mol. Genet. Metab. *104*, 448–456.
5. Shaham, O., Menuchin, Y., Farhy, C., and Ashery-Padan, R. (2012). Pax6: a multi-level regulator of ocular development. Prog. Retin. Eye Res. *31*, 351–376.
6. Morrison, D., FitzPatrick, D., Hanson, I., Williamson, K., van Heyningen, V., Fleck, B., Jones, I., Chalmers, J., and Campbell, H. (2002). National study of microphthalmia, anophthalmia, and coloboma (MAC) in Scotland: investigation of genetic aetiology. J. Med. Genet. *39*, 16–22.
7. Williamson, K.A., Hever, A.M., Rainger, J., Rogers, R.C., Magee, A., Fiedler, Z., Keng, W.T., Sharkey, F.H., McGill, N., Hill, C.J., et al. (2006). Mutations in SOX2 cause anophthalmia-esophageal-genital (AEG) syndrome. Hum. Mol. Genet. *15*, 1413–1422.
8. Chassaing, N., Golzio, C., Odent, S., Lequeux, L., Vigouroux, A., Martinovic-Bouriel, J., Tiziano, F.D., Masini, L., Piro, F., Maragliano, G., et al. (2009). Phenotypic spectrum of STRA6 mutations: from Matthew-Wood syndrome to non-lethal anophthalmia. Hum. Mutat. *30*, E673–E681.
9. Chassaing, N., Ragge, N., Kariminejad, A., Buffet, A., Ghaderi-Sohi, S., Martinovic, J., and Calvas, P. (2012). Mutation analysis of the STRA6 gene in isolated and non-isolated anophthalmia/microphthalmia. Clin. Genet. *9999*.
10. Ragge, N.K., Brown, A.G., Poloschek, C.M., Lorenz, B., Henderson, R.A., Clarke, M.P., Russell-Eggitt, I., Fielder, A., Gerrelli, D., Martinez-Barbera, J.P., et al. (2005). Heterozygous mutations of OTX2 cause severe ocular malformations. Am. J. Hum. Genet. *76*, 1008–1022.
11. Ragge, N.K., Lorenz, B., Schneider, A., Bushby, K., de Sanctis, L., de Sanctis, U., Salt, A., Collin, J.R., Vivian, A.J., Free, S.L., et al. (2005). SOX2 anophthalmia syndrome. Am. J. Med. Genet. A. *135*, 1–7, discussion 8.
12. Bakrania, P., Robinson, D.O., Bunyan, D.J., Salt, A., Martin, A., Crolla, J.A., Wyatt, A., Fielder, A., Ainsworth, J., Moore, A., et al. (2007). SOX2 anophthalmia syndrome: 12 new cases demonstrating broader phenotype and high frequency of large gene deletions. Br. J. Ophthalmol. *91*, 1471–1476.
13. Grün, F., Hirose, Y., Kawauchi, S., Ogura, T., and Umesono, K. (2000). Aldehyde dehydrogenase 6, a cytosolic retinaldehyde dehydrogenase prominently expressed in sensory neuroepithelia during development. J. Biol. Chem. *275*, 41210–41218.
14. Graham, C.E., Brocklehurst, K., Pickersgill, R.W., and Warren, M.J. (2006). Characterization of retinaldehyde dehydrogenase 3. Biochem. J. *394*, 67–75.
15. Cvekl, A., and Wang, W.L. (2009). Retinoic acid signaling in mammalian eye development. Exp. Eye Res. *89*, 280–291.
16. Duester, G. (2009). Keeping an eye on retinoic acid signaling during eye development. Chem. Biol. Interact. *178*, 178–181.
17. Fuhrmann, S. (2010). Eye morphogenesis and patterning of the optic vesicle. Curr. Top. Dev. Biol. *93*, 61–84.

18. Arnold, K., Bordoli, L., Kopp, J., and Schwede, T. (2006). The SWISS-MODEL workspace: a web-based environment for protein structure homology modelling. Bioinformatics *22*, 195–201.
19. Kiefer, F., Arnold, K., Künzli, M., Bordoli, L., and Schwede, T. (2009). The SWISS-MODEL Repository and associated resources. Nucleic Acids Res. *37*(Database issue), D387–D392.
20. Peitsch, M.C. (1995). Protein modeling by E-mail. Nature Biotechnology *13*, 658–660.
21. Dupé, V., Matt, N., Garnier, J.M., Chambon, P., Mark, M., and Ghyselinck, N.B. (2003). A newborn lethal defect due to inactivation of retinaldehyde dehydrogenase type 3 is prevented by maternal retinoic acid treatment. Proc. Natl. Acad. Sci. USA *100*, 14036–14041.
22. Molotkov, A., Molotkova, N., and Duester, G. (2006). Retinoic acid guides eye morphogenetic movements via paracrine signaling but is unnecessary for retinal dorsoventral patterning. Development *133*, 1901–1910.
23. Kawaguchi, R., Yu, J., Honda, J., Hu, J., Whitelegge, J., Ping, P., Wiita, P., Bok, D., and Sun, H. (2007). A membrane receptor for retinol binding protein mediates cellular uptake of vitamin A. Science *315*, 820–825.

AJHG, Volume 92

SUPPLEMENTAL DATA

ALDH1A3 Mutations Cause Recessive Anophthalmia and Microphthalmia

Lucas Fares-Taie, Sylvie Gerber, Nicolas Chassaing, Gill Clayton-Smith, Sylvain Hanein, Eduardo Silva, Margaux Serey, Valérie Serre, Xavier Gérard, Clarisse Baumann, Ghislaine Plessis, Bénédicte Demeer, Lionel Brétillon, Christine Bole, Patrick Nitschke, Arnold Munnich, Stanislas Lyonnet, Patrick Calvas, Josseline Kaplan, Nicola Ragge, and Jean-Michel Rozet

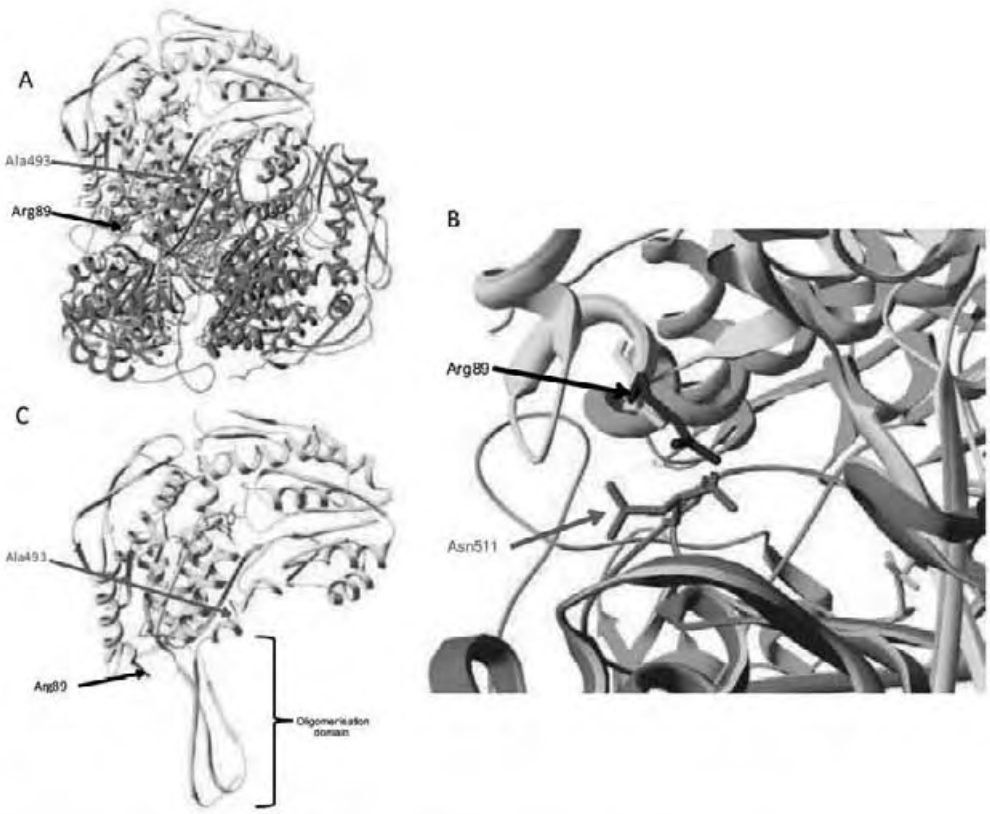

Figure S1. Ribbon Representation of the Human ALDH1A3 Tetramer

The 2.35 Å coordinate set for the tetrameric sheep liver class 1 aldehyde dehydrogenase with NAD bound (pdb code: 1BXS) was used as a template for modeling the human ALDH1A3 protein (71,3% sequence identity). (A) Each of the four monomers is shown in different colors (yellow, blue, green and red, respectively). . The four catalytic pockets are visualized with the four NAD co-crystallized with the sheep ALDH1 (1BXS) and are shown in light blue. (B) Magnification of the region around the Arg89 residue of a monomer. The interaction with the Asn511 residue at a distance of 5 Å in another monomer is shown. The replacement of the Arg89 by a cysteine is predicted to alter the interaction between the monomers. (C) Ribbon representation of a monomer (yellow) bound to NAD (light blue) showing the oligomerization domain and the position of the two residues affected by A/M mutations. The p.Ala493Pro mutation is predicted to alter severely the oligomerization domain of the enzyme.

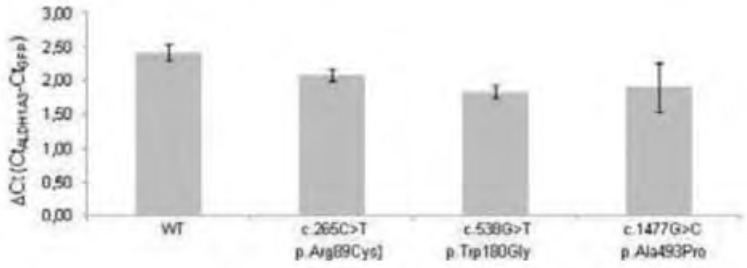

Figure S2. Relative Expression of GFP and ALDH1A3 mRNA in HEK293 Cells Measured by RT-qPCR

HEK293 cells were co-transfected with pCAG-GFP and pCMV6-Entry-ALDH1A3-WT-cMyc, pCMV6-Entry-ALDH1A3-Arg89Cys-cMyc, pCMV6-Entry-ALDH1A3-Trp180Gly-cMyc, pCMV6-Entry-ALDH1A3-Ala493Pro-cMyc plasmids, respectively. Total mRNA was extracted using the RNeasy Mini Kit (Qiagen, Courtaboeuf, France) according to manufacturer's protocol. cDNAs (5 µl of a 1:25 dilution in nuclease-free water) were subjected to real-time PCR amplification in a buffer (20 µl) containing MESA BLUE qPCR Master Mix Plus for Sybr Assay (Eurogentec, Angers, France) and 300 nmol/l of forward and reverse primers, on a Taqman 7900 HT Fast Real-Time PCR System (Applied Biosystems, Courtaboeuf, France). For each cDNA sample, the mean of cycle threshold (Ct) values was calculated from triplicates (SD <0.5 Ct). ALDH1A3 expression levels were normalized by using the relation ΔCt ($Ct_{ALDH1A3}$ - Ct_{GFP}). Amplification efficiency was calculated for each primer-pair using fourfold serial dilution curves (1:5, 1:25, 1:125, 1:625). No reverse transcriptase and no template control reaction were used as negative controls in each run. The quantitative data are the means ± SEM of three independent experiments. The graph shows that the expression of the wild-type and mutant *ALDH1A3* mRNAs are in the same range.

A

Filter	sub	del	ins	hom	het	Genes
None	47 594	197	199	20 268	27 722	16 634
Heterozygote variants excluded	20 268	0	0			9897
Variants with frequency ≥ 1% in dbSNP, EVS, 1000Genome excluded.	834	0	0			689
Variants in UTR, non-coding, intergenic and deep intronic regions and synonymous variants excluded	223	0	0			174
Polyphen and sift prediction begnin excluded	28	0	0			27

B

Gene	chr	Start	End	All	sub	ins	del	Coding	Silent	Splicing	Stop
NBPF8	1	144593863	144622156	1	1	0	0	0	0	0	0
OR2T35	1	248802088	248803059	1	1	0	0	1	0	0	0
SLC25A22	11	790975	798816	1	1	0	0	1	0	0	0
SORL1	11	121323412	121504887	1	1	0	0	1	0	0	0
OR10G7	11	123909273	123910217	1	1	0	0	1	0	0	0
MSANTD2	11	124636894	124671069	1	1	0	0	1	0	0	0
ZFHX2	14	23990569	24025901	1	1	0	0	1	0	0	0
AHNAK2	14	105404081	105445194	1	1	0	0	1	0	0	0
ITGA11	15	68594550	68725002	1	1	0	0	1	0	0	0
ALDH1A3	**15**	**101402629**	**101457331**	**1**	**1**	**0**	**0**	**1**	**0**	**0**	**0**
CTB-134H23.2	16	29050423	29064547	1	1	0	0	1	0	0	0
CLEC18B	16	74443029	74456149	1	1	0	0	1	0	0	0
FASN	17	80036715	80056606	1	1	0	0	1	0	0	0
TCEB3C	18	44555073	44556949	1	1	0	0	1	0	0	0
HIF3A	19	46800803	46847190	1	1	0	0	1	0	0	0
FUT2	19	49199728	49209707	1	1	0	0	1	0	0	0
RGPD4	2	108443888	108507797	1	1	0	0	1	0	0	0
PLEKHB2	2	131862920	132111782	1	1	0	0	1	0	0	0
KRTAP10-6	21	46011649	46012886	1	1	0	0	1	0	0	0
EIF4G1	3	184032783	184053646	1	1	0	0	1	0	0	0
LEAP2	5	132208514	132211238	1	1	0	0	1	0	0	0
PCDHB7	5	140552743	140556457	1	1	0	0	1	0	0	0
CTAGE9	6	132030081	132032706	1	1	0	0	1	0	0	0
TRGV9	7	38357118	38358962	1	1	0	0	1	0	0	0
ZAN	7	100331749	100395919	1	1	0	0	1	0	0	0
CPSF1	8	145618944	145635253	1	1	0	0	1	0	0	0
PCSK5	9	78506060	78977755	1	1	0	0	1	0	0	0

Table S1. Whole Exome Resequencing Summary. (A) Filtering strategy of the variants resulting in selection of 28 substitutions in 27 genes. sub: substitution, del: deletion, ins: insertion, hom: homozygous, het: heterozygous, UTR: untranslated region. (B) Genes harboring nonsynonymous

homozygote variants predicted to be deleterious or with unknown effect using the Polyphen and SIFT programs. *ALDH1A3* is the only gene located in the 15q26.3 region. Chr: chromosome.

Exon number	Forward sequence (5'-3')	Reverse sequence (5'-3')	Size of amplified product (bp)
1	GAGCGGGCTGCGCAGTGT	CCGAGACGTCCCGCGAAA	354
2	GGTGGACAAGATGGATAAGA	GCCAGTTCTGTCTTATAGCT	299
3	CCAAACTGCAGTCACCTCAA	CACGACCACACAAAACCAG	368
4-5	GGTGCATCTGACTGTGAG	GCTTGTTCAACGCTGGTG	745
6	CCTCCACAAAGGCATCGTTG	GCCACTGTCCCATCTCGT	392
7	GGATGAGAAGCCCAGGTC	GCCTGTCAAAGGAAAAGCTC	376
8	GAGAGCCAGGTGGTGGCA	GCACACATCTTACTCTCAGT	323
9	GCAGCTGTCACCAGTCCT	GGGACCCTGTAGGCGGTT	348
10	GGCTTGACAAGAACATGCAG	AAGGATTTCTGGGATCCCTG	371
11-12	GCTGAAGCAATGTTTGGACG	GCAGATTGGAGCCTGTGTC	1611
13	CTCCAACGGCCTGATGGA	CAGTAGATGTAAAGCCTCCAG	298

Table S2. Primers Used for MutationScreening of *ALDH1A3*.

Oligonucleotides	Sequence (5'-3')
ALDH1A3-c.265T_forward	GCCTTCCAGAGGGGCTCGCCATGG**T**GCCGGCTGGATGCCCTGAGTCGT
ALDH1A3-c.265A_reverse	CCCACGACTCAGGGCATCCAGCCGGC**A**CCATGGCGAGCCCCTCTGGAA
ALDH1A3-c.1477C_forward	GAAATGGCAGAGAACTAGGTGAATAC**C**CTTTGGCCGAATACACAGAAGTG
ALDH1A3-c.1477G_reverse	CACTTCTGTGTATTCGGCCAAAG**G**GTATTCACCTAGTTCTCTGCCATTTC
ALDH1A3-c.620C_forward	CATGGTCCTGAAGCCTGCGG**C**GCAGACACCTCTCACCGCCCTTT
ALDH1A3-c.620G_reverse	AGGGCGGTGAGAGGTGTCTGC**G**CCGCAGGCTTCAGGACCATGGT

Table S3. Primers Used for Site-Directed Mutagenesis of pCMV6-Entry-*ALDH1A3* Vector

The mutant nucleotides appear in bold underlined.

mRNA	Forward primer (5'-3')	Reverse primer (5'-3')
GFP	GFP-F_TCCAGCAGGACCATGTGATC	(GFP-R)_GTCCGCCCTGAGCAAAGA
ALDH1A3	ALDH1A3-ex12.13F_TGGCAGAGAACTAGGTGA	(c-Myc-R)_GCCAGATCCTCTTCTGAGAT

Table S4. RT-qPCR Primers Used to Assess *ALDH1A3* and *GFP* Expression in Transiently Transfected HEK293 Cells

The use of a primer located in the c-Myc tag with the ALDH1A3-ex12.13F allowed specific amplification of the *ALDH1A3* mRNA encoded by the plasmids.

ARTICLE 14

Recessive and dominant mutations in the retinoic acid receptor beta in cases with microphthalmia and diaphragmatic hernia

American Journal of Human Genetics

2013-93: 1–8

Myriam Srour*, David Chitayat*, Véronique Caron*, **Nicolas Chassaing***, Pierre Bitoun, Lysanne Patry, Marie-Pierre Cordier, José-Mario Capo-Chichi, Christine Francannet, Patrick Calvas, Nicola Ragge, Sylvia Dobrzeniecka, Fadi F. Hamdan, Guy A Rouleau, André Tremblay, Jacques L. Michaud

---

Pour cet article, nous avons été contactés par l'équipe du Pr Michaud (Montréal, Canada). Son équipe avait identifié dans une famille, par une combinaison d'homozygosity mapping et d'exome sequencing, un nouveau gène, *RARB* (Retinoic Acid Receptor beta), impliqué dans une AM syndromique (syndrome PDAC ou syndrome de Matthew-Wood). Ce syndrome de Matthew-Wood a initialement été associé à des mutations du gène *STRA6*, avec une hétérogénéité génétique probable puisque des mutations du gène *STRA6* ne sont pas retrouvées chez tous les patients atteints. Nous avions pu travailler sur le gène *STRA6* et avions des patients atteints du syndrome de Matthew-Wood sans mutation identifiée. Nous avons donc été contactés par l'équipe du Pr Michaud qui recherchait des patients appartenant cliniquement au spectre PDAC, sans mutation dans *STRA6*. Nous avons pu, en collaboration avec le Dr Nicola Ragge, inclure 15 patients (10 de Toulouse, 5 d'Oxford) correspondant à ces critères, ainsi que 15 patients avec anophtalmie ou microphtalmie extrême. Le séquençage du gène *RARB* chez ces patients a permis d'identifier chez 3 d'entre eux une variation faux-sens hétérozygote touchant le même codant du gène *RARB*. Ces variations n'étaient pas rapportées dans les bases de données, et la présence d'une variation hétérozygote du même codon (p.Arg387Cys et p.Arg387Ser) chez trois individus non apparentés suggérait un possible effet

dominant (mutation activatrice ou dominante négative). Cette hypothèse a été confortée par l'analyse parentale qui chez les trois patients a permis de montrer que le variant faux-sens de ce codon Arg387 étaient apparues *de novo*. Cette hypothèse a secondairement été confirmée par des analyses fonctionnelles démontrant l'effet activateur des mutations touchant ce codon, et l'effet perte de fonction des mutations récessives identifiées dans la première famille de cette étude. Cette étude implique ainsi un nouveau gène de la voie du métabolisme de l'acide rétinoïque dans l'AM. Des mutations de ce gène peuvent être transmises selon une transmission autosomique dominante ou récessive.

Please cite this article in press as: Srour et al., Recessive and Dominant Mutations in Retinoic Acid Receptor Beta in Cases with Microphthalmia and Diaphragmatic Hernia, The American Journal of Human Genetics (2013), http://dx.doi.org/10.1016/j.ajhg.2013.08.014

REPORT

Recessive and Dominant Mutations in Retinoic Acid Receptor Beta in Cases with Microphthalmia and Diaphragmatic Hernia

Myriam Srour,[1,12] David Chitayat,[2,3,12] Véronique Caron,[1,12] Nicolas Chassaing,[4,5,12] Pierre Bitoun,[6] Lysanne Patry,[1] Marie-Pierre Cordier,[7] José-Mario Capo-Chichi,[1] Christine Francannet,[8] Patrick Calvas,[4,5] Nicola Ragge,[9,10] Sylvia Dobrzeniecka,[11] Fadi F. Hamdan,[1] Guy A. Rouleau,[11] André Tremblay,[1] and Jacques L. Michaud[1,*]

Anophthalmia and/or microphthalmia, pulmonary hypoplasia, diaphragmatic hernia, and cardiac defects are the main features of PDAC syndrome. Recessive mutations in *STRA6*, encoding a membrane receptor for the retinol-binding protein, have been identified in some cases with PDAC syndrome, although many cases have remained unexplained. Using whole-exome sequencing, we found that two PDAC-syndrome-affected siblings, but not their unaffected sibling, were compound heterozygous for nonsense (c.355C>T [p.Arg119*]) and frameshift (c.1201_1202insCT [p.Ile403Serfs*15]) mutations in retinoic acid receptor beta (*RARB*). Transfection studies showed that p.Arg119* and p.Ile403Serfs*15 altered RARB had no transcriptional activity in response to ligands, confirming that the mutations induced a loss of function. We then sequenced *RARB* in 15 subjects with anophthalmia and/or microphthalmia and at least one other feature of PDAC syndrome. Surprisingly, three unrelated subjects with microphthalmia and diaphragmatic hernia showed de novo missense mutations affecting the same codon; two of the subjects had the c.1159C>T (Arg387Cys) mutation, whereas the other one carried the c.1159C>A (p.Arg387Ser) mutation. We found that compared to the wild-type receptor, p.Arg387Ser and p.Arg387Cys altered RARB induced a 2- to 3-fold increase in transcriptional activity in response to retinoic acid ligands, suggesting a gain-of-function mechanism. Our study thus suggests that both recessive and dominant mutations in *RARB* cause anophthalmia and/or microphthalmia and diaphragmatic hernia, providing further evidence of the crucial role of the retinoic acid pathway during eye development and organogenesis.

Anophthalmia or microphthalmia (A/M) refers to the absence or reduced size of the axial diameter of the globe in the ocular orbit, respectively. In over 50% of cases, A/M is associated with other congenital abnormalities.[1,2] The combination of pulmonary hypoplasia or agenesis, diaphragmatic hernia or eventration, A/M, and cardiac defects is characteristic of PDAC syndrome, which is also known as Matthew-Wood syndrome or Spear syndrome (MIM 601186).[3] In some individuals, PDAC syndrome is caused by autosomal-recessive mutations in *STRA6* (MIM 610745), encoding a membrane receptor for the retinol-binding protein.[4,5] Many cases of PDAC syndrome, however, remain unexplained.

In this study, we performed whole-exome sequencing in a nonconsanguineous family affected by PDAC syndrome to uncover the genetic cause (Figure 1A). The parents have two healthy daughters and four affected children, of whom two have all the features of PDAC syndrome and two have at least two features of PDAC syndrome (individuals II-1, II-4, II-5, and II-6 in family A, see Table 1 for clinical details). This family was described previously (cases 1A [II-4], 2A [II-5], and 3A [II-6] from family A in Chitayat et al.[3]). *STRA6* was previously sequenced in one affected individual of this family, and no mutation was identified.

This study was approved by our institutional ethics committee, and informed consent was obtained from each participant or legal guardian. Blood genomic DNA from affected individuals II-4 and II-5 and the unaffected sister (II-2) from family A was captured with the Agilent SureSelect Human All Exon Capture V4 Kit and sequenced (two paired-end 100 bp reads, three exomes per lane) with Illumina HiSeq2000 at the McGill University Genome Quebec Innovation Center (Montreal). Sequence processing, alignment (with a Burrows-Wheeler algorithm), and variant calling were done according to the Broad Institute Genome Analysis Toolkit (GATK v.4) best practices, and variant annotation was done with ANNOVAR.[6] The average exome coverage of the target bases was 111–114×, and 95% of the target bases were covered by at least 20 reads. Only the variants whose positions were covered ≥8× and supported by at least three variant reads constituting at least 20% of the total reads for each called

[1]Centre Hospitalier Universitaire Sainte-Justine Research Center, Montreal, QC H3T1C5, Canada; [2]Prenatal Diagnosis and Medical Genetics Program, Mount Sinai Hospital, Toronto, ON M5G 1X5, Canada; [3]Division of Clinical and Metabolic Genetics, The Hospital for Sick Children, Toronto, ON M5G 1X8, Canada; [4]Service de Génétique Médicale, Hôpital Purpan, Centre Hospitalier Universitaire de Toulouse, 31059 Toulouse, France; [5]Equipe d'Accueil 4555, Université Toulouse III - Paul-Sabatier, 31000 Toulouse, France; [6]Génétique Médicale, Hôpital Jean Verdier, Centre Hospitalier Universitaire Paris Nord, Assistance Publique – Hôpitaux de Paris, 93140 Bondy, France; [7]Service de Génétique, Hospices Civils de Lyon, F-69677 Bron, France; [8]Service de Génétique Médicale, Hôtel Dieu, 63058 Clermont-Ferrand, France; [9]School of Life Sciences, Oxford Brookes University, Oxford OX3 0BP, UK; [10]Clinical Genetics Unit, Birmingham Women's Hospital, Birmingham B15 2TG, UK; [11]Montreal Neurological Institute, McGill University, Montreal, QC H3A 2B4, Canada

[12]These authors contributed equally to this work

*Correspondence: jacques.michaud@recherche-ste-justine.qc.ca

http://dx.doi.org/10.1016/j.ajhg.2013.08.014.

Please cite this article in press as: Srour et al., Recessive and Dominant Mutations in Retinoic Acid Receptor Beta in Cases with Microphthalmia and Diaphragmatic Hernia, The American Journal of Human Genetics (2013), http://dx.doi.org/10.1016/j.ajhg.2013.08.014

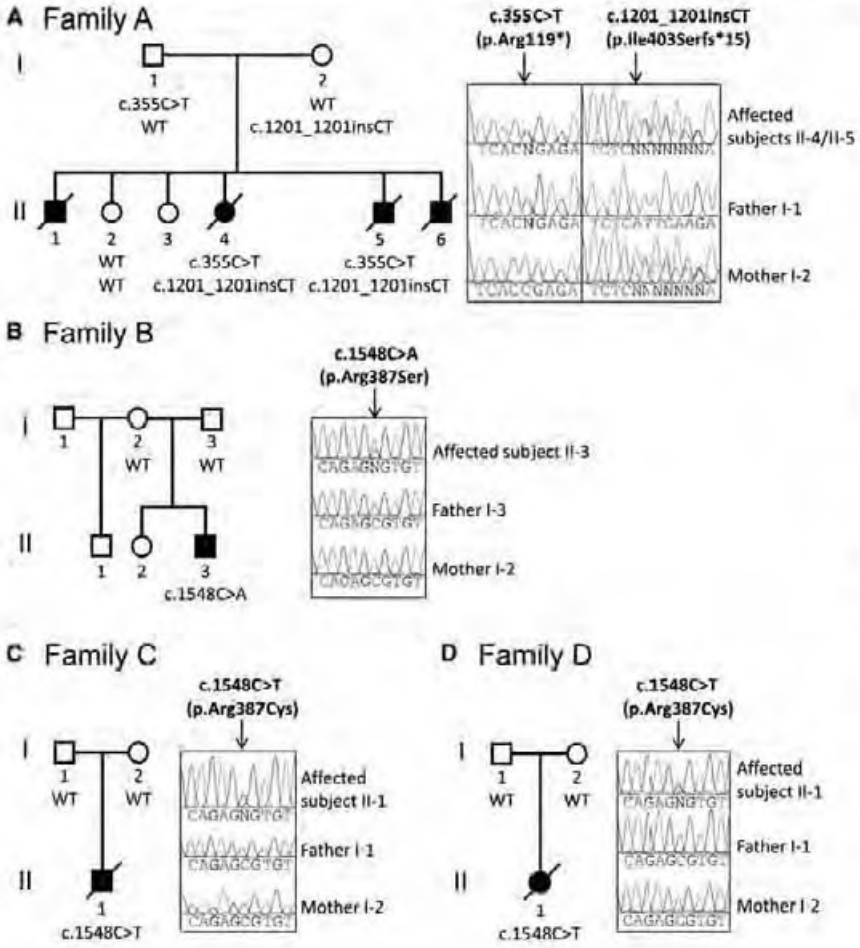

Figure 1. Mutations in *RARB* in Individuals with PDAC Syndrome

Sanger sequencing confirmed segregation of the recessive mutations in *RARB* in family A (A) and revealed that the mutations were de novo in families B (B), C (C), and D (D).

position were retained. To identify potentially pathogenic variants, we filtered out (1) synonymous variants or intronic variants other than those affecting the consensus splice sites, (2) variants seen in more than 2% of our in-house exomes (n = 1,000) from unrelated projects, and (3) variants with a minor allele frequency greater than 0.5% in either the 1000 Genomes Project or the National Heart, Lung, and Blood Institute (NHLBI) Exome Sequencing Project Exome Variant Server (EVS). The affected individuals did not share any rare coding or splicing variants in *STRA6* or *ALDH1A3* (MIM 600463), another gene involved in A/M and retinoic acid (RA) signaling.[7]

Given that transmission of the phenotype in this family was consistent with autosomal-recessive inheritance, we searched the whole-exome data sets for genes harboring homozygous or multiple rare variants in both affected probands, but not in their unaffected sibling. There were no such genes with rare homozygous variants. Only three genes containing multiple rare variants in both affected individuals were not shared by the unaffected sister: *PRPF39* (MIM 614907), *RARB* (MIM 180220), and *GAPVD1* (MIM 611714). Sanger sequencing in the parents and the siblings revealed that the variants in *PRPF39* were inherited in *cis*, thus excluding this gene as a candidate.

The affected probands, but not the unaffected sister, were compound heterozygous and the parents were singly heterozygous for the variants in *RARB* and *GAPVD1* (Figure 1A). *RARB* (RefSeq accession number NM_000965.3), which encodes RA receptor beta (RARB), was found to harbor two protein-truncating mutations: nonsense c.355C>T (p.Arg119*) and frameshift c.1201_1202insCT (p.Ile403Serfs*15). These variants are absent from all public SNP databases (1000 Genomes, EVS, and dbSNP138) and from our in-house exomes (n > 1,000). *RARB* has two major isoforms noted in the UCSC Genome Browser and three additional isoforms noted in the Ensembl Genome Browser. The major RefSeq isoform (RefSeq NM_000965.3) has eight exons and encodes a 448 aa protein. Both identified mutations affect all known *RARB* isoforms (Figure 2A). *GAPVD1* (RefSeq NM_015635), which encodes GTPase-activating protein and VPS9 domain 1, was found to harbor two rare missense variants, c.2809C>T (p.Arg937Trp) and c.3266G>T (p.Gly1089Val), in the probands. The p.Arg937Trp substitution is predicted to be damaging by both SIFT (score 0.0) and PolyPhen-2 (score 1.0), but the p.Gly1089Val substitution is predicted to be benign by both SIFT (score 0.2) and PolyPhen-2 (score 0.145). *GAPVD1* is involved in endocytosis,[8] phagosome maturation,[9] and regulation of the epidermal growth factor receptor[10] but is not known to have a role in eye development or embryogenesis. Because of the importance of the RA pathway for eye and diaphragm development (discussed below), mutations in *RARB* were deemed more likely to be pathogenic than those in *GAPVD1*.

RA receptors bind to DNA motifs known as RA response elements (RAREs) to modulate transcription of target genes by interacting with transcriptional corepressors and coactivators. Upon binding to RA, the corepressor docking site becomes hindered by helix 12 positioning, resulting in the recruitment of coactivators and an increase in transcription of target genes.[11] The c.355C>T (p.Arg119*) nonsense mutation is predicted to result in an inactive truncated receptor lacking the second zinc finger of the

Please cite this article in press as: Srour et al., Recessive and Dominant Mutations in Retinoic Acid Receptor Beta in Cases with Microphthalmia and Diaphragmatic Hernia, The American Journal of Human Genetics (2013), http://dx.doi.org/10.1016/j.ajhg.2013.08.014

Table 1. Clinical Characteristics of Subjects with Mutations in *RARB*

	Family A				Family B	Family C	Family D
	II-1	II-4	II-5	II-6	II-3	II-1	II-1
Ethnicity	French Canadian and English				French	African (Angola [father] and Congo [mother])	French
Consanguinity	–	–	–	–	–	–	–
Mutation(s)	NA	c.355C>T (p.Arg119*) and c.1201_1202insCT (p.Ile403Serfs*15)	c.355C>T (p.Arg119*) and c.1201_1202insCT (p.Ile403Serfs*15)	NA	c.1159 > A (p.Arg387Ser)[a]	c.1159C>T (p.Arg387Cys)[a]	c.1159C>T (p.Arg387Cys)[a]
Gender	male	female	male	male	male	male	female
Age (age at death)	(few hours; 34 weeks of gestation)[b]	(few hours; 38 weeks of gestation)	(21-week-old fetus)[c]	(few hours; term)	16 years	(34-week-old fetus)[c]	(few hours; 39 weeks of gestation)
Bilateral A/M	+	+	+	+	+	unilateral (left) microphthalmia; normal right eye	bilateral microphthalmia
Pulmonary hypoplasia	NA	–	+	NA	–	left lung with one hypoplastic lobe; normal right lung	bilateral (predominant on the left side)
Diaphragmatic hernia	NA	+	+	–	+	+ (left)	+ (left)
Cardiac abnormality	NA	+	–	NA	–	–	–
Intellectual disability	NA	NA	NA	NA	+	NA	NA
Other	–	cleft palate, dysmorphisms, small spleen, bicornate and small uterus	dysmorphisms, unfixed malrotated bowel	dysmorphisms	–	malrotated bowel, right cryptorchidy, mild IUGR (weight and length), and OFC at the fifth percentile	bicornate uterus

Abbreviations are as follows: NA, not available; IUGR, intrauterine growth restriction; and OFC, occipitofrontal circumference.
[a]De novo mutation.
[b]Died shortly after birth at 34 weeks as a result of a presumed tangled cord, although a diagnosis of PDAC was strongly suspected.
[c]Terminated pregnancy.

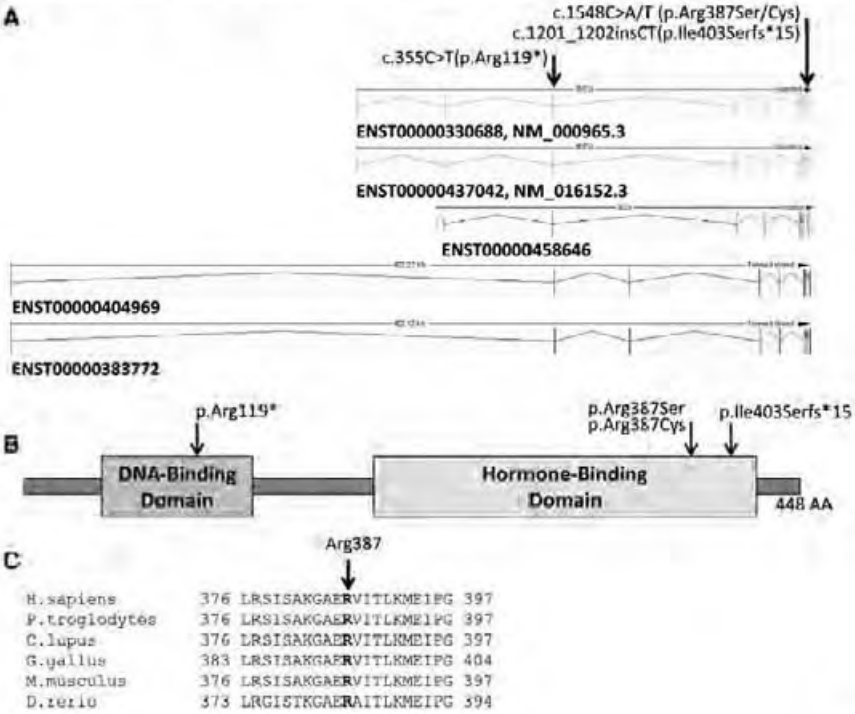

Figure 2. Localization and Impact of the Mutations in *RARB*

(A) Shown are the positions of the mutations with respect to the different *RARB* Ensembl-annotated transcripts that are predicted to produce proteins. Numbering on top is based on the cDNA positions of Ensembl ENST00000330688 (identical to RefSeq NM_000965.3).

(B) A schematic of RARB shows the DNA-binding and hormone-binding domains. Arrowheads above the protein show the positions of the variants.

(C) The HomoloGene-generated amino acid alignment of human RARB and its predicted orthologs shows the conservation of the p.Arg387 residue.

(D) The three-dimensional structure of RARB (Protein Data Bank ID 4DM8) in the presence of the RA ligand (purple) shows the proximity of the Arg387 residue in helix 11 to the RA ligand.

DNA-binding domain and the entire ligand-binding domain (Figure 2B). Moreover, this mutation has the potential to activate the nonsense-mediated mRNA decay pathway, resulting in the degradation of the corresponding transcript. The c.1201_1202insCT (p.Ile403Serfs*15) mutation results in the substitution of a hydrophobic isoleucine with serine, a polar residue, and the replacement of the last 52 amino acids with an aberrant extension of 15 amino acids (Figure 2B). As part of helix 12, residue Ile403 is thus predicted to play a key role in the recruitment of transcriptional cofactors and response to ligand. As such, in vitro studies have shown that Ile403 substitution with serine in RARB confers an increased binding to corepressor SMRT in the absence of ligand and thus results in reduced transcriptional activity.[12] Both mutations found in family A are thus predicted to disrupt *RARB* function.

We tested the impact of these truncating mutations on RARB activity by using a cellular one-hybrid luciferase-reporter transcriptional assay as previously described.[13] Expression plasmids encoding transcription factor Gal4 DNA-binding domain fusions to wild-type RARB or truncated variants p.Arg119* and p.Ile403Serfs*15 were generated and used for transfecting human embryonic kidney 293 (HEK293) cells in the presence of a luciferase reporter gene construct under the control of a Gal4-binding DNA upstream-activating sequence (UAStkLuc). This assay allowed transcriptional activity and response to ligand to be directly compared between variants and the wild-type receptor, avoiding any background effect of endogenously expressed RARB in cells. Transfected HEK293 cells were treated with the natural ligands all-*trans* RA (atRA) and its stereoisomer, 9-*cis* RA, which both act as pan-RAR agonists. As expected, compared to that of wild-type RARB, the transcriptional response of the p.Arg119* variant to the two RA ligands was completely abolished, correlating with its lack of ligand-binding domain (Figure 3). Similarly, compared to wild-type RARB, the p.Ile403Serfs*15 variant showed an impaired transcriptional response to retinoids. In the p.Ile403Serfs*15 variant, the disruption of helix 12 and its replacement with an aberrant extension most likely interfered with its ability to occlude the corepressor docking site. All together, these results strongly suggest that these truncating variants confer a loss of RARB function and explain the occurrence of PDAC syndrome in family A.

We next sequenced all the coding exons and intron-exon boundaries of *RARB* and the alternate exon 1

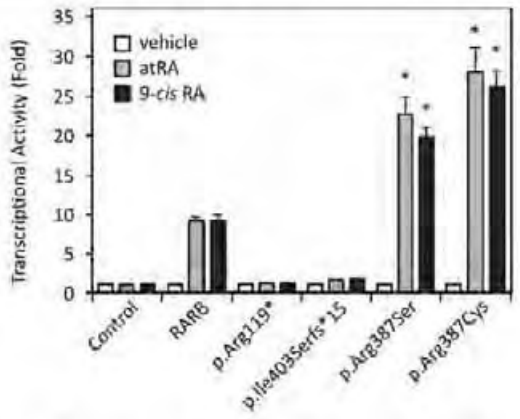

Figure 3. Transcriptional Response of Human RARB Variants to RA Ligands

HEK293 cells were seeded in 24-well plates and transfected with 100 ng per well of expression plasmid encoding either Gal4 fusion of wild-type human RARB or p.Arg119*, p.Ile403Serfs*15, p.Arg387Ser, or p.Arg387Cys RARB variants in the presence of 500 ng of UAStkLuc reporter-gene construct. All variant constructs, including p.Ile403Serfs*15 (carrying the additional out-of-frame amino acid extension), were generated by site-directed mutagenesis. Cells were treated with 1 μM atRA, 1 μM 9-*cis* RA, or vehicle (DMSO; 1/1,000, v/v) for 16 hr. Luciferase values were normalized to β-galactosidase activity and expressed as a fold response compared to those of empty Gal4-transfected control cells. Data were derived from three independent experiments performed in triplicate. *$p < 0.005$ versus wild-type RARB response to the respective RA ligand. Values represent means, and error bars represent SEs.

(Ensembl accession number ENST00000404969) in 15 additional individuals who had bilateral or unilateral A/M and at least one additional feature of PDAC (diaphragmatic hernia, cardiac defect, or lung hypoplasia) and who had been previously screened for mutations in *STRA6*.[14] In three unrelated subjects, who were all simplex cases, we identified single heterozygous *RARB* missense mutations affecting the same nucleotide. Of these, two subjects (II-1 from family C and II-1 from family D) harbored missense mutation c.1159C>T (p.Arg387Cys) and one individual (II-3 from family B) harbored missense mutation c.1159C>A (p.Arg387Ser) (Figures 1B and 1C). These mutations were absent from the genomic DNA of the parents, indicating that they occurred de novo. Using six informative unlinked microsatellite markers (D3S1754, D4S3351, D8S1179, D15S659, D14S587, and D19S215), we confirmed the paternity and maternity in these families, as previously described.[15] Both c.1159C>T (p.Arg387Cys) and c.1159C>A (p.Arg387Ser) are absent from public SNP databases (EVS, 1000 Genomes, and dbSNP138) and from our entire collection of in-house exomes (n >1,000). They are both predicted to be damaging by SIFT (score 0.0) and PolyPhen-2 (score 1.0) and affect a highly conserved amino acid in helix 11 of the ligand-binding domain (Figure 2C). Subject II-1 from family C was a fetus for whom pregnancy was terminated because of unilateral microphthalmia and left diaphragmatic hernia on prenatal ultrasound (Table 1). Autopsy also showed hypoplasia of a pulmonary lobe on the left side. Subject II-1 from family D was a newborn who passed away within a few hours after birth because of a left diaphragmatic hernia. This subject also showed bilateral microphthalmia and pulmonary hypoplasia. Subject II-3 from family B is currently a 14-year-old male with bilateral microphthalmia, corrected diaphragmatic hernia, and abnormal cognitive development with spasticity (for clinical details, see case 6 in Chitayat et al.[3]). We also sequenced *RARB* in 11 cases with isolated bilateral A/M, but we did not find any mutation in this gene.

The fact that the de novo mutations involved the same residue (Arg387) suggests that they confer a specific property to the protein. These mutations could induce a dominant-negative effect or act through a gain-of-function mechanism. In order to distinguish between these possibilities, we sought to study the impact of these mutations by using our one-hybrid functional assay. The p.Arg387Ser and p.Arg387Cys altered RARB exhibited a significant increase in their transcriptional response to atRA; they reached 23- and 28-fold induction, respectively, compared to 9-fold induction for wild-type RARB (Figure 3). Similar activation levels were also obtained with the 9-*cis* RA ligand. These results suggest that the two variants at Arg387 provide increased transcriptional potential to respond to retinoid ligands through a gain-of-function mechanism. Explaining such an increase in activity will require a more detailed mechanistic analysis.

We have identified compound-heterozygous truncating mutations and de novo mutations affecting the same *RARB* nucleotide in individuals with PDAC syndrome. The occurrence of such mutations in individuals with a similar and rare phenotype strongly suggests that they cause PDAC syndrome. Indeed, several observations indicate that the RA pathway plays a major role in the development of the eyes, diaphragm, and lungs. RA is a metabolite of retinol, a derivative of vitamin A. The importance of the RA pathway in embryogenesis has been recognized for decades, given that rats deficient in vitamin A give birth to progeny with multiple congenital malformations, including ocular abnormalities and diaphragmatic hernia.[16] Circulating retinol is bound to retinol-binding protein 4 (RBP4). The transmembrane protein STRA6 (stimulated by RA) facilitates the intracellular uptake of the retinol-RBP complex.[4] Mutations in *STRA6* have been identified in at least 24 individuals with A/M.[5,14,17–19] Most of these subjects showed other features of PDAC syndrome, but some of them had isolated A/M. Once transported into the cell, retinol is successively oxidized to retinaldehyde and RA. Mutations in *ALDH1A3*, which encodes a retinaldehyde dehydrogenase that is responsible for the oxidation of retinaldehyde into RA, have been found to be responsible for A/M with variable neurodevelopmental and cardiac features.[7]

In target cells, RA acts as a ligand for nuclear RA receptors. Several observations in mice suggest that these receptors play a major role in eye, diaphragm, and lung

development. Mice lacking all *Rarb* isoforms display microphthalmia.[20,21] RA is generated in the epithelial ocular compartment and diffuses in the neural-crest-cell-derived periocular mesenchyme to activate RARB and RARG. In turn, these receptors regulate the remodeling of the periocular mesenchyme, the growth of the ventral retina, and the expression of *Foxc1* and *Pitx2*, which play central roles in the development of the anterior eye segment.[22] Studies of mutant mice lacking both *Rara* and *Rarb* subtypes have also demonstrated the presence of diaphragmatic hernias in a subset of offspring.[23] Moreover, administration of nitrofen to pregnant rodents is thought to cause diaphragmatic hernias, in part through downregulation of RA receptor signaling (reviewed in Greer et al.[24]). Recent studies have indicated that *Rarb* functions along a pathway that directs development of the central tendon of the diaphragm.[25] Finally, *Rarb*$^{-/-}$ mice have smaller and more numerous alveoli in their lungs.[26] *Rarb* has been shown to have a critical role in lung morphogenesis by inducing *Fgf10* expression in bud fields.[27] Overall, these studies support our conclusion that loss of RARB function causes PDAC syndrome in family A.

Our transfection experiments suggest that the de novo mutations affecting Arg387 result in enhanced activity of RARB in response to RA ligands, suggesting a gain-of-function mechanism. Whether these two substitutions induce a conformational change that enhances protein stability, favors coactivator recruitment, and/or increases RA binding affinity remains to be determined. Consistent with this latter possibility, crystallographic studies have established that the Arg387 residue is facing inward relative to the ligand-binding pocket, in close proximity to the retinoid ligand (Figure 2D). Our model of gain-of-function mutations thus suggests that an increase in RARB response to retinoids might represent a primary cause of PDAC syndrome. Indeed, excess of vitamin A or RA during development in mice causes various malformations, including microphthalmia and diaphragmatic hernia.[28–32] Moreover, expression of a constitutively active RAR transgene in the developing eye results in animals that exhibit microphthalmia.[33] Similarly, zebrafish embryos exposed to 9-*cis*-RA develop multiple developmental abnormalities, including microphthalmia.[34] RA is also teratogenic in humans.[35] Interestingly, microphthalmia and diaphragmatic hernia have been reported in some babies from women exposed to RA during pregnancy.[35,36]

All together, our findings and the previous work described above therefore suggest that both decreased and increased RARB activity can result in PDAC syndrome. A recent study showed that RA exposure during embryonic development in mice was followed by decreased levels of *Raldh* transcripts encoding RA-synthesizing enzymes and increased levels of *Cyp26a1* and *Cyp26b1*, mRNAs encoding enzymes that catabolize RA.[32] Overall, these changes resulted in a decrease in RA levels. Restoration of RA levels by maternal supplementation with low doses of RA after the teratogenic insult rescued several developmental defects. Paradoxically, increased RARB signaling could thus result in a secondary state of RA deficiency, which could have an impact on this pathway at specific stages of development. Alternatively, it is possible that some developmental processes require a tight regulation of RARB targets, given that too little or too much signaling has the same consequence on these pathways.

In summary, we found that both recessive and dominant *RARB* mutations affect RARB function in the context of PDAC syndrome, opening a new window on the structural and mechanistic basis of RA receptor activity as it relates to human disease.

Acknowledgments

J.L.M. is a National Scientist of the Fonds de Recherche du Québec - Santé. M.S. holds a clinician-scientist award from the Canadian Institute for Health Research. We wish to thank the members of the bioinformatic analysis team of Réseau de Médecine Génétique Appliquée du Québec (Alexandre Dionne-Laporte, Dan Spiegelman, Edouard Henrion, and Ousmane Diallo) for the analysis of the exome sequencing data. This research was funded by a grant from the Canadian Institutes of Health Research (MOP 106499) to J.L.M. and by grants from the Clinical Research Hospital Program from the French Ministry of Health (PHRC 09 109 01) and Retina France to N.C.

Received: July 2, 2013
Revised: August 13, 2013
Accepted: August 22, 2013
Published: September 26, 2013

Web Resources

The URLs for data presented herein are as follows:

1000 Genomes Project, http://browser.1000genomes.org/index.html
dbSNP, http://www.ncbi.nlm.nih.gov/projects/SNP/
Ensembl Genome Browser, http://www.ensembl.org/index.html
GATK Best Practices, http://www.broadinstitute.org/gatk/guide/topic?name=best-practices
HomoloGene (NCBI), http://www.ncbi.nlm.nih.gov/homologene
NHLBI Exome Sequencing Project (ESP) Exome Variant Server (EVS), http://evs.gs.washington.edu/EVS/
Online Mendelian Inheritance in Man (OMIM), http://www.omim.org
PolyPhen-2, http://genetics.bwh.harvard.edu/pph2/
Protein Data Bank, http://www.rcsb.org/pdb
RefSeq, http://www.ncbi.nlm.nih.gov/RefSeq
SIFT, http://sift.jcvi.org/
UCSC Genome Browser, http://genome.ucsc.edu/

References

1. Shaw, G.M., Carmichael, S.L., Yang, W., Harris, J.A., Finnell, R.H., and Lammer, E.J. (2005). Epidemiologic characteristics of anophthalmia and bilateral microphthalmia among 2.5 million births in California, 1989-1997. Am. J. Med. Genet. A. *137*, 36–40.

2. Källén, B., Robert, E., and Harris, J. (1996). The descriptive epidemiology of anophthalmia and microphthalmia. Int. J. Epidemiol. *25*, 1009–1016.
3. Chitayat, D., Sroka, H., Keating, S., Colby, R.S., Ryan, G., Toi, A., Blaser, S., Viero, S., Devisme, L., Boute-Bénéjean, O., et al. (2007). The PDAC syndrome (pulmonary hypoplasia/agenesis, diaphragmatic hernia/eventration, anophthalmia/microphthalmia, and cardiac defect) (Spear syndrome, Matthew-Wood syndrome): report of eight cases including a living child and further evidence for autosomal recessive inheritance. Am. J. Med. Genet. A. *143A*, 1268–1281.
4. Kawaguchi, R., Yu, J., Honda, J., Hu, J., Whitelegge, J., Ping, P., Wiita, P., Bok, D., and Sun, H. (2007). A membrane receptor for retinol binding protein mediates cellular uptake of vitamin A. Science *315*, 820–825.
5. Pasutto, F., Sticht, H., Hammersen, G., Gillessen-Kaesbach, G., Fitzpatrick, D.R., Nürnberg, G., Brasch, F., Schirmer-Zimmermann, H., Tolmie, J.L., Chitayat, D., et al. (2007). Mutations in STRA6 cause a broad spectrum of malformations including anophthalmia, congenital heart defects, diaphragmatic hernia, alveolar capillary dysplasia, lung hypoplasia, and mental retardation. Am. J. Hum. Genet. *80*, 550–560.
6. Wang, K., Li, M., and Hakonarson, H. (2010). ANNOVAR: functional annotation of genetic variants from high-throughput sequencing data. Nucleic Acids Res. *38*, e164.
7. Fares-Taie, L., Gerber, S., Chassaing, N., Clayton-Smith, J., Hanein, S., Silva, E., Serey, M., Serre, V., Gérard, X., Baumann, C., et al. (2013). ALDH1A3 mutations cause recessive anophthalmia and microphthalmia. Am. J. Hum. Genet. *92*, 265–270.
8. Hunker, C.M., Galvis, A., Kruk, I., Giambini, H., Veisaga, M.L., and Barbieri, M.A. (2006). Rab5-activating protein 6, a novel endosomal protein with a role in endocytosis. Biochem. Biophys. Res. Commun. *340*, 967–975.
9. Kitano, M., Nakaya, M., Nakamura, T., Nagata, S., and Matsuda, M. (2008). Imaging of Rab5 activity identifies essential regulators for phagosome maturation. Nature *453*, 241–245.
10. Su, X., Kong, C., and Stahl, P.D. (2007). GAPex-5 mediates ubiquitination, trafficking, and degradation of epidermal growth factor receptor. J. Biol. Chem. *282*, 21278–21284.
11. Glass, C.K., and Rosenfeld, M.G. (2000). The coregulator exchange in transcriptional functions of nuclear receptors. Genes Dev. *14*, 121–141.
12. Farboud, B., and Privalsky, M.L. (2004). Retinoic acid receptor-alpha is stabilized in a repressive state by its C-terminal, isotype-specific F domain. Mol. Endocrinol. *18*, 2839–2853.
13. Demers, A., Caron, V., Rodrigue-Way, A., Wahli, W., Ong, H., and Tremblay, A. (2009). A concerted kinase interplay identifies PPARgamma as a molecular target of ghrelin signaling in macrophages. PLoS ONE *4*, e7728.
14. Chassaing, N., Ragge, N., Kariminejad, A., Buffet, A., Ghaderi-Sohi, S., Martinovic, J., and Calvas, P. (2013). Mutation analysis of the STRA6 gene in isolated and non-isolated anophthalmia/microphthalmia. Clin. Genet. *83*, 244–250.
15. Berryer, M.H., Hamdan, F.F., Klitten, L.L., Møller, R.S., Carmant, L., Schwartzentruber, J., Patry, L., Dobrzeniecka, S., Rochefort, D., Neugnot-Cerioli, M., et al. (2013). Mutations in SYNGAP1 cause intellectual disability, autism, and a specific form of epilepsy by inducing haploinsufficiency. Hum. Mutat. *34*, 385–394.
16. Wilson, J.G., Roth, C.B., and Warkany, J. (1953). An analysis of the syndrome of malformations induced by maternal vitamin A deficiency. Effects of restoration of vitamin A at various times during gestation. Am. J. Anat. *92*, 189–217.
17. Chassaing, N., Golzio, C., Odent, S., Lequeux, L., Vigouroux, A., Martinovic-Bouriel, J., Tiziano, F.D., Masini, L., Piro, F., Maragliano, G., et al. (2009). Phenotypic spectrum of STRA6 mutations: from Matthew-Wood syndrome to non-lethal anophthalmia. Hum. Mutat. *30*, E673–E681.
18. Casey, J., Kawaguchi, R., Morrissey, M., Sun, H., McGettigan, P., Nielsen, J.E., Conroy, J., Regan, R., Kenny, E., Connican, P., et al. (2011). First implication of STRA6 mutations in isolated anophthalmia, microphthalmia, and coloboma: a new dimension to the STRA6 phenotype. Hum. Mutat. *32*, 1417–1426.
19. White, T., Lu, T., Metlapally, R., Katowitz, J., Kherani, F., Wang, T.Y., Tran-Viet, K.N., and Young, T.L. (2008). Identification of STRA6 and SKI sequence variants in patients with anophthalmia/microphthalmia. Mol. Vis. *14*, 2458–2465.
20. Ghyselinck, N.B., Dupé, V., Dierich, A., Messaddeq, N., Garnier, J.M., Rochette-Egly, C., Chambon, P., and Mark, M. (1997). Role of the retinoic acid receptor beta (RARbeta) during mouse development. Int. J. Dev. Biol. *41*, 425–447.
21. Zhou, G., Strom, R.C., Giguere, V., and Williams, R.W. (2001). Modulation of retinal cell populations and eye size in retinoic acid receptor knockout mice. Mol. Vis. *7*, 253–260.
22. Matt, N., Dupé, V., Garnier, J.M., Dennefeld, C., Chambon, P., Mark, M., and Ghyselinck, N.B. (2005). Retinoic acid-dependent eye morphogenesis is orchestrated by neural crest cells. Development *132*, 4789–4800.
23. Mendelsohn, C., Lohnes, D., Décimo, D., Lufkin, T., LeMeur, M., Chambon, P., and Mark, M. (1994). Function of the retinoic acid receptors (RARs) during development (II). Multiple abnormalities at various stages of organogenesis in RAR double mutants. Development *120*, 2749–2771.
24. Greer, V.P., Mason, P., Kirby, A.J., Smith, H.J., Nicholls, P.J., and Simons, C. (2003). Some 1,2-diphenylethane derivatives as inhibitors of retinoic acid—metabolising enzymes. J. Enzyme Inhib. Med. Chem. *18*, 431–443.
25. Coles, G.L., and Ackerman, K.G. (2013). Kif7 is required for the patterning and differentiation of the diaphragm in a model of syndromic congenital diaphragmatic hernia. Proc. Natl. Acad. Sci. USA *110*, E1898–E1905.
26. Massaro, G.D., Massaro, D., Chan, W.Y., Clerch, L.B., Ghyselinck, N., Chambon, P., and Chandraratna, R.A. (2000). Retinoic acid receptor-beta: an endogenous inhibitor of the perinatal formation of pulmonary alveoli. Physiol. Genomics *4*, 51–57.
27. Desai, T.J., Chen, F., Lü, J., Qian, J., Niederreither, K., Dollé, P., Chambon, P., and Cardoso, W.V. (2006). Distinct roles for retinoic acid receptors alpha and beta in early lung morphogenesis. Dev. Biol. *291*, 12–24.
28. Padmanabhan, R., Singh, G., and Singh, S. (1981). Malformations of the eye resulting from maternal hypervitaminosis A during gestation in the rat. Acta Anat. (Basel) *110*, 291–298.
29. Sulik, K.K., Dehart, D.B., Rogers, J.M., and Chernoff, N. (1995). Teratogenicity of low doses of all-trans retinoic acid in presomite mouse embryos. Teratology *51*, 398–403.
30. Ozeki, H., and Shirai, S. (1998). Developmental eye abnormalities in mouse fetuses induced by retinoic acid. Jpn. J. Ophthalmol. *42*, 162–167.

31. Ozeki, H., Shirai, S., Ikeda, K., and Ogura, Y. (1999). Critical period for retinoic acid-induced developmental abnormalities of the vitreous in mouse fetuses. Exp. Eye Res. *68*, 223–228.
32. Lee, L.M., Leung, C.Y., Tang, W.W., Choi, H.L., Leung, Y.C., McCaffery, P.J., Wang, C.C., Woolf, A.S., and Shum, A.S. (2012). A paradoxical teratogenic mechanism for retinoic acid. Proc. Natl. Acad. Sci. USA *109*, 13668–13673.
33. Balkan, W., Klintworth, G.K., Bock, C.B., and Linney, E. (1992). Transgenic mice expressing a constitutively active retinoic acid receptor in the lens exhibit ocular defects. Dev. Biol. *151*, 622–625.
34. Shi, H., Zhu, P., Sun, Z., Yang, B., and Zheng, L. (2012). Divergent teratogenicity of agonists of retinoid X receptors in embryos of zebrafish (Danio rerio). Ecotoxicology *21*, 1465–1475.
35. Benke, P.J. (1984). The isotretinoin teratogen syndrome. JAMA *251*, 3267–3269.
36. Loureiro, K.D., Kao, K.K., Jones, K.L., Alvarado, S., Chavez, C., Dick, L., Felix, R., Johnson, D., and Chambers, C.D. (2005). Minor malformations characteristic of the retinoic acid embryopathy and other birth outcomes in children of women exposed to topical tretinoin during early pregnancy. Am. J. Med. Genet. A. *136*, 117–121.

ARTICLE 15

A male with unilateral microphthalmia reveals a role for *TMX3* in eye development

PLoS One

2010- 11;5(5):e10565

R. Chao, L. Nevin, P. Agarwal, J. Riemer, X. Bai, A. Delaney, M. Akana, N. JimenezLopez,

T. Bardakjian, A. Schneider, **N. Chassaing**, D. F. Schorderet, D. FitzPatrick, P. Y. Kwok,

L. Ellgaard, D. B. Gould, Y. Zhang, J. Malicki, H. Baier and A. Slavotinek

---

Nous avons été contactés par l'équipe du Pr. Anne Slavotinek (San Francisco, USA). Cette équipe venait de mettre en évidence, par CGH-array, une délétion sur le bras long du chromosome 18 chez un patient atteint d'AM. Dans cette délétion était inclus le gène *TMX3* exprimé au cours du développement dans la rétine et le cristallin. Cette équipe a recruté des patients AM pour séquencer ce gène chez eux à la recherche de mutation ponctuelles. Nous avions pu inclure 36 patients AM dans cette étude. L'implication de ce gène *TMX3* dans les défauts du développement oculaire a pu secondairement être validée par des expériences d'inactivation de l'expression de ce gène à l'aide de morpholinos dans un modèle de poisson zèbre.

PERSPECTIVES ET CONCLUSION

Perspectives

Les approches qui ont été développées au cours de ma thèse visaient à identifier des gènes candidats pouvant être impliqués dans les AM. J'ai décrit dans cette thèse, les différentes approches utilisées (gènes candidats fonctionnels, gènes candidats positionnels, gènes cibles des 4 FTs majeurs du développement oculaire).

Ces différentes approches nous ont permis d'obtenir de nombreux résultats dont certains, n'ont pas pu être totalement explorées. Il serait ainsi intéressant de se pencher plus spécifiquement sur le rôle au cours du développement oculaire des autres gènes (autres que *PTCH1*) pour lesquels des variations considérées comme possiblement pathogènes ont été identifiées chez les patients AM. Un travail spécifique sur le rôle des variations identifiées dans les régions régulatrices pourrait également être envisagé. Enfin, les résultats obtenus par ChIP-seq montrent une interaction forte entre les facteurs de transcription SOX2 et OTX2, similaire à celle déjà identifiée pour SOX2 et CHD7 [184]. Les données obtenues sur la co-régulation de gènes cibles par ces deux facteurs de transcription (démontrée précédemment pour la régulation de l'expression du gène *RAX*[173]) mériteraient d'être approfondies.

Avec la révolution du séquençage haut débit, la recherche de gènes impliqués dans des pathologies a totalement été modifiée. Le travail de réflexion n'est plus en amont du projet (recherche de gènes candidats pouvant être impliqués dans la pathologie), mais en aval du projet (recherche parmi les gènes porteur de mutations délétères d'un patient, ceux qui pourraient être impliqués dans la pathologie). Il convient donc de valider *a postériori* le rôle potentiel d'un gène porteur de mutations délétères dans une pathologie donnée.

Le séquençage haut débit peut être envisagé façon ciblée, mais de plus en plus, on a recours à des approches pangénomiques ("whole exome" ou "whole genome"). Devant le nombre important (plusieurs centaines) de variations potentiellement causales identifiées pour chaque patient, différentes stratégies ont été élaborées[185] :

- Recherche de mutations hétérozygotes en commun chez plusieurs patients atteints d'une même pathologie à transmission autosomique dominante. Cette approche n'est qu'exceptionnellement réalisable dans le cadre des AM en l'absence de grandes familles.
- Recherche de mutations présentes dans un gène en commun chez des patients non apparentés présentant la même pathologie. Cette approche, à moins de disposer d'un très grand nombre de patients, paraît aléatoire dans le cas des AM compte tenu de

l'hétérogénéité génétique majeure. Elle peut parfois être envisagée pour des formes syndromiques spécifiques de malformation oculaires.

- Recherche de mutations récessives homozygotes chez des patients issus de parents apparentés. La sensibilité de cette approche peut être augmentée en testant en parallèle plusieurs membres d'une même famille.
- Recherche de mutations hétérozygotes *de novo*. Cette approche est particulièrement indiquée pour les pathologies à forte hétérogénéité génétique et a démontré son efficacité dans des pathologies aussi génétiquement hétérogènes que la déficience intellectuelle[186] ou l'autisme[187].

Toutes ces approches ont permis un bond des connaissances et la description de dizaines de nouveaux gènes de pathologie humaine. Nous les avons utilisées dans plusieurs projets qui sont en cours et que je vais brièvement décrire ici :

- *Recherches de mutations causales d'AM*

En collaboration avec le Dr Nicola Ragge (Oxford UK), nous avons initié un projet de séquençage d'exome chez 24 patients AM. 12 sont des cas sporadiques étudiés en trio avec les parents (recherche de mutations *de novo*) et 12 sont des patients issus de parents apparentés (recherche de mutations homozygotes). Les résultats du séquençage haut débit ont été validés par séquençage Sanger. Ces analyses ont permis d'identifier une nouvelle mutation faux-sens délétère *de novo* de *PAX6* chez un patient, une mutation faux-sens hétérozygote du gène *BCOR* chez une patiente ainsi qu'une mutation faux-sens homozygote délétère (analyses fonctionnelles réalisées) du gène *ALDH1A3*. Ainsi pour 3 des 24 patients testés, l'approche par séquençage d'exome a permis d'identifier des mutations dans un gène connu d'AM (ce qui confirme le pouvoir de cette approche). Nous avons de nombreux gènes candidats parmi les 21 autres patients. Pour valider ces candidats, un séquençage (séquençage moyen débit) de ces gènes candidats dans une cohorte de 96 nouveaux patients AM est en cours d'organisation. En parallèle des analyses fonctionnelles des variants les plus intéressants vont être entreprises.

- *Recherches de mutations causales d'AM syndromique (Matthew-Wood)*

Nous avons initié en collaboration avec l'équipe du Pr. Jacques Michaud (Montréal, Canada), la recherche de mutation par séquençage d'exome chez 5 patients atteints de syndrome de Matthew-Wood (spectre PDAC), sans mutation identifiée dans *STRA6* ni *RARB*.

- *Recherches de mutations causales de dysgénésie du segment antérieur*

Nous avons initié en collaboration avec l'équipe du Dr. Josseline Kaplan et du Dr. Jean-Michel Rozet (Paris, France), la recherche de mutation par séquençage d'exome chez des patients atteints de dysgénésie du segment antérieur. 5 patients non apparentés atteints d'aniridie sans mutation de *PAX6* vont être analysés. De plus, des analyses de trio pour des patients atteints de dysgénésie du segment antérieur (anomalies de Peters, Rieger ou Axenfeld) est en cours.

- *Recherches de mutations causales d'aniridie syndromique*

En collaboration avec la même équipe du Dr. Josseline Kaplan et du Dr. Jean-Michel Rozet, nous avons débuté un projet visant à identifier un gène pour le syndrome de Gillespie associant aniridie et ataxie cérébelleuse. 4 patients atteints non apparentés vont être analysés.

Comme précédemment mentionné, il conviendra de valider l'implication des gènes identifiés par ces techniques de séquençage haut débit. De multiples approches sont possibles (recherche de mutation du même gène chez d'autres patients, validation fonctionnelle de la mutation, modèles animaux [zebrafish ou souris le plus fréquemment]…). Les approches utilisées pour valider nos gènes dépendent du type de mutation, de la fonction du gène, et de la pathologie étudiée. C'est dans le choix des meilleures techniques de validation des résultats haut débit que se fait maintenant la réflexion du chercheur.

Conclusion

Les AM sont les malformations embryonnaires oculaires les plus sévères. L'importante hétérogénéité génétique et la variabilité phénotypique rendent difficile l'optimisation de la prise en charge des patients et le conseil génétique. Nous avions fixés différents objectifs pour ce travail de thèse, visant à améliorer les connaissances sur les aspects cliniques et moléculaires de cette pathologie.

La première partie de mon travail a permis de montrer la fréquence de l'implication des principaux gènes d'AM dans la plus grande cohorte de patients rapportée. Cette analyse a permis de connaître le poids de chaque gène étudié dans l'AM. Cette analyse a également souligné la proportion importante de patients (80 %) chez qui l'AM ne peut pas être expliquée par des mutations des gènes couramment étudiés.

La deuxième partie de mon travail a été d'exploiter les résultats moléculaires obtenus chez les patients de notre cohorte pour essayer de mieux définir les phénotypes associés à chaque gène. Nous avons ainsi pu décrire précisément le phénotype de 32 patients porteurs de mutation dans ces gènes ce qui augmente fortement les données cliniques disponibles dans la littérature. En raison de présentations cliniques atypiques dans deux familles, nous nous sommes plus particulièrement intéressés aux variations phénotypiques observées pour les mutations des gènes *STRA6* et *OTX2*. Ceci nous a conduits à développer deux projets de recherche spécifiques concernant chacun de ces gènes et l'effet de leurs mutations et à décrire une étendue insoupçonnée des spectres phénotypiques en comparaison avec les descriptions initiales. En effet les mutations du gène *STRA6* se sont avérées pouvoir être responsables d'AM isolées, de manière surprenantes celles d'*OTX2* d'une atteinte développementale mandibulaire extrême, l'otocéphalie. Tout comme auparavant nous avions montré l'implication de *SOX2* dans des lésions cérébrales isolées ou le spectre AEG dans une même fratrie.

Enfin, la troisième partie de mon travail a visé à identifier de nouveaux gènes d'AM. Pour cela plusieurs approches ont été utilisées. Notre approche expérimentale (ChIP et transcriptomique) a permis d'obtenir des données précieuses sur les gènes régulés par les FTs Sox2, Otx2, Pax6 et Rax. Elle a conduit à sélectionner un certain nombre de gènes candidats, avant que la révolution du séquençage haut débit n'introduise un changement radical dans la progression de nos travaux. Ces données demeureront une aide précieuse lorsqu'il faudra interpréter les données de séquençage haut débit des projets en cours. Elles permettront en effet de corréler les résultats des différentes techniques et d'orienter plus aisément la sélection de gènes candidats. Deux éléments nous démontrent que la stratégie que nous avions imaginée était une bonne voie pour identifier de nouveaux gènes d'AM :

- Premièrement, notre approche expérimentale a permis d'identifier de nombreuses cibles des FTs étudiés. Parmi ces gènes cibles, une 15^{aine} de gènes avait été sélectionnés sur des arguments fonctionnels comme "meilleurs candidats" (voir chapitres correspondants). Le patron d'expression embryonnaire (œil, cerveau, membres) avait alors été étudié pour ces gènes. Seul l'un d'entre eux avait une expression cantonnée à l'œil, le gène *Aldh1a3* (voir Fig. 32), lui conférant ainsi le statut de candidat le plus probable à une anomalie restreinte à cet organe. Nous avons secondairement participé à la description de l'implication de ce gène dans l'AM. Elle a été prouvée par l'identification, par analyse de liaison et séquençage d'exome, de mutations délétères de ce gène dans une famille AM. Plusieurs autres patients AM porteurs de mutations dans *ALDH1A3* ont été rapportés depuis.
- Le deuxième élément correspond aux gènes choisis comme gènes candidats pour le séquençage haut débit ciblé sur 407 gènes. Depuis la sélection des gènes candidats et de l'élaboration de notre kit de capture, 9 gènes ont été impliqués dans des AM isolées (*ALDH1A3, ODZ3, SIX6*) ou syndromiques (*c12orf57, FNBP4, FREM1, SMOC1, VAX1*). Il est intéressant de noter que nous avions sélectionné la candidature de 6 de ces 9 gènes (*ALDH1A3, FREM1, RARB, SIX6, SMOC1, VAX1)* avant que leur implication dans l'AM n'ait été démontrée.

Cette stratégie expérimentale nous a également permis d'identifier le gène *PTCH1* comme le deuxième gène majeur des défauts du développement embryonnaire de l'œil (10 % des patients). Les mutations de ce gène ont une pénétrance incomplète et donnent des phénotypes variables allant de dysgénésies isolées du segment antérieur à des AM syndromiques, associées à des cardiopathies et aux anomalies cérébrales touchant la ligne médiane bien connues dans les anomalies de ce gène. L'identification de *PTCH1*, pointe tous les acteurs de la voie de signalisation SHH comme pouvant être impliqués dans les malformations oculaires.

Les résultats obtenus ont remplis les objectifs que nous avions fixés à son initiation. Ils nous ont également permis de mesurer l'importance du travail restant à accomplir pour pouvoir répondre aux mieux aux patients et à leurs familles. Ainsi, le nombre des gènes d'AM restant à découvrir est probablement élevé. Les manifestations phénotypiques associées aux mutations des gènes d'AM restent à définir et la collection de nouveaux patients demeure essentielle. Il ne semble pas exister de corrélation entre les génotypes et les phénotypes, et un des challenges qu'il faudra relever sera de pouvoir expliquer les causes de la variabilité phénotypique observée. S'agit-il d'effets liés à l'environnement, à des gènes modulateurs, ou des effets stochastiques ? Identifier les causes de la

variabilité phénotypique permettrait, là aussi, de préciser la prise en charge des patients et de leurs familles. Il sera probablement encore long et difficile de répondre intégralement à ces questions, mais la première étape consistera à constituer et à suivre de grandes cohortes de patients porteurs de mutations dans un même gène. Compte tenu de l'implication faible (en dehors de *SOX2* et *PTCH1*) de chaque gène dans ces pathologies rares, ceci n'est envisageable qu'au travers de collaborations nationales et internationales. Cet aspect collaboratif a également été au cœur de mon projet que ce soit dans l'optique de recruter les patients AM au travers toute la France et souvent en dehors de nos frontières, dans l'optique de valider des résultats obtenus par notre équipe de recherche, ou dans l'optique de participer à l'identification de nouveaux gènes d'AM. Les projets présentés dans les perspectives reflètent bien cet état d'esprit, et ils ont tous été défini dans le cadre de projets collaboratifs avec des équipes nationales ou internationales. Cet échange de compétence me semble essentiel pour avancer dans les connaissances dans le cadre des maladies rares en général et des AM en particulier.

REFERENCES

1. Verma AS, Fitzpatrick DR. Anophthalmia and microphthalmia. *Orphanet J Rare Dis* 2007;**2**:47.
2. Weiss AH, Kousseff BG, Ross EA, Longbottom J. Simple microphthalmos. *Arch Ophthalmol* 1989;**107**(11):1625-30.
3. Weiss AH, Kousseff BG, Ross EA, Longbottom J. Complex microphthalmos. *Arch Ophthalmol* 1989;**107**(11):1619-24.
4. Fantes J, Ragge NK, Lynch SA, McGill NI, Collin JR, Howard-Peebles PN, Hayward C, Vivian AJ, Williamson K, van Heyningen V, FitzPatrick DR. Mutations in SOX2 cause anophthalmia. *Nat Genet* 2003;**33**(4):461-3.
5. Ragge NK, Lorenz B, Schneider A, Bushby K, de Sanctis L, de Sanctis U, Salt A, Collin JR, Vivian AJ, Free SL, Thompson P, Williamson KA, Sisodiya SM, van Heyningen V, Fitzpatrick DR. SOX2 anophthalmia syndrome. *Am J Med Genet A* 2005;**135**(1):1-7; discussion 8.
6. Graw J. The genetic and molecular basis of congenital eye defects. *Nat Rev Genet* 2003;**4**(11):876-88.
7. Idrees F, Vaideanu D, Fraser SG, Sowden JC, Khaw PT. A review of anterior segment dysgeneses. *Surv Ophthalmol* 2006;**51**(3):213-31.
8. Mann I. The Developmental Basis of Eye Malformations. *Philadelphia (PA): JB Lippincott* 1953.
9. Fitzpatrick DR, van Heyningen V. Developmental eye disorders. *Curr Opin Genet Dev* 2005;**15**(3):348-53.
10. Spagnolo A, Bianchi F, Calabro A, Calzolari E, Clementi M, Mastroiacovo P, Meli P, Petrelli G, Tenconi R. Anophthalmia and benomyl in Italy: a multicenter study based on 940,615 newborns. *Reprod Toxicol* 1994;**8**(5):397-403.
11. Kallen B, Robert E, Harris J. The descriptive epidemiology of anophthalmia and microphthalmia. *Int J Epidemiol* 1996;**25**(5):1009-16.
12. Busby A, Dolk H, Collin R, Jones RB, Winter R. Compiling a national register of babies born with anophthalmia/microphthalmia in England 1988-94. *Arch Dis Child Fetal Neonatal Ed* 1998;**79**(3):F168-73.
13. Dolk H, Busby A, Armstrong BG, Walls PH. Geographical variation in anophthalmia and microphthalmia in England, 1988-94. *Bmj* 1998;**317**(7163):905-9; discussion 910.
14. Lowry RB, Kohut R, Sibbald B, Rouleau J. Anophthalmia and microphthalmia in the Alberta Congenital Anomalies Surveillance System. *Can J Ophthalmol* 2005;**40**(1):38-44.
15. Bermejo E, Martinez-Frias ML. Congenital eye malformations: clinical-epidemiological analysis of 1,124,654 consecutive births in Spain. *Am J Med Genet* 1998;**75**(5):497-504.
16. Morrison D, FitzPatrick D, Hanson I, Williamson K, van Heyningen V, Fleck B, Jones I, Chalmers J, Campbell H. National study of microphthalmia, anophthalmia, and coloboma (MAC) in Scotland: investigation of genetic aetiology. *J Med Genet* 2002;**39**(1):16-22.
17. Slavotinek AM. Eye development genes and known syndromes. *Mol Genet Metab* 2011;**104**(4):448-56.
18. Shah SP, Taylor AE, Sowden JC, Ragge N, Russell-Eggitt I, Rahi JS, Gilbert CE. Anophthalmos, microphthalmos, and Coloboma in the United kingdom: clinical features, results of investigations, and early management. *Ophthalmology* 2011;**119**(2):362-8.
19. Kava MP, Nagarajan L. Microphthalmia and microcornea: in congenital cytomegalovirus. *Indian J Ophthalmol* 2009;**57**(4):323.
20. Suhardjo, Utomo PT, Agni AN. Clinical manifestations of ocular toxoplasmosis in Yogyakarta, Indonesia: a clinical review of 173 cases. *Southeast Asian J Trop Med Public Health* 2003;**34**(2):291-7.
21. Duszak RS. Congenital rubella syndrome--major review. *Optometry* 2009;**80**(1):36-43.
22. Stromland K. Visual impairment and ocular abnormalities in children with fetal alcohol syndrome. *Addict Biol* 2004;**9**(2):153-7; discussion 159-60.

23. Lammer EJ, Chen DT, Hoar RM, Agnish ND, Benke PJ, Braun JT, Curry CJ, Fernhoff PM, Grix AW, Jr., Lott IT, et al. Retinoic acid embryopathy. *N Engl J Med* 1985;**313**(14):837-41.
24. Kallen B, Tornqvist K. The epidemiology of anophthalmia and microphthalmia in Sweden. *Eur J Epidemiol* 2005;**20**(4):345-50.
25. Maestro-de-Las-Casas C, Perez-Miguelsanz J, Lopez-Gordillo Y, Maldonado E, Partearroyo T, Varela-Moreiras G, Martinez-Alvarez C. Maternal folic acid-deficient diet causes congenital malformations in the mouse eye. *Birth Defects Res A Clin Mol Teratol* 2013;**97**(9):587-96.
26. Stoll C, Alembik Y, Dott B, Roth MP. Congenital eye malformations in 212,479 consecutive births. *Ann Genet* 1997;**40**(2):122-8.
27. Balikova I, de Ravel T, Ayuso C, Thienpont B, Casteels I, Villaverde C, Devriendt K, Fryns JP, Vermeesch JR. High frequency of submicroscopic chromosomal deletions in patients with idiopathic congenital eye malformations. *Am J Ophthalmol* 2011;**151**(6):1087-1094 e45.
28. Delahaye A, Bitoun P, Drunat S, Gerard-Blanluet M, Chassaing N, Toutain A, Verloes A, Gatelais F, Legendre M, Faivre L, Passemard S, Aboura A, Kaltenbach S, Quentin S, Dupont C, Tabet AC, Amselem S, Elion J, Gressens P, Pipiras E, Benzacken B. Genomic imbalances detected by array-CGH in patients with syndromal ocular developmental anomalies. *Eur J Hum Genet* 2012;**20**(5):527-33.
29. Raca G, Jackson CA, Kucinskas L, Warman B, Shieh JT, Schneider A, Bardakjian TM, Schimmenti LA. Array comparative genomic hybridization analysis in patients with anophthalmia, microphthalmia, and coloboma. *Genet Med* 2011;**13**(5):437-42.
30. Hever AM, Williamson KA, van Heyningen V. Developmental malformations of the eye: the role of PAX6, SOX2 and OTX2. *Clin Genet* 2006;**69**(6):459-70.
31. Williamson KA, Hever AM, Rainger J, Rogers RC, Magee A, Fiedler Z, Keng WT, Sharkey FH, McGill N, Hill CJ, Schneider A, Messina M, Turnpenny PD, Fantes JA, van Heyningen V, FitzPatrick DR. Mutations in SOX2 cause anophthalmia-esophageal-genital (AEG) syndrome. *Hum Mol Genet* 2006;**15**(9):1413-22.
32. Gerth-Kahlert C, Williamson K, Ansari M, Rainger JK, Hingst V, Zimmermann T, Tech S, Guthoff RF, van Heyningen V, FitzPatrick DR. Clinical and mutation analysis of 51 probands with anophthalmia and/or severe microphthalmia from a single center. *Molecular Genetics & Genomic Medicine* 2013;**1**:15-31.
33. Bakrania P, Robinson DO, Bunyan DJ, Salt A, Martin A, Crolla JA, Wyatt A, Fielder A, Ainsworth J, Moore A, Read S, Uddin J, Laws D, Pascuel-Salcedo D, Ayuso C, Allen L, Collin JR, Ragge NK. SOX2 anophthalmia syndrome: 12 new cases demonstrating broader phenotype and high frequency of large gene deletions. *Br J Ophthalmol* 2007;**91**(11):1471-6.
34. Mihelec M, Abraham P, Gibson K, Krowka R, Susman R, Storen R, Chen Y, Donald J, Tam PP, Grigg JR, Flaherty M, Gole GA, Jamieson RV. Novel SOX2 partner-factor domain mutation in a four-generation family. *Eur J Hum Genet* 2009;**17**(11):1417-22.
35. Schneider A, Bardakjian T, Reis LM, Tyler RC, Semina EV. Novel SOX2 mutations and genotype-phenotype correlation in anophthalmia and microphthalmia. *Am J Med Genet A* 2009;**149A**(12):2706-15.
36. Osborne RJ, Kurinczuk JJ, Ragge NK. Parent-of-origin effects in SOX2 anophthalmia syndrome. *Mol Vis* 2011;**17**:3097-106.
37. Jimenez NL, Flannick J, Yahyavi M, Li J, Bardakjian T, Tonkin L, Schneider A, Sherr EH, Slavotinek AM. Targeted 'next-generation' sequencing in anophthalmia and microphthalmia patients confirms SOX2, OTX2 and FOXE3 mutations. *BMC Med Genet* 2011;**12**:172.
38. Stark Z, Storen R, Bennetts B, Savarirayan R, Jamieson RV. Isolated hypogonadotropic hypogonadism with SOX2 mutation and anophthalmia/microphthalmia in offspring. *Eur J Hum Genet* 2011;**19**(7):753-6.
39. Adler R, Canto-Soler MV. Molecular mechanisms of optic vesicle development: complexities, ambiguities and controversies. *Dev Biol* 2007;**305**(1):1-13.
40. Chassaing N, Causse A, Vigouroux A, Delahaye A, Alessandri JL, Boespflug-Tanguy O, Boute-Benejean O, Dollfus H, Duban-Bedu B, Gilbert-Dussardier B, Giuliano F, Gonzales M, Holder-

Espinasse M, Isidor B, Jacquemont ML, Lacombe D, Martin-Coignard D, Mathieu-Dramard M, Odent S, Picone O, Pinson L, Quelin C, Sigaudy S, Toutain A, Thauvin-Robinet C, Kaplan J, Calvas P. Molecular findings and clinical data in a cohort of 150 patients with anophthalmia/microphthalmia. *Clin Genet* 2013.

41. Chassaing N, Gilbert-Dussardier B, Nicot F, Fermeaux V, Encha-Razavi F, Fiorenza M, Toutain A, Calvas P. Germinal mosaicism and familial recurrence of a SOX2 mutation with highly variable phenotypic expression extending from AEG syndrome to absence of ocular involvement. *Am J Med Genet A* 2007;**143**(3):289-91.
42. Kelberman D, Rizzoti K, Avilion A, Bitner-Glindzicz M, Cianfarani S, Collins J, Chong WK, Kirk JM, Achermann JC, Ross R, Carmignac D, Lovell-Badge R, Robinson IC, Dattani MT. Mutations within Sox2/SOX2 are associated with abnormalities in the hypothalamo-pituitary-gonadal axis in mice and humans. *J Clin Invest* 2006;**116**(9):2442-55.
43. Wang P, Liang X, Yi J, Zhang Q. Novel SOX2 mutation associated with ocular coloboma in a Chinese family. *Arch Ophthalmol* 2008;**126**(5):709-13.
44. Chassaing N, Ragge N, Kariminejad A, Buffet A, Ghaderi-Sohi S, Martinovic J, Calvas P. Mutation analysis of the STRA6 gene in isolated and non-isolated anophthalmia/microphthalmia. *Clin Genet* 2013;**83**(3):244-50.
45. Zenteno JC, Perez-Cano HJ, Aguinaga M. Anophthalmia-esophageal atresia syndrome caused by an SOX2 gene deletion in monozygotic twin brothers with markedly discordant phenotypes. *Am J Med Genet A* 2006;**140**(18):1899-903.
46. Faivre L, Williamson KA, Faber V, Laurent N, Grimaldi M, Thauvin-Robinet C, Durand C, Mugneret F, Gouyon JB, Bron A, Huet F, Hayward C, Heyningen V, Fitzpatrick DR. Recurrence of SOX2 anophthalmia syndrome with gonosomal mosaicism in a phenotypically normal mother. *Am J Med Genet A* 2006;**140**(6):636-9.
47. Ragge NK, Brown AG, Poloschek CM, Lorenz B, Henderson RA, Clarke MP, Russell-Eggitt I, Fielder A, Gerrelli D, Martinez-Barbera JP, Ruddle P, Hurst J, Collin JR, Salt A, Cooper ST, Thompson PJ, Sisodiya SM, Williamson KA, Fitzpatrick DR, van Heyningen V, Hanson IM. Heterozygous mutations of OTX2 cause severe ocular malformations. *Am J Hum Genet* 2005;**76**(6):1008-22.
48. Schilter KF, Schneider A, Bardakjian T, Soucy JF, Tyler RC, Reis LM, Semina EV. OTX2 microphthalmia syndrome: four novel mutations and delineation of a phenotype. *Clin Genet* 2011;**79**(2):158-68.
49. Henderson RH, Williamson KA, Kennedy JS, Webster AR, Holder GE, Robson AG, FitzPatrick DR, van Heyningen V, Moore AT. A rare de novo nonsense mutation in OTX2 causes early onset retinal dystrophy and pituitary dysfunction. *Mol Vis* 2009;**15**:2442-7.
50. Wyatt A, Bakrania P, Bunyan DJ, Osborne RJ, Crolla JA, Salt A, Ayuso C, Newbury-Ecob R, Abou-Rayyah Y, Collin JR, Robinson D, Ragge N. Novel heterozygous OTX2 mutations and whole gene deletions in anophthalmia, microphthalmia and coloboma. *Hum Mutat* 2008;**29**(11):E278-83.
51. Wyatt AW, Ragge N. MLGA: a cost-effective approach to the diagnosis of gene deletions in eye development anomalies. *Mol Vis* 2009;**15**:1445-8.
52. Tajima T, Ishizu K, Nakamura A. Molecular and Clinical Findings in Patients with LHX4 and OTX2 Mutations. *Clin Pediatr Endocrinol* 2013;**22**(2):15-23.
53. Chassaing N, Sorrentino S, Davis EE, Martin-Coignard D, Iacovelli A, Paznekas W, Webb BD, Faye-Petersen O, Encha-Razavi F, Lequeux L, Vigouroux A, Yesilyurt A, Boyadjiev SA, Kayserili H, Loget P, Carles D, Sergi C, Puvabanditsin S, Chen CP, Etchevers HC, Katsanis N, Mercer CL, Calvas P, Jabs EW. OTX2 mutations contribute to the otocephaly-dysgnathia complex. *J Med Genet* 2012;**49**(6):373-9.
54. Patat O, van Ravenswaaij-Arts CMA, Tantau J, Corsten-Janssen N, van Tintelen JP, Dijkhuizen T, Kaplan J, Chassaing N. Otocephaly-Dysgnathia Complex: description of four cases and confirmation of the role of OTX2. *Molecular Syndromology* In Press.

55. Bailey TJ, El-Hodiri H, Zhang L, Shah R, Mathers PH, Jamrich M. Regulation of vertebrate eye development by Rx genes. *Int J Dev Biol* 2004;**48**(8-9):761-70.
56. Lequeux L, Rio M, Vigouroux A, Titeux M, Etchevers H, Malecaze F, Chassaing N, Calvas P. Confirmation of RAX gene involvement in human anophthalmia. *Clin Genet* 2008;**74**(4):392-5.
57. Voronina VA, Kozhemyakina EA, O'Kernick CM, Kahn ND, Wenger SL, Linberg JV, Schneider AS, Mathers PH. Mutations in the human RAX homeobox gene in a patient with anophthalmia and sclerocornea. *Hum Mol Genet* 2004;**13**(3):315-22.
58. Abouzeid H, Youssef MA, Bayoumi N, ElShakankiri N, Marzouk I, Hauser P, Schorderet DF. RAX and anophthalmia in humans: evidence of brain anomalies. *Mol Vis* 2012;**18**:1449-56.
59. London NJ, Kessler P, Williams B, Pauer GJ, Hagstrom SA, Traboulsi EI. Sequence alterations in RX in patients with microphthalmia, anophthalmia, and coloboma. *Mol Vis* 2009;**15**:162-7.
60. Gonzalez-Rodriguez J, Pelcastre EL, Tovilla-Canales JL, Garcia-Ortiz JE, Amato-Almanza M, Villanueva-Mendoza C, Espinosa-Mattar Z, Zenteno JC. Mutational screening of CHX10, GDF6, OTX2, RAX and SOX2 genes in 50 unrelated microphthalmia-anophthalmia-coloboma (MAC) spectrum cases. *Br J Ophthalmol* 2010;**94**(8):1100-4.
61. Glaser T, Jepeal L, Edwards JG, Young SR, Favor J, Maas RL. PAX6 gene dosage effect in a family with congenital cataracts, aniridia, anophthalmia and central nervous system defects. *Nat Genet* 1994;**7**(4):463-71.
62. Dansault A, David G, Schwartz C, Jaliffa C, Vieira V, de la Houssaye G, Bigot K, Catin F, Tattu L, Chopin C, Halimi P, Roche O, Van Regemorter N, Munier F, Schorderet D, Dufier JL, Marsac C, Ricquier D, Menasche M, Penfornis A, Abitbol M. Three new PAX6 mutations including one causing an unusual ophthalmic phenotype associated with neurodevelopmental abnormalities. *Mol Vis* 2007;**13**:511-23.
63. Tzoulaki I, White IM, Hanson IM. PAX6 mutations: genotype-phenotype correlations. *BMC Genet* 2005;**6**:27.
64. Solomon BD, Pineda-Alvarez DE, Balog JZ, Hadley D, Gropman AL, Nandagopal R, Han JC, Hahn JS, Blain D, Brooks B, Muenke M. Compound heterozygosity for mutations in PAX6 in a patient with complex brain anomaly, neonatal diabetes mellitus, and microophthalmia. *Am J Med Genet A* 2009;**149A**(11):2543-6.
65. Vincent MC, Pujo AL, Olivier D, Calvas P. Screening for PAX6 gene mutations is consistent with haploinsufficiency as the main mechanism leading to various ocular defects. *Eur J Hum Genet* 2003;**11**(2):163-9.
66. Liu IS, Chen JD, Ploder L, Vidgen D, van der Kooy D, Kalnins VI, McInnes RR. Developmental expression of a novel murine homeobox gene (Chx10): evidence for roles in determination of the neuroretina and inner nuclear layer. *Neuron* 1994;**13**(2):377-93.
67. Ferda Percin E, Ploder LA, Yu JJ, Arici K, Horsford DJ, Rutherford A, Bapat B, Cox DW, Duncan AM, Kalnins VI, Kocak-Altintas A, Sowden JC, Traboulsi E, Sarfarazi M, McInnes RR. Human microphthalmia associated with mutations in the retinal homeobox gene CHX10. *Nat Genet* 2000;**25**(4):397-401.
68. Burkitt Wright EM, Perveen R, Bowers N, Ramsden S, McCann E, O'Driscoll M, Lloyd IC, Clayton-Smith J, Black GC. VSX2 in microphthalmia: a novel splice site mutation producing a severe microphthalmia phenotype. *Br J Ophthalmol* 2010;**94**(3):386-8.
69. Iseri SU, Wyatt AW, Nurnberg G, Kluck C, Nurnberg P, Holder GE, Blair E, Salt A, Ragge NK. Use of genome-wide SNP homozygosity mapping in small pedigrees to identify new mutations in VSX2 causing recessive microphthalmia and a semidominant inner retinal dystrophy. *Hum Genet* 2010;**128**(1):51-60.
70. Reis LM, Khan A, Kariminejad A, Ebadi F, Tyler RC, Semina EV. VSX2 mutations in autosomal recessive microphthalmia. *Mol Vis* 2011;**17**:2527-32.
71. Khan AO, Aldahmesh MA, Noor J, Salem A, Alkuraya FS. Lens Subluxation and Retinal Dysfunction in a Girl with Homozygous VSX2 Mutation. *Ophthalmic Genet* 2013.

72. Blixt A, Mahlapuu M, Aitola M, Pelto-Huikko M, Enerback S, Carlsson P. A forkhead gene, FoxE3, is essential for lens epithelial proliferation and closure of the lens vesicle. *Genes Dev* 2000;**14**(2):245-54.
73. Tholozan FM, Sanderson JM, Quinlan RA. Focus on molecules: FoxE3. *Exp Eye Res* 2007;**84**(5):799-800.
74. Ormestad M, Blixt A, Churchill A, Martinsson T, Enerback S, Carlsson P. Foxe3 haploinsufficiency in mice: a model for Peters' anomaly. *Invest Ophthalmol Vis Sci* 2002;**43**(5):1350-7.
75. Semina EV, Brownell I, Mintz-Hittner HA, Murray JC, Jamrich M. Mutations in the human forkhead transcription factor FOXE3 associated with anterior segment ocular dysgenesis and cataracts. *Hum Mol Genet* 2001;**10**(3):231-6.
76. Valleix S, Niel F, Nedelec B, Algros MP, Schwartz C, Delbosc B, Delpech M, Kantelip B. Homozygous nonsense mutation in the FOXE3 gene as a cause of congenital primary aphakia in humans. *Am J Hum Genet* 2006;**79**(2):358-64.
77. Iseri SU, Osborne RJ, Farrall M, Wyatt AW, Mirza G, Nurnberg G, Kluck C, Herbert H, Martin A, Hussain MS, Collin JR, Lathrop M, Nurnberg P, Ragoussis J, Ragge NK. Seeing clearly: the dominant and recessive nature of FOXE3 in eye developmental anomalies. *Hum Mutat* 2009;**30**(10):1378-86.
78. Reis LM, Tyler RC, Schneider A, Bardakjian T, Stoler JM, Melancon SB, Semina EV. FOXE3 plays a significant role in autosomal recessive microphthalmia. *Am J Med Genet A* 2010;**152A**(3):582-90.
79. Bremond-Gignac D, Bitoun P, Reis LM, Copin H, Murray JC, Semina EV. Identification of dominant FOXE3 and PAX6 mutations in patients with congenital cataract and aniridia. *Mol Vis* 2010;**16**:1705-11.
80. Ali M, Buentello-Volante B, McKibbin M, Rocha-Medina JA, Fernandez-Fuentes N, Koga-Nakamura W, Ashiq A, Khan K, Booth AP, Williams G, Raashid Y, Jafri H, Rice A, Inglehearn CF, Zenteno JC. Homozygous FOXE3 mutations cause non-syndromic, bilateral, total sclerocornea, aphakia, microphthalmia and optic disc coloboma. *Mol Vis* 2010;**16**:1162-8.
81. Doucette L, Green J, Fernandez B, Johnson GJ, Parfrey P, Young TL. A novel, non-stop mutation in FOXE3 causes an autosomal dominant form of variable anterior segment dysgenesis including Peters anomaly. *Eur J Hum Genet* 2011;**19**(3):293-9.
82. Cvekl A, Wang WL. Retinoic acid signaling in mammalian eye development. *Exp Eye Res* 2009;**89**(3):280-91.
83. Fares-Taie L, Gerber S, Chassaing N, Clayton-Smith J, Hanein S, Silva E, Serey M, Serre V, Gerard X, Baumann C, Plessis G, Demeer B, Bretillon L, Bole C, Nitschke P, Munnich A, Lyonnet S, Calvas P, Kaplan J, Ragge N, Rozet JM. ALDH1A3 mutations cause recessive anophthalmia and microphthalmia. *Am J Hum Genet* 2013;**92**(2):265-70.
84. Yahyavi M, Abouzeid H, Gawdat G, de Preux AS, Xiao T, Bardakjian T, Schneider A, Choi A, Jorgenson E, Baier H, El Sada M, Schorderet DF, Slavotinek AM. ALDH1A3 loss of function causes bilateral anophthalmia/microphthalmia and hypoplasia of the optic nerve and optic chiasm. *Hum Mol Genet* 2013;**22**(16):3250-8.
85. Aldahmesh MA, Khan AO, Hijazi H, Alkuraya FS. Mutations in ALDH1A3 cause microphthalmia. *Clin Genet* 2013;**84**(2):128-31.
86. Mory A, Ruiz FX, Dagan E, Yakovtseva EA, Kurolap A, Pares X, Farres J, Gershoni-Baruch R. A missense mutation in ALDH1A3 causes isolated microphthalmia/anophthalmia in nine individuals from an inbred Muslim kindred. *Eur J Hum Genet* 2013.
87. Roos L, Fang M, Dali CI, Jensen H, Christoffersen N, Wu B, Zhang J, Xu R, Harris P, Xu X, Gronskov K, Tumer Z. A homozygous mutation in a consanguineous family consolidates the role of ALDH1A3 in autosomal recessive microphthalmia. *Clin Genet* 2013.
88. Aldahmesh MA, Mohammed JY, Al-Hazzaa S, Alkuraya FS. Homozygous null mutation in ODZ3 causes microphthalmia in humans. *Genet Med* 2013;**14**(11):900-4.

89. Khan K, Logan CV, McKibbin M, Sheridan E, Elcioglu NH, Yenice O, Parry DA, Fernandez-Fuentes N, Abdelhamed ZI, Al-Maskari A, Poulter JA, Mohamed MD, Carr IM, Morgan JE, Jafri H, Raashid Y, Taylor GR, Johnson CA, Inglehearn CF, Toomes C, Ali M. Next generation sequencing identifies mutations in Atonal homolog 7 (ATOH7) in families with global eye developmental defects. *Hum Mol Genet* 2012;**21**(4):776-83.
90. Prasov L, Masud T, Khaliq S, Mehdi SQ, Abid A, Oliver ER, Silva ED, Lewanda A, Brodsky MC, Borchert M, Kelberman D, Sowden JC, Dattani MT, Glaser T. ATOH7 mutations cause autosomal recessive persistent hyperplasia of the primary vitreous. *Hum Mol Genet* 2012;**21**(16):3681-94.
91. Aldahmesh MA, Khan AO, Hijazi H, Alkuraya FS. Homozygous truncation of SIX6 causes complex microphthalmia in humans. *Clin Genet* 2013;**84**(2):198-9.
92. Hilton E, Johnston J, Whalen S, Okamoto N, Hatsukawa Y, Nishio J, Kohara H, Hirano Y, Mizuno S, Torii C, Kosaki K, Manouvrier S, Boute O, Perveen R, Law C, Moore A, Fitzpatrick D, Lemke J, Fellmann F, Debray FG, Dastot-Le-Moal F, Gerard M, Martin J, Bitoun P, Goossens M, Verloes A, Schinzel A, Bartholdi D, Bardakjian T, Hay B, Jenny K, Johnston K, Lyons M, Belmont JW, Biesecker LG, Giurgea I, Black G. BCOR analysis in patients with OFCD and Lenz microphthalmia syndromes, mental retardation with ocular anomalies, and cardiac laterality defects. *Eur J Hum Genet* 2009;**17**(10):1325-35.
93. Ng D, Thakker N, Corcoran CM, Donnai D, Perveen R, Schneider A, Hadley DW, Tifft C, Zhang L, Wilkie AO, van der Smagt JJ, Gorlin RJ, Burgess SM, Bardwell VJ, Black GC, Biesecker LG. Oculofaciocardiodental and Lenz microphthalmia syndromes result from distinct classes of mutations in BCOR. *Nat Genet* 2004;**36**(4):411-6.
94. Srour M, Chitayat D, Caron V, Chassaing N, Bitoun P, Patry L, Cordier MP, Capo-Chichi JM, Francannet C, Calvas P, Ragge N, Dobrzeniecka S, Hamdan FF, Rouleau GA, Tremblay A, Michaud JL. Recessive and Dominant Mutations in Retinoic Acid Receptor Beta in Cases with Microphthalmia and Diaphragmatic Hernia. *Am J Hum Genet* 2013.
95. Asai-Coakwell M, French CR, Ye M, Garcha K, Bigot K, Perera AG, Staehling-Hampton K, Mema SC, Chanda B, Mushegian A, Bamforth S, Doschak MR, Li G, Dobbs MB, Giampietro PF, Brooks BP, Vijayalakshmi P, Sauve Y, Abitbol M, Sundaresan P, van Heyningen V, Pourquie O, Underhill TM, Waskiewicz AJ, Lehmann OJ. Incomplete penetrance and phenotypic variability characterize Gdf6-attributable oculo-skeletal phenotypes. *Hum Mol Genet* 2009;**18**(6):1110-21.
96. Tassabehji M, Fang ZM, Hilton EN, McGaughran J, Zhao Z, de Bock CE, Howard E, Malass M, Donnai D, Diwan A, Manson FD, Murrell D, Clarke RA. Mutations in GDF6 are associated with vertebral segmentation defects in Klippel-Feil syndrome. *Hum Mutat* 2008;**29**(8):1017-27.
97. Asai-Coakwell M, French CR, Berry KM, Ye M, Koss R, Somerville M, Mueller R, van Heyningen V, Waskiewicz AJ, Lehmann OJ. GDF6, a novel locus for a spectrum of ocular developmental anomalies. *Am J Hum Genet* 2007;**80**(2):306-15.
98. Hayashi S, Okamoto N, Makita Y, Hata A, Imoto I, Inazawa J. Heterozygous deletion at 14q22.1-q22.3 including the BMP4 gene in a patient with psychomotor retardation, congenital corneal opacity and feet polysyndactyly. *Am J Med Genet A* 2008;**146A**(22):2905-10.
99. Bakrania P, Efthymiou M, Klein JC, Salt A, Bunyan DJ, Wyatt A, Ponting CP, Martin A, Williams S, Lindley V, Gilmore J, Restori M, Robson AG, Neveu MM, Holder GE, Collin JR, Robinson DO, Farndon P, Johansen-Berg H, Gerrelli D, Ragge NK. Mutations in BMP4 cause eye, brain, and digit developmental anomalies: overlap between the BMP4 and hedgehog signaling pathways. *Am J Hum Genet* 2008;**82**(2):304-19.
100. Reis LM, Tyler RC, Schilter KF, Abdul-Rahman O, Innis JW, Kozel BA, Schneider AS, Bardakjian TM, Lose EJ, Martin DM, Broeckel U, Semina EV. BMP4 loss-of-function mutations in developmental eye disorders including SHORT syndrome. *Hum Genet* 2011;**130**(4):495-504.
101. Zhang X, Li S, Xiao X, Jia X, Wang P, Shen H, Guo X, Zhang Q. Mutational screening of 10 genes in Chinese patients with microphthalmia and/or coloboma. *Mol Vis* 2009;**15**:2911-8.

102. Wyatt AW, Osborne RJ, Stewart H, Ragge NK. Bone morphogenetic protein 7 (BMP7) mutations are associated with variable ocular, brain, ear, palate, and skeletal anomalies. *Hum Mutat* 2010;**31**(7):781-7.
103. Rainger J, van Beusekom E, Ramsay JK, McKie L, Al-Gazali L, Pallotta R, Saponari A, Branney P, Fisher M, Morrison H, Bicknell L, Gautier P, Perry P, Sokhi K, Sexton D, Bardakjian TM, Schneider AS, Elcioglu N, Ozkinay F, Koenig R, Megarbane A, Semerci CN, Khan A, Zafar S, Hennekam R, Sousa SB, Ramos L, Garavelli L, Furga AS, Wischmeijer A, Jackson IJ, Gillessen-Kaesbach G, Brunner HG, Wieczorek D, van Bokhoven H, Fitzpatrick DR. Loss of the BMP antagonist, SMOC-1, causes Ophthalmo-acromelic (Waardenburg Anophthalmia) syndrome in humans and mice. *PLoS Genet* 2011;**7**(7):e1002114.
104. Okada I, Hamanoue H, Terada K, Tohma T, Megarbane A, Chouery E, Abou-Ghoch J, Jalkh N, Cogulu O, Ozkinay F, Horie K, Takeda J, Furuichi T, Ikegawa S, Nishiyama K, Miyatake S, Nishimura A, Mizuguchi T, Niikawa N, Hirahara F, Kaname T, Yoshiura K, Tsurusaki Y, Doi H, Miyake N, Furukawa T, Matsumoto N, Saitsu H. SMOC1 is essential for ocular and limb development in humans and mice. *Am J Hum Genet* 2011;**88**(1):30-41.
105. Abouzeid H, Boisset G, Favez T, Youssef M, Marzouk I, Shakankiry N, Bayoumi N, Descombes P, Agosti C, Munier FL, Schorderet DF. Mutations in the SPARC-related modular calcium-binding protein 1 gene, SMOC1, cause waardenburg anophthalmia syndrome. *Am J Hum Genet* 2011;**88**(1):92-8.
106. Kondo Y, Koshimizu E, Megarbane A, Hamanoue H, Okada I, Nishiyama K, Kodera H, Miyatake S, Tsurusaki Y, Nakashima M, Doi H, Miyake N, Saitsu H, Matsumoto N. Whole-exome sequencing identified a homozygous FNBP4 mutation in a family with a condition similar to microphthalmia with limb anomalies. *Am J Med Genet A* 2013;**161A**(7):1543-6.
107. Wimplinger I, Morleo M, Rosenberger G, Iaconis D, Orth U, Meinecke P, Lerer I, Ballabio A, Gal A, Franco B, Kutsche K. Mutations of the mitochondrial holocytochrome c-type synthase in X-linked dominant microphthalmia with linear skin defects syndrome. *Am J Hum Genet* 2006;**79**(5):878-89.
108. Indrieri A, van Rahden VA, Tiranti V, Morleo M, Iaconis D, Tammaro R, D'Amato I, Conte I, Maystadt I, Demuth S, Zvulunov A, Kutsche K, Zeviani M, Franco B. Mutations in COX7B cause microphthalmia with linear skin lesions, an unconventional mitochondrial disease. *Am J Hum Genet* 2012;**91**(5):942-9.
109. Slavotinek AM, Chao R, Vacik T, Yahyavi M, Abouzeid H, Bardakjian T, Schneider A, Shaw G, Sherr EH, Lemke G, Youssef M, Schorderet DF. VAX1 mutation associated with microphthalmia, corpus callosum agenesis, and orofacial clefting: the first description of a VAX1 phenotype in humans. *Hum Mutat* 2012;**33**(2):364-8.
110. Zahrani F, Aldahmesh MA, Alshammari MJ, Al-Hazzaa SA, Alkuraya FS. Mutations in c12orf57 cause a syndromic form of colobomatous microphthalmia. *Am J Hum Genet* 2013;**92**(3):387-91.
111. Akizu N, Shembesh NM, Ben-Omran T, Bastaki L, Al-Tawari A, Zaki MS, Koul R, Spencer E, Rosti RO, Scott E, Nickerson E, Gabriel S, da Gente G, Li J, Deardorff MA, Conlin LK, Horton MA, Zackai EH, Sherr EH, Gleeson JG. Whole-exome sequencing identifies mutated c12orf57 in recessive corpus callosum hypoplasia. *Am J Hum Genet* 2013;**92**(3):392-400.
112. Salih MA, Tzschach A, Oystreck DT, Hassan HH, AlDrees A, Elmalik SA, El Khashab HY, Wienker TF, Abu-Amero KK, Bosley TM. A newly recognized autosomal recessive syndrome affecting neurologic function and vision. *Am J Med Genet A* 2013;**161**(6):1207-13.
113. Sarkar A, Hochedlinger K. The sox family of transcription factors: versatile regulators of stem and progenitor cell fate. *Cell Stem Cell* 2013;**12**(1):15-30.
114. Masui S, Nakatake Y, Toyooka Y, Shimosato D, Yagi R, Takahashi K, Okochi H, Okuda A, Matoba R, Sharov AA, Ko MS, Niwa H. Pluripotency governed by Sox2 via regulation of Oct3/4 expression in mouse embryonic stem cells. *Nat Cell Biol* 2007;**9**(6):625-35.
115. Avilion AA, Nicolis SK, Pevny LH, Perez L, Vivian N, Lovell-Badge R. Multipotent cell lineages in early mouse development depend on SOX2 function. *Genes Dev* 2003;**17**(1):126-40.

116. Wood HB, Episkopou V. Comparative expression of the mouse Sox1, Sox2 and Sox3 genes from pre-gastrulation to early somite stages. *Mech Dev* 1999;**86**(1-2):197-201.
117. Yabuta Y, Kurimoto K, Ohinata Y, Seki Y, Saitou M. Gene expression dynamics during germline specification in mice identified by quantitative single-cell gene expression profiling. *Biol Reprod* 2006;**75**(5):705-16.
118. Kamachi Y, Uchikawa M, Collignon J, Lovell-Badge R, Kondoh H. Involvement of Sox1, 2 and 3 in the early and subsequent molecular events of lens induction. *Development* 1998;**125**(13):2521-32.
119. Furuta Y, Hogan BL. BMP4 is essential for lens induction in the mouse embryo. *Genes Dev* 1998;**12**(23):3764-75.
120. Ferri AL, Cavallaro M, Braida D, Di Cristofano A, Canta A, Vezzani A, Ottolenghi S, Pandolfi PP, Sala M, DeBiasi S, Nicolis SK. Sox2 deficiency causes neurodegeneration and impaired neurogenesis in the adult mouse brain. *Development* 2004;**131**(15):3805-19.
121. Taranova OV, Magness ST, Fagan BM, Wu Y, Surzenko N, Hutton SR, Pevny LH. SOX2 is a dose-dependent regulator of retinal neural progenitor competence. *Genes Dev* 2006;**20**(9):1187-202.
122. Lakowski J, Majumder A, Lauderdale JD. Mechanisms controlling Pax6 isoform expression in the retina have been conserved between teleosts and mammals. *Dev Biol* 2007;**307**(2):498-520.
123. Osumi N, Shinohara H, Numayama-Tsuruta K, Maekawa M. Concise review: Pax6 transcription factor contributes to both embryonic and adult neurogenesis as a multifunctional regulator. *Stem Cells* 2008;**26**(7):1663-72.
124. Hanson I, Van Heyningen V. Pax6: more than meets the eye. *Trends Genet* 1995;**11**(7):268-72.
125. Kioussi C, O'Connell S, St-Onge L, Treier M, Gleiberman AS, Gruss P, Rosenfeld MG. Pax6 is essential for establishing ventral-dorsal cell boundaries in pituitary gland development. *Proc Natl Acad Sci U S A* 1999;**96**(25):14378-82.
126. Dohrmann C, Gruss P, Lemaire L. Pax genes and the differentiation of hormone-producing endocrine cells in the pancreas. *Mech Dev* 2000;**92**(1):47-54.
127. Estivill-Torrus G, Vitalis T, Fernandez-Llebrez P, Price DJ. The transcription factor Pax6 is required for development of the diencephalic dorsal midline secretory radial glia that form the subcommissural organ. *Mech Dev* 2001;**109**(2):215-24.
128. Thompson JA, Ziman M. Pax genes during neural development and their potential role in neuroregeneration. *Prog Neurobiol* 2011;**95**(3):334-51.
129. Ashery-Padan R, Marquardt T, Zhou X, Gruss P. Pax6 activity in the lens primordium is required for lens formation and for correct placement of a single retina in the eye. *Genes Dev* 2000;**14**(21):2701-11.
130. Lang RA. Pathways regulating lens induction in the mouse. *Int J Dev Biol* 2004;**48**(8-9):783-91.
131. Marquardt T, Ashery-Padan R, Andrejewski N, Scardigli R, Guillemot F, Gruss P. Pax6 is required for the multipotent state of retinal progenitor cells. *Cell* 2001;**105**(1):43-55.
132. Pratt T, Vitalis T, Warren N, Edgar JM, Mason JO, Price DJ. A role for Pax6 in the normal development of dorsal thalamus and its cortical connections. *Development* 2000;**127**(23):5167-78.
133. Molnar Z, Higashi S, Lopez-Bendito G. Choreography of early thalamocortical development. *Cereb Cortex* 2003;**13**(6):661-9.
134. Engelkamp D, Rashbass P, Seawright A, van Heyningen V. Role of Pax6 in development of the cerebellar system. *Development* 1999;**126**(16):3585-96.
135. Ericson J, Rashbass P, Schedl A, Brenner-Morton S, Kawakami A, van Heyningen V, Jessell TM, Briscoe J. Pax6 controls progenitor cell identity and neuronal fate in response to graded Shh signaling. *Cell* 1997;**90**(1):169-80.

136. St-Onge L, Sosa-Pineda B, Chowdhury K, Mansouri A, Gruss P. Pax6 is required for differentiation of glucagon-producing alpha-cells in mouse pancreas. *Nature* 1997;**387**(6631):406-9.
137. Inoue T, Nakamura S, Osumi N. Fate mapping of the mouse prosencephalic neural plate. *Dev Biol* 2000;**219**(2):373-83.
138. Grindley JC, Davidson DR, Hill RE. The role of Pax-6 in eye and nasal development. *Development* 1995;**121**(5):1433-42.
139. Quiring R, Walldorf U, Kloter U, Gehring WJ. Homology of the eyeless gene of Drosophila to the Small eye gene in mice and Aniridia in humans. *Science* 1994;**265**(5173):785-9.
140. Hill RE, Favor J, Hogan BL, Ton CC, Saunders GF, Hanson IM, Prosser J, Jordan T, Hastie ND, van Heyningen V. Mouse small eye results from mutations in a paired-like homeobox-containing gene. *Nature* 1991;**354**(6354):522-5.
141. Schedl A, Ross A, Lee M, Engelkamp D, Rashbass P, van Heyningen V, Hastie ND. Influence of PAX6 gene dosage on development: overexpression causes severe eye abnormalities. *Cell* 1996;**86**(1):71-82.
142. Favor J, Peters H, Hermann T, Schmahl W, Chatterjee B, Neuhauser-Klaus A, Sandulache R. Molecular characterization of Pax6(2Neu) through Pax6(10Neu): an extension of the Pax6 allelic series and the identification of two possible hypomorph alleles in the mouse Mus musculus. *Genetics* 2001;**159**(4):1689-700.
143. Halder G, Callaerts P, Gehring WJ. Induction of ectopic eyes by targeted expression of the eyeless gene in Drosophila. *Science* 1995;**267**(5205):1788-92.
144. Chow RL, Altmann CR, Lang RA, Hemmati-Brivanlou A. Pax6 induces ectopic eyes in a vertebrate. *Development* 1999;**126**(19):4213-22.
145. Beby F, Lamonerie T. The homeobox gene Otx2 in development and disease. *Exp Eye Res* 2013;**111**:9-16.
146. Zuber ME, Gestri G, Viczian AS, Barsacchi G, Harris WA. Specification of the vertebrate eye by a network of eye field transcription factors. *Development* 2003;**130**(21):5155-67.
147. Martinez-Morales JR, Dolez V, Rodrigo I, Zaccarini R, Leconte L, Bovolenta P, Saule S. OTX2 activates the molecular network underlying retina pigment epithelium differentiation. *J Biol Chem* 2003;**278**(24):21721-31.
148. Acampora D, Mazan S, Lallemand Y, Avantaggiato V, Maury M, Simeone A, Brulet P. Forebrain and midbrain regions are deleted in Otx2-/- mutants due to a defective anterior neuroectoderm specification during gastrulation. *Development* 1995;**121**(10):3279-90.
149. Simeone A, Acampora D, Mallamaci A, Stornaiuolo A, D'Apice MR, Nigro V, Boncinelli E. A vertebrate gene related to orthodenticle contains a homeodomain of the bicoid class and demarcates anterior neuroectoderm in the gastrulating mouse embryo. *Embo J* 1993;**12**(7):2735-47.
150. Joyner AL, Liu A, Millet S. Otx2, Gbx2 and Fgf8 interact to position and maintain a mid-hindbrain organizer. *Curr Opin Cell Biol* 2000;**12**(6):736-41.
151. Martinez-Morales JR, Signore M, Acampora D, Simeone A, Bovolenta P. Otx genes are required for tissue specification in the developing eye. *Development* 2001;**128**(11):2019-30.
152. Matsuo I, Kuratani S, Kimura C, Takeda N, Aizawa S. Mouse Otx2 functions in the formation and patterning of rostral head. *Genes Dev* 1995;**9**(21):2646-58.
153. Nishida A, Furukawa A, Koike C, Tano Y, Aizawa S, Matsuo I, Furukawa T. Otx2 homeobox gene controls retinal photoreceptor cell fate and pineal gland development. *Nat Neurosci* 2003;**6**(12):1255-63.
154. Chuang JC, Raymond PA. Zebrafish genes rx1 and rx2 help define the region of forebrain that gives rise to retina. *Dev Biol* 2001;**231**(1):13-30.
155. Chuang JC, Mathers PH, Raymond PA. Expression of three Rx homeobox genes in embryonic and adult zebrafish. *Mech Dev* 1999;**84**(1-2):195-8.
156. Martinez-De Luna RI, Kelly LE, El-Hodiri HM. The Retinal Homeobox (Rx) gene is necessary for retinal regeneration. *Dev Biol* 2011;**353**(1):10-8.

157. Nelson SM, Park L, Stenkamp DL. Retinal homeobox 1 is required for retinal neurogenesis and photoreceptor differentiation in embryonic zebrafish. *Dev Biol* 2009;**328**(1):24-39.
158. Mathers PH, Grinberg A, Mahon KA, Jamrich M. The Rx homeobox gene is essential for vertebrate eye development. *Nature* 1997;**387**(6633):603-7.
159. Tucker P, Laemle L, Munson A, Kanekar S, Oliver ER, Brown N, Schlecht H, Vetter M, Glaser T. The eyeless mouse mutation (ey1) removes an alternative start codon from the Rx/rax homeobox gene. *Genesis* 2001;**31**(1):43-53.
160. Chase HB. Studies on an Anophthalmic Strain of Mice. IV. a Second Major Gene for Anophthalmia. *Genetics* 1944;**29**(3):264-9.
161. Loosli F, Winkler S, Burgtorf C, Wurmbach E, Ansorge W, Henrich T, Grabher C, Arendt D, Carl M, Krone A, Grzebisz E, Wittbrodt J. Medaka eyeless is the key factor linking retinal determination and eye growth. *Development* 2001;**128**(20):4035-44.
162. Loosli F, Staub W, Finger-Baier KC, Ober EA, Verkade H, Wittbrodt J, Baier H. Loss of eyes in zebrafish caused by mutation of chokh/rx3. *EMBO Rep* 2003;**4**(9):894-9.
163. Andreazzoli M, Gestri G, Cremisi F, Casarosa S, Dawid IB, Barsacchi G. Xrx1 controls proliferation and neurogenesis in Xenopus anterior neural plate. *Development* 2003;**130**(21):5143-54.
164. Lesnik Oberstein SA, Kriek M, White SJ, Kalf ME, Szuhai K, den Dunnen JT, Breuning MH, Hennekam RC. Peters Plus syndrome is caused by mutations in B3GALTL, a putative glycosyltransferase. *Am J Hum Genet* 2006;**79**(3):562-6.
165. Ueda Y, Yamaguchi R, Ikawa M, Okabe M, Morii E, Maeda Y, Kinoshita T. PGAP1 knock-out mice show otocephaly and male infertility. *J Biol Chem* 2007;**282**(42):30373-80.
166. Petryk A, Anderson RM, Jarcho MP, Leaf I, Carlson CS, Klingensmith J, Shawlot W, O'Connor MB. The mammalian twisted gastrulation gene functions in foregut and craniofacial development. *Dev Biol* 2004;**267**(2):374-86.
167. Sergi C, Kamnasaran D. PRRX1 is mutated in a fetus with agnathia-otocephaly. *Clin Genet* 2011;**79**(3):293-5.
168. Golzio C, Martinovic-Bouriel J, Thomas S, Mougou-Zrelli S, Grattagliano-Bessieres B, Bonniere M, Delahaye S, Munnich A, Encha-Razavi F, Lyonnet S, Vekemans M, Attie-Bitach T, Etchevers HC. Matthew-Wood syndrome is caused by truncating mutations in the retinol-binding protein receptor gene STRA6. *Am J Hum Genet* 2007;**80**(6):1179-87.
169. Pasutto F, Sticht H, Hammersen G, Gillessen-Kaesbach G, Fitzpatrick DR, Nurnberg G, Brasch F, Schirmer-Zimmermann H, Tolmie JL, Chitayat D, Houge G, Fernandez-Martinez L, Keating S, Mortier G, Hennekam RC, von der Wense A, Slavotinek A, Meinecke P, Bitoun P, Becker C, Nurnberg P, Reis A, Rauch A. Mutations in STRA6 cause a broad spectrum of malformations including anophthalmia, congenital heart defects, diaphragmatic hernia, alveolar capillary dysplasia, lung hypoplasia, and mental retardation. *Am J Hum Genet* 2007;**80**(3):550-60.
170. Kirchhoff M, Bisgaard AM, Stoeva R, Dimitrov B, Gillessen-Kaesbach G, Fryns JP, Rose H, Grozdanova L, Ivanov I, Keymolen K, Fagerberg C, Tranebjaerg L, Skovby F, Stefanova M. Phenotype and 244k array-CGH characterization of chromosome 13q deletions: an update of the phenotypic map of 13q21.1-qter. *Am J Med Genet A* 2009;**149A**(5):894-905.
171. Porter FD, Drago J, Xu Y, Cheema SS, Wassif C, Huang SP, Lee E, Grinberg A, Massalas JS, Bodine D, Alt F, Westphal H. Lhx2, a LIM homeobox gene, is required for eye, forebrain, and definitive erythrocyte development. *Development* 1997;**124**(15):2935-44.
172. Yun S, Saijoh Y, Hirokawa KE, Kopinke D, Murtaugh LC, Monuki ES, Levine EM. Lhx2 links the intrinsic and extrinsic factors that control optic cup formation. *Development* 2009;**136**(23):3895-906.
173. Danno H, Michiue T, Hitachi K, Yukita A, Ishiura S, Asashima M. Molecular links among the causative genes for ocular malformation: Otx2 and Sox2 coregulate Rax expression. *Proc Natl Acad Sci U S A* 2008;**105**(14):5408-13.
174. Chao R, Nevin L, Agarwal P, Riemer J, Bai X, Delaney A, Akana M, JimenezLopez N, Bardakjian T, Schneider A, Chassaing N, Schorderet DF, FitzPatrick D, Kwok PY, Ellgaard L, Gould DB,

Zhang Y, Malicki J, Baier H, Slavotinek A. A male with unilateral microphthalmia reveals a role for TMX3 in eye development. *PLoS One* 2010;**5**(5):e10565.
175. Barabasi AL, Oltvai ZN. Network biology: understanding the cell's functional organization. *Nat Rev Genet* 2004;**5**(2):101-13.
176. Tabata Y, Ouchi Y, Kamiya H, Manabe T, Arai K, Watanabe S. Specification of the retinal fate of mouse embryonic stem cells by ectopic expression of Rx/rax, a homeobox gene. *Mol Cell Biol* 2004;**24**(10):4513-21.
177. Ko BS, Chang TC, Shyue SK, Chen YC, Liou JY. An efficient transfection method for mouse embryonic stem cells. *Gene Ther* 2009;**16**(1):154-8.
178. Irizarry RA, Hobbs B, Collin F, Beazer-Barclay YD, Antonellis KJ, Scherf U, Speed TP. Exploration, normalization, and summaries of high density oligonucleotide array probe level data. *Biostatistics* 2003;**4**(2):249-64.
179. Carvalho BS, Irizarry RA. A framework for oligonucleotide microarray preprocessing. *Bioinformatics* 2010;**26**(19):2363-7.
180. Smyth GK, Michaud J, Scott HS. Use of within-array replicate spots for assessing differential expression in microarray experiments. *Bioinformatics* 2005;**21**(9):2067-75.
181. Li H, Durbin R. Fast and accurate short read alignment with Burrows-Wheeler transform. *Bioinformatics* 2009;**25**(14):1754-60.
182. Wen J, Hu Q, Li M, Wang S, Zhang L, Chen Y, Li L. Pax6 directly modulate Sox2 expression in the neural progenitor cells. *Neuroreport* 2008;**19**(4):413-7.
183. Ciani L, Patel A, Allen ND, ffrench-Constant C. Mice lacking the giant protocadherin mFAT1 exhibit renal slit junction abnormalities and a partially penetrant cyclopia and anophthalmia phenotype. *Mol Cell Biol* 2003;**23**(10):3575-82.
184. Engelen E, Akinci U, Bryne JC, Hou J, Gontan C, Moen M, Szumska D, Kockx C, van Ijcken W, Dekkers DH, Demmers J, Rijkers EJ, Bhattacharya S, Philipsen S, Pevny LH, Grosveld FG, Rottier RJ, Lenhard B, Poot RA. Sox2 cooperates with Chd7 to regulate genes that are mutated in human syndromes. *Nat Genet* 2011;**43**(6):607-11.
185. Boycott KM, Vanstone MR, Bulman DE, Mackenzie AE. Rare-disease genetics in the era of next-generation sequencing: discovery to translation. *Nat Rev Genet* 2013;**14**(10):681-91.
186. de Ligt J, Willemsen MH, van Bon BW, Kleefstra T, Yntema HG, Kroes T, Vulto-van Silfhout AT, Koolen DA, de Vries P, Gilissen C, del Rosario M, Hoischen A, Scheffer H, de Vries BB, Brunner HG, Veltman JA, Vissers LE. Diagnostic exome sequencing in persons with severe intellectual disability. *N Engl J Med* 2012;**367**(20):1921-9.
187. Michaelson JJ, Shi Y, Gujral M, Zheng H, Malhotra D, Jin X, Jian M, Liu G, Greer D, Bhandari A, Wu W, Corominas R, Peoples A, Koren A, Gore A, Kang S, Lin GN, Estabillo J, Gadomski T, Singh B, Zhang K, Akshoomoff N, Corsello C, McCarroll S, Iakoucheva LM, Li Y, Wang J, Sebat J. Whole-genome sequencing in autism identifies hot spots for de novo germline mutation. *Cell* 2012;**151**(7):1431-42.

ANNEXES

Client: Chiasma
Date réalisation: 19/03/2012
Nb de gènes retenus: 230
Critère p value ajustée: Benjamini & Hochberg

Seuil p value ajustée: 0,05
Log2 fold change: 0,5

Nom gène	Log2 intensité moyenne dans la condition souris SOX2	Log2 intensité moyenne dans la condition souris SCRUMBLE	Log2 du fold change	Fold change	P value brute	P value ajustée BH	Annotations										
ProbeSet	Souris_SOX2	Souris_SCRUMBLE	logFC	FC	p.value	adj.P.Val	Gene_Accession	Gene_Symbol	Gene_Description	mrna_assignr	GO_bio_proc	GO_cel_com	GO_mol_fun	pathway	total_probes	crosshyb_typ	seqname	strand
10346594	8,30858592	6,559496475	1,74908945	3,36146341	9,27E-12	2,63E-07	NM_001033373	Cdk15	cyclin-dependent kinase	NM_0010333	NM_0010333	NM_0010333	NM_0010333	---	33	1	chr1	+
10458663	7,012533124	5,906889563	0,89435644	0,53798713	5,42E-09	3,03E-05	NM_009468	Dpysl3	dihydropyrimidinase-like	NM_009468	NM_009468	NM_009468	NM_009468	---	32	1	chr18	-
10514576	8,600285423	7,413036213	1,18724921	2,27718138	6,41E-09	3,03E-05	NM_172872	Kank4	KN motif and ankyrin rep	NM_172872	NM_172872	NM_172872	NM_172872	---	33	1	chr4	-
10515003	8,628789002	7,670569792	0,95821921	1,94291018	4,46E-09	3,03E-05	NM_001099303	Fam159a	family with sequence sim	NM_0010993	NM_0010993	NM_0010993	NM_0010993	---	26	1	chr4	-
10539850	9,164835806	10,15699738	-0,99216157	0,50272198	3,33E-09	3,03E-05	8C024401	8430410A17Rik	RIKEN cDNA 8430410A17	BC024401	BC024401 //	BC024401 //	BC024401 //	---	27	1	chr6	+
10582649	8,559326753	7,393441243	1,16588551	2,2437089	4,13E-09	3,03E-05	NM_171824	Pgbd5	piggyBac transposable el	NM_171824	NM_171824	NM_171824	NM_171824	---	29	1	chr8	-
10357249	10,06581649	8,878602423	1,18721407	2,27712591	8,56E-09	3,18E-05	NM_001085409	Steap3	STEAP family member 3	NM_0010854	NM_0010854	NM_0010854	NM_0010854	---	42	1	chr1	-
10569429	10,20076118	8,916463745	1,28429744	2,43563413	7,89E-09	3,18E-05	NM_001161624	Cdkn1c	cyclin-dependent kinase	NM_0011616	NM_0011616	NM_0011616	NM_0011616	NM_0011616	34	1	chr7	-
10574780	9,257630075	7,664922629	1,59270745	3,01614842	1,02E-08	3,22E-05	NM_008289	Hsd11b2	hydroxysteroid 11-beta d	NM_008289	NM_008289	NM_008289	NM_008289	BC014753 //	33	1	chr8	+
10381140	7,555003674	6,614159007	0,94084467	1,91965182	4,05E-08	8,97E-05	NM_028918	Ttc25	tetratricopeptide repeat	NM_028918	NM_028918	NM_028918	NM_028918	---	25	1	chr11	+
10385036	9,444078043	8,794766803	0,64931124	1,56841924	5,02E-08	8,97E-05	NM_008005	Fgf18	fibroblast growth factor	NM_008005	NM_008005	NM_008005	NM_008005	---	26	1	chr11	-
10390519	8,605719666	7,73581794	0,86990173	1,82753841	3,49E-08	8,97E-05	NM_001163608	Plxdc1	plexin domain containing	NM_0011636	---	NM_0011636	---	---	30	1	chr11	-
10399691	10,66973959	9,80500375	0,86473584	1,8210062	4,96E-08	8,97E-05	NM_010496	Id2	inhibitor of DNA binding	NM_010496	NM_010496	NM_010496	NM_010496	---	21	1	chr12	-
10402514	8,098327954	9,153381569	-1,05505362	0,48127934	5,06E-08	8,97E-05	NM_009337	Tcf1	T-cell lymphoma breakpo	NM_009337	NM_009337	NM_009337	---	---	25	1	chr12	-
10451665	8,969934932	7,538001757	1,43193317	2,69808009	4,09E-08	8,97E-05	NM_009694	Apobec2	apolipoprotein B mRNA e	NM_009694	NM_009694	---	NM_009694	---	28	1	chr17	-
10527323	8,650453077	7,512805881	1,1376472	2,2002191	4,26E-08	8,97E-05	NM_010800	Bhlha15	basic helix-loop-helix fan	NM_010800	NM_010800	NM_010800	NM_010800	---	25	1	chr5	+
10570516	6,050226625	6,714120064	-0,66389344	0,63117263	5,75E-08	9,59E-05	NM_029116	Kbtbd11	kelch repeat and BTB (PO	NM_029116	NM_029116	NM_029116	NM_029116	---	24	1	chr8	+
10354677	8,279972419	7,15401152	1,1259609	2,1824686	8,04E-08	9,96E-05	NM_001081433	Ankrd44	ankyrin repeat domain 44	NM_0010814	NM_0010814	NM_0010814	NM_0010814	---	26	1	chr1	-
10472350	11,01497168	10,16818008	0,8467916	1,7984968	8,22E-08	9,96E-05	NM_145523	Gca	grancalcin	NM_145523	---	NM_145523	NM_145523	---	30	1	chr2	+
10477252	11,20695159	10,29452054	0,91243095	1,88221438	8,43E-08	9,96E-05	NM_010407	Hck	hemopoietic cell kinase	NM_010407	NM_010407	NM_010407	NM_010407	---	26	1	chr2	+
10481518	10,11895528	8,693649959	1,42630532	2,68757557	8,00E-08	9,96E-05	NM_022415	Ptges	prostaglandin E synthase	NM_022415	NM_022415	NM_022415	NM_022415	NM_022415	25	1	chr2	-
10506725	10,06305578	9,323437481	0,7396183	1,66973401	8,04E-08	9,96E-05	NM_198037	Cachd1	cache domain containing	NM_198037	NM_198037	NM_198037	NM_198037	---	28	1	chr4	+
10538959	9,954391681	8,982748585	0,9716431	1,9610728	8,43E-08	9,96E-05	NM_001101464	Foxl3	forkhead box l3	NM_0011014	NM_0011014	NM_0011014	NM_0011014	---	26	1	chr6	+
10600205	11,88531827	11,04026009	0,84505817	1,79633717	7,91E-08	9,96E-05	NM_029352	Dusp9	dual specificity phosphat	NM_029352	NM_029352	NM_029352	NM_029352	---	25	1	chrX	+
10567359	10,04171705	9,207864483	0,83385256	1,78243882	9,85E-08	0,0001168	NM_022420	Gprc5b	G protein-coupled recept	NM_022420	NM_022420	NM_022420	NM_022420	---	26	1	chr7	-
10594418	8,410115431	7,468183409	0,94193203	1,92109921	1,04E-07	0,00011347	NM_008542	Smad6	MAD homolog 6 (Drosop	NM_008542	NM_008542	NM_008542	NM_008542	NM_008542	31	1	chr9	-
10490129	8,38029232	7,386084549	0,99420777	1,99198638	1,36E-07	0,0001376	NM_007557	Bmp7	bone morphogenetic pro	NM_007557	NM_007557	NM_007557	---	---	29	1	chr2	-
10590031	8,407967525	9,183836201	-0,77586868	0,58403686	1,35E-07	0,0001376	NM_133721	Itga9	integrin alpha 9	NM_133721	NM_133721	NM_133721	NM_133721	NM_133721	28	1	chr9	+
10474048	8,036443748	7,290396915	0,74604883	1,67719081	1,43E-07	0,00013962	NM_030725	Syt13	synaptotagmin XIII	NM_030725	NM_030725	NM_030725	NM_030725	---	32	1	chr2	+
10517153	9,246089224	9,886429374	-0,6403401	0,65051753	1,49E-07	0,00014093	NM_145833	Lin28a	lin-28 homolog A (C. eleg	NM_145833	NM_145833	NM_145833	NM_145833	---	25	1	chr4	-
10457686	6,87674485	6,149033658	0,72770917	1,65600631	1,67E-07	0,00014756	NM_013505	Dsc2	desmocollin 2	NM_013505	NM_013505	NM_013505	NM_013505	---	39	1	chr18	-
10501827	7,261230101	5,922235767	1,33899433	2,52978915	1,82E-07	0,00014756	NR_036456	A730020M07Rik	RIKEN cDNA A730020M07	NR_036456	NR_036456 //	NR_036456 //	NR_036456 //	---	28	1	chr3	-
10505705	8,055114562	8,996414593	-0,94130003	0,5207634	1,81E-07	0,00014756	NM_019535	Sh3gl2	SH3-domain GRB2-like 2	NM_019535	NM_019535	NM_019535	NM_019535	---	33	1	chr4	+
10519123	8,6089087	7,526070959	1,08283822	2,11819913	1,69E-07	0,00014756	NM_011303	Dhrs3	dehydrogenase/reductas	NM_011303	NM_011303	NM_011303	NM_011303	---	31	1	chr4	+
10540833	8,301480751	9,225150825	-0,92367007	0,52716625	1,77E-07	0,00014756	NM_178703	Slc6a1	solute carrier family 6 (ne	NM_178703	NM_178703	NM_178703	NM_178703	---	32	1	chr6	+
10449551	8,765634572	8,048535379	0,71709919	1,6438734	2,25E-07	0,00017325	NM_153166	Cpne5	copine V	NM_153166	NM_153166	NM_153166	NM_153166	---	44	1	chr17	-
10485695	6,757399236	7,697945148	-0,94054591	0,52103568	2,26E-07	0,00017325	NR_033473	Gm13939	predicted gene 13939	NR_033473	NR_033473 /	NR_033473 /	---	---	25	1	chr2	-
10501811	7,980213669	7,258219579	0,72199409	1,64946034	2,57E-07	0,00019203	NM_145394	Slc44a3	solute carrier family 44,	NM_145394	NM_145394	NM_145394	NM_145394	---	30	1	chr3	-
10346001	7,589842789	6,741553352	0,84828943	1,80036501	2,75E-07	0,00020022	NM_028450	Gulp1	GULP, engulfment adapt	NM_028450	NM_028450	NM_028450	---	---	36	1	chr1	+
10393904	7,253790945	8,337358301	-1,08356736	0,47186061	3,14E-07	0,00022277	NM_175263	Notum	notum pectinacetylester	NM_175263	NM_175263	NM_175263	NM_175263	---	32	1	chr11	-
10366545	7,599023002	6,892965507	0,70605749	1,63134	3,39E-07	0,00023431	NM_027468	Cpm	carboxypeptidase M	NM_027468	NM_027468	NM_027468	NM_027468	---	28	1	chr10	+
10535065	7,256991607	8,03743033	-0,78043872	0,58218372	3,29E-07	0,00025558	NM_172723	Adap1	ArfGAP with dual PH dor	NM_172723	NM_172723	NM_172723	NM_172723	---	39	1	chr5	-
10495042	8,395344076	9,137203886	-0,74185981	0,597968	4,03E-07	0,00026597	NM_027982	Ppm1j	protein phosphatase 1J	NM_027982	NM_027982	---	NM_027982	---	31	1	chr3	+
10358213	8,903252494	9,784445594	-0,881881	0,54292014	4,50E-07	0,00027734	NM_030676	Nr5a2	nuclear receptor subfam	NM_030676	NM_030676	NM_030676	NM_030676	M81385 // G	33	1	chr1	-
10392221	9,737257007	8,969019839	0,76823713	1,70318731	4,40E-07	0,00027734	NM_008816	Pecam1	platelet/endothelial cell	NM_008816	NM_008816	NM_008816	---	---	37	1	chr11	-
10477985	9,019846831	8,337717728	0,6821291	1,60450591	4,34E-07	0,00027734	NM_010923	Nnat	neuronatin	NM_010923	NM_010923	NM_010923	---	---	39	1	chr2	+
10556302	9,362722009	8,532842925	0,82987908	1,77753638	4,60E-07	0,00027734	NM_009667	Ampd3	adenosine monophospha	NM_009667	NM_009667	---	NM_009667	---	35	1	chr7	+
10555981	10,39036523	9,746605251	0,64375998	1,5623958	5,40E-07	0,00031907	NM_008624	Mras	muscle and microspikes I	NM_008624	NM_008624	NM_008624	NM_008624	---	32	1	chr9	-
10506433	8,496233349	9,229991179	-0,73175783	0,60216978	5,58E-07	0,00032099	NM_177259	Dab1	disabled homolog 1 (Dro	NM_177259	NM_177259	NM_177259	NM_177259	---	50	1	chr4	+
10354897	10,27965732	9,507395657	0,77226169	1,70794536	5,55E-07	0,00032234	NM_172406	Trak2	trafficking protein, kines	NM_172406	NM_172406	NM_172406	NM_172406	---	35	1	chr1	-
10390117	10,42216473	9,70496727	0,71719746	1,64388533	5,55E-07	0,00032234	NM_013565	Itga3	integrin alpha 3	NM_013565	NM_013565	NM_013565	NM_013565	NM_013565	29	1	chr11	-
10603492	9,547776363	10,36207286	-0,8142969	0,56868573	6,03E-07	0,00032234	NM_016913	Porcn	porcupine homolog (Dro	NM_016913	NM_016913	NM_016913	NM_016913	---	30	1	chrX	-
10605988	11,55639467	12,54849776	-0,99210309	0,50274437	6,64E-07	0,00034834	NM_007515	Slc7a3	solute carrier family 7 (ca	NM_007515	NM_007515	NM_007515	NM_007515	---	24	1	chrX	-

10524327	8,123549225	7,302860635	0,82068859	1,76624881	7,62E-07	0,00039257	NM_001081235	Mn1	meningioma 1	NM_0010812	NM_0010812	---	---	---	27	1	chr5	+
10368317	10,85495861	11,40211821	-0,5471596	0,68436619	8,29E-07	0,00041956	NM_134005	Enpp3	ectonucleotide pyrophos	NM_134005	NM_134005	NM_134005	NM_134005	---	48	1	chr10	-
10382435	9,121458706	8,297876269	0,82358244	1,76979522	8,87E-07	0,00044125	NM_001110337	Gprc5c	G protein-coupled recept	NM_0011103	NM_0011103	NM_0011103	NM_0011103	---	25	1	chr11	+
10356475	6,76675608	6,062968369	0,70378771	1,62877544	9,21E-07	0,00045021	NM_177305	Arl4c	ADP-ribosylation factor-li	NM_177305	NM_177305	NM_177305	NM_177305	---	34	1	chr1	-
10585851	7,216398337	6,483334415	0,73306392	1,66216537	9,56E-07	0,00045682	NM_001081192	Hcn4	hyperpolarization-activat	NM_0010811	NM_0010811	NM_0010811	NM_0010811	---	31	1	chr9	+
10600707	11,98812688	12,54017915	-0,55205227	0,68204921	9,67E-07	0,00045682	NM_007430	Nr0b1	nuclear receptor subfam	NM_007430	NM_007430	NM_007430	NM_007430	M1568 // Ge	25	1	chrX	+
10492689	9,968671303	9,300917742	0,66775356	1,58859742	9,86E-07	0,00045828	NM_019971	Pdgfc	platelet-derived growth f	NM_019971	NM_019971	NM_019971	NM_019971	---	26	1	chr3	+
10383214	9,693391739	9,095709562	0,59768218	1,51328338	1,02E-06	0,00046489	AK173199	Rnf213	ring finger protein 213	AK173199	AK173199 //	AK173199 //	AK173199 //	---	49	1	chr11	+
10381603	8,343433501	7,504147279	0,83928622	1,78916475	1,05E-06	0,00046829	NM_020510	Fzd2	frizzled homolog 2 (Droso	NM_020510	NM_020510	NM_020510	NM_020510	NM_020510	36	1	chr11	+
10382328	8,167519271	7,180930592	0,98658868	1,98149411	1,06E-06	0,00046829	NM_011448	Sox9	SRY-box containing gene	NM_011448	NM_011448	NM_011448	NM_011448	---	25	1	chr11	+
10502780	10,19306672	10,88541846	-0,69235174	0,61884425	1,15E-06	0,00049336	NM_001081298	Lphn2	latrophilin 2	NM_0010812	NM_0010812	NM_0010812	NM_0010812	---	25	1	chr3	-
10595979	9,115087736	8,181511231	0,93357651	1,91000512	1,15E-06	0,00049336	NM_008624	Mras	muscle and microspikes R	NM_008624	NM_008624	NM_008624	NM_008624	---	25	1	chr9	-
10387170	7,591815482	8,289694659	-0,6978791	0,61647779	1,18E-06	0,00049738	NM_008744	Ntn1	netrin 1	NM_008744	NM_008744	NM_008744	NM_008744	---	27	1	chr11	-
10482144	10,38174234	9,879830361	0,50191198	1,41608904	1,23E-06	0,00051451	NM_001100591	Rc3h2	ring finger and CCCH-type	NM_0011005	NM_0011005	NM_0011005	NM_0011005	---	44	1	chr2	-
10346564	8,952638172	8,178227453	0,77441072	1,71049124	1,29E-06	0,00052188	NM_009812	Casp8	caspase 8	NM_009812	NM_009812	NM_009812	NM_009812	NM_009812	29	1	chr1	+
10572800	9,374075748	9,99458662	-0,62051087	0,65044056	1,59E-06	0,00063504	NM_008452	Klf2	Kruppel-like factor 2 (lun	NM_008452	NM_008452	NM_008452	NM_008452	---	26	1	chr8	+
10356484	9,975186346	10,56629275	-0,5911064	0,66383362	1,66E-06	0,00065218	NM_010262	Gbx2	gastrulation brain homeo	NM_010262	NM_010262	NM_010262	NM_010262	---	25	1	chr1	-
10492341	6,403379909	7,194828042	-0,7914481	0,57776386	1,78E-06	0,00068914	NM_001081295	4631416L12Rik	RIKEN cDNA 4631416L12	NM_0010812	NM_0010812	NM_0010812	NM_0010812	---	26	1	chr3	+
10495675	8,71347369	7,954602186	0,7588715	1,69216647	1,82E-06	0,00068914	NM_010171	F3	coagulation factor III	NM_010171	NM_010171	NM_010171	NM_010171	---	27	1	chr3	+
10517727	7,080952863	6,253250509	0,82770235	1,77485646	1,82E-06	0,00068914	NM_173427	Klhdc7a	kelch domain containing	NM_173427	NM_173427	NM_173427	NM_173427	---	27	1	chr4	-
10382300	8,100990984	7,361895149	0,73909583	1,66912944	1,89E-06	0,00069445	NM_011943	Map2k6	mitogen-activated protei	NM_011943	NM_011943	---	NM_011943	NM_011943	30	1	chr11	+
10458731	9,046076152	9,603136446	-0,55706029	0,67968571	1,87E-06	0,00069445	NM_001085373	Mcc	mutated in colorectal can	NM_0010853	---	---	---	---	64	1	chr18	-
10584288	9,445323083	8,810599015	0,63472407	1,55264076	1,96E-06	0,00070347	NM_028783	Robo4	roundabout homolog 4 (	NM_028783	NM_028783	NM_028783	NM_028783	---	40	1	chr9	+
10364346	10,98340516	11,56250804	-0,57910289	0,66937989	2,01E-06	0,00071255	NM_019448	Dnmt3l	DNA (cytosine-5-)-methy	NM_019448	NM_019448	NM_019448	NM_019448	---	27	1	chr10	+
10434993	7,503942118	6,871891543	0,63205058	1,54976619	2,04E-06	0,00071573	NM_172822	Pigz	phosphatidylinositol glyc	NM_172822	NM_172822	NM_172822	NM_172822	---	26	1	chr16	+
10383233	9,402341537	8,682570178	0,71977136	1,64692101	2,11E-06	0,00071904	AK173199	Rnf213	ring finger protein 213	AK173199	AK173199 //	AK173199 //	AK173199 //	---	25	1	chr11	+
10439732	7,303329897	6,857493798	0,50583609	1,41994603	2,19E-06	0,0007344	NM_001134480	Plcxd2	phosphatidylinositol-spe	NM_001134	NM_001134	NM_001134	NM_001134	---	26	1	chr16	-
10471721	6,500969591	7,082613694	-0,5816441	0,66820186	2,20E-06	0,0007344	NM_008969	Ptgs1	prostaglandin-endopero	NM_008969	NM_008969	NM_008969	NM_008969	M34141 // Ge	36	1	chr2	+
10502748	8,820747808	9,357249248	-0,53650144	0,68944079	2,27E-06	0,00074018	NM_001081298	Lphn2	latrophilin 2	NM_0010812	NM_0010812	NM_0010812	NM_0010812	---	33	1	chr3	-
10506274	9,408401347	9,951539915	-0,54313857	0,6862763	2,25E-06	0,00074018	NM_001164565	Dnajc6	DnaJ (Hsp40) homolog, s	NM_0011645	NM_0011645	NM_0011645	NM_0011645	---	42	1	chr4	+
10553450	6,335609583	5,553790725	0,78181886	1,71929709	2,36E-06	0,00075853	NM_001037906	Nell1	NEL-like 1 (chicken)	NM_0010379	NM_0010379	NM_0010379	NM_0010379	---	40	1	chr7	+
10360227	9,479099744	8,921937146	0,5571626	1,47137257	2,50E-06	0,00079683	NM_011063	Pea15a	phosphoprotein enriched	NM_011063	NM_011063	NM_011063	NM_011063	---	27	1	chr1	-
10416541	8,349267767	8,906414735	-0,55714747	0,67964465	2,63E-06	0,0008128	NM_172813	Enox1	ecto-NOX disulfide-thiol (	NM_172813	NM_172813	NM_172813	NM_172813	NM_172813	47	1	chr14	+
10421416	9,037321231	9,602158643	-0,56483741	0,6760316	2,60E-06	0,0008128	NM_013514	Epb41l3	erythrocyte protein band	NM_013514	NM_013514	NM_013514	NM_013514	---	33	1	chr14	-
10496262	7,860141946	8,279991189	-0,41984394	0,65073861	2,64E-06	0,0008128	NM_178877	Nhedc2	Na+/H+ exchanger do ma	NM_178877	NM_178877	NM_178877	NM_178877	---	25	1	chr3	+
10360748	6,835831986	6,152897912	0,68293407	1,60540141	2,84E-06	0,00085753	NM_013734	Atp1a4	ATPase, Na+/K+ transpor	NM_013734	NM_013734	NM_013734	NM_013734	---	42	1	chr1	-
10406277	8,450230959	7,870765103	0,57946586	1,4942399	2,83E-06	0,00085753	NM_053108	Glrx	glutaredoxin	NM_053108	NM_053108	NM_053108	NM_053108	---	23	1	chr13	+
10558481	8,02505365	7,471198714	0,55385494	1,46800302	3,01E-06	0,00089811	NM_011993	Dpysl4	dihydropyrimidinase-like	NM_011993	NM_011993	NM_011993	NM_011993	---	27	1	chr7	+
10361807	6,492358842	5,809626036	0,68274274	1,60518852	3,28E-06	0,00091047	NM_010437	Hivep2	human immunodeficienc	NM_010437	NM_010437	NM_010437	NM_010437	---	32	1	chr10	+
10368383	8,187689441	7,521856683	0,66583276	1,55648377	3,26E-06	0,00091047	NM_172787	L3mbtl3	l(3)mbt-like 3 (Drosophila	NM_172787	NM_172787	NM_172787	---	---	48	1	chr10	-
10379886	9,824305177	9,742140669	0,58216451	1,49709369	3,14E-06	0,00091047	NM_007607	Car4	carbonic anhydrase 4	NM_007607	NM_007607	NM_007607	NM_007607	---	32	1	chr11	+
10410039	11,63954518	11,11005289	0,52959228	1,44352139	3,25E-06	0,00091047	NM_008957	Ptch1	patched homolog 1	NM_008957	NM_008957	NM_008957	NM_008957	---	46	1	chr13	-
10606203	7,285603355	8,151908157	-0,8663048	0,51895968	3,17E-06	0,00091047	DQ975302	C77370	expressed sequence C77	DQ975302	DQ975302 //	DQ975302 //	DQ975302 //	---	26	1	chrX	-
10382425	8,490911379	7,887261937	0,60364944	1,51955558	3,45E-06	0,00094934	NM_001110337	Gprc5c	G protein-coupled recept	NM_0011103	NM_0011103	NM_0011103	NM_0011103	---	53	1	chr11	+
10443785	8,375652054	8,958895703	-0,5832385	0,66285322	3,64E-06	0,00099344	NM_008804	Pde9a	phosphodiesterase 9A	NM_008804	NM_008804	NM_008804	NM_008804	---	40	1	chr17	+
10349932	5,900601883	6,484495824	-0,5838939	0,66716063	4,04E-06	0,00107161	NM_175443	Etnk2	ethanolamine kinase 2	NM_175443	NM_175443	NM_175443	NM_175443	---	37	1	chr1	+
10381096	8,174079569	7,420149951	0,75392961	1,68637954	3,99E-06	0,00107161	NM_010517	Igfbp4	insulin-like growth factor	NM_010517	NM_010517	NM_010517	NM_010517	NM_010517	26	1	chr11	+
10587633	6,460992175	7,22694946	-0,7659572	0,58806304	4,15E-06	0,00107232	NM_011851	Nt5e	5'-nucleotidase, ecto	NM_011851	NM_011851	NM_011851	NM_011851	---	32	1	chr9	+
10602429	10,085721	9,531594459	0,55412653	1,44806517	4,11E-06	0,00107232	BC043119	Wnk3-ps	WNK lysine deficient prot	BC043119	---	---	---	---	25	1	chrX	+
10604694	8,725204022	9,453529332	-0,7283253	0,59943478	4,16E-06	0,00107232	NM_177293	Mtap7d3	MAP7 domain containing	NM_177293	NM_177293	NM_177293	NM_177293	---	36	1	chrX	-
10361829	11,77284561	11,26614377	0,50632191	1,42042427	4,56E-06	0,00113779	NM_010828	Cited2	Cbp/p300-interacting tra	NM_010828	NM_010828	NM_010828	NM_010828	---	26	1	chr10	+
10383208	6,789601389	6,181793748	0,60780764	1,52344163	4,53E-06	0,00113779	ENSMUST00000131035	Rnf213	ring finger protein 213	ENSMUST000	ENSMUST000	ENSMUST000	ENSMUST000	---	25	1	chr11	+
10499811	8,381744639	7,680479636	0,701265	1,62592384	4,58E-06	0,00113779	NM_008727	Npr1	natriuretic peptide recep	NM_008727	NM_008727	NM_008727	NM_008727	---	27	1	chr3	-
10352318	10,42457928	9,857801291	0,56687799	1,48131452	4,85E-06	0,00115146	NM_010094	Lefty1	left right determination f	NM_010094	NM_010094	NM_010094	NM_010094	---	22	1	chr1	+
10421774	8,99312092	9,713109176	-0,7199882	0,60710238	4,82E-06	0,00115146	NM_001081330	Dgkh	diacylglycerol kinase, eta	NM_0010813	NM_0010813	NM_0010813	NM_0010813	---	31	1	chr14	-
10527332	9,60132956	9,069137754	0,53219181	1,44612454	4,93E-06	0,00115146	NM_016789	Nptx2	neuronal pentraxin 2	NM_016789	---	NM_016789	NM_016789	---	25	1	chr5	+
10546417	9,411071248	9,984531055	-0,5734598	0,67200329	4,86E-06	0,00115146	NM_009426	Trh	thyrotropin releasing hor	NM_009426	NM_009426	NM_009426	NM_009426	---	29	1	chr6	-
10597575	10,21349434	9,577165686	0,63632865	1,55436859	4,89E-06	0,00115146	NM_019676	Plcd1	phospholipase C, delta 1	NM_019676	NM_019676	NM_019676	NM_019676	NM_019676	32	1	chr9	-
10561009	8,658549987	9,185627649	-0,5270776	0,693359	5,05E-06	0,00116504	NM_001039185	Ceacam1	carcinoembryonic antige	NM_0010391	NM_0010391	NM_0010391	---	---	22	1	chr7	-
10424628	8,400303575	7,895216454	0,50508711	1,41920905	5,49E-06	0,00122229	NM_174991	Bai1	brain-specific angiogenes	NM_174991	NM_174991	---	NM_174991	---	35	1	chr15	+
10529497	7,975134512	7,375350127	0,59978438	1,51549006	5,72E-06	0,00125722	NM_194344	Sh3tc1	SH3 domain and tetratric	NM_194344	NM_194344	NM_194344	NM_194344	---	34	1	chr5	-
10385772	5,931347062	5,220775277	0,71057178	1,63645257	5,90E-06	0,00128698	NR_034155	Olfr1372-ps1	olfactory receptor 1372	NR_034155	---	---	---	---	12	1	chr11	-
10382375	9,334128476	8,73820973	0,59591825	1,5114348	6,08E-06	0,00130685	NM_053273	Ttyh2	tweety homolog 2 (Droso	NM_053273	NM_053273	NM_053273	NM_053273	---	32	1	chr11	+
10518113	8,959411385	8,400588828	0,55882256	1,4730865	6,37E-06	0,00135688	NM_144531	9030409G11Rik	RIKEN cDNA 9030409G11	NM_144531	NM_144531	NM_144531	---	---	47	1	chr4	-
10600765	9,265112457	9,776963112	-0,5118506	0,70132222	6,47E-06	0,00136882	NM_211138	Pcyt1b	phosphate cytidylyltransf	NM_211138	NM_211138	NM_211138	NM_211138	---	33	1	chrX	+
10477854	9,300459609	8,785857454	0,51460214	1,42860012	6,59E-06	0,00138375	NM_013510	Epb41	erythrocyte protein band	NM_013510	NM_013510	NM_013510	NM_013510	---	32	1	chr2	+
10592802	8,330879786	7,798368056	0,53251173	1,44644526	6,85E-06	0,00142713	NM_027909	C2cd2l	C2 calcium-dependent do	NM_027909	NM_027909	NM_027909	NM_027909	---	25	1	chr9	-

10523490	8,506164943	7,991656178	-0,51450882	1,4285077	7,16E-06	0,00148238	NM_010203	Fgf5	fibroblast growth factor 5	NM_010203	NM_010203	NM_010203	NM_010203	---	28	1	chr5	+
10443598	6,602488691	7,184353952	-0,58186526	0,6680994	7,46E-06	0,00148931	NM_013811	Dnahc8	dynein, axonemal, heavy	NM_013811	NM_013811	NM_013811	NM_013811	---	91	1	chr17	+
10502776	9,750786586	10,32581558	-0,575029	0,67127276	7,42E-06	0,00148931	NM_001081298	Lphn2	latrophilin 2	NM_0010812	NM_0010812	NM_0010812	NM_0010812	---	25	1	chr3	-
10549836	8,839772551	9,400045756	-0,5602732	0,67817372	7,37E-06	0,00148931	NM_001177416	Gm6792	predicted gene 6792	NM_0011774	NM_0011774	NM_0011774	NM_0011774	---	25	1	chr7	+
10383198	9,07613098	8,482389739	-0,59374126	1,5091552	7,57E-06	0,0014904	ENSMUST00000131035	Rnf213	ring finger protein 213	ENSMUST000	ENSMUST000	ENSMUST000	ENSMUST000	---	25	1	chr11	+
10433445	8,884005448	8,283827294	0,60017815	1,5159037	7,62E-06	0,0014904	NM_172961	Abat	4-aminobutyrate aminotr	NM_172961	NM_172961	NM_172961	NM_172961	---	32	1	chr16	+
10585099	9,963261074	10,75834551	-0,79508443	0,5763094	7,57E-06	0,0014904	NM_175482	Usp28	ubiquitin specific peptida	NM_175482	NM_175482	NM_175482	NM_175482	---	29	1	chr9	+
10407327	10,8208031	10,23084912	0,58995398	1,5051987	8,14E-06	0,00154822	NM_010330	Emb	embrigin	NM_010330	NM_010330	NM_010330	---	---	27	1	chr13	+
10383206	8,266605128	7,661432379	0,60517275	1,5211608	8,32E-06	0,00157157	ENSMUST00000131035	Rnf213	ring finger protein 213	ENSMUST000	ENSMUST000	ENSMUST000	ENSMUST000	---	25	1	chr11	+
10537231	7,497680461	6,855188427	0,64249203	1,5610232	8,76E-06	0,00161469	NM_009292	Stra8	stimulated by retinoic ac	NM_009292	NM_009292	NM_009292	---	---	29	1	chr6	+
10587880	8,875148727	9,46490987	-0,58976114	0,6644529	8,77E-06	0,00161469	NM_029620	Pcolce2	procollagen C-endopepti	NM_029620	---	NM_029620	NM_029620	---	33	1	chr9	+
10528864	7,472941505	8,342295209	-0,8693537	0,5473920	9,44E-06	0,0017161	NM_175651	Cnoy1	canopy 1 homolog (zebra	NM_175651	NM_175651	NM_175651	NM_175651	---	34	1	chr5	-
10602704	8,392106933	8,893000346	-0,50089341	0,7066690	9,71E-06	0,00175282	NM_173780	Klf8	Kruppel-like factor 8	NM_173780	NM_173780	NM_173780	NM_173780	---	40	1	chrX	+
10480477	7,34845925	8,157817945	-0,8093587	0,5706354	1,01E-05	0,00180815	NM_011040	Paa8	paired box gene 8	NM_011040	NM_011040	NM_011040	NM_011040	---	36	1	chr2	-
10511560	7,382728234	8,056669714	-0,6739414	0,6267919	1,09E-05	0,00190381	NM_194055	Esrp1	epithelial splicing regulat	NM_194055	NM_194055	NM_194055	NM_194055	---	43	1	chr4	-
10456756	8,149225289	7,545014913	0,60421038	1,5201465	1,11E-05	0,00190857	NM_145356	Zbtb7c	zinc finger and BTB doma	NM_145356	---	NM_145356	NM_145356	---	29	1	chr18	+
10353713	7,02260936	7,551044645	-0,5284352	0,6933062	1,13E-05	0,00192328	NM_010827	Msr	musculin	NM_010827	NM_010827	NM_010827	NM_010827	---	25	1	chr1	-
10496091	9,664327442	10,28271985	-0,6183924	0,6513963	1,17E-05	0,00195998	NM_010703	Lef1	lymphoid enhancer bindi	NM_010703	NM_010703	NM_010703	NM_010703	NM_010703	35	1	chr3	+
10440427	8,465254066	9,023171688	-0,5579176	0,6792819	1,21E-05	0,00200609	NM_025967	D16Ertd472e	DNA segment, Chr 16, ER	NM_025967	NM_025967	NM_025967	NM_025967	---	26	1	chr16	-
10511870	6,762389215	7,388255023	-0,6258658	0,6480307	1,31E-05	0,00213262	NM_010243	Fut9	fucosyltransferase 9	NM_010243	NM_010243	NM_010243	NM_010243	---	31	1	chr4	-
10358027	8,916660177	8,331017351	0,5856428	1,5007075	1,33E-05	0,002147	NM_001163131	Elf3	E74-like factor 3	NM_001163	NM_001163	NM_001163	NM_001163	---	28	1	chr1	-
10587038	8,741506561	8,158163814	0,58334275	1,4983168	1,38E-05	0,00221829	NM_025890	2410004A20Rik	RIKEN cDNA 2410004A20	NM_025890	NM_025890	NM_025890	NM_025890	---	25	1	chr9	+
10427796	7,536024101	6,947542625	0,58848147	1,5036632	1,41E-05	0,00222627	NM_008728	Npr3	natriuretic peptide recep	NM_008728	NM_008728	NM_008728	NM_008728	---	30	1	chr15	-
10408610	9,055584657	8,390869917	0,66471474	1,5852547	1,43E-05	0,00224715	NM_009450	Tubb2a	tubulin, beta 2A	---	---	---	---	---	16	1	chr13	-
10459827	9,549466781	10,08263925	-0,5331724	0,6910334	1,48E-05	0,00229067	NM_001164504	Rnf165	ring finger protein 165	NM_0011645	NM_0011645	NM_0011645	NM_0011645	---	27	1	chr18	-
10543017	9,226092116	8,715548798	0,5105433	1,4245855	1,51E-05	0,0023207	NM_013743	Pdx4	pyruvate dehydrogenase	NM_013743	NM_013743	NM_013743	NM_013743	NM_013743	33	1	chr6	-
10518201	9,082686729	8,558796279	0,5238904	1,4378273	1,61E-05	0,00240797	NM_029948	Pramef12	PRAME family member 1	NM_029948	---	---	---	---	25	1	chr4	-
10383168	9,620154707	9,036860992	0,5832937	1,4982659	1,65E-05	0,00242766	ENSMUST00000131035	Rnf213	ring finger protein 213	ENSMUST000	ENSMUST000	ENSMUST000	ENSMUST000	---	45	1	chr11	+
10419446	3,399928417	3,900033323	-0,5001049	0,7070553	1,84E-05	0,00265328	NM_146363	Olfr731	olfactory receptor 731	NM_146363	NM_146363	NM_146363	NM_146363	---	25	1	chr14	-
10383632	8,49508288	7,980219067	0,5148637	1,4288592	1,92E-05	0,00269801	NM_030207	Sfi1	Sfi1 homolog, spindle ass	NM_030207	NM_030207	NM_030207	NM_030207	---	38	1	chr11	-
10605104	8,777592342	9,369335613	-0,5917432	0,6635406	1,92E-05	0,00269801	NM_001029868	Pdlim4	PDZ domain containing 4	NM_0010298	NM_0010298	NM_0010298	NM_0010298	---	32	1	chrX	-
10484894	8,402048169	9,012692284	-0,6106441	0,6549042	1,99E-05	0,00276003	NM_008982	Ptprj	protein tyrosine phospha	NM_008982	NM_008982	NM_008982	NM_008982	---	34	1	chr2	-
10383152	8,649931842	8,145206898	0,5047249	1,4188628	2,00E-05	0,00276022	ENSMUST00000131035	Rnf213	ring finger protein 213	ENSMUST000	ENSMUST000	ENSMUST000	ENSMUST000	---	30	1	chr11	+
10462217	10,27494242	9,772155634	0,5027867	1,4169479	2,30E-05	0,00300394	NM_015826	Dmrt1	doublesex and mab-3 rel	NM_015826	NM_015826	NM_015826	NM_015826	---	35	1	chr19	+
10408873	6,776406755	7,379403202	-0,8029994	0,6583850	2,36E-05	0,0030555	NM_001033399	Gfod1	glucose-fructose oxidore	NM_0010333	NM_0010333	NM_0010333	NM_0010333	---	25	1	chr13	-
10397264	6,93365571	7,551230621	-0,6176149	0,6517475	2,43E-05	0,00311425	NM_001168588	7420416P09Rik	RIKEN cDNA 7420416P09	NM_0011685	NM_0011685	NM_0011685	NM_0011685	---	26	1	chr12	+
10458767	5,669144707	6,442079838	-0,7729351	0,5852256	2,54E-05	0,00320531	NM_178872	Trim36	tripartite motif-containin	NM_178872	NM_178872	NM_178872	NM_178872	---	27	1	chr18	-
10456045	8,130198475	7,42377467	0,7064238	1,6317542	2,80E-05	0,00335045	NM_001146268	Pdgfrb	platelet derived growth f	NM_0011462	NM_0011462	NM_0011462	NM_0011462	---	48	1	chr18	+
10456392	6,798853037	6,181908455	0,6169485	1,5336258	2,82E-05	0,00335045	NM_007702	Cidea	cell death-inducing DNA	NM_007702	NM_007702	NM_007702	NM_007702	---	26	1	chr18	+
10456513	6,898667103	7,443532256	-0,9448651	0,6854554	3,06E-05	0,00351057	NM_013596	Mc5r	melanocortin 5 receptor	NM_013596	NM_013596	NM_013596	NM_013596	---	25	1	chr18	+
10383202	9,321887299	8,764365471	0,5875218	1,4717385	3,12E-05	0,00352544	ENSMUST00000131035	Rnf213	ring finger protein 213	ENSMUST000	ENSMUST000	ENSMUST000	ENSMUST000	---	25	1	chr11	+
10586781	9,938900442	9,437172753	0,5017276	1,4159083	3,09E-05	0,00352544	NM_181072	Myo1e	myosin IE	NM_181072	NM_181072	NM_181072	NM_181072	---	30	1	chr9	+
10562469	8,769317284	9,538544407	-0,7692271	0,5867317	3,17E-05	0,00356792	NM_028034	Tdrd12	tudor domain containing	NM_028034	NM_028034	NM_028034	NM_028034	---	32	1	chr7	-
10456021	6,897342433	6,359778702	0,5293637	1,4432925	3,44E-05	0,0037461	NM_177407	Camk2a	calcium/calmodulin-depe	NM_177407	NM_177407	NM_177407	NM_177407	NM_177407	55	1	chr18	+
10476935	8,347503493	8,985677533	-0,6381740	0,6425256	3,68E-05	0,0039109	NM_001085521	Tmem90b	transmembrane protein 9	NM_0010855	NM_0010855	NM_0010855	NM_0010855	---	27	1	chr2	+
10383195	8,467661471	7,966492937	0,5011684	1,4153539	3,74E-05	0,00392369	ENSMUST00000131035	Rnf213	ring finger protein 213	ENSMUST000	ENSMUST000	ENSMUST000	ENSMUST000	---	25	1	chr11	+
10411226	9,45314333	9,970369127	-0,5172258	0,6987141	3,87E-05	0,00401661	NM_007974	F2rl1	coagulation factor II (thro	NM_007974	NM_007974	NM_007974	NM_007974	NM_007974	25	1	chr13	-
10471067	8,136100488	7,585496634	0,5506038	1,4664986	4,23E-05	0,00421917	NM_009116	Prrx2	paired related homeoboo	NM_009116	NM_009116	NM_009116	NM_009116	---	25	1	chr2	+
10478633	7,225914429	6,649725257	0,5761891	1,4909056	4,24E-05	0,00421917	NM_013599	Mmp9	matrix metallopeptidase	NM_013599	NM_013599	NM_013599	NM_013599	NM_013599	26	1	chr2	+
10348733	8,170148546	8,824081055	-0,6539325	0,6355455	4,40E-05	0,00428579	NM_172463	Sned1	sushi, nidogen and EGF-li	NM_172463	NM_172463	NM_172463	NM_172463	---	35	1	chr1	+
10604564	9,504376523	8,853257493	0,6511180	1,5617018	4,45E-05	0,00428771	NM_008150	Gpc4	glypican 4	NM_008150	---	NM_008150	NM_008150	---	33	1	chrX	-
10542885	9,995224715	9,463816492	0,5314082	1,4453393	4,64E-05	0,00435627	NM_001081237	Klhdc5	kelch domain containing	NM_0010812	NM_0010812	NM_0010812	NM_0010812	---	26	1	chr6	+
10509204	9,117609018	9,621758303	-0,5041492	0,7058760	4,76E-05	0,00440038	NM_011542	Tcea3	transcription elongation	NM_011542	NM_011542	NM_011542	NM_011542	---	34	1	chr4	+
10444828	8,110110999	7,609286161	0,5008248	1,4150223	4,84E-05	0,00445621	NM_207648	H2-Q6	histocompatibility 2, Q re	NM_207648	NM_207648	NM_207648	---	---	19	1	chr17	+
10594068	7,877172122	7,347193446	0,5299788	1,4439078	4,87E-05	0,00447208	NM_010729	Loxl1	lysyl oxidase-like 1	NM_010729	NM_010729	NM_010729	NM_010729	---	32	1	chr9	-
10497994	6,916169641	6,399025455	0,5171441	1,4311195	4,99E-05	0,00452162	NM_001101479	Pabpc4l	poly(A) binding protein, c	NM_0011014	NM_0011014	NM_0011014	NM_0011014	---	25	1	chr3	-
10518735	8,367274013	7,810189457	0,5570845	1,4712929	5,84E-05	0,0049557	NM_029035	Spsb1	spla/ryanodine receptor	NM_029035	NM_029035	NM_029035	NM_029035	---	31	1	chr4	-
10453811	7,621742224	7,096651632	0,5250905	1,4390239	5,91E-05	0,00497691	NM_001083628	Greb1l	growth regulation by est	NM_0010836	NM_0010836	NM_0010836	NM_0010836	---	26	1	chr18	+
10348194	6,865453586	7,629850934	-0,7643974	0,5886992	6,03E-05	0,00502818	NM_028889	Efhd1	EF hand domain containi	NM_028889	NM_028889	NM_028889	NM_028889	---	27	1	chr1	+
10522908	3,941692283	4,561758556	-0,6200662	0,6506410	6,33E-05	0,00517293	ENSMUST00000007601	2310003L06Rik	RIKEN cDNA 2310003L06	ENSMUST000	ENSMUST000	ENSMUST000	ENSMUST000	---	27	1	chr5	+
10569499	7,737913934	7,230817905	0,5070960	1,4211866	6,28E-05	0,00517293	NM_001166273	Csgp5	chondroitin sulfate prote	NM_0011662	NM_0011662	NM_0011662	---	---	38	1	chr9	+
10439082	6,123945049	6,664812383	-0,5408673	0,6873575	7,18E-05	0,00562415	BC025912	Osta	organic solute transporte	ENSMUST000	BC025912 //	BC025912 //	BC025912 //	---	15	1	chr16	-
10366313	8,729026442	8,2221626	0,5068638	1,4209579	7,54E-05	0,0059872	NM_175489	Osbpl8	oxysterol binding protein	NM_175489	NM_175489	NM_175489	NM_175489	---	48	1	chr10	+
10362372	6,359450098	6,894231648	-0,5347815	0,6902633	8,11E-05	0,00618363	NM_001162537	9330159F19Rik	RIKEN cDNA 9330159F19	NM_0011625	NM_0011625	NM_0011625	NM_0011625	---	25	1	chr10	+
10498575	8,331781446	7,804753735	0,5270277	1,4409574	8,13E-05	0,00618363	NM_016753	Lan	latexin	NM_016753	NM_016753	NM_016753	NM_016753	---	28	1	chr3	-
10534862	11,10454778	10,52056247	0,5839853	1,4988343	8,16E-05	0,00618363	NM_008788	Pcolce	procollagen C-endopepti	NM_008788	NM_008788	---	---	NM_008788	28	1	chr5	-
10362363	7,719239697	8,327784318	-0,6085446	0,6558579	8,75E-05	0,00651053	NM_026138	6330407I23Rik	RIKEN cDNA 6330407I23	NM_026138	NM_026138	NM_026138	NM_026138	---	29	1	chr10	+

10453797	7,416683383	6,829990782	-0,5866926	1,5017999	8,75E-05	0,00651053	NM_001083628	Gretzl	growth regulation by est	NM_0010836	NM_0010836	NM_0010836	NM_0010836	---	26	1	chr18	+
10375360	8,755085478	8,149262814	0,605822666	1,5218463	8,80E-05	0,00652946	NM_007897	Ebf1	early B-cell factor 1	NM_007897	NM_007897	NM_007897	NM_007897	---	38	1	chr11	+
10506335	6,587537980	6,008810867	0,57872712	1,49353095	8,97E-05	0,0066195	NM_019840	Pde4b	phosphodiesterase 4B, c	NM_019840	NM_019840	NM_019840	NM_019840	NM_019840	47	1	chr4	+
10425138	9,743285049	9,120705093	0,62257996	1,53962602	9,48E-05	0,00689249	NM_009164	Sh3bp1	SH3-domain binding prot	NM_009164	NM_009164	NM_009164	NM_009164	---	38	1	chr15	+
10548105	8,806944482	9,391282983	-0,5843385	0,66695508	9,83E-05	0,0070582	NM_009829	Ccnd2	cyclin D2	NM_009829	NM_009829	NM_009829	NM_009829	BC049086 //	27	1	chr6	-
10532765	3,158960042	3,668007159	-0,50904712	0,7026864	0,00010663	0,00746439	---	NA	NA	ENSMUST000	---	---	---	---	18	1	chr5	-
10548038	6,863939645	6,080420195	0,78351945	1,72132492	0,00010886	0,00754556	NM_001164035	Ntf3	neurotrophin 3	NM_001164(	NM_001164(	NM_001164(	NM_001164(	---	25	1	chr6	-
10502778	7,717130048	8,30935863	-0,59222858	0,66331747	0,00010947	0,00756269	NM_001081298	Lphn2	latrophilin 2	NM_0010812	NM_0010812	NM_0010812	NM_0010812	---	25	1	chr3	-
10362350	5,828345795	6,349061948	-0,52071615	0,69702575	0,00010994	0,00756486	NM_178666	Themis	thymocyte selection ass	NM_178666	NM_178666	NM_178666	NM_178666	---	30	1	chr10	+
10497149	6,899402783	6,388467226	0,51093556	1,42497396	0,00012365	0,00822687	NM_026582	Wls	wntless homolog (Droso	NM_026582	NM_026582	NM_026582	NM_026582	---	29	1	chr3	+
10600777	8,45167720	7,880016375	0,57166089	1,48623359	0,00012445	0,00824323	NR_028320	AU015836	expressed sequence AU0	NR_028320	NR_028320 //	NR_028320 //	NR_028320 //	---	26	1	chrX	+
10503520	6,855602028	7,483113122	-0,62751109	0,64729215	0,00013922	0,00886944	NM_015767	Ttpa	tocopherol (alpha) transf	NM_015767	NM_015767	NM_015767	NM_015767	---	25	3	chr4	+
10450904	7,715096168	8,342450878	-0,62735471	0,64736232	0,00014689	0,00922871	NM_001039137	Scoc	short coiled-coil protein	NM_0010391	NM_0010391	NM_0010391	NM_0010391	---	39	3	chr17	-
10550818	4,517892881	3,873972132	0,64392075	1,56256992	0,00016327	0,00978584	NM_207548	Vmn1r174	vomeronasal 1 receptor 1	NM_207548	NM_207548	NM_207548	NM_207548	---	8	1	chr7	+
10580765	5,82779415	6,351946863	-0,52415271	0,69536738	0,00017211	0,01016522	NM_026385	Pilp	plasma membrane prote	NM_026385	NM_026385	NM_026385	NM_026385	---	26	1	chr8	-
10540472	8,261090306	7,501520742	0,75956956	1,69298544	0,00017724	0,01039932	NM_011498	Bhlhe40	basic helix-loop-helix fan	NM_011498	NM_011498	NM_011498	NM_011498	---	25	1	chr6	+
10390783	7,356630085	6,797179591	0,55945048	1,47370779	0,00018969	0,0108422	NM_007719	Ccr7	chemokine (C-C motif) re	NM_007719	NM_007719	NM_007719	NM_007719	NM_007719	25	1	chr11	-
10456904	7,687628206	7,102201051	0,585427161	1,50048319	0,00019448	0,01099753	NM_013831	Pstpip2	proline-serine-threonine	NM_013831	NM_013831	NM_013831	NM_013831	---	65	1	chr18	+
10597251	7,057240679	6,389335955	0,66790472	1,58876387	0,00021052	0,01150075	NM_001029838	Pknox2	Pbx/knotted 1 homeobox	NM_0010298	NM_0010298	NM_0010298	NM_0010298	---	27	1	chr9	-
10352302	8,653457082	8,094755773	0,55870131	1,4728422	0,00025532	0,01303797	NM_177099	Lefty2	left-right determination f	NM_177099	NM_177099	NM_177099	NM_177099	---	15	1	chr1	+
10396606	6,181381219	6,793389617	-0,6120084	0,65428523	0,00029436	0,01427011	NM_001005510	Sybe2	synaptic nuclear envelop	NM_0010055	NM_0010055	NM_0010055	NM_0010055	---	25	1	chr12	+
10517731	9,216004516	8,684604018	0,5314005	1,44533157	0,00037992	0,01680295	NM_198610	Igsf21	immunoglobin superfam	NM_198610	NM_198610	NM_198610	NM_198610	---	30	1	chr4	-
10383192	7,848322874	7,291578004	0,55474487	1,48890884	0,00038515	0,01695506	ENSMUST00000131035	Rnf213	ring finger protein 213	ENSMUST000	ENSMUST000	ENSMUST000	ENSMUST000	---	26	1	chr11	+
10606163	6,885446024	7,664085396	-0,77863937	0,58291629	0,00039772	0,01714783	BC107248	4930519F16Rik	RIKEN cDNA 4930519F16	BC107248	BC107248 //	BC107248 //	BC107248 //	---	39	1	chrX	-
10400987	8,39043836	7,836937994	0,55350037	1,46764227	0,00043859	0,01839148	NM_009189	Six1	sine oculis-related home	NM_009189	NM_009189	NM_009189	NM_009189	---	25	1	chr12	-
10572046	2,902330885	3,413711026	-0,51138014	0,70155098	0,00046118	0,01897588	---	NA	NA	ENSMUST000	---	---	---	---	4	1	chr8	+
10388212	9,082312317	8,546729097	0,53558322	1,44952802	0,00046778	0,01910879	ENSMUST00000131035	Rnf213	ring finger protein 213	ENSMUST000	ENSMUST000	ENSMUST000	ENSMUST000	---	25	1	chr11	+
10414651	8,086656247	7,566964174	0,51969207	1,43364922	0,00050508	0,02013024	NM_001033805	G630016D24Rik	RIKEN cDNA G630016D24	NM_0010338	NM_0010338	NM_0010338	NM_0010338	---	28	1	chr14	+
10434975	7,430249451	6,857621529	0,57262792	1,48723015	0,00051791	0,02037717	NM_013900	Mf2	antigen p97 (melanoma a	NM_013900	NM_013900	NM_013900	NM_013900	---	34	1	chr16	+
10998087	6,892950639	7,621145418	-0,72819478	0,60365876	0,00062058	0,02284879	ENSMUST00000082419	ND6	NADH dehydrogenase su	ENSMUST000	ENSMUST000	ENSMUST000	ENSMUST000	---	22	1	chrM	-
10506929	6,380506723	5,851827376	0,52867885	1,44260752	0,00067041	0,0241908	NM_001033226	Calr4	calreticulin 4	NM_0010332	NM_0010332	NM_0010332	NM_0010332	---	25	1	chr4	+
10535623	4,811955065	4,23944625	0,57250881	1,48710737	0,00067148	0,0241908	NM_001101463	Gm4871	predicted gene 4871	NM_0011014	NM_0011014	NM_0011014	NM_0011014	---	9	1	chr5	-
10452879	6,101546741	6,756152812	-0,65460607	0,63524892	0,00067864	0,02438492	NM_001033367	Nlrc4	NLR family, CARD domain	NM_0010333	NM_0010333	---	NM_0010333	---	29	1	chr17	-
10523297	7,58737498	7,078823215	0,50855177	1,42262139	0,00077878	0,02691737	NM_007635	Ccng2	cyclin G2	NM_007635	NM_007635	NM_007635	---	NM_007635	37	1	chr5	+
10432175	7,344059689	8,028336754	-0,68427656	0,62231781	0,00080133	0,02737072	NR_034051	Snora34	small nucleolar RNA, H/A	NR_034051	NR_034051 /	NR_034051 /	NR_034051 /	---	25	1	chr15	-
10400472	7,655556656	8,185041691	-0,52948504	0,69280198	0,00088729	0,02901342	NM_008701	Nkx2-9	NK2 transcription factor	NM_008701	NM_008701	NM_008701	NM_008701	---	18	1	chr12	-
10459835	7,747349448	8,302854063	-0,5605046	0,67806495	0,00090769	0,02937651	---	NA	NA	BC080318	---	---	---	---	25	1	chr18	-
10542965	8,314657046	7,758964221	0,55569282	1,46987434	0,00091889	0,02960278	NM_001130190	Sgcb	sarcoglycan, epsilon	NM_0011303	---	NM_0011303	NM_0011303	---	27	1	chr6	-
10452432	8,522031862	9,02767313	-0,50564127	0,70434725	0,00095248	0,03027212	NM_015794	Fbxl17	F-box and leucine-rich re	NM_015794	NM_015794	NM_015794	NM_015794	---	27	1	chr17	-
10523563	6,497530741	7,011360355	-0,51382961	0,70036087	0,00105342	0,03214701	NM_173370	Cds1	CDP-diacylglycerol synth	NM_173370	NM_173370	NM_173370	NM_173370	---	26	1	chr5	+
10435787	4,78709286	5,573634799	-0,78664194	0,57973201	0,00176229	0,04525447	---	NA	NA	ENSMUST000	---	---	---	---	7	1	chr16	+
10442069	7,596489683	7,007552184	0,5889379	1,50413895	0,0017998	0,04605096	NM_025681	Lix1	limb expression 1 homol	NM_025681	NM_025681	NM_025681	NM_025681	---	15	1	chr17	+
10598085	5,994997883	6,548487259	-0,55348939	0,68137015	0,00190097	0,04736768	---	NA	NA	BC104337	---	---	---	---	25	3	chrM	-

Etude Chassaing - Souris - Projet 64-10

Etude des gènes différentiellement exprimés entre les conditions :
- souris siPAX6
- souris SCRUMBLE

Puce : Affymetrix Gene Mouse 1.0 ST

Client:	Chassaing
Date réalisation:	25/04/2012
Nb de gènes retenus:	24
Critère p value ajustée:	Benjamini & Hochberg
Seuil p value ajustée:	0,05
Log2 fold change	-

Nom gène	Log2 intensité moyenne dans la condition souris siPAX6	Log2 intensité moyenne dans la condition souris SCRUMBLE	Log2 du fold change	Fold change	P value brute	P value ajustée BH	Annotations										
ProbeSet	Souris_siPAX6	Souris_SCRUMBLE	logFC	FC	p.value	adj.P.Val	Gene_Access	Gene_Symbol	Gene_Description	mrna_assign	GO_bio_proc	GO_cel_comp	GO_mol_func	pathway	total_probes	crosshyb_ty	seqname	strand
10385271	12,14608754	12,59915207	-0,45306452	0,73048952	6,62E-08	0,00093845	NM_009831	Ccng1	cyclin G1	NM_009831	NM_009831	NM_009831	NM_009831	---	31	1	chr11	-
10578922	7,277681896	7,915134444	-0,63745255	0,64284706	4,43E-08	0,00093845	NM_178633	Klhl2	kelch-like 2, Mayven (D	NM_178633	NM_178633	NM_178633	NM_178633	---	28	1	chr8	-
10359961	9,433100867	8,926074262	0,5070266	1,42111825	2,25E-07	0,0021108	NM_010633	Uhmk1	U2AF homology motif (	NM_010633	NM_010633	NM_010633	NM_010633	NM_010633	30	1	chr1	-
10389627	8,231054365	8,672026744	-0,44097238	0,73663795	2,98E-07	0,0021108	NM_053269	Rad51c	RAD51 homolog c (S. ce	NM_053269	NM_053269	NM_053269	NM_053269	---	31	1	chr11	-
10494306	10,92739355	11,33174175	-0,4043482	0,75557758	4,52E-07	0,00256243	NM_008562	Mcl1	myeloid cell leukemia s	NM_008562	NM_008562	NM_008562	NM_008562	NM_008562	25	1	chr3	+
10382508	8,692606136	9,050233349	-0,35762721	0,78044712	2,30E-06	0,00933384	NM_026729	Ict1	immature colon carcino	NM_026729	NM_026729	NM_026729	NM_026729	---	32	1	chr11	+
10389775	7,419690937	7,753215605	-0,33352467	0,79359527	2,27E-06	0,00933384	NM_008796	Pctp	phosphatidylcholine tra	NM_008796	NM_008796	NM_008796	NM_008796	---	28	1	chr11	-
10400572	7,919918771	8,462087081	-0,54216831	0,68673799	3,15E-06	0,01076985	NM_025707	Klhl28	kelch-like 28 (Droscphil	NM_025707	NM_025707	NM_025707	NM_025707	---	29	1	chr12	-
10403466	8,194801645	8,618353769	-0,42355212	0,74558662	3,42E-06	0,01076985	NM_0010814	Dip2c	DIP2 disco-interacting p	NM_0010814	NM_0010814	NM_0010814	NM_0010814	---	28	1	chr13	+
10461078	8,458507641	9,049065807	-0,59055817	0,66408593	3,93E-06	0,01113672	NM_146091	Atl3	atlastin GTPase 3	NM_146091	NM_146091	NM_146091	NM_146091	---	28	1	chr19	+
10561008	9,732432762	9,37401299	0,35841977	1,28202089	4,38E-06	0,01128193	NM_0010391	Ceacam1	carcinoembryonic antig	NM_0010391	NM_0010391	NM_0010391	NM_0010391	---	22	1	chr7	-
10465263	11,01177635	11,30555023	-0,29377388	0,81576534	8,89E-06	0,02100489	NM_011262	Dpf2	D4, zinc and double PHD	NM_011262	NM_011262	NM_011262	NM_011262	---	28	1	chr19	-
10355806	11,53422355	11,27112418	0,26309937	1,20005403	1,01E-05	0,02201036	NM_009447	Tuba4a	tubulin, alpha 4A	NM_009447	NM_009447	NM_009447	NM_009447	---	24	1	chr1	-
10415411	8,869104923	8,601503818	0,26760111	1,20380449	1,10E-05	0,02220372	NM_0010400	Nynrin	NYN domain and retrovi	NM_0010400	NM_0010400	NM_0010400	NM_0010400	---	25	1	chr14	+
10495111	11,09747191	11,45224374	-0,35477183	0,78199331	1,21E-05	0,02292845	NM_027432	Wdr77	WD repeat domain 77	NM_027432	NM_027432	NM_027432	NM_027432	---	22	1	chr3	+
10425161	10,72882744	10,4573127	0,27151474	1,20707451	1,42E-05	0,02509009	NM_008495	Lgals1	lectin, galactose birding	NM_008495	NM_008495	NM_008495	NM_008495	---	25	1	chr15	+
10400926	8,453116109	8,759961734	-0,30684562	0,80840737	1,53E-05	0,02550039	NM_153457	Rtn1	reticulon 1	NM_153457	NM_153457	NM_153457	NM_153457	---	37	1	chr12	-
10354897	8,895024236	9,59166963	0,30335455	1,23401039	1,97E-05	0,03097458	NM_172406	Trak2	trafficking protein, ine	NM_172406	NM_172406	NM_172406	NM_172406	---	35	1	chr1	-
10355456	10,78417114	11,07237264	-0,2882015	0,81692231	2,42E-05	0,03430528	NM_0010054	Mreg	melanoregulin	NM_0010054	NM_0010054	NM_0010054	---	---	29	1	chr1	-
10427026	9,692620238	9,338616165	0,35400407	1,27E10297	2,35E-05	0,03430528	NM_019518	Grasp	GRP1 (general receptor	NM_019518	NM_019518	NM_019518	NM_019518	---	32	1	chr15	+
10498284	8,659516755	8,317310337	0,34220642	1,26769389	2,55E-05	0,03438785	NM_133784	Wwtr1	WW domain containing	NM_133784	NM_133784	NM_133784	NM_133784	---	29	1	chr3	-
10419790	10,76265762	10,49785193	0,26480569	1,20147422	3,21E-05	0,04134638	NM_010590	Jub	ajuba	NM_010590	NM_010590	NM_010590	NM_010590	---	35	1	chr14	-
10472195	7,732764539	8,015855999	-0,28309146	0,82182809	3,76E-05	0,04569498	NM_172527	Nudt15	nudix (nucleoside dipho	NM_172527	NM_172527	NM_172527	NM_172527	---	45	3	chr2	+
10554945	9,05526374	9,326543091	-0,27127935	0,82258445	3,87E-05	0,04569498	NM_028243	Prcp	prolylcarboxypeptidase	NM_028243	NM_028243	NM_028243	NM_028243	---	34	1	chr7	+

Etude Chassaing - Souris - Projet 64-10

[redacted]

Puce: Affymetrix Gene Mouse 1.0 ST

Client: Chassaing
Date réalisation: 25/04/2012
Nb de gènes retenus: 57
Critère p value ajustée: Benjamini & Hochberg

Seuil p value ajustée: 0,05
Log2 fold change: -

10529215	8,972311005	9,740065888	-0,76775488	0,58733077	1,35E-08	7,65E-05	---	NA	NA	ENSMUST00(	---	---	---	---	32	1	chr5	-
10603492	10,06938602	10,51122103	-0,44183502	0,73619762	3,76E-08	0,00017749	NM_016913	Porcn	porcupine homolog (Dr	NM_016913	NM_016913	NM_016913	NM_016913	---	30	1	chrX	-
10569646	11,21000549	11,61987758	-0,40987209	0,75269011	4,58E-07	0,00185513	NM_007631	Ccnd1	cyclin D1	NM_007631	NM_007631	NM_007631	NM_007631	BC044841 //	28	1	chr7	
10589685	10,15643988	10,53904014	-0,38260026	0,76705384	5,53E-07	0,00196059	NM_028838	Lrrc2	leucine rich repeat cont	NM_028838	NM_028838	NM_028838	NM_028838	---	27	1	chr9	+
10404763	8,027595848	8,49635087	-0,46875502	0,72258789	9,51E-07	0,00269496	NM_0011635	Tmem170b	transmembrane protein	NM_0011635	NM_0011635	NM_0011635	NM_0011635	---	25	1	chr13	+
10523490	7,669547317	8,213771261	-0,54422394	0,68576019	9,41E-07	0,00269496	NM_010203	Fgf5	fibroblast growth factor	NM_010203	NM_010203	NM_010203	NM_010203	---	28	1	chr5	+
10474295	8,601624819	9,087011228	-0,48538641	0,71430573	1,21E-06	0,00311754	NM_144783	Wt1	Wilms tumor 1 homolog	NM_144783	NM_144783	NM_144783	NM_144783	---	33	1	chr2	+
10458843	7,7571815	8,32930548	-0,57212398	0,6726258	1,57E-06	0,00357557	NM_018744	Sema6a	sema domain, transmer	NM_018744	NM_018744	NM_018744	NM_018744	---	26	1	chr18	-
10465916	10,73688241	11,24036402	-0,5034816	0,7054024	1,64E-06	0,00357557	NM_0010334	Gm98	predicted gene 98	NM_0010334	NM_0010334	NM_0010334	NM_0010334	---	26	1	chr19	-
10437804	9,112562018	9,465055523	-0,35249351	0,78322922	1,84E-06	0,00372821	NM_011987	Pla2g10	phospholipase A2, grou	NM_011987	NM_011987	NM_011987	NM_011987	---	31	1	chr16	-
10544148	9,268195177	9,81296255	-0,54476737	0,68550193	2,62E-06	0,00494551	NM_0010334	Jhdm1d	jumonji C domain-conta	NM_0010334	NM_0010334	NM_0010334	NM_0010334	---	25	1	chr6	-
10385500	6,410815944	7,052902632	-0,64208669	0,64078546	3,23E-06	0,00508144	NM_008326	Irgm1	immunity-related GTPa	NM_008326	NM_008326	NM_008326	NM_008326	---	25	1	chr11	-
10394209	11,01851623	11,32984369	-0,31132746	0,80589989	3,20E-06	0,00508144	NM_007872	Dnmt3a	DNA methyltransferase	NM_007872	NM_007872	NM_007872	NM_007872	---	46	1	chr12	+
10447437	8,847512159	8,548378025	0,29913413	1,23040574	3,06E-06	0,00508144	NM_028658	Klraq1	KLRAQ motif containing	NM_028658	NM_028658	NM_028658	NM_028658	---	45	1	chr17	+
10355456	10,7101382	11,07237264	-0,36223444	0,77795875	3,96E-06	0,00590495	NM_0010054	Mreg	melanoregulin	NM_0010054	NM_0010054	NM_0010054	---	---	29	1	chr1	-
10403291	4,185561214	4,713970559	-0,52840934	0,69331874	6,16E-06	0,00766464	NM_134072	Akr1c14	aldo-keto reductase fan	NM_134072	NM_134072	NM_134072	NM_134072	---	31	1	chr13	+
10425161	10,77454949	10,4573127	0,31723679	1,2459419	5,51E-06	0,00766464	NM_008495	Lgals1	lectin, galactose birding	NM_008495	NM_008495	NM_008495	NM_008495	---	25	1	chr15	+
10602428	9,256758111	9,661502719	-0,40474461	0,75537	5,69E-06	0,00766464	BC043119	Wnk3-ps	WNK lysine deficient pr	BC043119	---	---	---	---	25	1	chrX	+
10604694	9,139711247	9,587344305	-0,44763306	0,73324485	6,22E-06	0,00766464	NM_177293	Mtap7d3	MAP7 domain containin	NM_177293	NM_177293	NM_177293	NM_177293	---	36	1	chrX	-
10376060	7,751865869	8,239482376	-0,48781651	0,71310355	6,57E-06	0,00775876	NM_008390	Irf1	interferon regulatory fa	NM_008390	NM_008390	NM_008390	NM_008390	M21065 // G	36	1	chr11	+
10362372	6,278657671	6,844194256	-0,56553658	0,67570405	6,96E-06	0,00778709	NM_0011625	9330159F19Rik	RIKEN cDNA 9330159F1	NM_0011625	NM_0011625	NM_0011625	NM_0011625	---	25	1	chr10	+
10427606	10,44622343	10,76829142	-0,32206799	0,79592243	7,42E-06	0,00778709	NM_145468	Skp2	S-phase kinase-associat	NM_145468	NM_145468	NM_145468	NM_145468	NM_145468	30	1	chr15	-
10548105	8,99588891	9,581689649	-0,58580074	0,66627943	7,29E-06	0,00778709	NM_009829	Ccnd2	cyclin D2	NM_009829	NM_009829	NM_009829	NM_009829	BC049086 //	27	1	chr6	-
10546417	9,674708563	10,18884814	-0,51413958	0,70221041	8,08E-06	0,00818196	NM_009426	Trh	thyrotropin releasing ho	NM_009426	NM_009426	NM_009426	NM_009426	---	29	1	chr6	-
10373604	2,109658532	2,716139024	-0,60548049	0,65679703	9,13E-06	0,00892996	ENSMUST000	Olfr227	olfactory receptor 227	ENSMUST000	ENSMUST000	ENSMUST000	ENSMUST000	---	15	1	chr10	-
10507500	9,217858427	9,536260417	-0,31836199	0,80397991	9,49E-06	0,00896891	NM_008135	Slc6a9	solute carrier family 6 (n	NM_008135	NM_008135	NM_008135	NM_008135	---	33	1	chr4	+
10475144	7,533642364	7,822184285	-0,28854192	0,8187291	1,04E-05	0,00950475	NM_007601	Capn3	calpain 3	NM_007601	NM_007601	NM_007601	NM_007601	NM_007601	76	1	chr2	+
10380560	10,59474432	10,91847545	-0,32373113	0,79600081	1,30E-05	0,01147308	NM_201609	Zfp652	zinc finger protein 652	NM_201609	NM_201609	NM_201609	NM_201609	---	25	1	chr11	+
10486203	10,44237851	10,73109068	-0,28871217	0,81863249	1,44E-05	0,01238666	NM_026574	Ino80	INO80 homolog (S. cere	NM_026574	NM_026574	NM_026574	NM_026574	---	37	1	chr2	-
10348670	8,710084304	8,340738423	0,36934588	1,23176701	1,63E-05	0,01360794	NM_181405	Rnpepl1	arginyl aminopeptidase	NM_181405	NM_181405	NM_181405	NM_181405	BC031789 //	31	1	chr1	+
10397264	7,027255006	7,573867848	-0,54557284	0,68464459	1,75E-05	0,01416675	NM_0011685	7420416P09Rik	RIKEN cDNA 7420416P0	NM_0011685	NM_0011685	NM_0011685	NM_0011685	---	26	1	chr12	+
10402808	7,909551628	7,61591635	0,29363527	1,22572494	2,48E-05	0,01901455	NM_010588	Jag2	jagged 2	NM_010588	NM_010588	NM_010588	NM_010588	---	26	1	chr12	-
10506150	8,93072245	9,316862794	-0,38614034	0,76517395	2,48E-05	0,01901455	NM_010425	Foxd3	forkhead box D3	NM_010425	NM_010425	NM_010425	NM_010425	---	25	1	chr4	+
10482687	9,292546838	9,709870665	-0,41732383	0,74881237	3,06E-05	0,02279971	NM_182994	Arl5a	ADP-ribosylation factor-	NM_182994	NM_182994	NM_182994	NM_182994	---	27	1	chr2	-
10499935	5,056733804	5,524895044	-0,46816124	0,72288535	3,25E-05	0,02365362	NM_029667	Lce1i	late cornified envelope	NM_029667	NM_029667	NM_029667	NM_029667	---	13	1	chr3	-
10404127	11,99298641	12,34488234	-0,35189592	0,78355371	3,36E-05	0,02383949	NM_175658	Hist1h2aa	histone cluster 1, H2aa	NM_175658	NM_175658	NM_175658	NM_175658	---	25	1	chr13	+
10453256	7,800064897	8,273859397	-0,4737945	0,72006822	3,48E-05	0,02409722	NM_153512	Kcng3	potassium voltage-gate	NM_153512	NM_153512	NM_153512	NM_153512	---	25	1	chr17	-
10356163	8,434890018	8,828128864	-0,39322858	0,76142367	3,59E-05	0,02425101	NM_175328	Slc6a15	solute carrier family 6 (n	NM_175328	NM_175328	NM_175328	NM_175328	---	28	1	chr10	+
10354677	7,522820098	7,157348083	0,36547201	1,28830806	3,71E-05	0,02442937	NM_0010814	Ankrd44	ankyrin repeat domain 4	NM_0010814	NM_0010814	NM_0010814	NM_0010814	---	26	1	chr1	-
10538227	8,352779758	8,643135752	-0,29035599	0,81770026	3,90E-05	0,02510377	NM_0011629	Dennd4a	DENN/MADD domain co	NM_0011629	NM_0011629	NM_0011629	NM_0011629	---	43	1	chr9	+
10584162	10,98735427	11,39986585	-0,41251157	0,75131428	4,38E-05	0,02760996	NM_019770	Tmed2	transmembrane emp24	NM_019770	NM_019770	NM_019770	---	---	55	3	chr9	+
10607089	10,00595403	10,24534416	-0,23939013	0,84710833	4,93E-05	0,03037616	NM_207625	Acsl4	acyl-CoA synthetase lon	NM_207625	NM_207625	NM_207625	NM_207625	NM_207625	40	1	chrX	-
10368096	3,988585367	4,437297242	-0,44871188	0,73269675	5,13E-05	0,03096082	NM_0011950	Ect2l	epithelial cell transform	NM_0011950	NM_0011950	NM_0011950	NM_0011950	---	27	1	chr10	-
10345777	6,057882842	6,54313034	-0,4852375	0,71437946	5,38E-05	0,03175247	NM_133193	Il1rl2	interleukin 1 receptor-li	NM_133193	NM_133193	NM_133193	NM_133193	---	35	1	chr1	+
10525744	10,52467384	10,928503	-0,40382916	0,75684947	5,51E-05	0,03765998	NM_019770	Tmed2	transmembrane emp24	NM_019770	NM_019770	NM_019770	---	---	53	3	chr5	+
10458808	10,3835245	10,64492319	-0,26139828	0,83427893	6,65E-05	0,03769099	NM_173423	Fem1c	fem-1 homolog c (C.eleg	NM_173423	NM_173423	NM_173423	NM_173423	---	32	1	chr18	-
10496605	8,987902634	9,245751961	-0,2578493	0,83633374	7,13E-05	0,03812056	NM_173763	Ccbl2	cysteine conjugate-beta	NM_173763	NM_173763	NM_173763	NM_173763	---	30	1	chr3	+
10507784	9,924373994	9,574041012	0,35033298	1,27485484	7,11E-05	0,03812056	NM_008917	Ppt1	palmitoyl-protein thioe	NM_008917	NM_008917	NM_008917	NM_008917	---	36	1	chr4	+
10546855	7,963760943	7,719421563	0,24433937	1,18455023	6,90E-05	0,03812056	NM_080448	Srgap3	SLIT-ROBO Rho GTPase	NM_080448	NM_080448	NM_080448	NM_080448	---	75	1	chr6	-
10431659	7,058350734	7,396747103	-0,33839637	0,79091997	8,22E-05	0,04314828	NM_0011090	Kif21a	kinesin family member 2	NM_0011090	NM_0011090	NM_0011090	NM_0011090	---	37	1	chr15	-
10424439	10,11111485	10,36369928	-0,2525844	0,83639139	9,27E-05	0,04776891	NM_133766	Efr3a	EFR3 homolog A (S. cere	NM_133766	NM_133766	NM_133766	NM_133766	---	51	1	chr15	+
10506714	8,532828975	8,202612795	0,33021618	1,25720175	9,67E-05	0,04808254	NR_033496	Lrp8	low density lipoprotein	NR_033496	NR_033496 /	NR_033496 /	NR_033496 /	---	42	1	chr4	+
10551514	8,15147897	8,473664768	-0,3221858	0,79685711	9,52E-05	0,04808254	NM_207238	Fbxo27	F-box protein 27	NM_207238	NM_207238	NM_207238	NM_207238	---	30	1	chr7	+

Etude Chassaing - Souris - Projet 64-10

Liste des gènes différentiellement exprimés entre les conditions :
- souris siRAX
- souris SCRUMBLE

Puce : Affymetrix Gene Mouse 1.0 ST

Client:	Chassaing
Date réalisation:	25/04/2012
Nb de gènes retenus:	57
Critère p value ajustée:	Benjamini & Hochberg
Seuil p value ajustée:	0,05
Log2 fold change	-

Nom gène	Log2 intensité moyenne dans la condition souris siRAX	Log2 intensité moyenne dans la condition souris SCRUMBLE	Log2 du fold change	Fold change	P value brute	P value ajustée BH	Annotations											
ProbeSet	Souris_siRAX	Souris_SCRUMBLE	logFC	FC	p.value	adj.P.Val	Gene_Access	Gene_Symbol	Gene_Description	mrna_assigni	GO_bio_proc	GO_cel_com	GO_mol_fun	pathway	total_probes	crosshyb_ty	seqname	strand
10372600	12,14295999	12,67658381	-0,53362383	0,69081733	5,47E-08	0,001449	NM_007636	Cct2	chaperonin containing T	NM_007636	NM_007636	NM_007636	NM_007636	---	34	1	chr10	-
10459471	8,788831814	9,452639711	-0,6638079	0,63121006	2,04E-07	0,001449	NM_013833	Rax	retina and anterior neu	NM_013833	NM_013833	NM_013833	NM_013833	---	25	1	chr18	-
10470547	9,764204188	10,18384942	-0,41964523	0,74760844	1,83E-07	0,001449	NM_080452	Mrps2	mitochondrial ribosoma	NM_080452	NM_080452	NM_080452	NM_080452	---	34	1	chr2	+
10571312	9,154302994	8,660244503	0,49405849	1,40840133	1,04E-07	0,001449	NM_176933	Dusp4	dual specificity phospha	NM_176933	NM_176933	NM_176933	NM_176933	---	25	1	chr8	+
10497831	11,82960738	12,16842478	-0,3388174	0,79068918	6,30E-07	0,003574	NM_009828	Ccna2	cyclin A2	NM_009828	NM_009828	NM_009828	NM_009828	NM_009828	36	1	chr3	-
10584288	9,334116842	8,908723398	0,42539344	1,34293869	7,74E-07	0,003659	NM_028783	Robo4	roundabout homolog 4	NM_028783	NM_028783	NM_028783	NM_028783	---	40	1	chr9	+
10519747	7,542701128	7,949477824	-0,4067767	0,75430678	1,09E-06	0,004434	NM_011348	Sema3e	sema domain, immunog	NM_011348	NM_011348	NM_011348	NM_011348	---	42	1	chr5	+
10507500	9,18123298	9,536260417	-0,35502744	0,78185477	2,47E-06	0,007792	NM_008135	Slc6a9	solute carrier family 6 (r	NM_008135	NM_008135	NM_008135	NM_008135	---	33	1	chr4	+
10594988	10,8978883	11,24338363	-0,34549533	0,78703771	2,20E-06	0,007792	NM_015806	Mapk6	mitogen-activated prot	NM_015806	NM_015806	NM_015806	NM_015806	NM_027418	26	1	chr9	-
10424363	9,837022627	9,496857084	0,34016554	1,26590184	2,85E-06	0,007919	NM_026746	Nsmce2	non-SMC element 2 hor	NM_026746	NM_026746	NM_026746	NM_026746	---	19	1	chr15	+
10426301	11,75184447	12,07213387	-0,3202894	0,8009092	3,07E-06	0,007919	NM_011541	Tcea1	transcription elongation	NM_011541	NM_011541	NM_011541	NM_011541	---	28	3	chr15	+
10354897	9,957989211	9,59166969	0,36631942	1,28906	5,19E-06	0,011413	NM_172406	Trak2	trafficking protein, kine	NM_172406	NM_172406	NM_172406	NM_172406	---	35	1	chr1	-
10591806	7,635504065	8,200606475	-0,56510241	0,67590749	5,23E-06	0,011413	NM_018739	rp9	retinitis pigmentosa 9 (h	NM_018739	---	NM_018739	NM_018739	---	26	1	chr9	-
10405535	10,06468651	10,43151757	-0,36683105	0,77548401	5,73E-06	0,011595	BC051430	B230219D22Rik	RIKEN cDNA B230219D2	BC051430	BC051430 //	BC051430 //	BC051430 //	---	25	1	chr13	+
10382890	10,03186126	10,40474676	-0,37288561	0,77223636	6,30E-06	0,011868	NM_001166	Sec14l1	SEC14-like 1 (S. cerevisi	NM_001166	NM_001166	NM_001166	NM_001166	---	42	1	chr11	+
10412251	11,28313471	11,87726537	-0,59413066	0,66244351	7,41E-06	0,011868	NM_010887	Ndufs4	NADH dehydrogenase ((	NM_010887	NM_010887	NM_010887	NM_010887	---	26	1	chr13	-
10548118	6,58197031	7,106578704	-0,52460839	0,69514778	7,03E-06	0,011868	NM_201371	Prmt8	protein arginine N-methl	NM_201371	NM_201371	NM_201371	NM_201371	---	27	1	chr6	-
10606195	9,926576446	10,30695208	-0,38037564	0,76823754	7,54E-06	0,011868	NM_011276	Rlim	ring finger protein, LIM	NM_011276	NM_011276	NM_011276	NM_011276	---	28	1	chrX	-
10587073	8,549065093	8,981370261	-0,43230417	0,74107725	9,31E-06	0,013884	NM_023635	Rab27a	RAB27A, member RAS c	NM_023635	NM_023635	NM_023635	NM_023635	---	37	1	chr9	+
10360110	9,602314459	10,00965297	-0,40733851	1,7540131	1,22E-05	0,014728	NR_033728	Nit1	nitrilase 1	NR_033728	NR_033728 //	NR_033728 //	NR_033728 //	---	34	1	chr1	-
10362372	5,304711125	6,844194256	-0,53948301	0,68801742	1,23E-05	0,014728	NM_001162	9330159F19Rik	RIKEN cDNA 9330159F1	NM_001162	NM_001162	NM_001162	NM_001162	---	25	1	chr10	+
10455912	10,55384704	10,8985512	-0,34470416	0,78746944	1,12E-05	0,014728	NM_025478	Isoc1	isochorismatase domai	NM_025478	NM_025478	NM_025478	NM_025478	---	28	1	chr18	+
10500800	4,397543881	4,036833824	0,36071006	1,28405772	1,25E-05	0,014728	---	NA	NA	ENSMUST00	---	---	---	---	25	1	chr3	-
10506215	9,649595286	9,34482965	0,30476564	1,23521796	1,05E-05	0,014728	NM_198037	Cachd1	cache domain containir	NM_198037	NM_198037	NM_198037	NM_198037	---	28	1	chr4	+
10415099	5,850895638	6,231335855	-0,38043922	0,76820368	1,35E-05	0,015324	ENSMUST00	Gm10332	predicted gene 10332	ENSMUST00	ENSMUST00	ENSMUST00	ENSMUST00	---	33	1	chr14	+
10539850	10,11744723	10,50884547	-0,39139824	0,76239035	1,76E-05	0,017799	BC024401	8430410A17Rik	RIKEN cDNA 8430410A1	BC024401	BC024401 //	BC024401 //	BC024401 //	---	27	1	chr6	+
10553301	13,37377859	13,63298489	-0,2592063	0,83554747	1,70E-05	0,017799	NM_001136	Ldha	lactate dehydrogenase A	NM_001136	NM_001136	NM_001136	NM_001136	U13687 // Ge	21	1	chr7	+
10583478	4,048428122	4,511180062	-0,46275194	0,72560085	1,69E-05	0,017799	NM_146339	Olfr77	olfactory receptor 77	NM_146339	NM_146339	NM_146339	NM_146339	---	25	1	chr9	+
10458663	7,63038387	8,027342365	-0,3969585	0,75945769	1,84E-05	0,017983	NM_009468	Dpysl3	dihydropyrimidinase-lik	NM_009468	NM_009468	NM_009468	NM_009468	---	32	1	chr18	-
10358210	9,659537544	9,915202398	-0,25566485	0,83760104	2,09E-05	0,019765	NM_030676	Nr5a2	nuclear receptor subfar	NM_030676	NM_030676	NM_030676	NM_030676	M81385 // Ge	33	1	chr1	-
10360914	9,535876541	9,824403537	-0,288527	0,81873757	2,32E-05	0,021179	NM_146106	Lyplal1	lysophospholipase-like	NM_146106	NM_146106	NM_146106	NM_146106	---	26	1	chr1	-
10473281	9,965923446	9,662423906	0,30349954	1,23413442	2,61E-05	0,023108	NM_008402	Itgav	integrin alpha V	NM_008402	NM_008402	NM_008402	NM_008402	U14135 // Ge	30	1	chr2	+
10498284	8,632120442	8,317310337	0,3148101	1,23771212	2,96E-05	0,025395	NM_133784	Wwtr1	WW domain containing	NM_133784	NM_133784	NM_133784	NM_133784	---	29	1	chr3	-
10443463	10,93666279	10,20255183	0,33411096	1,26060034	3,19E-05	0,026569	NM_007669	Cdkn1a	cyclin-dependent kinase	NM_007669	NM_007669	NM_007669	NM_007669	BC002043 //	30	1	chr17	+
10422781	9,890464493	9,63802153	0,2524429	1,19122249	3,38E-05	0,027408	NM_030168	Rictor	RPTOR independent cor	NM_030168	NM_030168	NM_030168	NM_030168	---	40	1	chr15	+
10349711	10,63693623	10,88377556	-0,24679326	0,84276759	3,69E-05	0,02882	NM_173865	Slc41a1	solute carrier family 41	NM_173865	NM_173865	NM_173865	NM_173865	---	36	1	chr1	+
10383233	9,204357704	8,829404282	0,37495343	1,2967977	3,76E-05	0,02882	AK173199	Rnf213	ring finger protein 213	AK173199	AK173199 //	AK173199 //	AK173199 //	---	25	1	chr11	+
10589494	7,610984843	7,274250835	0,33673401	1,2628944	3,58E-05	0,029692	NM_001166	Csgs5	chondroitin sulfate prot	NM_001166	NM_001166	---	---	---	38	1	chr9	+
10554704	10,23495896	10,59531729	-0,36035832	0,77897108	4,31E-05	0,029883	NM_023403	Mesdc2	mesoderm developmen	NM_023403	NM_023403	---	---	---	25	1	chr7	+
10451665	8,271513265	7,850941179	0,42057199	1,33845811	4,37E-05	0,030994	NM_009694	Apobec2	apolipoprotein B mRNA	NM_009694	NM_009694	---	NM_009694	---	28	1	chr17	-
10607004	9,319890472	9,634661943	-0,31477147	0,80397833	4,78E-05	0,033047	NM_016883	Psmd10	proteasome (prosome,	NM_016883	NM_016883	NM_016883	NM_016883	NM_016883	28	1	chrX	-
10390560	8,207983649	7,925638012	0,28234564	1,21617061	5,12E-05	0,034567	NM_146028	Stac2	SH3 and cysteine rich d	NM_146028	NM_146028	NM_146028	NM_146028	---	35	1	chr11	-
10359428	10,42123754	10,6933009	-0,27206306	0,82813447	5,53E-05	0,036435	NM_146104	Aph1a	anterior pharynx defect	NM_146104	NM_146104	NM_146104	NM_146104	---	34	3	chr1	-
10434998	9,655818433	9,945340902	-0,28952247	0,81817283	6,47E-05	0,038839	NM_026554	Ncbp2	nuclear cap binding pro	NM_026554	NM_026554	NM_026554	NM_026554	NM_026554	24	1	chr16	+
10489569	10,53223156	10,22348822	0,30874334	1,23662832	6,55E-05	0,038839	NM_011125	Pltp	phospholipid transfer p	NM_011125	NM_011125	NM_011125	NM_011125	---	37	1	chr2	-
10494312	10,09522254	10,36909973	-0,27387719	0,82709377	6,46E-05	0,038839	NM_146104	Aph1a	anterior pharynx defect	NM_146104	NM_146104	NM_146104	NM_146104	---	37	3	chr3	+
10524314	11,0260581	11,31792115	-0,29186305	0,81684653	6,16E-05	0,038839	NM_019640	Pitpnb	phosphatidylinositol tra	NM_019640	NM_019640	NM_019640	NM_019640	---	29	1	chr5	+
10604564	9,252045126	8,883375647	0,36866948	1,29316151	6,58E-05	0,038839	NM_008150	Gpc4	glypican 4	NM_008150	---	NM_008150	NM_008150	---	33	1	chrX	-

10401244	11,25312384	11,50541893	-0,25229509	0,83955975	7,08E-05	0,040845	NM_134156	Actn1	actinin, alpha 1	NM_134156	NM_134156	NM_134156	NM_134156	NM_134156	44	1	chr12	-
10401803	6,263396151	5,939464816	0,32393134	1,25173688	7,20E-05	0,040845	---	NA	NA	mmu-mir-300	---	---	---	---	25	1	chr12	-
10488029	8,869131684	9,227730472	-0,35859879	0,77992171	8,00E-05	0,043601	NM_025512	Zfand1	zinc finger, AN1-type do	NM_025512	NM_025512	NM_025512	NM_025512	---	29	3	chr2	-
10569646	11,35197056	11,61987758	-0,26790701	0,83052355	7,89E-05	0,043601	NM_007631	Ccnd1	cyclin D1	NM_007631	NM_007631	NM_007631	NM_007631	BC044841 //	28	1	chr7	-
10360227	9,416748878	9,122345605	0,29440327	1,22637762	8,24E-05	0,044101	NM_011063	Pea15a	phosphoprotein enriche	NM_011063	NM_011063	NM_011063	NM_011063	---	27	1	chr1	-
10562461	9,361509242	9,078092807	0,28341644	1,21707362	8,60E-05	0,045124	NM_178643	C230052I12Rik	RIKEN cDNA C230052I1	NM_178643	NM_178643	NM_178643	NM_178643	---	26	1	chr7	-
10497300	9,035058059	9,412028152	-0,37697009	0,77005314	9,06E-05	0,046724	NM_025512	Zfand1	zinc finger, AN1-type do	NM_025512	NM_025512	NM_025512	NM_025512	---	31	3	chr3	-
10350697	7,65081605	8,029839219	-0,37902317	0,76895807	9,47E-05	0,047927	NM_175460	Nmnat2	nicotinamide nucleotide	NM_175460	NM_175460	NM_175460	NM_175460	---	35	1	chr1	+
10486875	8,550642872	8,874721499	-0,32407863	0,79880838	0,0001005	0,049984	NM_172673	Frmd5	FERM domain containin	NM_172673	NM_172673	NM_172673	NM_172673	---	38	1	chr2	-

[redacted]

[redacted]
- souris PAX6
- souris VV

Puce: Affymetrix Gene Mouse 1.0 ST

Client:	Chassaing
Date réalisation:	10/04/2012
Nb de gènes retenus:	385
Critère p value ajustée:	Benjamini & Hochberg
Seuil p value ajustée	0,05
Log2 fold change	-

Nom gène	Log2 intensité moyenne dans la condition souris PAX6	Log2 intensité moyenne dans la condition souris VV	Log2 du fold change	Fold change	P value brute	P value ajustée BH	Annotations											
ProbeSet	Souris_PAX6	Souris_VV	logFC	FC	p.value	adj.P.Val	Gene_Access	Gene_Symbol	Gene_Description	mrna_assigne	GO_bio_proc	GO_cel_comp	GO_mol_fun	pathway	total_probes	crosshyb_typ	seqname	strand
10548105	11,74510947	9,78096823	1,96414124	3,90180382	1,31E-18	3,72E-14	NM_009829	Ccnd2	cyclin D2	NM_009829	NM_009829	NM_009829	NM_009829	BC049086 //	27	1	chr6	-
10348194	9,927889235	8,74208344	1,1858058	2,27490421	8,10E-14	7,65E-10	NM_028889	Efhd1	EF hand domain containi	NM_028889	NM_028889	NM_028889	NM_028889	---	27	1	chr1	+
10459866	7,223335784	5,80608545	1,41725034	2,67076	6,65E-14	7,65E-10	NM_0011710	Slc14a1	solute carrier family 14 (	NM_0011710	NM_0011710	NM_0011710	NM_0011710	---	35	1	chr18	-
10475144	9,444299529	8,33387984	1,11041969	2,15908448	2,19E-13	1,56E-09	NM_007601	Capn3	calpain 3	NM_007601	NM_007601	NM_007601	NM_007601	NM_007601	76	1	chr2	+
10469672	7,620121513	6,23890414	1,38121738	2,60488083	2,07E-12	1,18E-08	NM_008078	Gad2	glutamic acid decarboxyl	NM_008078	NM_008078	NM_008078	NM_008078	D42051 // Ge	38	1	chr2	+
10462507	8,168400298	6,50051687	1,66788343	3,17748084	1,36E-11	6,45E-08	NM_011864	Papss2	3'-phosphoadenosine 5'-	NM_011864	---	---	NM_011864	---	35	1	chr19	+
10457077	9,816184784	9,04559288	0,77059319	1,70596955	1,68E-11	6,80E-08	NM_015798	Fbxo15	F-box protein 15	NM_015798	---	NM_015798	NM_015798	---	32	1	chr18	+
10570855	7,629920837	6,16620912	1,46371172	2,75817065	1,98E-11	7,00E-08	NM_008872	Plat	plasminogen activator, ti	NM_008872	NM_008872	NM_008872	NM_008872	NM_008872	27	1	chr8	+
10502655	8,635544211	7,74100814	0,89453607	1,85901198	2,73E-11	8,59E-08	NM_010516	Cyr61	cysteine rich protein 61	NM_010516	NM_010516	NM_010516	NM_010516	---	26	1	chr3	-
10579894	7,684655293	6,64540294	1,03925235	2,05516233	5,68E-11	1,61E-07	NM_020259	Hhip	Hedgehog-interacting pr	NM_020259	NM_020259	NM_020259	NM_020259	---	30	1	chr8	-
10360248	7,99092013	6,80542523	1,1854949	2,27441403	9,00E-11	2,32E-07	NM_013734	Atp1a4	ATPase, Na+/K+ transpor	NM_013734	NM_013734	NM_013734	NM_013734	---	42	1	chr1	-
10453811	8,432967134	7,85584655	0,57712059	1,49186872	1,93E-10	4,57E-07	NM_0010836	Greb1l	growth regulation by est	NM_0010836	NM_0010836	NM_0010836	NM_0010836	---	26	1	chr18	+
10346843	7,877507638	7,05848951	0,81901813	1,7642049	2,62E-10	5,72E-07	NM_0010774	Nrp2	neuropilin 2	NM_0010774	NM_0010774	NM_0010774	NM_0010774	---	44	1	chr1	+
10350516	7,929257838	6,47739405	1,45186379	2,73561231	3,18E-10	6,45E-07	NM_011198	Ptgs2	prostaglandin-endoperox	NM_011198	NM_011198	NM_011198	NM_011198	M88242 // Ge	26	1	chr1	+
10565102	8,293833832	7,40591802	0,88791581	1,85050087	4,20E-10	7,94E-07	NM_021492	Ap3b2	adaptor-related protein c	NM_021492	NM_021492	NM_021492	NM_021492	---	29	1	chr7	-
10422272	9,154350188	8,2652C849	0 8891417	1,852073B5	4,63E-10	8,21E-07	NM_177753	Sox21	SRY-box containing gene	NM_177753	NM_177753	NM_177753	NM_177753	---	30	1	chr14	-
10431659	9,342272321	8,78542314	0,55684918	1,47105296	5,85E-10	9,75E-07	NM_0011090	Kif21a	kinesin family member 2	NM_0011090	NM_0011090	NM_0011090	NM_0011090	---	37	1	chr15	-
10492738	10,75598852	10,0318579	0,72413163	1,65190604	6,68E-10	1,05E-06	NM_009144	Sfrp2	secreted frizzled-related	NM_009144	NM_009144	NM_009144	NM_009144	---	25	1	chr3	+
10440491	8,512251369	7,94627076	0,56598051	1,4803934	1,25E-09	1,86E-06	NM_007471	App	amyloid beta (A4) precur	NM_007471	NM_007471	NM_007471	NM_007471	---	41	1	chr16	-
10411274	7,408107057	6,61457691	0,79343015	1,7331904	1,56E-09	2,21E-06	NM_029210	Sv2c	synaptic vesicle glycopro	NM_029210	NM_029210	NM_029210	NM_029210	---	36	1	chr13	-
10393904	9,183753121	8,58813835	0,59561477	1,51111637	2,12E-09	2,87E-06	NM_175263	Notum	notum pectinacetylester	NM_175263	NM_175263	NM_175263	NM_175263	---	32	1	chr11	-
10534852	10,83645422	10,2027692	0,633685	1,5515229	3,40E-09	4,38E-06	NM_008788	Pcolce	procollagen C-endopeptid	NM_008788	---	---	---	NM_008788	28	1	chr5	-
10355984	9,128336635	8,49517747	0,63315917	1,55095751	3,88E-09	4,59E-06	NM_009255	Serpine2	serine (or cysteine) pept	NM_009255	NM_009255	NM_009255	NM_009255	---	33	1	chr1	-
10453737	8,76646951	8,04097436	0,72549515	1,65346802	3,87E-09	4,59E-06	NM_0010836	Greb1l	growth regulation by est	NM_0010836	NM_0010836	NM_0010836	NM_0010836	---	26	1	chr18	+
10564661	10,42491528	9,89935807	0,5255572	1,43948944	4,81E-09	5,46E-06	NM_0011642	Tpm1	tropomyosin 1, alpha	NM_0011642	NM_0011642	NM_0011642	NM_0011642	NM_0011642	38	1	chr9	-
10458704	7,498574055	6,5722883	0,92648575	1,9006406	6,02E-09	6,56E-06	NM_009258	Spink3	serine peptidase inhibito	NM_009258	NM_009258	NM_009258	NM_009258	---	25	1	chr18	-
10466886	8,048659222	7,1155553	0,93310392	1,90937956	7,58E-09	7,96E-06	ENSMUST000	Glis3	GLIS family zinc finger 3	ENSMUST000	ENSMUST000	ENSMUST000	ENSMUST000	---	25	1	chr19	-
10360235	7,809678056	7,21665139	0,59302666	1,50840795	8,17E-09	8,27E-06	NM_009813	Casq1	calsequestrin 1	NM_009813	NM_009813	NM_009813	NM_009813	---	36	1	chr1	-
10423353	8,756653961	8,18810069	0,56885327	1,48334406	1,10E-08	1,04E-05	NM_020332	Ank	progressive ankylosis	NM_020332	NM_020332	NM_020332	NM_020332	---	30	1	chr15	+
10568436	9,0630674	8,58742479	0,47559261	1,39048327	1,09E-08	1,04E-05	NM_010207	Fgfr2	fibroblast growth factor r	NM_010207	NM_010207	NM_010207	NM_010207	---	48	1	chr7	-
10458828	7,847392079	7,05739023	0,79000185	1,72907568	1,16E-08	1,06E-05	NM_033037	Cdo1	cysteine dioxygenase 1, c	NM_033037	NM_033037	NM_033037	NM_033037	---	25	1	chr18	-
10390175	9,878502189	9,17559793	0,70290426	1,62777834	1,21E-08	1,07E-05	NM_033217	Ngfr	nerve growth factor rece	NM_033217	NM_033217	NM_033217	NM_033217	NM_033217	29	1	chr11	-
10585186	9,523269872	8,82946079	0,69380908	1,61754862	1,33E-08	1,15E-05	NM_029639	1600029D21Rik	RIKEN cDNA 1600029D2	NM_029639	---	---	NM_029639	---	30	1	chr9	+
10466888	8,228411468	7,76170562	0,46670585	1,38195041	1,48E-08	1,24E-05	NM_175459	Glis3	GLIS family zinc finger 3	NM_175459	NM_175459	NM_175459	NM_175459	---	36	1	chr19	-
10405633	7,246586601	6,69981934	0,54716726	1,46121378	2,19E-08	1,78E-05	NM_0010250	Ntrk2	neurotrophic tyrosine kir	NM_0010250	NM_0010250	NM_0010250	NM_0010250	---	52	1	chr13	+
10496736	9,96589656	9,56094001	0,40495655	1,32404904	2,86E-08	2,25E-05	NM_138744	Ssx2ip	synovial sarcoma, X brea	NM_138744	NM_138744	NM_138744	NM_138744	---	31	1	chr3	+
10574220	8,155648879	7,55967994	0,59626893	1,51180172	2,98E-08	2,28E-05	NM_009142	Cx3cl1	chemokine (C-X3-C moti	NM_009142	NM_009142	NM_009142	NM_009142	---	32	1	chr8	+
10458590	8,488232989	7,82763352	0,66059947	1,58073931	3,55E-08	2,65E-05	NM_010197	Fgf1	fibroblast growth factor	NM_010197	NM_010197	NM_010197	NM_010197	---	29	1	chr18	-
10478997	7,610991288	6,8579847	0,75300659	1,68530135	4,36E-08	3,12E-05	NM_009335	Tcfap2c	transcription factor AP-2	NM_009335	NM_009335	NM_009335	NM_009335	---	30	1	chr2	+
10546855	8,48102273	8,02564654	0,45537619	1,37114029	4,40E-08	3,12E-05	NM_080448	Srgap3	SLIT-ROBO Rho GTPase a	NM_080448	NM_080448	NM_080448	NM_080448	---	75	1	chr6	-
10372503	6,915311365	5,13203456	0,78327681	1,72103544	4,88E-08	3,38E-05	NM_010195	Lgr5	leucine rich repeat conta	NM_010195	NM_010195	NM_010195	NM_010195	---	40	1	chr10	-
10585981	9,371261488	8,90626464	0,46489685	1,38031434	5,16E-08	3,48E-05	NM_008624	Mras	muscle and microspikes	NM_008624	NM_008624	NM_008624	NM_008624	---	32	1	chr9	-
10480275	7,087255766	6,52351122	0,56374455	1,47810069	5,87E-08	3,87E-05	NM_028757	Nebl	nebulette	NM_028757	NM_028757	NM_028757	NM_028757	---	32	1	chr2	-
10360277	9,856461508	9,42735072	0,42911079	1,34640346	6,08E-08	3,92E-05	NM_011063	Pea15a	phosphoprotein enriche	NM_011063	NM_011063	NM_011063	NM_011063	---	27	1	chr1	-
10396952	7,705928599	7,05431303	0,65161557	1,57092538	6,23E-08	3,92E-05	NM_0010331	Ttc9	tetratricopeptide repeat	NM_0010331	NM_0010331	NM_0010331	NM_0010331	---	26	1	chr12	+
10489204	8,121558256	7,22938662	0,89217154	1,85596774	7,87E-08	4,85E-05	NM_009373	Tgm2	transglutaminase 2, C po	NM_009373	NM_009373	NM_009373	NM_009373	---	28	1	chr2	-

10565089	7,633785118	7,05616745	0,57761767	1,49238283	1,10E-07	6,60E-05	NM_007755	Cpeb1	cytoplasmic polyadenyla	NM_007755	NM_007755	NM_007755	NM_007755	NM_007755	36	1	chr7	-
10466735	7,724681918	7,17884734	0,54583458	1,45986461	1,15E-07	6,79E-05	NM_0011141	Fam189a2	family with sequence sir	NM_0011141	NM_0011141	NM_0011141	NM_0011141	---	25	1	chr19	-
10551891	7,726644771	8,10021529	-0,37357052	0,77186983	1,37E-07	7,95E-05	NM_172142	Nfkbid	nuclear factor of kappa li	NM_172142	NM_172142	NM_172142	NM_172142	---	37	1	chr7	+
10442069	7,519458526	7,07115598	0,44830254	1,36443393	1,74E-07	9,88E-05	NM_025681	Lix1	limb expression 1 homol	NM_025681	NM_025681	NM_025681	NM_025681	---	15	1	chr17	+
10374366	7,942669756	7,54798415	0,39468561	1,31465624	2,36E-07	0,00013113	NM_207655	Egfr	epidermal growth factor	NM_207655	NM_207655	NM_207655	NM_207655	---	51	1	chr11	+
10475653	9,227655574	8,67356904	0,55486853	1,4682387	2,67E-07	0,00014574	NM_011978	Slc27a2	solute carrier family 27 (	NM_011978	NM_011978	NM_011978	NM_011978	---	33	1	chr2	+
10530819	8,160242505	7,68934446	0,47089804	1,38597194	2,79E-07	0,00014903	NM_175606	Hopx	HOP homeobox	NM_175606	NM_175606	NM_175606	NM_175606	---	33	1	chr5	-
10490826	8,552831154	7,87273825	0,6800929	1,60224293	3,15E-07	0,00016549	NM_177660	Zbtb10	zinc finger and BTB doma	NM_177660	NM_177660	NM_177660	NM_177660	---	26	1	chr3	+
10571705	6,660791167	6,16632797	0,4944682	1,40880135	3,35E-07	0,00017279	NM_008391	Irf2	interferon regulatory fac	NM_008391	NM_008391	NM_008391	NM_008391	J03168 // Ge	26	1	chr8	+
10470834	11,13403172	10,78452	0,3495117	1,27412931	3,56E-07	0,00017707	NM_0010769	Spna2	spectrin alpha 2	NM_0010769	NM_0010769	NM_0010769	NM_0010769	---	58	1	chr2	+
10561008	9,414632416	8,87457692	0,5400555	1,45402845	3,52E-07	0,00017707	NM_0010391	Ceacam1	carcinoembryonic antige	NM_0010391	NM_0010391	NM_0010391	NM_0010391	---	22	1	chr7	-
10546853	8,220618928	7,60931318	0,61130575	1,52764122	3,63E-07	0,00017738	NM_080448	Srgap3	SLIT-ROBO Rho GTPase a	NM_080448	NM_080448	NM_080448	NM_080448	---	25	1	chr6	-
10464391	6,469509738	5,74819856	0,72131118	1,64867974	3,73E-07	0,00017918	NM_010132	Emx2	empty spiracles homolog	NM_010132	NM_010132	NM_010132	NM_010132	---	25	1	chr19	+
10489484	10,12363194	9,75953926	0,36409268	1,28707193	3,80E-07	0,0001794	NM_011521	Sdc4	syndecan 4	NM_011521	NM_011521	NM_011521	NM_011521	---	30	1	chr2	-
10425317	7,852780473	6,99954641	0,85323406	1,80654609	3,91E-07	0,00018175	---	NA	NA	ENSMUST000	---	---	---	---	25	1	chr15	+
10457644	8,954466455	8,59719771	0,35726875	1,28099847	4,80E-07	0,00021937	NM_007664	Cdh2	cadherin 2	NM_007664	NM_007664	NM_007664	NM_007664	---	34	1	chr18	-
10556456	11,40175255	11,0173415	0,38441103	1,30532678	5,49E-07	0,00024707	NM_0011665	Tead1	TEA domain family mem	NM_0011665	NM_0011665	NM_0011665	NM_0011665	---	25	1	chr7	+
10434229	8,56184987	8,0257302	0,53611967	1,45006711	5,80E-07	0,00025688	NM_013805	Cldn5	claudin 5	NM_013805	NM_013805	NM_013805	NM_013805	NM_013805	25	1	chr16	+
10459999	8,827307569	8,42307389	0,40423368	1,32338578	6,53E-07	0,00028497	NM_178280	Sall3	sal-like 3 (Drosophila)	NM_178280	NM_178280	NM_178280	NM_178280	---	32	1	chr18	-
10606600	7,151124665	6,54570592	0,60541874	1,52142028	9,00E-07	0,00038649	NM_0011052	Pcdh19	protocadherin 19	NM_0011052	NM_0011052	NM_0011052	NM_0011052	---	25	1	chrX	-
10362186	8,034004397	7,64416523	0,38983917	1,31024733	9,55E-07	0,00040392	NM_021509	Moxd1	monooxygenase, DBH-lik	NM_021509	NM_021509	NM_021509	NM_021509	---	28	1	chr10	+
10382838	9,594667081	9,26034237	0,33432471	1,26078713	1,10E-06	0,00045665	NR_027821	1810032O08Rik	RIKEN cDNA 1810032O0	NR_027821	NR_027821 /	NR_027821 /	NR_027821 /	---	19	1	chr11	+
10513739	6,536944805	5,99301059	0,54393421	1,45794289	1,25E-06	0,00051409	NM_011607	Tnc	tenascin C	NM_011607	NM_011607	NM_011607	NM_011607	---	30	1	chr4	-
10453057	6,892243471	6,35338812	0,53885535	1,45281938	1,29E-06	0,00051748	NM_009994	Cyp1b1	cytochrome P450, family	NM_009994	NM_009994	NM_009994	NM_009994	---	26	1	chr17	-
10588226	9,407207808	9,0694615	0,3377463	1,26378084	1,30E-06	0,00051748	NM_019764	Amotl2	angiomotin-like 2	NM_019764	NM_019764	NM_019764	NM_019764	---	32	1	chr9	+
10447317	11,46806382	11,7280398	-0,2599756	0,83510184	1,39E-06	0,00054911	NM_010137	Epas1	endothelial PAS domain	NM_010137	NM_010137	NM_010137	NM_010137	---	38	1	chr17	+
10381608	10,26036204	10,6014582	-0,3410961	0,78944126	1,42E-06	0,00055325	NM_0011275	Gm1564	predicted gene 1564	NM_0011275	NM_0011275	NM_0011275	NM_0011275	---	25	1	chr11	+
10372796	9,196299575	8,77058202	0,42571755	1,34324042	1,46E-06	0,00055768	NM_010441	Hmga2	high mobility group AT-h	NM_010441	NM_010441	NM_010441	NM_010441	---	24	1	chr10	-
10390117	9,974352703	9,6002958	0,3740569	1,29599208	1,56E-06	0,00059048	NM_013565	Itga3	integrin alpha 3	NM_013565	NM_013565	NM_013565	NM_013565	NM_013565	29	1	chr11	-
10530059	6,963286968	6,63726234	0,32602463	1,25355442	1,77E-06	0,00065966	NM_172710	Sel1l3	sel-1 suppressor of lin-12	NM_172710	NM_172710	NM_172710	NM_172710	---	27	1	chr5	-
10420413	8,109667797	7,72852405	0,38114375	1,30237395	1,86E-06	0,00068424	NM_015771	Lats2	large tumor suppressor 2	NM_015771	NM_015771	NM_015771	NM_015771	---	33	1	chr14	-
10553148	8,546648886	8,82072645	-0,2740775	0,82697851	1,97E-06	0,00071448	NM_0010332	Ccdc114	coiled-coil domain conta	NM_0010332	NM_0010332	NM_0010332	NM_0010332	---	40	1	chr7	+
10518201	8,347897638	8,7104974	-0,3629997	0,77776178	2,17E-06	0,00078026	NM_029948	Pramef12	PRAME family member 1	NM_029948	---	---	---	---	25	1	chr4	-
10485042	9,125108228	9,4523578	-0,3272495	0,79705458	2,23E-06	0,00078529	NM_027982	Ppm1j	protein phosphatase 1J	NM_027982	NM_027982	---	NM_027982	---	31	1	chr3	+
10524684	10,29539025	9,84552115	0,4498691	1,36591532	2,27E-06	0,00078529	NM_008629	Msi1	Musashi homolog 1(Dros	NM_008629	NM_008629	NM_008629	NM_008629	D49654 // Ge	26	1	chr5	+
10504587	5,532734285	5,89149948	-1,3587652	0,38891588	2,26E-06	0,00078529	NR_029853	Mir363	microRNA 363	NR_029853	---	---	---	---	25	1	chrX	-
10420688	7,398173758	8,06693089	-0,6685709	0,62904839	2,31E-06	0,00078742	NR_029733	Mir15a	microRNA 15a	NR_029733	---	---	---	---	27	1	chr14	-
10448925	8,249978151	7,90147171	0,34830644	1,27324181	2,71E-06	0,00089372	NM_021415	Cacna1h	calcium channel, voltage	NM_021415	NM_021415	NM_021415	NM_021415	---	37	1	chr17	-
10499158	8,983040337	8,68002071	0,30301963	1,23372365	2,66E-06	0,00089372	NM_0011709	Kirrel	kin of IRRE like (Drosoph	NM_0011709	NM_0011709	NM_0011709	NM_0011709	---	35	1	chr3	-
10528008	9,824847757	10,2383976	-0,4135498	0,75077375	2,76E-06	0,00089372	NM_0011031	Steap2	six transmembrane epith	NM_0011031	NM_0011031	NM_0011031	NM_0011031	---	27	1	chr5	-
10570434	10,11255767	9,51665641	0,5958126	1,51141648	2,77E-06	0,00089372	NM_026820	Ifitm1	interferon induced trans	NM_026820	NM_026820	NM_026820	NM_026820	---	26	3	chr8	+
10573128	8,574887907	8,31681287	0,25807504	1,195882	2,75E-06	0,00089372	NM_0011113	Tbc1d9	TBC1 domain family, mer	NM_0011113	NM_0011113	NM_0011113	NM_0011113	---	46	1	chr8	+
10466248	9,93826068	10,1844365	-0,2461758	0,84312834	2,97E-06	0,00094537	NM_0010253	Stx3	syntaxin 3	NM_0010253	NM_0010253	NM_0010253	NM_0010253	---	45	1	chr19	-
10422412	8,250552926	7,64849647	0,60205646	1,51787865	3,00E-06	0,00094551	NM_053079	Slc15a1	solute carrier family 15 (	NM_053079	NM_053079	NM_053079	NM_053079	---	44	1	chr14	-
10464471	7,651489384	7,05388068	0,59760871	1,51320532	3,06E-06	0,00095391	NM_010253	Gal	galanin	NM_010253	NM_010253	NM_010253	NM_010253	---	26	1	chr19	-
10502240	8,110549234	7,66026076	0,45028847	1,36631343	3,10E-06	0,00095481	NM_033525	Npnt	nephronectin	NM_033525	NM_033525	NM_033525	NM_033525	---	31	1	chr3	-
10420935	7,4595263	6,88460591	0,57482039	1,43959526	3,43E-06	0,00104524	NM_007940	Ephx2	epoxide hydrolase 2, cyt	NM_007940	NM_007940	NM_007940	NM_007940	---	42	1	chr14	-
10436182	9,207472879	8,86692645	0,34054643	1,2662361	4,21E-06	0,00127112	NM_010581	Cd47	CD47 antigen (Rh-related	NM_010581	NM_010581	NM_010581	NM_010581	---	26	1	chr16	+
10558759	11,36573993	10,7758237	0,58961624	1,50515935	4,63E-06	0,00138136	NM_026820	Ifitm1	interferon induced trans	NM_026820	NM_026820	NM_026820	NM_026820	---	24	1	chr7	+
10538842	10,80123172	10,5432066	0,25802508	1,19584059	5,13E-06	0,00151514	NM_0011775	Gng12	guanine nucleotide bind	NM_0011775	NM_0011775	NM_0011775	NM_0011775	NM_0011775	25	1	chr6	+
10505625	8,211537373	7,75971659	0,45182083	1,36776543	5,81E-06	0,00167992	BC030404	D4Bwg0951e	DNA segment, Chr 4, Brig	BC030404	---	---	---	---	27	1	chr4	+
10597420	7,573035905	7,10806321	0,4649727	1,38029123	5,76E-06	0,00167992	NM_009916	Ccr4	chemokine (C-C motif) re	NM_009916	NM_009916	NM_009916	NM_009916	X90862 // Ge	34	1	chr9	-
10415572	7,708421872	7,31488608	0,39353579	1,31360889	5,89E-06	0,00158632	ENSMUST000	2410022M11Rik	RIKEN cDNA 2410022M1	ENSMUST000	ENSMUST000	ENSMUST000	ENSMUST000	---	13	1	chr14	+
10454782	8,75475512	8,12677317	0,62798195	1,54540176	6,06E-06	0,00171899	NM_007913	Egr1	early growth response 1	NM_007913	NM_007913	NM_007913	NM_007913	NM_007913	35	1	chr18	+
10553833	10,46841644	10,1150123	0,35340412	1,27757157	6,27E-06	0,00175419	NM_010882	Ndn	necdin	NM_010882	NM_010882	NM_010882	NM_010882	---	25	1	chr7	+
10567316	9,004035636	9,35956653	-0,3556308	0,78158198	6,31E-06	0,00175419	NM_172476	Tmc7	transmembrane channel	NM_172476	NM_172476	NM_172476	NM_172476	---	34	1	chr7	-
10496438	6,776626113	6,3309156	0,44571053	1,36198471	6,38E-06	0,00175512	NM_007409	Adh1	alcohol dehydrogenase 1	NM_007409	NM_007409	NM_007409	NM_007409	---	32	1	chr3	+
10502830	5,321773485	4,60364445	0,71812903	1,64504726	6,76E-06	0,00184381	NM_199465	Nexn	nexilin	NM_199465	NM_199465	NM_199465	NM_199465	---	26	1	chr3	-
10406481	6,520189468	7,06621662	-0,5462715	0,6849036	6,99E-06	0,00188855	NR_029545	Mir9-2	microRNA 9-2	NR_029545	---	---	---	---	30	1	chr13	+
10510422	8,641507097	8,29950616	0,34200094	1,26751335	7,36E-06	0,00196745	NM_0011593	Casz1	castor homolog 1, zinc fi	NM_0011593	NM_0011593	NM_0011593	NM_0011593	NM_0011593	49	1	chr4	+
10536635	8,58038534	8,93172437	-0,3513390	0,78385523	7,69E-06	0,00203798	BC151018	A430107O13Rik	RIKEN cDNA A430107O1	BC151018	BC151018 //	BC151018 //	BC151018 //	---	44	1	chr6	+
10435733	7,731378358	7,2713915	0,45998686	1,37552929	8,06E-06	0,0021159	NM_170599	Igsf11	immunoglobulin superfa	NM_170599	NM_170599	NM_170599	NM_170599	---	27	1	chr16	+

10382435	8,82428961	8,48755906	0,33673055	1,26289137	8,15E-06	0,00212061	NM_0011103	Gprc5c	G protein-coupled recep	NM_0011103	NM_0011103	NM_0011103	NM_0011103	---	25	1	chr11	+
10362201	10,6880709	10,3426172	0,34545375	1,27055053	8,35E-06	0,00215095	NM_010217	Ctgf	connective tissue growth	NM_010217	NM_010217	NM_010217	NM_010217	---	27	1	chr10	+
10578539	11,0664028	10,7452161	0,32118678	1,24935786	8,68E-06	0,0022169	NM_007450	Slc25a4	solute carrier family 25 (	NM_007450	NM_007450	NM_007450	NM_007450	U27315 // Ge	25	1	chr8	-
10352314	10,9663089	10,6588617	0,30744724	1,23751606	8,91E-06	0,00225453	NM_010094	Lefty1	left right determination f	NM_010094	NM_010094	NM_010094	NM_010094	---	22	1	chr1	+
10400006	9,02768715	9,28859113	-0,26090398	0,83456483	9,31E-06	0,00233641	NM_013464	Ahr	aryl-hydrocarbon recepto	NM_013464	NM_013464	NM_013464	NM_013464	---	32	1	chr12	-
10542335	8,08996154	7,60394982	0,48601172	1,4005677	9,79E-06	0,0024342	NM_181444	Gprc5a	G protein-coupled recep	NM_181444	NM_181444	NM_181444	NM_181444	---	27	1	chr6	+
10404913	8,88669115	8,63008254	0,25660861	1,19466706	1,04E-05	0,00256985	NM_026056	Cap2	CAP, adenylate cyclase-a	NM_026056	NM_026056	NM_026056	NM_026056	---	27	1	chr13	+
10422227	10,751904	10,4831151	0,26878977	1,20479674	1,07E-05	0,00261705	NM_011897	Spry2	sprouty homolog 2 (Dros	NM_011897	NM_011897	NM_011897	NM_011897	---	25	1	chr14	-
10474671	11,0642560	10,7555897	0,30866634	1,23856222	1,10E-05	0,00267271	NM_033524	Spred1	sprouty protein with EVH	NM_033524	NM_033524	NM_033524	NM_033524	---	31	1	chr2	+
10468668	7,14966566	6,76292907	0,3867366	1,30743262	1,16E-05	0,00275053	NM_146102	Afap1l2	actin filament associated	NM_146102	NM_146102	NM_146102	NM_146102	---	43	1	chr19	-
10498119	8,53811021	8,13441312	0,40369709	1,32289366	1,16E-05	0,00275053	NM_172862	Frem2	Fras1 related extracellula	NM_172862	NM_172862	NM_172862	NM_172862	---	26	1	chr3	-
10606083	9,69085944	9,342799	0,34860644	1,27284826	1,15E-05	0,00275053	NM_007709	Cited1	Cbp/p300-interacting tra	NM_007709	NM_007709	NM_007709	NM_007709	---	29	1	chrX	-
10457733	11,2866298	11,0150345	0,27159533	1,20714194	1,21E-05	0,0028389	NM_019737	B4galt6	UDP-Gal:betaGlcNAc bet	NM_019737	NM_019737	NM_019737	NM_019737	---	32	1	chr18	-
10489961	8,48772512	8,71918857	-0,23146344	0,85177043	1,27E-05	0,00294779	NM_010899	Nfatc2	nuclear factor of activate	NM_010899	NM_010899	NM_010899	NM_010899	---	59	1	chr2	-
10485312	7,00356965	7,42731623	-0,42374657	0,74548614	1,31E-05	0,0030307	NR_030431	Mir670	microRNA 670	NR_030431	---	---	---	---	25	1	chr2	-
10538959	10,4699192	10,7986564	-0,3287371	0,79623318	1,34E-05	0,00303214	NM_0011014	Foxi3	forkhead box I3	NM_0011014	NM_0011014	NM_0011014	NM_0011014	---	26	1	chr6	+
10555460	9,84563635	9,56493559	0,28070076	1,2147848	1,33E-05	0,00303214	NM_019990	Stard10	START domain containin	NM_019990	---	NM_019990	---	---	33	1	chr7	+
10456513	7,70115888	7,237761	0,46339788	1,37878536	1,50E-05	0,00336702	NM_013596	Mc5r	melanocortin 5 receptor	NM_013596	NM_013596	NM_013596	NM_013596	---	25	1	chr18	+
10497590	6,05122523	5,70909301	0,34213222	1,26762869	1,53E-05	0,00341147	NM_007963	Mecom	MDS1 and EVI1 complex	NM_007963	NM_007963	NM_007963	NM_007963	---	46	1	chr3	-
10468691	7,35932851	7,11957902	0,2397495	1,18078762	1,63E-05	0,00359199	NM_178688	Ablim1	actin-binding LIM protein	NM_178688	NM_178688	NM_178688	NM_178688	---	30	1	chr19	-
10600936	8,74582215	8,42192178	0,32390037	1,25171001	1,63E-05	0,00359199	NM_010110	Efnb1	ephrin B1	NM_010110	NM_010110	NM_010110	NM_010110	---	28	1	chrX	+
10463729	5,89537868	5,29292748	0,60245121	1,51829403	1,72E-05	0,00375285	NM_0011643	Nt5c2	5'-nucleotidase, cytosolic	NM_0011643	NM_0011643	NM_0011643	NM_0011643	---	26	1	chr19	+
10352798	7,42055233	6,96089876	0,45965358	1,37521156	1,76E-05	0,00378988	NM_010600	Kcnh1	potassium voltage-gated	NM_010600	NM_010600	NM_010600	NM_010600	---	28	1	chr1	+
10388718	9,99171275	10,2595722	0,26785942	0,83055095	1,76E-05	0,00378988	NM_008952	Pipox	pipecolic acid oxidase	NM_008952	NM_008952	NM_008952	NM_008952	---	35	1	chr11	-
10479981	7,08036193	6,60961808	0,47074386	1,38582382	1,87E-05	0,00399398	NM_008091	Gata3	GATA binding protein 3	NM_008091	NM_008091	NM_008091	NM_008091	---	25	1	chr2	-
10587792	10,3343000	10,0535216	0,28077843	1,2148502	2,13E-05	0,00451385	NM_011636	Plscr1	phospholipid scramblase	NM_011636	NM_011636	NM_011636	NM_011636	---	18	1	chr9	+
10521678	9,75879189	9,48480136	0,27399053	1,20914774	2,20E-05	0,00461924	NM_007646	Cd38	CD38 antigen	NM_007646	NM_007646	NM_007646	NM_007646	---	31	1	chr5	+
10415857	7,11534587	6,84017246	0,27517341	1,21013954	2,34E-05	0,00480595	NM_177628	Fam167a	family with sequence sim	NM_177628	NM_177628	NM_177628	NM_177628	---	30	1	chr14	+
10438753	8,35208973	7,92689392	0,42519582	1,34275474	2,33E-05	0,00480595	NM_173379	Leprel1	leprecan-like 1	NM_173379	NM_173379	NM_173379	NM_173379	---	30	1	chr16	-
10581538	8,87685674	8,38437306	0,49248368	1,40686479	2,32E-05	0,00480595	NM_008706	Nqo1	NAD(P)H dehydrogenase	NM_008706	NM_008706	NM_008706	NM_008706	---	30	1	chr8	-
10471129	8,35797568	7,92310135	0,43487434	1,35179309	2,36E-05	0,00480748	NM_019681	Ncs1	neuronal calcium sensor	NM_019681	NM_019681	NM_019681	NM_019681	---	31	1	chr2	+
10454535	9,97524756	9,73736582	0,23788174	1,17925992	2,39E-05	0,00483664	NM_010928	Notch2	Notch gene homolog 2 (	NM_010928	NM_010928	NM_010928	NM_010928	---	36	1	chr3	+
10348999	6,61864559	6,0404978	0,57814779	1,49293131	2,48E-05	0,00496549	NM_011800	Cdh20	cadherin 20	NM_011800	NM_011800	NM_011800	NM_011800	---	27	1	chr1	+
10552276	10,5599515	10,2806547	0,27929681	1,21360321	2,49E-05	0,00496549	NM_009459	Ube2h	ubiquitin-conjugating en	NM_009459	NM_009459	ENSMUST000	NM_009459	---	48	3	chr7	+
10485138	7,23813071	6,89506306	0,34306765	1,26845088	2,54E-05	0,00503649	NM_183180	Tspan18	tetraspanin 18	NM_183180	NM_183180	NM_183180	NM_183180	---	37	1	chr2	-
10389025	9,03634590	8,5968193	0,4395256	1,40398411	2,66E-05	0,00521985	NM_007763	Crip1	cysteine-rich protein 1 (i	NM_007763	---	---	NM_007763	---	25	1	chr12	+
10530641	9,56119936	9,17453174	0,3865876	1,3072926	2,67E-05	0,00521985	NM_177561	Usp46	ubiquitin specific peptida	NM_177561	NM_177561	NM_177561	NM_177561	---	30	1	chr5	-
10419356	11,8950690	12,2249064	-0,3298373	0,79562616	2,77E-05	0,00537633	NM_144841	Otx2	orthodenticle homolog 2	NM_144841	NM_144841	NM_144841	NM_144841	---	33	1	chr14	-
10353311	9,33865043	9,58060625	-0,24195582	0,84559818	2,82E-05	0,00541821	NM_020604	Jph1	junctophilin 1	NM_020604	NM_020604	NM_020604	NM_020604	---	28	1	chr1	-
10539850	10,3908265	10,1001196	0,29070698	1,22323957	2,83E-05	0,00541821	BC024401	8430410A17Rik	RIKEN cDNA 8430410A17	BC024401	BC024401 //	BC024401 //	BC024401 //	---	27	1	chr6	+
10504606	7,61955585	7,88452183	-0,26496587	0,83221842	2,90E-05	0,00552662	NM_028270	Aldh1b1	aldehyde dehydrogenase	NM_028270	NM_028270	NM_028270	NM_028270	---	25	1	chr4	+
10555510	8,75511888	8,43011358	0,32500531	1,25266305	2,94E-05	0,00556311	NM_0011438	Pde2a	phosphodiesterase 2A, c	NM_0011438	NM_0011438	NM_0011438	NM_0011438	---	37	1	chr7	+
10586158	11,4286002	10,9454816	0,48311854	1,39776191	3,05E-05	0,00572998	NR_028548	Snord16a	small nucleolar RNA, C/D	NR_028548	NR_028548 /	NR_028548 /	NR_028548 /	---	34	1	chr9	+
10353132	8,55030665	8,12094027	0,47936644	1,34664207	3,12E-05	0,00581528	NM_010164	Eya1	eyes absent 1 homolog (	NM_010164	NM_010164	NM_010164	NM_010164	---	40	1	chr1	-
10500327	7,23149255	7,97482476	-0,7433322	0,59735804	3,18E-05	0,0058908	NM_054045	Hist2h3c2-ps	histone cluster 2, H3c2, p	NM_054045	---	---	---	---	13	1	chr3	-
10478525	7,48504128	7,12596799	0,35907334	1,2826018	3,25E-05	0,00598715	NM_026323	Wfdc2	WAP four-disulfide core d	NM_026323	NM_026323	NM_026323	NM_026323	---	30	1	chr2	+
10356082	9,73385598	9,44370355	0,29015243	1,22276946	3,37E-05	0,00616637	NM_011636	Plscr1	phospholipid scramblase	NM_011636	NM_011636	NM_011636	NM_011636	---	28	3	chr1	-
10567546	8,24396177	8,55496296	-0,3110118	0,80603217	3,38E-05	0,00616637	NM_016669	Crym	crystallin, mu	NM_016669	NM_016669	NM_016669	NM_016669	---	27	1	chr7	-
10423230	7,80566319	8,07439515	-0,26873196	0,83004879	3,48E-05	0,00627752	NM_009869	Cdh9	cadherin 9	NM_009869	NM_009869	NM_009869	NM_009869	---	35	1	chr15	+
10440513	9,43491302	9,70280727	-0,26789425	0,8305309	3,50E-05	0,00627752	NM_144853	Cyyr1	cysteine and tyrosine-ric	NM_144853	NM_144853	NM_144853	NM_144853	---	27	1	chr16	-
10410450	7,64727538	7,37291549	0,2743595	1,20545735	3,79E-05	0,0067542	NM_0011451	Ube2ql1	ubiquitin-conjugating en	NM_0011451	NM_0011451	NM_0011451	NM_0011451	---	26	1	chr13	-
10387737	9,21630056	9,4818885	-0,26558794	0,83185966	3,92E-05	0,00691759	NM_007528	Bcl6b	B-cell CLL/lymphoma 6, r	NM_007528	NM_007528	NM_007528	NM_007528	---	27	1	chr11	-
10467538	6,62146319	6,20903811	0,41242509	1,33092114	3,93E-05	0,00691759	NM_008528	Blnk	B-cell linker	NM_008528	NM_008528	NM_008528	NM_008528	---	39	1	chr19	-
10496625	9,65700626	9,8842611	-0,22725483	0,85425883	4,07E-05	0,00703046	NM_173763	Ccbl2	cysteine conjugate-beta (	NM_173763	NM_173763	NM_173763	NM_173763	---	30	1	chr3	+
10529824	8,04924592	7,81666456	0,23258137	1,17493534	4,06E-05	0,00703046	NM_0011635	Prom1	prominin 1	NM_0011635	NM_0011635	NM_0011635	NM_0011635	---	33	1	chr5	-
10549889	7,92732264	7,65547896	0,27184368	1,20734976	4,04E-05	0,00703046	NM_0010809	Aurkc	aurora kinase C	NM_0010809	NM_0010809	NM_0010809	NM_0010809	---	44	3	chr7	+
10388532	11,7262799	11,5266357	0,19964422	1,14841511	4,12E-05	0,00707947	NM_008750	Nxn	nucleoredoxin	NM_008750	NM_008750	NM_008750	NM_008750	---	34	1	chr11	-
10474720	8,10362024	7,80088099	0,30273925	1,23348422	4,17E-05	0,0071157	NM_011580	Thbs1	thrombospondin 1	NM_011580	NM_011580	NM_011580	NM_011580	NM_011580 /	48	1	chr2	+
10558548	7,64445124	7,88884859	-0,24439735	0,84416835	4,19E-05	0,0071157	NM_177261	Kndc1	kinase non-catalytic C-lob	NM_177261	NM_177261	NM_177261	NM_177261	---	31	1	chr7	+
10376950	9,58434587	9,27018367	0,31416225	1,24328848	4,32E-05	0,00729017	NM_008885	Prnp22	peripheral myelin protein	NM_008885	NM_008885	---	---	---	26	1	chr11	+
10482172	8,90110585	9,2223048	-0,32119897	0,80040442	4,38E-05	0,00734106	NM_199025	Zbtb26	zinc finger and BTB doma	NM_199025	NM_199025	NM_199025	NM_199025	---	27	1	chr2	-
10349834	8,87552277	8,62788735	0,24763543	1,1872596	4,45E-05	0,00742114	NM_0010992	Pik3c2b	phosphoinositide-3-kinas	NM_0010992	NM_0010992	NM_0010992	NM_0010992	---	33	1	chr1	+

10501802	5,271412076	4,912856591	0,358555481	1,282141491	4,55E-05	0,007506031	NM_178936	Tmem56	transmembrane protein	NM_178936	NM_178936	NM_178936	NM_178936	---	32	1	chr3	-
10587266	11,31462154	11,10436541	0,210256151	1,156893571	4,54E-05	0,007506031	NM_010295	Gclc	glutamate-cysteine ligase	NM_010295	NM_010295	NM_010295	NM_010295	---	34	1	chr9	+
10450579	9,564163318	9,275193241	0,288970081	1,221767761	4,67E-05	0,007648291	NM_007584	Ddr1	discoidin domain recepto	NM_007584	NM_007584	NM_007584	NM_007584	---	44	1	chr17	-
10389087	8,337680442	8,028112981	0,309567461	1,239336071	4,78E-05	0,007770821	NM_001164	Rffl	ring finger and FYVE like	NM_001164	NM_001164	NM_001164	NM_001164	---	43	1	chr11	-
10446928	8,110554501	7,815786871	0,294767641	1,226687391	4,80E-05	0,007770821	NM_019919	Ltbp1	latent transforming grow	NM_019919	NM_019919	NM_019919	NM_019919	NM_019919	36	1	chr17	+
10415396	8,396760472	8,096773491	-0,300911301	0,811738521	4,86E-05	0,007822931	NM_023699	Nfatc4	nuclear factor of activate	NM_023699	NM_023699	NM_023699	NM_023699	---	32	1	chr14	+
10373542	10,20664758	10,47623141	-0,269583841	0,82955881	5,15E-05	0,008214841	NM_016811	Dgka	diacylglycerol kinase, alp	NM_016811	NM_016811	NM_016811	NM_016811	---	26	1	chr10	-
10446473	9,326267211	9,053329121	0,272938091	1,208265991	5,16E-05	0,008214841	NM_008480	Lama1	laminin, alpha 1	NM_008480	NM_008480	NM_008480	NM_008480	---	63	1	chr17	+
10461856	7,031374566	6,547794171	0,483580441	1,398209361	5,21E-05	0,008256241	NM_008137	Gna14	guanine nucleotide bindi	NM_008137	NM_008137	NM_008137	NM_008137	NM_008137	30	1	chr19	+
10356020	7,605250308	7,926293781	-0,321043471	0,800490691	5,35E-05	0,008340331	NM_175291	Dock10	dedicator of cytokinesis 1	NM_175291	NM_175291	NM_175291	NM_175291	---	61	1	chr1	-
10446190	6,785421427	6,425023371	0,360398061	1,283780061	5,34E-05	0,008340331	BC116283	1700061G19Rik	RIKEN cDNA 1700061G19	BC116283	BC116283 //	BC116283 //	BC116283 //	---	31	1	chr17	+
10462313	6,986807487	6,687051591	0,29975591	1,230936131	5,31E-05	0,008340331	NM_009199	Slc1a1	solute carrier family 1 (ne	NM_009199	NM_009199	NM_009199	NM_009199	---	32	1	chr19	+
10384398	12,06849348	12,27915741	-0,210663941	0,864139461	5,51E-05	0,008536021	NM_010345	Grb10	growth factor receptor b	NM_010345	NM_010345	NM_010345	NM_010345	---	44	1	chr11	-
10404874	8,396614043	8,091623291	0,304990751	1,235410721	5,82E-05	0,008971351	NM_153789	Mylip	myosin regulatory light c	NM_153789	NM_153789	NM_153789	NM_153789	---	27	1	chr13	+
10560685	8,540422094	8,216315511	0,324106581	1,251888941	5,88E-05	0,009008311	NM_033601	Bcl3	B-cell leukemia/lymphon	NM_033601	NM_033601	NM_033601	NM_033601	---	27	1	chr7	-
10362896	9,546580501	9,179602891	0,366977611	1,289648241	6,01E-05	0,009106311	NM_009846	Cd24a	CD24a antigen	NM_009846	NM_009846	NM_009846	NM_009846	---	19	1	chr10	+
10380289	7,356300315	7,033375911	0,322924021	1,250863551	5,99E-05	0,009106311	NM_026178	Mmd	monocyte to macrophag	NM_026178	NM_026178	NM_026178	NM_026178	---	28	1	chr11	+
10391914	8,189074681	7,928026741	0,261047731	1,198348661	6,14E-05	0,009261131	NM_183288	Sh3d20	SH3 domain containing 2	NM_183288	NM_183288	NM_183288	NM_183288	---	25	1	chr11	-
10487722	8,194709824	7,956647321	0,238062511	1,179407681	6,33E-05	0,009500431	NM_001081	Slc4a11	solute carrier family 4, so	NM_001081	NM_001081	NM_001081	NM_001081	---	25	1	chr2	-
10496091	12,00805974	12,21329391	-0,205234171	0,867397881	6,56E-05	0,009789481	NM_010703	Lef1	lymphoid enhancer bind	NM_010703	NM_010703	NM_010703	NM_010703	NM_010703	35	1	chr3	+
10424082	8,542602958	8,117559471	0,425043491	1,342612981	6,95E-05	0,010322361	NM_175503	Aard	alanine and arginine rich	NM_175503	NM_175503	NM_175503	NM_175503	---	25	1	chr15	+
10458731	9,92689279	9,687131051	0,239761741	1,180797641	7,19E-05	0,010559751	NM_0010853	Mcc	mutated in colorectal can	NM_0010853	---	---	---	---	64	1	chr18	-
10538356	7,794842864	7,538226961	0,256615911	1,19467311	7,19E-05	0,010559751	NM_0011636	Chn2	chimaerin (chimaerin) 2	NM_0011636	NM_0011636	NM_0011636	NM_0011636	---	40	1	chr6	+
10364346	12,40346269	12,61681811	0,213355311	0,86252891	7,24E-05	0,010574681	NM_019448	Dnmt3l	DNA (cytosine-5-)-methy	NM_019448	NM_019448	NM_019448	NM_019448	---	27	1	chr10	+
10351368	10,36095505	10,11963911	0,241316	1,182070431	7,33E-05	0,010632461	NM_021610	Gpa33	glycoprotein A33 (transm	NM_021610	---	NM_021610	---	---	32	1	chr1	+
10365833	9,672419868	9,898957061	-0,226537191	0,854683881	7,46E-05	0,010632461	NM_183199	Usp44	ubiquitin specific peptide	NM_183199	NM_183199	NM_183199	NM_183199	---	41	1	chr10	+
10366163	8,701277463	8,942126151	-0,240848691	0,846247351	7,44E-05	0,010632461	NM_175328	Slc6a15	solute carrier family 6 (ne	NM_175328	NM_175328	NM_175328	NM_175328	---	28	1	chr10	+
10469167	8,051795236	7,704873551	0,346921691	1,271843971	7,43E-05	0,010632461	NM_177386	Sfmbt2	Scm-like with four mbt d	NM_177386	NM_177386	NM_177386	NM_177386	---	49	1	chr2	+
10585048	9,895201128	9,638234991	0,256966141	1,194963161	7,36E-05	0,010632461	NM_207675	Cadm1	cell adhesion molecule 1	NM_207675	NM_207675	NM_207675	NM_207675	---	36	1	chr9	+
10485117	10,68395775	10,92437711	-0,240419341	0,846499231	7,60E-05	0,010768411	NM_011957	Creb3l1	cAMP responsive elemer	NM_011957	NM_011957	NM_011957	NM_011957	BC016447 //	26	1	chr2	-
10375065	8,241670361	7,994622111	0,247048251	1,186776491	7,88E-05	0,011116231	NM_177364	Sh3pxd2b	SH3 and PX domains 2B	NM_177364	NM_177364	NM_177364	NM_177364	---	26	1	chr11	+
10452404	6,561243265	6,964432751	-0,403189481	0,756184681	8,16E-05	0,011367921	NM_026497	Nudt12	nudix (nucleoside diphos	NM_026497	NM_026497	NM_026497	NM_026497	---	32	1	chr17	-
10489053	6,783863613	7,307145571	-0,523281961	0,69578721	8,18E-05	0,011367921	ENSMUST000	4930518I15Rik	RIKEN cDNA 4930518I15	ENSMUST000	ENSMUST000	ENSMUST000	ENSMUST000	---	25	1	chr2	-
10503178	10,73134881	10,39600681	0,335342061	1,261676511	8,16E-05	0,011367921	NM_0010814	Chd7	chromodomain helicase	NM_0010814	NM_0010814	NM_0010814	NM_0010814	---	25	1	chr4	+
10383472	8,961964075	8,669937931	0,292026151	1,224358581	8,22E-05	0,011371591	NM_133223	Rac3	RAS-related C3 botulinur	NM_133223	NM_133223	NM_133223	NM_133223	---	25	1	chr11	+
10396800	8,230338871	7,987259271	0,243079661	1,183516321	8,37E-05	0,011521321	NM_181073	Plekhh1	pleckstrin homology dom	NM_181073	NM_181073	NM_181073	NM_181073	---	30	1	chr12	+
10514020	7,739739793	7,504262061	0,235477731	1,172795521	8,44E-05	0,011554021	NM_010820	Mpdz	multiple PDZ domain pro	NM_010820	NM_010820	NM_010820	NM_010820	---	46	1	chr4	-
10384725	8,104398808	7,809692821	0,294705951	1,226634971	8,56E-05	0,011670171	NM_009044	Rei	reticuloendotheliosis one	NM_009044	NM_009044	NM_009044	NM_009044	---	30	1	chr11	-
10562532	6,348363886	6,852371421	-0,504007541	0,70514531	8,66E-05	0,011752761	NM_177890	Gm5114	predicted gene 5114	NM_177890	NM_177890	NM_177890	NM_177890	---	8	1	chr7	-
10570189	9,606138318	9,335286111	0,270852201	1,206520911	8,77E-05	0,011843511	NM_009233	Sox1	SRY-box containing gene	NM_009233	NM_009233	NM_009233	NM_009233	---	25	1	chr8	+
10362958	6,984957151	6,690435561	0,294521551	1,226478221	8,90E-05	0,011904111	NM_024285	Bves	blood vessel epicardial s	NM_024285	NM_024285	NM_024285	NM_024285	---	25	1	chr10	+
10413229	11,63497088	11,38232731	0,252643871	1,191388441	8,87E-05	0,011904111	NM_013469	Anxa11	annexin A11	NM_013469	NM_013469	NM_013469	NM_013469	---	14	1	chr14	+
10483215	7,548471347	7,756740031	-0,208268681	0,865575351	9,29E-05	0,012367391	NM_018732	Scn3a	sodium channel, voltage-	NM_018732	NM_018732	NM_018732	NM_018732	---	32	1	chr2	-
10459788	9,880649232	9,571032661	0,309616631	1,239378311	9,40E-05	0,012448661	---	NA	NA	ENSMUST000	---	---	---	---	35	1	chr18	-
10526514	6,996611199	6,720384531	0,276226571	1,211023341	9,49E-05	0,012508291	NM_021719	Cldn15	claudin 15	NM_021719	---	NM_021719	NM_021719	---	25	1	chr5	+
10587639	8,191354613	7,851745411	0,339609211	1,265413771	9,76E-05	0,012803941	NM_011851	Nt5e	5' nucleotidase, ecto	NM_011851	NM_011851	NM_011851	NM_011851	---	32	1	chr9	+
10437854	10,18737097	10,39288511	-0,205514171	0,867229561	0,00010098	0,013192571	NM_011987	Pla2g10	phospholipase A2, group	NM_011987	NM_011987	NM_011987	NM_011987	---	31	1	chr16	-
10370013	7,979592275	8,267139141	-0,287546831	0,819294011	0,00010346	0,013393481	NM_010361	Gstt2	glutathione S-transferase	NM_010361	NM_010361	NM_010361	NM_010361	---	31	1	chr10	-
10557058	8,321873711	8,768982571	-0,447108861	0,733511321	0,00010324	0,013393481	NM_025298	Polr3e	polymerase (RNA) III (DN	NM_025298	NM_025298	NM_025298	NM_025298	NM_025298	19	1	chr7	+
10401028	8,786276714	8,493012721	0,293263991	1,225409541	0,00010802	0,013879331	NM_030750	Sgpp1	sphingosine-1-phosphate	NM_030750	NM_030750	NM_030750	NM_030750	---	27	1	chr12	-
10504076	8,839442626	9,321787481	-0,482314851	0,715813251	0,0001082	0,013879331	NR_002900	Snora69	small nucleolar RNA, H/A	NR_002900	NR_002900 /	NR_002900 /	---	---	25	1	chrX	-
10504535	5,342339325	5,674823711	-0,332484381	0,794167721	0,00010933	0,013962351	NR_029657	Mir106a	microRNA 106a	NR_029657	---	---	---	---	31	1	chrX	-
10492231	7,043402713	6,831459461	0,211943261	1,158247251	0,00012587	0,015991141	NM_177855	Med12l	mediator of RNA polyme	NM_177855	NM_177855	NM_177855	NM_177855	---	49	1	chr3	+
10514177	11,7285845	11,94485871	-0,215927421	0,865785561	0,00012635	0,015991141	NM_172870	Bnc2	basonuclin 2	NM_172870	NM_172870	NM_172870	NM_172870	---	30	1	chr4	-
10446986	8,937456468	8,703611611	0,233843851	1,217434251	0,00012772	0,016093251	NM_015800	Crim1	cysteine rich transmemb	NM_015800	NM_015800	NM_015800	NM_015800	---	34	1	chr17	+
10478924	8,938383796	9,285561731	-0,347177941	0,786120331	0,00012987	0,016291431	ENSMUST000	Gm9873	predicted gene 9873	ENSMUST000	ENSMUST000	ENSMUST000	ENSMUST000	---	25	1	chr2	+
10354753	7,782403815	8,142294231	-0,359890411	0,779223771	0,00013125	0,016392411	NM_029267	Boll	bol, boule-like (Drosophi	NM_029267	NM_029267	NM_029267	NM_029267	NM_029267	41	1	chr1	-
10474211	7,912418862	7,553323111	0,377095751	1,25872481	0,00013249	0,016473861	NM_008505	Lmo2	LIM domain only 2	NM_008505	NM_008505	NM_008505	NM_008505	---	26	1	chr2	+
10359235	9,407016341	9,620392191	-0,213375851	0,862515611	0,00013664	0,016915891	NM_177644	Rasal2	RAS protein activator like	NM_177644	NM_177644	NM_177644	NM_177644	---	37	1	chr1	-
10453256	9,070258758	9,409655771	-0,339437011	0,790349671	0,00013956	0,017202211	NM_153512	Kcng3	potassium voltage-gated	NM_153512	NM_153512	NM_153512	NM_153512	---	25	1	chr17	-
10559357	12,07947857	12,35380981	-0,273611958	0,822241471	0,0001433	0,017587281	NM_010202	Fgf4	fibroblast growth factor	NM_010202	NM_010202	NM_010202	NM_010202	---	25	1	chr7	+
10358389	6,495423512	6,104871211	0,390552311	1,311089161	0,0001479	0,018020861	NM_009061	Rgs2	regulator of G-protein sig	NM_009061	NM_009061	NM_009061	NM_009061	NM_009061	34	1	chr1	-

10385175	8,850559649	8,59015977	0,26039988	1,19781066	0,00014811	0,01802086	NM_170779	Wwc1	WW, C2 and coiled-coil d	NM_170779	NM_170779	NM_170779	NM_170779	---	51	1	chr11	-
10380599	7,715267204	7,97570034	-0,26043314	0,83483724	0,00014926	0,01808386	NM_172799	Ttll6	tubulin tyrosine ligase-lik	NM_172799	NM_172799	NM_172799	NM_172799	---	28	1	chr11	+
10397703	5,381107567	5,06156849	0,31953908	1,24793179	0,00015318	0,01847895	ENSMUST000	3300002A11Rik	RIKEN cDNA 3300002A11	ENSMUST000	ENSMUST000	ENSMUST000	ENSMUST000	---	27	1	chr12	+
10387368	9,866475157	10,1253883	-0,25891319	0,83571725	0,00015735	0,01883338	NM_025915	Tmem88	transmembrane protein	NM_025915	NM_025915	NM_025915	NM_025915	---	27	1	chr11	-
10391301	10,01775399	9,76092184	0,25683215	1,19485218	0,00015744	0,01883338	NM_213659	Stat3	signal transducer and act	NM_213659	NM_213659	NM_213659	NM_213659	BC003806 //	30	1	chr11	-
10479833	8,305784075	8,53878532	-0,23300124	0,850863	0,0001509	0,01904646	NM_181848	Optn	optineurin	NM_181848	NM_181848	NM_181848	NM_181848	---	30	1	chr2	-
10384223	8,6712239	8,34909392	0,32212998	1,25017493	0,00016548	0,01943858	NM_008343	Igfbp3	insulin-like growth factor	NM_008343	NM_008343	NM_008343	NM_008343	NM_008343	26	1	chr11	-
10406590	7,784642475	7,50314107	0,28150141	1,21545915	0,00016593	0,01943858	NM_175455	Ankrd34b	ankyrin repeat domain 34	NM_175455	NM_175455	NM_175455	NM_175455	---	28	1	chr13	+
10455374	7,527501323	7,06591396	0,46158737	1,37705613	0,0001654	0,01943858	NM_178749	Stk32a	serine/threonine kinase	NM_178749	NM_178749	NM_178749	NM_178749	---	27	1	chr18	+
10469457	9,504053084	9,74000033	-0,23554725	0,84912729	0,00016429	0,01943858	NM_026162	Plxdc2	plexin domain containing	NM_026162	---	---	---	---	34	1	chr2	+
10415074	6,653896572	6,94749156	-0,29359499	0,8158665	0,00016832	0,01955718	NM_080726	Rem2	rad and gem related GTP	NM_080726	NM_080726	NM_080726	NM_080726	---	27	1	chr14	+
10585099	11,97806913	12,1699071	-0,19183794	0,87548967	0,00016773	0,01955718	NM_175482	Usp28	ubiquitin specific peptida	NM_175482	NM_175482	NM_175482	NM_175482	---	29	1	chr9	+
10458340	8,764315765	8,47243002	0,29188574	1,22423943	0,00016939	0,01960041	NM_010415	Hbegf	heparin-binding EGF-like	NM_010415	NM_010415	NM_010415	NM_010415	---	30	1	chr18	-
10440619	3,623216369	3,95014692	-0,32693055	0,79723085	0,00017135	0,01974737	---	NA	NA	ENSMUST000	---	---	---	---	25	1	chr16	-
10361771	8,562595459	8,25973531	0,30286015	1,23358759	0,00017788	0,02041602	NM_009538	Plagl1	pleiomorphic adenoma g	NM_009538	NM_009538	---	NM_009538	---	30	1	chr10	+
10437376	8,848239218	9,02145805	-0,17321884	0,88686177	0,00018	0,02057667	NM_175347	Srl	sarcalumenin	NM_175347	NM_175347	NM_175347	NM_175347	---	28	1	chr16	-
10503161	11,28210401	11,0746845	0,20741949	1,1546211	0,00018188	0,02070804	NM_0010814	Chd7	chromodomain helicase	NM_0010814	NM_0010814	NM_0010814	NM_0010814	---	28	1	chr4	+
10431051	8,020019677	7,64240113	0,37761855	1,29919551	0,00018571	0,0209753	NM_022723	Scube1	signal peptide, CUB dom	NM_022723	---	NM_022723	NM_022723	---	28	1	chr15	-
10528648	11,31091958	11,5502426	-0,239323	0,84714275	0,00018507	0,0209753	NM_013853	Abcf2	ATP-binding cassette, su	NM_013853	NM_013853	NM_013853	NM_013853	---	26	1	chr5	-
10411459	7,401517323	6,9988176	0,40269972	1,32197943	0,00018698	0,02103501	NM_0010256	Tmem171	transmembrane protein	NM_0010256	NM_0010256	NM_0010256	NM_0010256	---	29	1	chr13	-
10409557	11,22723952	10,951385	0,27585453	1,210711	0,00018909	0,02118879	NM_012015	H2afy	H2A histone family, mem	NM_012015	NM_012015	NM_012015	NM_012015	---	35	1	chr13	-
10543686	10,19412883	9,9351842	0,25894463	1,19660303	0,00019668	0,02195215	NM_009459	Ube2h	ubiquitin-conjugating en	NM_009459	NM_009459	ENSMUST000	NM_009459	---	60	3	chr6	-
10605571	8,621253313	8,31619075	0,30506257	1,23547222	0,00020178	0,02243281	NM_212444	Gyk	glycerol kinase	NM_212444	NM_212444	NM_212444	NM_212444	NM_212444	48	1	chrX	-
10375261	4,569235307	4,30035447	0,26888083	1,20487279	0,00020373	0,02256156	NM_008070	Gabrb2	gamma-aminobutyric aci	NM_008070	NM_008070	NM_008070	NM_008070	---	25	1	chr11	+
10428707	9,072855756	9,33446669	-0,26163094	0,83415597	0,00021023	0,0231905	NM_008216	Has2	hyaluronan synthase 2	NM_008216	NM_008216	NM_008216	NM_008216	---	27	1	chr15	-
10419240	9,230769588	8,99624884	0,23452075	1,17651585	0,00021202	0,02329802	NM_0010427	Ddhd1	DDHD domain containing	NM_0010427	NM_0010427	NM_0010427	NM_0010427	---	38	1	chr14	-
10574350	7,849078625	7,6125448	0,23653382	1,17815865	0,00021509	0,02354327	NM_008609	Mmp15	matrix metallopeptidase	NM_008609	NM_008609	NM_008609	NM_008609	BC047278 //	26	1	chr8	+
10598041	12,10348719	11,3222304	0,78125677	1,71862736	0,00021631	0,02358595	---	NA	NA	NC_005089	---	---	---	---	18	3	chrM	+
10393559	6,756535389	6,45453161	0,30200378	1,23285556	0,00021853	0,02365583	NM_011594	Timp2	tissue inhibitor of metall	NM_011594	NM_011594	NM_011594	NM_011594	NM_011594	31	1	chr11	-
10546510	8,790566466	8,5811384	0,20942807	1,15622972	0,00021862	0,02365583	NM_008377	Lrig1	leucine-rich repeats and	NM_008377	---	NM_008377	NM_008377	---	44	1	chr6	-
10382328	7,532612308	7,24988543	0,28272688	1,21649204	0,00022223	0,0238851	NM_011448	Sox9	SRY-box containing gene	NM_011448	NM_011448	NM_011448	NM_011448	---	25	1	chr11	+
10426557	10,39585034	10,5962806	-0,20043023	0,87029059	0,00022326	0,0238851	NM_0011634	Pfkm	phosphofructokinase, m	NM_0011634	NM_0011634	NM_0011634	NM_0011634	NM_021514	46	1	chr15	+
10523130	8,879341202	8,61727585	0,26206535	1,19919424	0,00022252	0,0238851	NM_145562	Parm1	prostate androgen-regul	NM_145562	NM_145562	NM_145562	NM_145562	---	27	1	chr5	+
10386422	7,279536806	7,6154932	-0,33556539	0,79225876	0,00022559	0,02395863	NM_008856	Prkch	protein kinase C, eta	NM_008856	NM_008856	---	NM_008856	NM_008856	32	1	chr12	+
10575052	11,99109418	12,174642	-0,1835478	0,88053497	0,00022564	0,02395863	NM_009864	Cdh1	cadherin 1	NM_009864	NM_009864	NM_009864	NM_009864	NM_009864	39	1	chr8	+
10544084	8,218728346	7,92025653	0,29847182	1,2298401	0,0002369	0,02506015	NM_172467	Zc3hav1l	zinc finger CCCH-type, an	NM_172467	NM_172467	NM_172467	NM_172467	---	25	1	chr6	-
10589610	8,279285923	8,6514224	-0,37213648	0,77263745	0,0002379	0,0250727	NM_153099	Prss42	protease, serine, 42	NM_153099	NM_153099	NM_153099	NM_153099	---	26	1	chr9	+
10575034	8,898289917	9,21834616	-0,32025624	0,80103865	0,00023898	0,0250932	NM_0010378	Cdh3	cadherin 3	NM_0010378	NM_0010378	NM_0010378	NM_0010378	---	34	1	chr8	+
10554655	8,244082132	7,95722782	0,28685431	1,21997731	0,00024494	0,02562387	NM_175366	Mex3b	mex3 homolog B (C. eleg	NM_175366	---	NM_175366	NM_175366	---	25	1	chr7	+
10417798	10,79420431	11,0007779	-0,20657362	0,86659293	0,00024838	0,02579288	NM_021542	Kcnk5	potassium channel, subf	NM_021542	NM_021542	NM_021542	NM_021542	---	29	1	chr14	-
10556442	11,11327113	10,917C459	0,19622526	1,14569577	0,00024813	0,02579288	NM_0011665	Tead1	TEA domain family mem	NM_0011665	NM_0011665	NM_0011665	NM_0011665	---	38	1	chr7	+
10379856	10,9223634	11,1484946	-0,22613116	0,85492445	0,00025083	0,02595225	NM_007607	Car4	carbonic anhydrase 4	NM_007607	NM_007607	NM_007607	NM_007607	---	32	1	chr11	+
10416850	5,503934867	5,13328591	0,37064836	1,29293429	0,00025674	0,02646729	NM_022886	Scel	scielfin	NM_022886	NM_022886	NM_022886	NM_022886	---	36	1	chr14	+
10503238	9,148086035	8,82120874	0,32687725	1,25429552	0,00026118	0,02682773	NM_0010814	Chd7	chromodomain helicase	NM_0010814	NM_0010814	NM_0010814	NM_0010814	---	25	1	chr4	+
10425161	10,11056076	9,85744637	0,25311439	1,19177707	0,00026522	0,02704631	NM_008495	Lgals1	lectin, galactose binding,	NM_008495	NM_008495	NM_008495	NM_008495	---	25	1	chr15	+
10425333	8,509207053	8,10568644	0,40352061	1,32273184	0,00026493	0,02704631	ENSMUST000	Apobec3	apolipoprotein B mRNA e	ENSMUST000	ENSMUST000	ENSMUST000	ENSMUST000	---	25	1	chr15	+
10349383	10,32588907	10,131639	0,19425007	1,14412928	0,00027394	0,02783578	NM_028787	Slc35f5	solute carrier family 35,	NM_028787	NM_028787	NM_028787	NM_028787	---	34	1	chr1	+
10367335	8,99740269	8,76612512	0,23127757	1,17387401	0,00027987	0,02828408	---	NA	NA	AK138466	---	---	---	---	25	1	chr10	+
10428619	8,247252544	8,50860743	-0,26135488	0,83430403	0,00028035	0,02828408	NM_015744	Enpp2	ectonucleotide pyrophos	NM_015744	NM_015744	NM_015744	NM_015744	---	28	1	chr15	-
10489620	9,956343957	9,79401732	0,17232663	1,12687433	0,00028359	0,02851013	NM_144892	Ncoa5	nuclear receptor coactiv	NM_144892	NM_144892	NM_144892	NM_144892	---	31	1	chr2	-
10386671	8,657046234	8,43294521	0,22410102	1,16804918	0,00028594	0,02854371	NM_153804	Plekhg3	pleckstrin homology dom	NM_153804	NM_153804	NM_153804	NM_153804	---	43	1	chr12	+
10411215	7,626884218	7,29036843	0,33661575	1,26279092	0,00028519	0,02854371	NM_198408	Crhbp	corticotropin releasing h	NM_198408	NM_198408	NM_198408	NM_198408	---	25	1	chr13	-
10410931	9,816851589	10,1027802	-0,28552863	0,82021349	0,00029147	0,02899402	NM_0010812	Vcan	versican	NM_0010812	NM_0010812	NM_0010812	NM_0010812	---	30	1	chr13	-
10469514	6,971789112	6,66096842	0,31082027	1,24041312	0,00029416	0,02915882	NM_007552	Bmi1	Bmi1 polycomb ring finge	NM_007552	NM_007552	NM_007552	NM_007552	---	13	1	chr2	+
10483023	9,610361704	9,29927944	0,31108226	1,24063804	0,00029948	0,02947979	ENSMUST000	Rbms1	RNA binding motif, single	ENSMUST000	ENSMUST000	ENSMUST000	ENSMUST000	---	25	1	chr2	-
10507189	8,882336039	9,1683965	-0,28606046	0,82013854	0,0002989	0,02947979	NM_153319	Amot	angiomotin	NM_153319	NM_153319	NM_153319	NM_153319	---	36	1	chrX	-
10372781	8,798856436	8,47743011	0,32142633	1,24856533	0,00030244	0,02957438	NM_028679	Irak3	interleukin-1 receptor-as	NM_028679	NM_028679	---	NM_028679	---	27	1	chr10	-
10402708	10,39818591	10,0719315	0,32625442	1,2537541	0,00030252	0,02957438	NM_021273	Ckb	creatine kinase, brain	NM_021273	NM_021273	NM_021273	NM_021273	---	17	1	chr12	-
10383379	8,430048017	8,20024946	0,22979855	1,1726712	0,00031681	0,03086466	NM_026280	Mxra7	matrix-remodelling assoc	NM_026280	NM_026280	NM_026280	NM_026280	---	34	1	chr11	-
10489085	6,976246039	6,67254509	0,30370095	1,23430573	0,0003221	0,03127233	NM_172682	Fam160a1	family with sequence sim	NM_172682	NM_172682	NM_172682	NM_172682	---	32	1	chr3	-
10382425	8,320866718	8,08212613	0,23874056	1,17896216	0,00032419	0,03136783	NM_0011103	Gprc5c	G protein-coupled recept	NM_0011103	NM_0011103	NM_0011103	NM_0011103	---	53	1	chr11	+
10504111	8,255072507	7,99239331	0,26283176	1,19966513	0,00032956	0,03177933	NM_0010250	Rhox1	reproductive homeobox	NM_0010250	NM_0010250	NM_0010250	NM_0010250	---	27	1	chrX	-

10551614	9,603365115	9,35925968	0,24410543	1,18435816	0,00033383	0,03208124	NM_016772	Ech1	enoyl coenzyme A hydrat	NM_016772	NM_016772	NM_016772	NM_016772	---	27	1	chr7	+
10413012	7,885081259	7,27528747	0,60979379	1,52604107	0,00034012	0,03252896	AK034234	Fut11	fucosyltransferase 11	AK034234	AK034234 //	AK034234 //	AK034234 //	---	21	1	chr14	+
10460057	6,160079223	5,89230931	0,26776992	1,20394536	0,00034078	0,03252896	NM_0010813	Tshz1	teashirt zinc finger family	NM_0010813	NM_0010813	NM_0010813	NM_0010813	---	27	1	chr18	-
10598251	8,492534009	8,67920722	-0,18667321	0,87862947	0,00034481	0,03280367	NM_177914	Dgkk	diacylglycerol kinase kap	NM_177914	NM_177914	---	NM_177914	---	27	1	chrX	+
10368193	7,680231664	7,91948412	-0,23925245	0,84718418	0,00034815	0,03301007	NM_145743	Lace1	lactation elevated 1	NM_145743	NM_145743	NM_145743	NM_145743	---	26	1	chr10	-
10508490	10,97232497	10,6597492	0,3125758	1,24192306	0,00035392	0,03344546	NM_0010796	Srsf5	serine/arginine-rich splic	NM_0010796	NM_0010796	NM_0010796	NM_0010796	---	37	3	chr4	+
10396740	9,493567144	9,71369	-0,22012286	0,85849233	0,00035808	0,03356444	NM_172952	Gphn	gephyrin	NM_172952	NM_172952	NM_172952	NM_172952	---	26	1	chr12	+
10492682	8,594723709	8,9064457	0,31172199	0,80567953	0,00035691	0,03356444	NM_133187	Fam198b	family with sequence sim	NM_133187	NM_133187	NM_133187	NM_133187	---	26	1	chr3	+
10600901	7,348727919	7,69589661	-0,34716869	0,78612537	0,00035873	0,03356444	NM_013476	Ar	androgen receptor	NM_013476	NM_013476	NM_013476	NM_013476	NM_013476	27	1	chrX	+
10455863	6,713966798	6,38565816	0,32830864	1,25554057	0,00036002	0,03357405	NM_0011346	Ctxn3	cortexin 3	NM_0011346	NM_0011346	NM_0011346	NM_0011346	---	25	1	chr18	+
10409833	8,733222133	8,41891662	0,31430551	1,24341295	0,00036546	0,03392678	NM_008086	Gas1	growth arrest specific 1	NM_008086	NM_008086	NM_008086	NM_008086	---	26	1	chr13	-
10441107	11,08869434	11,2882402	-0,19954584	0,87082466	0,00036619	0,03392678	NM_019537	Psmg1	proteasome (prosome, m	NM_019537	NM_019537	NM_019537	NM_019537	---	28	1	chr16	-
10456184	8,146579468	7,95801359	0,18856588	1,13963029	0,00036777	0,03396206	NM_133237	Apcdd1	adenomatosis polyposis (	NM_133237	NM_133237	NM_133237	---	---	31	1	chr18	+
10435641	10,34424584	10,0816766	0,26256922	1,19961313	0,00037971	0,03472679	NM_008047	Fstl1	follistatin-like 1	NM_008047	---	NM_008047	NM_008047	---	36	1	chr16	+
10485550	6,905874992	6,65946155	0,24641344	1,18625441	0,00037973	0,03472679	NM_0010333	D430041D05Rik	RIKEN cDNA D430041D0	NM_0010333	NM_0010333	NM_0010333	NM_0010333	---	33	1	chr2	-
10508052	10,66632755	10,4427189	0,22360864	1,1676506	0,0003792	0,03472679	NM_0010810	Grik3	glutamate receptor, ionc	NM_0010810	NM_0010810	NM_0010810	NM_0010810	---	32	1	chr4	+
10490129	7,725251287	7,43739241	0,28785888	1,22082709	0,00038265	0,03484103	NM_007557	Bmp7	bone morphogenetic pro	NM_007557	NM_007557	NM_007557	NM_007557	---	29	1	chr2	-
10535807	7,274495089	7,00216456	0,27233053	1,20775727	0,00038344	0,03484103	NM_010228	Flt1	FMS-like tyrosine kinase	NM_010228	NM_010228	NM_010228	NM_010228	---	33	1	chr5	-
10582811	9,925084653	9,73094582	0,19413884	1,14404106	0,00038926	0,035257	NM_0011645	Irf2bp2	interferon regulatory fac	NM_0011645	NM_0011645	NM_0011645	NM_0011645	---	26	1	chr8	-
10563891	9,993752869	9,72370903	0,27043841	1,20584447	0,00039778	0,03591443	NM_010879	Nck2	non-catalytic region of ty	NM_010879	NM_010879	NM_010879	NM_010879	---	14	1	chr7	-
10381154	9,780183078	9,4868921	0,29329098	1,22543246	0,00040041	0,03603721	NM_009923	Cnp	2',3'-cyclic nucleotide 3'	NM_009923	NM_009923	NM_009923	NM_009923	---	25	1	chr11	+
10549256	11,35795433	11,5371973	-0,17924296	0,88316631	0,00040404	0,0362487	NM_021284	Kras	v-Ki-ras2 Kirsten rat sarc	NM_021284	NM_021284	NM_021284	NM_021284	NM_021284	30	1	chr6	-
10603746	6,971975479	6,57985744	0,39211804	1,31231862	0,00040541	0,03625706	NM_172778	Maob	monoamine oxidase B	NM_172778	NM_172778	NM_172778	NM_172778	---	34	1	chrX	-
10458843	10,07578181	10,3198833	-0,24410149	0,84434149	0,00041374	0,03688537	NM_018744	Sema6a	sema domain, transmem	NM_018744	NM_018744	NM_018744	NM_018744	---	26	1	chr18	-
10543791	10,36199025	10,5795005	-0,21751024	0,8600484	0,00041773	0,03712447	NM_013723	Podxl	podocalyxin-like	NM_013723	NM_013723	NM_013723	---	---	29	1	chr6	-
10351801	9,612117777	9,84888675	-0,23676897	0,84864379	0,00042064	0,0372661	NM_033608	Igsf9	immunoglobulin superfa	NM_033608	NM_033608	NM_033608	---	---	46	1	chr1	+
10545780	10,03945849	10,2581285	-0,21867006	0,85935726	0,00042246	0,03731096	NM_177077	Exoc6b	exocyst complex compor	NM_177077	NM_177077	NM_177077	NM_177077	---	45	1	chr6	-
10364593	10,66400972	10,371681	0,29232869	1,22461536	0,00043178	0,03801517	NM_007725	Cnn2	calponin 2	NM_007725	NM_007725	NM_007725	NM_007725	BC009144 //	27	1	chr10	+
10402766	10,04524194	9,82592053	0,21932141	1,16418587	0,00043542	0,03821753	NM_009652	Akt1	thymoma viral proto-onc	NM_009652	NM_009652	NM_009652	NM_009652	NM_009652	32	1	chr12	-
10503654	6,58841845	6,24345155	0,3449669	1,27012184	0,00043773	0,03830154	---	NA	NA	ENSMUST000	---	---	---	---	16	1	chr4	+
10419719	4,767844067	5,03823837	-0,2703943	0,82909291	0,00044216	0,03856963	NM_020513	Olfr1508	olfactory receptor 1508	NM_020513	NM_020513	NM_020513	NM_020513	---	25	1	chr14	-
10514456	8,002091155	7,68659453	0,31549662	1,24443965	0,00044698	0,03887052	NM_010591	Jun	Jun oncogene	NM_010591	NM_010591	NM_010591	NM_010591	NM_010591	26	1	chr4	-
10476824	7,406260222	7,1132105	0,29304972	1,22522755	0,00044879	0,03890916	NM_008780	Pax1	paired box gene 1	NM_008780	NM_008780	NM_008780	NM_008780	---	26	1	chr2	+
10462086	4,095401236	3,73232829	0,36307295	1,28616251	0,00045136	0,03901221	---	NA	NA	AK164996	---	---	---	---	25	1	chr19	+
10365518	9,014014298	8,83131319	0,18270111	1,13500693	0,00045874	0,03918025	NM_175331	Nt5dc3	5'-nucleotidase domain c	NM_175331	NM_175331	NM_175331	NM_175331	---	31	1	chr10	+
10515429	9,953050184	9,68735576	0,26619443	1,201798	0,00045883	0,03918025	NR_030704	Snord55	small nucleolar RNA, C/D	NR_030704	NR_030704 //	NR_030704 //	NR_030704 //	---	25	1	chr4	-
10528015	8,03175703	8,47247657	-0,44091954	0,73676706	0,00045772	0,03918025	NM_027399	Steap1	six transmembrane epith	NM_027399	NM_027399	NM_027399	---	---	26	1	chr5	-
10574682	11,73451789	11,9106003	-0,17602838	0,88510322	0,0004563	0,03918025	NM_148952	E2f4	E2F transcription factor 4	NM_148952	NM_148952	NM_148952	NM_148952	NM_148952	32	1	chr8	+
10503176	11,16988603	10,838573	0,33131302	1,25815792	0,00046219	0,03923047	NM_0010814	Chd7	chromodomain helicase	NM_0010814	NM_0010814	NM_0010814	NM_0010814	---	25	1	chr4	+
10544875	8,406439681	8,23803577	0,16840391	1,12381449	0,00046153	0,03923047	NM_027268	Scrn1	secernin 1	NM_027268	NM_027268	NM_027268	NM_027268	---	33	1	chr6	-
10516054	8,185424651	7,88269031	0,30273434	1,23348002	0,00046905	0,03969416	NM_029662	Mfsd2a	major facilitator superfa	NM_029662	NM_029662	---	NM_029662	---	28	1	chr4	-
10460253	8,434232663	8,16718173	0,26705093	1,20934551	0,00047119	0,03975699	NM_027857	Acy3	aspartoacylase (aminoac	NM_027857	---	NM_027857	NM_027857	---	26	1	chr19	+
10352957	7,837631086	8,0893C228	-0,2516712	0,8399229	0,0047714	0,04013902	NM_0011777	Rgs20	regulator of G-protein sig	NM_0011777	NM_0011777	NM_0011777	NM_0011777	NM_0011777	34	1	chr1	-
10448748	11,25232263	10,992417	0,25930557	1,19740041	0,00048407	0,04050146	NM_011956	Nubp2	nucleotide binding prote	NM_011956	---	NM_011956	NM_011956	---	26	1	chr17	-
10418835	7,781371332	7,4950834	0,28628794	1,21949846	0,00049383	0,04105562	NM_021712	Slc18a3	solute carrier family 18 (	NM_021712	NM_021712	NM_021712	NM_021712	---	25	1	chr14	-
10475414	8,951593983	8,66693698	0,284657	1,21812063	0,00049276	0,04105562	NM_009735	B2m	beta-2 microglobulin	NM_009735	NM_009735	NM_009735	NM_009735	---	25	1	chr2	+
10548695	4,837253078	4,5319C403	0,30534905	1,23571757	0,00049379	0,04105562	NM_053211	Tas2r103	taste receptor, type 2, m	NM_053211	NM_053211	NM_053211	NM_053211	---	24	1	chr6	-
10396926	10,82239888	10,5284965	0,29390237	1,2259519	0,00049569	0,04106735	NM_0010796	Srsf5	serine/arginine-rich splic	NM_0010796	NM_0010796	NM_0010796	NM_0010796	---	43	3	chr12	+
10464030	7,176715562	6,80836105	0,36835451	1,29087965	0,00049686	0,04106735	NM_007417	Adra2a	adrenergic receptor, alpl	NM_007417	NM_007417	NM_007417	NM_007417	---	26	1	chr19	+
10503138	10,11753522	9,86631612	0,2512191	1,19021244	0,00050057	0,04125309	NM_0010814	Chd7	chromodomain helicase	NM_0010814	NM_0010814	NM_0010814	NM_0010814	---	25	1	chr4	+
10541258	7,631199595	7,30322406	0,32797553	1,2552507	0,00051297	0,0421525	NM_0010810	Slc25a18	solute carrier family 25 (	NM_0010810	NM_0010810	NM_0010810	NM_0010810	---	29	1	chr6	+
10582376	11,63461833	11,8073826	-0,1727642E	0,88714125	0,00052147	0,04272743	NM_0010372	Fam38a	family with sequence sim	NM_0010372	NM_0010372	NM_0010372	NM_0010372	---	25	1	chr8	-
10357579	9,6599086	9,4702E858	0,22964002	1,17254234	0,00052823	0,04303216	NM_008551	Mapkapk2	MAP kinase-activated pr	NM_008551	NM_008551	NM_008551	NM_008551	---	30	1	chr1	-
10538373	7,328418103	7,04616255	0,28225555	1,21609468	0,00052672	0,04303216	NM_030024	Prr15	proline rich 15	NM_030024	NM_030024	NM_030024	NM_030024	---	29	1	chr6	+
10379615	5,985662681	5,60092715	0,38473553	1,30562042	0,00053524	0,04328237	NM_183201	Slfn5	schlafen 5	NM_183201	NM_183201	NM_183201	NM_183201	---	31	1	chr11	+
10448034	8,546683814	8,24772188	-0,2013807	0,8699244	0,00053588	0,04328237	NM_007865	Dll1	delta-like 1 (Drosophila)	NM_007865	NM_007865	NM_007865	NM_007865	---	26	1	chr17	-
10564418	7,808756729	7,5415578	0,26719938	1,20346933	0,00053403	0,04328237	NM_008542	Smad6	MAD homolog 6 (Drosop	NM_008542	NM_008542	NM_008542	NM_008542	NM_008542	31	1	chr9	-
10411306	8,743108543	8,97247568	-0,22936714	0,853009	0,00054689	0,04392776	NM_012048	Polk	polymerase (DNA directe	NM_012048	NM_012048	NM_012048	NM_012048	---	44	1	chr13	-
10538214	8,836555533	8,57755903	0,2589965	1,19664506	0,00054697	0,04392776	NM_172727	D330028D13Rik	RIKEN cDNA D330028D1	NM_172727	NM_172727	NM_172727	NM_172727	---	28	1	chr6	+
10434523	9,654686735	9,47918378	0,18550236	1,13721336	0,00055176	0,04393913	NM_145632	Polr2h	polymerase (RNA) II (DNA	NM_145632	NM_145632	NM_145632	NM_145632	BC092087 //	17	1	chr16	+
10462406	10,27638402	10,4639441	-0,18706007	0,8783939	0,00055166	0,04393913	NM_0010813	C030046E11Rik	RIKEN cDNA C030046E11	NM_0010813	NM_0010813	NM_0010813	NM_0010813	---	28	1	chr19	+
10482530	9,118769707	8,85505464	0,26371506	1,20056629	0,00055019	0,04393913	NM_028810	Rnd3	Rho family GTPase 3	NM_028810	NM_028810	NM_028810	NM_028810	---	27	1	chr2	-

10369481	10,2180325	9,83529727	0,38273523	1,30381143	0,00055881	0,04437632	NM_207000	H2afy2	H2A histone family, mem	NM_207000	NM_207000	NM_207000	NM_207000	---	8	1	chr10	-
10475544	6,503370662	6,18595113	0,31741953	1,24609973	0,00057147	0,04525444	NM_199241	Sema6d	sema domain, transmem	NM_199241	NM_199241	NM_199241	NM_199241	---	44	1	chr2	+
10454807	9,312030929	9,77768709	-0,46565616	0,72414165	0,00058019	0,04574893	NR_002905	Snora74a	small nucleolar RNA, H/A	NR_002905	NR_002905 //	NR_002905 //	NR_002905 //	---	25	1	chr18	+
10553401	7,605394244	7,39256201	0,21283223	1,15896117	0,00058094	0,04574893	AK157552	F830223B06Rik	RIKEN cDNA F830223B06	AK157552	AK157552 //	AK157552 //	AK157552 //	---	25	1	chr7	+
10491056	10,6204173	10,3734792	0,24693812	1,1866859	0,00058563	0,04575924	NM_030732	Tbl1xr1	transducin (beta)-like 1X	NM_030732	NM_030732	NM_030732	NM_030732	---	25	1	chr3	+
10497894	8,752427392	8,43550868	0,31691871	1,24566723	0,00058556	0,04575924	NM_145825	Cetn4	centrin 4	NM_145825	NM_145825	NM_145825	NM_145825	---	8	1	chr3	-
10513869	7,923479559	7,60402656	0,31945299	1,24785733	0,00058574	0,04575924	NM_172694	Megf9	multiple EGF-like-domain	NM_172694	NM_172694	NM_172694	NM_172694	---	28	1	chr4	-
10551872	8,859799636	8,67807978	0,18171986	1,13423522	0,00058753	0,04575924	NM_153577	AI428936	expressed sequence AI42	NM_153577	NM_153577	NM_153577	NM_153577	---	32	1	chr7	+
10361075	8,799267106	8,62097646	0,17829065	1,1315424	0,00058935	0,04577551	NM_0010812	Mfsd7b	major facilitator superfar	NM_0010812	NM_0010812	NM_0010812	NM_0010812	---	25	1	chr1	-
10345675	6,340114574	6,02896052	0,31115405	1,24069977	0,00060843	0,04712846	NM_008719	Npas2	neuronal PAS domain pr	NM_008719	NM_008719	NM_008719	NM_008719	---	43	1	chr1	+
10380560	11,55025237	11,7316329	-0,18138052	0,88185874	0,00061556	0,04755045	NM_201609	Zfp652	zinc finger protein 652	NM_201609	NM_201609	NM_201609	NM_201609	---	25	1	chr11	+
10463911	9,765496393	9,45176317	0,31373323	1,24291982	0,00062805	0,04812248	NM_0011640	Add3	adducin 3 (gamma)	NM_0011640	NM_0011640	NM_0011640	NM_0011640	---	35	1	chr19	+
10553533	8,280472345	7,55807911	0,72239324	1,64991676	0,00062602	0,04812248	XM_885168	Gm6181	predicted pseudogene 61	ENSMUST000	---	---	---	---	9	1	chr7	+
10604591	4,452327761	5,08567417	-0,63334641	0,64467931	0,00062723	0,04812248	NR_029715	Mir19b-2	microRNA 19b-2	NR_029715	---	---	---	---	30	1	chrX	-
10526797	10,11758512	10,3345064	-0,2169213	0,86039956	0,00063665	0,04858133	NM_016964	Stag3	stromal antigen 3	NM_016964	NM_016964	NM_016964	NM_016964	---	34	1	chr5	+
10595803	10,08587361	9,76182516	0,32404845	1,2518385	0,00063747	0,04858133	NM_011279	Rnf7	ring finger protein 7	NM_011279	NM_011279	NM_011279	NM_011279	---	8	1	chr9	-
10407782	7,406396481	7,00631229	0,4000842	1,31958492	0,00064106	0,04870583	NM_133643	Edaradd	EDAR lectodysplasin-A re	NM_133643	NM_133643	NM_133643	NM_133643	---	27	1	chr13	-
10544002	8,63626112	8,30394095	0,33232017	1,25903656	0,00064254	0,04870583	NM_178661	Creb3l2	cAMP responsive elemer	NM_178661	NM_178661	NM_178661	NM_178661	---	36	1	chr6	-
10576051	6,529801849	6,18447745	0,3453244	1,27043662	0,00064502	0,04876328	NM_013519	Foxc2	forkhead box C2	NM_013519	NM_013519	NM_013519	NM_013519	---	33	1	chr8	+
10482448	7,404530194	7,0923525	0,31217769	1,2415804	0,00065704	0,04953996	NM_015753	Zeb2	zinc finger E-box binding	NM_015753	NM_015753	NM_015753	NM_015753	NM_015753	63	1	chr2	-
10369761	8,773724001	8,54928939	0,22443461	1,1683193	0,00067488	0,04995496	NM_178606	Reep3	receptor accessory prote	NM_178606	NM_178606	NM_178606	NM_178606	---	33	1	chr10	-
10371201	9,504735247	9,662836	-0,15810075	0,89620411	0,00067329	0,04995496	NM_134009	Ncln	nicalin homolog (zebrafis	NM_134009	NM_134009	NM_134009	NM_134009	---	30	1	chr10	-
10388310	7,631251529	7,31888566	0,31236587	1,24174236	0,00067	0,04995496	NM_0010150	Rap1gap2	RAP1 GTPase activating p	NM_0010150	NM_0010150	NM_0010150	NM_0010150	---	26	1	chr11	-
10433597	8,329154317	8,55626816	-0,22711384	0,85434232	0,00067185	0,04995496	NM_028964	Snx29	sorting nexin 29	NM_028964	NM_028964	NM_028964	NM_028964	---	32	1	chr16	+
10449926	8,619360238	8,83389198	-0,21453174	0,86182584	0,00067066	0,04995496	NM_177359	Zfp799	zinc finger protein 799	NM_177359	NM_177359	NM_177359	NM_177359	---	29	1	chr17	-
10487879	8,24648282	8,00156017	0,24492265	1,18502924	0,00066903	0,04995496	NM_178607	Rnf24	ring finger protein 24	NM_178607	NM_178607	NM_178607	NM_178607	---	25	1	chr2	-
10527940	6,688752967	6,42966651	0,25908646	1,19672068	0,00067311	0,04995496	NM_011074	Cdk14	cyclin-dependent kinase	NM_011074	NM_011074	NM_011074	NM_011074	---	36	1	chr5	-

Export Classeur - Souris - Redressé

Liste de gènes différentiellement exprimés (test de Student)
- souris OTX2
- souris VV

Puce : Affymetrix Gene Atlas 1.0 ST

Client :	Chassaing
Date réalisation :	16/04/2012
Nb de gènes retenus :	101
Critère p value ajustée :	Benjamini & Hochberg
Seuil p value ajustée :	0,05
Log2 fold change :	-

Nom gène	Log2 intensité moyenne dans la condition souris OTX2	Log2 intensité moyenne dans la condition souris VV	Log2 du fold change	Fold change	P value brute	P value ajustée BH	Annotations										
ProbeSet	Souris_OTX2	Souris_VV	logFC	FC	p.value	adj.P.Val	Gene_Access	Gene_Symbol	Gene_Description	mrna_assigne	GO_bio_proc	GO_cel_comp	GO_mol_fun	pathway	total_probes	crosshyb_typ	seqname	strand
10478633	8,64619964	7,77078783	0,8754118	1,83453166	1,36E-09	2,69E-05	NM_013599	Mmp9	matrix metallopeptidas	NM_013599	NM_013599	NM_013599	NM_013599	NM_013599	26	1	chr2	+
10597575	9,79867763	9,18573566	0,61294197	1,52937476	1,90E-09	2,69E-05	NM_019676	Plcd1	phospholipase C, delta	NM_019676	NM_019676	NM_019676	NM_019676	NM_019676	32	1	chr9	-
10379866	11,6596313	10,1484946	0,51113675	1,4251727	4,15E-09	3,92E-05	NM_007607	Car4	carbonic anhydrase 4	NM_007607	NM_007607	NM_007607	NM_007607	---	32	1	chr11	+
10546417	10,7887946	10,3555015	0,43329306	1,35031225	3,05E-08	0,00021615	NM_009426	Trh	thyrotropin releasing h	NM_009426	NM_009426	NM_009426	NM_009426	---	29	1	chr6	-
10375578	8,05192161	7,62043063	0,43149098	1,34862662	6,73E-08	0,00035933	NM_008029	Flt4	FMS-like tyrosine kinas	NM_008029	NM_008029	NM_008029	NM_008029	---	29	1	chr11	+
10524621	8,29022523	7,65578993	0,63443529	1,55233001	7,60E-08	0,00035933	NM_011854	Oasl2	2'-5' oligoadenylate syn	NM_011854	NM_011854	NM_011854	NM_011854	NM_011854	35	1	chr5	+
10604595	5,13554263	5,67482371	-0,53928108	0,68811372	2,10E-07	0,00085091	NR_029657	Mir106a	microRNA 106a	NR_029657	---	---	---	---	31	1	chrX	-
10425317	7,87262755	6,99954641	0,87308114	1,83157038	2,80E-07	0,0009918	---	NA	NA	ENSMUST000	---	---	---	---	25	1	chr15	+
10523490	9,6992828	9,14757718	0,55170563	1,46581764	3,41E-07	0,00107329	NM_010203	Fgf5	fibroblast growth factor	NM_010203	NM_010203	NM_010203	NM_010203	---	28	1	chr5	+
10362896	9,70958959	9,17960289	0,5299867	1,44391588	5,20E-07	0,0012294	NM_009846	Cd24a	CD24a antigen	NM_009846	NM_009846	NM_009846	NM_009846	---	19	1	chr10	+
10376326	6,97722212	6,36242846	0,61479366	1,53133896	4,53E-07	0,0012294	NM_019440	Irgm2	immunity-related GTPa	NM_019440	---	NM_019440	NM_019440	---	37	1	chr11	+
10496592	7,86476258	7,039499	0,82526357	1,77185872	5,05E-07	0,0012294	NM_010260	Gbp2	guanylate binding prote	NM_010260	---	NM_010260	NM_010260	---	33	1	chr3	+
10383214	10,0424693	9,67676762	0,36570163	1,28850812	5,82E-07	0,00126989	AK173199	Rnf213	ring finger protein 213	AK173199	AK173199 //	AK173199 //	AK173199 //	---	49	1	chr11	+
10531994	6,2998445	5,90502242	0,39482208	1,31478061	7,26E-07	0,00146965	NM_194336	Mpa2l	macrophage activation	NM_194336	NM_0010396	NM_0010396	NM_0010396	---	53	3	chr5	-
10510129	8,74585805	8,33731852	0,40853952	1,32734143	8,81E-07	0,00166495	NM_011303	Dhrs3	dehydrogenase/reduct	NM_011303	NM_011303	NM_011303	NM_011303	---	31	1	chr4	+
10361186	8,37544673	8,06330154	0,31214519	1,24155243	2,38E-06	0,0040361	NM_198247	Sertad4	SERTA domain containi	NM_198247	NM_198247	NM_198247	NM_198247	---	26	1	chr1	-
10382838	9,5759298	9,26034237	0,31558743	1,24451829	2,42E-06	0,0040361	NR_027821	1810032O08Rik	RIKEN cDNA 1810032O	NR_027821	NR_027821 /	NR_027821 /	NR_027821 /	---	19	1	chr11	+
10395659	8,48292102	7,9903458	0,49257523	1,40695406	2,76E-06	0,00435056	NM_007728	Coch	coagulation factor C ho	NM_007728	NM_007728	NM_007728	---	---	36	1	chr12	+
10383204	8,75309334	8,28374134	0,469352	1,38448747	3,23E-06	0,00481662	ENSMUST000	Rnf213	ring finger protein 213	ENSMUST000	ENSMUST000	ENSMUST000	ENSMUST000	---	25	1	chr11	+
10383158	9,90949936	9,57109001	0,33840935	1,26436179	4,04E-06	0,00573352	ENSMUST000	Rnf213	ring finger protein 213	ENSMUST000	ENSMUST000	ENSMUST000	ENSMUST000	---	45	1	chr11	+
10378549	8,01716951	7,62657722	0,39059229	1,31084063	5,68E-06	0,00703191	NM_177708	Rtn4rl1	reticulon 4 receptor-like	NM_177708	NM_177708	NM_177708	NM_177708	---	27	1	chr11	+
10382435	8,83506174	8,48755906	0,34750267	1,27235625	5,43E-06	0,00703191	NM_0011103	Gprc5c	G protein-coupled rece	NM_0011103	NM_0011103	NM_0011103	NM_0011103	---	25	1	chr11	+
10441487	9,97713413	9,71605649	0,26107764	1,19837351	5,70E-06	0,00703191	NM_054040	Tulp4	tubby like protein 4	NM_054040	NM_054040	NM_054040	NM_054040	---	21	1	chr17	+
10420030	11,1743918	10,7883351	0,38605671	1,30681662	6,12E-06	0,00722453	NM_011190	Psme2	proteasome (prosome,	NM_011190	NM_011190	---	NM_011190	NM_011190	9	1	chr14	-
10385511	10,1008194	9,6701135	0,43070592	1,34789295	7,27E-06	0,00824595	NM_011190	Psme2	proteasome (prosome,	NM_011190	NM_011190	---	NM_011190	NM_011190	25	1	chr11	-
10383196	8,81241762	8,41598992	0,3964277	1,31624468	8,57E-06	0,00871737	ENSMUST000	Rnf213	ring finger protein 213	ENSMUST000	ENSMUST000	ENSMUST000	ENSMUST000	---	25	1	chr11	+
10383233	9,6490584	9,28763241	0,36142599	1,28469509	8,17E-06	0,00871737	AK173199	Rnf213	ring finger protein 213	AK173199	AK173199 //	AK173199 //	AK173199 //	---	25	1	chr11	+
10415282	10,4200703	10,1378658	0,28220453	1,21605167	8,61E-06	0,00871737	NM_011189	Psme1	proteasome (prosome,	NM_011189	NM_011189	NM_011189	NM_011189	NM_011189	28	1	chr14	+
10592251	7,77471581	7,36982993	0,40488588	1,32398418	9,72E-06	0,00950129	NM_0010298	Pknox2	Pbx/knotted 1 homeob	NM_0010298	NM_0010298	NM_0010298	NM_0010298	---	27	1	chr9	-
10485886	7,5011973	7,17857508	0,32262222	1,25060156	1,09E-05	0,01027919	NM_0010254	Camk2d	calcium/calmodulin-de	NM_0010254	NM_0010254	NM_0010254	NM_0010254	NM_0010254	51	1	chr3	+
10345037	5,74000764	6,02091441	-0,28090677	0,82307353	1,35E-05	0,01032558	NM_153154	Tcfap2d	transcription factor AP-	NM_153154	NM_153154	NM_153154	NM_153154	---	32	1	chr1	+
10352302	9,39578535	8,80882426	0,58696109	1,50207941	1,21E-05	0,01032558	NM_177099	Lefty2	left-right determination	NM_177099	NM_177099	NM_177099	NM_177099	---	15	1	chr1	+
10352314	10,9594465	10,6588617	0,30058485	1,23164361	1,18E-05	0,01032558	NM_010094	Lefty1	left right determination	NM_010094	NM_010094	NM_010094	NM_010094	---	22	1	chr1	+
10390246	7,51578735	7,03429235	0,481495	1,39618973	1,30E-05	0,01032558	NM_029755	Calcoco2	calcium binding and co	NM_029755	NM_029755	NM_029755	NM_029755	---	18	1	chr11	-
10406220	9,26343533	8,73695627	0,52647906	1,44040954	1,32E-05	0,01032558	NM_053108	Glrx	glutaredoxin	NM_053108	NM_053108	NM_053108	NM_053108	---	23	1	chr13	+
10408220	7,14668124	6,4387201	0,70796114	1,63349398	1,20E-05	0,01032558	NM_178189	Hist1h2ac	histone cluster 1, H2ac	NM_178189	NM_178189	NM_178189	NM_178189	---	14	1	chr13	-
10514177	11,6811919	11,9448587	-0,26366677	0,83296815	1,25E-05	0,01032558	NM_172870	Bnc2	basonuclin 2	NM_172870	NM_172870	NM_172870	NM_172870	---	30	1	chr4	-
10349345	7,67418988	7,3454868	0,32770108	1,25501367	1,49E-05	0,01084096	NM_010133	En1	engrailed 1	NM_010133	NM_010133	NM_010133	NM_010133	---	26	1	chr1	+
10477189	9,30964472	8,85193513	0,4577096	1,37335976	1,46E-05	0,01084096	NM_010495	Id1	inhibitor of DNA bindin	NM_010495	NM_010495	NM_010495	NM_010495	---	35	1	chr2	+
10383192	8,42275077	7,98546135	0,48728943	1,40180864	1,63E-05	0,01125761	ENSMUST000	Rnf213	ring finger protein 213	ENSMUST000	ENSMUST000	ENSMUST000	ENSMUST000	---	26	1	chr11	+
10512067	9,13366328	8,77442287	0,35924041	1,28275034	1,63E-05	0,01125761	NM_172689	Ddx58	DEAD (Asp-Glu-Ala-Asp	NM_172689	NM_172689	NM_172689	NM_172689	---	39	1	chr4	-
10404036	8,66230392	8,2680219	0,39428202	1,31428852	1,83E-05	0,01237298	NM_178196	Hist1h2bg	histone cluster 1, H2bg	NM_178196	NM_178196	NM_178196	NM_178196	---	25	1	chr13	+
10502655	8,11019179	7,74100814	0,36918365	1,29162176	1,91E-05	0,01256564	NM_010516	Cyr61	cysteine rich protein 61	NM_010516	NM_010516	NM_010516	NM_010516	---	26	1	chr3	-
10376050	10,2713687	9,93256624	0,33867249	1,26459244	2,09E-05	0,01257019	NM_008390	Irf1	interferon regulatory fa	NM_008390	NM_008390	NM_008390	NM_008390	M21065 // G	36	1	chr11	+
10379728	5,09902231	4,51406935	0,58495296	1,49999008	2,01E-05	0,01257019	---	NA	NA	ENSMUST000	---	---	---	---	25	1	chr11	+

10447317	11,5165314	12,7280398	-0,21150841	0,86363379	2,05E-05	0,01257019	NM_010137	Epas1	endothelial PAS domain	NM_010137	NM_010137	NM_010137	NM_010137	---	38	1	chr17	+
10519555	8,56597255	8,26634992	0,29962263	1,23082242	1,98E-05	0,01257019	NM_011075	Abcb1b	ATP-binding cassette, s	NM_011075	NM_011075	NM_011075	NM_011075	---	22	1	chr5	+
10588226	9,34194355	9,0694615	0,27248205	1,2078841	2,13E-05	0,01257019	NM_019764	Amotl2	angiomotin-like 2	NM_019764	NM_019764	NM_019764	NM_019764	---	32	1	chr9	+
10571214	9,35964169	9,04248318	0,31715851	1,24587429	2,26E-05	0,01309693	NM_175136	Rnf122	ring finger protein 122	NM_175136	NM_175136	NM_175136	NM_175136	---	26	1	chr8	+
10521498	10,6531992	10,9046819	-0,25148279	0,84003259	2,62E-05	0,01475978	NM_007765	Crmp1	collapsin response med	NM_007765	NM_007765	NM_007765	NM_007765	---	31	1	chr5	+
10568553	9,93132322	9,61163659	0,31968663	1,24805942	2,71E-05	0,01475978	NM_029935	Chst15	carbohydrate (N-acetyl	NM_029935	NM_029935	NM_029935	NM_029935	---	37	1	chr7	-
10584435	8,44641579	8,01089565	0,43552014	1,85239833	2,66E-05	0,01475978	NM_172767	Vwa5a	von Willebrand factor A	NM_172767	NM_172767	NM_172767	NM_172767	---	42	1	chr9	+
10404059	10,3029299	9,97690948	0,32602047	1,2535508	2,76E-05	0,01477271	NM_015786	Hist1h1c	histone cluster 1, H1c	NM_015786	NM_015786	NM_015786	NM_015786	---	25	1	chr13	+
10547469	8,80071434	8,40643595	0,3942784	1,31428522	2,83E-05	0,01484965	BC146009	Wnk1	WNK lysine deficient pr	BC146009	BC146009 //	BC146009 //	BC146009 //	---	25	1	chr6	-
10348194	9,08244274	8,74208344	0,3403593	1,26607187	2,92E-05	0,01504274	NM_028889	Efhd1	EF hand domain contai	NM_028889	NM_028889	NM_028889	NM_028889	---	27	1	chr1	+
10458731	9,42943968	9,68713105	-0,25769137	0,83642531	3,12E-05	0,01580766	NM_0010853	Mcc	mutated in colorectal c	NM_0010853	---	---	---	---	64	1	chr18	-
10399691	11,3911301	11,0819047	0,30922543	1,23904229	3,38E-05	0,01623994	NM_010496	Id2	inhibitor of DNA bindin	NM_010496	NM_010496	NM_010496	NM_010496	---	21	1	chr12	-
10433709	9,90454632	10,1281569	-0,22361057	0,85641943	3,32E-05	0,01623994	BC022741	2900011O08Rik	RIKEN cDNA 2900011O0	BC022741	BC022741 //	BC022741 //	BC022741 //	---	26	1	chr16	+
10478525	7,48412204	7,12596795	0,3581541	1,28178483	3,35E-05	0,01623994	NM_026323	Wfdc2	WAP four-disulfide core	NM_026323	NM_026323	NM_026323	NM_026323	---	30	1	chr2	+
10436978	7,84217001	7,54768773	0,29448228	1,22644478	3,98E-05	0,01867236	NM_173047	Cbr3	carbonyl reductase 3	NM_173047	NM_173047	---	NM_173047	---	25	1	chr16	+
10491915	10,3193124	10,567965	-0,24865256	0,84168216	4,08E-05	0,01867236	NM_009834	Ccrn4l	CCR4 carbon catabolite	NM_009834	NM_009834	---	---	---	26	1	chr3	+
10601581	7,57131974	7,09351614	0,4778036	1,39262188	4,07E-05	0,01867236	NM_0011460	9230105E10Rik	RIKEN cDNA 9230105E1	NM_0011460	---	---	ENSMUST000	---	25	3	chrX	+
10509163	9,40751588	8,75850297	0,64901291	1,56809494	4,21E-05	0,01896737	NM_008321	Id3	inhibitor of DNA bindin	NM_008321	NM_008321	NM_008321	NM_008321	---	27	1	chr4	+
10475414	9,02250949	8,66693698	0,35557251	1,27949322	4,69E-05	0,02075614	NM_009735	B2m	beta-2 microglobulin	NM_009735	NM_009735	NM_009735	NM_009735	---	25	1	chr2	+
10383198	9,63746751	9,19838284	0,43908466	1,35574389	4,87E-05	0,0212595	ENSMUST000	Rnf213	ring finger protein 213	ENSMUST000	ENSMUST000	ENSMUST000	ENSMUST000	---	25	1	chr11	+
10353899	9,49462868	9,21495464	0,27967404	1,21392058	5,05E-05	0,02168934	NM_0011260	Sema4c	sema domain, immuno	NM_0011260	NM_0011260	NM_0011260	NM_0011260	---	29	1	chr1	-
10370000	8,53377962	8,27747527	0,25630435	1,19441514	5,44E-05	0,0229987	NM_008185	Gstt1	glutathione S-transfera	NM_008185	NM_008185	NM_008185	NM_008185	---	27	1	chr10	-
10400967	8,39081993	7,90991755	0,48090237	1,39561632	5,90E-05	0,0238823	NM_009189	Six1	sine oculis-related hom	NM_009189	NM_009189	NM_009189	NM_009189	---	25	1	chr12	-
10462623	6,93871055	6,24779226	0,6909183	1,61431072	5,84E-05	0,0238823	NM_008331	Ifit1	interferon-induced pro	NM_008331	NM_008331	---	NM_008331	---	24	1	chr19	+
10550059	7,90221582	7,47703031	0,42518551	1,34274519	5,89E-05	0,0238823	NM_029809	2310014L17Rik	RIKEN cDNA 2310014L1	NM_029809	NM_029809	NM_029809	NM_029809	---	25	1	chr7	+
10363000	11,3781009	11,0866098	0,29149107	1,22390456	6,32E-05	0,02523427	NM_0010377	Gpx4	glutathione peroxidase	NM_0010377	NM_0010377	NM_0010377	NM_0010377	---	40	3	chr10	+
10570189	9,05695708	9,33528611	-0,27832903	0,82454548	6,47E-05	0,02545883	NM_009233	Sox1	SRY-box containing gen	NM_009233	NM_009233	NM_009233	NM_009233	---	25	1	chr8	+
10431659	9,03268835	8,78542314	0,24726521	1,18695497	6,70E-05	0,02601284	NM_0011090	Kif21a	kinesin family member	NM_0011090	NM_0011090	NM_0011090	NM_0011090	---	37	1	chr15	-
10381603	9,03278235	8,73422491	0,29855744	1,229914	6,82E-05	0,02613495	NM_020510	Fzd2	frizzled homolog 2 (Dro	NM_020510	NM_020510	NM_020510	NM_020510	NM_020510	36	1	chr11	+
10423243	7,99760176	7,6712534	0,32634836	1,25383574	7,74E-05	0,02923415	NM_009865	Cdh10	cadherin 10	NM_009865	NM_009865	NM_009865	NM_009865	---	28	1	chr15	+
10457644	8,83717013	8,59719771	0,23997242	1,18097009	7,94E-05	0,02923415	NM_007664	Cdh2	cadherin 2	NM_007664	NM_007664	NM_007664	NM_007664	---	34	1	chr18	-
10570434	9,97117222	9,51655641	0,45451581	1,37032283	7,85E-05	0,02923415	NM_026820	Ifitm1	interferon induced tran	NM_026820	NM_026820	NM_026820	NM_026820	---	26	3	chr8	+
10457077	9,31654607	9,04559288	0,27095318	1,20660476	8,91E-05	0,03197031	NM_015798	Fbxo15	F-box protein 15	NM_015798	---	NM_015798	NM_015798	---	32	1	chr18	+
10504713	5,58234263	4,76274649	0,81959614	1,76491186	8,81E-05	0,03197031	NR_002903	Snord61	small nucleolar RNA, C/	NR_002903	NR_002903 /	NR_002903 /	NR_002903 /	---	25	1	chrX	-
10521602	7,84843738	7,59657454	0,25186285	1,19074364	9,05E-05	0,03207864	NM_175937	Cpeb2	cytoplasmic polyadenyl	NM_175937	NM_175937	NM_175937	NM_175937	---	36	1	chr5	+
10496595	7,10378265	6,59052044	0,51316221	1,42717496	0,00010208	0,03572906	NM_010259	Gbp1	guanylate binding prote	NM_010259	NM_010259	NM_010259	NM_010259	---	36	1	chr3	+
10515003	8,79972348	8,51515697	0,28456651	1,21804422	0,00010675	0,03680517	NM_0010993	Fam159a	family with sequence si	NM_0010993	NM_0010993	NM_0010993	NM_0010993	---	26	1	chr4	-
10444088	9,95558548	9,65381301	0,30177247	1,2326579	0,00011039	0,03770487	NM_0010253	Tapbp	TAP binding protein	NM_0010253	NM_0010253	NM_0010253	---	---	27	1	chr17	+
10435271	7,48778498	7,17759152	0,31019347	1,23987396	0,00011373	0,03838255	NM_175256	Heg1	HEG homolog 1 (zebraf	NM_175256	---	---	---	---	32	1	chr16	+
10356020	7,62710573	7,32629378	-0,29918805	0,81270966	0,00011761	0,03868949	NM_175291	Dock10	dedicator of cytokinesis	NM_175291	NM_175291	NM_175291	NM_175291	---	61	1	chr1	-
10435266	7,5761722	7,3154669	0,2597053	1,19723412	0,0001167	0,03868949	NM_175256	Heg1	HEG homolog 1 (zebraf	NM_175256	---	---	---	---	25	1	chr16	+
10444695	10,1825558	9,80095518	0,38160058	1,30278641	0,00011873	0,03868949	NM_0011904	Ddah2	dimethylarginine dimet	NM_0011904	NM_0011904	NM_0011904	NM_0011904	---	30	1	chr17	+
10586039	10,839234	10,6204738	0,21876019	1,16373308	0,0001207	0,03888407	NM_0010839	Tle3	transducin-like enhance	NM_0010839	NM_0010839	NM_0010839	NM_0010839	---	48	1	chr9	+
10385530	8,90493454	8,3978204	0,50711413	1,42120447	0,00013104	0,04092672	NM_008326	Irgm1	immunity-related GTPa	NM_008326	NM_008326	NM_008326	NM_008326	---	25	1	chr11	-
10457686	6,59196974	6,59196242	0,35972932	1,28318512	0,00012881	0,04092672	NM_013505	Dsc2	desmocollin 2	NM_013505	NM_013505	NM_013505	NM_013505	---	39	1	chr18	-
10490826	8,29655354	7,87273825	0,42381528	1,34147046	0,00013137	0,04092672	NM_177660	Zbtb10	zinc finger and BTB dor	NM_177660	NM_177660	NM_177660	NM_177660	---	26	1	chr3	+
10502770	8,17186837	7,86336781	0,50850056	1,4225709	0,00013925	0,04250944	NM_0010812	Lphn2	latrophilin 2	NM_0010812	NM_0010812	NM_0010812	NM_0010812	---	21	1	chr3	-
10559736	10,2023747	9,87492576	0,22744898	1,17076294	0,00013945	0,04250944	NM_008817	Peg3	paternally expressed 3	NM_008817	NM_008817	NM_008817	NM_008817	---	36	1	chr7	-
10383256	8,81501898	8,41575829	0,3992607	1,31883191	0,00014651	0,04372106	ENSMUST000	Rnf213	ring finger protein 213	ENSMUST000	ENSMUST000	ENSMUST000	ENSMUST000	---	25	1	chr11	+
10490599	8,70477338	8,42389405	0,28083279	1,21489597	0,00014548	0,04372106	NM_015730	Chrna4	cholinergic receptor, ni	NM_015730	NM_015730	NM_015730	NM_015730	---	26	1	chr2	-
10567514	3,70781144	3,35611142	0,35170002	1,27606341	0,00015812	0,04669462	---	NA	NA	XM_355934	---	---	---	---	25	1	chr7	-
10380639	8,76420332	8,50728431	0,25691901	1,19492412	0,00016338	0,04678727	NM_019877	Copz2	coatomer protein comp	NM_019877	NM_019877	NM_019877	NM_019877	---	30	1	chr11	+
10550801	7,93030709	7,56300218	0,26730491	1,20355737	0,00016323	0,04678727	NM_007464	Birc3	baculoviral IAP repeat-c	NM_007464	NM_007464	NM_007464	NM_007464	U28908 // Ge	18	1	chr9	-
10592489	6,01758407	6,40436156	-0,38677749	0,76483509	0,00016178	0,04678727	---	NA	NA	GENSCAN000	---	---	---	---	15	1	chr9	-
10364675	11,2828295	11,0147449	0,26808453	1,20420793	0,00016576	0,0467881	NM_008162	Gpx4	glutathione peroxidase	NM_008162	NM_008162	NM_008162	NM_008162	---	39	3	chr10	+
10458245	7,23633103	6,51283076	0,72350027	1,65118329	0,00016669	0,0467881	---	NA	NA	ENSMUST000	---	---	---	---	25	1	chr18	-

Étude Chassaing - Souris - [illegible]

Liste des gènes différentiellement exprimés entre les conditions:
- souris RAX
- souris VV

Puce: Affymetrix Gene Mouse 1.0 ST

Client:	Chassaing
Date réalisation:	15/04/2012
Nb de gènes retenus:	363
Critère p value ajustée:	Benjamini & Hochberg
Seuil p value ajustée:	0,05
Log2 fold change:	-

Nom gène	Log2 intensité moyenne dans la condition souris RAX	Log2 intensité moyenne dans la condition souris VV	Log2 du fold change	Fold change	P value brute	P value ajustée BH	Annotations														
ProbeSet	Souris_RAX	Souris_VV	logFC	FC	p.value	adj.P.Val	Gene_Access	Gene_Symbol	Gene_Description	mrna_assign	GO_bio_proc	GO_cel_comp	GO_mol_func	pathway	total_probes	crosshyb_typ	seqname	strand
10450365	11,3234925	12,1217935	-0,79830101	0,57502596	3,03E-10	8,60E-06	---	NA	NA	ENSMUST000	---	---	---	---	30	1	chr17	-
10405211	8,87293835	8,13378397	0,73915437	1,66919716	2,63E-09	2,21E-05	NM_011817	Gadd45g	growth arrest and DNA-da	NM_011817	NM_011817 /	NM_011817 /	NM_011817 /	---	25	1	chr13	+
10425317	8,13775734	6,99954641	1,13821093	2,201079	4,68E-09	2,21E-05	---	NA	NA	ENSMUST000	---	---	---	---	25	1	chr15	+
10502655	8,4081913	7,74100814	0,66718315	1,58796945	3,77E-09	2,21E-05	NM_010516	Cyr61	cysteine rich protein 61	NM_010516	NM_010516 /	NM_010516 /	NM_010516 /	---	26	1	chr3	-
10551891	7,63414756	8,10021529	-0,46606774	0,7239351	4,38E-09	2,21E-05	NM_172142	Nfkbid	nuclear factor of kappa lig	NM_172142	NM_172142 /	NM_172142 /	NM_172142 /	---	37	1	chr7	+
10588226	9,57116813	9,0694615	0,50170663	1,41588749	3,23E-09	2,21E-05	NM_019764	Amotl2	angiomotin-like 2	NM_019764	NM_019764 /	NM_019764 /	NM_019764 /	---	32	1	chr9	+
10375127	10,1012306	9,30472056	0,79651003	1,73689438	5,54E-09	2,24E-05	AK006938	1700072H12Rik	RIKEN cDNA 1700072H12	AK006938	---	---	---	---	25	1	chr11	+
10420668	7,08510866	8,06693085	-0,98182219	0,50633981	7,67E-09	2,42E-05	NR_029733	Mir15a	microRNA 15a	NR_029733	---	---	---	---	27	1	chr14	-
10541268	8,07552117	7,30322406	0,7722971	1,70798713	6,91E-09	2,42E-05	NM_0010810	Slc25a18	solute carrier family 25 (m	NM_0010810	NM_0010810	NM_0010810	NM_0010810	---	29	1	chr6	+
10352314	11,1186182	10,6588617	0,45975653	1,3753097	2,90E-08	8,23E-05	NM_010094	Lefty1	left right determination fa	NM_010094	NM_010094 /	NM_010094 /	NM_010094 /	---	22	1	chr1	+
10584578	10,8073658	11,6220987	-0,81473281	0,56851377	3,20E-08	8,25E-05	NR_028276	Snord14c	small nucleolar RNA, C/D	NR_028276	M13967 // G	M13967 // G	M13967 // G	NR_028276 /	25	3	chr9	+
10579089	8,44215516	9,04852076	-0,6063656	0,65684934	3,61E-08	8,54E-05	NM_177899	Zfp866	zinc finger protein 866	NM_177899	NM_177899 /	NM_177899 /	NM_177899 /	---	34	1	chr8	-
10450199	6,89386413	7,61900763	-0,7251435	0,60493687	4,26E-08	9,28E-05	NM_0010816	Btnl7	butyrophilin-like 7	NM_0010816	NM_0010816	NM_0010816	NM_0010816	---	21	1	chr17	-
10409059	7,58721791	6,83979681	0,7474211	1,67878921	6,27E-08	0,00012615	NR_029656	Mirlet7d	microRNA let7d	NR_029656	---	---	---	---	25	1	chr13	-
10450829	8,13226046	8,65398899	-0,52172853	0,69653679	6,67E-08	0,00012615	---	NA	NA	ENSMUST000	---	---	---	---	26	1	chr17	-
10522465	8,08394295	8,76231678	-0,67837384	0,62486921	8,02E-08	0,00013383	NR_031758	Snora26	small nucleolar RNA, H/A	NR_031758	NR_031758 /	NR_031758 /	NR_031758 /	---	25	1	chr5	+
10584576	10,8160984	11,6174651	-0,80136667	0,57380535	7,79E-08	0,00013383	NR_028276	Snord14c	small nucleolar RNA, C/D	NR_028276	M13967 // G	M13967 // G	M13967 // G	NR_028276 /	25	3	chr9	+
10509014	9,54373876	10,1986222	-0,65488341	0,63512582	1,06E-07	0,00016738	BC043057	D4Wsu53e	DNA segment, Chr 4, Way	BC043057	BC043057 //	BC043057 //	BC043057 //	---	28	1	chr4	+
10382838	9,64927639	9,26034237	0,38893402	1,30942554	1,22E-07	0,00018262	NR_027821	1810032O08Rik	RIKEN cDNA 1810032O08	NR_027821	NR_027821 /	NR_027821 /	NR_027821 /	---	19	1	chr11	+
10453604	9,29657183	8,79487817	0,50169367	1,41587477	2,40E-07	0,00033327	NM_026505	Bambi	BMP and activin membra	NM_026505	NM_026505 /	NM_026505 /	---	NM_026505 /	26	1	chr18	+
10457077	9,47225678	9,04559288	0,4266639	1,34412182	2,47E-07	0,00033327	NM_015798	Fbxo15	F-box protein 15	NM_015798	---	NM_015798 /	NM_015798 /	---	32	1	chr18	+
10404059	9,52095265	9,97690948	-0,45595683	0,7290265	3,16E-07	0,00039003	NM_015786	Hist1h1c	histone cluster 1, H1c	NM_015786	NM_015786 /	NM_015786 /	NM_015786 /	---	25	1	chr13	+
10459602	6,92396878	7,2999705	-0,37600173	0,77057019	3,03E-07	0,00039003	NM_0011271	Ptpn2	protein tyrosine phospha	NM_0011271	NM_0011271	NM_0011271	NM_0011271	---	25	1	chr18	-
10362201	10,7792948	10,3426172	0,43667756	1,35348374	3,38E-07	0,00039274	NM_010217	Ctgf	connective tissue growth	NM_010217	NM_010217 /	NM_010217 /	NM_010217 /	---	27	1	chr10	+
10458340	8,94904234	8,47243002	0,47661232	1,39147242	3,46E-07	0,00039274	NM_010415	Hbegf	heparin-binding EGF-like	NM_010415	NM_010415 /	NM_010415 /	NM_010415 /	---	30	1	chr18	-
10384566	6,75604673	7,44585718	-0,68981045	0,6199353	5,22E-07	0,00052856	---	NA	NA	BC106119	---	---	---	---	27	1	chr11	-
10500327	6,95814395	7,97482476	-1,01668081	0,49425217	5,18E-07	0,00052856	NM_054045	Hist2h3c2-ps	histone cluster 2, H3c2, p	NM_054045	---	---	---	---	13	1	chr3	-
10584580	9,62676514	10,2178419	-0,59107673	0,66384727	4,96E-07	0,00052856	NR_028275	Snord14e	small nucleolar RNA, C/D	NR_028275	---	---	---	NR_028275 /	25	1	chr9	+
10378570	8,94171698	8,12309272	0,81862426	1,76372332	7,43E-07	0,0006348	---	NA	NA	ENSMUST000	---	---	---	---	25	1	chr11	+
10415572	7,77298439	7,31488608	0,45809831	1,37372984	7,47E-07	0,0006348	ENSMUST000	2410022M11Rik	RIKEN cDNA 2410022M11	ENSMUST000	ENSMUST000	ENSMUST000	ENSMUST000	---	13	1	chr14	+
10424370	9,17347863	8,85816087	0,31531775	1,24428568	7,02E-07	0,0006348	NM_144549	Trib1	tribbles homolog 1 (Droso	NM_144549	NM_144549 /	NM_144549 /	NM_144549 /	---	27	1	chr15	+
10478934	6,82914606	6,3211814	0,50796466	1,42204257	6,57E-07	0,0006348	BC137932	1700029J11Rik	RIKEN cDNA 1700029J11	BC137932	BC137932 //	BC137932 //	BC137932 //	---	25	1	chr2	+
10482172	8,78292201	9,2223048	-0,43938279	0,73745004	7,61E-07	0,0006348	NM_199025	Zbtb26	zinc finger and BTB doma	NM_199025	NM_199025 /	NM_199025 /	NM_199025 /	---	27	1	chr2	-
10598041	12,5683318	11,3222304	1,24610138	2,37199568	6,80E-07	0,0006348	---	NA	NA	NC_005089	---	---	---	---	18	1	chrM	+
10447317	11,4579267	11,7280398	-0,27011305	0,82925456	8,17E-07	0,00066194	NM_010137	Epas1	endothelial PAS domain p	NM_010137	NM_010137 /	NM_010137 /	NM_010137 /	---	38	1	chr17	+
10379956	5,25738225	4,64426025	0,613122	1,52956562	9,08E-07	0,00071472	NR_029652	Mir301	microRNA 301	NR_029652	---	---	---	---	25	1	chr11	+
10415640	9,71657301	10,1437157	-0,42714269	0,74373332	9,90E-07	0,00075872	NR_002898	Snora65	small nucleolar RNA, H/A	NR_002898	NR_002898 /	NR_002898 /	NR_002898 /	NR_002898 /	29	3	chr14	+
10504076	8,63115045	9,32178748	-0,69063703	0,61958021	1,24E-06	0,00092335	NR_002900	Snora69	small nucleolar RNA, H/A	NR_002900	NR_002900 /	NR_002900 /	---	---	25	1	chrX	-
10373702	9,75922534	10,0675593	-0,30833398	0,80757381	1,49E-06	0,00108302	NR_003517	Pisd-ps1	phosphatidylserine decar	NR_003517	---	---	---	---	20	1	chr11	+
10453738	7,66338328	7,3008624	0,36252088	1,28567044	1,56E-06	0,00110636	NM_008058	Fzd8	frizzled homolog 8 (Droso	NM_008058	NM_008058 /	NM_008058 /	NM_008058 /	---	25	1	chr18	+
10523746	7,02291999	7,55271535	-0,52979536	0,69265298	1,64E-06	0,00113277	NM_0011665	BC005561	cDNA sequence BC005561	NM_0011665	NM_0011665	NM_0011665	NM_0011665	---	26	1	chr5	+
10450363	7,69247687	8,41861908	-0,72614222	0,60451824	1,80E-06	0,00121664	NR_028527	Snord52	small nucleolar RNA, C/D	NR_028527	NR_028527 /	NR_028527 /	NR_028527 /	---	25	1	chr17	-
10485312	6,93570029	7,42731623	-0,49161594	0,71122802	1,88E-06	0,00124048	NR_030431	Mir670	microRNA 670	NR_030431	---	---	---	---	25	1	chr2	-
10478957	7,42412469	6,8579847	0,56613999	1,48055696	2,71E-06	0,00174358	NM_009335	Tcfap2c	transcription factor AP-2,	NM_009335	NM_009335 /	NM_009335 /	NM_009335 /	---	30	1	chr2	+
10478924	8,80901746	9,28556173	-0,47654427	0,71869708	2,78E-06	0,00174911	ENSMUST000	Gm9873	predicted gene 9873	ENSMUST000	ENSMUST000	ENSMUST000	ENSMUST000	---	25	1	chr2	+

10520521	11,2965108	12,0511546	0,24535619	1,18538535	3,64E-06	0,00224326	NM_007681	Cenpa	centromere protein A	NM_007681	NM_007681	NM_007681	NM_007681	---	25	1	chr5	+
10566488	9,39116221	9,6239994	-0,23283719	0,85095978	3,81E-06	0,00229591	NM_018880	Trim3	tripartite motif-containing	NM_018880	NM_018880	NM_018880	NM_018880	---	26	1	chr7	-
10461152	10,0121094	9,35837677	0,65373265	1,57323332	4,06E-06	0,00239719	AK051045	Snhg1	small nucleolar RNA host	AK051045	AK051045 //	AK051045 //	AK051045 //	---	25	1	chr19	+
10550059	8,00359992	7,47703031	0,5265696	1,44049994	4,22E-06	0,00242579	NM_029809	2310014L17Rik	RIKEN cDNA 2310014L17	NM_029809	NM_029809	NM_029809	NM_029809	---	25	1	chr7	+
10551355	7,58700235	8,07718132	-0,49017897	0,71193677	4,28E-06	0,00242579	NM_133210	Sertad3	SERTA domain containing	NM_133210	NM_133210	NM_133210	NM_133210	---	25	1	chr7	+
10380560	11,4523805	12,7316329	-0,27925243	0,82401789	4,72E-06	0,00252459	NM_201609	Zfp652	zinc finger protein 652	NM_201609	NM_201609	NM_201609	NM_201609	---	25	1	chr11	+
10489053	6,64466533	7,30714557	-0,66248024	0,63179121	4,64E-06	0,00252459	ENSMUST00(	4930518I15Rik	RIKEN cDNA 4930518I15	ENSMUST00(	ENSMUST00(	ENSMUST00(	ENSMUST00(	---	25	1	chr2	-
10597420	7,58046141	7,10806321	0,4723982	1,38741386	4,68E-06	0,00252459	NM_009916	Ccr4	chemokine (C-C motif) rec	NM_009916	NM_009916	NM_009916	NM_009916	X90862 // Ge	34	1	chr9	-
10604961	8,23076537	8,67123515	-0,44046978	0,73689462	5,16E-06	0,00270851	NM_008067	Gabra3	gamma-aminobutyric acid	NM_008067	NM_008067	NM_008067	NM_008067	---	33	1	chrX	-
10497894	8,91317072	8,43550868	0,47766204	1,39248529	5,81E-06	0,00299619	NM_145825	Cetn4	centrin 4	NM_145825	NM_145825	NM_145825	NM_145825	---	8	1	chr3	-
10416954	6,42250361	5,75715844	0,66534517	1,58594767	5,99E-06	0,00303471	NR_029737	Mir20a	microRNA 20a	NR_029737	---	---	---	---	25	1	chr14	+
10356457	6,49559654	6,8785111	-0,38291456	0,76688675	6,49E-06	0,00309698	NM_008299	Dnajb3	DnaJ (Hsp40) homolog, su	NM_008299	---	---	NM_008299	---	25	1	chr1	-
10554240	7,70906642	7,25511136	0,45395506	1,36979031	6,55E-06	0,00309698	NM_020583	Isg20	interferon-stimulated pro	NM_020583	NM_020583	NM_020583	NM_020583	---	30	1	chr7	+
10586168	11,4933628	10,9454816	0,54788118	1,46193704	6,39E-06	0,00309698	NR_028548	Snord16a	small nucleolar RNA, C/D	NR_028548	NR_028548 /	NR_028548 /	NR_028548 /	---	34	1	chr9	+
10587880	9,47240078	9,15767846	0,31472232	1,24377224	6,32E-06	0,00309698	NM_029620	Pcolce2	procollagen C-endopeptid	NM_029620	---	NM_029620	NM_029620	---	33	1	chr9	+
10604587	5,6410572	6,89149948	-1,25044229	0,42031933	6,80E-06	0,00316122	NR_029853	Mir363	microRNA 363	NR_029853	---	---	---	---	25	1	chrX	-
10346876	5,91951573	6,55855079	-0,63903506	0,6421423	6,99E-06	0,00319708	NR_028558	Snora41	small nucleolar RNA, H/A	NR_028558	NR_028558 /	NR_028558 /	NR_028558 /	---	15	1	chr1	+
10463729	5,93811848	5,29292748	0,64519101	1,56394633	7,26E-06	0,00326776	NM_001164	Nt5c2	5'-nucleotidase, cytosolic	NM_001164	NM_001164	NM_001164	NM_001164	---	26	1	chr19	+
10364824	11,4344634	12,7131701	-0,27870667	0,82432967	8,34E-06	0,0036003	NM_134002	Csnk1g2	casein kinase 1, gamma 2	NM_134002	NM_134002	NM_134002	NM_134002	---	32	1	chr10	+
10379708	5,14075801	4,51406935	0,62668866	1,54401703	8,51E-06	0,0036003	---	NA	NA	ENSMUST00(	---	---	---	---	25	1	chr11	+
10410092	9,70125081	9,4348905	0,26636032	1,20276961	8,45E-06	0,0036003	NM_175494	Zfp367	zinc finger protein 367	NM_175494	NM_175494	NM_175494	NM_175494	---	25	1	chr13	-
10563338	8,78567477	8,38896881	0,39770596	1,31741142	8,23E-06	0,0036003	NM_008654	Ppp1r15a	protein phosphatase 1, re	NM_008654	NM_008654	NM_008654	---	---	25	1	chr7	-
10414953	4,29842099	3,7574845	0,54093649	1,45491663	9,25E-06	0,00385436	ENSMUST00(	Gm16591	predicted gene, 16591	ENSMUST00(	---	---	---	---	9	1	chr14	+
10516484	7,86396378	7,3194987	0,54446508	1,45847947	9,59E-06	0,0039406	NM_008126	Gjb3	gap junction protein, beta	NM_008126	NM_008126	NM_008126	NM_008126	NM_011600	25	1	chr4	-
10578539	11,0624115	10,7452161	0,31719538	1,24590614	1,02E-05	0,00412073	NM_007450	Slc25a4	solute carrier family 25 (m	NM_007450	NM_007450	NM_007450	NM_007450	U27315 // Ge	25	1	chr8	-
10568461	10,8376778	11,0885068	-0,25082905	0,84041333	1,07E-05	0,00425317	NM_146218	Rfwd3	ring finger and WD repeat	NM_146218	NM_146218	NM_146218	NM_146218	---	51	3	chr7	-
10489018	11,7778705	12,4493831	0,32848735	1,2556961	1,10E-05	0,00426619	NM_133242	Rbm39	RNA binding motif protein	NM_133242	NM_133242	NM_133242	NM_133242	NM_133242	104	1	chr2	-
10575326	8,9971131	8,66130775	0,33580534	1,26208173	1,09E-05	0,00426619	---	NA	NA	AK156953	---	---	---	---	25	1	chr8	+
10604154	8,50729991	8,15849457	0,34880534	1,27350563	1,22E-05	0,00466467	NM_023894	Rhox9	reproductive homeobox 9	NM_023894	NM_023894	NM_023894	NM_023894	---	14	1	chrX	-
10399224	9,61502961	10,0446914	-0,42966175	0,74243583	1,25E-05	0,00469615	NR_030694	1110002L01Rik	RIKEN cDNA 1110002L01	NR_030694	NR_030694 /	NR_030694 /	NR_030694 /	---	9	1	chr12	-
10588691	7,59926286	8,00964078	-0,41037792	0,75742625	1,26E-05	0,00469615	NM_008317	Hyal1	hyaluronoglucosaminidas	NM_008317	NM_008317	NM_008317	NM_008317	---	25	1	chr9	+
10581800	10,838676	11,0831288	-0,24445287	0,84413587	1,32E-05	0,00484947	NM_146218	Rfwd3	ring finger and WD repeat	NM_146218	NM_146218	NM_146218	NM_146218	---	52	3	chr8	-
10384208	7,82151273	8,34397997	-0,52246724	0,69618023	1,36E-05	0,00495363	---	NA	NA	ENSMUST00(	---	---	---	---	19	1	chr11	-
10528648	11,2504967	11,5502426	-0,29974591	0,81239546	1,40E-05	0,00502914	NM_013853	Abcf2	ATP-binding cassette, sub	NM_013853	NM_013853	NM_013853	NM_013853	---	26	1	chr5	-
10425383	8,62454522	8,10568644	0,51885878	1,43282139	1,56E-05	0,00552164	ENSMUST00(	Apobec3	apolipoprotein B mRNA e	ENSMUST00(	ENSMUST00(	ENSMUST00(	ENSMUST00(	---	25	1	chr15	+
10556581	7,86253446	8,25376803	-0,39123357	0,76247737	1,59E-05	0,0055567	ENSMUST00(	Gm10589	predicted gene 10589	ENSMUST00(	ENSMUST00(	ENSMUST00(	ENSMUST00(	---	25	1	chr7	+
10554588	9,66650985	9,44317547	0,22333438	1,16742865	1,70E-05	0,00588292	NM_017400	Sh3gl3	SH3-domain GRB2-like 3	NM_017400	NM_017400	NM_017400	NM_017400	---	30	1	chr7	+
10445944	7,77095617	8,08622431	-0,31526814	0,8037016	1,97E-05	0,006721	NM_172829	St6gal2	beta galactoside alpha 2,6	NM_172829	NM_172829	NM_172829	NM_172829	---	29	1	chr17	+
10493282	10,4742245	10,6906966	-0,21647207	0,86066752	2,11E-05	0,00713764	NM_028814	2810403A07Rik	RIKEN cDNA 2810403A07	NM_028814	NM_028814	NM_028814	NM_028814	---	27	1	chr3	+
10445507	7,17855009	6,85050868	0,3279414	1,25522101	2,31E-05	0,00766537	BC147714	Gm88	predicted gene 88	BC147714	BC147714 //	BC147714 //	BC147714 //	---	30	1	chr17	+
10485830	11,4899001	11,2112263	0,2786738	1,21307925	2,35E-05	0,00766537	NM_026519	Tmem85	transmembrane protein 8	NM_026519	NM_026519	NM_026519	NM_026519	---	24	1	chr2	-
10511808	6,83744206	6,45159892	0,38584314	1,30662318	2,34E-05	0,00766537	NR_028384	4930528A17Rik	RIKEN cDNA 4930528A17	NR_028384	NR_028384 /	NR_028384 /	NR_028384 /	---	25	1	chr4	-
10374400	6,25258772	6,71105144	-0,45846372	0,72776081	2,58E-05	0,00804495	NM_176982	Fbxo48	F-box protein 48	NM_176982	NM_176982	NM_176982	NM_176982	---	25	1	chr11	+
10419631	10,4022552	10,6203324	-0,21807712	0,85971053	2,57E-05	0,00804495	NM_019721	Mettl3	methyltransferase like 3	NM_019721	NM_019721	NM_019721	NM_019721	NM_019721	36	1	chr14	-
10488254	8,24316051	7,7370615	0,50609891	1,42020472	2,51E-05	0,00804495	---	NA	NA	ENSMUST00(	---	---	---	---	32	1	chr2	-
10586331	8,67594166	8,32506498	0,35087668	1,27533538	2,58E-05	0,00804495	NM_008988	Igdcc3	immunoglobulin superfan	NM_008988	NM_008988	NM_008988	NM_008988	---	30	1	chr9	+
10589927	6,39242801	6,89208871	-0,4996607	0,7072731	2,72E-05	0,00837585	---	NA	NA	BC005774	---	---	---	---	25	1	chr9	+
10419465	9,95854339	10,3297711	-0,37122767	0,77312432	2,82E-05	0,00859025	NM_001111	Ccnb1ip1	cyclin B1 interacting prote	NM_001111	NM_001111	NM_001111	NM_001111	---	24	1	chr14	-
10442087	7,47384594	7,90685541	-0,43300946	0,74071504	3,07E-05	0,0090667	NM_001162	Ncrna00085	non-protein coding RNA 8	NM_001162	NM_001162	NM_001162	NM_001162	---	35	1	chr17	+
10499130	8,88601756	8,13659134	0,75057378	0,59436712	3,05E-05	0,0090667	NR_004418	Rnu73b	U73B small nuclear RNA	NR_004418	NR_004418 /	NR_004418 /	NR_004418 /	---	25	1	chr3	-
10514054	9,25027535	9,59402222	-0,34374687	0,78799213	3,06E-05	0,0090667	NM_011132	Nfib	nuclear factor I/B	NM_011132	NM_011132	NM_011132	NM_011132	---	38	1	chr4	-
10376887	8,54557938	9,24402979	-0,69845041	0,70786569	3,19E-05	0,00923831	NR_028550	Snord49a	small nucleolar RNA, C/D	NR_028550	NR_028550 /	NR_028550 /	NR_028550 /	---	25	1	chr11	+
10507477	5,75133642	5,20338589	0,74795053	1,67940539	3,18E-05	0,00923831	---	NA	NA	ENSMUST00(	---	---	---	---	10	1	chr4	+
10356423	8,26099517	8,52797215	-0,26697698	0,83105912	3,46E-05	0,00960924	NM_011985	Usp40	ubiquitin specific peptida	NM_011985	NM_011985	NM_011985	NM_011985	---	33	1	chr1	-
10370025	10,779368	11,017233	-0,237865	0,84799931	3,54E-05	0,00960924	NM_011418	Smarcb1	SWI/SNF related, matrix a	NM_011418	NM_011418	NM_011418	NM_011418	---	33	1	chr10	-
10424082	8,56939452	8,11755947	0,45183505	1,36577891	3,43E-05	0,00960924	NM_175503	Aard	alanine and arginine rich	NM_175503	NM_175503	NM_175503	NM_175503	---	25	1	chr15	+
10461454	7,56383937	7,98137176	-0,41747239	0,74873526	3,64E-05	0,00960924	NM_026919	1810006K21Rik	RIKEN cDNA 1810006K21	NM_026919	NM_026919	NM_026919	NM_026919	---	21	1	chr19	+
10502135	5,31030591	5,81466497	-0,49564094	1,40094701	3,69E-05	0,00960924	NM_009102	Rrh	retinal pigment epithelium	NM_009102	NM_009102	NM_009102	NM_009102	NM_009102	38	1	chr3	-
10513320	9,32752962	9,02356492	0,3039447	1,23451529	3,51E-05	0,00960924	NM_025968	Ptgr1	prostaglandin reductase 1	NM_025968	NM_025968	NM_025968	NM_025968	---	33	1	chr4	-
10516022	7,24599284	7,78896193	-0,54296908	0,68635592	3,67E-05	0,00960924	---	NA	NA	ENSMUST00(	---	---	---	---	37	1	chr4	-
10549615	9,9125537	10,1938254	-0,28727173	0,81945025	3,58E-05	0,00960924	NM_172736	Leng8	leukocyte receptor cluste	NM_172736	NM_172736	---	NM_172736	---	34	1	chr7	+
10563829	9,83544326	9,54323639	0,29220688	1,22451197	3,45E-05	0,00960924	NM_010270	Mrps33	mitochondrial ribosomal p	NM_010270	NM_010270	NM_010270	NM_010270	---	31	3	chr7	-

10572332	8,44024774	8,67489066	-0,23464293	0,84989533	3,69E-05	0,00960924	NM_172755	Sugp2	SURP and G patch domain	NM_172755	NM_172755	NM_172755	NM_172755	---	36	1	chr8	+
10584405	6,3253477	6,76521928	-0,43987158	0,73720023	3,36E-05	0,00960924	NM_146869	Olfr147	olfactory receptor 147	NM_146869	NM_146869	NM_146869	NM_146869	---	25	1	chr9	+
10440619	3,57614689	3,95014692	-0,37400004	0,77164007	3,83E-05	0,00988245	---	NA	NA	ENSMUST000	---	---	---	---	25	1	chr16	-
10543676	7,5217679	7,14386364	0,37790426	1,29945283	3,92E-05	0,01000134	ENSMUST000	1700080G18Rik	RIKEN cDNA 1700080G18	ENSMUST000	ENSMUST000	ENSMUST000	ENSMUST000	---	25	1	chr6	-
10352954	8,79470334	8,38801045	0,40669289	1,32564354	4,02E-05	0,01004707	NM_008253	Hmgb3	high mobility group box 3	NM_008253	NM_008253	NM_008253	NM_008253	---	45	3	chr1	-
10365833	9,65994825	9,89895706	-0,2390088	0,84732726	4,04E-05	0,01004707	NM_183199	Usp44	ubiquitin specific peptida	NM_183199	NM_183199	NM_183199	NM_183199	---	41	1	chr10	+
10581448	7,5032923	7,12676985	0,37652245	1,29820881	4,00E-05	0,01004707	---	NA	NA	ENSMUST000	---	---	---	---	19	1	chr8	-
10359235	9,38335269	9,62039219	-0,2370395	0,84848467	4,21E-05	0,01038265	NM_177644	Rasal2	RAS protein activator like	NM_177644	NM_177644	NM_177644	NM_177644	---	37	1	chr1	-
10420097	10,2626036	10,4898213	-0,22721776	0,85428079	4,26E-05	0,01042218	NM_145705	Tinf2	Terf1 (TRF1)-interacting n	NM_145705	NM_145705	NM_145705	NM_145705	---	42	1	chr14	-
10468881	8,70681961	9,13829115	-0,43147154	0,74150507	4,82E-05	0,01164362	BC086681	Zfp826	zinc finger protein 826	BC086681	BC086681 //	BC086681 //	BC086681 //	---	24	1	chr19	-
10529819	6,41749337	5,95601355	0,46147983	1,37695345	4,85E-05	0,01164362	NM_008009	Fgfbp1	fibroblast growth factor b	NM_008009	NM_008009	NM_008009	NM_008009	---	29	1	chr5	-
10357875	9,6799239	9,91483724	-0,23491334	0,84973604	5,16E-05	0,01199852	NM_007570	Btg2	B-cell translocation gene	NM_007570	NM_007570	---	NM_007570	---	25	1	chr1	-
10416948	6,60835742	6,05250821	0,55584922	1,47003369	5,14E-05	0,01199852	NR_029785	Mir17	microRNA 17	NR_029785	---	---	---	---	26	1	chr14	+
10446739	8,83158846	9,15759285	-0,32600439	0,79774281	5,21E-05	0,01199852	NM_030179	Clip4	CAP-GLY domain containi	NM_030179	NM_030179	NM_030179	NM_030179	---	32	1	chr17	+
10489484	10,0097684	9,75953926	0,25022909	1,18939597	5,09E-05	0,01199852	NM_011521	Sdc4	syndecan 4	NM_011521	NM_011521	NM_011521	NM_011521	---	30	1	chr2	-
10506452	6,88251151	7,48954742	-0,60703591	0,65654422	5,20E-05	0,01199852	AY512949	AY512949	cDNA sequence AY512949	AY512949	AY512949 //	AY512949 //	AY512949 //	---	25	1	chr4	+
10425161	10,1510075	9,85744637	0,29356111	1,22566194	5,34E-05	0,0122076	NM_008495	Lgals1	lectin, galactose binding,	NM_008495	NM_008495	NM_008495	NM_008495	---	25	1	chr15	+
10466248	9,98987064	10,1844365	-0,19456588	0,8738358	5,55E-05	0,01249775	NM_001025	Stx3	syntaxin 3	NM_001025	NM_001025	NM_001025	NM_001025	---	45	1	chr19	-
10548128	9,1328642	8,91682284	0,21604136	1,16154203	5,54E-05	0,01249775	NM_175414	Tspan9	tetraspanin 9	NM_175414	NM_175414	NM_175414	NM_175414	---	30	1	chr6	-
10552353	9,17044063	9,45678784	-0,28634721	0,81997554	5,79E-05	0,01292137	---	NA	NA	GENSCAN000	---	---	---	---	38	3	chr7	+
10546088	11,3008236	11,5341691	0,23334552	0,85065998	5,88E-05	0,01297718	NM_198622	H1fx	H1 histone family, membe	NM_198622	NM_198622	NM_198622	NM_198622	---	26	1	chr6	-
10551542	8,29195812	8,04560276	0,24635536	1,18620664	5,90E-05	0,01297718	NM_015796	Fbxo17	F-box protein 17	NM_015796	NM_015796	NM_015796	NM_015796	---	41	1	chr7	+
10413229	11,1208488	11,382327	-0,26147818	0,83423273	6,03E-05	0,01305287	NM_013469	Anxa11	annexin A11	NM_013469	NM_013469	NM_013469	NM_013469	---	14	1	chr14	+
10458828	7,48277302	7,05739023	0,42538279	1,34292877	6,03E-05	0,01305287	NM_033037	Cdo1	cysteine dioxygenase 1, c	NM_033037	NM_033037	NM_033037	NM_033037	---	25	1	chr18	-
10356020	7,61102104	7,92629378	-0,31527274	0,80369904	6,58E-05	0,01372373	NM_175291	Dock10	dedicator of cytokinesis 1	NM_175291	NM_175291	NM_175291	NM_175291	---	61	1	chr1	-
10371662	5,68009028	5,21636317	0,46372711	1,37910003	6,56E-05	0,01372373	NM_011461	Spic	Spi-C transcription factor	NM_011461	NM_011461	NM_011461	NM_011461	---	28	1	chr10	-
10449148	8,27303703	7,96657932	0,3064577	1,23666754	6,49E-05	0,01372373	NM_0011004	Wfikkn1	WAP, FS, Ig, KU, and NTR	NM_0011004	NM_0011004	NM_0011004	NM_0011004	---	27	1	chr17	-
10462995	5,57214933	4,94364731	0,62850203	1,54595897	6,42E-05	0,01372373	---	NA	NA	GENSCAN000	---	---	---	---	27	1	chr19	+
10534966	8,03780997	8,36131316	-0,32350319	0,79912706	6,53E-05	0,01372373	NM_019747	Zfp113	zinc finger protein 113	NM_019747	NM_019747	NM_019747	NM_019747	---	26	1	chr5	-
10366409	9,72256881	10,003461	-0,28089223	0,82308183	6,83E-05	0,01403676	NM_0010332	Zfc3h1	zinc finger, C3H1-type con	NM_0010332	NM_0010332	NM_0010332	NM_0010332	---	36	1	chr10	+
10417829	9,79830636	9,6162149	0,18209147	1,13452741	6,89E-05	0,01403676	NM_134081	Dnajc9	DnaJ (Hsp40) homolog, su	NM_134081	NM_134081	NM_134081	NM_134081	---	26	1	chr14	-
10557058	8,30555633	8,76838257	-0,46342624	0,7252518	6,93E-05	0,01403676	NM_025298	Polr3e	polymerase (RNA) III (DNA	NM_025298	NM_025298	NM_025298	NM_025298	NM_025298	19	1	chr7	+
10564877	8,32660478	8,59333682	-0,26673204	0,83120023	6,81E-05	0,01403676	NM_173445	Rccd1	RCC1 domain containing 1	NM_173445	NM_173445	NM_173445	NM_173445	---	29	1	chr7	-
10368616	8,72418058	8,9881601	-0,26397952	0,83278759	7,14E-05	0,0142558	NM_028287	Zufsp	zinc finger with UFM1-spe	NM_028287	NM_028287	NM_028287	NM_028287	---	35	1	chr10	-
10546936	8,01079397	7,76105227	0,24974169	1,18899421	7,13E-05	0,0142558	NM_172487	Prrt3	proline-rich transmembra	NM_172487	NM_172487	NM_172487	NM_172487	---	33	1	chr6	-
10593988	3,70580036	3,35577339	0,24997103	0,84091214	7,35E-05	0,01457491	NM_007713	Clk3	CDC-like kinase 3	NM_007713	NM_007713	NM_007713	NM_007713	NM_007713	24	1	chr9	-
10359425	10,1008576	10,3149523	-0,21409485	0,86208598	7,69E-05	0,01514319	NM_0010394	Klhl20	kelch-like 20 (Drosophila)	NM_0010394	NM_0010394	NM_0010394	NM_0010394	---	26	1	chr1	-
10437852	10,6235736	10,8257164	-0,20214286	0,86925848	7,75E-05	0,01514554	NM_0010811	4921513D23Rik	RIKEN cDNA 4921513D23	NM_0010811	NM_0010811	NM_0010811	NM_0010811	---	32	1	chr16	-
10465831	9,63389479	10,0041936	-0,37029883	0,77362224	7,80E-05	0,01514554	NR_027866	5730408K05Rik	RIKEN cDNA 5730408K05	NR_027866	NR_027866 /	NR_027866 /	NR_027866 /	---	26	1	chr19	-
10526514	7,00134367	6,72038453	0,28095914	1,21500238	7,86E-05	0,0151512	NM_021719	Cldn15	claudin 15	NM_021719	---	NM_021719	NM_021719	---	25	1	chr5	+
10475414	9,00561044	8,66693698	0,33867346	1,26459328	8,15E-05	0,01560689	NM_009735	B2m	beta-2 microglobulin	NM_009735	NM_009735	NM_009735	NM_009735	---	25	1	chr2	+
10572605	8,04843552	8,24776577	-0,19928025	0,87098498	8,41E-05	0,01589277	NM_172756	Ankle1	ankyrin repeat and LEM d	NM_172756	NM_172756	NM_172756	NM_172756	---	27	1	chr8	+
10573210	7,3869025	6,88971755	0,49718495	1,31693574	8,37E-05	0,01589277	NM_013641	Ptger1	prostaglandin E receptor	NM_013641	NM_013641	NM_013641	NM_013641	---	30	1	chr8	+
10506376	7,92790856	8,24121984	-0,31331128	0,80479247	8,52E-05	0,01599327	NM_025921	2610002M06Rik	RIKEN cDNA 2610002M06	NM_025921	NM_025921	NM_025921	NM_025921	---	26	1	chrX	-
10464030	7,24256485	6,80836105	0,4342038	1,35116494	9,12E-05	0,0170832	NM_007417	Adra2a	adrenergic receptor, alph	NM_007417	NM_007417	NM_007417	NM_007417	---	26	1	chr19	+
10376425	6,56082249	6,88715878	-0,32633629	0,79755931	9,54E-05	0,01767902	ENSMUST000	Gm12258	predicted gene 12258	ENSMUST000	ENSMUST000	ENSMUST000	ENSMUST000	---	25	1	chr11	+
10425799	7,1638965	6,83557973	0,32831677	1,25554764	9,87E-05	0,01816296	NR_004432	Rnu12	RNA U12, small nuclear	NR_004432	---	---	---	---	29	3	chr15	+
10448278	8,82981982	9,04997073	-0,22015091	0,85847563	0,00010128	0,01840544	NM_0010333	Mmp25	matrix metallopeptidase 2	NM_0010333	NM_0010333	NM_0010333	NM_0010333	---	35	1	chr17	-
10489946	8,92598025	9,15388415	-0,22786125	0,85389983	0,00010092	0,01840544	NM_010072	Dpm1	dolichol-phosphate (beta-	NM_010072	NM_010072	NM_010072	NM_010072	---	34	1	chr2	-
10552088	6,95370602	6,50734158	0,34636444	1,27135281	0,00010198	0,01841457	ENSMUST000	Gm10640	predicted gene 10640	ENSMUST000	ENSMUST000	ENSMUST000	ENSMUST000	---	25	1	chr7	+
10365003	7,10094201	7,72777225	-0,6268306	0,64759754	0,00010282	0,01844987	NR_028549	Scord37	small nucleolar RNA, C/D	NR_028549	NR_028549 /	NR_028549 /	NR_028549 /	---	25	1	chr10	+
10475981	9,95032512	10,2378633	-0,28753814	0,81929855	0,0001048	0,018463	NM_025395	Chchd5	coiled-coil-helix-coiled-co	NM_025395	NM_025395	NM_025395	NM_025395	---	25	1	chr2	+
10511175	11,4896818	11,2882534	0,20142844	1,14983527	0,00010485	0,018463	NM_025338	Aurkaip1	aurora kinase A interactin	NM_025338	NM_025338	NM_025338	NM_025338	---	26	1	chr4	+
10500901	7,30475837	7,69389661	-0,39113824	0,76252776	0,00010369	0,018463	NM_013476	Ar	androgen receptor	NM_013476	NM_013476	NM_013476	NM_013476	NM_013476	27	1	chrX	+
10465089	6,85066991	7,16543799	-0,31476808	0,80398022	0,00010591	0,01853461	NM_0010245	Snx32	sorting nexin 32	NM_0010245	NM_0010245	NM_0010245	NM_0010245	---	26	1	chr19	-
10595803	10,1475914	9,76182516	0,38576624	1,30655354	0,00010934	0,01901704	NM_011279	Rnf7	ring finger protein 7	NM_011279	NM_011279	NM_011279	NM_011279	---	8	1	chr9	-
10380549	5,51261883	5,9450505	-0,43343167	0,7404983	0,00011199	0,01926446	---	NA	NA	AK158420	---	---	---	---	25	1	chr11	+
10516256	7,60687203	7,89492445	-0,28805243	0,81900684	0,00011242	0,01926446	NM_153159	Zc3h12a	zinc finger CCCH type con	NM_153159	NM_153159	NM_153159	NM_153159	---	31	1	chr4	-
10600357	8,50153438	8,79335487	-0,29182049	0,81687063	0,0001128	0,01926446	NM_0011735	Taz	tafazzin	NM_0011735	NM_0011735	NM_0011735	NM_0011735	---	38	1	chrX	+
10458030	9,18453848	8,89642032	0,28811817	1,22104552	0,00011484	0,01946533	NM_007874	Reep5	receptor accessory protei	NM_007874	NM_007874	NM_007874	NM_007874	---	27	1	chr18	-
10533933	8,82858338	9,01316952	-0,18458614	0,87990145	0,00011752	0,01983176	NM_133895	Slc15a4	solute carrier family 15, m	NM_133895	NM_133895	NM_133895	NM_133895	---	32	1	chr5	-
10351045	5,01450827	6,07019104	-1,05568277	0,4810595	0,00011913	0,01998365	---	NA	NA	ENSMUST000	---	---	---	---	30	1	chr1	+

10400095	10,3516917	10,097425	0,25426673	1,19272937	0,00012522	0,02052009	NM_013562	Ifrd1	interferon-related develo	NM_013562	NM_013562	NM_013562	NM_013562	---	38	1	chr12	-
10426451	7,24319995	6,98374729	0,25945265	1,19702448	0,00012416	0,02052009	NM_029926	Irak4	interleukin-1 receptor-ass	NM_029926	NM_029926	---	NM_029926	---	30	1	chr15	+
10472313	6,34135156	6,00760401	0,33374755	1,26028284	0,00012517	0,02052009	NM_009322	Tbr1	T-box brain gene 1	NM_009322	NM_009322	NM_009322	NM_009322	---	25	1	chr2	+
10510019	5,89726605	5,42726249	0,47000357	1,38511288	0,00012464	0,02052009	NR_030695	B330016D10Rik	RIKEN cDNA B330016D10	NR_030695	NR_030695 //	NR_030695 //	NR_030695 //	---	25	1	chr4	+
10508797	8,73408277	8,2563674	0,47771537	1,39253672	0,00013018	0,02121055	ENSMUST000	Gm10151	predicted gene 10151	ENSMUST000	ENSMUST000	ENSMUST000	ENSMUST000	---	25	1	chr4	+
10519480	5,78583687	5,41765534	0,36818154	1,29072489	0,00013242	0,02145254	---	NA	NA	GENSCAN000	---	---	---	---	15	1	chr5	+
10346607	12,0414995	12,2148853	-0,17338579	0,88675914	0,00013572	0,02173848	NM_008057	Fzd7	frizzled homolog 7 (Droso	NM_008057	NM_008057	NM_008057	NM_008057	NM_008057	28	1	chr1	+
10353010	9,69556328	10,0553438	-0,35978055	0,77928311	0,00013531	0,02173848	NM_008651	Mybl1	myeloblastosis oncogene	NM_008651	NM_008651	NM_008651	NM_008651	---	33	1	chr1	-
10362896	9,52015857	9,17960289	0,34055568	1,26624421	0,00013717	0,02184741	NM_009846	Cd24a	CD24a antigen	NM_009846	NM_009846	NM_009846	NM_009846	---	19	1	chr10	+
10469453	4,5811949	4,99911326	-0,41791836	0,74850385	0,00013901	0,02201708	---	NA	NA	ENSMUST000	---	---	---	---	25	1	chr2	+
10584358	4,62347474	4,20805738	0,41541736	1,33368444	0,0001399	0,02203459	NM_146417	Olfr877	olfactory receptor 877	NM_146417	NM_146417	NM_146417	NM_146417	---	25	1	chr9	+
10404069	11,9918495	12,7551125	-0,23673699	1,17832457	0,00014307	0,02240945	NM_030609	Hist1h1a	histone cluster 1, H1a	NM_030609	NM_030609	NM_030609	NM_030609	---	25	1	chr13	+
10361110	11,5527339	12,3410907	-0,21164317	1,15800635	0,00014787	0,02266767	NM_029766	Dtl	denticle ess homolog (Dro	NM_029766	NM_029766	NM_029766	---	---	36	1	chr1	-
10389882	10,7211892	10,9847159	-0,26352669	0,83304903	0,0001473	0,02266767	NM_026313	Luc7l3	LUC7-like 3 (S. cerevisiae)	NM_026313	NM_026313	NM_026313	NM_026313	---	33	1	chr11	-
10455094	5,44491985	5,20844645	0,2364734	1,1781093	0,00014728	0,02266767	NM_053138	Pcdhb13	protocadherin beta 13	NM_053138	NM_053138	NM_053138	---	---	28	1	chr18	+
10468584	9,75798352	9,55441005	0,20357347	1,15154714	0,00014988	0,02266767	NM_0010335	Zdhhc6	zinc finger, DHHC domain	NM_0010335	NM_0010335	NM_0010335	NM_0010335	---	24	1	chr19	-
10472277	11,4404579	12,2418802	-0,19857763	1,1475664	0,00015032	0,02266767	NM_020575	March7	membrane-associated rin	NM_020575	NM_020575	NM_020575	NM_020575	---	32	1	chr2	+
10490986	7,56924921	7,88970544	-0,32045624	0,80081659	0,00014911	0,02266767	NR_027985	4632415L05Rik	RRS1 ribosome biogenesis	NR_027985	NR_027985 //	NR_027985 //	NR_027985 //	---	26	1	chr3	+
10586967	8,23437256	8,80812824	-0,57375568	0,67186548	0,00015003	0,02266767	AK087684	Gm7265	predicted gene 7265	AK087684	AK087684 //	AK087684 //	AK087684 //	---	25	1	chr9	+
10528864	8,99513073	9,2179371	-0,22280637	0,85689696	0,00015249	0,0228733	NM_175651	Cnpy1	canopy 1 homolog (zebraf	NM_175651	NM_175651	NM_175651	NM_175651	---	34	1	chr5	-
10450622	8,52882905	8,74476284	-0,21593379	0,8609887	0,00015629	0,02320302	NM_0011427	Atat1	alpha tubulin acetyltransf	NM_0011427	NM_0011427	NM_0011427	NM_0011427	---	44	1	chr17	-
10573451	11,3303036	12,1539326	-0,17637102	1,13003779	0,00015714	0,02320302	NM_0011682	Syce2	synaptonemal complex ce	NM_0011682	NM_0011682	NM_0011682	NM_0011682	---	26	1	chr8	+
10584584	7,27466288	7,02249205	0,25217083	1,19099787	0,00015681	0,02320302	NM_178245	Bsx	brain specific homeobox	NM_178245	NM_178245	NM_178245	NM_178245	---	26	1	chr9	+
10437073	7,37213835	7,10697669	0,26516166	1,20177071	0,00016054	0,02358241	NM_133229	Ripply3	ripply3 homolog (zebrafis	NM_133229	NM_133229	NM_133229	NM_133229	---	27	1	chr16	+
10392241	7,65393022	7,95701745	-0,30308724	0,81051611	0,00016226	0,0237114	NM_015810	Polg2	polymerase (DNA directed	NM_015810	NM_015810	NM_015810	NM_015810	---	33	1	chr11	-
10393125	10,0229146	10,2365008	-0,21358615	0,8623909	0,00016467	0,02394036	NM_024177	Mrpl38	mitochondrial ribosomal g	NM_024177	NM_024177	NM_024177	NM_024177	---	76	1	chr11	-
10354792	9,73045284	9,39284593	0,33760691	1,26365874	0,00016939	0,02425396	NR_004860	1110034B05Rik	RIKEN cDNA 1110034B05	NR_004860	NR_004860 //	NR_004860 //	NR_004860 //	---	35	1	chr1	-
10402560	7,39723248	7,86109504	-0,46386256	0,72504245	0,00016883	0,02425396	AK079474	A130014H13Rik	RIKEN cDNA A130014H13	AK079474	AK079474 //	AK079474 //	AK079474 //	---	25	1	chr12	-
10586458	9,28617878	9,56033872	-0,27415994	0,82693169	0,00016855	0,02425396	NM_173185	Csnk1g1	casein kinase 1, gamma 1	NM_173185	NM_173185	NM_173185	NM_173185	---	35	1	chr9	+
10571221	8,43733442	8,70491671	-0,26758229	0,83071051	0,00017481	0,02490454	NM_0011127	BC019943	cDNA sequence BC019943	NM_0011127	NM_0011127	NM_0011127	NM_0011127	NM_0011127	32	1	chr8	+
10542836	9,72337698	9,97702936	-0,25365238	0,83877026	0,0001787	0,02533104	NM_0010812	Klhdc5	kelch domain containing 5	NM_0010812	NM_0010812	NM_0010812	NM_0010812	---	26	1	chr6	+
10434782	8,43048025	8,64334244	-0,21286219	0,86282376	0,0001819	0,0256656	NM_178665	Lpp	LIM domain containing pr	NM_178665	NM_178665	NM_178665	NM_178665	---	31	1	chr16	+
10367434	8,47469702	8,8597458	-0,38504878	0,76575311	0,00018309	0,0256964	---	NA	NA	AK086046	---	---	---	---	25	1	chr10	+
10361091	7,67348119	7,32756199	0,3459192	1,2709505	0,00018731	0,02588822	NM_007498	Atf3	activating transcription fa	NM_007498	NM_007498	NM_007498	NM_007498	BC019946 //	25	1	chr1	-
10410124	11,4258689	12,2422502	-0,18361813	1,135729	0,00018903	0,02588822	NM_009984	Ctsl	cathepsin L	NM_009984	NM_009984	NM_009984	NM_009984	---	25	1	chr13	-
10454238	9,44213683	9,73216577	-0,29004894	0,81787431	0,00018817	0,02588822	NM_027007	Zfp397	zinc finger protein 397	NM_027007	NM_027007	NM_027007	NM_027007	---	28	1	chr18	+
10480601	7,25226723	7,52615467	-0,27458744	0,82668569	0,00018838	0,02588822	NM_146115	A830007P12Rik	RIKEN cDNA A830007P12	NM_146115	NM_146115	NM_146115	NM_146115	---	26	1	chr2	-
10515429	9,97759169	9,68785576	0,28973593	1,32241551	0,00018871	0,02588822	NR_030704	Snord55	small nucleolar RNA, C/D	NR_030704	NR_030704 /	NR_030704 /	NR_030704 /	---	25	1	chr4	-
10370920	11,4619594	11,6933169	-0,23135744	0,85183302	0,00019373	0,02627805	NM_145361	Btbd2	BTB (POZ) domain contain	NM_145361	NM_145361	NM_145361	NM_145361	---	30	1	chr10	-
10401052	6,9839581	6,57190524	0,31205286	1,24147298	0,00019354	0,02627805	NM_019784	Tex21	testis expressed gene 21	NM_019784	---	---	---	---	30	1	chr12	-
10466885	8,31915133	8,50268531	-0,28353397	0,82157605	0,00019577	0,02642918	NM_011265	Rfx3	regulatory factor X, 3 (infl	NM_011265	NM_011265	NM_011265	NM_011265	---	39	1	chr19	-
10562005	10,5642493	10,7658231	-0,20157376	0,86960144	0,00019749	0,02653476	NM_029274	Wbp7	WW domain binding prot	NM_029274	NM_029274	NM_029274	NM_029274	---	38	1	chr7	-
10481654	11,1983499	10,9552057	0,24314419	1,1835593	0,00019976	0,02671337	NM_010236	Fpgs	folylpolyglutamyl synthet	NM_010236	NM_010236	NM_010236	NM_010236	---	30	1	chr2	-
10409039	11,2103153	11,3970124	-0,18669711	0,87861491	0,00020569	0,0271218	NM_0010332	Fam120a	family with sequence sim	NM_0010332	---	NM_0010332	NM_0010332	---	36	1	chr13	-
10552736	7,57395222	7,29879475	0,27515747	1,21012617	0,00020391	0,0271218	NM_0010775	Tsks	testis-specific serine kinas	NM_0010775	NM_0010775	---	NM_0010775	---	35	1	chr7	+
10580365	9,11264466	8,83422171	0,27842295	1,21286834	0,00020495	0,0271218	NM_025722	4921524J17Rik	RIKEN cDNA 4921524J17	NM_025722	NM_025722	NM_025722	NM_025722	---	10	1	chr8	-
10386633	8,02654987	8,29956506	-0,27301519	0,8275881	0,00020827	0,02733531	NR_027800	Gm16516	predicted gene, Gm16516	NR_027800	NR_027800 /	NR_027800 /	NR_027800 /	---	25	1	chr11	-
10401781	11,0961904	10,836203	0,19958742	1,14868834	0,0002164	0,02810374	NM_011479	Sptic2	serine palmitoyltransferas	NM_011479	NM_011479	NM_011479	NM_011479	---	26	1	chr12	-
10416956	7,3484147	6,81535041	0,73306429	1,66216579	0,00021599	0,02810374	NR_029815	Mir19b-1	microRNA 19b-1	NR_029815	---	---	---	---	30	1	chr14	+
10495935	9,20386207	9,41285693	-0,20899486	0,86513977	0,00021712	0,02810374	NM_197997	4930422G04Rik	RIKEN cDNA 4930422G04	NM_197997	NM_197997	NM_197997	NM_197997	---	27	1	chr3	+
10502235	11,3487061	11,5299938	-0,18128775	0,88191545	0,00021809	0,02810374	NM_139144	Ogt	O-linked N-acetylglucosar	NM_139144	NM_139144	NM_139144	NM_139144	---	28	1	chrX	+
10510339	7,52199691	7,76288822	-0,2408913	0,84622235	0,00021914	0,02811122	NM_0010038	Masp2	mannan-binding lectin se	NM_0010038	NM_0010038	NM_0010038	NM_0010038	NM_145556	48	1	chr4	+
10461071	8,98184776	8,75328722	0,22856054	1,17166533	0,0002205	0,02815907	NM_175381	2700081O15Rik	RIKEN cDNA 2700081O15	NM_175381	NM_175381	NM_175381	NM_175381	---	27	1	chr19	+
10589610	8,27689004	8,6514224	-0,37453136	0,7713554	0,00022273	0,02831607	NM_153099	Prss42	protease, serine, 42	NM_153099	NM_153099	NM_153099	NM_153099	---	26	1	chr9	+
10409508	10,6800498	10,8680487	-0,18799896	0,87782243	0,00022446	0,02840829	NM_134059	Ddx41	DEAD (Asp-Glu-Ala-Asp) b	NM_134059	NM_134059	NM_134059	NM_134059	NM_134059	33	1	chr13	-
10355310	7,5158894	7,18679315	0,32909626	1,25622619	0,00022997	0,02854824	---	NA	NA	ENSMUST000	---	---	---	---	9	1	chr1	-
10421555	4,71273749	5,22351873	-0,51078124	0,70184228	0,00022987	0,02854824	NR_030459	Mir687	microRNA 687	NR_030459	---	---	---	---	25	1	chr14	-
10542880	8,92534828	9,29333037	-0,36798208	0,77486555	0,00022919	0,02854824	BC048711	4833442J19Rik	RIKEN cDNA 4833442J19	BC048711	BC048711 //	BC048711 //	BC048711 //	---	26	1	chr6	+
10543017	9,26869346	8,92521	0,34348346	1,26881652	0,00022671	0,02854824	NM_013743	Pdk4	pyruvate dehydrogenase (	NM_013743	NM_013743	NM_013743	NM_013743	NM_013743	33	1	chr6	-
10548180	9,91540723	9,70263445	0,21277277	1,1589134	0,0002306	0,02854824	NM_133927	Itfg2	integrin alpha FG-GAP rep	NM_133927	NM_133927	NM_133927	NM_133927	---	35	1	chr6	-
10560043	8,30113717	8,59812109	-0,29678392	0,8140551	0,00023328	0,0287549	NM_026046	Zfp329	zinc finger protein 329	NM_026046	NM_026046	NM_026046	NM_026046	---	25	1	chr7	-
10491056	10,6441738	10,3734792	0,27099463	1,20663943	0,00023539	0,02876391	NM_030732	Tbl1xr1	transducin (beta)-like 1X-	NM_030732	NM_030732	NM_030732	NM_030732	---	25	1	chr3	+

10491300	10,8980605	12,0762918	-0,1782313	0,88378583	0,00023515	0,02876391	NM_011386	Ski	Ski-like	NM_011386	NM_011386	NM_011386	NM_011386	U36203 // Ge	36	1	chr3	+
10409643	10,2123908	10,0122165	0,20017431	1,14883715	0,0002375	0,02889808	NM_029872	Hnrnpa0	heterogeneous nuclear ri	NM_029872	NM_029872	NM_029872	NM_029872	NM_029872	25	1	chr13	-
10552276	10,5085871	10,2806547	0,22793236	1,17115527	0,00023959	0,02902694	NM_009459	Ube2h	ubiquitin-conjugating enz	NM_009459	NM_009459	ENSMUST000	NM_009459	---	48	3	chr7	+
10350146	10,7331694	10,4693473	0,26382213	1,20065539	0,00024415	0,0293479	NM_013750	Phlda3	pleckstrin homology-like d	NM_013750	NM_013750	NM_013750	NM_013750	---	26	1	chr1	+
10457853	10,0567879	9,77101918	0,2857687	1,21905964	0,00024431	0,0293479	NM_172625	Ino80c	INO80 complex subunit C	NM_172625	NM_172625	NM_172625	NM_172625	---	26	1	chr18	-
10501963	8,13402468	8,34820754	-0,21418286	0,86203427	0,00024826	0,02957181	NM_011674	Ugt8a	UDP galactosyltransferase	NM_011674	NM_011674	NM_011674	NM_011674	---	27	1	chr3	-
10557655	11,5188438	11,6858822	-0,16703838	0,89066921	0,00024802	0,02957181	ENSMUST000	Srcap	Snf2-related CREBBP activ	ENSMUST000	ENSMUST000	ENSMUST000	ENSMUST000	---	47	1	chr7	+
10347552	11,0292184	11,2465829	-0,21736452	0,86013528	0,00025571	0,03033234	NM_011494	Strk16	serine/threonine kinase 1	NM_011494	NM_011494	NM_011494	NM_011494	---	33	1	chr1	+
10398693	10,7282323	10,1424688	0,58576353	1,50083308	0,00025913	0,03061018	NR_033168	Snora28	small nucleolar RNA, H/A	NR_033168	NR_033168 /	NR_033168 /	NR_033168 /	---	25	1	chr12	+
10349752	8,36384975	8,59596484	-0,23211509	0,85138579	0,00026164	0,03077781	NM_007923	Elk4	ELK4, member of ETS onc	NM_007923	NM_007923	NM_007923	NM_007923	---	33	1	chr1	+
10353923	9,57713697	9,79605599	-0,21891902	0,85920898	0,00026836	0,03130866	NM_201365	Fam178b	family with sequence sim	NM_201365	NM_201365	NM_201365	NM_201365	---	30	1	chr1	-
10480971	9,517407	9,73369274	-0,21628574	0,86077869	0,00026768	0,03130866	NR_033572	Snapc4	small nuclear RNA activat	NR_033572	NR_033572 /	NR_033572 /	NR_033572 /	---	50	1	chr2	-
10452417	6,57071947	6,85546873	-0,28474926	0,82088426	0,00027154	0,03154993	---	NA	NA	ENSMUST000	---	---	---	---	26	1	chr17	-
10460517	8,70586978	8,91211375	-0,20624397	0,86679097	0,00027446	0,03175915	NM_134155	Brms1	breast cancer metastasis-	NM_134155	NM_134155	---	---	---	32	1	chr19	+
10416958	7,89476081	7,35387211	0,54088871	1,45486845	0,00027816	0,03192671	NR_029816	Mir92-1	microRNA 92-1	NR_029816	NR_029382 /	NR_029382 /	NR_029382 /	---	30	1	chr14	+
10485261	8,64604928	8,85276342	-0,20671414	0,86650853	0,00027751	0,03192671	NM_0010334	Accsl	1-aminocyclopropane-1-c	NM_0010334	NM_0010334	NM_0010334	NM_0010334	---	29	1	chr2	-
10412517	10,6321583	10,9195248	-0,2873665	0,81939642	0,00028034	0,03204699	NR_033388	Gm3002	alpha-takusan pseudogen	NR_033388	ENSMUST000	ENSMUST000	ENSMUST000	---	30	3	chr14	+
10355214	11,4178659	11,0640201	0,35384572	1,27796269	0,00028347	0,03227419	NM_010497	Idh1	isocitrate dehydrogenase	NM_010497	NM_010497	NM_010497	NM_010497	---	30	1	chr1	-
10542875	8,5777668	8,20018849	0,37757831	1,29915927	0,00028461	0,03227506	BC106181	3010003L21Rik	RIKEN cDNA 3010003L21	BC106181	BC106181 //	BC106181 //	BC106181 //	---	26	1	chr6	+
10527801	9,94571267	10,1462081	-0,20049543	0,87025166	0,00028638	0,03234606	NM_0010810	Brca2	breast cancer 2	NM_0010810	NM_0010810	NM_0010810	NM_0010810	---	30	1	chr5	+
10386359	9,88435943	9,66876687	0,21559256	1,16118075	0,00029182	0,03270003	NM_008193	Guk1	guanylate kinase 1	NM_008193	NM_008193	NM_008193	NM_008193	---	30	1	chr11	-
10430536	11,4398083	11,7230543	-0,28324592	0,82174011	0,00029136	0,03270003	NM_199080	Ddx17	DEAD (Asp-Glu-Ala-Asp) b	NM_199080	NM_199080	NM_199080	NM_199080	---	60	1	chr15	-
10458755	7,09010685	6,76376231	0,32634454	1,25383242	0,00029321	0,0327261	NM_0011630	Ythdc2	YTH domain containing 2	NM_0011630	NM_0011630	NM_0011630	NM_0011630	---	25	1	chr18	-
10451650	11,3149676	11,5277146	-0,21274705	0,86289263	0,00030479	0,03388591	NM_0011108	Nfya	nuclear transcription fact	NM_0011108	NM_0011108	NM_0011108	NM_0011108	---	36	1	chr17	-
10604751	6,93188578	7,1623084	-0,23042261	0,85238516	0,00031191	0,03454171	NM_010200	Fgf13	fibroblast growth factor 1	NM_010200	NM_010200	NM_010200	NM_010200	---	31	1	chrX	-
10378568	7,36467991	7,02007343	0,34460647	1,26980457	0,0003141	0,03464888	NR_029739	Mir22	microRNA 22	NR_029739	NR_030711 /	NR_030711 /	NR_030711 /	---	25	1	chr11	+
10380558	6,74176906	7,11796119	-0,37619212	0,7704685	0,00031752	0,03488979	NR_028263	B130006D01Rik	RIKEN cDNA B130006D01	NR_028263	NR_028263 /	NR_028263 /	NR_028263 /	---	25	1	chr11	+
10398402	3,0422006	3,45322247	-0,41102187	0,75209048	0,00031958	0,03493189	NR_030446	Mir495	microRNA 495	NR_030446	---	---	---	---	18	1	chr12	+
10585680	7,15059186	6,84456532	0,30602653	1,236298	0,00032036	0,03493189	---	NA	NA	ENSMUST000	---	---	---	---	25	1	chr9	+
10356512	7,0481811	6,78577634	0,26240476	1,19947639	0,00032348	0,03500258	NM_029122	Iqca	IQ motif containing with A	NM_029122	NM_029122	NM_029122	NM_029122	---	25	1	chr1	-
10443527	11,4519654	11,2647351	0,18723028	1,13857575	0,00032278	0,03500258	NM_008842	Pim1	proviral integration site 1	NM_008842	NM_008842	NM_008842	NM_008842	---	26	1	chr17	+
10453811	8,06233825	7,85584655	0,20649171	1,15387881	0,00033039	0,03561391	NM_0010836	Greb1l	growth regulation by estr	NM_0010836	NM_0010836	NM_0010836	NM_0010836	---	26	1	chr18	+
10487645	8,30458738	8,49930737	-0,19471999	0,87374246	0,00033235	0,03568949	NM_019696	Cpxm1	carboxypeptidase X 1 (M3	NM_019696	NM_019696	NM_019696	NM_019696	---	28	1	chr2	-
10384421	4,72674175	4,39123982	0,33550193	1,26181634	0,00033983	0,03635576	---	NA	NA	ENSMUST000	---	---	---	---	25	1	chr11	-
10553401	7,61744952	7,39256201	0,22488751	1,16868812	0,00034119	0,03636345	AK157552	F830223B06Rik	RIKEN cDNA F830223B06	AK157552	AK157552 //	AK157552 //	AK157552 //	---	25	1	chr7	+
10418702	8,41020354	8,17430428	0,23529926	1,17715089	0,0003438	0,03644962	NM_011894	Sh3bp5	SH3-domain binding prote	NM_011894	NM_011894	NM_011894	NM_011894	---	40	1	chr14	-
10520638	10,5559312	10,3015467	0,24738454	1,18705315	0,00034457	0,03644962	NM_027855	0610007C21Rik	RIKEN cDNA 0610007C21	NM_027855	NM_027855	NM_027855	NM_027855	---	34	1	chr5	+
10588505	6,68564746	7,00478574	-0,31913828	0,8015485	0,00034792	0,03666698	NM_029631	Abhd14b	abhydrolase domain cont	NM_029631	NM_029631	NM_029631	NM_029631	---	25	1	chr9	+
10536620	10,8073153	10,6352664	0,17204894	1,12665745	0,00035247	0,03687285	NM_023626	Ing3	inhibitor of growth family	NM_023626	NM_023626	NM_023626	NM_023626	---	27	1	chr6	+
10544243	9,54924664	9,31841579	0,23083085	1,17351058	0,00035136	0,03687285	NM_010270	Mrps33	mitochondrial ribosomal p	NM_010270	NM_010270	NM_010270	NM_010270	---	38	3	chr6	-
10566895	7,99734955	7,55907344	0,43827611	1,25424503	0,0003548	0,03698038	ENSMUST000	AA474408	expressed sequence AA47	ENSMUST000	ENSMUST000	ENSMUST000	ENSMUST000	---	25	1	chr7	-
10404083	7,3708778	7,78317313	-0,41229533	0,7514269	0,00035702	0,03707487	NM_145713	Hist1h1d	histone cluster 1, H1d	NM_145713	NM_145713	NM_145713	NM_145713	---	22	1	chr13	+
10424577	9,10033567	8,81108769	0,28924799	1,22200314	0,00036137	0,03721651	NM_053068	Chrac1	chromatin accessibility co	NM_053068	NM_053068	NM_053068	NM_053068	---	25	1	chr15	+
10444685	10,1433874	9,8009518	0,34243322	1,26789232	0,00036402	0,03721651	NM_0011904	Ddah2	dimethylarginine dimethy	NM_0011904	NM_0011904	NM_0011904	NM_0011904	---	30	1	chr17	+
10453114	9,71369325	9,30873279	-0,19503954	0,87354896	0,00036278	0,03721651	NM_0011637	Dhx57	DEAH (Asp-Glu-Ala-Asp/H	NM_0011637	NM_0011637	NM_0011637	NM_0011637	---	48	1	chr17	-
10517028	9,76646286	9,4779634	0,28849945	1,22136927	0,00036626	0,03721651	NM_025667	Tmem222	transmembrane protein 2	NM_025667	NM_025667	NM_025667	NM_025667	---	25	1	chr4	-
10557262	9,17436878	9,41495308	-0,24058431	0,84640244	0,00036295	0,03721651	NM_146198	Slc5a11	solute carrier family 5 (so	NM_146198	NM_146198	NM_146198	NM_146198	---	44	1	chr7	+
10504595	5,37887399	5,67482371	-0,29594972	0,81453595	0,00036589	0,03721651	NM_029657	Mir106a	microRNA 106a	NR_029657	---	---	---	---	31	1	chrX	-
10500017	8,95729375	8,67057463	0,28671912	1,21986299	0,00037674	0,0381445	NM_008253	Hmgb3	high mobility group box 3	NM_008253	NM_008253	NM_008253	NM_008253	---	56	3	chrX	+
10366519	6,98224997	6,63829015	0,34395983	1,26923554	0,00038193	0,03836444	NM_0010378	Cnot2	CCR4-NOT transcription c	NM_0010378	NM_0010378	NM_0010378	NM_0010378	---	25	1	chr10	+
10442082	7,56915237	7,82708537	-0,25788301	0,83631422	0,00038567	0,03836444	BC002059	BC002059	cDNA sequence BC002059	BC002059	BC002059 //	BC002059 //	BC002059 //	---	19	1	chr17	+
10485622	11,9583602	12,165907	-0,20754675	0,8660086	0,00038463	0,03836444	NM_0011233	Qser1	glutamine and serine rich	NM_0011233	NM_0011233	NM_0011233	NM_0011233	---	25	1	chr2	-
10539104	8,79208257	9,0273277	-0,23524513	0,84954064	0,00038419	0,03836444	NM_026696	0610030E20Rik	RIKEN cDNA 0610030E20	NM_026696	NM_026696	NM_026696	NM_026696	---	28	1	chr6	+
10540935	9,5632558	9,75680961	-0,19355381	0,87444903	0,00038326	0,03836444	NM_025958	Cand2	cullin-associated and ned	NM_025958	NM_025958	NM_025958	NM_025958	---	32	1	chr6	+
10362261	10,4873204	10,663498	-0,17617759	0,88504481	0,00040093	0,03971111	NM_025481	Smurf2	SMAD specific E3 ubiquiti	NM_025481	NM_025481	NM_025481	NM_025481	---	39	1	chr11	-
10404995	7,63535479	7,33550469	0,2997501	1,23093118	0,00040201	0,03971111	NM_031166	Id4	inhibitor of DNA binding 4	NM_031166	NM_031166	NM_031166	NM_031166	---	26	1	chr13	+
10392990	9,31846051	9,29805447	0,02040604	1,16506144	0,00040779	0,04014215	NM_008163	Grb2	growth factor receptor bo	NM_008163	NM_008163	NM_008163	NM_008163	BC052377 //	16	1	chr11	-
10494411	9,89194196	9,47623382	0,41570813	1,33395328	0,00041431	0,04022468	NR_004412	Rnu1b1	U1b1 small nuclear RNA	NR_004412	NR_004413 /	NR_004413 /	NR_004413 /	---	26	3	chr3	+
10494417	9,89194196	9,47623382	0,41570813	1,33395328	0,00041431	0,04022468	NR_004412	Rnu1b1	U1b1 small nuclear RNA	NR_004412	NR_004413 /	NR_004413 /	NR_004413 /	---	26	3	chr3	+
10500356	9,89194196	9,47623382	0,41570813	1,33395328	0,00041431	0,04022468	NR_004412	Rnu1b1	U1b1 small nuclear RNA	NR_004412	NR_004413 /	NR_004413 /	NR_004413 /	---	26	3	chr3	-
10553148	8,64683103	8,82072645	-0,17389541	0,88644596	0,00041245	0,04022468	NM_0010332	Ccdc114	coiled-coil domain contai	NM_0010332	NM_0010332	NM_0010332	NM_0010332	---	40	1	chr7	+
10411326	8,73679891	8,37247568	-0,23567677	0,84928551	0,00042157	0,04065159	NM_012048	Polk	polymerase (DNA directed	NM_012048	NM_012048	NM_012048	NM_012048	---	44	1	chr13	-

10533095	10,7115691	10,9069414	-0,19537227	0,87334751	0,00042053	0,04065159	NM_172721	Fbxw8	F-box and WD-40 domain	NM_172721	NM_172721	NM_172721	NM_172721	NM_172721	30	1	chr5	-
10468329	8,99549805	9,19976833	-0,20427028	0,8679776	0,00042341	0,04069053	NM_175360	Obfc1	oligonucleotide/oligosacc	NM_175360	NM_175360	NM_175360	NM_175360	---	36	1	chr19	-
10345065	7,40873496	7,22644296	0,182292	1,13468512	0,00042854	0,04102824	NM_0010773	Gsta3	glutathione S-transferase	NM_0010773	NM_0010773	NM_0010773	NM_0010773	---	32	1	chr1	+
10537452	7,59958527	7,99183564	-0,39225036	0,76194018	0,00042982	0,04102824	NM_026612	Ndufb2	NADH dehydrogenase (ub	NM_026612	NM_026612	NM_026612	NM_026612	NM_026612	28	1	chr6	+
10387363	9,5112362	9,87694427	-0,36570807	0,77608788	0,00043206	0,0411038	NM_0010455	Cyb5d1	cytochrome b5 domain co	NM_0010455	NM_0010455	NM_0010455	NM_0010455	---	30	3	chr11	-
10356712	8,93967791	9,19882981	-0,25915191	0,83557897	0,00043463	0,04120989	NM_008440	Kif1a	kinesin family member 1A	NM_008440	NM_008440	NM_008440	NM_008440	---	49	1	chr1	+
10515026	6,90330346	6,55329741	0,35000604	1,27456597	0,0004386	0,04144746	NM_177045	Cc2d1b	coiled-coil and C2 domain	NM_177045	NM_177045	NM_177045	NM_177045	---	25	1	chr4	-
10574682	11,7340963	12,9106003	-0,17650398	0,88484461	0,00044589	0,04199654	NM_148952	E2f4	E2F transcription factor 4	NM_148952	NM_148952	NM_148952	NM_148952	NM_148952	32	1	chr8	+
10594251	11,7497151	12,5376114	0,21210368	1,15837605	0,00044935	0,04218259	NM_024245	Kif23	kinesin family member 23	NM_024245	NM_024245	NM_024245	NM_024245	---	48	1	chr9	-
10557450	10,0119009	9,66770529	0,34419561	1,26944299	0,00046373	0,04338845	NM_175103	Bola2	bolA-like 2 (E. coli)	NM_175103	NM_175103	NM_175103	NM_175103	---	33	1	chr7	+
10405879	6,09658893	6,34206688	-0,24547795	0,8435363	0,00046709	0,04355949	NM_0011026	Vmn2r85	vomeronasal 2, receptor 8	NM_0011026	NM_0011026	NM_0011026	NM_0011026	AF011413 //	51	3	chr13	+
10415952	7,15642533	7,6606163	-0,50419098	0,70505564	0,00047473	0,0439824	---	NA	NA	GENSCAN000	---	---	---	---	17	1	chr14	+
10449926	8,61131342	8,83389198	-0,22257855	0,85703228	0,00047381	0,0439824	NM_177359	Zfp799	zinc finger protein 799	NM_177359	NM_177359	NM_177359	NM_177359	---	29	1	chr17	-
10350985	9,34664863	9,1250662	0,22158243	1,16601183	0,0004804	0,04424203	NM_025474	Mrps14	mitochondrial ribosomal p	NM_025474	NM_025474	NM_025474	NM_025474	---	22	1	chr1	+
10359826	9,38876872	9,89161626	-0,50334755	0,70546795	0,00048337	0,04424203	NM_025650	Uqcr11	ubiquinol-cytochrome c re	NM_025650	NM_025650	NM_025650	NM_025650	---	9	1	chr1	-
10503654	6,58463382	6,24345155	0,34118227	1,26679429	0,00048679	0,04424203	---	NA	NA	ENSMUST000	---	---	---	---	16	1	chr4	+
10506939	9,33727407	9,54850109	-0,21122702	0,86380225	0,0004869	0,04424203	NM_007943	Eps15	epidermal growth factor r	NM_007943	NM_007943	NM_007943	NM_007943	---	28	1	chr4	+
10508490	10,9622838	10,6597492	0,30253467	1,23330931	0,00048624	0,04424203	NM_0010796	Srsf5	serine/arginine-rich splici	NM_0010796	NM_0010796	NM_0010796	NM_0010796	---	37	3	chr4	+
10588466	11,5969057	12,8181454	-0,22123973	0,85782798	0,00048502	0,04424203	NM_011876	Twf2	twinfilin, actin-binding pr	NM_011876	NM_011876	NM_011876	NM_011876	---	30	1	chr9	+
10384577	8,22177242	8,51082938	-0,28905695	0,81843687	0,00049209	0,04428866	---	NA	NA	ENSMUST000	---	---	---	---	17	1	chr11	-
10445078	10,2822314	10,4438537	-0,16162224	0,89401923	0,00049366	0,04428866	NM_019439	Gabbr1	gamma-aminobutyric acid	NM_019439	NM_019439	NM_019439	NM_019439	BC054735 //	51	1	chr17	+
10515716	8,91475171	9,10830417	-0,19355247	0,87444984	0,0004918	0,04428866	NM_198170	Szt2	seizure threshold 2	NM_198170	---	NM_198170	---	---	36	1	chr4	-
10529287	8,4672882	8,75610633	-0,28881813	0,81857237	0,00049361	0,04428866	NM_178390	Fam53a	family with sequence sim	NM_178390	NM_178390	NM_178390	NM_178390	---	36	1	chr5	-
10492355	8,0434112	7,71564512	0,32776608	1,25506848	0,00049912	0,0446377	NM_008604	Mme	membrane metallo endop	NM_008604	NM_008604	NM_008604	NM_008604	---	48	1	chr3	+
10603485	8,74898256	8,50366301	0,24531955	1,18535529	0,00050543	0,04505958	NM_007898	Ebp	phenylalkylamine Ca2+ an	NM_007898	NM_007898	NM_007898	NM_007898	---	26	1	chrX	-
10427334	4,02905506	4,38599015	-0,35693509	0,78082162	0,00051028	0,04520734	NR_029766	Mir148b	microRNA 148b	NR_029766	---	---	---	---	25	1	chr15	+
10520622	8,19557982	8,49477923	-0,29919942	0,81270326	0,00050953	0,04520734	NR_003522	Abhd1	abhydrolase domain cont	NR_003522	NR_003522 //	NR_003522 //	NR_003522 //	---	26	1	chr5	+
10354286	8,80714077	9,10815289	-0,30101212	0,81168276	0,00051319	0,0452079	NM_023645	Kdelc1	KDEL (Lys-Asp-Glu-Leu) co	NM_023645	---	NM_023645	---	---	36	1	chr1	-
10412207	9,50185067	9,2398556	0,26199507	1,19913582	0,00051347	0,0452079	NM_027127	Gpx8	glutathione peroxidase 8	NM_027127	NM_027127	NM_027127	NM_027127	---	26	1	chr13	-
10409968	13,0481698	12,9010099	0,14715992	1,10738733	0,00052045	0,04544408	NM_011296	Rps18	ribosomal protein S18	NM_011296	NM_011296	NM_011296	NM_011296	---	34	3	chr13	-
10417933	6,6120372	6,33416673	0,27787047	1,21240396	0,00052096	0,04544408	NM_021508	Myoz1	myozenin 1	NM_021508	---	NM_021508	NM_021508	---	27	1	chr14	-
10484425	9,91282521	9,64946193	0,26334328	1,20025994	0,00051874	0,04544408	NM_0010331	2700094K13Rik	RIKEN cDNA 2700094K13	NM_0010331	NM_0010331	---	NM_0010331	---	27	1	chr2	-
10599321	9,28222073	9,52418985	-0,24196812	0,84559039	0,0005229	0,04547328	NM_020256	Zbtb33	zinc finger and BTB doma	NM_020256	NM_020256	NM_020256	NM_020256	---	25	1	chrX	+
10424457	8,53303485	8,75521088	-0,22217603	0,85727143	0,00052932	0,04589095	NM_0010814	Phf20l1	PHD finger protein 20-like	NM_0010814	NM_0010814	NM_0010814	NM_0010814	---	33	1	chr15	+
10452874	11,1633628	10,8745038	0,28845933	1,22133531	0,00053493	0,04595532	NM_025381	Atp6v1f	ATPase, H+ transporting,	NM_025381	NM_025381	NM_025381	NM_025381	---	25	3	chr17	-
10482144	10,7707302	10,9590509	-0,18832067	0,87762571	0,00053445	0,04595532	NM_0011005	Rc3h2	ring finger and CCCH-type	NM_0011005	NM_0011005	NM_0011005	NM_0011005	---	44	1	chr2	-
10546790	11,3690685	11,1218365	0,24723195	1,18692761	0,00053318	0,04595532	NM_010028	Ddx3x	DEAD/H (Asp-Glu-Ala-Asp	NM_010028	---	---	---	NM_010028	25	3	chrX	-
10384778	5,52379778	5,11097126	0,41282652	1,33129152	0,00053809	0,04608735	---	NA	NA	ENSMUST000	---	---	---	---	25	1	chr11	-
10468533	9,4550177	9,56786875	-0,21287105	0,86281846	0,00054341	0,04640268	NM_008149	Gpam	glycerol-3-phosphate acyl	NM_008149	NM_008149	NM_008149	NM_008149	---	47	1	chr19	-
10352333	9,73874022	9,52131612	0,2174241	1,16265583	0,00054785	0,0464254	NM_012058	Srp9	signal recognition particle	NM_012058	NM_012058	NM_012058	NM_012058	NM_012058	15	1	chr1	+
10419553	5,68871016	5,84828801	-0,24957784	0,84114251	0,00054859	0,0464254	NM_011271	Rnase1	ribonuclease, RNase A fan	NM_011271	NM_011271	NM_011271	NM_011271	---	25	1	chr14	-
10497622	7,26366014	7,05523919	0,20842095	1,15542286	0,00054692	0,0464254	NM_027941	Lrrc34	leucine rich repeat contai	NM_027941	NM_027941	NM_027941	NM_027941	---	37	1	chr3	-
10376507	7,20393905	7,47919988	-0,27526083	0,82630092	0,00055367	0,04669729	NM_172941	Zkscan17	zinc finger with KRAB and	NM_172941	NM_172941	NM_172941	NM_172941	---	25	1	chr11	+
10505315	10,3211787	9,36213725	0,3590414	1,28257341	0,0005551	0,04669729	NM_025410	Lage3	L antigen family, member	NM_025410	NM_025410	NM_025410	NM_025410	---	13	1	chrX	-
10361712	9,77180727	9,35361276	-0,18180549	0,88159901	0,00056553	0,04713223	NM_172937	Shprh	SNF2 histone linker PHD R	NM_172937	NM_172937	NM_172937	NM_172937	---	35	1	chr10	+
10388154	9,31842934	9,04873538	0,26969396	1,20555207	0,00056545	0,04713223	NM_026068	Med31	mediator of RNA polymer	NM_026068	NM_026068	NM_026068	NM_026068	---	25	1	chr11	-
10534988	7,32594234	7,04096102	0,28498131	1,21839448	0,00056692	0,04713223	NR_029658	Mir106b	microRNA 106b	NR_029658	---	---	---	---	25	1	chr5	-
10568202	10,4501386	10,1494697	0,30066889	1,23171535	0,00056387	0,04713223	NM_017461	Sept1	septin 1	NM_017461	NM_017461	NM_017461	NM_017461	---	36	1	chr7	-
10451238	11,8725068	11,697698	0,17480874	1,12881474	0,00057656	0,04779377	NM_009085	Polr1c	polymerase (RNA) I polyp	NM_009085	NM_009085	NM_009085	NM_009085	---	27	1	chr17	-
10355188	6,89444343	6,55159007	0,34075336	1,26641773	0,00058095	0,04787288	NM_007777	Cryge	crystallin, gamma E	NM_007777	NM_007777	---	NM_007777	---	25	3	chr1	-
10459758	9,82980086	9,5710329	0,25876825	1,19645676	0,00058735	0,04787288	---	NA	NA	ENSMUST000	---	---	---	---	35	1	chr18	-
10471333	7,34401775	7,55935307	-0,31533531	0,80366418	0,00058765	0,04787288	---	NA	NA	ENSMUST000	---	---	---	---	25	3	chr2	+
10471335	7,34401775	7,55935307	-0,31533531	0,80366418	0,00058765	0,04787288	---	NA	NA	ENSMUST000	---	---	---	---	25	3	chr2	+
10511252	9,8940691	9,52737977	0,26668933	1,20304393	0,00058642	0,04787288	NM_021402	Ube2j2	ubiquitin-conjugating enz	NM_021402	---	NM_021402	---	---	15	1	chr4	+
10595573	9,52227544	9,32374395	0,19853149	1,1475297	0,00058102	0,04787288	NM_172926	Snx14	sorting nexin 14	NM_172926	NM_172926	NM_172926	NM_172926	---	30	1	chr9	-
10372629	11,2566494	11,0802739	0,17637551	1,13004131	0,00059028	0,04794969	NM_026570	Yeats4	YEATS domain containing	NM_026570	NM_026570	NM_026570	NM_026570	---	27	1	chr10	-
10375157	7,74246653	7,99309334	-0,25062681	0,84053115	0,00060239	0,04824542	NM_0010253	Fam196b	family with sequence sim	NM_0010253	NM_0010253	NM_0010253	NM_0010253	---	25	1	chr11	+
10419704	9,62642193	9,84265843	-0,2162365	0,86080806	0,0006019	0,04824542	NM_015772	Sall2	sal-like 2 (Drosophila)	NM_015772	NM_015772	NM_015772	NM_015772	---	26	1	chr14	-
10420850	11,1737636	11,3374723	-0,16370869	0,89272721	0,00059935	0,04824542	NM_028811	Elp3	elongation protein 3 hom	NM_028811	NM_028811	NM_028811	NM_028811	---	32	1	chr14	-
10476122	9,00589829	8,59425593	0,41164236	1,33019925	0,00060216	0,04824542	---	NA	NA	ENSMUST000	---	---	---	---	22	1	chr2	+
10507976	9,25648902	9,04622649	0,21026253	1,15689869	0,00060243	0,04824542	NM_153566	Yrdc	yrdC domain containing (E	NM_153566	NM_153566	NM_153566	NM_153566	---	26	1	chr4	+
10495534	5,11728829	4,80761184	0,30967645	1,23942971	0,00060583	0,04838069	---	NA	NA	GENSCAN000	---	---	---	---	25	1	chr3	+

10369761	8,77614366	8,54928939	0,22685427	1,17028042	0,00061075	0,04863684	NM_178606	Reep3	receptor accessory protei	NM_178606	NM_178606	NM_178606	NM_178606	---	33	1	chr10	-
10445558	11,1999535	10,959394	0,24055946	1,18145073	0,00061398	0,04875758	NM_207161	BC048355	cDNA sequence BC048355	NM_207161	NM_207161	NM_207161	NM_207161	---	29	1	chr17	+
10399579	10,7130208	10,9376694	-0,22464867	0,85580341	0,0006234	0,04911207	ENSMUST000	1700030C10Rik	RIKEN cDNA 1700030C10	ENSMUST000	ENSMUST000	ENSMUST000	ENSMUST000	---	16	1	chr12	-
10468691	7,29099497	7,11957902	0,17141596	1,12616324	0,00062365	0,04911207	NM_178688	Ablim1	actin-binding LIM protein	NM_178688	NM_178688	NM_178688	NM_178688	---	30	1	chr19	-
10502772	8,66708153	8,25614244	0,41093909	1,32955098	0,00062039	0,04911207	NM_0010812	Lphn2	latrophilin 2	NM_0010812	NM_0010812	NM_0010812	NM_0010812	---	15	1	chr3	-
10367726	7,994456	7,72706728	0,26738871	1,20362728	0,00063643	0,0498862	ENSMUST000	6530403G13Rik	RIKEN cDNA 6530403G13	ENSMUST000	ENSMUST000	ENSMUST000	ENSMUST000	---	25	1	chr10	-
10552938	6,96768855	6,64710992	0,32057863	1,24883133	0,00063875	0,0498862	NM_198190	Ntf5	neurotrophin 5	NM_198190	NM_198190	NM_198190	NM_198190	---	27	1	chr7	+
10591754	9,8086483	10,014216	-0,20556773	0,86719736	0,00063775	0,0498862	NM_181419	Zfp599	zinc finger protein 599	NM_181419	NM_181419	NM_181419	NM_181419	---	25	1	chr9	-

Principaux pics détectés par ChIP-seq avec SOX2

Probe	Feature	Orientation	Distance	IgG	Ac anti-OTX2	Ac anti-PAX6	Ac anti-RAX	Ac anti-SOX2
Chr1:59505280-5	**Fzd7**	downstream	32703	9	571	4	16	161
Chr9:95326322-9	**Chst2**	downstream	18633	87	548	150	211	159
Chr10:85002152-	**Btbd11**	overlapping	0	4	142	3	5	159
Chr13:57463952-	**Spock1**	upstream	60109	1	54	2	5	159
Chr16:63312411-	**null**	Not found	0	88	462	120	156	159
Chr16:30646169-	**Fam43a**	upstream	43286	1	83	0	2	158
Chr1:5217707-52	**Atp6v1h**	upstream	65077	8	490	7	9	157
Chr2:25036020-2	**Nrarp**	overlapping	0	0	14	0	2	157
Chr16:13748825-	**1810007I06Rik**	upstream	11152	2	323	9	13	157
Chr19:50385111-	**Sorcs1**	overlapping	0	68	540	142	180	157
Chr1:22473497-2	**Rims1**	overlapping	0	6	106	5	5	156
Chr1:80233834-8	**Fam124b**	downstream	18786	12	72	6	7	156
Chr2:20417901-2	**Etl4**	overlapping	0	2	179	5	15	156
Chr3:87778127-8	**Nes**	overlapping	0	0	50	3	3	156
Chr8:19994752-1	**Gm10348**	overlapping	0	145	61	115	158	156
Chr2:81689006-8	**null**	Not found	0	1	70	2	9	155
Chr3:72662569-7	**Sis**	upstream	29413	1	150	2	12	155
Chr4:145265052-	**Gm13242**	overlapping	0	13	507	18	33	155
Chr5:27030253-2	**null**	Not found	0	1	178	2	7	155
Chr8:19882650-1	**6820431F20Rik**	overlapping	0	162	135	152	165	155
Chr6:20636629-2	**null**	Not found	0	0	366	9	6	154
Chr5:8488862-84	**Rundc3b**	upstream	1147	0	13	3	6	153
Chr8:75843550-7	**Large**	overlapping	0	35	126	55	79	153
Chr16:11144001-	**Zc3h7a**	overlapping	0	41	561	66	103	153
Chr2:44380712-4	**Gtdc1**	upstream	38538	2	297	4	20	152
Chr4:91114554-9	**Elavl2**	downstream	47879	1	137	0	5	152
Chr15:90908348-	**Kif21a**	downstream	27966	1	267	2	12	152
Chr1:78116487-7	**Pax3**	overlapping	0	3	118	3	18	151
Chr14:59277547-	**SNORA17.35**	downstream	8310	78	522	140	187	151

Chr1:3472912-34	**Xkr4**	overlapping	0	2	115	4	11	150
Chr3:127912958-	**null**	Not found	0	84	571	155	199	150
Chr6:144402859-	**Sox5**	overlapping	0	4	47	2	10	150
Chr10:90172224-	**Anks1b**	overlapping	0	2	127	3	11	150
Chr11:77707321-	**Pipox**	overlapping	0	4	82	5	9	150
Chr12:63808096-	**Spanxn4**	upstream	18865	2	192	5	12	150
Chr14:9569281-9	**4930455B14Rik**	upstream	63389	0	186	6	4	150
Chr2:171704622-	**1700028P15Rik**	upstream	77227	2	143	4	3	149
Chr5:110503501-	**Plcxd1**	downstream	25410	77	515	124	177	149
Chr6:94700576-9	**Lrig1**	downstream	50424	0	53	3	4	149
Chr7:59987449-5	**null**	Not found	0	2	284	12	7	149
Chr7:140951672-	**Dhx32**	overlapping	0	4	347	7	10	149
Chr8:91795307-9	**Gm5356**	downstream	83848	2	287	3	11	149
Chr8:19868583-1	**6820431F20Rik**	overlapping	0	132	129	124	197	148
Chr8:24672389-2	**Zmat4**	downstream	73697	4	95	2	5	148
Chr5:115914783-	**Pla2g1b**	downstream	1102	1	76	0	0	147
Chr9:115633139-	**n-R5s92**	downstream	97303	0	198	3	8	147
Chr9:120058507-	**Mobp**	downstream	44	1	25	1	1	147
Chr12:29502104-	**Tssc1**	overlapping	0	0	620	15	8	147
Chr14:50067247-	**Slc35f4**	overlapping	0	0	166	1	3	147
Chr16:13977060-	**Ifitm7**	upstream	4152	4	291	7	9	147
Chr4:118698849-	**Gm12862**	downstream	25759	2	571	9	10	146
Chr14:11968616:	**Hs6st3**	overlapping	0	58	408	118	135	146
Chr15:39560238-	**Tm7sf4**	downstream	16809	3	99	8	2	146
Chr16:26962061-	**Gm606**	overlapping	0	1	165	1	7	146
ChrX:166527167-	**Mid1**	upstream	83499	629	4168	1057	1540	1318
Chr4:126143043-	**Eif2c1**	overlapping	0	2	71	1	1	145
Chr17:3083675-3	**Pisd-ps2**	overlapping	0	16	425	29	46	145
Chr16:5709261-5	**null**	Not found	0	69	467	134	145	144
Chr1:72275660-7	**U2.23**	upstream	2656	2	61	3	8	143
Chr5:80929913-8	**null**	Not found	0	73	541	113	188	143
Chr7:36315527-3	**Tdrd12**	overlapping	0	1	199	4	8	143
Chr7:56603271-5	**Nav2**	overlapping	0	3	81	1	7	143
Chr12:27835953-	**Gm9866**	overlapping	0	3	200	8	6	143

Chr12:45741573-	**Nrcam**	upstream	38622	3	190	2	1	143
Chr12:94815435-	**null**	Not found	0	76	422	113	149	143
Chr18:31407655-	**Rit2**	overlapping	0	3	90	1	3	143
Chr1:53806761-5	**Stk17b**	upstream	5106	3	333	8	11	142
Chr1:106909110-	**Cdh20**	upstream	17052	3	87	5	10	142
Chr6:4873828-48	**Ppp1r9a**	overlapping	0	75	438	117	154	142
Chr6:34137477-3	**Gm13855**	upstream	1085	0	276	12	11	142
Chr8:58730478-5	**Hpgd**	downstream	41862	6	265	9	9	142
Chr9:90197157-9	**U4.28**	downstream	13513	84	518	142	197	142
Chr10:94334780-	**Plxnc1**	overlapping	0	58	411	103	159	142
Chr1:47133177-4	**null**	Not found	0	7	207	3	11	141
Chr7:3348052-33	**Cacng7**	overlapping	0	1	220	2	3	141
Chr7:87890225-8	**Iqgap1**	overlapping	0	6	380	6	6	141
Chr12:75904892-	**Kcnh5**	upstream	93241	137	71	137	176	141
Chr1:4140783-41	**null**	Not found	0	0	158	4	8	140
Chr3:64069063-6	**AC119863.1**	overlapping	0	3	369	9	9	140
Chr6:49186451-4	**Tra2a**	upstream	7315	37	365	60	79	140
Chr16:30829626-	**U6.127**	upstream	15272	83	539	142	203	140
Chr17:31194083-	**Abcg1**	downstream	145	1	40	0	4	140
Chr1:134097139-	**Lemd1**	overlapping	0	4	403	10	13	139
Chr6:65747257-6	**Prdm5**	overlapping	0	1	215	4	11	139
Chr12:66694542-	**SNORA17.70**	upstream	27334	1	126	6	10	139
Chr13:30161241-	**Gm11368**	upstream	6401	3	153	2	2	139
Chr14:74465728-	**null**	Not found	0	92	489	109	166	139
Chr2:170597502-	**Dok5**	overlapping	0	0	226	4	8	138
Chr3:18523942-1	**null**	Not found	0	4	122	2	4	138
Chr5:93718664-9	**Ccng2**	upstream	13407	79	473	136	167	138
Chr8:19872783-1	**6820431F20Rik**	overlapping	0	149	73	136	210	138
Chr11:11028357[illegible]	**Map2k6**	overlapping	0	68	460	104	175	138
Chr16:23504378-	**Masp1**	overlapping	0	1	159	2	5	138
Chr16:35981672-	**Gm15564**	downstream	447	39	573	39	52	138
Chr17:68090702-	**Lama1**	overlapping	0	88	483	113	160	138
ChrX:109484351-	**Apool**	overlapping	0	95	73	95	150	138
Chr2:41751722-4	**Lrp1b**	overlapping	0	75	421	111	154	137

Chr3:88085413-8	**Rhbg**	overlapping	0	0	299	3	10	137
Chr8:94740129-9	**null**	Not found	0	3	390	6	11	137
Chr11:80149174-	**Rhbdl3**	overlapping	0	2	117	1	3	137
Chr13:66515195-	**2410141K09Rik**	upstream	3578	7	246	7	5	137
Chr1:71125914-7	**Bard1**	overlapping	0	64	422	94	137	136
Chr5:106605801-	**null**	Not found	0	79	519	106	199	136
Chr10:11521395-	**null**	Not found	0	4	167	3	15	136
Chr14:10632007E	**Spry2**	downstream	24042	1	58	4	3	136
Chr15:91694501-	**Muc19**	overlapping	0	2	125	1	2	136
Chr16:57391242-	**2610528E23Rik**	overlapping	0	66	250	54	111	136
Chr16:72072157-	**null**	Not found	0	1	71	6	6	136
Chr2:45591885-4	**Gm13465**	overlapping	0	2	22	0	3	135
Chr8:19877986-1	**6820431F20Rik**	overlapping	0	105	79	117	148	135
Chr12:12184185-	**5S_rRNA.93**	upstream	70512	0	199	1	2	135
Chr13:52015931-	**Gm16767**	downstream	52030	0	210	1	5	135
Chr8:93194359-9	**null**	Not found	0	3	127	2	14	134
Chr10:94055180-	**Gm16154**	overlapping	0	62	435	107	147	134
Chr14:35173050-	**2200001I15Rik**	downstream	4431	1	165	5	4	134
Chr1:7116052-71	**Pcmtd1**	overlapping	0	3	124	1	7	133
Chr2:19430947-1	**4921504E06Rik**	overlapping	0	67	436	124	164	133
Chr9:8769992-87	**Trpc6**	upstream	89427	2	114	4	5	133
Chr3:83590975-8	**Gm16790**	overlapping	0	1	368	5	11	132
Chr8:19891839-1	**6820431F20Rik**	overlapping	0	44	249	64	93	132
Chr18:31728408-	**Slc25a46**	upstream	10937	4	121	7	9	132
Chr18:43073588-	**Ppp2r2b**	overlapping	0	62	436	154	159	132
Chr18:43135434-	**Ppp2r2b**	overlapping	0	54	33	72	99	132
Chr1:115860594-	**9330185C12Rik**	overlapping	0	6	359	11	12	131
Chr1:137404212-	**Nav1**	overlapping	0	4	284	7	21	131
Chr10:21465869-	**Gm5420**	upstream	52085	3	182	6	2	131
Chr10:33095300-	**Trdn**	overlapping	0	3	172	3	10	131
Chr13:44114102-	**null**	Not found	0	1	139	5	3	131
Chr13:90385569-	**null**	Not found	0	0	179	1	8	131
Chr1:135389759-	**Sox13**	downstream	68805	4	245	4	12	130
Chr3:5989017-59	**null**	Not found	0	0	114	5	4	130

Chr7:25664560-2	**Dmrtc2**	upstream	1890	7	164	8	8	130
Chr8:20018349-2	**Gm10348**	overlapping	0	72	165	70	82	130
Chr9:99671188-9	**Gm16004**	upstream	14726	3	34	4	2	130
Chr10:12985699[illegible]	**AC159473.1**	overlapping	0	4	99	6	8	130
Chr7:77736445-7	**null**	Not found	0	1	498	6	4	129
Chr12:12587598-	**null**	Not found	0	0	231	1	4	129
Chr17:71121658-	**Dlgap1**	overlapping	0	1	377	9	18	129
Chr5:142605901-	**Sdk1**	overlapping	0	3	163	4	2	128
Chr6:148940847-	**Dennd5b**	overlapping	0	0	86	3	7	128
Chr18:38308484-	**Pcdh1**	upstream	36615	1	143	2	4	128
Chr1:182863790-	**Lefty1**	downstream	889	3	56	2	2	127
Chr8:19893902-1	**Gm10348**	overlapping	0	109	74	98	147	127
Chr13:66648072-	**Gm16986**	downstream	27613	0	78	1	5	127
Chr14:78688768-	**Tnfsf11**	overlapping	0	0	121	3	6	127
Chr2:147118606-	**Nkx2-2as**	overlapping	0	3	85	9	6	126
Chr7:46563091-4	**U6.424**	upstream	23588	10	214	16	15	126
Chr18:3008483-3	**null**	Not found	0	116	92	115	170	126
Chr1:17922055-1	**null**	Not found	0	3	338	6	19	125
Chr3:96963415-9	**Acp6**	overlapping	0	0	32	2	6	125
Chr5:108505904-	**Mtf2**	overlapping	0	2	167	4	4	125
Chr1:22562741-2	**Rims1**	overlapping	0	56	371	89	127	124
Chr8:19976898-1	**Gm10348**	overlapping	0	120	80	101	156	124
Chr19:26682801-	**Smarca2**	overlapping	0	2	91	4	7	124
Chr1:4792427-47	**Lypla1**	downstream	4512	2	319	14	20	123
Chr4:118744040-	**Gm12866**	downstream	2324	1	301	9	5	123
Chr6:83840175-8	**Gm5138**	downstream	14754	1	282	3	7	123
Chr10:12917252[illegible]	**Olfr806**	upstream	2225	55	367	97	129	123
Chr15:5941320-5	**null**	Not found	0	2	437	11	15	123
Chr1:16814628-1	**null**	Not found	0	3	197	3	7	122
Chr1:77458330-7	**Epha4**	overlapping	0	4	197	4	8	122
Chr3:16841179-1	**null**	Not found	0	2	219	3	1	122
Chr4:50180272-5	**null**	Not found	0	112	79	110	117	122
Chr7:80545015-8	**Rgma**	overlapping	0	0	134	4	6	122
Chr8:19908016-1	**Gm10348**	overlapping	0	119	55	90	125	122

Chr14:8838646-8	**Abhd6**	overlapping	0	62	396	85	121	122
Chr2:15847143-1	**null**	Not found	0	2	327	1	9	121
Chr4:18322594-1	**Gm11867**	downstream	11430	2	132	5	7	121
Chr5:61273686-6	**null**	Not found	0	3	108	6	2	121
Chr8:20036574-2	**Gm10348**	downstream	16161	85	43	67	113	121
Chr1:5222877-52	**Atp6v1h**	upstream	70247	1	66	6	12	120
Chr1:135389089-	**Sox13**	downstream	68135	1	54	3	7	120
Chr3:30988202-3	**Skil**	downstream	5322	3	216	7	1	120
Chr7:67151141-6	**Snrpn**	overlapping	0	3	241	6	6	120
Chr11:3025328-3	**Pisd-ps1**	overlapping	0	46	250	52	95	120
Chr17:35640784-	**Pou5f1**	downstream	1795	0	72	1	3	120
Chr18:3006221-3	**null**	Not found	0	55	96	67	108	120
Chr19:10015441-	**AC132253.2**	upstream	32673	3	27	3	3	120
Chr10:36331196-	**Hs3st5**	overlapping	0	2	258	2	5	119
Chr13:4824960-4	**Gm5444**	overlapping	0	2	166	4	8	119
Chr16:90437456-	**Hunk**	overlapping	0	0	144	1	5	119
Chr1:69503316-6	**Ikzf2**	upstream	74343	81	460	121	157	118
Chr2:40766387-4	**Lrp1b**	overlapping	0	4	560	13	3	118
Chr11:34552445-	**Dock2**	overlapping	0	1	26	4	2	118
Chr8:20020249-2	**Gm10348**	overlapping	0	10	122	29	44	117
Chr13:65592624-	**Gm10139**	downstream	20436	9	246	9	17	117
Chr1:138466809-	**Kif14**	upstream	38721	1	260	2	10	116
Chr8:48812197-4	**n-R5s96**	upstream	7474	5	61	3	9	116
Chr11:12905255-	**null**	Not found	0	5	192	1	15	116
Chr14:16810875-	**null**	Not found	0	0	100	2	2	116
Chr1:58670757-5	**Ndufb3**	upstream	17949	37	100	46	78	115
Chr5:92541471-9	**5S_rRNA.86**	upstream	5102	2	224	8	16	115
Chr6:122574499-	**Y_RNA.10**	upstream	823	3	84	6	4	115
Chr9:88713216-8	**CT030259.2**	overlapping	0	1	122	8	8	115
Chr10:11417443[illegible]	**Trhde**	overlapping	0	55	310	101	117	115
Chr11:30391880-	**Acyp2**	upstream	13689	1	57	2	5	115

Principaux pics obtenus par ChIP-seq avec OTX2

Probe	Feature	Orientation	Distance	IgG	Ac anti-OTX2	Ac anti-PAX6	Ac anti-RAX	Ac anti-SOX2
Chr1:84214315-84	**Pid1**	overlapping	0	4	136	3	7	104
Chr4:22072010-22	**null**	Not found	0	3	136	4	5	98
Chr9:40047338-40	**Zfp202**	upstream	26149	4	136	1	6	68
Chr13:85175619-8	**CT009527.1**	downstream	10680	1	136	3	3	55
Chr17:63289344-6	**Efna5**	downstream	58678	4	136	3	8	55
Chr1:134930174-1	**AC137948.1**	upstream	1087	1	136	6	13	49
Chr2:166884296-1	**Znfx1**	overlapping	0	3	136	0	7	48
Chr1:10868295-10	**SNORA66.5**	downstream	43008	2	136	8	14	29
ChrX:71762801-71	**U6.286**	downstream	16247	3	136	1	9	28
Chr1:90736052-90	**null**	Not found	0	0	136	3	4	27
Chr10:19611586-1	**Pex7**	overlapping	0	2	136	1	7	23
Chr5:111268722-1	**Hscb**	overlapping	0	0	136	3	3	14
Chr4:133669317-1	**Ubxn11**	overlapping	0	1	136	0	1	11
Chr4:124322172-1	**Pou3f1**	downstream	12377	2	136	1	6	9
Chr11:113836119-	**Sdk2**	overlapping	0	0	136	6	3	4
Chr8:19882650-19	**6820431F20Rik**	overlapping	0	162	135	152	165	155
Chr3:75454386-75	**Serpini1**	upstream	6969	1	135	0	5	105
Chr11:8654561-86	**Pkd1l1**	upstream	71754	1	135	5	8	63
Chr18:24228714-2	**Ino80c**	upstream	33991	2	135	2	7	62
Chr5:25160452-25	**Gm10062**	upstream	4819	0	135	4	4	61
Chr1:137572071-1	**AC120405.1**	overlapping	0	4	135	3	7	57
Chr10:21874904-2	**H60b**	downstream	3097	6	135	1	14	57
Chr3:148006243-1	**SNORA17.150**	upstream	10187	4	135	10	5	55
Chr4:146932308-1	**Gm13154**	overlapping	0	4	135	7	6	49
Chr4:33043454-33	**Ankrd6**	downstream	5638	1	135	6	8	46
Chr1:72870119-72	**Igfbp2**	downstream	451	0	135	4	6	33
Chr7:29488251-29	**Fbxo27**	upstream	3894	1	135	2	0	17
Chr9:61164282-61	**Gm10655**	upstream	53981	0	135	5	2	14

Chr10:126962100-	**Nxph4**	upstream	86	1	135	1	4	12
Chr16:30205545-3	**Gm11179**	overlapping	0	2	135	0	2	11
Chr9:120528669-1	**5830454E08Rik**	upstream	41480	0	135	5	3	10
Chr3:135345289-1	**Nfkb1**	overlapping	0	0	135	0	3	9
Chr7:80545015-80	**Rgma**	overlapping	0	0	134	4	6	122
Chr1:130288815-1	**Dars**	overlapping	0	6	134	5	15	113
Chr1:36001124-36	**null**	Not found	0	1	134	8	10	95
Chr1:103525061-1	**null**	Not found	0	1	134	3	7	89
Chr10:8083973-80	**Ust**	overlapping	0	2	134	1	3	78
Chr12:64129206-6	**null**	Not found	0	1	134	2	5	45
Chr15:99704980-9	**Lima1**	overlapping	0	0	134	2	1	40
Chr11:9015974-90	**Upp1**	downstream	1705	0	134	4	4	32
Chr13:99786683-9	**7SK.315**	upstream	23362	2	134	0	5	27
Chr9:6832901-683	**Dync2h1**	upstream	95226	2	134	5	1	21
ChrX:11380380-11	**U6.388**	downstream	46892	1	134	0	2	17
Chr7:138377130-1	**Fgfr2**	overlapping	0	0	134	1	3	12
Chr4:120032757-1	**Scmh1**	downstream	44850	0	134	0	3	9
Chr3:15056813-15	**null**	Not found	0	1	133	3	2	105
Chr3:93884403-93	**Gm10697**	downstream	7837	4	133	9	17	99
Chr3:7805020-780	**null**	Not found	0	1	133	1	7	69
Chr2:153468800-1	**7530422B04Rik**	upstream	5161	0	133	1	6	67
Chr2:115549178-1	**BC052040**	overlapping	0	1	133	1	6	61
Chr11:31882685-3	**4930524B15Rik**	upstream	3034	3	133	1	1	52
Chr9:113170569-1	**null**	Not found	0	19	133	26	48	33
ChrX:106309167-1	**Sh3bgrl**	overlapping	0	1	133	0	3	23
Chr1:186320861-1	**U6.839**	upstream	82764	0	133	0	2	22
Chr4:23540210-23	**AL772326.1**	upstream	13225	0	133	13	9	20
Chr16:87208172-8	**null**	Not found	0	0	133	0	1	17
Chr7:150016956-1	**Gm6471**	overlapping	0	0	133	5	4	10
Chr4:18322594-18	**Gm11867**	downstream	11430	2	132	5	7	121
Chr4:135702676-1	**Id3**	upstream	1006	0	132	2	3	56
Chr7:138034402-1	**Fgfr2**	overlapping	0	3	132	7	9	48
Chr18:10866166-1	**Mib1**	upstream	47464	1	132	1	1	47
Chr16:76321915-7	**Nrip1**	overlapping	0	1	132	1	6	46

Chr7:146041818-1	**Ppp2r2d**	overlapping	0	0	132	1	5	41
Chr3:6116092-611	**null**	Not found	0	22	132	36	33	36
Chr4:145105817-1	**Gm13225**	overlapping	0	5	132	5	9	36
Chr3:87283132-87	**Fcrl5**	upstream	21374	6	132	4	5	35
Chr16:10975169-1	**Litaf**	overlapping	0	259	132	265	354	266
Chr15:96321553-9	**Srsf2ip**	downstream	30279	2	132	8	10	30
Chr2:86234484-86	**Olfr1058**	downstream	7911	2	132	4	12	28
Chr5:24083301-24	**Abcf2**	downstream	84	0	132	1	3	11
Chr17:17792523-1	**Lnpep**	downstream	31070	2	132	0	4	9
Chr1:39243676-39	**Npas2**	downstream	7136	3	132	3	1	7
Chr4:137322302-1	**Alpl**	overlapping	0	0	132	0	1	4
Chr1:99969790-99	**Pam**	overlapping	0	6	131	2	4	66
Chr1:11391188-11	**A830018L16Rik**	downstream	12575	2	131	2	8	49
Chr15:22691001-2	**Cdh18**	overlapping	0	3	131	2	8	40
Chr11:36845152-3	**Odz2**	overlapping	0	2	131	3	1	22
Chr7:70585262-70	**4930554H23Rik**	overlapping	0	0	131	5	7	14
Chr3:133196913-1	**Tet2**	overlapping	0	3	131	3	7	9
Chr12:12892454-1	**AC127270.1**	downstream	16709	0	131	1	5	6
Chr8:80622082-80	**null**	Not found	0	2	130	5	10	72
Chr1:73006881-73	**Tnp1**	upstream	54367	2	130	2	6	49
Chr10:13121915-1	**Phactr2**	overlapping	0	23	130	30	46	30
Chr8:64533868-64	**Anxa10**	upstream	1916	23	130	29	39	29
Chr4:3127003-312	**Vmn1r3**	downstream	14498	5	130	4	5	22
Chr6:98959660-98	**Foxp1**	overlapping	0	0	130	0	7	16
Chr1:78137055-78	**Pax3**	overlapping	0	1	130	5	10	13
Chr10:14687526-1	**SNORA17.465**	downstream	16642	1	130	7	1	13
Chr19:21685760-2	**1110059E24Rik**	overlapping	0	0	130	2	1	13
Chr1:120218125-1	**Mki67ip**	overlapping	0	1	130	4	1	12
Chr3:135188137-1	**Manba**	overlapping	0	1	130	6	1	8
Chr8:19868583-19	**6820431F20Rik**	overlapping	0	132	129	124	197	148
Chr9:106113553-1	**Twf2**	overlapping	0	5	129	3	4	81
Chr13:85286092-8	**Ccnh**	downstream	42392	7	129	4	5	43
Chr13:15487074-1	**Gli3**	downstream	67573	0	129	0	3	36
Chr17:17561917-1	**Lix1**	overlapping	0	1	129	2	3	20

Chr1:90709785-90	**null**	Not found	0	7	129	9	10	15
Chr7:146742952-1	**Inpp5a**	overlapping	0	0	129	1	1	12
Chr3:30828729-30	**Phc3**	overlapping	0	2	129	1	0	11
Chr14:122841689-	**Gm5089**	overlapping	0	0	129	3	0	8
Chr2:71128209-71	**Slc25a12**	overlapping	0	0	129	5	1	6
Chr3:95708496-95	**Car14**	overlapping	0	0	129	2	4	5
Chr14:124494224-	**Fgf14**	overlapping	0	2	129	1	4	4
Chr15:89486867-8	**Rabl2**	downstream	64513	2	128	3	4	96
Chr2:28763223-28	**Barhl1**	overlapping	0	2	128	4	8	70
Chr9:109079730-1	**Fbxw13**	upstream	1628	2	128	0	8	58
Chr11:107213961-	**Pitpnc1**	overlapping	0	1	128	1	3	50
Chr10:22303225-2	**Slc2a12**	downstream	61287	0	128	1	3	39
Chr15:38921812-3	**Cthrc1**	upstream	3145	4	128	0	4	39
Chr3:95467469-95	**Mcl1**	upstream	370	1	128	5	3	33
Chr8:19920032-19	**Gm10348**	overlapping	0	211	128	170	234	194
Chr1:134696878-1	**SNORA17.507**	upstream	13546	4	128	5	7	32
Chr2:17138884-17	**Gm13322**	downstream	31770	1	128	1	2	27
Chr8:111272778-1	**Zfhx3**	overlapping	0	3	128	7	4	26
Chr11:79140619-7	**Nf1**	downstream	12150	3	128	4	4	25
Chr2:30634654-30	**1700001O22Rik**	upstream	15277	2	128	1	2	13
Chr12:85981173-8	**7420416P09Rik**	downstream	448	1	128	4	3	4
Chr10:90172224-9	**Anks1b**	overlapping	0	2	127	3	11	150
Chr8:93194359-93	**null**	Not found	0	3	127	2	14	134
Chr6:13697998-13	**B630005N14Rik**	downstream	70032	3	127	1	3	99
Chr3:6768032-676	**null**	Not found	0	2	127	2	8	96
Chr1:116538202-1	**null**	Not found	0	1	127	4	19	89
Chr13:66421127-6	**AC192333.1**	downstream	28835	2	127	3	7	75
Chr7:137395580-1	**Fgfr2**	overlapping	0	3	127	1	3	69
Chr15:100094217-	**Atf1**	upstream	2542	3	127	3	7	55
Chr1:90969009-90	**Sh3bp4**	overlapping	0	1	127	6	13	51
Chr2:180475100-1	**Slc17a9**	overlapping	0	0	127	4	6	51
Chr1:70367529-70	**Spag16**	overlapping	0	3	127	5	2	46
Chr17:85656294-8	**1700106N22Rik**	overlapping	0	1	127	2	14	46
Chr9:20356658-20	**AC171206.1**	overlapping	0	2	127	0	2	34

Chr2:5300090-530	**Camk1d**	overlapping	0	31	127	31	90	170
Chr1:127169309-1	**null**	Not found	0	2	127	0	5	23
Chr7:53152462-53	**Tmem143**	overlapping	0	1	127	1	4	21
Chr8:75843550-75	**Large**	overlapping	0	35	126	55	79	153
Chr12:66694542-6	**SNORA17.70**	upstream	27334	1	126	6	10	139
Chr13:80862462-8	**null**	Not found	0	0	126	5	3	83
Chr17:29588038-2	**Gm16912**	upstream	10390	0	126	0	8	70
Chr5:61239359-61	**null**	Not found	0	20	126	32	47	38
Chr19:10244338-1	**Fads1**	downstream	12688	1	126	5	1	37
Chr6:144199796-1	**Sox5**	overlapping	0	0	126	2	4	36
Chr5:6328619-632	**AC132270.1**	upstream	41956	1	126	4	0	32
Chr9:37015491-37	**Tmem218**	downstream	51	0	126	1	6	27
Chr13:87147290-8	**null**	Not found	0	1	126	2	5	16
Chr8:111250637-1	**Zfhx3**	overlapping	0	0	126	1	5	15
Chr15:25679035-2	**Myo10**	overlapping	0	2	126	5	5	13
ChrX:154032520-1	**Mbtps2**	overlapping	0	0	126	1	0	13
Chr8:109127931-1	**Cdh1**	overlapping	0	1	126	1	1	8
Chr15:91694501-9	**Muc19**	overlapping	0	2	125	1	2	136
Chr6:63078770-63	**U6.767**	upstream	70804	0	125	5	9	82
Chr13:37865215-3	**Rreb1**	downstream	4617	2	125	0	5	80
Chr10:70911006-7	**Ipmk**	upstream	14931	3	125	2	6	63
Chr3:8005630-800	**null**	Not found	0	0	125	2	9	56
Chr8:35867921-35	**Dusp4**	downstream	1969	1	125	2	7	41
Chr2:94430648-94	**SNORA17.268**	downstream	31137	0	125	3	3	37
Chr1:12708592-12	**Sulf1**	overlapping	0	6	125	1	3	36
Chr2:102669529-1	**Cd44**	overlapping	0	2	125	9	17	32
Chr1:93444234-93	**Asb1**	overlapping	0	1	125	8	7	27
Chr13:25099639-2	**Mrs2**	overlapping	0	4	125	4	4	26
Chr15:27971116-2	**Trio**	downstream	15513	2	125	4	13	21
Chr4:100465921-1	**Cachd1**	overlapping	0	1	125	5	1	14
Chr1:7116052-711	**Pcmtd1**	overlapping	0	3	124	1	7	133
Chr11:78061228-7	**Sdf2**	overlapping	0	4	124	4	2	94
Chr3:101887774-1	**Casq2**	downstream	2148	2	124	7	6	86
Chr6:54046859-54	**Chn2**	overlapping	0	2	124	6	4	75

Chr1:42115348-42	**null**	Not found	0	1	124	3	5	73
Chr6:68802617-68	**Gm16904**	upstream	9157	5	124	2	6	72
Chr11:111705099-	**Gm11674**	downstream	42909	0	124	1	7	72
Chr6:140285264-1	**n-R5s168**	upstream	17010	1	124	1	0	65
Chr1:53638149-53	**Dnahc7a**	downstream	15608	4	124	2	3	64
Chr15:93350038-9	**Prickle1**	overlapping	0	1	124	3	7	41
Chr11:11781435-1	**Ddc**	overlapping	0	2	124	4	3	39
Chr5:125411393-1	**Zfp664**	upstream	28330	1	124	1	6	33
Chr16:19865477-1	**A930003A15Rik**	upstream	10857	1	124	1	6	33
Chr15:39612082-3	**Dpys**	overlapping	0	1	124	1	5	32
Chr9:118991281-1	**Plcd1**	overlapping	0	1	124	0	1	26
Chr11:53244534-5	**Gdf9**	overlapping	0	0	124	3	3	1
Chr5:128988925-1	**AC166933.1**	upstream	47714	3	123	2	7	94
Chr14:16629574-1	**null**	Not found	0	4	123	1	3	92
Chr1:95094184-95	**E030010N08Rik**	downstream	17797	3	123	8	12	75
Chr2:174086818-1	**Mir296**	upstream	5409	0	123	3	5	71
Chr3:14191211-14	**Ralyl**	upstream	8924	0	123	2	2	68
Chr7:123009384-1	**Sox6**	overlapping	0	1	123	6	7	61
Chr15:27925405-2	**Trio**	overlapping	0	1	123	3	5	44
Chr2:78149659-78	**Gm14461**	upstream	7272	1	123	3	0	36
Chr11:5462909-54	**SNORA17.91**	downstream	2171	1	123	2	0	36
Chr13:66405796-6	**AC173345.1**	upstream	40338	4	123	4	8	36
Chr16:31546298-3	**Bdh1**	upstream	87311	0	123	7	7	34
Chr2:54011120-54	**SNORA51.1**	upstream	58147	0	123	0	2	33
Chr4:146791314-1	**Gm16889**	overlapping	0	19	123	21	27	216
Chr10:26357343-2	**null**	Not found	0	1	123	2	2	26
Chr4:147167652-1	**Gm13157**	overlapping	0	8	123	7	3	19
Chr10:98725603-9	**Dusp6**	overlapping	0	1	123	3	6	16
Chr17:10937968-1	**Pacrg**	overlapping	0	1	123	7	2	15
Chr3:82928036-82	**Gm10710**	upstream	1085	1	123	9	12	14
Chr4:45599161-45	**U6.304**	upstream	37440	1	123	2	1	14
Chr1:73870892-73	**5S_rRNA.66**	upstream	60483	2	123	2	5	9
Chr11:79593345-7	**9130204K15Rik**	upstream	1853	1	123	1	1	9
Chr15:103197867-	**Itga5**	downstream	673	0	123	1	2	6

AUTEUR
Nicolas CHASSAING

TITRE
Anophthalmia-Microphthalmia :
genotypes and phenotypes ; identification of new genes involved in ocular development

DIRECTEURS DE THESE
Professeur Patrick CALVAS
Docteur Heather ETCHEVERS

LIEU ET DATE DE SOUTENANCE
Faculté de Médecine Purpan, 12 décembre 2013

RESUME

Anophthalmia and Microphthalmia (AM) are the most severe malformations of the eye. We analyzed the frequency with which known AM genes were implicated and detailed phenotypes associated with each gene in a large cohort of 150 patients.

Genetic causes are thought to account for most cases of AM but a genetic cause can be identified only in about 25% of patients. In order to find new AM genes we used direct candidate gene sequencing, array-CGH, transcriptomic analyses, ChIP and high throughput sequencing. We succeed identifying the second major AM gene, *PTCH1*, and participate to identification of other novel genes causing isolated and syndromic AM.

The finding that *PTCH1* mutations are found in numerous patients paves the way to new hypotheses concerning the pathophysiology of all ocular developmental defects. This information is important to following up patients and providing them with genetic counselling.

MOTS-CLES
Genetics, Ocular Development, Microphthalmia, Anophthalmia, Otocephaly, ChIP, Transcriptomic, High Throughput Sequencing, *PTCH1*, *OTX2*, *STRA6*

DISCIPLINE ADMINISTRATIVE
Gènes, cellules et développement

INTITULE ET ADRESSE DE L'U.F.R. OU DU LABORATOIRE
EA-4555, Université Paul-Sabatier Toulouse III, CPTP, Toulouse, France

AUTEUR
Nicolas CHASSAING

TITRE
Génétique des micro-anophtalmies : revue des phénotypes et des génotypes ; stratégies d'identification de nouveaux gènes impliqués dans le développement oculaire

DIRECTEURS DE THESE
Professeur Patrick CALVAS
Docteur Heather ETCHEVERS

LIEU ET DATE DE SOUTENANCE
Faculté de Médecine Purpan, 12 décembre 2013

RESUME

Les anophtalmies et microphtalmies (AM) sont les plus sévères malformations de l'œil. Nous avons étudié la fréquence des mutations des principaux gènes d'AM dans une grande cohorte de 150 patients et défini la variabilité phénotypique associée à ces mutations. Bien que l'origine génétique soit prépondérante, une anomalie moléculaire causale ne peut être identifiée que chez environ 25 % des patients.

Pour identifier de nouveaux gènes responsables d'AM, différentes approches ont été utilisées: gènes candidats, CGH-array, analyse du transcriptome, ChIP, et séquençage haut débit. Nous avons ainsi pu identifier un nouveau gène majeur du développement oculaire, *PTCH1*, et participer à l'identification d'autres gènes d'AM isolées ou syndromiques.

L'implication du gène PTCH1 introduit de nouvelles hypothèses physiopathologiques pour l'ensemble des malformations oculaires congénitales. Ces données sont importantes pour la prise en charge des patients et de leurs familles.

MOTS-CLES
Génétique, Développement oculaire, Microphtalmie, Anophtalmie, Otocéphalie, ChIP, Transcriptome, Séquençage haut débit, *PTCH1*, *OTX2*, *STRA6*

DISCIPLINE ADMINISTRATIVE
Gènes, cellules et développement

INTITULE ET ADRESSE DE L'U.F.R. OU DU LABORATOIRE
EA-4555, Université Paul-Sabatier Toulouse III, CPTP, Toulouse, France